# DIRECT-CURRENT MACHINES

By

MICHAEL LIWSCHITZ-GARIK, Dr-Ing.

*Professor at the Polytechnic Institute of Brooklyn; Consulting Engineer to the Westinghouse Electric Corporation, i.R.; Consulting Engineer to the National Electric Coil Company, Columbus, Ohio*

Assisted by

CLYDE C. WHIPPLE, E.E.

*Professor at the Polytechnic Institute of Brooklyn; Chairman of the Undergraduate Electrical Engineering Department*

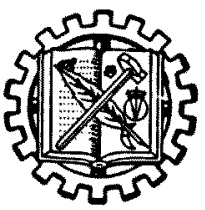

SECOND EDITION

D. VAN NOSTRAND COMPANY, INC.

PRINCETON, NEW JERSEY

TORONTO LONDON

NEW YORK

*All correspondence should be addressed to the principal office of the company at Princeton, N. J.*

D. VAN NOSTRAND COMPANY, INC.
120 Alexander St., Princeton, New Jersey
257 Fourth Avenue, New York 10, New York
25 Hollinger Rd., Toronto 16, Canada
Macmillan Co., Ltd., St. Martin's St., London, W.C. 2, England

Copyright, ©, 1946, 1956 by
D. VAN NOSTRAND COMPANY, INC.

Published simultaneously in Canada by
D. VAN NOSTRAND COMPANY (Canada), LTD.

*All Rights Reserved*

*This book, or any parts thereof, may not be reproduced in any form without written permission from the authors and the publishers.*

Library of Congress Catalogue Card No.: 56-9012

***First Edition, September 1946***
*Five Reprintings*
***Second Edition, July 1956***

PRINTED IN THE UNITED STATES OF AMERICA

To My Late Wife

OLGA LIWSCHITZ-GARIK

I dedicate my work

# PREFACE

This new edition of *Direct-Current Machines* is designed for college undergraduate courses in electrical engineering. The principal aim of the text is to provide a fundamental link between the basic laws of electrodynamics and the performance characteristics of the electric machines. Moreover, on the basis of our own teaching experience and on the advice of numerous college teachers, the organization of the present book has been extensively rearranged from that of the previous edition. The book is divided into two parts: "The Fundamentals of D-C Machines" and "Some Advanced Topics"; the first part is designed for undergraduate study, whereas the second part deals with problems of interest for advanced undergraduate and postgraduate students and also for practicing engineers.

In comparison with the first edition, new material has been added on commutation, heating, and tangential forces in the electric machines. Furthermore, the present d-c volume has been made entirely independent of the a-c companion volume, which is separately published. In the first part of the text is contained the necessary material for a one-semester undergraduate course on d-c machines. It is written from the viewpoint of enabling the student to understand the physical principles of operation, as well as the terminal characteristics of the d-c machine. The second part is written with the viewpoint of giving the graduate student, as well as the practicing engineer and designer, information of specific value not ordinarily available.


## ACKNOWLEDGMENTS

The preparation of this new edition has been greatly aided by the help of my colleague, Professor Clyde C. Whipple. Professor Whipple has critically read all the material and has made many valuable suggestions. He has provided the examples, together with the problems and answers. He prepared the material on motor starting, control, and application. I also wish to express my appreciation to my colleagues, Professors F. Wahlers and J. Hostetter, as well as to Professor R. T. Weil, Jr., of Manhattan College, for their suggestions and critical reading of the manuscript.

I am also indebted to Dr. H. S. Rogers, President of the Polytechnic Institute of Brooklyn, and to Dr. E. Weber, head of the Department of Electrical Engineering at the Polytechnic Institute of Brooklyn, for their kind assistance in offering the facilities of the Institute necessary for the completion of this work. The Westinghouse Electric Corporation generously supported my efforts and supplied information and photographs for which I am deeply grateful.

Finally, I wish to express my gratitude to the General Electric Company, the National Electric Coil Company, the Allis Chalmers Corporation, the Century Electric Company, Robbins and Meyers, Inc., and Wagner Electric Corporation, and the Cutler-Hammer Company for their contribution of cuts, data, and photographs.

*Brooklyn, New York*
*May, 1956*

MICHAEL LIWSCHITZ-GARIK

CONTENTS

## *PART I FUNDAMENTALS OF D-C MACHINES*

### CHAPTER 1 THE FUNDAMENTAL LAWS


| | | PAGE |
|---|---|---|
| 1-1 | Faraday's Law of Induction | 1 |
| 1-2 | Kirchhoff's Mesh Law | 8 |
| 1-3 | Circuital Law of the Magnetic Field (Ampére's Law) | 8 |
| 1-4 | Forces on Conductors in a Magnetic Field (Biot-Savart's Law) | 10 |
| 1-5 | Electromagnetic Power of the Electrical Machine | 12 |
| 1-6 | Summary | 13 |

CHAPTER 2 MECHANICAL ELEMENTS OF THE D-C MACHINE 17

### CHAPTER 3 D-C ARMATURE AND FIELD WINDINGS

| | | |
|---|---|---|
| 3-1 | Homopolar Machine for Generating a Direct Current | 26 |
| 3-2 | Two Types of D-C Armature Windings. Lap Winding and Wave Winding | 26 |
| 3-3 | Winding Pitch | 29 |
| 3-4 | Number of Parallel Paths in the Lap and Wave Windings | 31 |
| 3-5 | The Field Displacement and the Number of Parallel Paths | 38 |
| 3-6 | Series-Parallel or Duplex-Wave Winding | 42 |
| 3-7 | The Split-Coil Winding | 46 |
| 3-8 | Operation of the Commutator | 46 |
| 3-9 | Equalizer Connections. Condition for Symmetry | 49 |
| 3-10 | Insulation of D-C Armature Windings | 51 |
| 3-11 | D-C Field Windings | 51 |

### CHAPTER 4 EMF INDUCED IN A D-C ARMATURE WINDING (APPLICATION OF FARADAY'S LAW OF INDUCTION); ELECTROMAGNETIC TORQUE PRODUCED BY A D-C MACHINE (APPLICATION OF BIOT-SAVART'S LAW)

| | | |
|---|---|---|
| 4-1 | Emf Induced in a D-C Armature Winding | 55 |
| 4-2 | Electromagnetic Torque Produced by a D-C Machine | 57 |

## Chapter 5 The Magnetic Circuit (Application of Ampére's Law)


| | | PAGE |
|---|---|---|
| 5-1 | The Magnetic Circuit of the D-C Machine at No-Load | 61 |
| 5-2 | No-Load Characteristic | 67 |
| 5-3 | Mmf of the Armature Winding | 67 |
| 5-4 | Field and Armature Both Carry Current | 70 |
| | (a) Cross Magnetizing Effect of the Armature | 70 |
| | (b) Demagnetizing Effect of the Armature | 72 |
| | (c) Calculation of the Field Mmf Under Load | 73 |


## Chapter 6 Methods of Excitation; Direction of Rotation of the Shunt and Series Machine


| | | |
|---|---|---|
| 6-1 | Methods of Excitation | 77 |
| | (a) Series Excitation | 77 |
| | (b) Shunt Excitation | 78 |
| | (c) Compound Excitation | 78 |
| 6-2 | Direction of Rotation of a Shunt and Series Machine as Generator and Motor | 80 |


## Chapter 7 The D-C Generator


| | | |
|---|---|---|
| 7-1 | The Voltage Equation of the D-C Generator | 82 |
| 7-2 | Characteristic Curves of the D-C Generator | |
| | (a) Regulation | 83 |
| 7-3 | Separately Excited Generator | 84 |
| | (a) The No-Load Characteristic | 84 |
| | (b) The Load Characteristic | 85 |
| | (c) The External Characteristic | 86 |
| 7-4 | Series Generator | 91 |
| | (a) The No-Load Characteristic | 91 |
| | (b) The Load Characteristic | 91 |
| | (c) The External Characteristic | 91 |
| 7-5 | Shunt Generator | 91 |
| | (a) The No-Load Characteristic and Building Up of Voltage | 91 |
| | (b) Influence of Speed on the Induced Emf at No Load | 93 |
| | (c) The Load Characteristic | 94 |
| | (d) The External Characteristic | 94 |
| | (e) The Regulation Curve | 97 |
| | (f) Influence of Speed on the External Characteristic | 97 |
| 7-6 | The Cumulative Compound Generator | 97 |
| | (a) The No-Load Characteristic | 97 |
| | (b) The External Characteristic | 97 |

PAGE

7-7 Parallel Connection and Operation of D-C Generators ..... 100
7-8 Applications of the Different Types of Generators ..... 103
(a) Separately Excited Generator and Shunt Generator ..... 103
(b) Cumulative Compound Generator ..... 104
(c) Differential Compound Generator ..... 104
(d) Series Generator ..... 104

## Chapter 8 The D-C Motor

8-1 Voltage and Torque Equation of the D-C Motor ..... 107
8-2 Characteristics of the Shunt Motor ..... 109
8-3 Characteristics of the Series Motor ..... 115
8-4 Characteristics of the Cumulative Compound Motor ..... 117
8-5 Comparison Between the Different Types of Motors ..... 120
8-6 Stability of a Motor ..... 122
8-7 Speed Control of the D-C Motors ..... 122
(a) Separately Excited, Shunt and Cumulative Compound Motor 123
(b) Series Motor ..... 124
8-8 Motor Application ..... 125
8-9 Characteristics of Load ..... 125
8-10 Motor Types, Sizes, and Costs ..... 129

## Chapter 9 Commutation

9-1 The Short-circuited Winding Elements ..... 135
9-2 The Commutation Curve ..... 137
9-3 Resistance Commutation ..... 138
9-4 Conditions Necessary for Zero Current Density at the Trailing Brush Edge ..... 141
9-5 Effects of the Various Emf's on the Commutation ..... 143
(a) Influence of the Emf of Self-Induction on the Commutation 143
(b) Influence of the Armature Flux on Commutation ..... 144
9-6 Production of a Commutating Flux by Means of Interpoles. Compensating Winding ..... 145
9-7 The Magnitude of the Emf or Self- and Mutual-Induction in the Short-Circuited Winding Element. The Magnitude of Interpole Flux-Density ..... 148
9-8 The Brush Curve ..... 151
9-9 Reaction of Current in the Short-Circuited Winding Elements Upon Main Flux ..... 152

## Chapter 10 Special D-C Machines and Rotating Amplifiers

### A. SPECIAL D-C MACHINES

PAGE

10-1 Three-Wire Generator . . . . 154
10-2 Train-Lighting Generators 157
10-3 Arc-Welding Generators . 161
10-4 Diverter-Pole Generator . . . . 163
10-5 Dynamotor . . . . 164
10-6 Tuned Generators (Rototrol, Regulex) . 164

### B. ROTATING AMPLIFIERS

10-7 Amplidyne . . . . 169
10-8 Rototrol (Two-Stage and Three-Stage) . 170

## Chapter 11 Losses

11-1 Losses Due to the Main Flux . . . . 172
(a) Iron Losses in the Armature 172
(b) Pole-Face Losses . . . . 175
(c) Copper Losses . . . . 175
(d) Eddy-Current Losses in Structural Parts 176
11-2 Losses Due to the Armature Current . . 176
(a) $I^rR$-Losses in the Armature, Interpole, Series Field, and Compensating Windings . . . . 176
(b) Skin-Effect Losses . . . . 176
(c) Copper Losses in the Armature Winding Due to Flux Distortion . . . . 178
11-3 Friction and Windage Losses . . . . 179
11-4 No-Load and Load Losses. Stray Load Losses . . 179
11-5 Examples of Loss Distribution and Efficiencies . . . 180

## Chapter 12 Heating and Cooling

12-1 Influence of the Heat Conductivity of the Materials and of the Heat Transfer to the Air . . . . 182
12-2 Heating and Cooling of a Homogeneous Body . . . . 184
12-3 Temperature Rise of the Windings . . . . 188
12-4 Cooling (Ventilation) of D-C Machines
(a) Different Types of Enclosures . . . . 188

## Chapter 13 Starting of D-C Motors

13-1 Starting a Motor . . . . 194
(a) Shunt Motor . . . . 194
(b) Series Motor . . . . 198

PAGE

13-2 Manual Type Starters for D-C Motors . . . . . 199
(a) Three-Terminal Starter . . . . . 200
(b) Four-Terminal Starter . . . . . 201
(c) Drum-Type Starter . . . . . 203
13-3 Automatic Starters for D-C Motors . . . . . 207
(a) Counter-Emf Type . . . . . 208
(b) Definite-Time Starter . . . . . 209
(c) Dynamic Braking Controller . . . . . 212
13-4 Definitions . . . . . 214

*PART II SOME ADVANCED TOPICS*

CHAPTER 14 TANGENTIAL FORCES IN THE ELECTRIC MACHINES

14-1 Biot-Savart's Law . . . . . 219
14-2 Stresses in the Magnetic Field . . . 219
14-3 Forces at the Boundary Surface Between Air and Iron 221
14-4 Forces on the Teeth . . . . . 224

CHAPTER 15 LIMITATIONS OF THE WAVE WINDING WITH RESPECT TO THE NUMBER OF WINDING ELEMENTS PER LAYER PER SLOT 227

CHAPTER 16 DETERMINATION OF THE NO-LOAD FIELD MMF

16-1 Cross-Sectional Area of the Gap. Gap Mmf . . . . . 228
16-2 Teeth Mmf . . . . . 233
16-3 Armature Core Mmf . . . . . 236
16-4 Pole Leakage. Pole and Yoke Mmf's . . . . . 236

CHAPTER 17 COMMUTATION

17-1 General Formulae for $L$ and $M$ . . . . . 240
17-2 The Slot Leakage Flux . . . . . 241
(a) Single-Layer Winding . . . . . 241
(b) Two-Layer Winding with One Winding Element per Layer 243
(c) Two-Layer Winding with Several Winding Elements per Layer . . . . . 245
17-3 The Tooth-Top Leakage Fluxes . . . . . 245
17-4 The End-Winding Leakage Fluxes . . . . . 247
17-5 Standard (Non-Split) Coil . . . . . 248
17-6 Example of Calculation of $(L + \Sigma M)_{av}$ . . . . . 253
17-7 Split Coils . . . . . 257
17-8 Comparison Between Not-Chorded Standard Coil, Chorded Standard Coil, and Split Coil . . . . . 260

PAGE

17-9 Reactance Voltage ..... 265
17-10 Interpole-AT ..... 266

CHAPTER 18 LOSSES DUE TO SLOT-OPENINGS AND SKIN-EFFECT

18-1 Pole-Face Losses ..... 268
18-2 Copper Losses Due to the Main Flux ..... 270
18-3 Skin-Effect Losses ..... 271
18-4 Example of Calculation ..... 272

CHAPTER 19 HEAT FLOW AND TEMPERATURE RISES OF THE WINDINGS AND IRON

19-1 Data on Heat Conductivities and Heat Transfer Coëfficients . 274
19-2 Assumptions for the Investigation ..... 275
19-3 The Equation of Heat Flow ..... 276
19-4 Temperature Rises of Stator Copper and Iron ..... 276
19-5 Temperature Rises of Rotor Copper and Iron ..... 283
19-6 Temperature Rise of Concentric Field Windings ..... 284
19-7 Example of Calculation ..... 284

CHAPTER 20 APPROXIMATE DETERMINATION OF THE FIELD-DISTRIBUTION CURVE ..... 289

CHAPTER 21 THE TWO-STAGE AND THREE-STAGE ROTOTROLS

21-1 The Two-Stage Rototrol ..... 291
21-2 Multi-Stage Amplifier (Multi-Stage Rototrol) ..... 297

# LIST OF SYMBOLS

## *A, a*

| | |
|---|---|
| $A$ | ampere-conductors per unit of circumference |
| $A$ | area |
| $a$ | number of parallel paths in the d-c armature winding |
| $a$ | area |

## *B, b*

| | |
|---|---|
| $B$ | flux density |
| $B$ or $B_g$ | flux density in the gap |
| $B'_t$ | fictitious flux density in the tooth |
| $B_t$ | actual flux density in the tooth |
| $B_i$ | flux density in the air gap of the interpole |
| $B_c$ | flux density in the core |
| $B_o$ | variation of flux density due to slot openings |
| $b$ | width |
| $b_e$ | equivalent pole arc |
| $b_v$ | width of a radial ventilating duct |
| $b_p$ | width of pole shoe (arc) |
| $b_s$ | slot width |
| $b_i$ | width of interpole |
| $b_o$ | slot width at the air gap |
| $b_b$ | brush width |
| $b'_b$ | brush width referred to the armature |
| $b_{cz}$ | width of the commutating zone |

## *C, c*

| | |
|---|---|
| $c$ | specific heat |
| $c$ | chording of the armature coil |

## *D, d*

| | |
|---|---|
| $D$ | outside diameter of the armature core |
| $d$ | air space between two insulated coil ends |
| $d_M$ | current density corresponding to copper loss due to main flux |

## *E, e*

| | |
|---|---|
| $E$ | induced emf (for a-c effective value) |
| $E_m$ | magnetic energy |

| | |
|---|---|
| $e$ | induced emf, instantaneous value |
| $e_i$ | voltage induced in the short-circuited winding element by the interpole flux |
| $e_r$ | reactance voltage |
| $e_s$ | emf of self-induction |

## *F, f*

| | |
|---|---|
| $F$ | force |
| $f$ | force on a single conductor |
| $f$ | pull on the surface of iron |
| $f$ | frequency in cycles per second |

## *g*

| | |
|---|---|
| $g$ | air gap length |
| $g_i$ | interpole air gap length |

## *H, h*

| | |
|---|---|
| $H$ | field intensity |
| $HP$ | output in horsepower |
| $h$ | height |
| $h_p$ | length of magnetic path in a pole |
| $h_t$ | length of magnetic path in a tooth |
| $h_1$ | height of the slot occupied by the conductors |
| $h_s$ | depth of the slot |
| $h$ | heat transfer coefficient |

## *I, i*

| | |
|---|---|
| $I$ | current |
| $I_a$ | total current of a d-c armature winding |
| $I_f$ | field current |
| $I_n$ | rated current |
| $i$ | current, instantaneous value |
| $i_a$ | current per path in the d-c armature winding |

## *K, k*

| | |
|---|---|
| $K$ | number of commutator bars |
| $k_c$ | Carter factor |
| $k_v$ | vent factor (see p. 230) |
| $k_t$ | ratio of cross section of slot to cross section of tooth |
| $k_i$ | stacking factor |

$k_s$ ratio of total length of armature $L$ to the length effective for slot leakage

$k$ constant

## $L$, $l$

$L$ coefficient of self-inductance

$L$ total length of armature core

$L_s$ coefficient of self-inductance for the slot leakage flux

$L_s$ pole-face loss

$L_{st}$ coefficient of self-inductance of the top coil side for the slot leakage flux

$L_{sb}$ coefficient of self-inductance of the bottom coil side for the slot leakage flux

$L_{tt}$ coefficient of self-inductance for the tooth top leakage flux

$L_e$ coefficient of self-inductance for the end winding leakage flux

$L_{sk}$ loss due to skin effect

$l$ length

$l$ length of armature core without radial ventilating ducts

$l_e$ equivalent length of armature core

$l_c$ length of magnetic path in a core

$l_y$ length of magnetic path in a yoke

$l_s$ effective length of the armature for slot leakage flux

$l_e$ length of the end winding for half a coil

$l_t$ mean length of a turn

## $M$, $m$

$M$ coefficient of mutual inductance

$M$ magnetomotive force (mmf)

$M_g$ mmf for the air gap

$M_t$ mmf for the teeth

$M_y$ mmf for the yoke

$M_c$ mmf for the core

$M_{tb} = M_{bt}$ coefficient of mutual inductance between the top and bottom coil side for the slot leakage

$M_d$ total mmf of armature reaction

$M'_d$ total mmf of armature reaction measured in shunt field amperes

$M_f$ field mmf

## $N$, $n$

$N$ number of turns in a coil

$N$ number of turns in series between two brushes

$N_e$ number of turns per winding element

$N_x$ number of turns linked with a flux $\phi_x$

$N_f$ number of turns in a concentrated field winding
$n$ rpm
$n_c$ number of turns per coil
$n_n$ normal or rated speed
$n_0$ no-load speed
$n_v$ number of radial ventilating ducts

## $P$, $p$

$P$ power
$P_{Fe}$ iron losses
$P_W$ windage losses
$P_F$ friction losses
$p$ number of poles

## $Q$, $q$

$Q$ total number of slots
$Q$ heat produced in a body per second

## $R$, $r$

$R$ resistance
$R$ radius
$R_f$ resistance of shunt field rheostat
$R_c$ resistance of choke coil
$r$ resistance
$r_a$ resistance of armature winding
$r_e$ reduction factor for eddy current loss
$r_s$ resistance of series field winding
$r_i$ resistance of interpole winding
$r_f$ resistance of the shunt field winding

## $S$, $s$

$S$ cooling surface
$s$ current density

## $T$, $t$

$T$ period of a wave
$T_c$ period of commutation
$T$ torque
$T$ thermal time constant
$t$ time in seconds

### *U, u*

| | |
|---|---|
| $u$ | number of conductors side by side in the slot |

### *V, v*

| | |
|---|---|
| $V$ | terminal voltage |
| $\Delta V$ | voltage drop under all the brushes of same polarity |
| $\Delta V$ | voltage drop between the outer wires for the 3-wire generator |
| $v$ | terminal voltage, instantaneous value |
| $v_c$ | surface velocity of the commutator |

### *W*

| | |
|---|---|
| $W$ | weight |

### *Y, y*

| | |
|---|---|
| $y$ | winding pitch |
| $y_b$ | back pitch |
| $y_f$ | front pitch |

### *Z, z*

| | |
|---|---|
| $Z$ | total number of conductors on an armature |

### Delta

| | |
|---|---|
| $\Delta$ | thickness of laminations |
| $\delta'$ | distance between two conductors in the same slot |
| $\delta''$ | distance between the conductors of two adjacent slots |

### Epsilon

| | |
|---|---|
| $\epsilon$ | voltage regulation |
| $\epsilon$ | voltage drop |
| $\epsilon$ | basis of the natural logarithms |

### Zeta

| | |
|---|---|
| $\zeta$ | permeance per unit length for the leakage fluxes during commutation |

### Eta

| | |
|---|---|
| $\eta$ | efficiency |

### Theta

| | |
|---|---|
| $\theta$ | temperature |
| $\theta_s$ | temperature at the surface |
| $\theta_{air}$ | temperature of the cooling air |
| $\theta$ | temperature rise |

### Lambda

| | |
|---|---|
| $\Lambda$ | permeance |
| $\lambda$ | permeance per unit length |
| $\lambda_s$ | permeance per unit length for the slot leakage flux |
| $\lambda_{st}$ | permeance per unit length of the top coil side for the slot leakage flux |
| $\lambda_{sb}$ | permeance per unit length of the bottom coil side for the slot leakage flux |
| $\lambda_{tt}$ | permeance per unit length for the tooth top leakage flux |
| $\lambda_{bt} = \lambda_{tb}$ | permeance per unit length for mutual induction between bottom and top coil side in the slot |
| $\lambda_h$ | heat conductivity |

### Mu

| | |
|---|---|
| $\mu$ | relative permeability |

### Rho

| | |
|---|---|
| $\rho$ | resistivity |

### Tau

| | |
|---|---|
| $\tau$ | pitch |
| $\tau$ | pole pitch |
| $\tau_v$ | vent pitch (width of one stack of laminations plus width of one ventilating duct) |
| $\tau_s$ | slot pitch |
| $\tau_{sg}$ | slot pitch at the gap |
| $\tau_c$ | commutator pitch |

### Phi

| | |
|---|---|
| $\Phi$ | flux per pole in the air gap |
| $\Phi'$ | flux within a slot pitch |
| $\Phi_p$ | flux in the pole core |
| $\phi$ | flux |

### Omega

| | |
|---|---|
| $\omega$ | electrical angular velocity |

# *Chapter 1*

## THE FUNDAMENTAL LAWS

*All electric machines, direct- as well as alternating-current, operate on the same basic principles, and only a few fundamental laws govern the behavior of these machines. A thorough understanding of these fundamental laws is essential for the study of electric machines.* These laws are treated in this chapter and are listed below:

1. Faraday's law of induction.
2. Kirchhoff's law of the electric circuit.
3. Circuital law of the magnetic field (Ampère's law).
4. Law of force on a conductor in a magnetic field (Biot-Savart's law).

**1–1. Faraday's Law of Induction.** (a) *Electromotive force induced in a closed conducting circuit by a flux produced by a magnet.* **Faraday's law of induction** states: *If the magnetic flux linking a closed conducting circuit is changing, an electromotive force is induced in the circuit.*

If $\phi$ represents the flux linking the circuit and $d\phi$ the change in flux during the time $dt$, then the magnitude of the induced emf is proportional to the rate of change of the flux, $d\phi/dt$.

The direction of the induced emf is determined by Lenz's law, which states that the current produced by the induced emf opposes the change in flux. This will be explained by several simple examples.

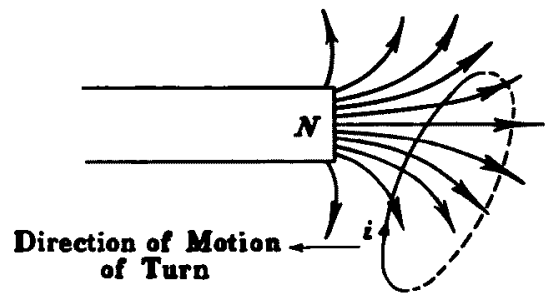


FIG. 1–1. Induction of an emf in a simple circuit.

**Example 1–1.** Consider Fig. 1–1. Shown here are an isolated north pole and a closed circuit of one turn which may be moved relative to this pole. The lines of force proceed outward from the north pole.

It should be remembered that the direction of the current and the direction of the lines of force produced by the current bear the same relation to one another as the direction of progress and direction of rotation of a right-hand screw (such as a corkscrew); if the forward motion of the screw and the direction of the current coincide, then the direction of the lines of force about the conductor is the same as the direction of rotation of the screw.

If the magnet and circuit (Fig. 1–1) are now brought closer to one another so that the flux linking the circuit is increased, the current produced by the induced voltage has a direction as shown by the arrow and tends to produce a flux which reduces the number of lines of force linking the circuit. On the other hand, if the magnet and the circuit are moved farther apart so that the number of lines of force linking the circuit is reduced, the induced current $i$ has the opposite direction and tends to produce a flux which increases the number of lines of force linking the circuit. In both cases the induced current opposes the change in flux.

**Example 1–2.** Consider an elementary machine (Fig. 1–2). A coil $ab$ mounted on an iron core rotates between a north and a south pole. The flux interlinked with the coil is a maximum when the plane of the coil is horizontal and is a minimum

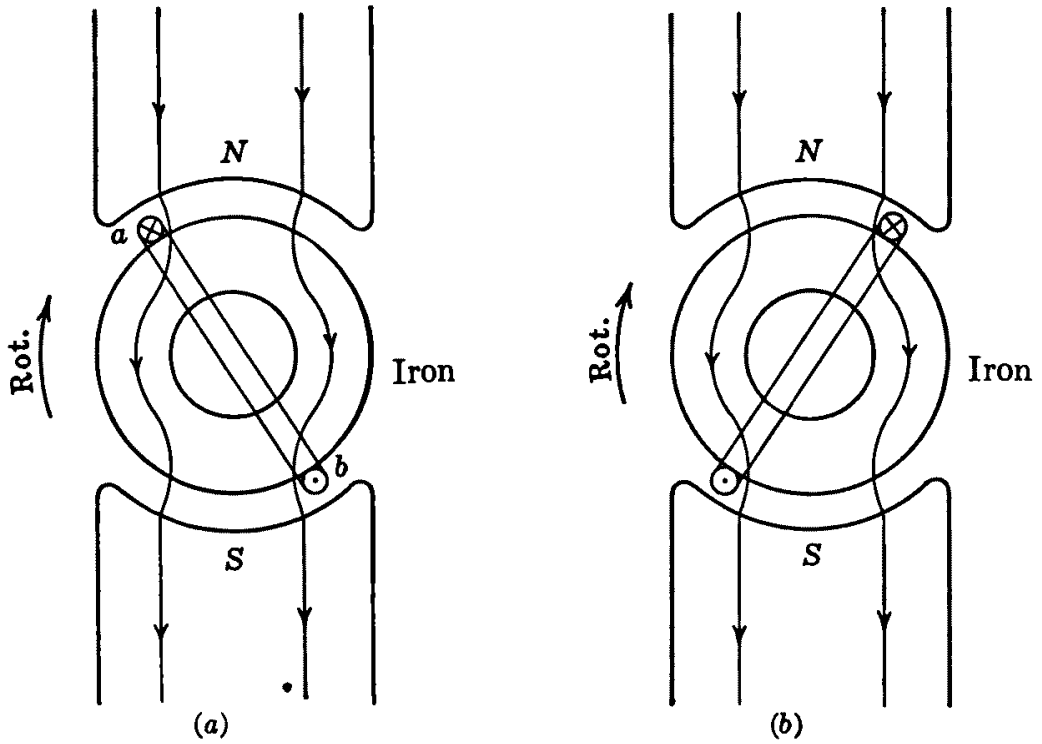


FIG. 1–2. Induction of an emf in a coil of an electric machine.

when the plane is vertical. When the coil is in the position shown in Fig. 1–2a, the flux linking the coil is decreasing. The induced emf and resultant current, therefore, will have a direction as indicated by the cross and dot* since current flowing in this direction tends to oppose the reduction in flux linkages.

Fig. 1–2b shows the direction of emf and current for another position of the coil. In this position the flux interlinked with the coil is increasing. The direction of the current is the same as in Fig. 1–2a because a current in this direction tends to oppose the increase in flux linkages.

In both examples considered, the induced emf has the same direction as the current, and therefore this emf must be considered negative with respect to the change of flux interlinkage. If the flux linked with the circuit increases, i.e., $d\phi/dt$ is positive, the current produced by the induced emf decreases the flux; if the

* The cross represents a current flowing away from the observer, and the dot represents a current flowing toward the observer.

flux linked with the circuit decreases, i.e., $d\phi/dt$ is negative, the current produced by the induced emf increases the flux. Accordingly, Faraday's law of induction must be written :

$$e = -\frac{d\phi}{dt}\,10^{-8} \text{ volt} \qquad (1\text{–}1)$$

i.e., *the emf induced in the circuit is equal to the rate of decrease of the flux interlinked with the circuit.* In this equation $\phi$ is in maxwells and $t$ in seconds.

**Example 1–3.** Consider Fig. 1–3. A conductor $ab$ moves downward between two poles. Since the flux interlinked with the circuit is diminishing, for the chosen direction of movement, the current in the conductor will be in the direction from $b$ to $a$ because this would oppose the reduction of flux linking the circuit.

For this case, Faraday's law of induction may be expressed in a different way. If the conductor $ab$ moves downward a distance $dx$ in a time $dt$, the change in flux interlinkage is $d\phi = -Bl\ dx$, where $B$ is the flux density in gausses and $l$ is the length of the conductor within the flux, in centimeters. Hence,

$$e = -\frac{d\phi}{dt}\,10^{-8} = Bl\frac{dx}{dt}\,10^{-8} \text{ volt}$$

in which $dx/dt$ is the velocity $v$ with which the conductor moves. Thus, the instantaneous value of $e$ is proportional to $B$ and $v$,

$$e = Blv10^{-8} \text{ volt} \qquad (1\text{–}2a)$$

or

$$e = \tfrac{1}{3}Blv10^{-8} \text{ volt} \qquad (1\text{–}2b)$$

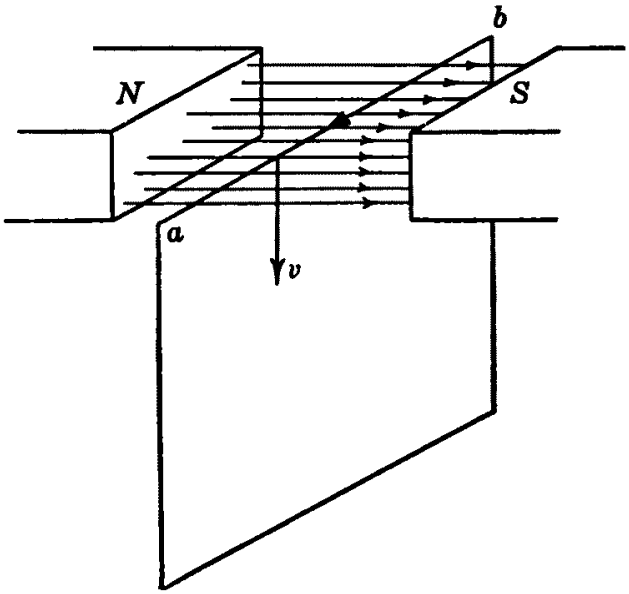


FIG. 1–3. Induction of an emf in a simple circuit.

if $B$ expressed in lines per square inch, $l$ in inches, and $v$ in feet per minute. $Bldx$ is the flux cut by the conductor in the time $dt$. Therefore, Eq. 1–2 can be interpreted as follows: *The emf induced in the conductor is equal to the flux cut by it per second.*

Eq. 1–2 can be applied also to the second example where a coil rotates between two poles. It should be noted that Eq. 1–1, which is based on flux interlinkages, is more general, while the flux cutting Eqs. 1–2a and 1–2b are applicable where there is relative motion between conductors and a flux which is constant with time.

The *average emf* induced in the coil of Fig. 1–2 can be readily determined from Eq. 1–1. When the coil lies in the horizontal, it is interlinked with the total pole-flux $\Phi$. When it moves from the horizontal position a quarter of a revolution, it lies in the vertical and its flux interlinkage is zero. A quarter of a revolution further in the same direction brings the coil again to the horizontal; the flux interlinkage is again $\Phi$ but in the opposite direction. Thus, during a half revolution, $\Delta\phi = 2\Phi$. If the speed of the armature is

$n/60$ rps, ($n$ in rpm), the duration of a half-revolution is $\Delta t = 30/n$ seconds and

$$E_{av} = \frac{2\Phi}{30/n} 10^{-8} = 4\Phi \frac{n}{60} 10^{-8} \text{ volt} \tag{1–3}$$

The average emf depends upon the total flux per pole and is independent of the way the flux is distributed around the periphery of the armature, i.e., of the magnitude of the flux density $B$ around the armature. The instantaneous values of the induced emf, on the contrary, depend upon the distribution of $B$, as indicated by Eq. 1–2.

Eq. 1–3 assumes that there are only two poles. If the number of poles is $p$, then, during a half revolution, $\Delta\Phi = 2\Phi(p/2)$, and $E_{av}$ becomes $p/2$ times the value given by Eq. 1–3, so that

$$E_{av} = \left(4\Phi \frac{p}{2}\right) \frac{n}{60} 10^{-8} \text{ volt} \tag{1–3a}$$

Consider Fig. 1–4 which shows the normal flux distribution in a d-c machine. $B$ is zero in the middle of the interpolar space (see Fig. 1–2) and is a maximum in the center of the pole. If both coil sides lie at all times in fields of equal strength, the instantaneous value of the emf induced in the coil is (Eq. 1–2a)

$$e = 2B_x lv 10^{-8} \text{ volt} \tag{1–4}$$

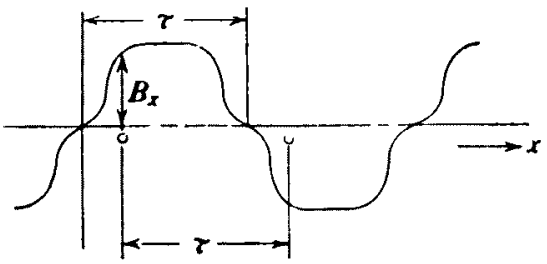


FIG. 1–4. Flux distribution in a d-c machine.

i.e., it is proportional to $B_x$, and the emf curve has exactly the same shape as the $B$ curve.

If $D$ = diameter of the armature and $p$ = number of poles, then the arc $\tau$

$$\tau = \frac{\pi D}{p} \tag{1–5}$$

is the *pole pitch*. In order that both sides of a coil lie in flux densities of the same strength, its coil span, measured as an *arc*, must be equal to the pole pitch. This is the case in Fig. 1–2.

If the flux distribution along the armature is *sinusoidal*, the emf of the coil also will be sinusoidal (Fig. 1–5). Since the ratio of amplitude to average value of a sinusoidal function is $\pi/2$, the amplitude of the sinusoidal emf induced in the coil is, from Eq. 1–3a,

$$E_m = 2\pi\Phi \frac{pn}{120} 10^{-8} \text{ volt} \tag{1–6}$$

Consider Fig. 1–2. While the coil is making one revolution, it generates one cycle of the emf (Fig. 1–5). If the armature rotates at $n$ revolutions per

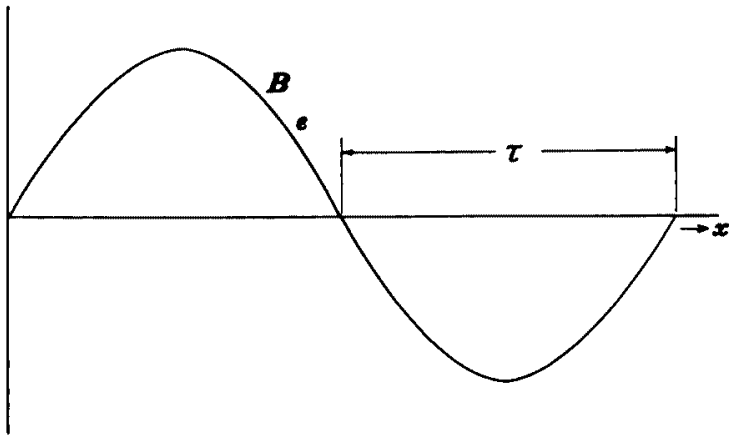


FIG. 1–5. Sinusoidal flux distribution.

minute, the frequency of the emf, in cycles per second, will be $f=n/60$. This applies to a 2-pole machine. If the number of poles is $p$ instead of 2, it still holds that the emf goes through a complete cycle when the coil passes *two* poles of the machine and therefore the frequency of the induced emf is

$$f=\frac{p}{2}\frac{n}{60}=\frac{pn}{120} \text{ cps} \tag{1–7}$$

When Eq. 1–7 is introduced into Eq. 1–6, the amplitude of the emf becomes

$$E_m=2\pi f\Phi 10^{-8} \text{ volt} \tag{1–6a}$$

and its effective value

$$E=\frac{Em}{\sqrt{2}}=4.44f\Phi 10^{-8} \text{ volt} \tag{1–8}$$

Eqs. 1–3a, 1–6a, and 1–8 assume that the coil consists of two conductors making one turn. If the number of series-connected turns of the coil is $N$ and these $N$ turns are so concentrated that they are all interlinked with the same number of flux lines at any instant of time, the induced emf will be $N$ times that given by these equations, i.e.,

$$E_{av}=4\Phi N\frac{p}{2}\frac{n}{60}10^{-8} \text{ volt} \tag{1–9}$$

$$E_m=2\pi fN\Phi 10^{-8} \text{ volt} \tag{1–10}$$

and

$$E=4.44Nf\Phi 10^{-8} \text{ volt} \tag{1–11}$$

**Example 1–4.** A coil with five series-connected turns rotates at a speed of 1200 rpm. The flux per pole is $\Phi=3\times10^6$ maxwells; the number of poles is $p=6$. What is the average emf induced in the coil? What is the amplitude and the effective value of the emf induced in the coil if the flux is sinusoidally distributed?

From Eq. 1–9, with $p=6$ and $N=5$,

$$E_{av}=4\times3\times10^6\times5\times\frac{6}{2}\times\frac{1200}{60}\times10^{-8}=36 \text{ volts}$$

From Eq. 1–7

$$f = \frac{6 \times 1200}{120} = 60 \text{ cps}$$

From Eq. 1–10

$$E_m = 2\pi \times 60 \times 5 \times 3 \times 10^6 \times 10^{-8} = 56.6 \text{ volts}$$

and

$$E = \frac{56.5}{\sqrt{2}} = 40 \text{ volts}$$

For a sinusoidally distributed flux, $E_{av}$ must be $\frac{2}{\pi} E_m$.

Faraday's law of induction, Eq. 1–1, can be interpreted also in another manner. In this interpretation, $e$ is the total emf induced in the closed circuit; i.e., if the circuit were opened somewhere and an oscillograph inserted, the value of $e$ measured at each instant would be for the entire circuit. In reality, $e$ is the sum of all elemental emf's $de$ which are induced in the individual elements $dl$ of the circuit, and Eq. 1–1 can be written:

$$e = \oint E_l dl = -\frac{d\phi}{dt} 10^{-8} \text{ volt} \qquad (1–12)$$

where $E_l$ is the component of the electric field intensity $E$ in the direction of $dl$. This equations states that every change in the lines of flux linking a circuit produces an electric field within the circuit, and that the line integral of the intensity of this electric field (the induced emf) is equal to $-\frac{d\phi}{dt}$. (See references on Electromagnetic Field Theory.)

(b) *Electromotive force of self-induction and mutual induction.* In the previous examples (Figs. 1–1 to 1–3), the flux is produced by a magnet, and the change of flux interlinkage is caused by a relative movement between a coil and a magnet. According to Faraday's law of induction, it is only the *change of flux interlinkage* that causes an emf to appear in a circuit, no matter what the source of the flux is. Therefore, an emf will be induced in a circuit if its own flux is changed by changing its current, or if the flux of an adjacent circuit is changed by changing the current in this latter circuit. In the first case this will be an emf of *self-induction*; in the second case, an emf of *mutual induction.*

In the case of self-induction, the *flux interlinkage* of the circuit is determined by its own current:

$$(N\phi) = Li \quad \text{or} \quad L = \frac{(N\Phi)}{i} \qquad (1–13)$$

$L$ is the *coefficient of self-inductance.* According to Eq. 1–13 it is the *flux interlinkage per unit current.* The magnitude of $L$ depends upon the geometrical arrangement of the conductors, upon the number of turns, and upon the

magnetic nature of the surroundings. The last-mentioned factor plays a great part in the magnitude of the flux $\Phi$ and the flux interlinkage. If the surroundings contain ferromagnetic materials, the magnetic resistance (reluctance) is much lower and the flux $\Phi$ is much larger for the same current than when there are no ferromagnetic materials. This is discussed in Art. 1–3. It is also shown that, when there are no ferromagnetic materials, the flux is directly proportional to the magnetizing force (the current), and therefore, in this case, the coefficient of self-inductance $L$ in Eq. 1–13 is a constant. On the other hand, in ferromagnetic materials flux and magnetizing force are coordinated through the magnetization curve of the material (Fig. 1–8) which has a non-linear character; therefore the coefficient of self-inductance $L$ is not a constant in this case, but varies with the magnetizing force. For constant $L$, according to Eq. 1–1, the emf of self-induction is

$$e_s = -\frac{d\phi}{dt}\,10^{-8} = -L\frac{di}{dt}\text{ volt} \tag{1–14}$$

where $L$ is measured in henries.

In the case of mutual induction, the flux interlinking circuit 1 (the circuit considered) is:

$$(N\phi)_1 = Mi_2 \tag{1–15}$$

The coefficient of mutual inductance $M$ depends upon the same quantities as does $L$, and also upon the relative position of both circuits with respect to each other. For constant $M$, according to Eq. 1–1, the emf of mutual induction is

$$e_{M1} = -M\frac{di_2}{dt}\text{ volt} \tag{1–16a}$$

and vice versa

$$e_{M2} = -M\frac{di_1}{dt}\text{ volt} \tag{1–16b}$$

where $M$ is measured in henries.

**Example 1–5.** A solenoid with 400 turns carries a 60-cycle current of $I = 6$ amp. The maximum flux interlinked with each of the 400 turns is $4 \times 10^6$ maxwells. The surrounding environment is air. What is the coefficient of self-inductance of the coil? What is the effective value of emf of self-induction?

From Eq. 1–13

$$L = \frac{400 \times 4 \times 10^6}{\sqrt{2} \times 6} \times 10^{-8} = 1.886 \text{ henries}$$

From Eq. 1–6a

$$E_s = 6 \times 2\pi \times 60 \times 1.886 = 4270 \text{ volts}$$

**Example 1–6.** The field circuit of a d-c generator has an inductance of 4 henries.

Its field current of 8 amp is interrupted in 0.06 sec. What is the average emf induced in the winding?

From Eq. 1–14

$$e_{s,\,av} = 4\,\frac{8}{0.06} = 534 \text{ volts}$$

**1–2. Kirchhoff's Mesh Law.** This law states: In each mesh of a network, the sum of all impressed and induced emf's is equal to the sum of all resistive voltage drops.

$$\Sigma(V + E) = \Sigma IR \tag{1–17}$$

Examples showing the application of Kirchhoff's mesh law will be given later throughout the text.

**1–3. Circuital Law of the Magnetic Field (Ampère's Law).** A relation similar to Eq. 1–12 also holds for the magnetic circuit, i.e., for a closed circuit carrying a magnetic flux.

If $H_l$ is the magnetic field intensity at the element $dl$ of the magnetic circuit, $N$ the number of turns which are linked by the magnetic flux, and $I$ the current which flows in the winding, then the equation referred to above is

$$\oint H_l\, dl = NI \tag{1–18}$$

This equation states that *the line integral of the magnetic field strength along a closed path is equal to the sum of the ampere-turns with which this path is linked.* (See references on Electromagnetic Field Theory.)

Fig. 1–6 shows a solenoid and the flux produced by it. The line integral $\int H_l dl$ is the same for all three closed lines (1, 2, and 3) because all three are linked by the entire turns of the solenoid and therefore $NI$ is the same for all three. The value of the integral $\int H_l dl$ is not affected by the shape or the length of the force line selected, provided the force line links all of the $N$ turns. For a long line, such as 3, the number of terms $dl$ appearing in the sum will increase, but the field intensity becomes smaller as the distance from the coil increases.

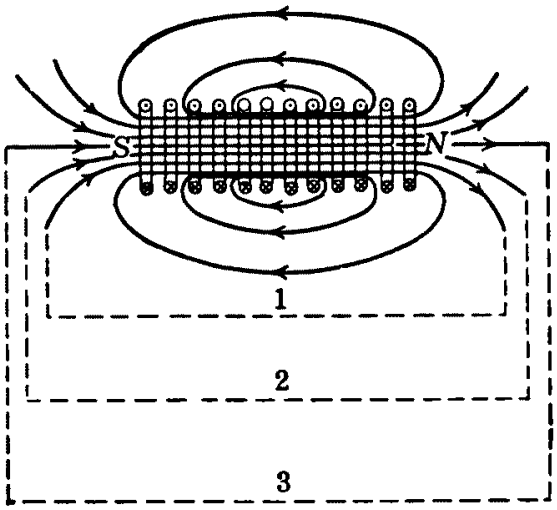


FIG. 1–6. Flux produced by a solenoid.

Eq. 1–18 can be put easily into a form which is similar to Ohm's law for the electric circuit. For the magnetic induction $B$, the relation holds that

$$B = \mu_0 \mu H \tag{1–19}$$

where $\mu_0$ is a constant equal to $0.4\pi$, and $\mu$ is the relative permeability of the material, i.e., the ratio of its permeability to that of free space (vacuum). In Eqs. 1–18 and 1–19, the current $I$ is expressed in amperes, $H$ in ampere-turns per centimeter, which, as far as fundamental dimensions are concerned, is the same as amperes per centimeter, $B$ in gausses, and $\mu_0$ in gauss centimeter per ampere.

For air $\mu = 1$, while for iron $\mu$ is a variable which depends upon the saturation. As an example, Fig. 1–7 shows the value of $\mu$ as a function of the field

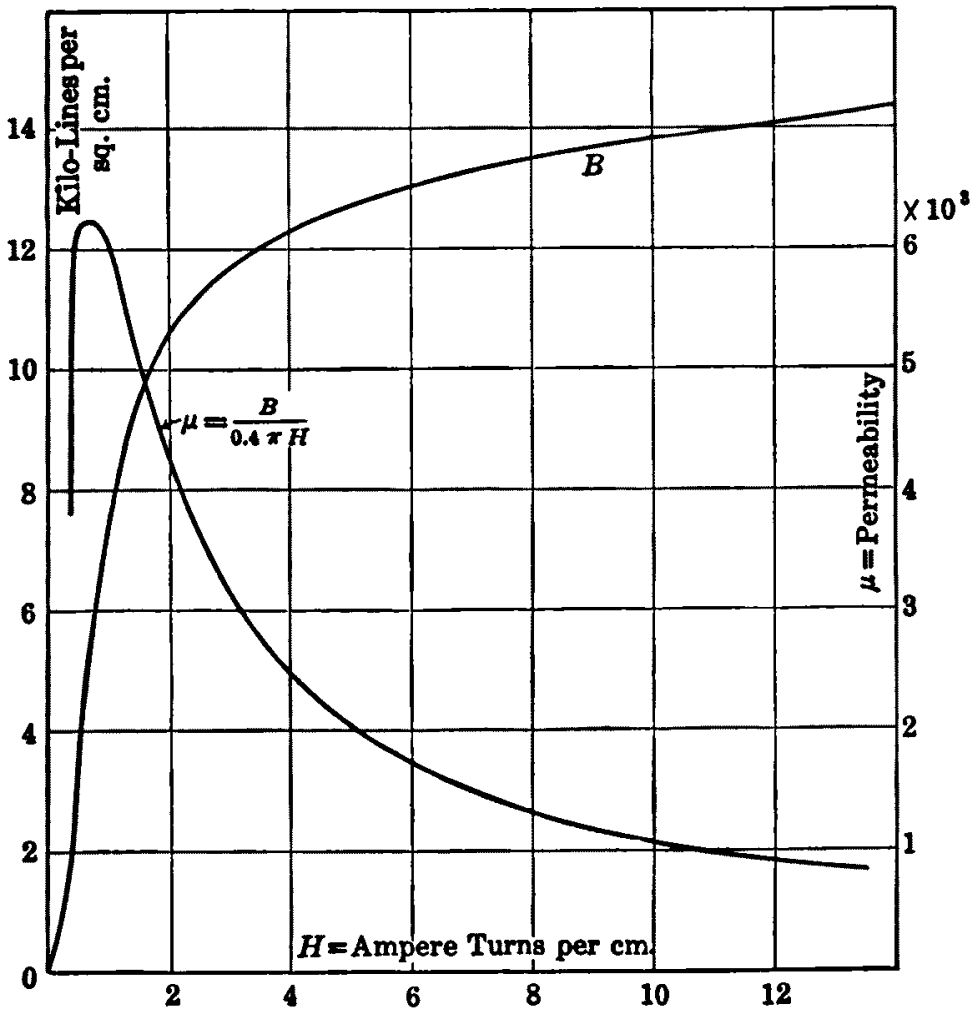


FIG. 1–7. Induction $B$ and permeability $\mu$ as a function of field intensity $H$.

strength $H$ for electrical sheet steel (1.0% silicon); in this case $\mu$ has a maximum value of 6100. The values of $B$ are also shown in Fig. 1–7. The $BH$ curve is called the *magnetization curve* of the material in question. This curve is used in making calculations for magnetic circuits.

The relation between magnetic flux $\phi$, cross-section $A$, and magnetic induction (flux density) $B$ is given by

$$\phi = BA \tag{1–20}$$

Substituting Eqs. 1–19 and 1–20 in Eq. 1–18 results in

$$\phi = \frac{0.4\pi NI}{R_m} \tag{1–21}$$

where

$$R_m = \int \frac{dl}{\mu A} = \Sigma \frac{l}{\mu A} \tag{1–22}$$

Eq. 1–21 is *Ohm's law of the magnetic circuit.* The factor $NI$ is analogous to the emf in the electric circuit and is called the *magnetomotive force.* It is usually symbolized by $M$. $R_m$ is the magnetic resistance or reluctance of the magnetic circuit. $R_m$, similar to the electric resistance, depends upon the length, cross-section, and magnetic conductivity or permeability of the flux path. Notice that $R_m$ depends upon the value of $\mu$. Since in ferromagnetic materials $\mu$ varies with the magnetizing force, $R_m$ also varies with the magnetizing force in these materials. An example of the application of the circuital law of the magnetic field is given in Chap. 5.

**1–4. Forces on Conductors in a Magnetic Field (Biot-Savart's Law).** (a) *Magnitude and direction of the force.* When a current-carrying conductor is placed in a magnetic field, a force is exerted upon it. If the direction of the lines of induction makes an angle $\alpha$ with the direction of the current-carrying conductor (Fig. 1–8), this force is

$$f = 8.85 \times 10^{-8} BlI \sin \alpha \quad \text{lb} \tag{1–23a}$$

where $l$ is the length of the conductor within the magnetic field, in inches, $I$

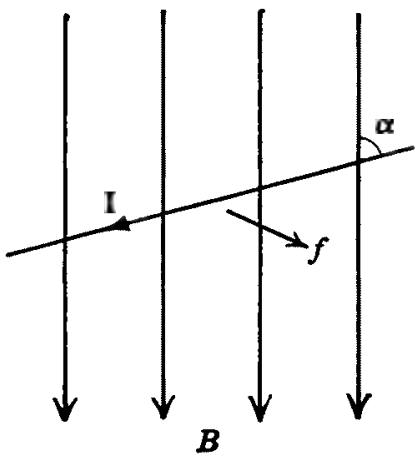


FIG. 1–8. Force on a current-carrying conductor in a magnetic field.

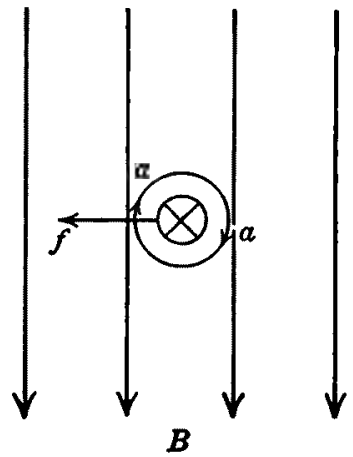


FIG. 1–9. Determination of the direction of the force on a current-carrying conductor in a magnetic field.

the current in amperes, and $B$ the density of the flux (in lines per square inch) in which the conductor is located.

In electric machines, the lines of induction and the conductors are always perpendicular to each other. Thus, in electric machines,

$$f = 8.85 \times 10^{-8} BlI \quad \text{lb} \tag{1-23b}$$

The direction of the force $f$ on the conductor can be determined with the aid of the left-hand rule: open the left hand, keep the fingers together and the thumb in the same plane as the palm but pointing at right angles to the fingers. If the fingers point in the direction of current, and the flux enters the palm at right angles to it, the thumb points in the direction of the force.

Another rule for the determination of the direction of the force $f$ is the following (Fig. 1–9): draw some lines of induction $B$, draw a circle between the lines to represent the cross-section of the conductor, and show by two arrows *aa* the direction of the field due to the current in the conductor. The conductor will tend to move *toward the region of opposing fields.*

It follows from these rules that the force $f$ is always perpendicular to the plane through $I$ and $B$.

(b) *Direction of the force in an electric machine.* The force on the coil between two poles in Fig. 1–2 will be considered. Fig. 1–10 shows the direction of the forces exerted upon the two coil sides. Because of the large difference between the permeabilities of air and iron, the lines of induction in the air-gap are perpendicular to the iron and therefore the forces are *tangential* to the armature. The forces on both sides act as a couple and tend to rotate the coil about the armature axis. The torque on each conductor, corresponding to the force $f$, is equal to $fR$, when $R$ is the radius of the armature. In accordance with the law of action and reaction, this torque acts not only upon the conductors but also upon the magnetic poles.

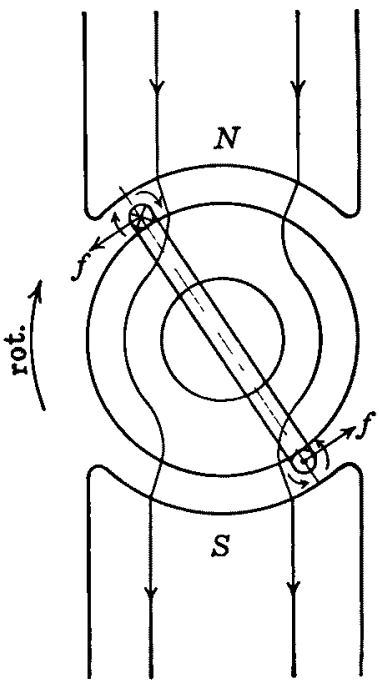


FIG. 1–10. Force on a coil of an electric machine.

In the case of an alternating field and a conductor carrying alternating current (both sinusoidal), the instantaneous values of the flux density $B$ and the current $I$ must be used in Eq. 1–23. If the average value of the force is calculated for a single period, it is found to depend upon the effective values of $B$ and $I$, and upon the time phase displacement between these quantities, i.e.,

$$F_{av} = 8.85 \times 10^{-8} l B_{eff} I \cos (B,I) \tag{1-24}$$

The torque produced by the couple in Fig. 1–10 is greatest when the flux and current are in time phase.

Eq. 1–23 for the force and Figs. 1–8 and 1–9 show that the direction of the torque changes if the direction of either the flux or the current is changed.

Changing the direction of the current and flux simultaneously does not change the direction of the torque. This explains why a unidirectional torque is possible in an a-c machine.

The forces shown in Fig. 1–10 refer to a generator that is driven (by a prime mover) in clockwise direction. Fig. 1–10 also shows the direction of the torque produced by the generated current: it is counterclockwise. Thus, in the case of a generator, the torque developed between the conductors and the flux (the electromagnetic torque) acts in a direction opposite to the direction of rotation and has to be overcome by the prime mover. In the case of a motor, the torque developed between the conductors and the flux is in the same direction as the direction of rotation and is delivered to its shaft. The balance of torques thus occurs in such a manner that in the generator the torque delivered by the prime mover is balanced by the opposing electromagnetic torque of the armature; in the motor the electromagnetic torque produced by the armature is balanced by the opposing torque of the load. It is well to remember that the generator converts mechanical power into electrical power and the motor converts electrical power into mechanical power.

**1–5. Electromagnetic Power of the Electric Machine.** Eq. 1–24 which gives the average value of the tangential force permits the derivation of a useful formula for the *electromagnetic power* of the electric machine. The torque produced by both sides of the coil (Fig. 1–10) is, in lb-ft,

$$T = 2 \times 8.85 \times 10^{-8} B_{\text{eff}} l I \cos (B,I) \times \frac{R}{12} \tag{1–25}$$

where $R = D/2$ is the radius of the rotor in inches. The relation between torque and power is given by the fundamental equation of mechanics:

$$T = \frac{5250 P_{\text{hp}}}{n} = \frac{7.04 P_{\text{watts}}}{n} \tag{1–26}$$

Observe that the *area of the flux distribution curve*, i.e., of the $B$ curve (Fig. 1–4 or Fig. 1–5), is the *flux per pole per unit of length* parallel to the axis of the machine, so that for a sinusoidal flux distribution

$$\Phi = \frac{2}{\pi} \tau l B \tag{1–27}$$

where $B$ is the amplitude of the sinusoidal $B$ curve. The pole pitch $\tau$ is given by Eq. 1–5; $l$ is the length of the armature within the flux parallel to the axis of rotation. The speed $n$ in Eq. 1–26 can be expressed by the frequency $f$ by using Eq. 1–7 with $p = 2$, since a 2-pole structure is considered.

Combining Eqs. 1–25, 1–26, and 1–27 and introducing Eq. 1–8, we have the following result for the power $P$:

$$P = EI \cos (B,I) \text{ watts}$$

It is seen from Fig. 1–5 that $E$ is in phase with $B$, so that the electromagnetic power of the electric machine is

$$P = EI \cos \psi \text{ watts} \tag{1–28}$$

where $\psi$ is the angle between $E$ and $I$.

Eq. 1–28, although derived for an elementary machine with two poles and a single coil under the assumption of a sinusoidal flux distribution, applies also to the actual electric machine. It will be seen later that the angle $\psi$ is smaller than 90° in a generator and larger than 90° in a motor.

**1–6. Summary.** The four fundamental laws:

1. Faraday's law of induction,
2. Kirchhoff's law of the electric circuit,
3. Circuital law of the magnetic field (Ampère's law),
4. Law of force on a conductor in a magnetic field (Biot-Savart's law),

can be correlated by a simple figure which is very helpful for memorizing the four laws and their relations. This representation has been proposed by L. V. Bewley.

If, in the triangle of Fig. 1–11, the left side represents the current, the right side represents the voltage, and the base represents the magnetic

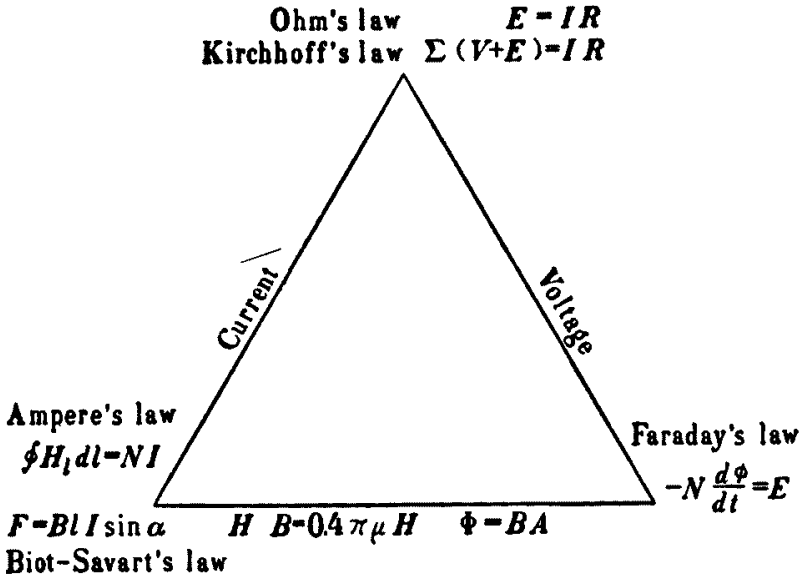


FIG. 1–11. Graphical correlation of the fundamental laws.

field intensity $H$ as well as the flux density $B = 0.4\pi\mu H$ and also the flux $\Phi = B \times$ Area, then the top corner which connects current and voltage is to be assigned to Kirchhoff's mesh law, the left corner which connects current and $H$ is to be assigned to Ampère's law (circuital law of the magnetic field), and the right corner which connects flux and voltage is to be assigned to Faraday's induction law. Since the left corner connects not only current

and $H$, but also current and $B$, it represents Ampère's law *and* Biot-Savart's law (law of force on a conductor in a magnetic field).

## PROBLEMS

**1.** A conductor 10 in. long is moving with a velocity of 80 fpm perpendicular to a magnetic flux whose average density is 60,000 lines per sq. in. Determine the average voltage generated.

**2.** Determine the velocity of a conductor 15 in. long moving perpendicularly across a magnetic flux of 40,000 lines per sq. in. average density if an average voltage of 0.05 volt is to be induced.

**3.** A 4-pole generator having a coil of 60 turns on the armature produces a maximum coil voltage of 28.3 volts with a pole flux of $10^6$ maxwells. The flux distribution is sinusoidal. Determine the generator speed.

**4.** A conductor is "cutting flux" at an average rate of 150,000 lines per sec. Determine the average voltage induced in the conductor.

**5.** It is desired to induce an average voltage of 3.5 volts in a coil linking a certain magnetic circuit. The flux changes from $+200{,}000$ lines to $-200{,}000$ lines in a time interval of 1/3 sec. Determine the number of turns on the coil.

**6.** A 6-pole generator has a flux per pole of $2 \times 10^6$ maxwells. The armature rotates at 720 rpm. The flux distribution is sinusoidal. Determine the average emf and the maximum emf induced in a full pitch coil of 5 turns.

**7.** A square coil 10 in. on each edge has 25 turns and rotates at a speed of 1000 rpm in a magnetic field of 2000 lines per sq. in. Determine the maximum flux passing through the coil, and the average emf induced in the coil. What is the voltage if flux and speed are both increased 50%.

**8.** A 4-pole generator has a flux of $3.5 \times 10^6$ maxwells per pole. The armature rotates at 600 rpm. (a) Calculate the average voltage generated in a turn when it travels one pole pitch. (b) What is the average voltage generated in one conductor in 1/4 revolution of the armature?

**9.** An armature conductor 15 in. long moves in a flux the density of which is 50,000 lines per sq. in. under the center of the pole. The diameter of the coil of which the conductor is a part is 15 in. and the armature rotates at 1200 rpm. What is the emf induced in the conductor when it lies under the center of the pole?

**10.** At what speed must the armature of Problem 9 move in order that the emf induced in the conductor be 12 volts.

**11.** A square coil, 8 in. on each edge, has 50 turns and its plane lies perpendicular to a uniform magnetic flux with a density of 5000 lines per sq. in. The coil rotates $\frac{1}{4}$ turn about its axis in 0.08 sec. Determine: (a) maximum flux interlinked with the coil; (b) average emf induced during this 0.08 sec; (c) average emf induced if the coil is made to rotate at 150 rpm; (d) instantaneous emf when coil is perpendicular to the flux and also when it is parallel to the flux.

**12.** A current of 10 amp flowing in a 400-turn coil produced a flux of 8000 lines interlinking these 400 turns. Determine: (a) the flux linkages in maxwell turns; (b) the self-inductance in henries.

**13.** If the number of turns in the coil of Problem 12 is doubled and the current remains the same, determine the flux linkages and self-inductance in henries. Assume all flux lines link all turns.

**14.** 1000 turns are wound upon an iron core magnetic circuit of 3 sq. in. cross-section. A current of 9 amp produces a flux density of 85,000 lines per sq. in. and a current of 4 amp produces 65,000 lines per sq. in. Determine the coefficient of self-inductance for each current.

**15.** The field of a shunt generator has a self-inductance of 35 henries. The current in the field winding is changed from 1.5 amp to 0.80 amp in 0.01 sec. Determine the emf of self-induction.

**16.** What is the emf of self-induction in Problem 15 if the current changes to zero in the same time?

**17.** The four shunt field coils of a generator are connected in series and each has 1000 turns. A direct current of 4.0 amp produces $0.5 \times 10^6$ lines of flux linking each coil. Determine: (a) the coefficient of self-inductance of the entire winding; (b) the total energy storage. If the field circuit is opened and the current decays to zero in 0.25 sec, what is the average value of voltage generated across the field?

**18.** Two field coils of a 2-pole machine are wound with 1500 turns each. A field current of 3.0 amp produces a flux of $3 \times 10^6$ maxwells linking each coil. What is the self-inductance of the field circuit?

**19.** A 4-pole generator having 2000 field turns per pole produces a pole flux of $3 \times 10^6$ maxwells when the field current is 2.80 amp. Determine: (a) maxwell-turn linkages per pole; (b) total maxwell-turn linkages; (c) coefficient of self-inductance of the field circuit.

**20.** A mutual inductance of 3.1 henries magnetically couples two circuits. If the current in the first circuit changes from 2.75 to 1.0 amp in 0.015 sec, what is the average voltage induced in the second circuit?

**21.** A cast-iron ring has a mean diameter of 12 in. and a circular cross-section of 3.5 sq. in. area. Determine the number of ampere-turns required to produce a total flux of 110,000 maxwells.

**22.** Solve Problem 21 for the case where an air gap 0.10 in. is cut in the cast-iron ring. (Neglect fringing.)

**23.** How many additional ampere-turns are required in Problem 21 if the total flux is (a) increased 20%, (b) decreased 20%.

**24.** A cast-steel ring having a mean diameter of 5.5 in. and a circular cross-sectional area of 0.85 sq. in. has an air gap 0.10 in. long cut in the ring. (a) Determine the number of ampere-turns necessary to produce fluxes of 30, 50, 80, 100 and 105 kilolines per sq. in. (b) If the winding on the ring has 250 turns, plot the curve of total flux vs. exciting current.

**25.** A 200-turn, single-layer coil is wound uniformly upon the entire of a wooden toroidal ring having a mean diameter of 6 in. and a square cross-section of 1 sq. in. area. Determine: (a) flux density in core when coil current is 4 amp; (b) flux density if the wooden ring is replaced by a cast-steel ring of the same dimensions and the coil carries 4 amp.

**26.** A cast-steel ring having a mean radius of 10 in. and a circular cross-section 2 in. in diameter is wound with a coil of 700 turns carrying 10 amp. Determine the flux density and the total flux.

**27.** If an air gap 0.50 in. long is cut in a cast-iron ring of 10 in. mean radius and 3.5 sq. in. circular cross-section, determine the total flux and flux density when 2500 ampere-turns are impressed upon the magnetic circuit.

**28.** A conductor 25 in. long carries a current of 15 amp and is acted upon by a

force of 2 lb when placed in a magnetic flux perpendicular to the flux lines. Determine the flux density in gausses and in lines per square inch.

**29.** Determine the current carried by a conductor 15 in. long if a force of 0.001 lb acts upon it when it is placed in a magnetic flux of 5000 lines per sq. in. flux density so that the lines of flux make an angle of 45° with the normal to the conductor.

**30.** A flat, square coil of 20 turns having an area of 60 sq. in. is placed in a uniform magnetic flux, so that the plane of the coil is parallel to the flux lines and the two active coil sides lie perpendicular to the lines of flux. The flux density is 5000 lines per sq. in. and the coil current is 10 amp. Determine: (a) the force in pounds acting on each side of the coil; (b) the torque in pound-feet acting to turn the coil.

**31.** The coil in Problem 30 is replaced by a 25-turn rectangular coil having dimensions 12″ × 18″, with the longer sides being the active conductors. Determine the turning torque in pound-feet when the current is 15 amp.

**32.** Repeat Problem 31 with the plane of the coil making an angle of 45° with the direction of the flux lines.

**33.** Repeat Problem 31 with the plane of the coil making an angle of 60° with the direction of the flux lines.

**34.** A 15-in. conductor carrying 20 amp lies in a uniform magnetic flux. A force of 0.25 lb tends to move the conductor perpendicular to the flux and to itself. Determine the flux density.

# *Chapter 2*

## MECHANICAL ELEMENTS OF THE D-C MACHINE

It follows from Art. 1–4 that the magnetic flux and the current-carrying conductors are the two indispensable elements of the electric machine. The part of the machine on which the conductors producing the tangential forces (Eq. 1–23a) are placed is called the *armature*. In the d-c machine this is the rotating inner part of the machine. The electro-magnets (poles) are stationary and are connected with the outer part of the machine or frame.

Figs. 2–1 and 2–2 show the magnetic paths of a 2-pole and of a 6-pole

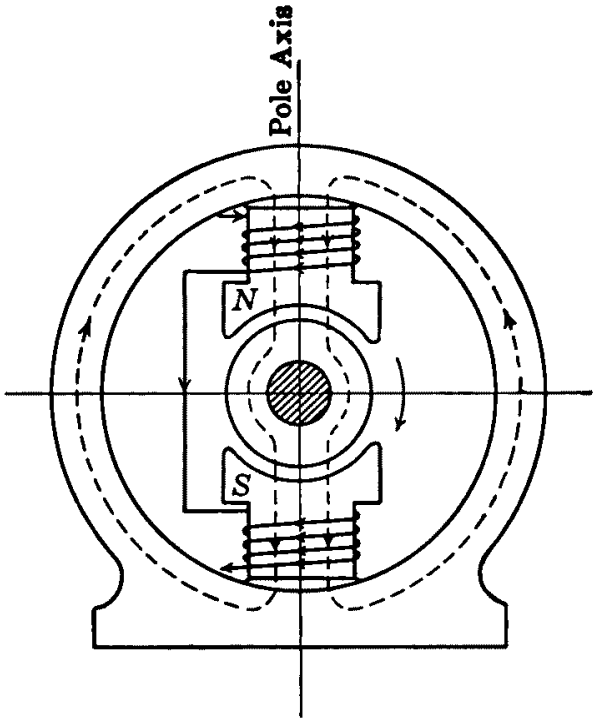


FIG. 2–1. Main flux paths of a 2-pole d-c machine.

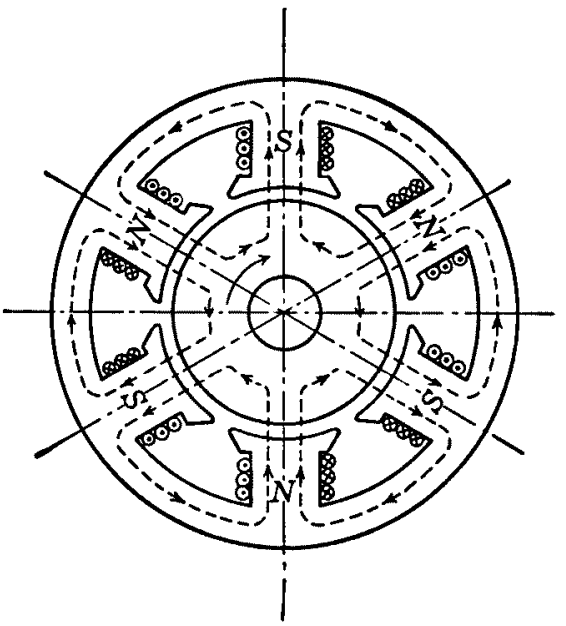


FIG. 2–2. Main flux paths of a 6-pole d-c machine.

d-c machine. The flux originates in the poles which are mounted on the frame and on which field-exciting coils are placed. The armature is the inner and rotating part of the machine. The armature conductors are placed in slots punched in the armature laminations. The path of the magnetic flux (Fig. 2–1) consists of: a part of the frame, two poles, two air-gaps

between the poles and the armature, two sets of teeth on the armature, and a part of the armature core.

The material of the armature conductors and field coils is copper, since, among the relatively cheap materials, copper has the lowest resistivity and thus the lowest $I^2R$ losses.

The slots and armature conductors are usually placed parallel to the axis of the armature, but sometimes are skewed at a slight angle to the axis. The armature iron must be laminated and the laminations insulated;

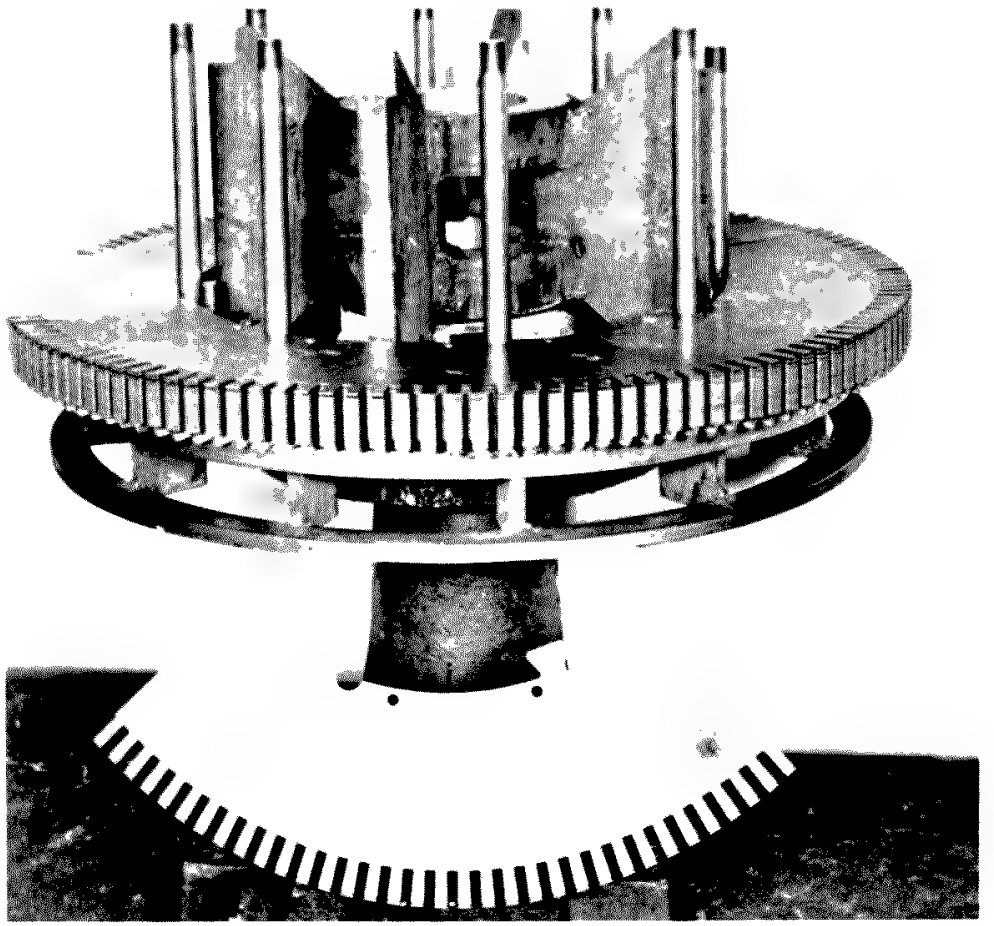

FIG. 2–3. Punched laminated segment of a large d-c armature. Partially assembled stack of laminations of a large d-c armature.

otherwise the pole flux induces an emf in the iron (just as it does in the conductors) which will produce large eddy currents and corresponding $I^2R$ losses at the surface of the iron. Laminating the core increases the resistance of the eddy-current path and reduces the magnitude of these eddy currents. For similar reasons (see Art. 11–1) the poles of d-c machines are usually laminated, but the frame is usually solid.

At the bottom of Fig. 2–3 is shown a punched, laminated segment of a large d-c armature and, at the top, the process of stacking such laminations. Fig. 2–4 shows the assembled core for a small, 2-pole, d-c armature with slot

insulation inserted. In small machines where the length of the core is small the entire core consists of a single stack. Fig. 2–5 shows a complete armature core, with commutator, for a large machine. Here the core assembly is divided into five stacks, separated by ventilating ducts. The purpose of these ducts is to transfer the heat developed in the iron (see Chap. 12) to the circulating air. It will be explained in Chap. 3 that the induced emf in a d-c machine is an a-c emf. The purpose of the commutator is to make the machine act, with respect to an external circuit, as though it produces a constant voltage.

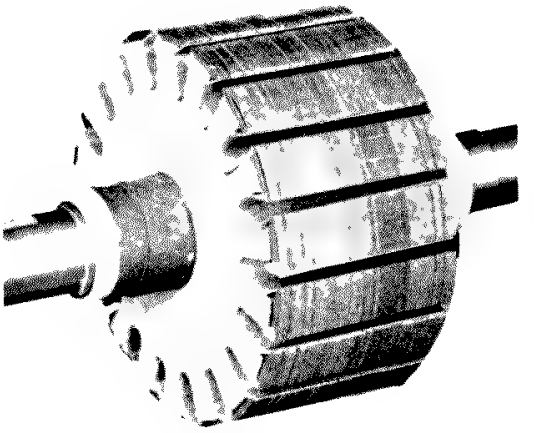

FIG. 2–4. Assembled armature core for a small d-c machine.

Fig. 2–6 shows a partially wound d-c armature. Fig. 2–7 shows a complete armature of a larger machine with the winding connected to the commutator. In Fig. 2–7 some of the wedges which hold the winding in place are partially inserted; the band wires which hold the end windings have not yet been put on. Fig. 2–8 shows a complete d-c armature for a small machine, with a ventilating fan. The slots are skewed in order to reduce noise.

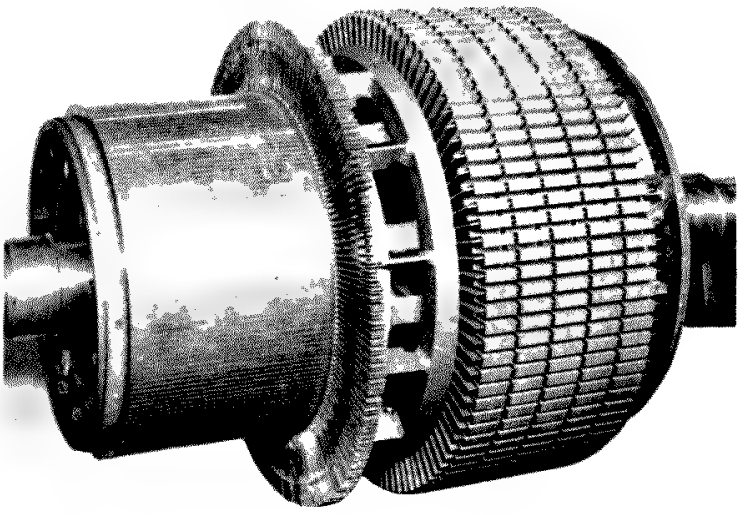

FIG. 2–5. Completely assembled armature core and commutator for a large d-c machine.

A complete pole, assembled from laminations and held together by rivets, is shown in Fig. 2–9, which also shows a field coil consisting of two windings, one a shunt coil of fine wire over which is wound a series coil of heavy wire (see Art. 6–1). Whereas the armature laminations *must* be

insulated, the pole laminations are not insulated from each other because the main flux does not vary with time. Fig. 2–10 shows a complete field pole assembly for a larger d-c machine. Here the series coil is made up of

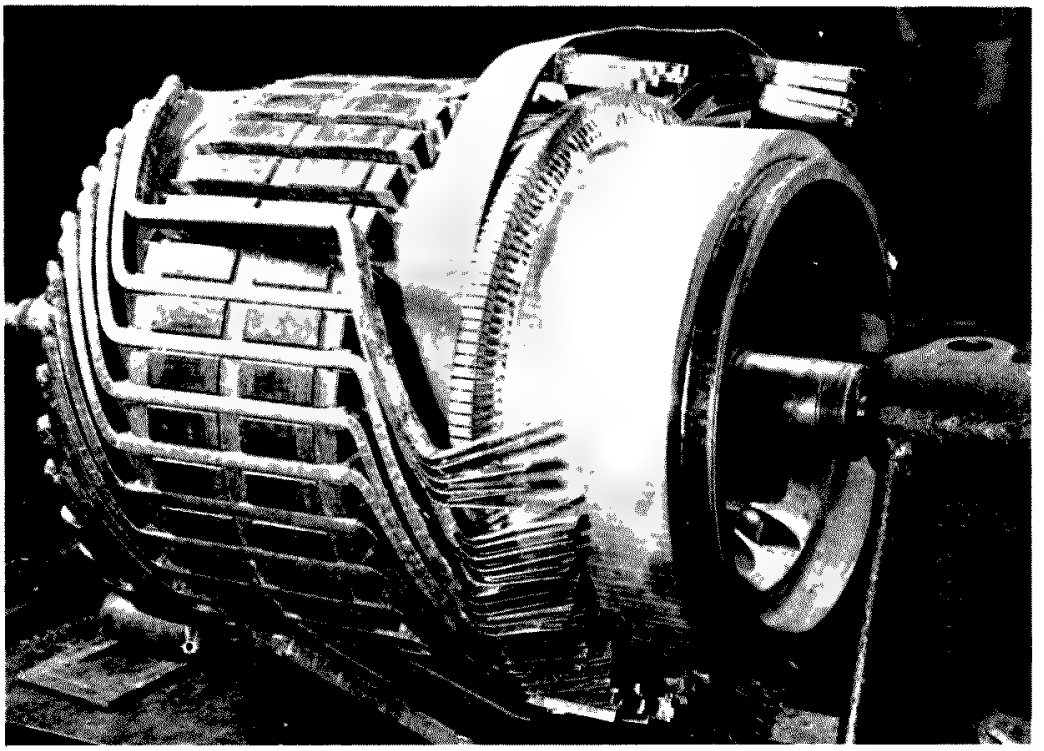

FIG. 2–6. Partially wound d-c armature.

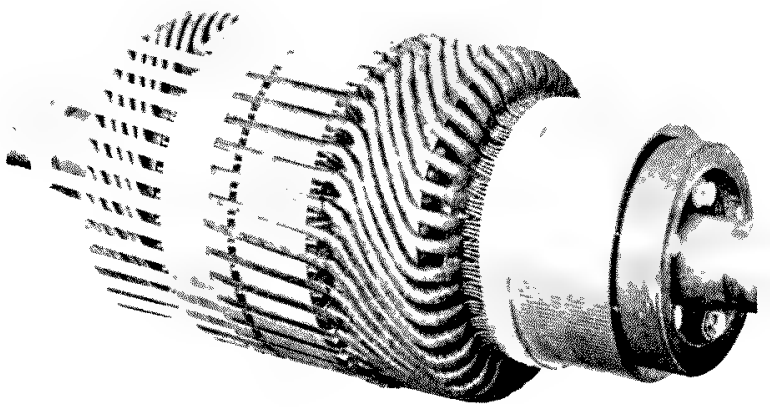

FIG. 2–7. Completely wound d-c armature, slot wedges partly in place.

copper ribbon. Fig. 2–11 shows a completely assembled stator—that is, the stationary outer part of the machine consisting of the frame, four main poles with their field windings, and four small poles called interpoles or

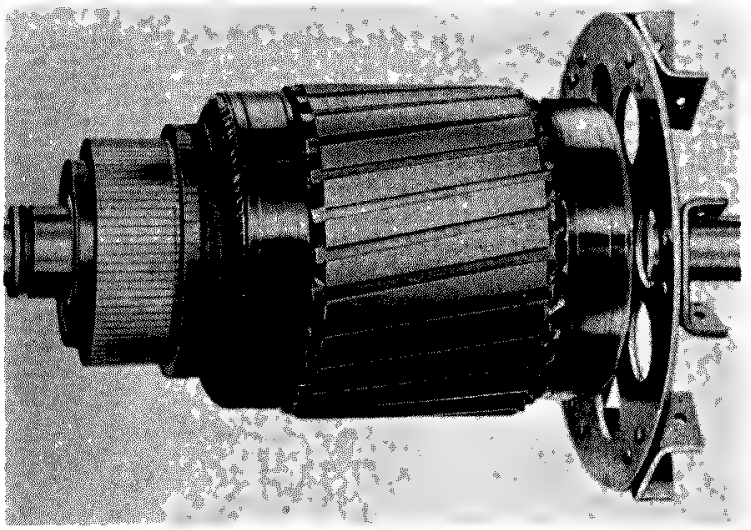

FIG. 2–8. Small d-c armature with skewed slots and ventilating fan.

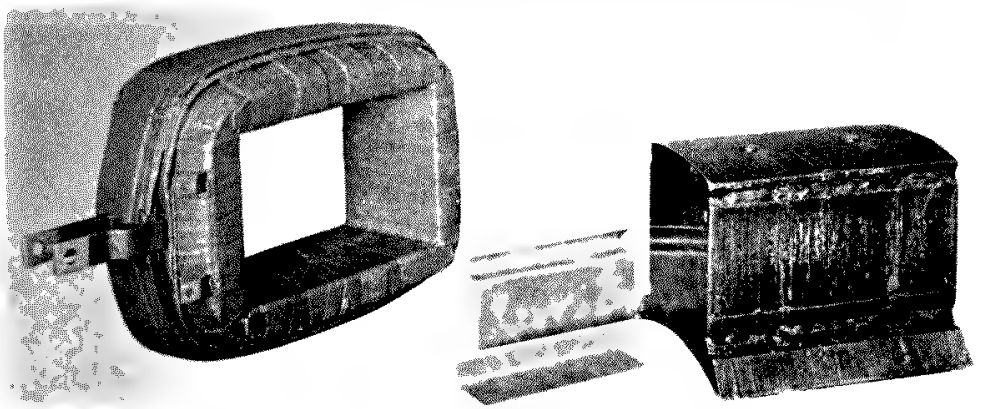

FIG. 2–9. Field coil and field pole for a d-c machine.

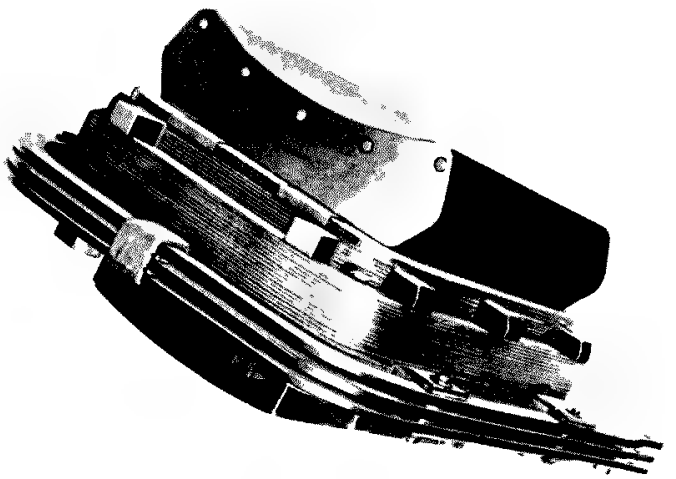

FIG. 2–10. Completely assembled pole core and field windings for a d-c machine, showing shunt and series windings.

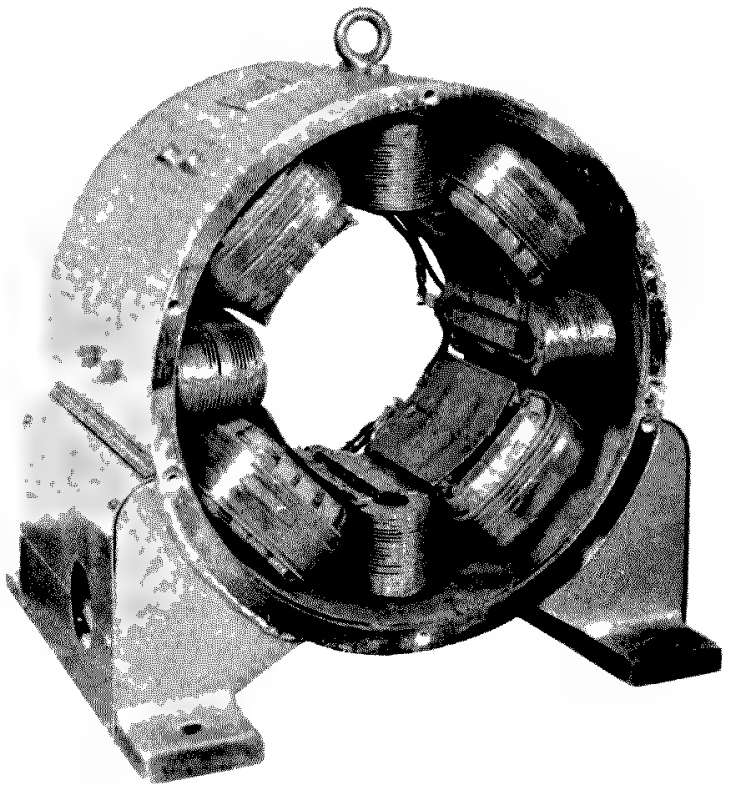

FIG. 2–11. Completely assembled stator for a 50-hp, 850-rpm, 230-volt d-c machine showing main poles and interpoles.

FIG. 2–12. Carbon brush mounted in a brush holder.

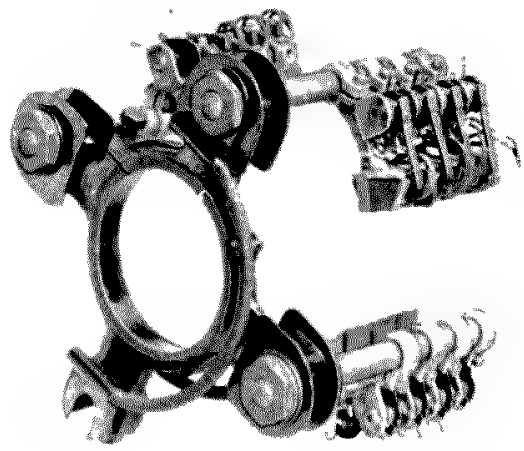

FIG. 2–13. Partially assembled brush rigging for a d-c machine.

commutating poles. The purpose of the interpoles is to avoid sparking at the commutator which may be caused when the armature coils are short-circuited by the brushes on the commutator (see Art. 9–6).

Fig. 2–12 shows a single carbon brush mounted in a brush holder. The

FIG. 2–14. Parts of a 2-pole fractional-horsepower d-c motor.

FIG. 2–15. Parts of a small integral-horsepower d-c motor.

current is conducted from the brush to the brush holder by a flexible copper pigtail. In order to produce the necessary pressure for smooth running of the

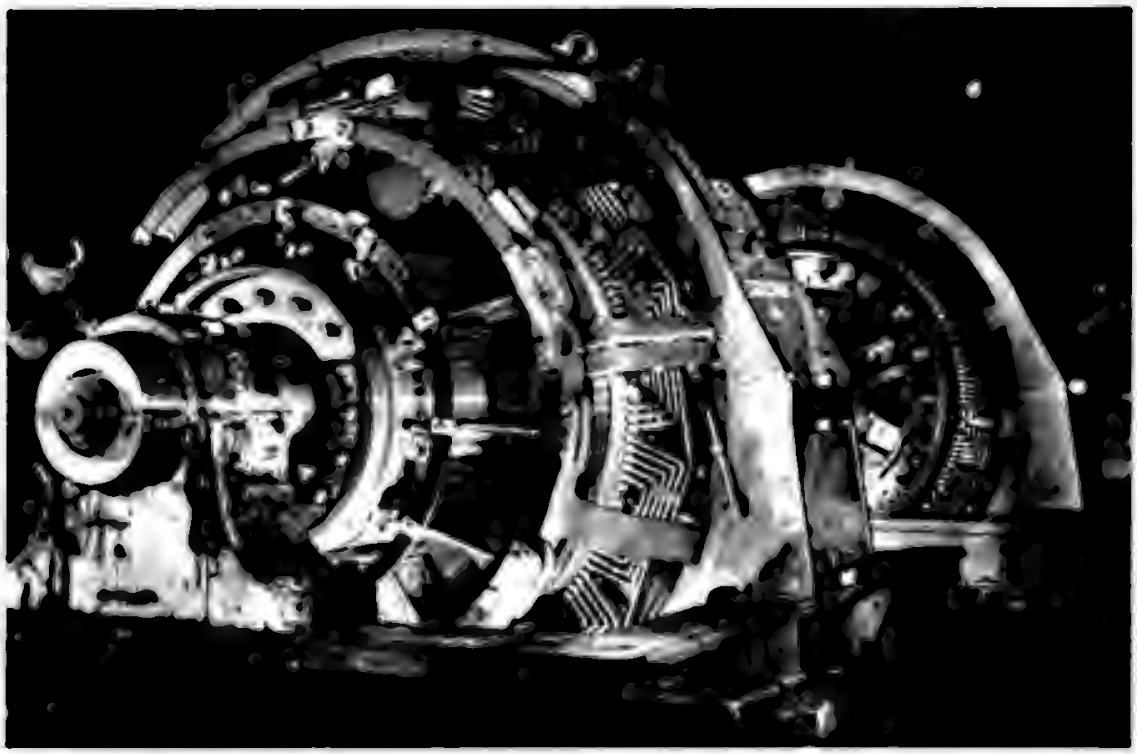

FIG. 2–16. 2500-hp, 225/450-rpm d-c mill motor.

brush on the commutator, an adjustable spring bears on the top of the brush. Fig. 2–13 shows a brush rigging consisting of a rocker ring, four brush studs

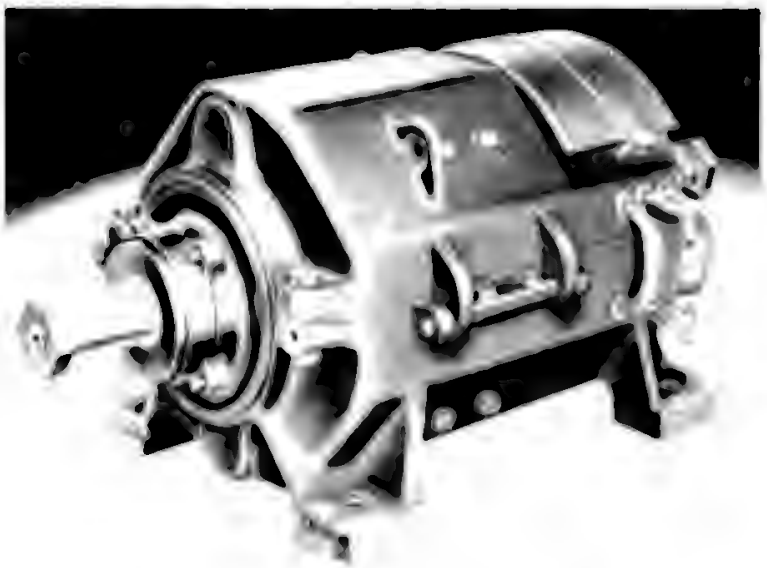

FIG. 2–17. Smaller mill-type totally enclosed d-c motor.

(one not shown), and four brushes on each stud. Current passes from the brush holder to the stud, which is insulated from the rocker ring. All positive

studs are connected together, as well as all negative studs, to form the positive and negative, + and −, terminals of the machine.

Fig. 2–14 shows all the parts of a 2-pole, fractional-horsepower motor with no interpoles. Fig. 2–15 shows the parts of a small, integral-horsepower motor with two main poles and one interpole. Fig. 2–16 shows a large d-c mill motor, and Fig. 2–17 a smaller mill-type motor, which is totally enclosed.

# *Chapter 3*

## D-C ARMATURE AND FIELD WINDINGS

**3–1. Homopolar Machine for Generating a Direct Current.** Theoretically it is possible to produce direct current directly without resorting to the use of a commutator. Consider Fig. 1–3; if the conductor *ab* is moved downward with constant velocity $v$, a constant emf will be induced in the circuit, provided $B$ is constant.

$$e = Blv \tag{3–1}$$

Fig. 3–1 shows an arrangement by means of which the conductor $AB$ moves

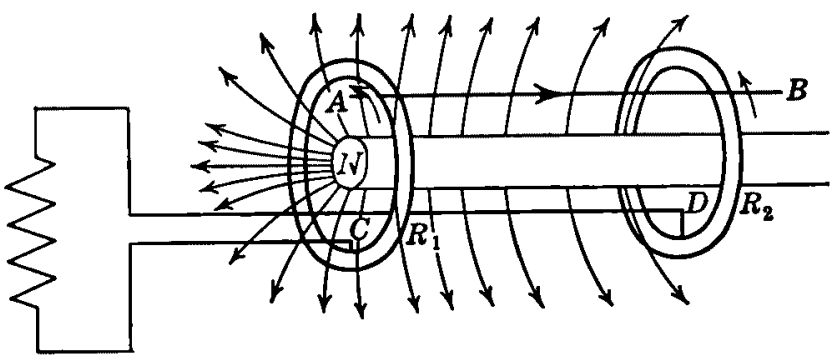


FIG. 3–1. Scheme of a homopolar generator.

in a circular path, around a north pole $N$. The circuit consists of the conductor $AB$, two rings $R_1$ and $R_2$, connections to the load, and the load. Machines which operate upon this principle are called *homopolar machines* because the conductor always moves in a field of the same polarity. This type of machine design has not been adopted practically to any extent, because the voltages produced are necessarily low and the currents usually high, and it is difficult to increase the voltage and reduce the current.

*The d-c machines which are used in practice are, in reality, a-c machines with a special device, the commutator, which makes it possible to pick up from the winding a fixed instantaneous value of the a-c voltage. With respect to the external circuit, the voltage then appears as a constant quantity.* The operation of the commutator will be studied in Art. 3–4.

**3–2. Two Types of D-c Armature Windings. Lap Winding and Wave Winding.** Windings which are adapted for connection to a commutator

are usually called *d-c armature windings*, although they may be used also in a-c machines.

In order that the commutator may accomplish its purpose, the d-c armature winding must be a *closed* one, i.e., if, starting at any point, the winding is followed through all its turns, the starting point is reached again. From points on one side of the winding, connections are made at regular intervals to the commutator.

The emf induced in a coil is *greatest* when the *coil width is equal to the pole pitch*. Such a winding is called a *full-pitch* winding. In this case when the plane of the coil is perpendicular to the pole axis, the coil is linked by the entire flux penetrating the armature (Fig. 1–2). If the coil width is either less or greater than the pole pitch (*chorded-type*, or *fractional-pitch winding*), then the maximum flux which links the coil is less than the pole flux. In the first case (Fig. 3–2a), where the coil width is less than a pole pitch, it can never

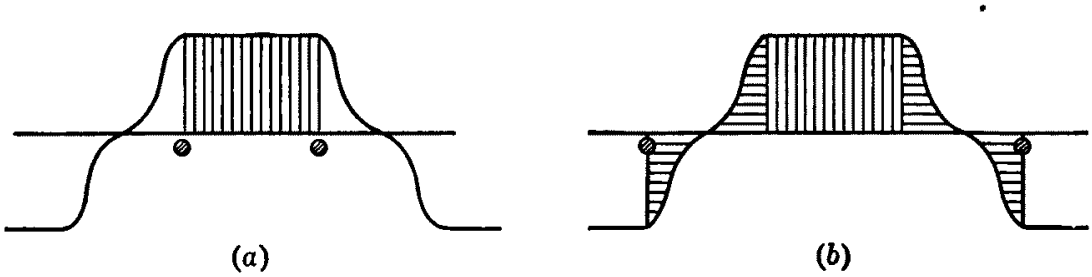


FIG. 3–2. Influence of fractional pitch on the induced emf.

embrace the entire pole flux; in the second case, the coil embraces the flux of an entire pole and, in addition, a part of the lines of force of the neighboring pole. Since the neighboring poles are of opposite polarity, the maximum flux linked by a coil the pitch of which is greater than the pole pitch is also less than the pole flux (Fig. 3–2b). In this latter figure, as well as in Fig. 3–2a, the vertically hatched part of the field curve is a measure of the maximum flux which links the coil, because the area under the field curve is directly proportional to the flux per unit length of the armature (Art. 1–5).

For this reason the coil width is always made nearly equal to or equal to the pole pitch. In addition the individual winding elements must be connected to one another in such a manner that the emf's within each armature path are *aiding*. This is the case if, after passing through the end of a winding element, the connection goes next either to the same pole where this element started or to another pole which is of the same polarity as this one. In this way two kinds of d-c armature windings result: the *lap winding* and the *wave winding*.

Fig. 3–3 shows the lap winding. Turn $a$ consists of conductors $a'$–$a''$, turn $b$ consists of conductors $b'$–$b''$, and so forth. The end $a''$ of turn $a$ is connected with the beginning $b'$ of turn $b$ which lies under the same pole as the beginning of turn $a$; the end of turn $b(b'')$ is connected with the

beginning of turn $c(c')$, and so forth. The end of the last turn of the winding is then connected with the beginning of the first turn and the winding is closed.

As mentioned, it is important that the end of a turn and the beginning of the next following turn lie under poles of *different* polarity, otherwise the emf's of two consecutive turns will not add. This is achieved in the lap winding, Fig. 3–3, by connecting the end of turn $a(a'')$ with the beginning of turn $b(b')$ which lies under the same pole as the beginning of the turn $a(a')$.

The addition of the emf's of consecutive turns can also be achieved in the way shown in Fig. 3–4. Here the end $a''$ of turn $a$ which lies under a S-pole

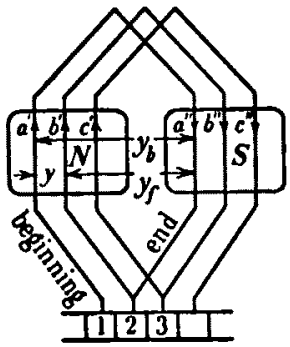


FIG. 3–3. Elements of a lap winding.

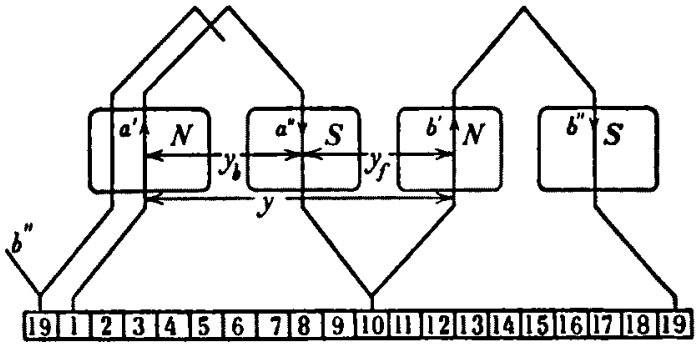


FIG. 3–4. Elements of a wave winding.

is connected with a turn-beginning $(b')$ which lies under a N-pole; however, the latter N-pole is not the N-pole under which the beginning of coil $a(a')$ lies but *the next following N-pole*. The coil connection of Fig. 3–4 is that of the wave winding.

Two steps are necessary in order to follow through from the beginning of a turn to the beginning of the next following turn. The steps are one forward and one backward step in the lap winding; there are two forward steps in the wave winding.

The wave winding of Fig. 3–4, just as the lap winding, is a closed winding. The first wave is connected to the commutator bars 1, 10, 19; the second wave is connected to the commutator bars 19, 9, 18; and so forth. The last wave is connected to commutator bars 12, 2, 11, and the last turn is connected to commutator bars 11 and 1, closing the winding (see also Fig. 3–17).

The lap and wave windings are electrically different. For the same number of turns, same pole-flux, and same speed, the lap winding generates a lower voltage than the wave winding. This is due to the fact that the lap winding has more parallel circuits than the wave winding, i.e., fewer coils are connected in series in each path of the lap winding than in the wave winding, thus yielding a lower voltage. This will be explained in some detail in the following articles.

**3–3. Winding Pitch.** *Back Pitch and Front Pitch.* The distance between the beginnings of two consecutive turns is called the *winding pitch* ($y$). The distances which correspond to the two steps necessary to follow through from the beginning of one turn to the beginning of the next following turn are called *back pitch* ($y_b$) and *front pitch* ($y_f$). The three pitches are shown in Figs. 3–3 and 3–4. Since in the lap winding one of the two steps is a forward step, and the other is a backward step, the winding pitch ($y$) of the lap winding is equal to the difference between the back pitch and front pitch.

$$y = y_b - y_f \text{ lap winding} \tag{3–2}$$

Since in the wave winding both of these steps are forward steps, the winding pitch of the wave winding is equal to the sum of the back pitch and front pitch.

$$y = y_b + y_f \text{ wave winding} \tag{3–3}$$

In larger machines, a *winding element* has one turn. In smaller machines, the winding element may have more than one turn, as shown in Figs. 3–5 and 3–6.

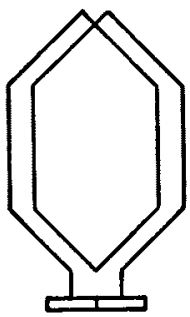

FIG. 3–5. Element of a lap winding with two turns.

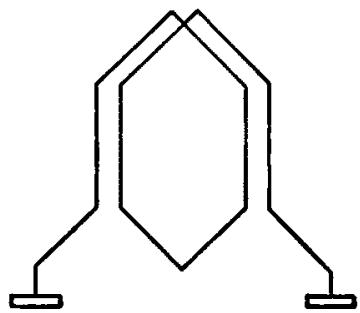

FIG. 3–6. Element of a wave winding with two turns.

In these latter cases, the statements made in the foregoing with respect to the beginnings and ends of a turn refer to the beginnings and ends of the *winding element*, i.e., of the coil consisting of several turns. It will become clear from Art. 3–8 that the beginning and the end of each winding element must be connected to a commutator bar. Therefore, there are *as many commutator bars* ($K$) *as winding elements* for both the lap and wave windings.

On the basis of the foregoing, the *winding element will be defined as that part of the winding the beginning and end of which are connected to commutator bars.* The winding element consists of at least 1 turn. It may, however, consist of 2, 3, or more turns in series. A turn consists of 2 conductors in series. The conductor may be solid or consist of several insulated strands in parallel, which may be of either round or rectangular shape.

The 3 pitches, $y$, $y_b$ and $y_f$ may be expressed in several ways. They may be expressed in any linear dimension measured at the surface of the armature,

or in slot pitches, or in degrees, or in commutator bars (commutator pitches). In this text these pitches will be measured in commutator bars.

It is seen from Fig. 3–3 that the winding pitch of the lap winding is equal to one commutator bar.

$$y = 1 \text{ (lap winding)} \tag{3–4}$$

In the lap winding, (Fig. 3–3), the end of the winding element returns to a slot under the starting pole and consequently is connected to commutator bar 2 *adjacent* to the starting commutator bar shown as bar 1 in Fig. 3–3. In the wave winding (Fig. 3–4) the end of the winding element goes to a slot under the *next pole of same polarity* and is connected there to commutator bar $(1+y)$, which is located *about 2 pole pitches* distant (measured on the commutator) from the starting commutator bar 1. In the wave winding, the commutator bar adjacent to the starting bar is reached after progressing through a number of winding elements equal to the number of pole pairs $p/2$ (Figs. 3–4 and 3–17). The winding pitch $y$ of the wave winding *must deviate somewhat from 2 times the pole pitch* (measured in terms of commutator bars), or else the starting bar 1 would be reached after progressing through $p/2$ elements. The latter would result at once in a closed circuit, and a series connection of all the coils of the armature paths would not be achieved. Therefore, in the wave winding $y \neq \dfrac{K}{p/2}$, but

$$y = \frac{K \mp 1}{p/2} = \frac{K}{p/2} \mp \frac{1}{p/2} \quad \text{(wave winding)} \tag{3–5}$$

i.e., the resultant pitch $y$ of a wave winding differs from the number of bars in 2 pole pitches by the $\dfrac{1}{p/2}$ part of a bar. The minus or plus sign in Eq. 3–5 depends upon whether the progress through the $p/2$ winding elements brings the winding to the commutator bar at the left or at the right of the starting bar, respectively. If it brings it to the left of the starting bar, the winding is called *retrogressive*; if to the right, *progressive*.

The *back pitch* (coil width) of the lap as well as of the wave winding must be equal or approximately equal to the number of *commutator bars per pole*, i.e., $y_b \approx \dfrac{K}{p}$, in order that the coil span be equal or approximately equal to a pole pitch.

As a rule, two coil sides are placed one above the other in each slot of a drum winding (Fig. 3–7). The coil is to be understood here as a group of winding elements insulated together and put into the slot as a unit. In Fig. 3–7 each coil contains 3 winding elements. Each winding element has one side in the upper layer and the other side in the lower layer (Fig. 3–8). Such a winding is called a *2-layer winding* to distinguish it from a *single-layer winding* (Fig. 3–9), which is seldom used in d-c machines. The 2-layer

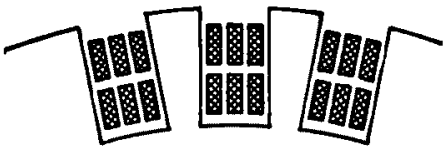

FIG. 3–7. Two-layer winding.

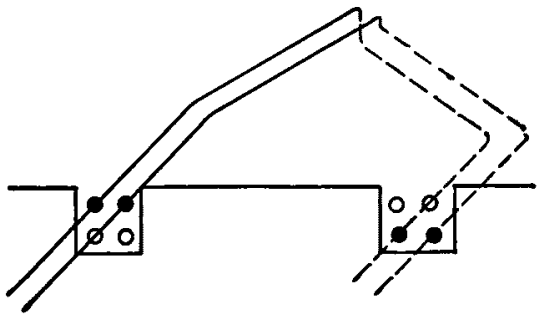

FIG. 3–8. Two-layer winding.

winding has as many coils as slots. The single-layer winding has half as many coils as slots. The number of conductors per coil side (winding elements per coil) is optional.

Since one commutator bar must be provided for each winding element, the total number of commutator bars $K$ is determined by the total number of conductors $Z$ and the number of turns per winding element $N_e$:

$$K = \frac{Z}{2N_e} \qquad (3\text{–}6)$$

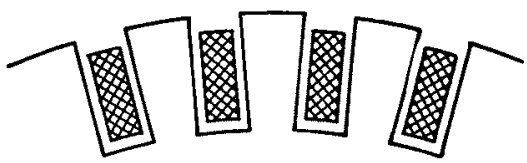

FIG. 3–9. Single-layer winding.

**Example 3–1.** 4-pole machine with 36 winding elements and lap winding. What are the back and front pitches of this winding, expressed in commutator bars?

Since there are 36 winding elements, the number of commutator bars is 36. The number of commutator bars per pole is then $36/4 = 9$, making the back pitch $y_b = 9$; the front pitch becomes (Eq. 3–2) $y_f = y_b - 1 = 8$ commutator pitches.

**Example 3–2.** 4-pole machine with 37 winding elements and wave winding. What are the three pitches of this winding expressed in commutator bars?

Since there are 37 winding elements, the number of commutator bars is equal to 37. From Eq. 3–5

$$\text{winding pitch} \quad y = \frac{37 \mp 1}{2} = 18 \text{ or } 19$$

The number of commutator bars per pole is $37/4 = 9.25$.
The back pitch is made $y_b = 9$.
Therefore (Eq. 3–3) the front pitch is either $y_f = 18 - 9 = 9$ or $19 - 9 = 10$ commutator pitches.

**3–4. Number of Parallel Paths in the Lap and Wave Winding.** It follows from Faraday's law, Art. 1–1, Fig. 1–2, that all conductors lying under poles of the same polarity have emf's of the same direction and that conductors lying under poles of different polarity have emf's of different directions (Fig. 3–10), i.e., a reversal in the direction of the induced emf appears after each pole pitch.

The winding of Fig. 3–10 which is shown developed in Fig. 3–11 has 2

poles and is arranged in 10 slots. The number of conductors in each layer of the slot is one. The total number of conductors is $10 \times 2 = 20$, and, therefore, the number of turns (winding elements) as well as the number of commutator bars is 10. A pole pitch is $10/2 = 5$ commutator bars, and the back pitch (coil span) is chosen to be equal to 5 commutator bars (full pitch winding). Since there is only 1 conductor per layer in the slot, the back pitch is also equal to 5 *slot* pitches. The front pitch must be equal to 4 commutator bars or slot pitches, in order that the winding pitch be equal to one, Eq. 3–2.

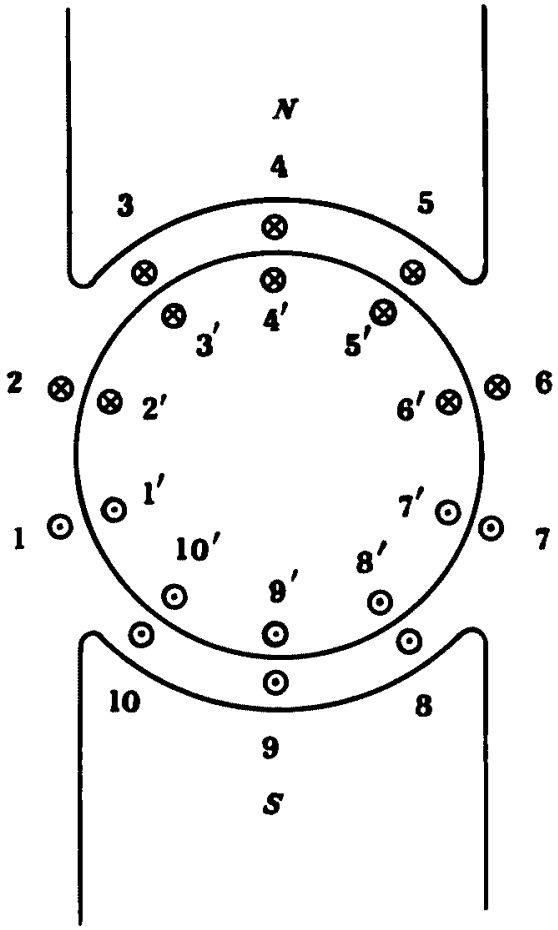


FIG. 3–10. Two-pole, 2-layer lap winding with Q = 10. Current distribution.

In Fig. 3–11, the upper and lower layers are shown next to each other, with the upper layer represented by a full line and the lower layer by a dotted line. Corresponding to the coil span, $y_b = 5$ commutator bars $= 5$ slot pitches, upper conductor 1 is connected to lower conductor $1 + y_b = 1 + 5 = 6$, then this lower conductor to upper conductor $6 - y_f = 6 - 4 = 2$, and so forth, until the winding is closed.

For reasons which will be explained later (Art. 3–8), the brushes are placed on the commutator in such a manner that they are connected with the conductors lying at or close to the reversal points of the induced emf's. So in Fig. 3–11 one brush contacts commutator bar 2 which is connected with conductors 2 and 6′ and the other brush contacts commutator bar 7 which is connected with conductors 7 and 1′. It could appear from Fig. 3–10 that a brush connected to the conductors lying at the reversal-point of the emf's is connected with conductors of different polarity. Fig. 3–11 shows that this is not the case: both the upper and lower conductors of the turns lying at the reversal points and the connections between the consecutive turns must be taken into account. It is then found that each of the brushes contacts a commutator bar which is connected to 2 conductors of the *same* emf direction (Fig. 3–11), but the emf direction is *opposite* for the 2 brushes. This means that, with respect to the brushes, the armature consists of *2 parallel paths*. The conductors lying in each path are shown in Fig. 3–12. A 2-pole winding is a lap winding. Thus a 2-pole lap winding has 2 parallel paths.

Fig. 3–13 shows a 4-pole lap winding, developed. Fig. 3–14 shows the

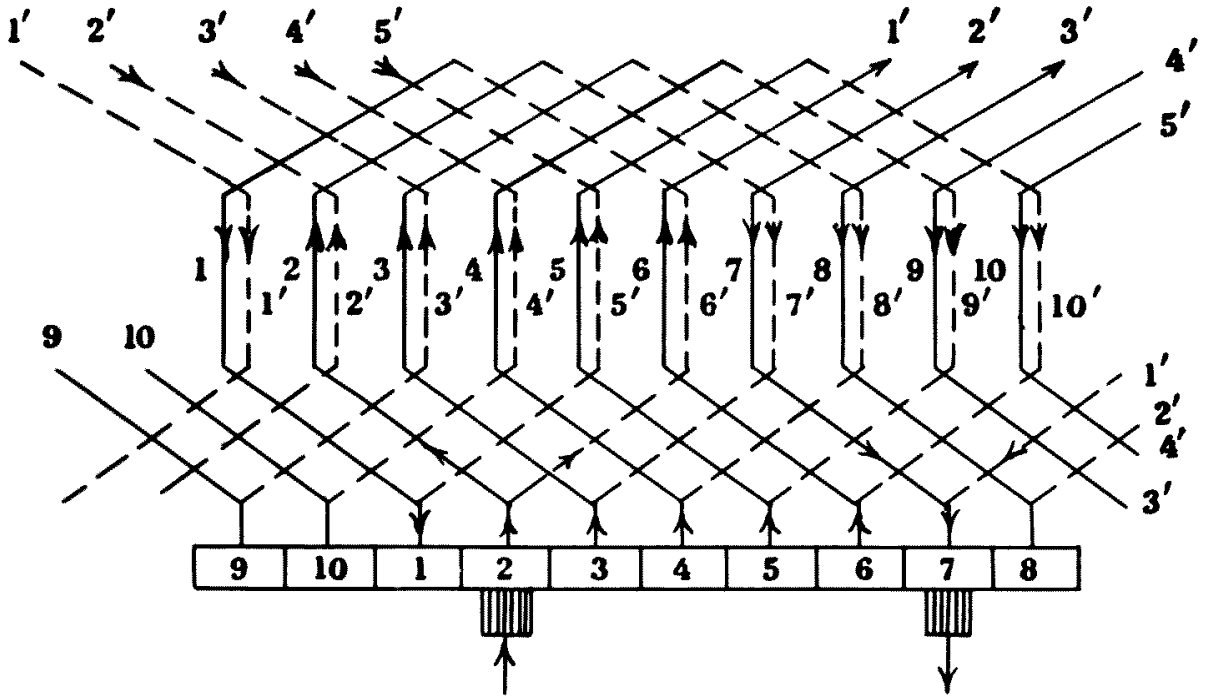


FIG. 3–11. Winding of Fig. 3–10, developed.

same winding in a polar diagram. The number of slots is 20 and the number of conductors in each layer of the slot is one. The total number of conductors is $20 \times 2 = 40$, and therefore the number of turns (winding elements) as well as the number of commutator bars is 20. A pole pitch is $20/4 = 5$ commutator bars. The back pitch (coil span) is chosen to be equal to 5 commutator bars (full pitch winding); the front pitch is then equal to 4 commutator bars.

As in Fig. 3–11, the emf's of consecutive poles have different directions. No emf direction is given to the conductors which lie close to the middle of the interpolar space, because there the flux density is very small and the induced emf negligible (see Fig. 1–4 and Eq. 1–4).

By starting at point *a* in Fig. 3–13 and following through the winding, Fig. 3–15 is obtained for the sequence of the *upper* conductors and for the direction of the induced emf's (indicated by arrows). It is not necessary here to consider also the lower conductors, since the coil span is equal to a pole pitch and the emf of each lower conductor is equal to and automatically adds to the emf of its upper conductor. (Conductors lying between poles do not contribute to the emf and are not included.)

Consider Fig. 3–15; there are four groups of turns, each group consisting of four turns in which an emf is

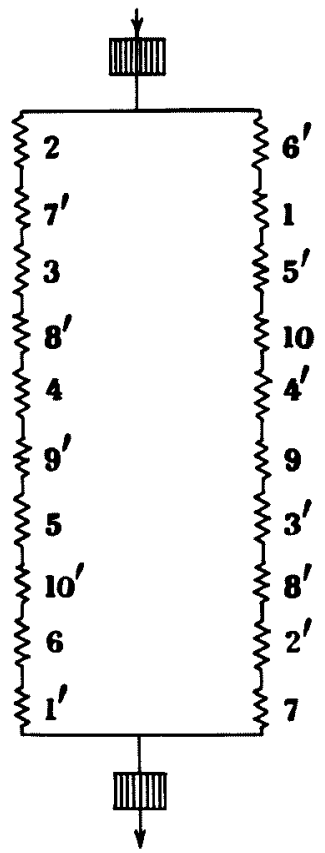


FIG. 3–12. The two parallel circuits of the winding Fig. 3–10.

induced. A voltage difference exists between the points $a$ and $b$, $a$ and $c$, $d$ and $b$, and $d$ and $c$, but there is no voltage difference between the points $a$ and $d$ or between the points $b$ and $c$. Points $a$ and $d$ and points $b$ and $c$ can be connected, respectively, yielding the grouping of Fig. 3–16, which shows that the winding has four parallel circuits, i.e., as many as there are poles. It is a characteristic feature of the *lap winding* that the *number of parallel cir-*

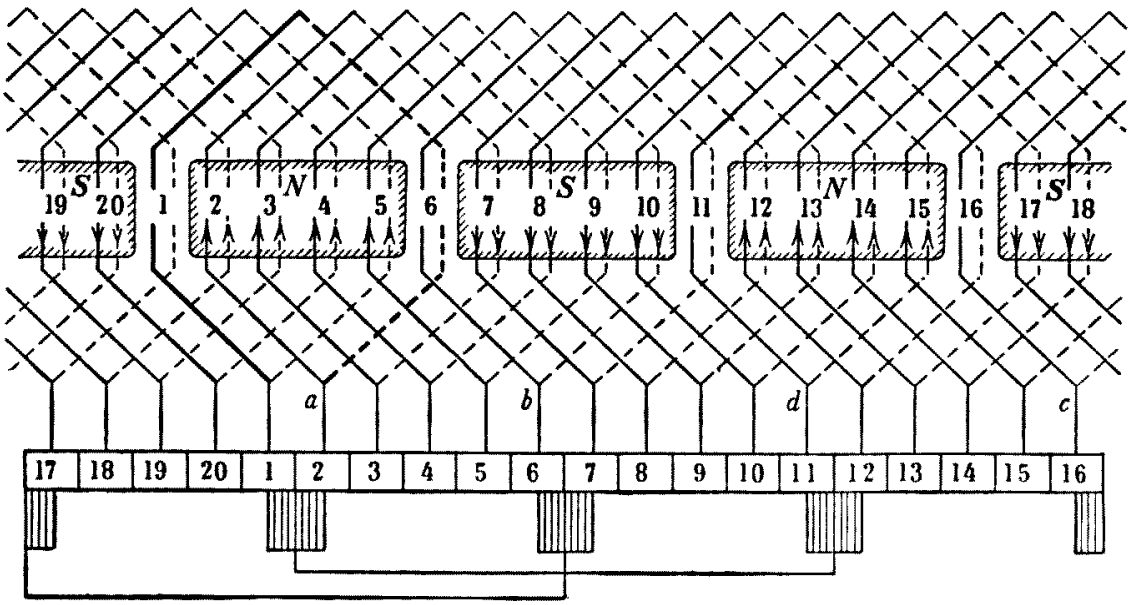


FIG. 3–13. Developed diagram of a 4-pole, 2-layer lap winding with 20 slots and one conductor per layer.

*cuits is equal to the number of poles.* Thus, a lap winding will have 8 parallel circuits in an 8-pole machine, 16 parallel circuits in a 16-pole machine, and so forth.

Fig. 3–17 shows a 4-pole wave winding developed, and Fig. 3–18 shows the same winding in a polar diagram. The number of slots is 19 and the number of conductors in each layer of a slot is 1. The total number of conductors is $19 \times 2 = 38$, and, therefore, the number of turns (winding elements) as well as the number of commutator bars is 19. According to Eq. 3–5, the winding pitch is

$$y = \frac{19 - 1}{2} = 9 = y_b + y_f$$

commutator bars. In one pole pitch there are $19/4 = 4\frac{3}{4}$ commutator bars. The coil span $y_b$ is chosen as 5 commutator bars, i.e., close to the pole pitch but slightly larger than the pole pitch. The front pitch is then $9 - 5 = 4$ commutator bars. Since there is only 1 conductor per layer in the slot, the back pitch and front pitch are 5 and 4 slots, respectively, if they are expressed in slot pitches. Thus, starting with upper conductor 1, a connection must be made to lower conductor $1 + y_b = 1 + 5 = 6$ on the side opposite the commutator (back end), then to upper conductor $6 + y_f = 6 + 4 = 10$ on the

commutator side, then again to lower conductor $10+y_b=10+5=15$, next to upper conductor $15+4=19$, and so forth, until the winding is closed.

Starting at point $a$ in Fig. 3–17 and tracing through the winding, the sequence of the upper and lower conductors and the direction of the induced

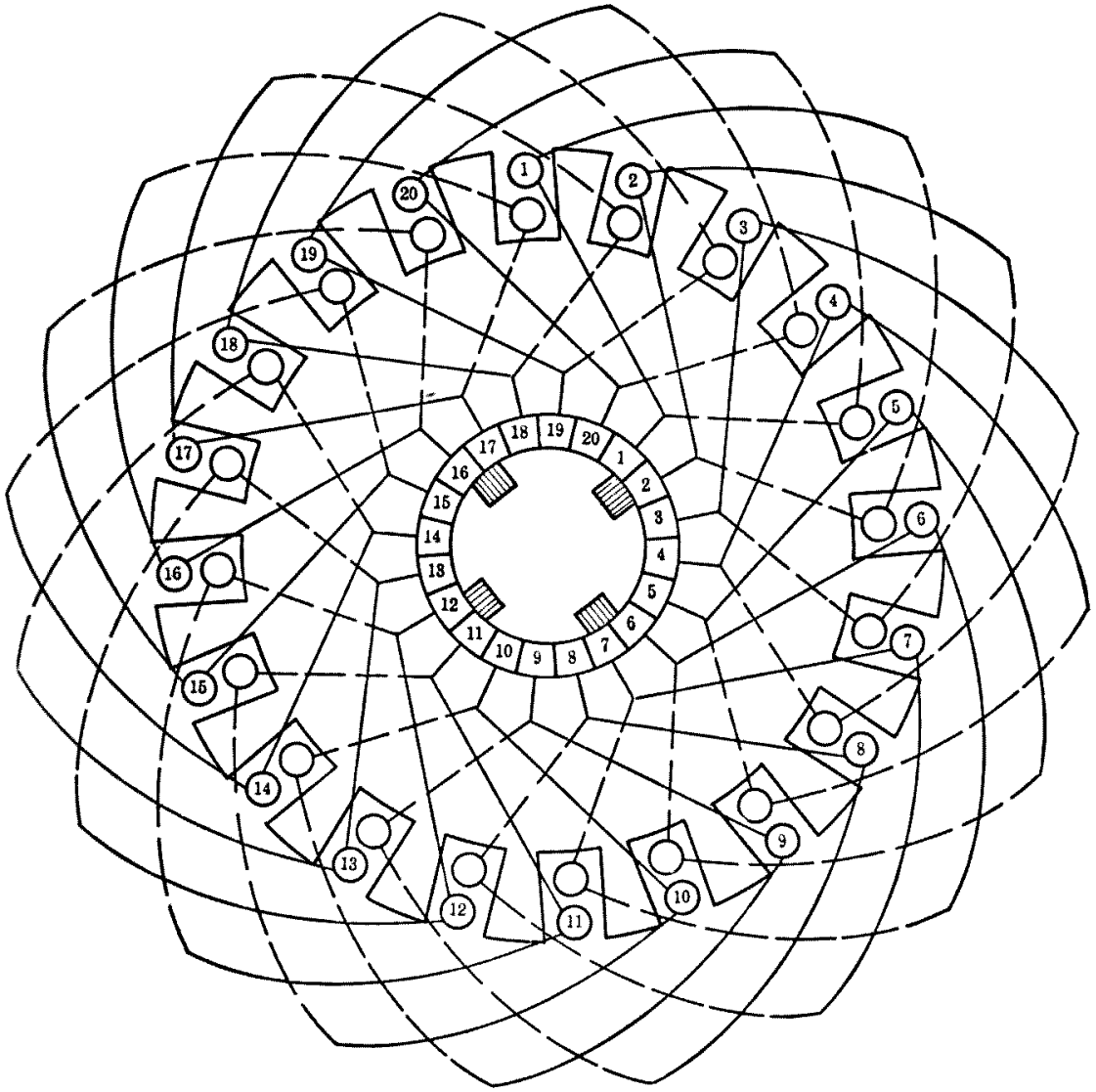


FIG. 3–14. Polar diagram of the winding shown in Fig. 3–13.

emf's is as shown in Fig. 3–19. Upper and lower conductors must be considered here because the coil span is not equal to the pole pitch. It is seen from this figure that here there are only two parallel circuits as compared with the four parallel circuits of the 4-pole lap winding (Figs. 3–13 and 3–16). It is a characteristic feature of the *wave winding* that it *has only two parallel circuits*, regardless of the number of poles. This feature of the wave winding is the reason why it is designated as a *series winding*, and the lap winding is designated as a *parallel winding*.

It is seen from Figs. 3–16 and 3–19 that four external connections to the

winding, i.e., four brush studs on the commutator, are necessary for the 4-pole lap winding and only two brush studs for the 4-pole wave winding.

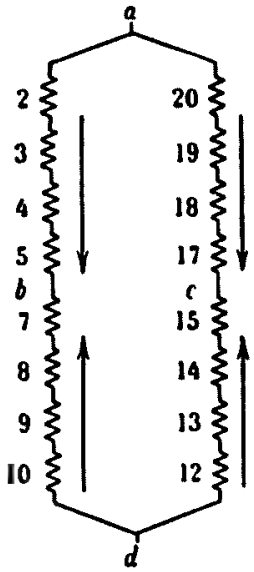


FIG. 3–15. Sequence of upper conductors and direction of the emf's of winding shown in Fig. 3–13.

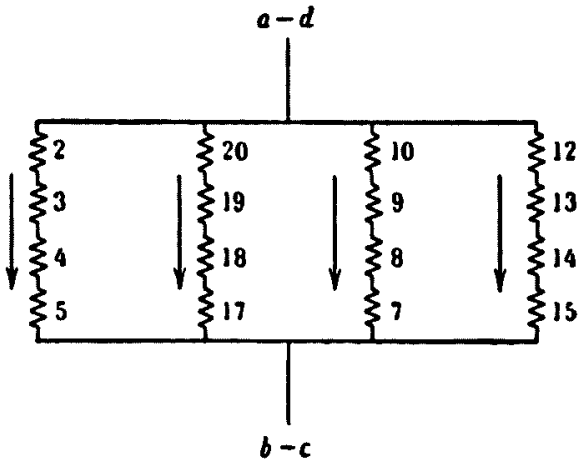


FIG. 3–16. The four parallel circuits of the winding shown in Fig. 3–13.

In general, the *lap winding needs as many brush studs as there are poles*, since it has as many parallel circuits as poles. Half of the brush studs are of

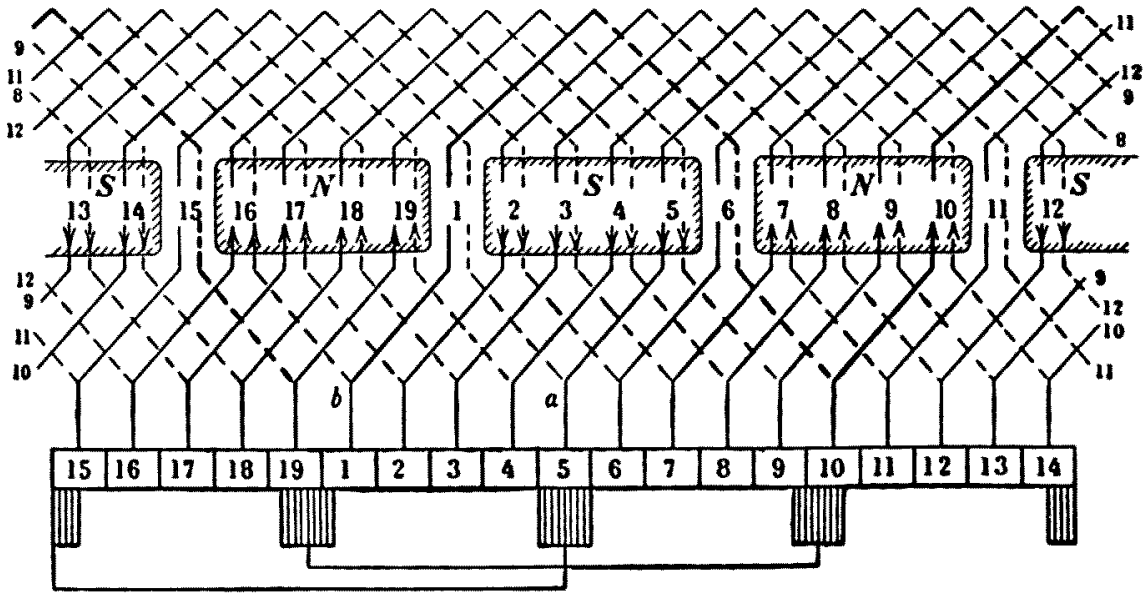


FIG. 3–17. Developed diagram of a 4-pole, 2-layer wave winding with 19 slots and one conductor per layer.

positive polarity; half, of negative. As to the wave winding, two brush studs, one positive and one negative, suffice for any number of poles. How-

ever, normally the wave winding has also as many brush studs as poles. This has the advantage that, for a given current, the commutator is shorter. The positive as well as the negative brush studs are then seen to be internally connected by the winding elements short-circuited by the brushes (see Fig. 3–17).

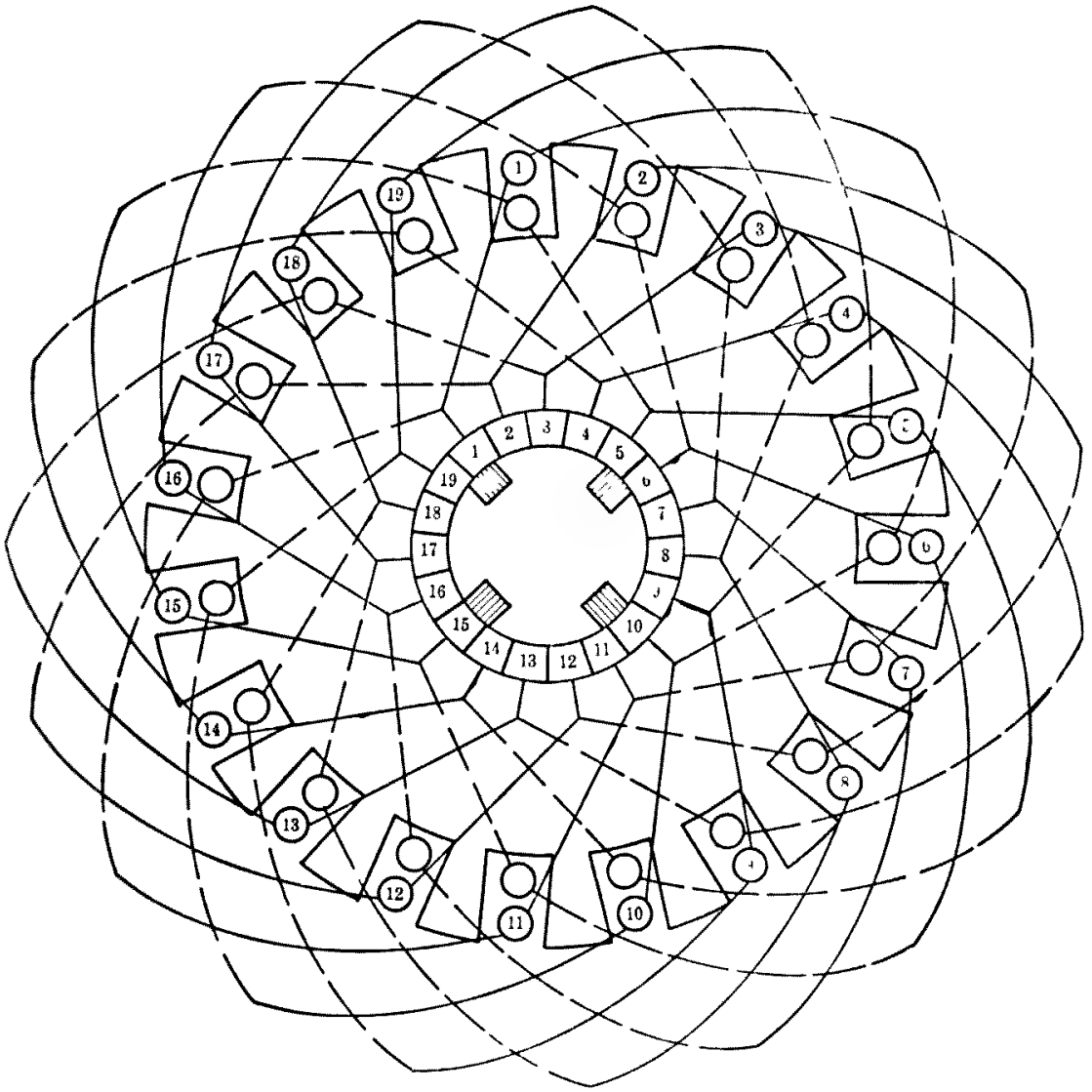


Wave Winding

FIG. 3–18. Polar diagram of the winding shown in Fig. 3–17.

It is seen from Figs. 3–11, 3–13, and 3–17 that in the diamond-shape coils the brushes *physically* lie at the center lines of the poles. The active (in iron embedded) parts of the winding elements connected to the brushes then lie in the interpolar spaces at the reversal points of the induced emf's. In schematic diagrams (see Art. 6–1) the brushes are usually placed in the center lines of the interpolar spaces to indicate the conductors to which they are connected. In Figs. 3–13, 3–14, 3–17, and 3–18, the polarity of the brushes is definitely determined by the pole polarities and the direction

of rotation of the armature. In the schematic diagrams, the polarity of the brushes is not definitely determined and may be assigned arbitrarily.

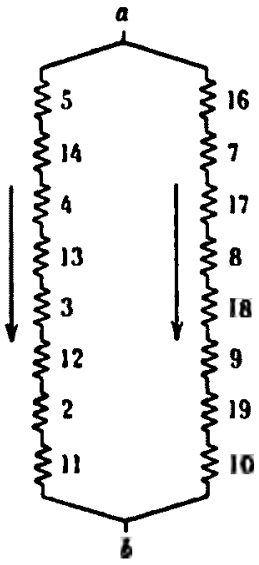


FIG. 3–19. The two parallel circuits of the winding shown in Fig. 3–17.

**Example 3–3.** 8-pole armature with 132 slots; 2-layer winding with three conductors per layer in the slot. Lap winding.

Determine the number of commutator bars and the back and front pitches. Show the sequence in which the conductors are connected.

Since there are three conductors per layer in the slot, the total number of winding elements is $132 \times 3 = 396$; therefore, the number of commutator bars is

$$K = 396$$

The number of commutator bars per pole is $396/8 = 49\frac{1}{2}$, and the back pitch must be close to this figure. The number of slots per pole is $132/8 = 16\frac{1}{2}$, and the back pitch, if measured in slot pitches, must be also close to this figure. The back pitch is chosen as 16 slot pitches $= 16 \times 3 = 48$ commutator pitches. Fig. 3–20 shows the arrangement of the conductors in the slots. Since the back pitch is 16 slot pitches, upper conductor 1 is connected with a lower conductor lying in slot $1 + 16 = 17$ and, since the back pitch is 48 commutator pitches, upper conductor 1 is connected with lower conductor $1 + 48 = 49'$. According to Eqs. 3–1 and 3–3, the front pitch is $y_f = 47$. Thus lower conductor 49′ must be connected with upper conductor $49' - 47 = 2$, and so forth. The sequence in which the conductors are connected is

1-49′-2-50′-3-51′-4-52′-5-53′ . . .

The three turns 1-49′, 2-50′, and 3-51′ lie in the same slots (1 and 17); they are insulated together and placed in the slots together. Such a group is called a coil (see page 46). The same applies for the turns 4-52′, 5-53′, 6-54′, and so forth.

FIG. 3–20. Example—Arrangement of conductors in slots.

**3–5. The Field Displacement and the Number of Parallel Paths.** The difference in the number of parallel paths of the lap and wave winding has been demonstrated in the last article by tracing through the winding and determining the number of parallel circuits. The real reason for the difference in the number of parallel paths of the two winding types lies in the *selection of the number of slots and the resulting difference of the position in the magnetic field.* Notice that the 4-pole lap winding (Fig. 3–13) has 20 slots, while the 4-pole wave winding (Fig. 3–17) has 19 slots. The 4-pole lap winding cannot be made with 19 slots, and the 4-pole wave winding cannot be made with 20 slots.

Consider the position of the individual winding elements in the magnetic

field; each winding element has a different position in the field in relation to the adjacent winding element. This displacement in the magnetic field between two consecutive winding elements is equal to the distance between the beginnings of those two elements; i.e., it is equal to the resultant winding pitch $y = 1$ for the lap winding (see Fig. 3–21), and to the difference between twice the pole pitch $2\tau$ (measured in commutator bars) and the resultant winding pitch $y$ for the wave winding (see Fig. 3–22). Thus, the field displacement is the distance (in commutator bars) by which corresponding sides of consecutive winding elements (such as $a$ and $b$ in Figs. 3–21 and 3–22) fail to lie in exactly the same positions under the poles of the same polarity. In terms of commutator bars the field displacement is equal to 1 in the case of the lap winding, and equal to (Eq. (3–5))

$$y - \frac{K}{p/2} = \mp\frac{1}{p/2}$$

in the case of the wave winding; i.e., the field displacement is a whole commutator bar for the lap winding, and a fraction of a commutator bar for the wave winding.

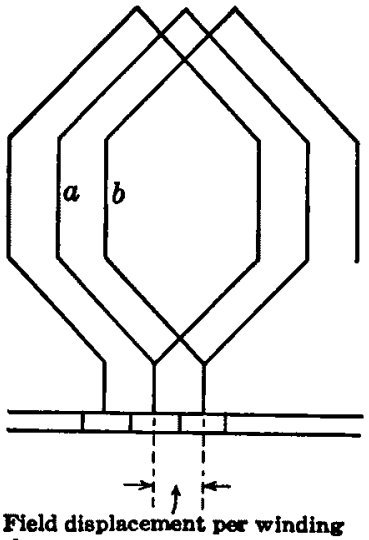


FIG. 3–21. Field displacement of the lap winding. Field displacement per winding element = 1 commutator pitch 4 poles, 20 slots, 20 winding elements. Lap winding.

The total field displacement of a winding is obtained by starting at any bar, progressing through the whole winding, and adding up the field displacements of all winding elements. It is this *total field displacement which determines the number of parallel paths of a d-c armature winding*. If the winding has a field displacement of $p$ pole pitches, the winding will have $p$ parallel paths. If the winding has a displacement of 2 pole pitches, the winding will have only 2 parallel paths. It is seen from Fig. 3–12 that 2 is the minimum number of parallel paths of a d-c armature winding.

Starting at any bar and progressing through the 4-pole lap winding (Fig. 3–13), the entire field displacement is equal to 20 commutator bars, i.e., to $20/5 = 4$ pole pitches (measured in commutator bars). Therefore, the number of parallel paths will be 4.

If the number of winding elements or commutator bars per pole is not a whole number, then the lap winding cannot be designed as a full-pitch winding. The winding then must be designed as a fractional-pitch winding, and in this case the coil width is made less than the pole pitch. With regard to the arrangement of equalizers (see Art. 3–9), the number of commutator bars *per pole pair* in the lap winding is always made an integer.

Consider the 4-pole wave winding, Fig. 3–17. Starting at any commutator

segment such as 1 and progressing through one winding element, the end of the winding element does not terminate at the adjacent bar 2 or 19, as in the case of the lap winding, but rather at bar 10 that is distant by almost double the pole pitch (measured in commutator bars). *The adjacent bar* 19 *is reached after progressing through* two (in general, $p/2$) *winding elements.* The field displacement per winding element is here $y - K/(p/2) = 9 - 9\frac{1}{2} = \frac{1}{2}$ commutator pitch (Fig. 3–22). By progressing through the whole winding

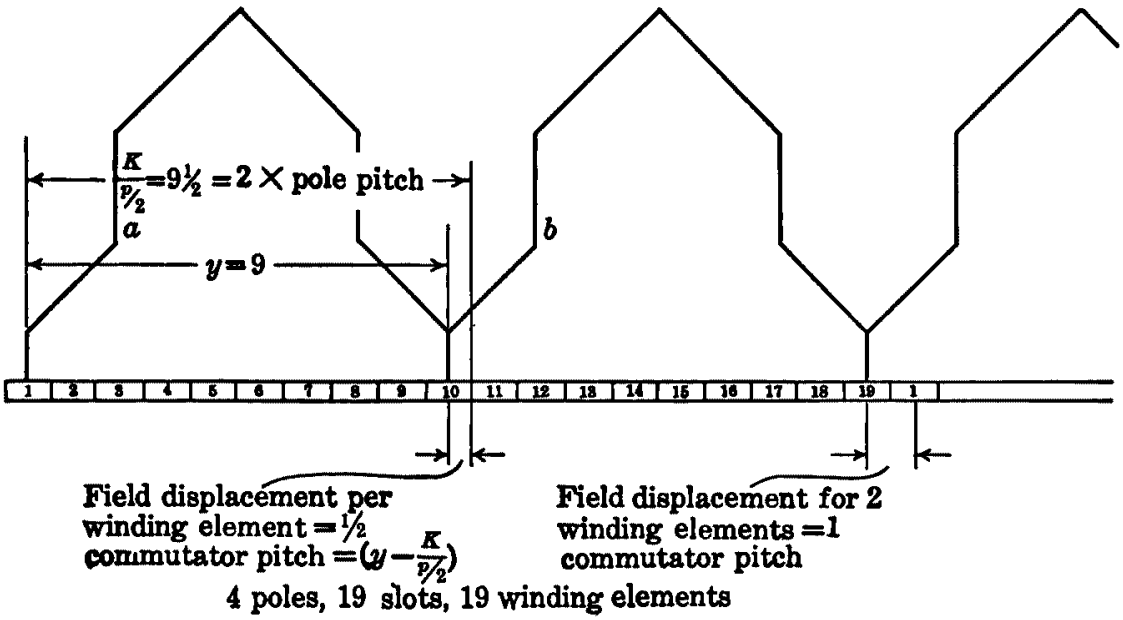
K/p/2 = 9½ = 2 × pole pitch
a
b
y = 9
1 2 3 4 5 6 7 8 9 10 11 12 13 14 15 16 17 18 19 1
Field displacement per winding element = ½ commutator pitch = (y − K/p/2)
Field displacement for 2 winding elements = 1 commutator pitch
4 poles, 19 slots, 19 winding elements

FIG. 3–22. Field displacement of the simple wave winding.

Field displacement per winding element $= \frac{1}{2}$ commutator pitch $= \left(y - \frac{K}{p/2}\right)$

Field displacement for 2 winding elements $= 1$ commutator pitch

4 poles, 19 slots, 19 winding elements.

(through all 19 winding elements) the entire field displacement here is only $19 \times \frac{1}{2} = 9\frac{1}{2}$ commutator pitches. A single pole corresponds to $19/4 = 4\frac{3}{4}$ commutator pitches. The entire field displacement is thus equal to $9\frac{1}{2}/4\frac{3}{4} = 2$ pole pitches, and therefore there will be *only two* parallel paths ($a = 2$) in the wave winding.

This result is independent of the number of poles. Each wave winding which follows the rule $y = (K \mp 1)/(p/2)$ has only two parallel circuits. The field displacement per winding element is equal to $1/(p/2)$ commutator pitches. The total number of winding elements is $K$, and, therefore, the entire field displacement is $K \times 1/(p/2)$. Since there are $K/p$ commutator pitches per pole, the total field displacement will be $\frac{2K}{p} \Big/ \frac{K}{p} = 2$ pole pitches, or $a = 2$.

A further clarification of the difference between the lap and wave winding is obtained, when it is assumed that the flux distribution around the arma-

ture is sinusoidal. In this case the emf's of the individual conductors are sinusoidal (Art. 1–1) and the amplitudes of the emf's can be represented by phasors; i.e., by quantities whose values are represented by complex numbers.

The emf's of conductors lying in 2 consecutive slots are out of phase by an angle which corresponds to a slot pitch, i.e., to $\alpha_s = 180p/Q$ electrical degrees, where $Q$ is the total number of slots. For our purpose, it is satisfactory to consider only either the upper or the lower conductors. The upper conductors will be the ones considered.

Refer to the 4-pole lap winding Fig. 3–13; the angle between 2 slots is $\frac{4 \times 180}{20} = 36$ electrical degrees. By placing the phasor of upper conductor 1 in the horizontal to the left and drawing the phasors of conductors 2, 3, 4, . . . 20, each 36° apart from the other, the complete phasor diagram of the winding (Fig. 3–23) is obtained. It is seen from this diagram that the phasors

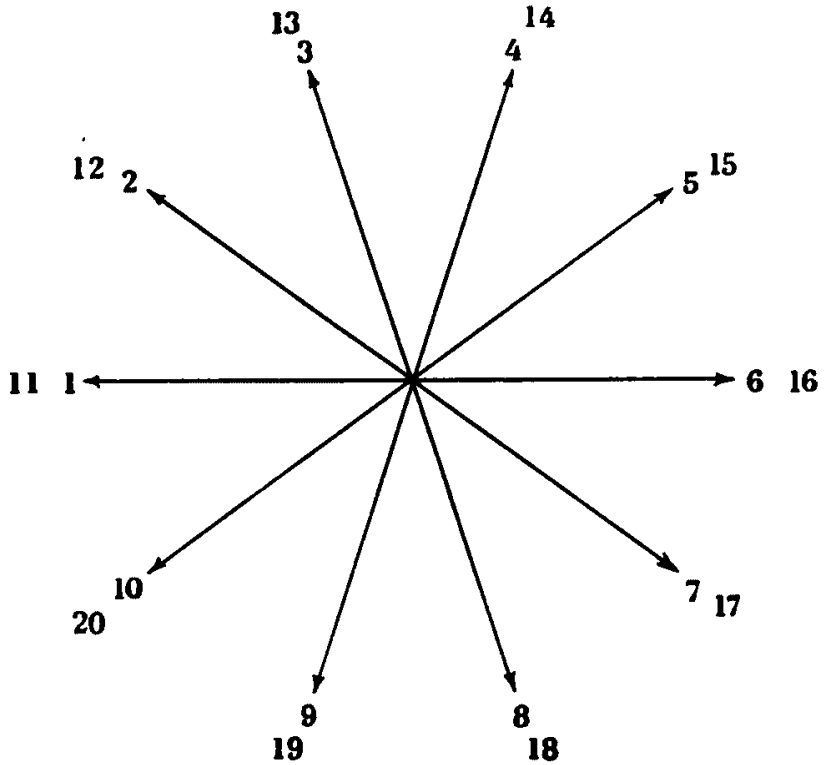


FIG. 3–23. Phasor diagram of the 4-pole lap winding Fig. 3–13.

of 2 poles make a circle and that the phasor-circle of poles 3 and 4 coincides with the phasor-circle of poles 1 and 2. Since there is a fixed relation between the number of slots and number of commutator bars, the phasor diagram is simply another representation of the field displacement of the winding. One complete phasor circle corresponds to 2 poles phase-displacement. The 4-pole lap winding (Fig. 3–13) is represented by 2 circles; it has a phase displacement of 4 poles and, therefore, 4 parallel paths.

In the 4-pole wave winding of Fig. 3–17, the angle between 2 slots is

$\frac{4 \times 180}{19} = 37\frac{17}{19}$ electrical degrees. Starting again with upper conductor 1 and drawing the 19 conductors $37\frac{17}{19}$ degrees apart from each other, not 2 phasor-circles but *one single phasor-circle is obtained* (Fig. 3–24). The phasor

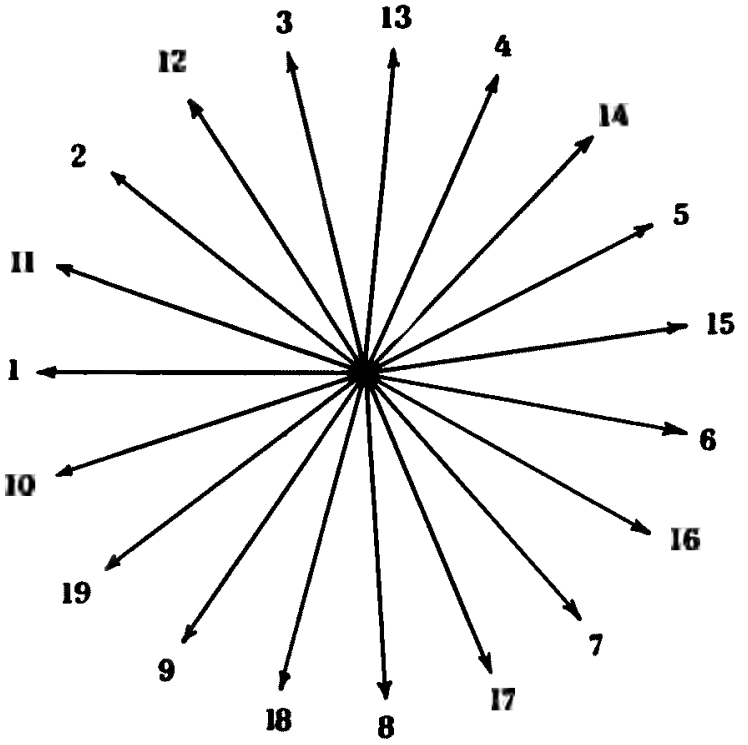


FIG. 3–24. Phasor diagram of the 4-pole wave winding Fig. 3–17.

diagram is the same which is obtained for a 2-pole winding with 19 conductors and, therefore, the 4-pole wave winding (Fig. 3–17) has only 2 parallel paths.

Fig. 3–25 shows the phasor diagram of a 6-pole wave winding in 31 slots with 1 conductor per layer. The total number of conductors per layer is 31 and the angle between 2 adjacent slots is $\frac{6 \times 180}{31} = 34\frac{26}{31}$ electrical degrees. The phasor diagram of all 6 poles is again represented by a single circle, just as the phasor diagram of a 2-pole winding with 31 conductors per layer, and the number of parallel paths is 2. Between 2 consecutive phasors, for example 1 and 2, lie 2 other phasors (12 and 22). Independent of the number of poles, the phasor diagram of the wave winding is represented by a single circle and between 2 consecutive phasors lie $\left(\frac{p}{2} - 1\right)$ other phasors belonging to other poles.

**3–6. Series-Parallel or Duplex-Wave Winding.** If the total field displacement is increased in the case of the wave winding, a number of armature paths greater than two is obtained. The field displacement per winding

element of the simple wave winding ($a=2$) is $1/(p/2)$ commutator pitches, and this results in two parallel paths. If the field displacement is made $2 \times 1/(p/2)$ commutator pitches, the number of paths will be 2 times as large,

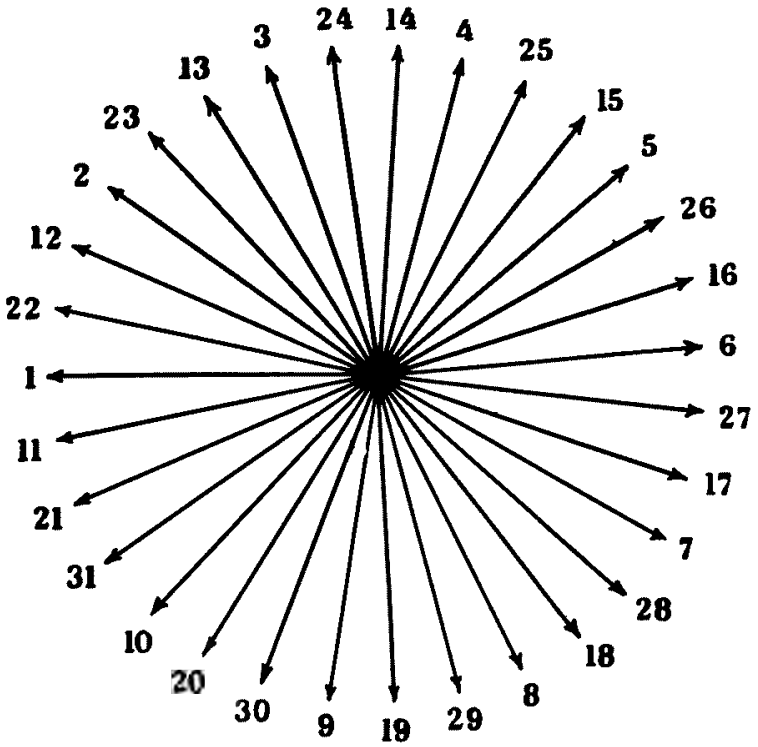


FIG. 3–25. Phasor diagram of a 6-pole wave winding in 31 slots.

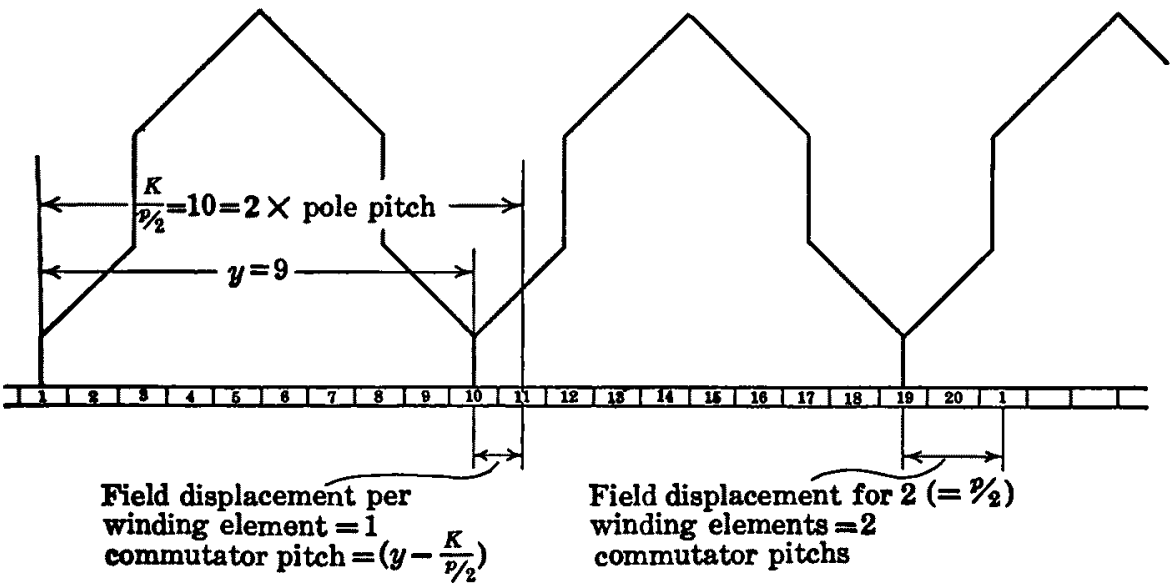
$\frac{K}{p/2}$=10=2 × pole pitch
$y$=9
1 2 3 4 5 6 7 8 9 10 11 12 13 14 15 16 17 18 19 20 1
Field displacement per winding element = 1 commutator pitch = $(y-\frac{K}{p/2})$
Field displacement for 2 (= $p/2$) winding elements = 2 commutator pitchs
Series parallel or duplex wave winding

FIG. 3–26. Field displacement of a 4-pole duplex wave winding with 20 slots and 20 winding elements.

Field displacement per winding element = 1 commutator pitch $= \left(y - \frac{K}{p/2}\right)$

Field displacement for 2 ($=p/2$) winding elements = 2 commutator pitches

namely, 4. This means that if the resultant pitch $y$ is selected in such a manner that, after progressing through $p/2$ winding elements, the winding arrives, not at a segment adjacent to the starting segment, but at a segment which is $x$ commutator pitches distant from the starting point, the wave winding has $2x$ armature paths. Figs. 3–26 and 3–27 show such a 4-pole wave winding with 4 instead of 2 armature paths. Twenty commutator

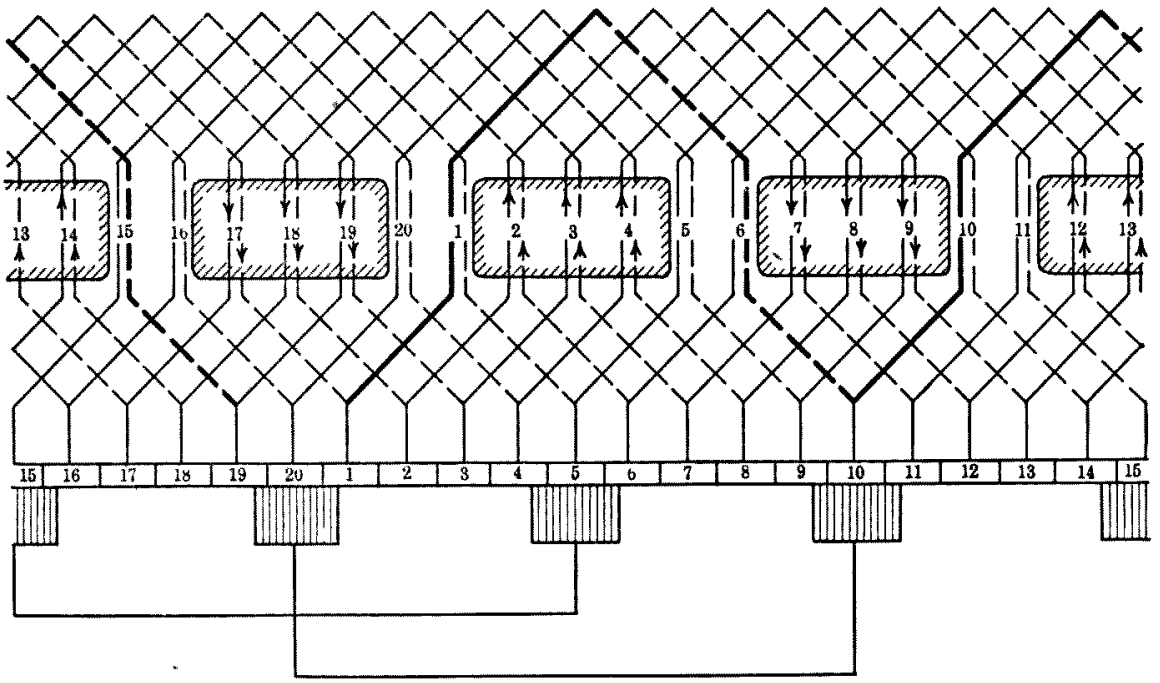


FIG. 3–27. Developed diagram of a 4-pole 2-layer series-parallel or duplex wave winding with 20 slots and 1 conductor per layer.

segments (winding elements) are used in the winding. In this winding, by starting at commutator segment 1 and progressing through $p/2=2$ winding elements, the winding does not reach the adjacent bar 20, but rather bar 19. The total field displacement is 2 times as great as in the case of the customary series winding, and consequently there are 4 armature paths present. The phasor diagram of this winding is shown in Fig. 3–28. Contrary to the wave winding with $a=2$ (Figs. 3–24 and 3–25) it consists of 2 circles coinciding with each other just as in the case of a 4-pole lap winding (Fig. 3–23). This means that $a$ is equal to 4. A wave winding with more than 2 armature paths is called a series-parallel winding, or *duplex-wave* winding when the number of paths is 4 and *triplex-wave* winding when the number of paths is 6.

The resultant winding pitch $y$ of the series-parallel winding is, in accordance with the displacement per winding element,

$$y-\frac{K}{p/2}=\mp\frac{a/2}{p/2}$$

or

$$y=\frac{K\mp a/2}{p/2} \tag{3–7}$$

The usual wave winding ($a=2$) closes on itself after progressing through as many circuits, each having $p/2$ winding elements, as is contained in $y$ commutator pitches. For example, starting with commutator bar 1 (Fig.

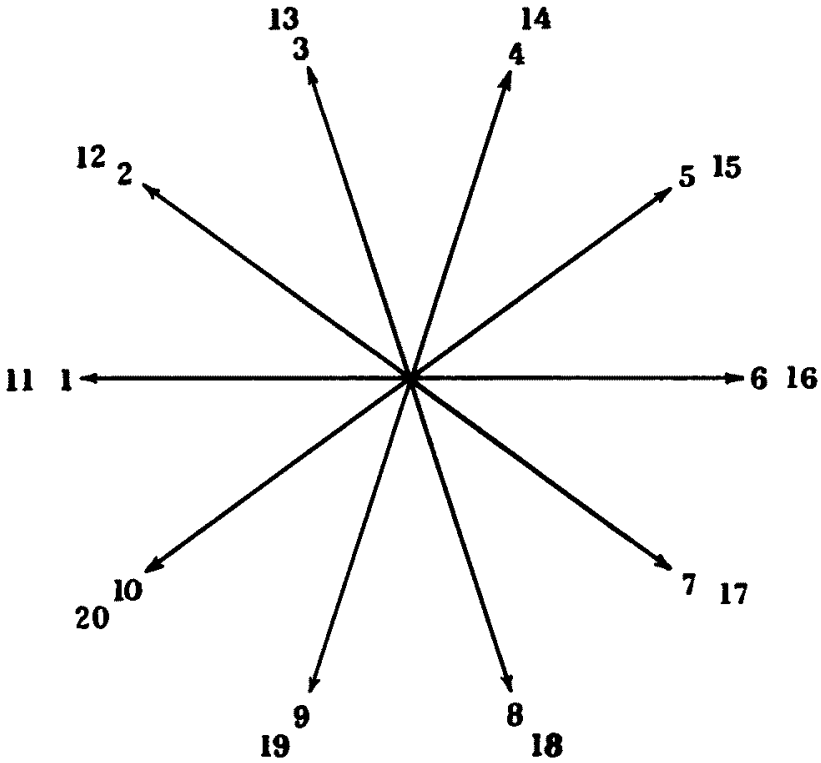


FIG. 3–28. Phasor diagram of the 4-pole duplex wave winding Figs. 3–26 and 3–27.

3–17), the winding closes after the neighboring 9 commutator bars numbers 19, 18, 17, 16, 15, 14, 13, 12, and 11 have been passed in tracing through the winding. If, in the series-parallel winding, $y$ is divisible by $a/2$, the winding closes on itself after progressing through $y/(a/2)$ circuits, each having $p/2$ winding elements, without traversing *all* winding elements of the armature. Should the series-parallel winding form a single closed path (meaning it would be *singly re-entrant*), then $y$ and $a/2$ should have no common divisor. With regard to improving the commutation in a-c commutator machines, doubly closed (*doubly re-entrant*) windings are sometimes employed.

The maximum number of parallel paths for the lap winding as well as for the multiplex wave winding is $p$. By arranging a lap winding and a multiplex wave winding with $p$ paths in the same slots and connecting both windings to the same commutator, $2p$ parallel paths can be obtained. Since both windings are connected in parallel, they must have the same position in the magnetic field in order to avoid circulating currents, i.e., back and front pitches of the two windings must be respectively the same. Each of the two separate windings cross-connects the other winding so that equalizers (see

Art. 3–9) are not necessary. A winding of this kind is referred to as *frog-leg winding.*

**3–7. The Split-Coil Winding.** If, as is usually the case, several winding elements lie side by side in each layer within a slot (Fig. 3–7), then two different designs are possible for both the lap and the wave winding. Either the sides of the winding elements which lie adjacent to each other in the upper layer of a slot are also together in the lower layer of a slot, distant by the back pitch $y_b$ (as Fig. 3–29a shows), or they lie in the lower layers of different slots (as Figs. 3–29b and 3–29c show for the case of two and three

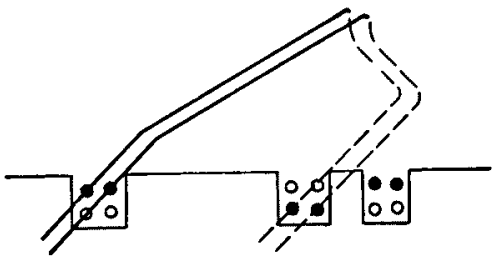

(*a*)

FIG. 3–29a. Normal winding.

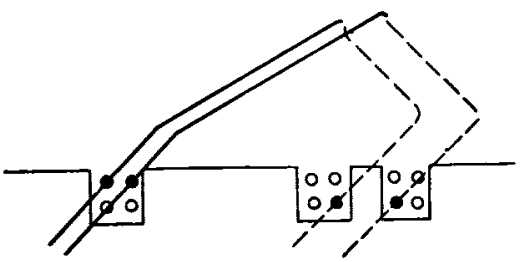

(*b*)

FIG. 3–29b. Split-coil winding.

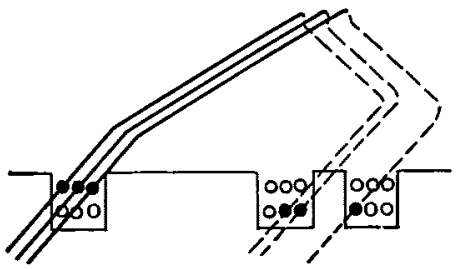

(*c*)

FIG. 3–29c. Split-coil winding.

winding elements, respectively). In the first case, all winding elements are identical; in the case of open slots, all winding elements can be insulated together to form a coil before they are placed in the slot. In the second case, winding elements of different widths are necessary, and the insulation of the winding elements becomes more complicated. This type of design is called a *split-coil winding.* It has certain advantages with respect to commutation but is more costly to manufacture.

**3–8. Operation of the Commutator.** Fig. 3–30 shows a 2-pole machine with 12 winding elements in 12 slots. It will be assumed that the flux is sinusoidally distributed over the armature. Then the emf's induced in the individual winding elements are sinusoidal functions of time and their amplitudes can be represented by phasors (see Art. 3–5).

Only the upper conductors are shown in Fig. 3–30. The lower conductors lie a pole pitch apart from the upper conductors of the same winding element. So, for example, the lower conductor of winding element 1 lies in the same slot as upper conductor 7; the lower conductor of winding element 2 lies in the same slot as upper conductor 8, and so forth (see Fig. 3–10). For the position of the conductors shown in Fig. 3–30, winding elements 1 and 7 have maximum instantaneous emf, since they are cut by the amplitude of $B$ (see Art. 1–1). On the other hand, winding elements 4 and 10 have zero induced emf, since they lie under $B=0$.

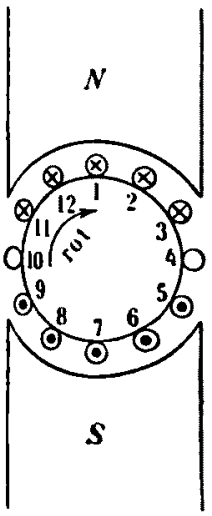


FIG. 3–30. Two-pole machine with 12 winding elements. One layer shown.

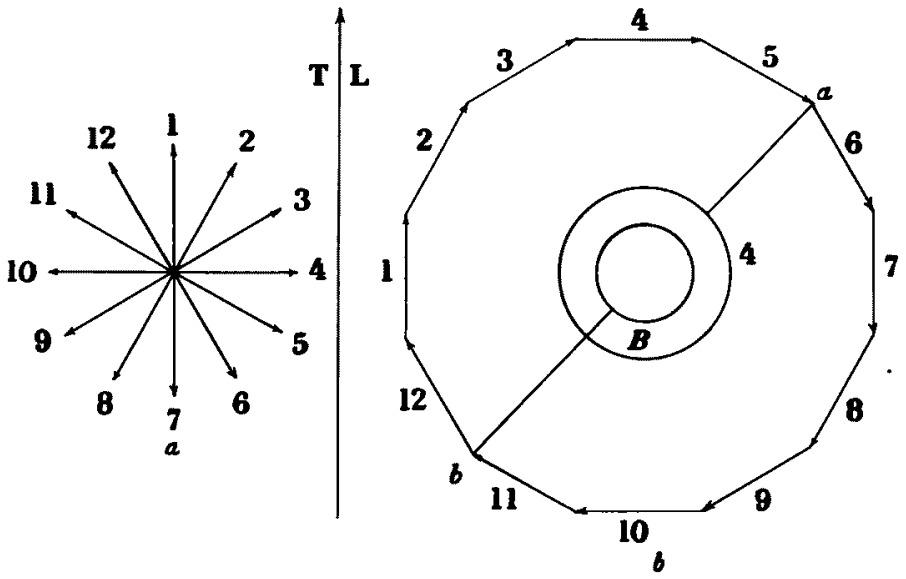


Fig. 3–31. Voltage star and voltage polygon of the winding—Fig. 3–30.

The phasors representing the amplitudes of the emf's of the individual winding elements are shifted with respect to each other by an angle corresponding to a slot pitch. The phasors of all winding elements taken together yield a voltage star, as shown in Fig. 3–31a. The time line (T.L.) is placed corresponding to Fig. 3–30, i.e., in such a position that the instantaneous value of the emf is maximum in winding elements 1 and 7.

If the phasors of Fig. 3–31a are arranged in succession in the same order in which they follow one another in the winding, the *voltage polygon* (Fig. 3–31b) is obtained.

Consider two diametrically opposite points, such as $a$ and $b$, $a$ being at the junction point between winding elements 5 and 6, and $b$ at the junction of elements 11 and 12, respectively. If each of these points $a$ and $b$ are joined to separate slip rings $A$ and $B$ (Fig. 31b) *which rotate with the winding*, and a voltage is taken from these slip rings by means of brushes, this voltage is an alternating voltage. The amplitude of this voltage is equal to the length of

the connecting line *a-b* in Fig. 3–31b, which in turn is the geometric sum of the individual voltages 12, 1, 2, 3, 4, and 5, or 6, 7, 8, 9, 10, and 11. This alternating voltage is a maximum when the armature winding is so located in the field that the line *a-b* is parallel to the time line, and is zero when the armature winding is so located that the line *a-b* is perpendicular to the time line.

The action is quite different if the voltage is taken from two points which are *at standstill* rather than from two winding points which rotate with the winding. Theoretically, two such points can be obtained, if at one end of the armature the insulation is removed from the surface of all conductors and two brushes are held against the bare copper conductor. The voltage between these two brushes will have a *constant* value, because looking into the winding through the brushes, the winding always appears *to be the same*, i.e. always having the same number of conductors, and these conductors always are in the same position in the magnetic field. The constant voltage between the brushes is the *instantaneous value* of the a-c emf which corresponds to the *position of the two brushes with respect to the time line.* The brushes will pick up the amplitude of the a-c emf, when they are oriented parallel to the time line.

However, it is impractical to remove the insulation from the conductors at one end of the armature in this manner. The practical solution consists in tapping the closed armature winding at all points at which the adjacent winding elements are connected to each other and connecting these tap points to bare bars insulated from each other, i.e., to a commutator. Brushes resting on the commutator then pick up continuously a *fixed instantaneous* value of the a-c voltage generated in the winding. The picking up of a fixed instantaneous value of an a-c voltage is the function of the commutator with its brushes.

It has been previously pointed out (Art. 3–3) that in the diamond-shaped 2-layer winding the brushes must lie in the pole axes. In this position they are connected to the conductors which lie in or close to center lines of the interpolar spaces (*neutral axes*) (in Fig. 3–30 close to the conductors 4 and 10). It is seen from the voltage polygon (Fig. 3–31b) that the instantaneous voltage between conductors close to 4 and 10 is the amplitude of the induced alternating emf, since their connection line is parallel to the time line. Thus the *brushes pick up the maximum voltage* (the amplitude of the a-c voltage) *when they are connected to the conductors lying in or close to the center lines of the interpolar spaces* (*neutral axes*).

The voltage between the brushes is not absolutely constant. There is a slight variation in this voltage because the brush covers alternately one or two commutator bars (Fig. 3–10). This changes the form of the voltage polygon with respect to the brushes, as shown in Fig. 3–32. The voltage between the brushes is alternately equal to chord 3–10 or to diameter 4–10. The magnitude of this variation decreases with an increase in the number of commutator bars (winding elements). With a large number of winding

elements the voltage polygon approaches a circle and the variation is very small. Most practical machines closely approach this condition. This variation is commonly referred to as a commutator ripple.

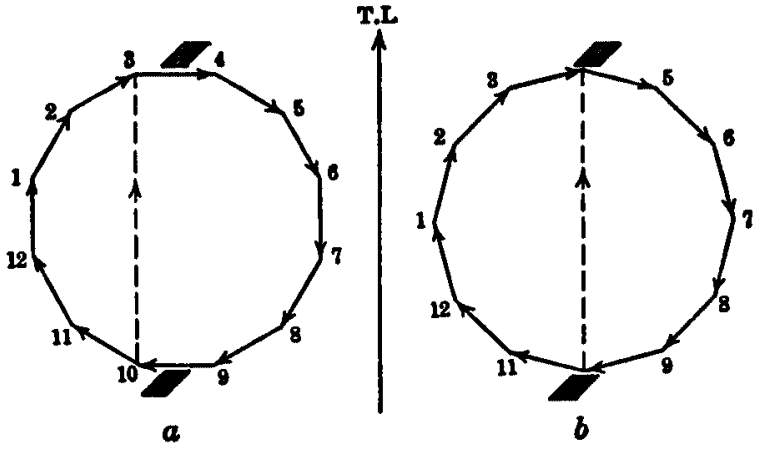


FIG. 3–32. Explanation of the voltage variation of a d-c machine.

**3–9. Equalizer Connections. Conditions for Symmetry.** A 2-pole winding is considered in Figs. 3–30 and 3–31. If the voltage polygon is drawn for a 4-pole *lap* winding, it is found that the polygon closes after passing through only two poles (two armature circuits) and that the total winding is represented by two identical polygons which coincide, if placed one above the other (Fig. 3–23). On the other hand, a 4-pole *wave* winding yields only one voltage polygon (Fig. 3–24). In general, there are as many voltage polygons as there are pairs of parallel circuits, i.e., $p/2$ polygons, in the lap winding, and only one polygon, independent of the number of poles, in the simple wave winding ($a=2$). The duplex-wave winding has two identical voltage polygons.

The points of the voltage polygons which coincide when placed one above the other are *in-phase* points. In the case of the 4-pole lap winding, there is a large number of pairs of in-phase points; in the 6-pole lap winding, there is a large number of triplets of in-phase points and so forth. The simple wave winding has no in-phase points.

If the field (pole) system is not symmetrical or if the armature bearings are eccentric, asymmetry between the pole fluxes of the machine results. This asymmetry has no effect on the magnitude of the emf's induced in the individual paths of a *simple wave* winding, because in this winding the winding elements of each parallel path are distributed under *all* poles of the machine. The effect of flux asymmetry is quite different in lap windings. Here the winding elements which belong to a single armature path lie only under *two adjacent* poles. Because of the flux asymmetry, the emf's of the various individual paths are no longer equal, and the points of the winding which were in-phase points under conditions of complete symmetry are no longer in phase. Since some of these points are connected by brushes of the

same polarity, circulating current will flow through the brushes. Sparking at the commutator can easily result in this event, if individual brushes are overloaded.

In order to rid the brushes of these circulating currents, some in-phase points of the winding, between which no voltage difference would exist under conditions of complete symmetry, are tied together by *equalizer connections* having negligible resistance. An alternating current then flows through the winding and the equalizers, which leads to an improvement of the commutation but gives rise to additional heating losses.

It follows from the foregoing that equalizer connections should be applied to the multiple-pole lap windings and to the wave windings with more than two parallel circuits (duplex wave windings, triplex wave windings, etc.).

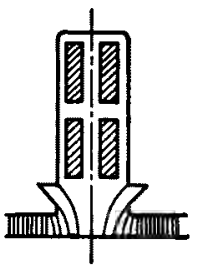

FIG. 3–33. Flux in the tooth and in the slot space.

The preceding consideration of the voltage polygon was applied to the case where the slot contains only one winding element per layer. Fig. 3–33 shows that the flux passes almost entirely through the teeth and not through the slot space. Therefore, if there are several winding elements in each layer, the emf's induced in all winding elements within any one slot are in phase and they are represented in the voltage diagram by in-phase phasors. The previous coniderations thus apply also when there are several winding elements per layer.

D-c armature windings *must be symmetrical* in order to give sparkless commutation. The conditions for symmetry can be derived from the preceding consideration of the voltage polygon.

Since each two parallel paths make one voltage polygon, the number of winding elements (commutator bars) in two parallel paths must be an integer, i.e.,

$$\frac{K}{a/2} \text{ must be an integer} \tag{3–8}$$

In order that the number of winding elements per layer be the same for all slots also

$$\frac{Q}{a/2} \text{ must be an integer} \tag{3–9}$$

These two conditions for symmetry must be fulfilled by the lap as well as by the wave winding. The wave winding with $a>2$ (duplex and triplex windings) must fulfill the further condition that $\frac{p/2}{a/2}=$ integer, i.e., for the *wave* winding in general

$$\frac{p}{a} \text{ must be an integer} \tag{3–10}$$

Further information on the wave winding is given in Chap. 15.

In general practice the lap winding has been applied widely. High-voltage machines and almost all small machines which contain a comparatively large number of series-connected conductors usually are designed with the simple wave winding.

**3–10. Insulation of D-c Armature Windings.** The insulation of an electric machine must have the following characteristics: It must have a certain dielectric strength, in order to withstand the voltage differences between the conductors themselves and between the conductors and core iron. The A.I.E.E. standards require that the d-c armature windings shall be able to withstand, for 1 minute, a voltage difference between the conductors and the core iron of 2 times the rated voltage plus 1000 volts. The insulation must be able to withstand certain temperature rises (see Art. 12–1), and it must have a high heat conductivity; it must be able to resist moisture and, under certain conditions, oil, conductive and abrasive dust, and different kinds of chemicals. Further, it should occupy as little space as possible.

D-c armature coils are wound either with insulated wire of round or rectangular cross section or with bare rectangular strap copper (Figs. 3–34 to 3–36). Round wire is used generally in smaller machines. The rectangular cross section gives a better space factor and a mechanically stronger coil. The insulation of the wire is a coating of enamel plus a single cotton covering for smaller machines and double cotton covering for larger machines; for Class B insulation (see Art. 12–1) the wire insulation consists of a double glass covering. Straps are taped with 0.005- to 0.007-inch-thick cotton tape and, for Class B insulation, with mica tape; however, in order to save space not all straps are taped (see Fig. 3–36).

The insulation between coil and iron consists of cloth treated with varnish, or of fish-paper and mica, or of mica. The thickness of one layer is about 0.010 to 0.012 inch. It can be used in the form of a sheet or a tape which is wrapped around the coil side. In large machines, even with Class A insulation, mica usually is used for the wrapper. The finished coils as well as the complete armature are further impregnated with varnish.

For mechanical protection of the coil insulation against the edges of the punchings, a slot cell of paraffined fishpaper or other tough paper 0.008 to 0.010 inch thick is placed into the slots. Typical examples of complete insulation are shown in Figs. 3–34 to 3–36.

Wire-wound coils often are wound so that both coil sides lie at first in the same plane and then are pulled into the desired diamond shape by a pulling machine. Bare strap copper coils are formed on a mould.

**3–11. D-c Field Windings.** The field coils of d-c machines are concentrated coils. Round, square, or rectangular conductors are used. The insulation is enamel or single cotton covering for small conductors and double cotton

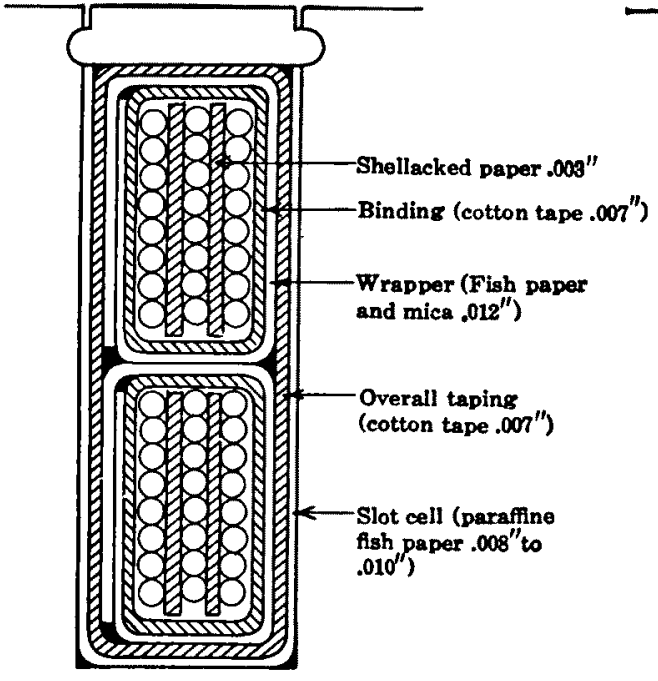
Shellacked paper .003"
Binding (cotton tape .007")
Wrapper (Fish paper and mica .012")
Overall taping (cotton tape .007")
Slot cell (paraffine fish paper .008" to .010")

FIG. 3–34. Example of insulation of armature coils with round conductors.

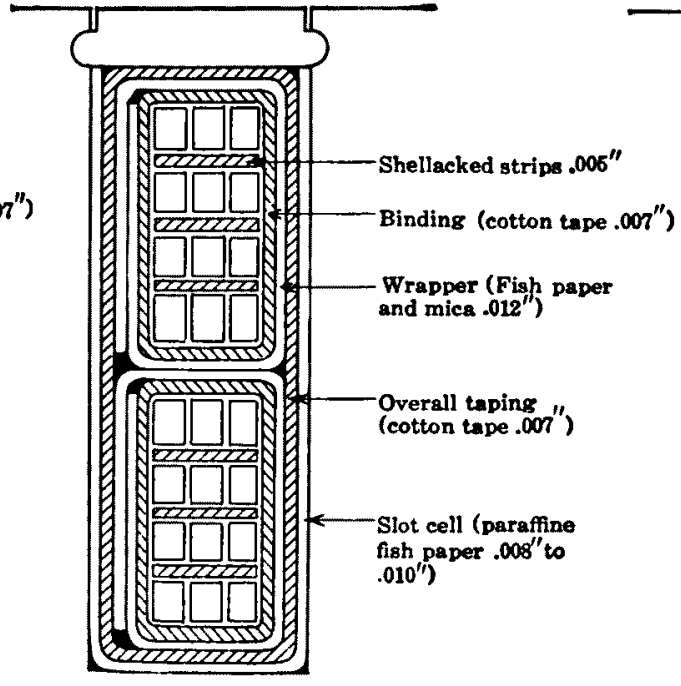
Shellacked strips .005"
Binding (cotton tape .007")
Wrapper (Fish paper and mica .012")
Overall taping (cotton tape .007")
Slot cell (paraffine fish paper .008" to .010")

FIG. 3–35. Example of insulation of armature coils with rectangular conductors.
Shellacked strips .005"
Binding (cotton tape .007")
Wrapper (Fish paper and mica .012")
Overall taping (cotton tape .007")
Slot cell (paraffine fish paper .008" to .010")

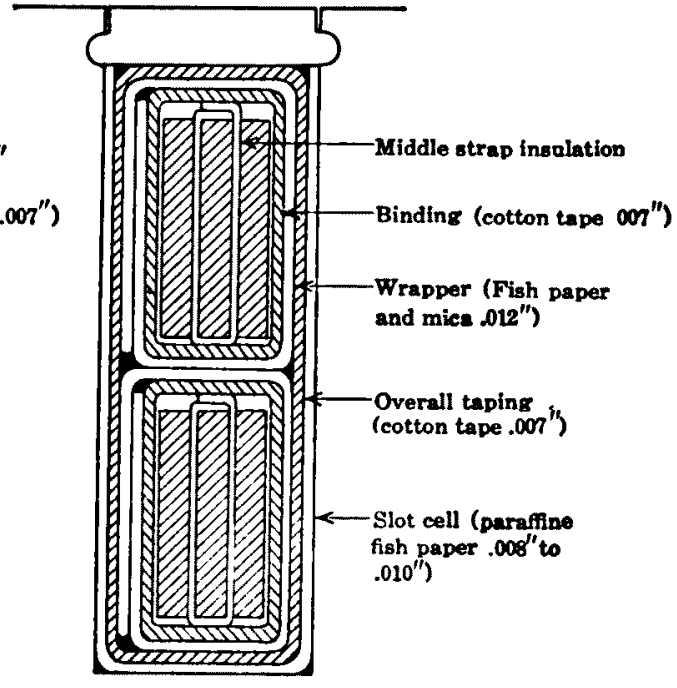
Middle strap insulation
Binding (cotton tape .007")
Wrapper (Fish paper and mica .012")
Overall taping (cotton tape .007")
Slot cell (paraffine fish paper .008" to .010")

FIG. 3–36. Example of insulation of armature coils with bare rectangular strap copper.
Middle strap insulation
Binding (cotton tape .007")
Wrapper (Fish paper and mica .012")
Overall taping (cotton tape .007")
Slot cell (paraffine fish paper .008" to .010")

covering for larger conductors. The complete coil must be carefully impregnated in order to avoid air spaces between the conductors, since such air spaces would permit moisture to penetrate the coil and also prevent the flow of heat from the interior of the coil to its surface, where it is dissipated. Examples of field coils of d-c machines are shown in Figs. 2–9 and 2–10.

## PROBLEMS

**1.** The armature of a 4-pole machine has 24 slots, 2 conductors per slot, 1 turn per element. Determine for a two-layer lap winding the following: (1) total number of conductors $Z$, (2) number of winding elements $K$, (3) number of commutator bars $K$, (4) the winding pitch $y$, (5) the back pitch $y_b$, (6) the front pitch $y_f$, (7) the coil width expressed in terms of (a) slot pitches, (b) mechanical degrees, (c) electrical degrees, (d) commutator pitches.

**2.** Repeat Problem 1 if there are 6 conductors per slot and 3 turns per element.

**3.** Repeat Problem 1 if there are 8 conductors per slot and 2 turns per element.

**4.** The armature of a 6-pole generator has 72 slots with 6 conductors per slot and 1 turn per winding element, two-layer, lap. Determine:

(1) total number of conductors, $Z$,
(2) number of winding elements $K$,
(3) number of commutator bars,
(4) winding pitch, $y$,
(5) back pitch, $y_b$,
(6) front pitch, $y_f$,
(7) the coil width expressed in terms of
  (a) slot pitches,
  (b) mechanical degrees,
  (c) electrical degrees,
  (d) commutator pitches.

**5.** Repeat Problem 4 if there are 3 turns per element.

**6.** The armature of a 6-pole machine has 37 slots, 2 conductors per slot, 1 turn per element. Determine for a two-layer, simple wave winding:

(1) number of conductors on the armature,
(2) number of winding elements,
(3) number of commutator bars,
(4) the back pitch, $y_b$,
(5) the winding pitch, $y$,
(6) the front pitch, $y_f$,
(7) the width of the winding element expressed in
  (a) slot pitches,
  (b) mechanical degrees,
  (c) electrical degrees,
  (d) commutator pitches.

**7.** Repeat Problem 6 if there are 6 conductors per slot and 3 turns per element.

**8.** Repeat Problem 6 if there are 8 conductors per slot and 2 turns per element.

**9.** Repeat Problem 6 if there are 36 slots.

**10.** Repeat Problem 7 using 1 turn per element.

**11.** The resistance of each winding element in Problem 1 is 0.006 ohm. What is the total resistance of the armature winding as measured between the terminals?

**12.** In Problem 3 the resistance of each element is 0.008 ohm. What is the total resistance of the armature winding as measured between the terminals?

**13.** In Problem 6 the resistance of each winding element is 0.006 ohm. What is the total resistance of the armature winding as measured between the terminals?

# *Chapter 4*

## EMF INDUCED IN A D-C ARMATURE WINDING

(APPLICATION OF FARADAY'S LAW OF INDUCTION)

## ELECTROMAGNETIC TORQUE PRODUCED BY A D-C MACHINE

(APPLICATION OF BIOT-SAVART'S LAW)

**4–1. Emf Induced in a D-c Armature Winding.** It has already been stated that the practical d-c machine is an a-c machine with a special device (the commutator) which permits a d-c voltage to be picked up by means of brushes on the commutator. The emf induced in a d-c armature winding, therefore, can be obtained either from Eq. 1–11

$$E = \frac{2\pi}{\sqrt{2}} Nf\Phi 10^{-8} \text{ volt} \tag{4–1}$$

for the effective value of the induced emf, assuming sinusoidal flux distribution, or considering only the fundamental wave of a non-sinusoidal distribution, or from Eq. 1–9

$$E_{avg} = 4\Phi \frac{p}{2} N \frac{n}{60} 10^{-8} \text{ volt} \tag{4–2}$$

for the average value of the induced emf, where $N$ is the number of turns in series between two brushes of different polarity (number of turns per circuit). If $Z$ = total number of conductors of the armature and $a$ = number of parallel circuits, then the total number of turns is $Z/2$, and the number of turns between two brushes of different polarity (number of turns per circuit) is $Z/2a$.

It is presumed in Eqs. 4–1 and 4–2 that the $N$ turns are concentrated in such a manner that they are all interlinked with the same number of flux lines at any instant of time (see Art. 1–1). This is apparently not the case in an actual d-c machine: the $Z/2a$ turns of a circuit are shifted with respect to each other and the emf's induced in them are not in phase. Consider the voltage polygon, Figs. 3–31 and 3–32: the brushes pick up a voltage corresponding to the diameter of a circle, while the *algebraic* sum of the voltages of all winding elements between the brushes approaches a value equal to half

the circumference of the circle. This means that, because of the shift of the $Z/2a$ winding elements with respect to each other, the voltage between the two brushes is reduced in the ratio

$$\frac{\text{diameter}}{\text{half of the circle}} = \frac{2}{\pi}$$

and both Eqs. 4–1 and 4–2 must be multiplied by this factor.

Remembering that the brushes are placed in such a position that they pick up the amplitude of the induced a-c voltage, we see that Eq. 4–1 must be multiplied by $\sqrt{2}$ and Eq. 4–2 by $\pi/2$.

If we replace $N$ by $Z/2a$ and multiply Eq. 4–1 by $2/\pi$ and $\sqrt{2}$, or multiply Eq. 4–2 by $2/\pi$ and $\pi/2$, the emf between two brushes of different polarity of a d-c armature becomes

$$E = Z \frac{p}{a} \frac{n}{60} \Phi 10^{-8} \text{ volt} \tag{4–3}$$

The derivation of Eq. 4–3 is based on the voltage polygon, Fig. 3–31; this means that sinusoidal flux distribution is assumed. However, this equation holds for any flux distribution, as can be seen from the following discussion which gives another derivation for the emf between brushes of different polarity of the d-c machine.

If $Z$ is the total number of conductors (in both layers), then the number of conductors per layer per path is $Z/2a$. Since an armature path covers a pole pitch ($\tau$) (Fig. 3–10), there are $(Z/2a\tau)\,dx$ conductors per layer in the arc $dx$ of the armature circumference. Applying Eq. 1–2a to the conductors lying in the arc $dx$, the induced instantaneous emf is

$$e_x = B_x l v \times 10^{-8} \times \frac{Z}{2a\tau} dx$$

where $B_x$ is the flux density at the element $dx$. The total instantaneous emf induced in *the path per layer* is found by integrating $e_x$ over the length of the path, $\tau$, since instantaneous emf's add up algebraically. Thus

$$E' = \frac{Zv}{2a\tau} 10^{-8} \int_{x=0}^{x=\tau} B_x l \, dx$$

The integral is the flux per pole $\Phi$ (see Fig. 1–4 or 1–5), because $\int_0^\tau B_x \, dx$ is the area of the flux distribution curve, i.e., the flux per unit of armature length. Therefore, the emf induced in a path per layer is

$$E' = \frac{Zv}{2a\tau} \Phi \times 10^{-8}$$

If the winding is full-pitch, i.e., if the back pitch of the winding (width of the coil) is equal to the pole pitch, both conductors of a turn (which lie in different

layers) lie in flux densities of the same magnitude and the emf's induced in them are equal at any instant of time (see Art. 1–1). Therefore, the total emf per path (for both layers) is $2 \times E'$. Introducing for $v$

$$v = \frac{\pi D n}{60} = \frac{p \tau n}{60}$$

the resultant instantaneous emf per path is

$$E = Z \frac{p}{a} \frac{n}{60} \Phi 10^{-8} \text{ volt} = C_1 \Phi n \qquad (4\text{–}3a)$$

where $C_1 = Z \frac{p}{a} \frac{1}{60} 10^{-8}$ is a constant for a given machine. Since 2 brushes of different polarity pick up continuously the instantaneous emf of a path as a constant quantity (see Art. 3–8), Eq. 4–3a represents the constant emf of the d-c armature winding. Eq. 4–3a may be arranged as

$$E = \left( \frac{p \Phi n}{60 \times 10^8} \right) \times \frac{Z}{a}$$

from which it is to be observed that $\left( \frac{p \Phi n}{60 \times 10^8} \right)$ is the average voltage contributed by each conductor, and $\frac{Z}{a}$ the number of conductors per path.

Equation (4–3a) is the same as Eq. 4–3. However, the first derivation, on the basis of Eq. 4–1 or 4–2 and the voltage polygon, is general and applies to d-c as well as a-c windings, while the second derivation for $E$ applies only to the voltage between two brushes of the d-c machine.

D-c armature windings usually are full-pitch or only slightly chorded. Since the air gap flux density is very small in the interpolar space, a little chording does not materially influence the value of $E$ as given by Eq. 4–3.

It is evident from the preceding derivations that Eq. 4–3 applies only when the brushes lie in the neutral axis, i.e., when they are connected to conductors lying at the reversal points of the induced emf's, because only in this position do the brushes pick up the amplitude of the a-c voltage. If the brushes are placed in such a manner that they are connected to the conductors lying under the middle of the pole, the voltage between them is zero (see Art. 3–8).

**4–2. Electromagnetic Torque Produced by a D-c Machine.** The electromagnetic (developed) torque produced by a d-c machine can be calculated from the basic law of force on a conductor in a magnetic field (Art. 1–4). According to Eq. 1–23b, the tangential force exerted on a single conductor is

$$f = 8.85 B l I \times 10^{-8} \text{ lb} \qquad (4\text{–}4)$$

where $B$ is in lines per square inch, $l$ is in inches, and $I$ is in amperes. In the

d-c machine, the current per conductor, i.e., the total armature current $I_a$ divided by the number of parallel paths $a$, has to be introduced for $I$.

With the armature diameter $D$ expressed in inches, the torque in pound-feet produced by a *single conductor* of a *smooth* armature is

$$T_c = f \times \frac{D}{2 \times 12} = \frac{D}{2 \times 12} 8.85 Bl \frac{I_a}{a} 10^{-8} \text{ lb-ft} \tag{4–5}$$

where $B$ is the flux density in the air gap around the armature (Fig. 1–4).

The conductors lying under a pole of a given polarity all have currents in the same direction (Fig. 3–10) and their torques add. Also, all conductors lying under poles of different polarity add their torques (see Art. 1–4). Thus the total torque is obtained by adding up the torques of all $Z$ conductors around the armature.

$B$ is not the same for all conductors (Fig. 1–4). Considering an arc of the length $dx$ on the armature circumference at the distance $x$ from the center of the interpolar space, the flux density there is $B_x$ and the torque produced by the $\frac{Z}{\pi D} dx$ conductors lying in this arc $dx$ is

$$\frac{D}{24} 8.85 \frac{I_a}{a} 10^{-8} \frac{Z}{\pi D} B_x l \, dx \text{ lb-ft}$$

The total torque is obtained by integrating this equation from $x = 0$ to $x = \pi D = p\tau$. Since the flux distribution curve $B_x = f(x)$ has the length $\tau$ and repeats itself around the armature circumference $p$ times, the integration can be extended from $x = 0$ to $x = \tau$ and the result multiplied by $p$. Thus, the total electromagnetic torque is

$$T = 0.1174 \times 10^{-8} \frac{p}{a} Z I_a \int_{x=0}^{x=\tau} B_x l \, dx \text{ lb-ft}$$

As in the previous consideration (Art. 4–1), the integral is the flux per pole, $\Phi$. Hence the electromagnetic torque produced by the d-c machines is

$$T = 0.1174 \times 10^{-8} \frac{p}{a} Z \Phi I_a \text{ lb-ft} \tag{4–6}$$

The electromagnetic torque of the machine is proportional to its total flux ($p\Phi$) and to its total ampere-conductors $(I_a/a)Z$. For a given machine $0.1174 \times 10^{-8}(p/a)Z$ is a constant so that

$$T = C_2 \Phi I_a = 7.04 C_1 \Phi I_a \tag{4–7}$$

The foregoing derivation of the torque is based on the assumption that the conductors lie directly in the pole-flux (smooth armature). In the actual machine the conductors are placed in slots. The pole flux takes its path mainly through the teeth, and the flux density in the slots, where the con-

ductors lie, is small. Despite this fact, Eq. 4–6 yields correct results for the torque. For further information see Chap. 14.

Notice that the (developed) torque can be calculated also from the electromagnetic power. It follows from Eqs. 1–26 and 1–28

$$T = \frac{7.04}{n} EI_a \text{ lb-ft} \tag{4–8}$$

This equation also can be obtained from Eq. 4–6 by substituting for $\Phi$ the value which follows from Eq. 4–3.

## PROBLEMS

**1.** If the average induced emf per conductor in Problem 1, Chap. 3, is 2 volts, what will be the terminal voltage?

**2.** If the average induced emf per conductor in Problem 3, Chap. 3, is 2 volts, what will be the terminal voltage? What is the voltage per winding element?

**3.** If the average induced emf per conductor in Problem 6, Chap. 3 is 2 volts, what will be the terminal voltage? What is the voltage per winding element?

**4.** The armature of a 6-pole machine has 72 slots with 6 conductors per slot connected in a simple lap winding. If the machine has a flux per pole of $2.78 \times 10^6$ lines, and operates at 1200 rpm, what will be the induced voltage?

**5.** If the machine of Problem 4 were reconnected as a simple wave winding, what would be the terminal voltage?

**6.** What will be the ratio of the armature current in Problem 4 to that in Problem 5?

**7.** A 500-kw, 250-volt, 4-pole, 900-rpm shunt generator has a 2-layer lap winding with 90 slots and one turn per winding element. The flux per pole is $\Phi = 4.65 \times 10^6$ maxwells. If the voltage is 250 volts at 900 rpm, determine the number of conductors per slot that are necessary. How many commutator bars are used?

**8.** A 230-volt, 8-pole, 514-rpm shunt generator has 100 slots and $\Phi = 3.36 \times 10^6$ maxwells. Each slot contains eight conductors and the winding is 2-layer with one turn per winding element. What type of winding is used and what are the pitches.

**9.** A 220-volt, 4-pole, 900-rpm shunt generator has a 2-layer lap winding with 99 slots and two conductors per slot. The pole flux is $\Phi = 3.7 \times 10^6$ maxwells. Determine the type of winding used to produce 220 volts at no-load, the number of commutator bars, and the front and back pitches.

**10.** A 4-pole shunt generator is to produce a voltage of 220 volts at 1750 rpm. The armature has a 2-layer wave winding placed in 35 slots with 10 conductors per slot. Determine the flux per pole.

**11.** A d-c generator has the following data: effective armature length 6.26 in., effective pole arc 8.1 in., air gap flux density = 5300 lines per sq. in., 8 poles, 72 slots, 6 conductors per slot and a 2-layer lap winding. Determine the torque developed for an armature current of 500 amp.

**12.** Determine the electromagnetic torque developed by the generator of Problem 11 for an armature current of 1000 amp and a pole-flux $\Phi = 2 \times 10^6$ maxwells.

**13.** A 4-pole generator with a simplex wave winding operates at 250 rpm and

delivers 250 amp at 550 volts. Assume an armature resistance drop of 3%. Determine the electromagnetic torque developed.

**14.** Determine the electromagnetic torque developed by a 6-pole d-c machine with 360 conductors arranged in a lap winding. The conductor current is 75 amp, and the flux per pole is $3.0 \times 10^6$ maxwells.

**15.** If the armature current of the machine in Problem 4 is 1042 amp, what is the electromagnetic torque?

# *Chapter 5*

## THE MAGNETIC CIRCUIT

### (Application of Ampère's Law)

The d-c machine has 2 basic windings: the field winding which is placed on the poles, and the armature winding. When both windings carry current, as is the case when the armature is loaded, the flux of the machine is determined by the resultant magnetomotive force (mmf) of both windings. When the armature is not loaded, the flux is determined only by the field winding. This latter case will be considered first.

**5–1. The Magnetic Circuit of the D-c Machine at No-Load.** Figs. 2–1 and 2–2 show a 2-pole and a 6-pole machine, respectively, with their magnetic circuits. The magnetic flux of each pole has its path through the stator yoke, pole body, air gap between pole body and armature, armature teeth, armature core, then back through the armature teeth, air gap, and pole body to the stator yoke. This closed magnetic circuit passes twice through the air gap, teeth, and pole body. The pole flux is divided into two parts in the stator yoke as well as in the armature core.

The emf to be induced in the armature winding is known: it is approximately equal to the terminal voltage (see Art. 7–1). Then if the magnitude of the emf is known for a given machine, the flux is also known: it is determined by Eq. 4–3. *A certain mmf is necessary to drive this flux through the magnetic circuit of the machine.* The determination of the magnitude of this mmf, i.e., of the ampere-turns to be placed on the poles, is the object of this article.

The fundamental law which connects magnetic flux and mmf is Ampère's law, Eq. 1–18. If this law is applied in the form of Eqs. 1–21 and 1–22, it is seen that the sum in the equation

$$\Phi \Sigma \frac{l}{\mu A} = 0.4\pi NI \tag{5–1}$$

has to be extended over five terms in each of which the permeability $\mu$, the length of the magnetic path $l$, and the cross-section $A$ are different. The flux density $B$ is usually different for the stator yoke, pole body, armature teeth, and armature core; therefore $\mu$ is also different for these parts of the

magnetic circuit; for the air gap, $\mu$ is equal to 1. Thus Eq. 5–1 can be written in the form

$$\Phi\left(\frac{l_y}{\mu_y A_y}+\frac{2l_p}{\mu_p A_p}+\frac{2g}{A_g}+\frac{2l_t}{\mu_t A_t}+\frac{l_c}{\mu_c A_c}\right)=0.4\pi NI \qquad (5\text{–}2)$$

where $l_p$, $g$, and $l_t$ are lengths of the path for 1 pole, 1 air gap, and 1 armature tooth. It follows from Eqs. 1–20 and 5–2

$$\frac{B_y}{0.4\pi\mu_y}l_y+2\frac{B_p}{0.4\pi\mu_p}l_p+2\frac{B_g}{0.4\pi}g+2\frac{B_t}{0.4\pi\mu_t}l_t+\frac{B_c}{0.4\pi\mu_c}l_c=NI \qquad (5\text{–}3)$$

$$H_y l_y+2H_p l_p+2H_g g+2H_t l_t+H_c l_c=NI \qquad (5\text{–}4)$$

$H$ is the ampere-turns per unit length. Eq. 5–4 states that, in order to find the total ampere-turns $NI$ necessary to force the flux through the structure, the ampere-turns for each of the five components are to be determined separately and then added up.

Eq. 5–2 to 5–4 describe how to determine the five ampere-turn components. First divide the flux $\Phi$ by the cross-section area of each of the five parts, in order to determine the five values of $B$ to be used in Eq. 5–3. Then determine from the saturation curves of the iron used for the yoke, pole body, and armature, the values of $H=B/0.4\pi\mu$ (in ampere-turns per unit length) which correspond to the values of $B$ given by Eq. 5–3. Finally, multiply the values of $H$ found from the saturation curves by $l$, their path lengths, and add the five components. This yields the field (pole) mmf of one complete magnetic circuit. A 2-pole machine has only one magnetic circuit, and the $NI$ ampere-turns are placed half on each pole. A multipole machine has $p/2$ magnetic circuits, and the total number of necessary ampere-turns is $p/2$ times the ampere-turns necessary for one circuit.

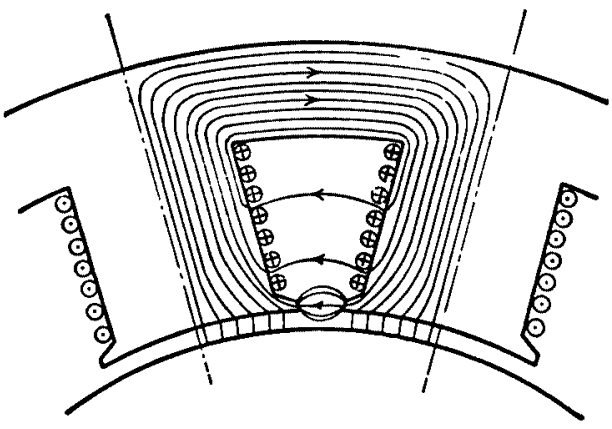

FIG. 5–1. Main flux and leakage flux.

The term $2(B_g/0.4\pi)g=2H_g g$ which represents the ampere-turns necessary to drive the flux $\Phi$ through the two air gaps is the largest of the five terms. Its magnitude is from 65% to 80% of the total $NI$.

The flux $\Phi$ in Eqs. 4–3, 5–1, and 5–2 is the flux which is necessary to induce the emf $E$ of Eq. 4–3 in the armature winding, i.e., the flux which crosses the gap and goes through the teeth into the armature where it is *interlinked with the armature winding*. The flux which goes through the pole and stator yoke is larger than this flux $\Phi$, owing to leakage. Fig. 5–1 shows the flux distribution between two poles. It is seen that some of the lines of force go from pole tip to pole tip and from pole body to pole body without

passing through the gap and armature. These lines of force are not interlinked with the armature winding and do not contribute to the armature emf; they represent a *leakage* flux.

The pole-leakage flux is not negligible: it can be as high as 15 to 25% of the useful flux $\Phi$. Therefore, it is not correct to assume the flux to be the same, namely, equal to $\Phi$, for all five parts of the magnetic circuit, as is done in Eqs. 5–1 and 5–2. The flux densities in the yoke and pole, $B_y$ and $B_p$, should be calculated with (1.15 to 1.25) $\times \Phi$. The calculation of the field ampere-turns $NI$ will now be demonstrated by an example.

**Example 5–1.** As an example, a 250-kw, 6-pole, 240-volt, 1200-rpm generator will be considered. The dimensions of this generator, in inches, are listed below: (also see Fig. 5–2).

| | | | |
|---|---|---|---|
| Outside diameter of armature core | $D = 22.5$ | Pole length | $l_p = 7.0$ |
| Inside diameter of armature core | $d_i = 12.5$ | Pole width | 6.0 |
| Gross core length | $L = 7.0$ | Frame $ID$ | $37\frac{11}{16}$ |
| Number of radial vents | $n_v = 2$ | Frame $OD$ | $42\frac{7}{16}$ |
| Width of each vent | $b_v = \frac{3}{8}$ | Frame width | 10 |
| Net length of core $l = 7 - 2 \times \frac{3}{8}$ | 6.25 | No. of arm. slots | 72 |
| Single air gap | $g = 0.218$ | Slot depth | 2.0 |
| Pole embrace (arc) | $b_p = 7.65$ | Slot width | 0.36 |

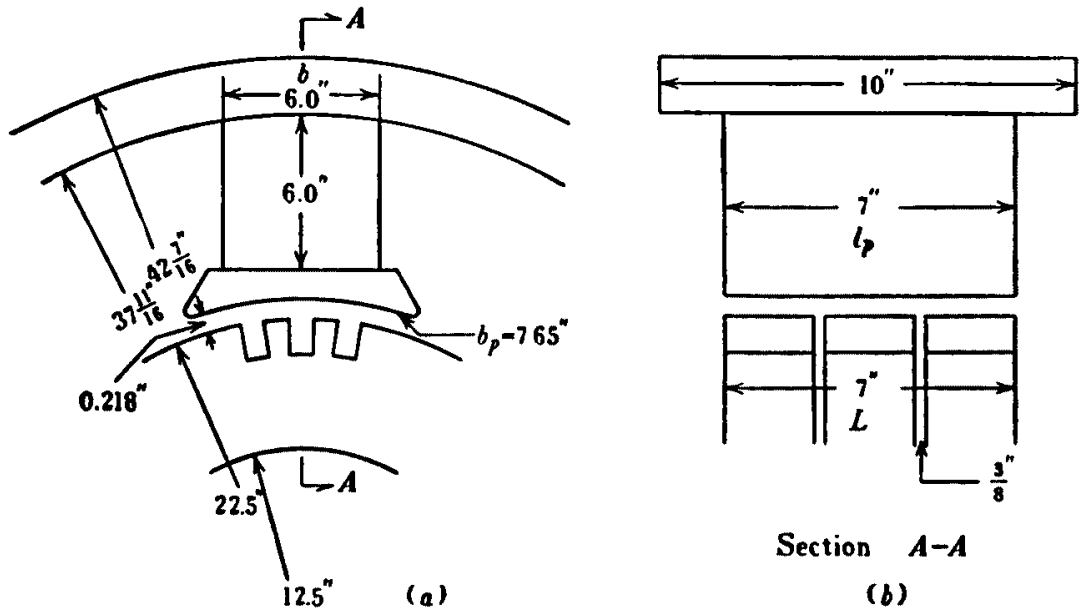


FIG. 5–2. Example—machine dimensions.

Electrical steel is used for the armature. USS hot-rolled steel is used for the poles and frame. The $B$-$H$ curves of these materials are given at the end of this text.

(a) *Flux per pole.* The armature has a lap winding and, therefore, $a = p = 6$. Each slot has six conductors, three per layer. The total number of conductors is, then, $Z = 6 \times 72 = 432$. According to Eq. 4–3, the flux necessary to induce an emf of 240 volts at no-load in the armature winding is

$$\Phi = \frac{240 \times 10^8}{432} \times \frac{60}{1200} \times \frac{6}{6} = 2.78 \times 10^6 \text{ maxwells}$$

(b) Ampere-turns necessary to drive the pole flux through the two gaps.

It has been mentioned that the ampere-turns necessary to drive the flux $\Phi$ through the air-gap is the largest of the 5 components. Therefore, the area of the gap $A_g$ must be determined with satisfactory accuracy.

Setting

$$A_g = l_e b_e \tag{5–5}$$

and

$$B_g = \frac{\Phi}{l_e b_e} \tag{5–6}$$

the *effective armature length* $l_e$ and the *effective pole arc* $b_e$ are obtained from the following considerations.

It has been explained in Chap. 2 (Fig. 2–5) that the laminated core of the armature of medium size and larger machines is divided into several stacks by radial vents. The flux density in the vents is much smaller than that in the gap between pole and armature iron (Fig. 5–3a). The *effective* armature length $l_e$ is, therefore, smaller than the gross core length $L$ and larger than the net core length $l = L - n_v b_v$. A more accurate method for calculating $l_e$ is given in Chap. 16. It will be assumed here that $l_e = (L + l)/2$.

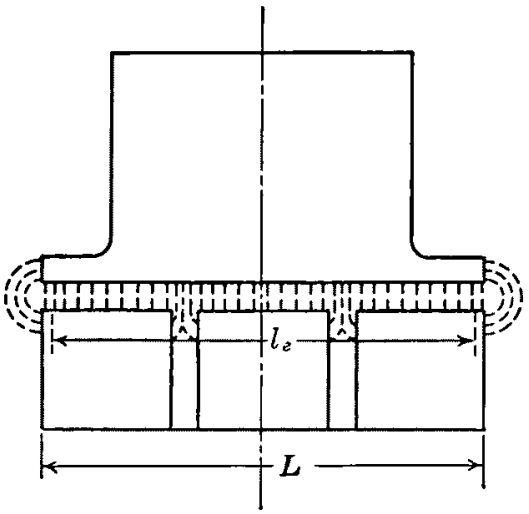


FIG. 5–3a. Determination of the equivalent armature length.

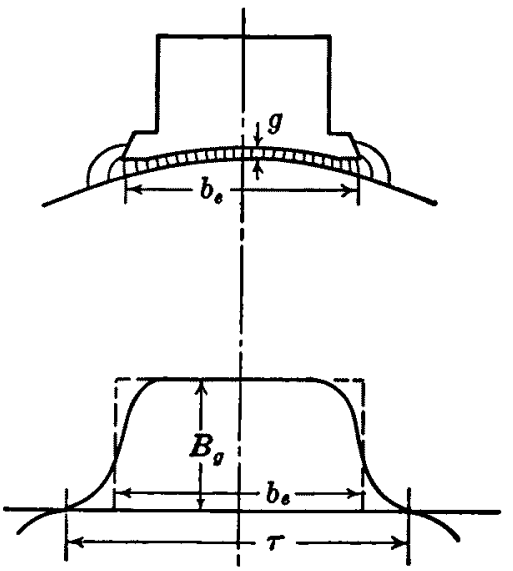


FIG. 5–3b. Field-distribution curve of a d-c machine.

Because of fringing on both sides of the pole shoe (Fig. 5–3b) the *effective* pole arc $b_e$ is larger than the actual pole arc $b_p$. It can be assumed that $b_e = b_p + 2g$. Thus

$$l_e = \frac{7 + 6.25}{2} = 6.62 \text{ in.}$$

$$b_e = 7.65 + (2 \times 0.218) = 8.1 \text{ in.}$$

and

$$B_g = \frac{\Phi}{A_g} = \frac{2.78 \times 10^6}{6.62 \times 8.1} = 51{,}800 \text{ lines/in.}^2$$

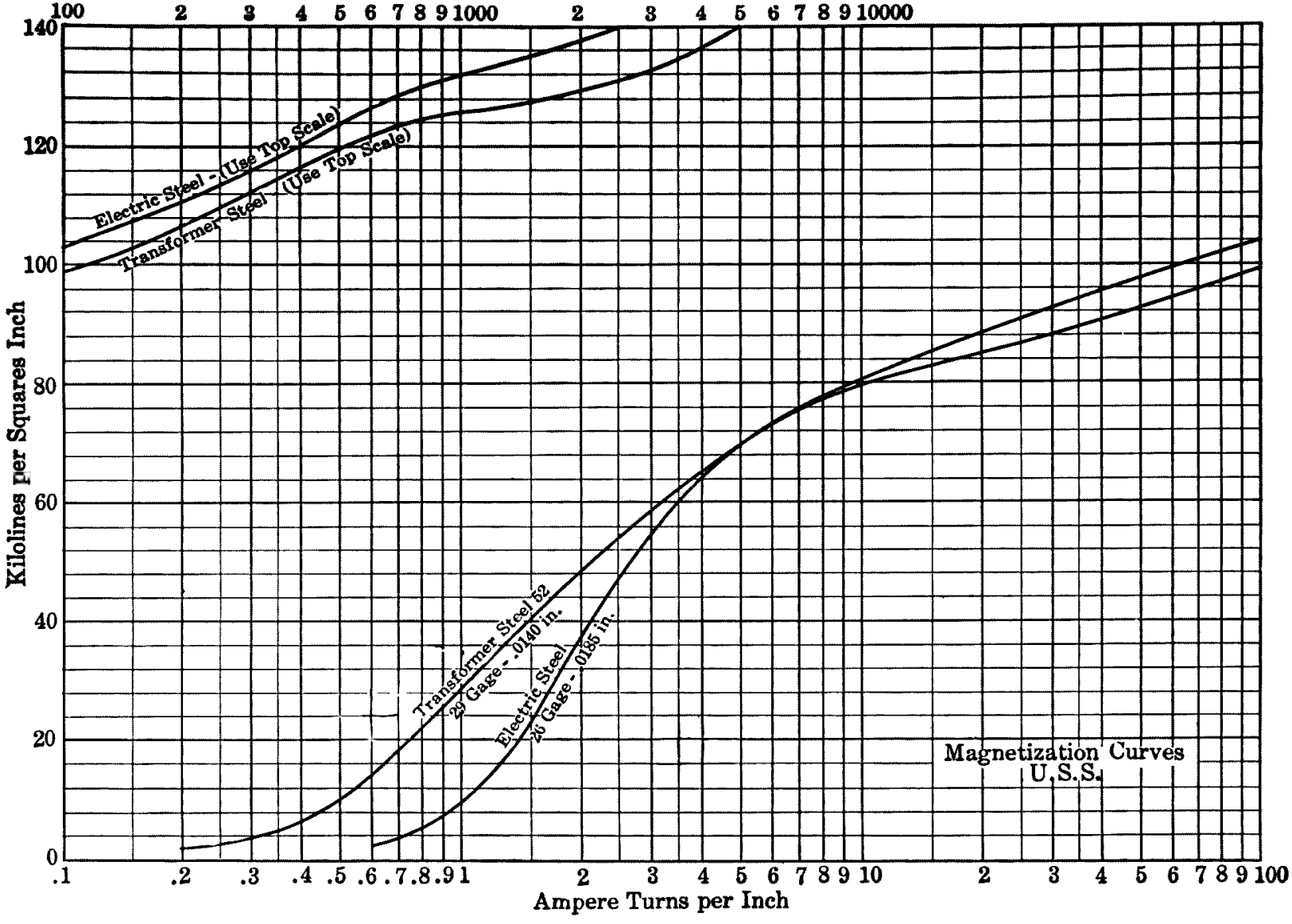


FIG. 5-2a. Magnetization curves for transformer steel and dynamo steel.

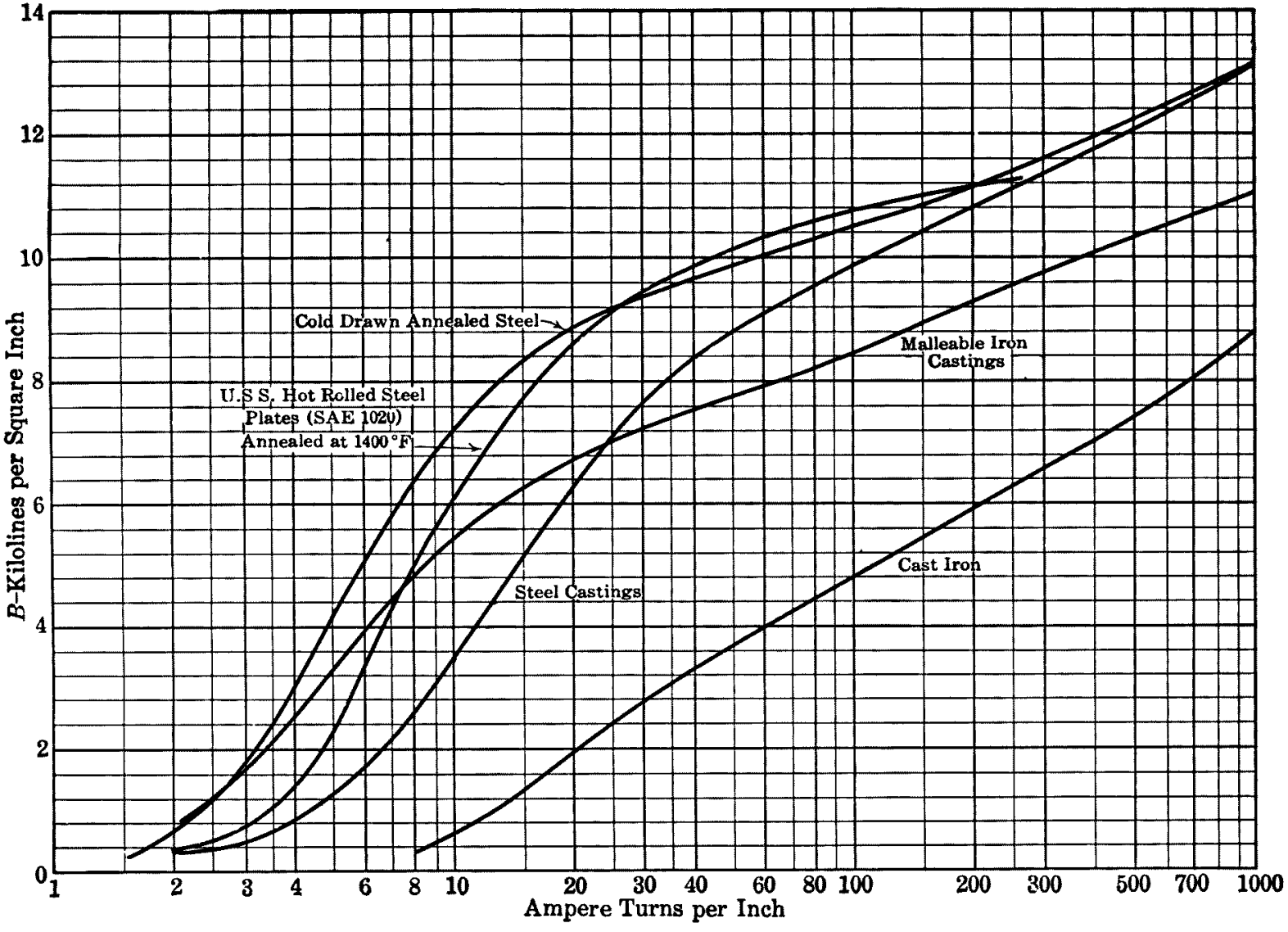


FIG. 5-2b. Magnetization curves for cast iron, steel castings, cold-drawn annealed steel, and hot-rolled steel.

The ampere-turns for two gaps (see Eq. 5–3) are:

$$AT_g = \frac{51{,}800}{0.4\pi \times (2.54)^2} \times 2 \times 0.218 \times 2.54 \times 1.10 = 7780 \text{ AT}$$

2.54 is the conversion factor from inches to centimeters. The last factor 1.10 takes into account the fact that the gap appears increased at the points opposite the slots, so that the effective air gap is larger than 0.218 in.

(c) *Ampere-turns for the teeth.* The pole flux $\Phi$ goes into the armature through the teeth lying within the pole arc $b_e = 8.1$ in. The pole pitch is

$$\tau = \frac{\pi D}{6} = \frac{\pi \times 22.5}{6} = 11.8 \text{ in.}$$

Thus the pole flux $\Phi$ goes through $\frac{72}{6} \times \frac{8.1}{11.8}$ teeth. The width of a tooth in the middle of the tooth is equal to 0.534 in. The iron length of the core is somewhat smaller than the net core length $l = 6.25$ in., because of the insulation between the laminations. Assuming a loss due to insulation of 8%, the cross-section of the teeth per pole is

$$A_t = \frac{72}{6} \times \frac{8.1}{11.8} \times 0.534 \times 6.25 \times 0.92 = 25.3 \text{ in.}^2$$

and

$$B_t = \frac{\Phi}{A_t} = \frac{2.78 \times 10^6}{25.3} = 111{,}000 \text{ lines/in.}^2$$

The *B-H* curve for electrical steel yields for $B = 110{,}000$ lines/in.$^2$ 180 AT per in. The length of the magnetic path in a tooth is equal to 2 in. (=slot depth). Thus the AT necessary to drive the flux through the teeth twice is

$$AT_t = 2 \times 2 \times 180 = 720 \text{ AT}$$

(d) *Ampere-turns for the armature core.* The height of the armature core below the teeth is equal to $\frac{22.5 - 12.5}{2} - 2 = 3.0$ in. The iron length of the core is the same as that of the teeth, i.e., $6.25 \times 0.92$ in. The cross-section of the core is thus

$$(3 \times 6.25 \times 0.92)$$

sq. in. Since the pole flux $\Phi$ divides into two parts within the core

$$B_c = \frac{2.78 \times 10^6}{2 \times 3 \times 6.25 \times 0.92} = 80{,}600 \text{ lines/in.}^2$$

The *B-H* curve for electrical steel yields, for $B = 80{,}600$ lines, 10 AT per in. The length of the path in the core is equal to the pole pitch in the middle of the core, i.e., to

$$\frac{\pi(d_i + h_c)}{p} = \frac{\pi(12.5 + 3.0)}{6} = 8.1 \text{ in.}$$

Thus the ampere-turns necessary to drive the flux through the core are

$$AT_c = 10 \times 8.1 = 81 \text{ AT}$$

(e) *Ampere-turns for the poles.* It will be assumed that the leakage flux between the poles shoes and pole bodies is equal to 20% of the armature flux. Therefore, the flux through the pole and the yoke is

$$\Phi_p = 1.2 \times 2.78 \times 10^6 = 3.34 \times 10^6 \text{ maxwells}$$

The pole laminations are not insulated. The loss of iron thickness due to air layers between the laminations can be assumed 5%. The cross-section of a pole is, therefore, equal to $(0.95 \times 7 \times 6)$ sq. in. (see Fig. 5–2), and the flux density in the pole is

$$B_p = \frac{3.34 \times 10^6}{0.95 \times 7 \times 6} = 83{,}600 \text{ lines/in.}^2$$

The *B-H* curve for USS hot-rolled steel yields, for $B = 83{,}600$ lines, 18 AT per in. The length of the path in the pole is assumed equal to the height of the pole without pole shoe (the flux density is low in the pole shoe). This length is equal to 6.0 in., and thus the ampere-turns necessary for two poles are

$$\text{AT}_p = 2 \times 18 \times 6.0 = 216 \text{ AT}$$

(f) *Ampere-turns for the yoke (frame).* The height of the yoke is

$$\frac{(42\frac{7}{16} - 37\frac{11}{16})}{2} = 2\tfrac{3}{8} \text{ in.}$$

The yoke is of solid steel. Thus the flux density in the yoke is

$$B_y = \frac{3.34 \times 10^6}{2 \times 2.375 \times 10} = 70{,}000 \text{ lines/in.}^2$$

The *B-H* curve for USS hot-rolled steel yields, for $B = 70{,}000$ lines, 13.0 AT per in. The length of the magnetic path in the yoke is $\frac{\pi(42\frac{7}{16} - 2\frac{3}{8})}{6} = 20.9$ in., and the ampere-turns necessary to drive the flux through the yoke are

$$\text{AT}_y = 13 \times 20.9 = 270 \text{ AT}$$

(g) *Total ampere-turns.* The ampere-turns for two poles (for one magnetic circuit) are

$$\begin{aligned}\text{AT}_{\text{cir}} &= \text{AT}_y + \text{AT}_p + \text{AT}_g + \text{AT}_t + \text{AT}_c \\ &= 270 + 216 + 7780 + 720 + 81 = 9067 \text{ AT}\end{aligned}$$

and for all six poles (all three magnetic circuits)

$$\text{AT}_{\text{total}} = 3 \times 9067 = 27{,}200 \text{ AT}$$

It does not matter whether these AT are produced by a large number of turns on the poles and a small current in the conductors or by a small number of turns and a large current in the conductors. It is necessary, however, that the product of the number of turns and the current in the conductors is equal to the required number of ampere-turns. The machine considered has 1064 turns per pole. Therefore, the field current necessary to drive the flux $\Phi = 2.78 \times 10^6$ maxwells through the magnetic path is

$$I_f = \frac{9067}{2 \times 1064} = \frac{27{,}200}{6 \times 1064} = 4.25 \text{ amp}$$

A more accurate method for calculating the field AT at no-load is given in Chap. 16.

**5–2. No-load Characteristic.** If the field AT are calculated for several values of the armature flux $\Phi$ and the flux $\Phi$ is plotted against the field AT, a curve is obtained which is similar to the *B-H* curve of iron. Fig. 5–4 shows such a curve which is called the *no-load characteristic* or magnetization curve. The emf $E$ induced in the armature or the flux density in the air gap $B_g$ can be plotted along the axis of ordinates instead of $\Phi$, since both these quantities are proportional to $\Phi$ for a given machine at constant speed (see Eq. 4–3). Along the axis of abscissae, either the total field AT, or the field AT per circuit, or the field AT per pole (half of the AT of a circuit), or only the field current $I_f$ can be plotted, since all of these quantities are proportional to each other for a given machine.

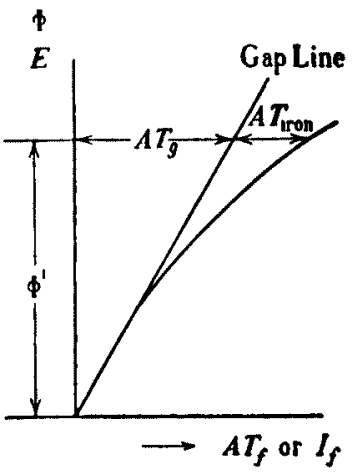


FIG. 5–4. No-load characteristic and air-gap line.

The lower part of the no-load characteristic, Fig. 5–4, follows practically a straight line. This is due to the fact that, at small values of $\Phi$, the AT necessary for the four iron parts of the magnetic circuit are negligible in comparison to those necessary for the air gap. As the flux $\Phi$ becomes larger, the iron AT increase and the no-load characteristic bends to the right of the air-gap line. In Fig. 5–4 the AT necessary for the air gap and the AT necessary for the iron are indicated for one value $\Phi'$ of the flux.

It has been assumed in the considerations of this article and also of Art. 5–1 that the armature conductors do not carry current, i.e., that the armature is not loaded (this explains the name "no-load characteristic").

**5–3. Mmf of the Armature Winding.** It will now be assumed that only the armature winding carries current. Fig. 5–5 shows a developed d-c machine. A generator with conductors moving to the right will have the current direction assumed in this figure. A line of force symmetrical with respect to the interpolar space, as indicated by the line $a'a'$, cannot be produced by the armature since the resultant mmf for this line of force is zero. On the other hand, a line of force symmetrical to the pole axis (line of force $aa$) can be produced by the armature. The mmf of the armature winding for the lines of force symmetrical to the pole axis increases with the distance $x$ from the pole axis. Therefore, if a finely distributed winding is assumed, the mmf of the armature winding will have triangular shape (Fig. 5–5b) with the zero points in the pole axes and the maxima in the axes of the interpolar spaces.

Fig. 5–5b applies to the mmf curve only. The field curve, i.e., the flux density as a function of distance $x$, is determined by the mmf curve and the magnetic reluctance for the different tubes of force. Since the magnetic reluctance is very high in the interpolar space, the flux density there will be

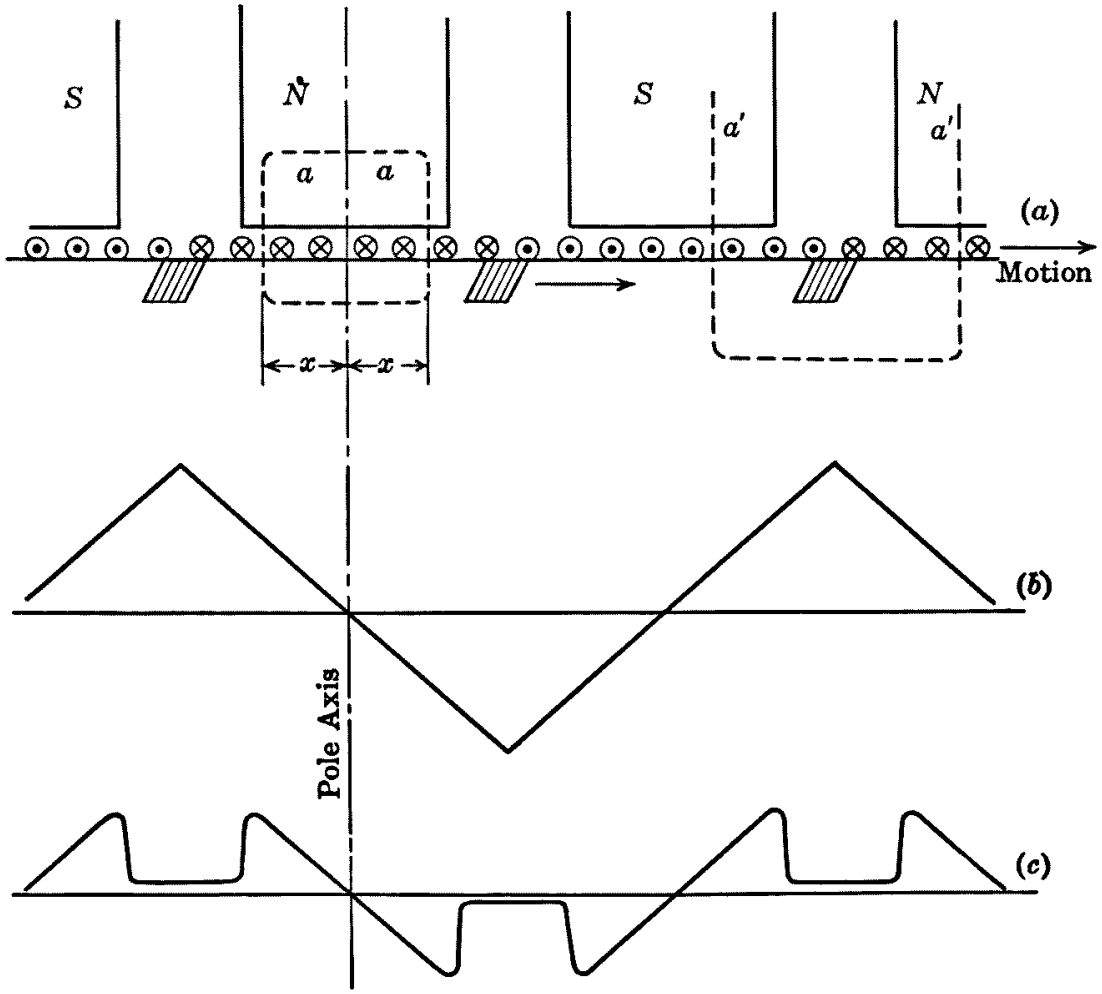


FIG. 5–5. Mmf and field curve of a d-c machine with a finely distributed winding.

very small. The approximate shape of the field curve which corresponds to the mmf curve in Fig. 5–5b is shown in Fig. 5–5c.

The smooth triangular curve for the mmf (Fig. 5–5b) was obtained under the assumption of a finely distributed winding. Usually the conductors are located in slots and the mmf changes from slot to slot by a certain amount. If the assumption is made that the change occurs abruptly in the middle of the slot, the shape of the mmf curve becomes *stepped*. Fig. 5–6 shows such a curve.

In Fig. 5–5 it is assumed that the brushes are in the neutral axis. If the brushes are shifted from the neutral axis, the *shape* of the mmf curve (Fig. 5–5b) will not be changed, but its zero and maximum points will not coincide with the pole axes and the axes of the interpolar spaces. The shape of the field curve, therefore, will be different from that in Fig. 5–5c. This follows from the following consideration.

In accordance with Faraday's law for an induced emf, all conductors lying under north poles will have induced emf's in one direction and all those under south poles will have their induced emf's in the opposite direction. If the brushes lie in the neutral axis, the same rule applies also to the currents;

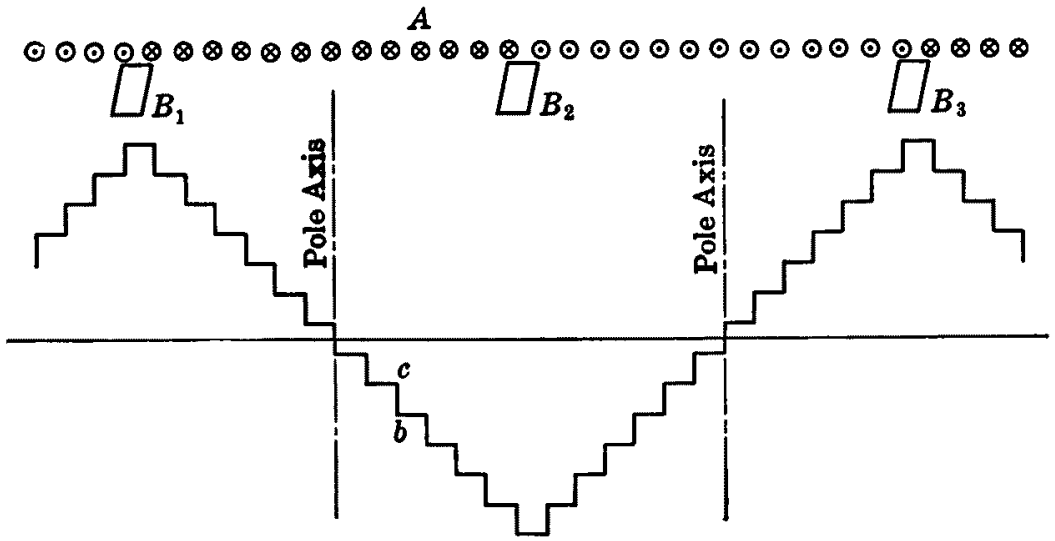


FIG. 5–6. Stepped mmf curve of a d-c machine.

thus, considering Fig. 5–7, all conductors above (or below) the neutral axis have currents in the same direction. If the brushes are shifted from the neutral axis, as shown in Fig. 5–8, the rule dictated by Faraday's law for the emf's

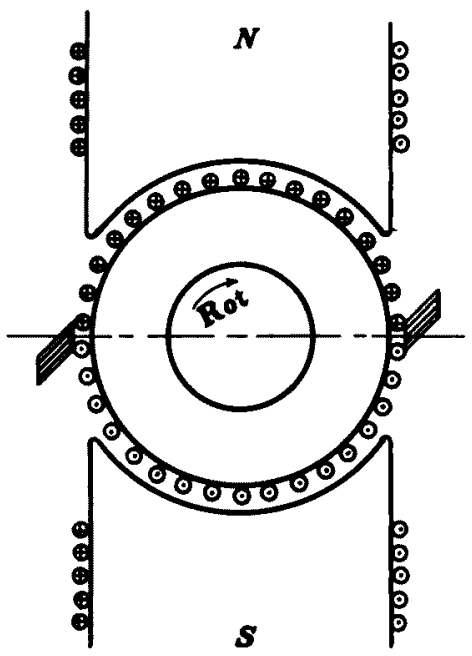


FIG. 5–7. Current distribution in a 2-pole generator with brushes in the neutral.

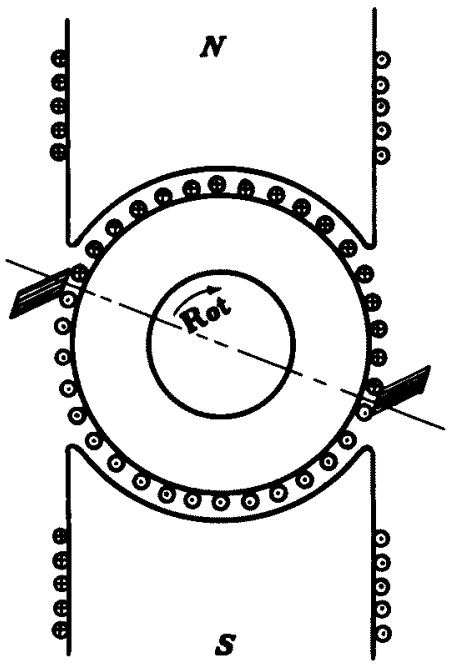


FIG. 5–8. Current distribution in a 2-pole generator with brushes shifted from the neutral.

no longer holds for the currents. This is due to the fact that *the brushes* determine, and are the *connection points between, the parallel circuits*. Since the current direction is the same for all conductors within any one of the parallel circuits, all conductors lying above (or below) the brush axis (*BB* in

Fig. 5–8) must have currents of the same direction, i.e., it is *the brush axis which determines the direction of the currents in the conductors.* Comparing Fig. 5–8 with 5–7, we see that, because of the brush shift, some conductors carry a current the direction of which is opposite to the direction of their induced emf. If now the mmf-curve of the armature winding is drawn for the current distribution of Fig. 5–8, the peaks of the triangles (*the axes of the armature mmf*) do not lie in the neutral axes, as in Fig. 5–5b, but at the points where the brushes lie.

Considering Figs. 5–7 and 5–8, the armature behaves magnetically like a solenoid with turns of varying enclosed area, the area being the smallest close to the brushes. The axis of this solenoid, i.e., *the axis of the armature mmf, coincides with the brush axis.*

**5–4. Field and Armature Both Carry Current. Armature Reaction.** When the armature is loaded, the flux distribution is determined by the mmf's of the field *and* armature winding and is different from that at no-load. The effect of the armature mmf upon the flux distribution due to the field winding alone is called *armature reaction.*

(a) *Cross-magnetizing Effect of the Armature.* Fig. 5–9 shows the flux distribution of a 2-pole generator when only the field winding carries current. Fig. 5–10 shows the flux distribution when only the armature carries current

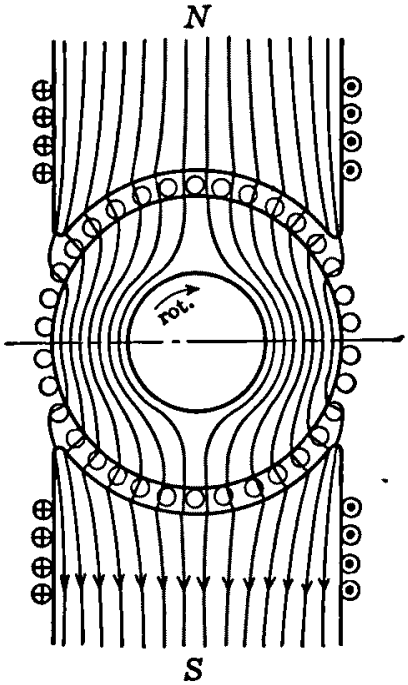


Fig. 5–9. Flux distribution when only the main poles are excited.

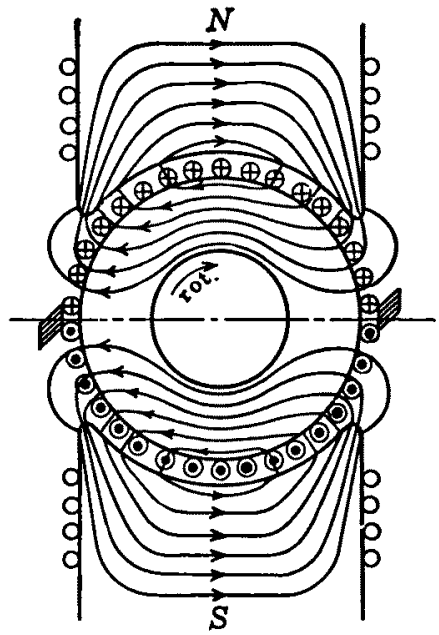


Fig. 5–10. Flux distribution when only the armature is excited.

and the brushes are in the neutral axis. The armature flux is a *cross* flux with respect to the main (field) flux. It can be further seen that the armature mmf

strengthens one half of a pole and weakens the other half. When the iron is saturated, the effect of the armature mmf in weakening one pole half is greater than the effect of this mmf in strengthening the other pole half. The result is a reduction in the main flux.

Fig. 5–10 shows that in a generator the armature cross flux weakens the leading pole half and strengthens the trailing pole half. In a motor where the current and induced emf are in opposite directions the inverse is true. Moreover, the armature mmf not only weakens the pole flux and the air-gap flux but also *distorts* them and causes a *displacement of the neutral zone*. This is shown in Fig. 5–11 which is obtained by superposition of

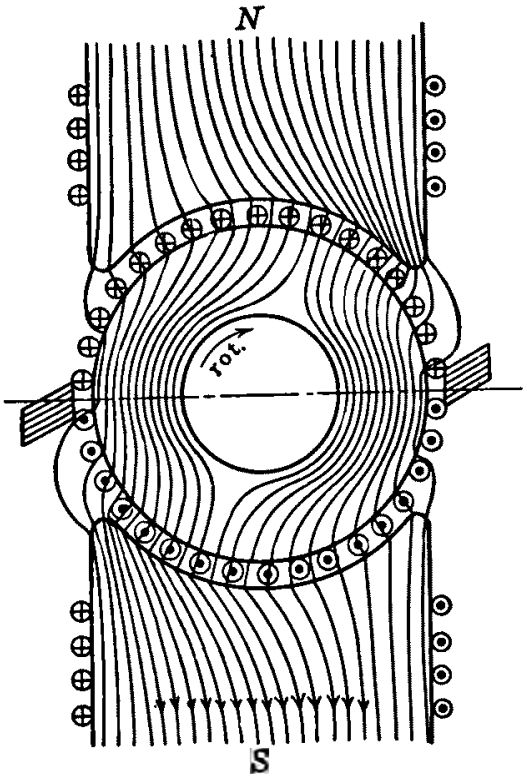


FIG. 5–11. Flux distribution under load.

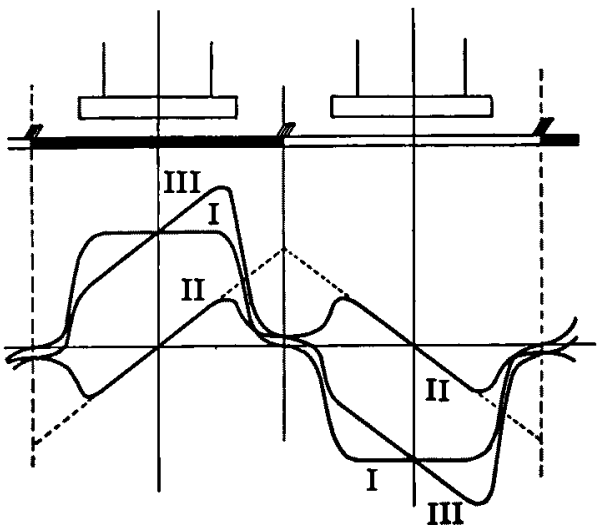


FIG. 5–12. Field curve at load. Brushes in the neutral.

Figs. 5–9 and 5–10. In a generator the neutral zone is displaced in the direction of rotation, while in a motor it is displaced in a direction opposite to that of rotation. It will be shown that this is significant in the consideration of commutation. In a machine without interpoles the neutral axis of the field coincides with the perpendicular to the pole axis *only* at no-load.

The armature cross flux produces a non-uniform distribution of the pole flux and, as a result, the air-gap flux density under one pole half is greater than that under the other pole half. As a result of this non-uniform distribution, the instantaneous emf induced in the coils while they are in the field of greatest flux density may become high enough to cause a spark to take place

between the commutator bars in which the coil terminates, and may ultimately lead to ring fire (flash-over).

It has been shown in Art. 5–3 that the mmf curve of a d-c armature winding is triangular. If there is low saturation in the armature teeth and in the pole shoe, both mmf's and their fluxes can be considered separately. The armature flux distribution is then a straight line under the pole and a saddle-shaped curve in the interpolar space (see Fig. 5–5c). The flux distribution curve due to the field pole mmf alone is trapezoidal. Fig. 5–12 represents schematically 2 poles and a part of the armature winding of a multipolar machine. The current directions of consecutive armature paths are different and are indicated by black or white areas. The brushes are in the neutral axis. The lower part of the figure shows the pole flux distribution (curve I), the armature flux distribution (curve II), and the resultant flux distribution (curve III). This latter curve is distorted in shape when compared with that at no-load (curve I). Since low saturation of the iron is assumed, the armature flux is symmetrical with respect to the axis of abscissa and the area under curve III is equal to the area under curve I; that is, the magnitude of the air gap flux, which is proportional to the area of the flux distribution curve, remains the same under load as at no-load.

If the armature teeth and pole shoes are saturated, the area of the part of curve III which lies above curve I will be *less* than that lying below curve I (Fig. 5–12) and as a result of armature reaction, the resultant air gap flux under load will be less than that at no-load.

(b) *Demagnetizing Effect of the Armature.* The armature reaction is much greater when the brushes are displaced from the neutral axis, as is sometimes done (see Art. 9–5). If in Fig. 5–13 a line *GG* is drawn at the same angle $\beta$ to the horizontal as that of the brush axis *BB*, the armature conductors are divided into four groups which comprise two solenoids. The two groups lying under the poles constitute a solenoid the axis of which is *perpendicular* to the pole axis. Therefore, its mmf produces a cross flux, the same as that in Fig. 5–10 where the brushes are in the neutral axis. The two remaining groups which lie in the interpolar space constitute a solenoid the axis of which *coincides* with the pole axis. The mmf of this solenoid consequently acts along the same axis as the field winding.

Thus, if the brushes are displaced from the neutral axis, a part of the armature conductors produces cross magnetization and the remaining conductors produce an mmf the effect of which acts along the pole axis. This latter action may either oppose or aid the mmf of the field winding and consequently alter the flux $\Phi$. Fig. 5–13 represents a generator in which the brushes are displaced in the direction of rotation, producing a demagnetizing armature mmf and a consequent reduction in the flux.

In general, *if the brushes of a generator are displaced in the direction of rotation or if the brushes of a motor are displaced opposite to rotation, the flux is weakened.* Displacing the brushes of a generator opposite to the direction of

rotation and displacing those of a motor in the direction of rotation strengthens the flux.

It will be shown later that, with regard to the commutation, strengthening the flux by shifting the brushes of a generator opposite to the direction of rotation and shifting those of a motor in the direction of rotation is not permissible. If, in order to improve the commutation, the brushes are displaced from the neutral axis, then the shift is in the direction of rotation in the generator and opposite to the direction of rotation in the motor, in both cases weakening the flux.

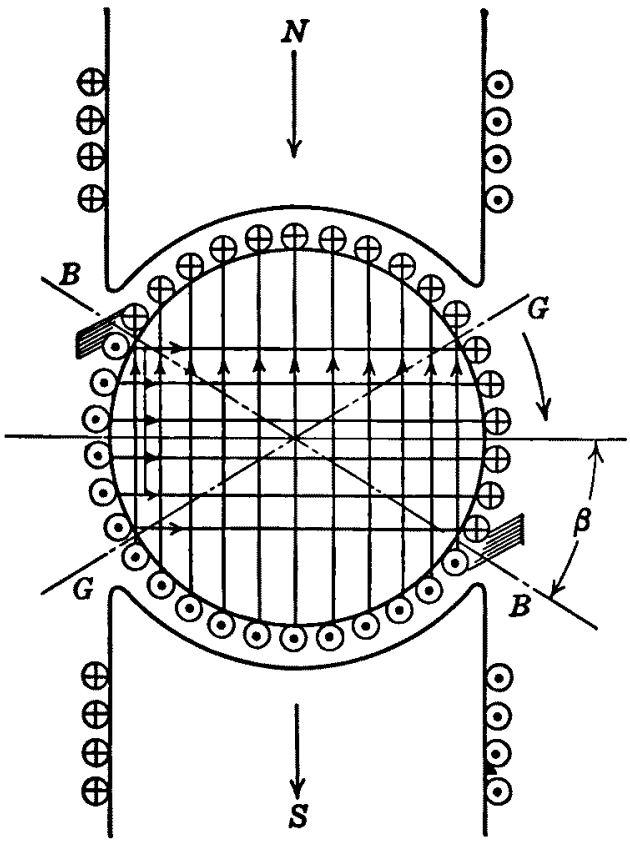


FIG. 5–13. Armature reaction with brushes shifted from the neutral axis.

Fig. 5–14 shows the pole-flux distribution (curve I), armature flux distribution (curve II), and resultant flux distribution (curve III), of a machine with the brushes displaced from the neutral axis, as just considered in the foregoing.

(c) *Calculation of the Field Mmf Under Load.* If the terminal voltage of a d-c generator under load is to be the same as that at no-load, the field current must be increased because of the demagnetizing effect of the armature mmf and the voltage drop in the windings (see Art. 7–3). The amount by which the field current must be increased to take care of the armature cross flux will be determined first.

It is evident from Figs. 5–10 and 5–13 that only the part of the armature

conductors lying under the pole shoes is of main importance in the determination of the cross flux. The total armature mmf per pair of poles (and, therefore, for a magnetic circuit) is $\tau A$ ampere turns, where $A$ is the number of ampere-conductors per inch of armature circumference $\left(=\frac{ZI/a}{\pi D}\right)$ and $\tau$ is the pole pitch in inches. Of these $\tau A$ ampere turns, the cross-magnetizing effect is produced chiefly by $b_e A$ ampere turns in such a manner that all $b_e A$ ampere turns affect each pole (see Fig. 5–10), i.e., each half-pole is affected by $b_e A/2$ ampere turns. It is to be recalled that $b_e$ is the effective pole arc. (See Example 5–1.)

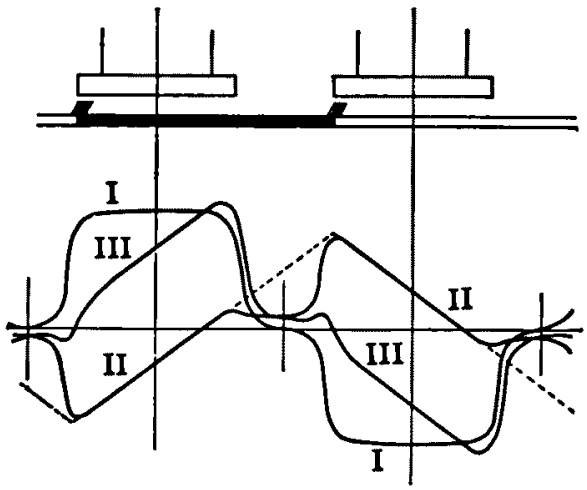


FIG. 5–14. Field curve at load with brushes shifted.

Since the armature mmf affects only a part of the magnetic path of the machine, mainly the air-gap and the armature teeth, $B_g$ is drawn as a function of $(M_g + M_t)$ (Fig. 5–15a), i.e., as a function of the air-gap and tooth mmf *per pole* (half circuit). As explained in Example 5–1

$$B_g = \frac{\Phi}{b_e l_e} \tag{5–6}$$

Thus, if, in Fig. 5–15a, $OC$ is the flux density in the air-gap corresponding to the rated voltage, then $CD$ is the air-gap and tooth mmf per pole at no-load.

At no-load the flux density $B_g$ is constant under the entire pole arc $b_e$ and is equal to $OC$. A picture of the distribution of the air-gap density $B_g$ under load is obtained by laying off the mmf $b_e A/2$ to the right and to the left of the point $D$ in Fig. 5–15a. The distribution of $B_g$ under the pole shoe then is given by the curve $aDb$ (see Fig. 5–12). The point $D$ corresponds to the center of the pole; at this point the armature mmf is zero and the air-gap density is the same as that for zero armature current. Points $a$ and $b$ correspond to the pole edges: for a generator, $a$ is the leading pole edge and $b$ the trailing pole edge; for a motor the reverse condition holds true. The resultant mmf at one pole edge is $CD - b_e A/2$, and at the other $CD + b_e A/2$.

The area $F_1 = Dmb$ is less than the area $F_2 = Dla$: the demagnetizing effect of the one pole half is greater than the magnetizing effect of the other pole half. If the line segment $lm = b_e A$ is shifted to the right, using a pair of dividers, until the area $F_1$ is equal to the area $F_2$ (Fig. 5–15b), then the line segment $DD' = \Delta M_f$ is the increase in the field mmf per pole necessary to compensate for the cross-magnetizing effect of the armature mmf. Therefore, in order to produce the same flux under load as at no-load, the field mmf per pole under load must be $CD'$ instead of $CD$.

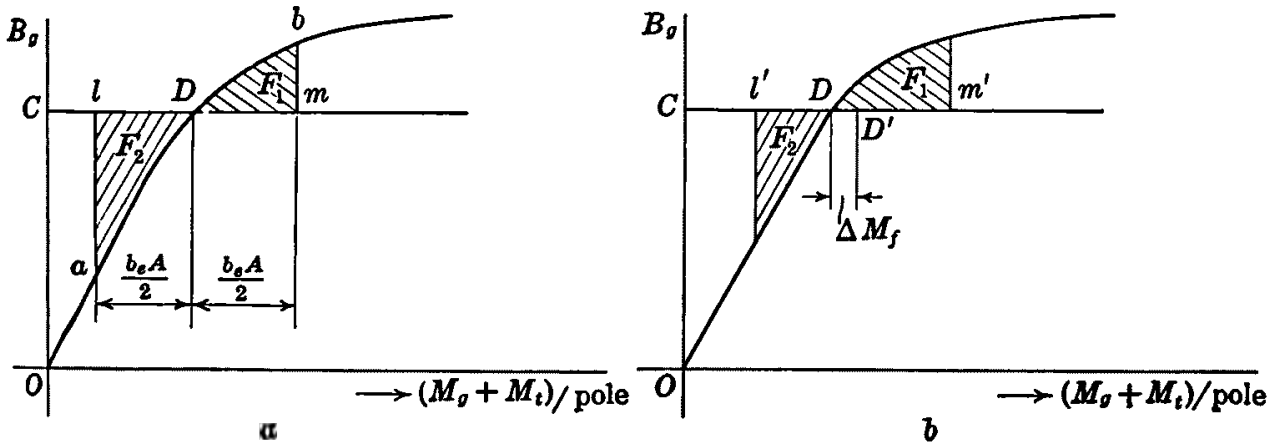


FIG. 5–15. Determination of increase of field mmf necessary to compensate for the cross mmf of the armature.

If the axis of abscissa of Fig. 5–15 is in mmf per pole pair, i.e., if $2(M_g + M_t)$ is taken as the abscissa, the line $lm$ must be made equal to $2b_e A$. $DD'$ is then the increase in field mmf per circuit (pole pair) necessary to compensate for the cross-magnetizing effect of the armature mmf. Knowing the number of turns on the field coils, the increase in field current may be determined.

The increase of the field mmf necessary to compensate for the component of the armature mmf acting along the pole axis, when the brushes are shifted from the neutral axes, can be determined from Fig. 5–13.

If $b_\beta$ is the arc corresponding to the brush-displacement angle $\beta$, then $2b_\beta A$ is the number of demagnetizing ampere turns per pole pair (per circuit). The field mmf per pole pair (per circuit) must be increased by this amount in order to compensate for the demagnetizing effect of the armature mmf along the pole axis.

It has been mentioned that the brushes usually lie in or close to the neutral axis. This means that the arc $b_\beta$ is usually small. In small machines without interpoles, however, it may become considerable.

The influence of armature reaction on the operating characteristics of d-c machines will be taken up later when we consider the different kinds of machines (Chaps. 7 and 8).

## PROBLEMS

Data and machine dimensions are listed below for several d-c machines. Using Fig. 5–2 and Example 5–1 determine the no-load ampere-turns required at 85% and 100% of rated voltage.

| *Problem No.* | 1 | 2 | 3 | 4 |
|---|---|---|---|---|
| Machine | Generator | Generator | Generator | Motor |
| Rating | 7.5 kw | 300 kw | 250 kw | 1 HP |
| Volts | 250 | 230 | 275 | 230 |
| Amperes | 30 | 1305 | 909 | 4.3 |
| Number of poles | 4 | 8 | 6 | 2 |
| Speed (rpm) | 1750 | 514 | 1200 | 1750 |
| Outside diameter of armature core ($D$) | 7.50″ | 38″ | 22.5″ | 4.75″ |
| Inside diameter of armature core ($d_i$) | 3.10″ | 26″ | 12.5″ | 1.20″ |
| Gross core length ($L$) | 5″ | 8″ | 7″ | 3″ |
| Number of radial vents | 0 | 2 | 2 | 0 |
| Width of vents | | $\frac{3}{8}$″ | $\frac{3}{8}$″ | |
| Net core length | 5″ | 7.25″ | 6.25″ | 3″ |
| Air gap (single) ($g$) | 0.078″ | 0.28″ | 0.125″ | 0.04″ |
| Pole embrace (arc) ($b_p$) | 4.20″ | 9.75″ | 7.70″ | 4.63″ |
| Pole length ($l_p$) | 5″ | 7.50″ | 7″ | 2.585″ |
| Pole width | 2.25″ | 8.0″ | 6″ | 2.25″ |
| Frame inside diameter (ID) | 14″ | 59″ | $37\frac{11}{16}$″ | 8.0″ |
| Frame outside diameter (OD) | 15.75″ | 64.75″ | $42\frac{7}{16}$″ | 9.375″ |
| Frame width | 8″ | 13″ | 10″ | 4.5″ |
| Number of armature slots | 31 | 100 | 75 | 20 |
| Slot depth | 0.920″ | 1.93″ | 1.97″ | 0.855″ |
| Slot width (in middle of tooth) | 0.318″ | 0.45″ | 0.343″ | 0.30″ |
| Winding | wave | lap | lap | wave |
| Number of circuits ($a$) | 2 | 8 | 6 | 2 |
| Conductors per slot | 18 | 8 | 6 | 70 |
| Effective air gap (equals air gap times factor) | 1.23 | 1.1 | 1.15 | 1.18 |
| Leakage flux between pole shoes and pole bodies in percent of armature flux | 18% | 20% | 20% | 15% |
| Height of pole (without pole shoe) | 2.8″ | 9.6″ | 7.1″ | 1.3″ |
| Loss of iron length: | | | | |
| (a) due to insulation between armature laminations | 4% | 8% | 8% | 4% |
| (b) due to air layers in pole. | 5% | 5% | 5% | 5% |

# *Chapter 6*

# METHODS OF EXCITATION

## DIRECTION OF ROTATION OF THE SHUNT AND SERIES MACHINE

**6–1. Methods of Excitation.** A d-c motor gets its field current for excitation as well as the armature current from an external source of power. A d-c generator can also be excited from an external source of power: this is the separately excited generator. However, a d-c generator is also able to produce its own excitation, i.e., it is capable of *self-excitation*. This ability is due to the emf induced in the d-c armature by the residual magnetism which remains in the field poles after the machine has been once separately excited. It will be shown that under proper conditions the emf induced in the armature winding by the residual magnetism produces a field current in such a direction that the residual magnetism is *strengthened*; this increases the armature emf as well as the field current, and the growth of both quantities continues until a voltage is reached whose magnitude depends upon the saturation of the iron of the machine and, for the excitation listed below under (b), also upon the resistance of the field winding (see Art. 7–5).

Thus, the d-c generator may be separately-excited or *self-excited*. According to the manner of connection of the field winding with respect to the armature winding and the load, three separate cases of self-excitation are available:

(a) Series excitation.
(b) Shunt excitation.
(c) Compound excitation.

(a) *Series Excitation.* For series excitation the field winding and armature winding are connected in series as shown in Fig. 6–1. If the residual magnetism is such that the top pole is a north pole (N) and the bottom pole a south pole (S), the field winding must be connected in series with the armature so that the field current produces a north pole at the top and a south pole at the bottom. Fig. 6–1 shows the connection of both windings as well as the direction of the current in the field winding. $T_1$ and $T_2$ are the terminals of the machine which are connected to the load circuit.

If the field winding is connected in reverse so that end $b$ of the field winding rather than end $a$ is connected to the positive pole of the armature,

the magnetism will not build up and no rise in voltage will be obtained. An interchange of the terminals of the field winding reverses the field current, provided the residual magnetism has not been completely destroyed by the previous wrong connection, and the machine then builds up voltage. If the machine does not build up, a separate source of field current must then be employed to restore the residual magnetism. *Self-excitation can result only when the field current aids the residual magnetism.*

(b) *Shunt Excitation.* For shunt excitation the field winding is placed in parallel with the armature winding as shown in Fig. 6–2. While the resistance

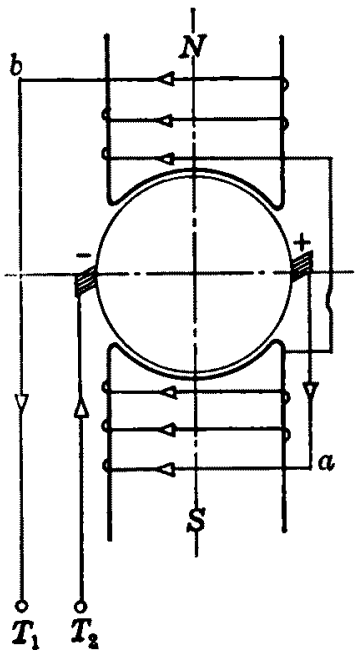


FIG. 6–1. D-c machine with series excitation.

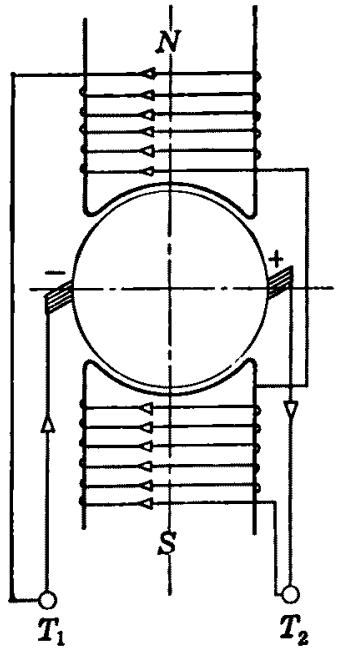


FIG. 6–2. D-c machine with shunt excitation.

of a series field winding is made low, in order to prevent a large voltage drop across it, the resistance of the field winding used for shunt excitation is high. Fig. 6–2 shows that the armature furnishes not only the load current but the field current also. If the resistance of the field winding were low, it would take a high current and this would load the armature winding. Normally the field current of shunt-wound machines is 1 to 5% of the armature current, the higher values applying to small machines.

To produce the field flux an mmf is necessary. It does not matter whether this mmf is produced by the large current and small number of turns of the series winding or by the low current and correspondingly large number of turns of the shunt winding.

(c) *Compound Excitation.* In the case of compound excitation the machine has both a series and a shunt field winding. The greater part of the excitation mmf is usually furnished by the shunt field winding. The series winding serves to make the field flux dependent, within narrow limits, on the load

current. The series winding may be connected to the armature winding so that it produces an mmf of the same direction as that of the shunt winding (*cumulative compound connection*) or an mmf opposite to that of the shunt winding (*differential compound connection*). It will be shown later, Art. 7–6, that the cumulative compound-wound generator, in contrast to the shunt-wound generator, offers the possibility to compensate for the voltage drop in the armature winding as well as to overcome the demagnetizing effect of the armature reaction.

The three methods of excitation of a d-c generator as just described are used also in d-c motors. It will be shown in Art. 8–4 that the compound-wound motor, in contrast to the shunt-wound motor, offers the possibility of maintaining the same speed at no-load and rated load.

In the cumulative compound-wound machine the shunt field winding may be connected either directly across the armature terminals (*short-shunt connection*) or across the terminals $T_1$ and $T_2$ which connect to the external circuit or the line (*long-shunt connection*). The first case is shown schematically in Fig. 6–3a and the second in Fig. 6–3b. "Sh" is the shunt field winding and "Se" the series field winding. There is no essential difference between the operating characteristics of the short- and long-shunt connection.

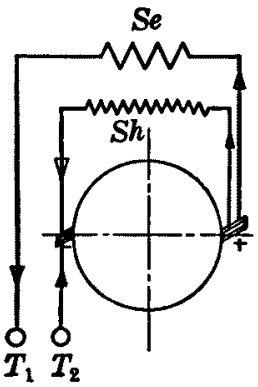


FIG. 6–3a. D-c machine with compound excitation, short-shunt connection.

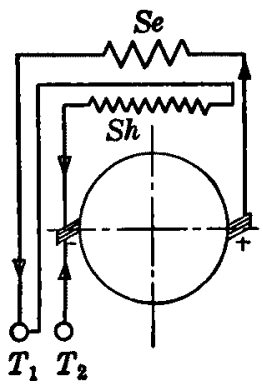


FIG. 6–3b. D-c machine with compound excitation, long-shunt connection.

The *polarity* of the self-excited d-c generator depends upon its residual magnetism and the direction of rotation. With respect to the build-up of the voltage the following additional condition must be satisfied. It has been shown that the self-excited d-c generator can build up its voltage only when the field winding is connected to the armature winding in such a manner that the field current assists the residual magnetism. An incorrect connection between the field and armature windings will tend to demagnetize the machine and then it will not build up its voltage. The same demagnetizing effect and resulting failure to build up occur in a machine which has been operating

with self-excitation, if the direction of rotation of the armature were reversed, because a reversal of the direction of rotation changes the polarity of the armature.

In order that a self-excited generator may build up its voltage, there must be the proper direction of rotation of the armature and the proper connection of the field winding to the armature terminals. If one of these factors is changed in a correctly running machine, the machine will tend to demagnetize itself. If both factors are changed, the machine builds up its voltage but with opposite polarity.

**6–2. Direction of Rotation of a Shunt and Series Machine as Generator and Motor.** If a generator is to deliver a certain power output, it must receive this power plus its losses from the prime mover. The prime mover must overcome the electromagnetic torque produced by the armature conductors which are rotating in the magnetic field of the generator (see Art. 1–4). Under steady-load conditions, the prime mover torque is always opposite in direction but equal to the sum of the electromagnetic torque and the loss torque of the generator.

Fig. 6–4 shows one pole of the generator previously drawn in Fig. 5–11.

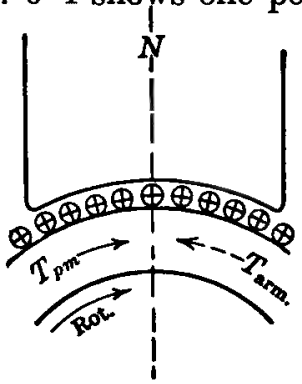


FIG. 6–4. Balance of torques in a generator.

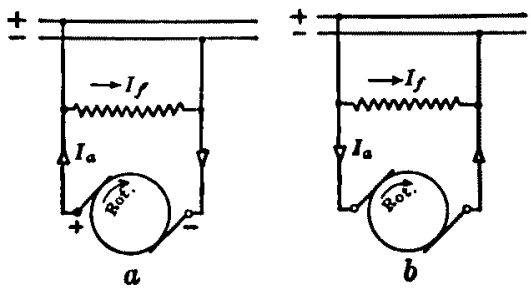


FIG. 6–5. Direction of rotation of a shunt machine as generator and motor.

The direction of rotation of the armature is clockwise. The prime mover torque $T_{pm}$ also must be clockwise. The electromagnetic torque of the armature $T_{arm}$ is counter-clockwise and is shown by the dotted arrow. If the prime mover torque is removed and the direction of the field and armature currents is assumed to remain unchanged, the armature will rotate in a direction opposite to that of the prime mover and will produce a motor torque. Therefore, *for the same direction of the field and armature currents, the direction of rotation of the machine as a motor is opposite to its direction of rotation as a generator.*

Since the direction of the armature torque changes when the direction of either the field or the armature current is changed, it is a simple matter to determine the direction of rotation of the shunt or series machine when operating as a generator or as a motor.

It is assumed for the shunt-wound machine of Fig. 6–5a that, for the direction of rotation shown, it operates as a generator and produces the polarity given in the figure, which must correspond to the polarity of the bus-bars. For this condition of operation, the directions of armature and field currents are as shown in the figure. If the machine is operated as a motor with the same connection to the line, the armature current reverses while the field current is in the same direction, as shown in Fig. 6–5b. Since the direction of the armature current reverses when this machine operates as a motor, while the field current remains the same, the direction of rotation as a motor is the same as that when operating as a generator. Consequently *the shunt machine, without any change in the connections, will operate in the same direction either as a motor or as a generator.*

Figure 6–6a shows the direction of the current in the armature and field of a series-connected machine when operated as a generator. If the series machine is operated as a motor from lines of the same polarity (Fig. 6–6b), the current is reversed in both the armature and the field winding; therefore, *the series machine when operated as a motor without changing the connections rotates in a direction opposite to that as a generator.*

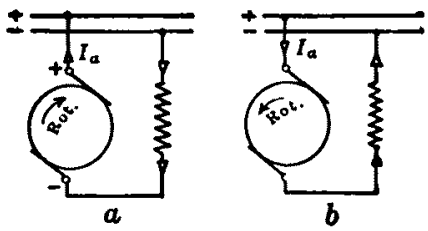


FIG. 6–6. Direction of rotation of a series machine as generator and motor.

If a shunt machine operating as a motor loses the opposing torque of its load, it may be made to operate as a generator in the same direction by supplying it with mechanical power and adjusting the field current so that the induced emf is greater than the line voltage (see Art. 7–1). In the series motor, in order to operate in the same direction as a generator, either the armature current or field current must be reversed in direction.

It follows from the foregoing that the *direction of either the armature current or field current must be reversed, in order to reverse the direction of rotation of a motor.* Interchanging the connections to the bus-bars will not reverse the direction of rotation, since this reverses the direction of the current in both windings.

# *Chapter 7*

## THE D-C GENERATOR

**7–1. The Voltage Equation of the D-c Generator.** The emf induced in the armature winding under load does not appear in its full amount at the terminals of the generator. This is due to the fact that, under load, there are voltage drops in the various resistances.

The armature current $I_a$ flowing in the armature winding produces a voltage drop $I_a r_a$. If the machine is series wound or compound wound, the series winding which is connected in series with the armature produces a voltage drop $I_s r_s$. It will be shown later, Art. 9–6, that d-c machines have a special winding—the interpole winding—for the purpose of improving the commutation. This winding is also connected in series with the armature and produces a voltage drop $I_i r_i$. If there is a compensating winding (see Art. 9–6), this winding will also be connected in series with the armature and will produce a voltage drop $I_c r_c$. Furthermore, there is a voltage drop in the contact resistance between the brushes and commutator. The voltage drop between all the brushes of each polarity and commutator will be denoted by $\Delta V$. Thus, the total voltage drop is

$$I_a r_a + I_s r_s + I_i r_i + I_c r_c + 2\Delta V = \Sigma Ir + 2\Delta V \tag{7–1}$$

Applying Kirchhoff's law to the armature circuit, we have

$$E = V + (\Sigma Ir + 2\Delta V) \tag{7–2a}$$

where $V$ is the terminal voltage of the armature, i.e., the voltage applied to the load. Thus the terminal voltage

$$V = E - (\Sigma Ir + 2\Delta V) \tag{7–2b}$$

The magnitude of the induced emf is given by Eq. 4–3:

$$E = Z \frac{p}{a} \frac{n}{60} \Phi 10^{-8} = C_1 n \Phi \tag{7–3}$$

where $C_1$ is a constant quantity for a given machine and $\Phi$ is the flux per pole produced by the resultant mmf of field and armature winding.

In a shunt generator, the field winding is connected in parallel with the armature winding (and load). The armature current ($I_a$) of a shunt generator is, therefore, slightly larger than its load current ($I_L$), i.e.,

$$I_L = I_a - I_f \tag{7-4}$$

The same applies to the compound generator.

**7–2. Characteristic Curves of the D-c Generator; Regulation.** The following characteristic curves of a d-c generator will be considered.

(a) No-load characteristic, or magnetization curve, $E = f(I_f)$; $n$ = constant
(b) Load characteristic, $V = f(I_f)$; $I_a$ and $n$ = constant
(c) External characteristic, $V = f(I_L)$; $n$ = constant
(d) Regulation curve, $I_f = f(I_a)$; $V$ and $n$ = constant

The no-load characteristic has been treated in Art. 5–2. Its shape depends upon the dimensions of the different parts of the magnetic circuit and the materials used. The shape of all other characteristic curves depends upon the shape of the no-load characteristic and upon the load.

The influence of the load appears as:

(a) Armature reaction (Art. 5–3).
(b) Voltage drop in the armature, series, interpole, and compensating windings ($\Sigma Ir$).
(c) Voltage drop at the contact surfaces of the brushes ($2\Delta V$).

As has been explained in Art. 5–4, the armature reaction consists of two parts, one due to the cross flux, the other due to the demagnetizing or magnetizing armature mmf within the angle $2\beta$ (Fig. 5–13). The armature reaction due to the cross flux depends upon the saturation of the machine. When the magnetic circuit is unsaturated, the effect of the cross-magnetizing ampere turn is to distort the flux distribution without changing the value of the total flux per pole; with saturation there is also a reduction of the air gap flux due to the cross mmf. The demagnetizing or magnetizing armature mmf due to the brush shift depends upon the load current; it is usually demagnetizing and subtracts from the field mmf.

In the following there will be given the constructions of the characteristic curves for the different types of d-c generators. Since these constructions are based on the magnetization curve (no-load characteristic), the variation of the cross-flux armature reaction with saturation appears as a factor which considerably complicates the problem. In order to simplify it, the assumption will be made that the influence of saturation on the cross-flux armature reaction is constant and equal to that which occurs near the bend of the no-load characteristic and that the cross-flux mmf is proportional to the armature current. This assumption is justified by the fact that the d-c generator normally operates near the bend of the no-load characteristic. The sum of the two parts of the armature reaction mmf will be denoted by $M_d$ when expressed in ampere turns. This combined effect of armature reaction may also be expressed as a *reduction* in field current which would produce the same reduction in flux or emf. The quantity $M_d$, expressed in equivalent

field current then will be $M'_d = \frac{M_d}{N_f}$, where $N_f$ is the number of turns of the field winding.

The voltage drop $\Delta V$ at the contact surface of the brushes depends on the brush material. For the usual carbon brush it is as given in Fig. 7–1, where it is shown as a function of the current density in the brush. $\Delta V$ increases with increasing current density, but it will be assumed equal to 1 volt for the brushes of each polarity, i.e., to 2 volts for the total machine, since the current density in the brushes usually does not exceed 50 amperes per square inch at normal load.

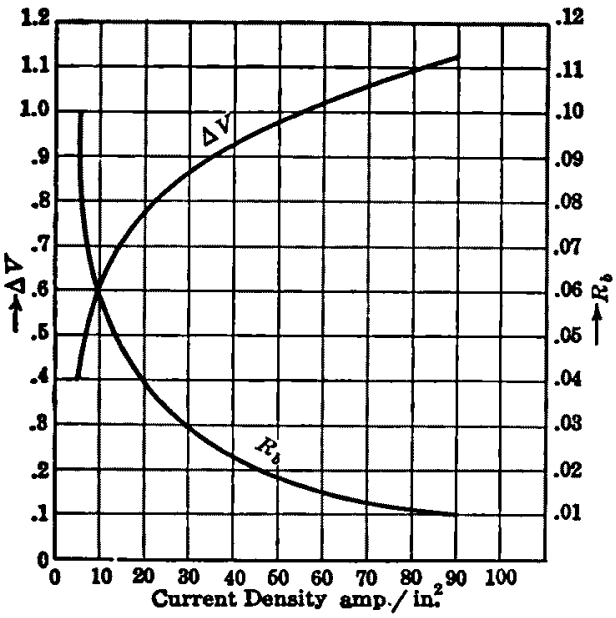


FIG. 7–1. Characteristics of a carbon brush.

In the case of a generator, besides the characteristic curves, the *voltage regulation* is of considerable importance, that is, the change in voltage from no-load to full-load expressed as a percentage of the full-load voltage. The regulation is a measure of the stiffness of the machine with respect to variation of voltage with variation of load. The regulation is closely related to the external characteristic of the machine and will be determined in connection with the treatment of this characteristic.

The characteristic curves of the different types of generators will be considered in the following paragraphs.

**7–3. Separately Excited Generator.** (a) *The No-load Characteristic.* The emf induced in the armature is given by Eq. (7–3):

$$E = C_1 n \Phi$$

Since the armature carries no current, the flux $\Phi$ depends only upon the field mmf, or, since the number of field turns is constant for a given machine, upon the field current $I_f$. If $n$ is constant,

$$E = C'_1 f(I_f) \tag{7–5}$$

where $C'_1 = C_1 n$. This is the no-load characteristic; it shows the terminal voltage at no-load as a function of the field current and it is obtained using the connections shown in Fig. 7–2a: $A$ is the armature, $FW$ the field winding, and $B$ the source which supplies the field current. The resistance $R_f$ is used to vary the field current.

In Fig. 7–2b which shows the no-load characteristic, curve $a$ shows the voltage $E_0$ as a function of $I_f$ when the field current is increased from zero

to $I_{fm}$; and curve $b$ shows the voltage $E_0$ as a function of $I_f$ when the field current is reduced from this $I_{fm}$ value to zero. Because of the effect of the residual magnetism the two curves do not coincide. The residual magnetism is also the cause of the plot of curve $a$ usually starting above the zero point for zero field current.

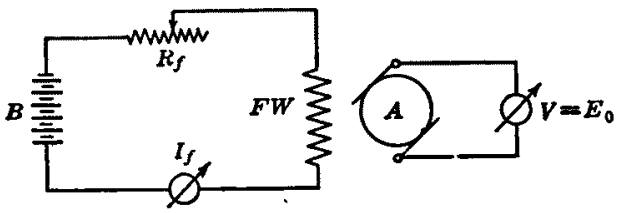


FIG. 7–2a. Connection diagram for the determination of the no-load characteristic of a separately excited generator by test.

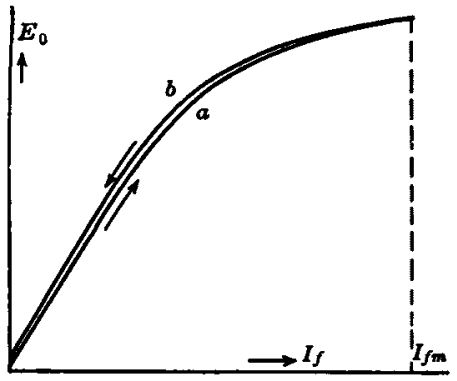


FIG. 7–2b. No-load characteristic of a separately excited generator.

(b) *The Load Characteristic.* If the armature is loaded, the terminal voltage is no longer equal to the emf induced in the armature winding, but is less than this value because of the armature reaction ($M_d$), the voltage drop in the armature and other windings ($\Sigma I_a r$), and the contact-resistance drop due to the brushes ($2\Delta V$). The curve of terminal voltage as a function of field current for constant speed and constant armature current is known as the *load characteristic.* Fig. 7–3a shows the connections used for taking the load characteristic. The load current is adjusted by means of the resistance $R_L$.

Curve III in Fig. 7–3b is a load characteristic. Curve I is the no-load characteristic of the same machine. If the quantity $AB=(\Sigma I_a r+2\Delta V)$ is added to the load-characteristic curve, curve II thus obtained is the emf induced in the armature winding by the resultant flux. The distance $BC$ between curve II and the no-load-characteristic curve I is the voltage drop produced by armature reaction. In order to maintain the terminal voltage $CH$ at both no-load and full-load, $CD$ is required as the increase in the field current necessary to compensate for the effect of armature reaction ($M_d$) and the voltage drops.

The load characteristic (curve III, Fig. 7–3b) can be found approximately in the following way: At point $m$ of the load characteristic, $V$ is equal to zero (armature is short-circuited). In order that the current $I_a$, for which the load characteristic is to be determined, may flow in the armature at this condition of operation, the emf

$$AB=\Sigma I_a r+2\Delta V$$

must be induced in the armature and the field current $OA$ is necessary for this. Moreover, an additional field-current component

$$Bl = Am = \frac{M_d}{N_f} = M'_d$$

is necessary to compensate for armature reaction.

The sides of the triangle $Blm$ are proportional to the load current $I$, and, since this current is constant, the triangle $Blm$ is the same for any value of $V$. The load characteristic therefore can be found by moving the triangle

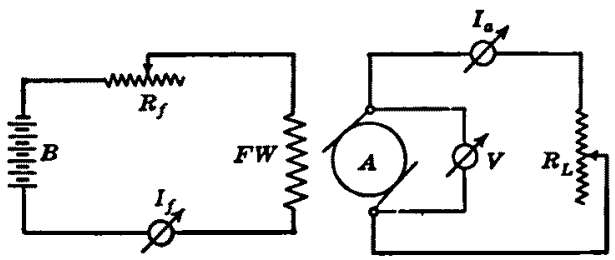


FIG. 7–3a. Connection diagram for the determination of the load characteristic of a separately excited generator by test.

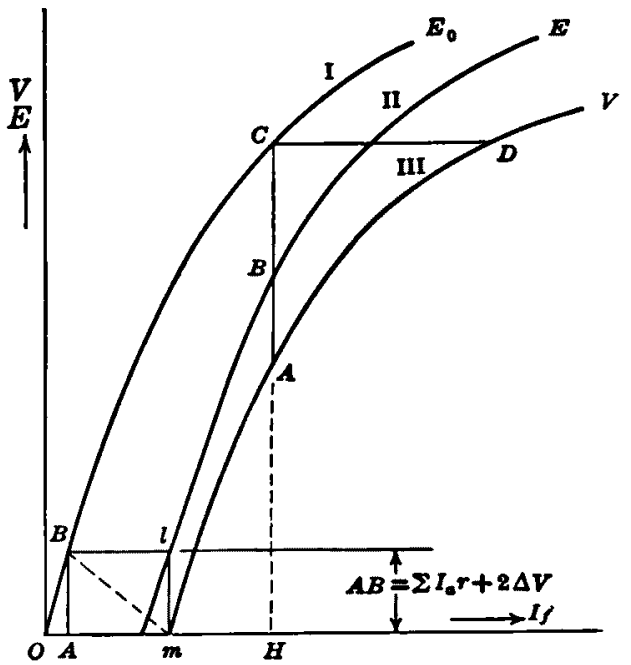


FIG. 7–3b. Load characteristic of a separately excited d-c generator.

$Blm$ parallel to itself along the no-load characteristic (curve I, Fig. 7–3b). Point $m$ of the triangle then traces the load characteristic (curve III, Fig. 7–3b). It is to be noted that the load characteristic so obtained is correct only near the bend since $M_d$ is determined for this part of the characteristic. For lower saturation the values of $V$ are too low; for higher saturation, too high.

(c) *The External Characteristic.* The curve showing the terminal voltage as a function of the load current at constant speed and field current, $V = f(I_a)$, is called the *external characteristic* (curve III, Fig. 7–4). With increasing load current, the armature reaction, as well as the resistance drops in the armature winding, increases. Consequently the terminal voltage $V$ drops with increasing load current.

If the voltage drop $AB = (\Sigma I_a r + 2\Delta V)$ is added to the external characteristic, the value of the emf $E$ induced in the armature winding by the resultant flux is obtained (curve II). $BC$, the difference between curve I,

which corresponds to the no-load voltage $E_0$, and curve II, is the voltage drop caused by the armature reaction. With the aid of the external characteristic, the voltage regulation ($\epsilon$) of the machine can be determined. It is (Fig. 7–4):

$$\epsilon\% = 100\frac{E_0 - AA}{AA},$$

where $AA$ is the value of the terminal voltage at rated load. The connections used to obtain the external characteristic are the same as those used for the load characteristic (Fig. 7–3a).

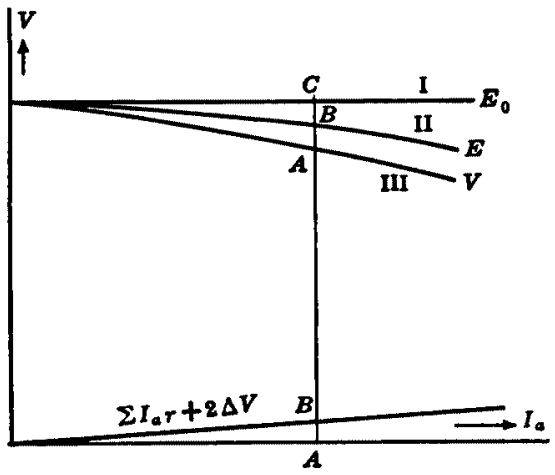


FIG. 7–4. External characteristic of a separately excited generator.

With the aid of the no-load characteristic, the external characteristic can be approximately determined in the following way: In Fig. 7–5 $OP$ is the constant field current for which the external characteristic is to be found. The no-load voltage for this field current is $PC = OC'$. Assume any load current $I' = OS$. For this current determine

$$\Sigma I' r + 2\Delta V = A'B'$$

and

$$M'_a = \frac{M_a}{N_f} = Q'B'.$$

If the triangle $A'B'Q'$ is placed in such a manner that $A'B'$ lies on $PC$, $B'Q'$ is parallel to the axis of abscissa, and $Q'$ lies on the no-load characteristic, then $PA'$ is the terminal voltage for the load current $I'$. To the left make

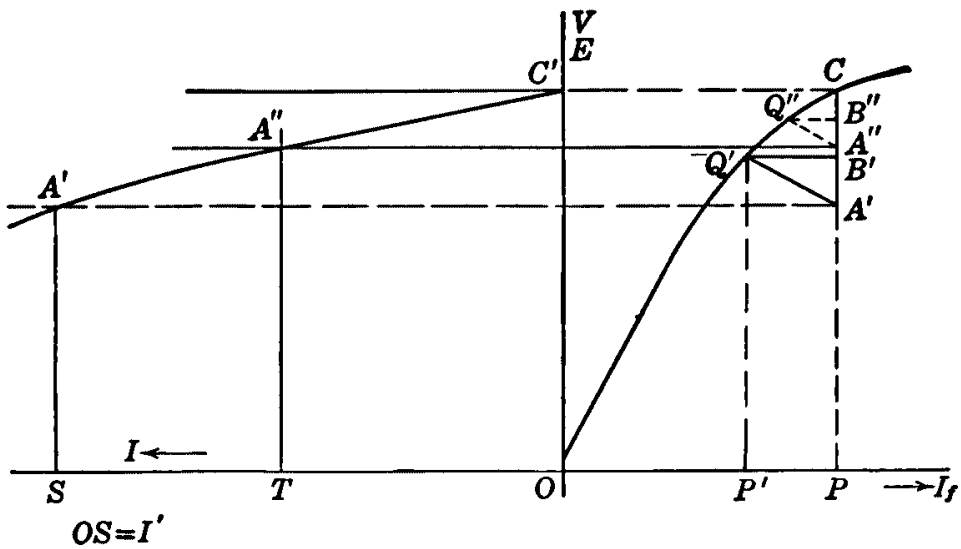


FIG. 7–5. Construction of the external characteristic of a separately excited d-c generator from its no-load characteristic.

$SA' = PA'$. For the assumed load current $I'$, the terminal voltage is $SA' = PA'$, corresponding to a drop of $A'C$ from no-load. The component drop $A'B'$ is due to $\Sigma Ir + 2\Delta V$ and $B'C$ is due to the effect of armature reaction in reducing the flux. Since the induced emf is $PB' = P'Q'$ the effective field current may be considered to be $OP'$, corresponding to a reduction of $PP' = M'_d$ from the actual field current $OP$.

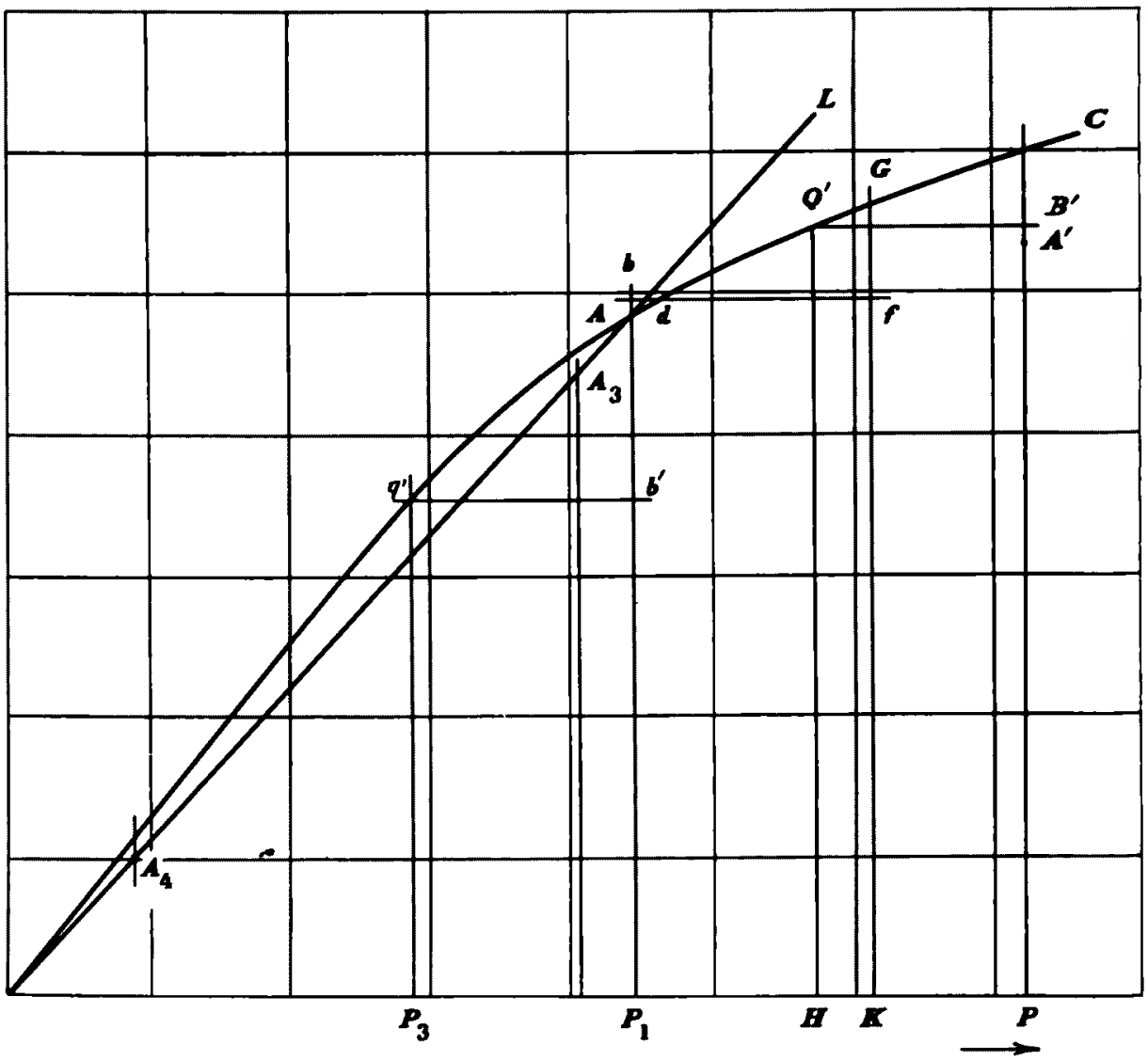


FIG. 7–6a. No-load characteristic of the machine of Example 1.

In the triangle $A'B'Q'$, $A'B'$ is nearly proportional to the load current while $B'Q'$ is not exactly proportional to the load current, for the cross-flux armature reaction is not exactly proportional to the load current. The assumption will be made, however, that $B'Q'$ is also proportional to the load current. Then for any other assumed load current, $OT$, a new triangle such as $A''B''Q''$ may be constructed, for which $A''P = A''T$ will be the terminal voltage. The assumption that the armature reaction mmf is proportional

to the load current is approximately correct for higher saturation, but it is incorrect for lower saturation. The construction used above, therefore, gives correct results for the points which lie above the bend of the no-load characteristic.

**Example 1.** The no-load characteristic of a 250-kw, 6-pole, 1200-rpm, d-c generator, obtained by test, is shown in Fig. 7–6a. The total resistance of the shunt

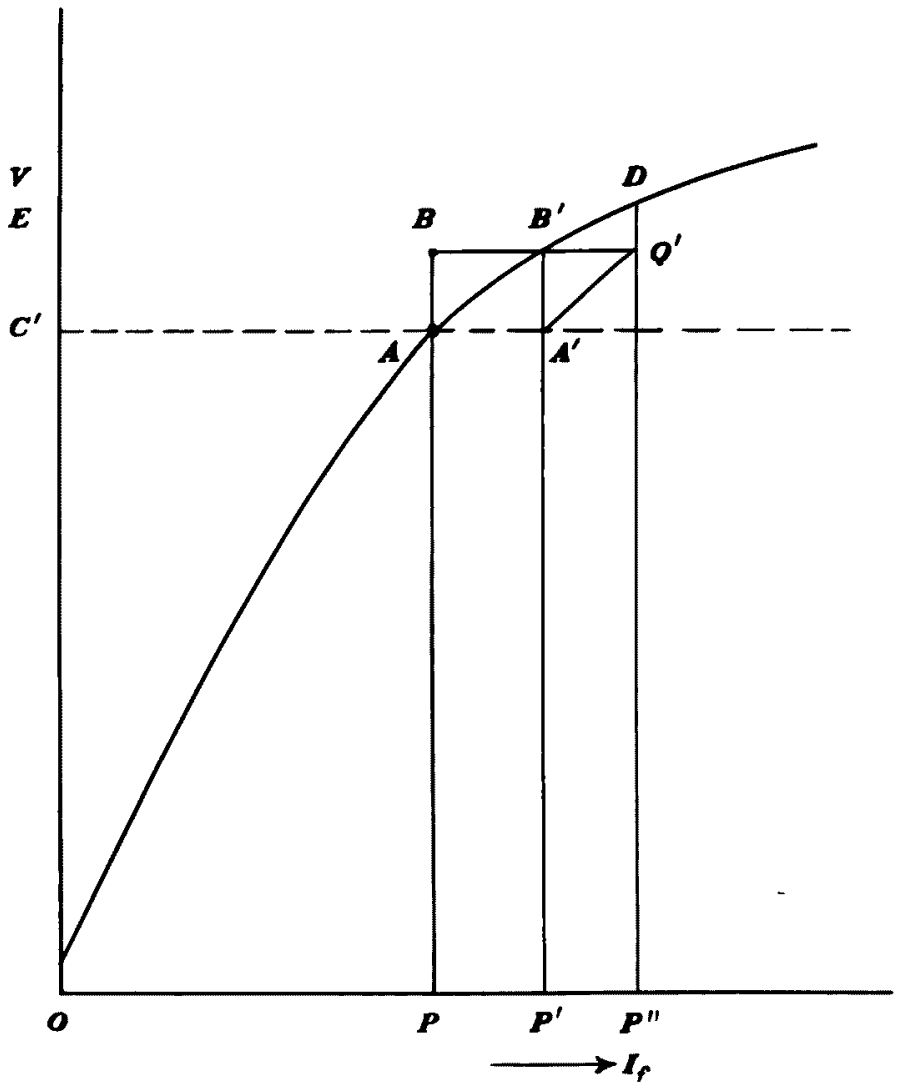


FIG. 7–6b. Construction of regulation curve (Example 1d).

field circuit is 47.9 ohms at 75° C; there are 1064 shunt turns per pole; the resistance of the armature winding is 0.00366 ohm at 75° C, and that of the interpole winding is 0.00163 ohm. The total demagnetizing effect of the armature is 1600 AT per pole at full-load armature current of 1042 amp, and it is assumed to vary directly with the armature current. Assuming that the machine operates as a separately excited generator at rated speed, with the field current constant and V = 300 volts at no-load, the field current will be 7.2 amp = $OP$ (Fig. 7–6a) and this will provide 7670 AT per pole. The voltage required at the field terminals will be $7.2 \times 47.9 = 344$. The terminal voltage $V$ at full load $I_a$ will be obtained as follows: referring to

Figs. 7–5 and 7–6a, $Q'B' = M'_d = 1600/1064 = 1.5$ amps, the demagnetizing effect of armature reaction expressed in terms of shunt field current. The line $Q'B'$ is fitted in between the no-load curve and the vertical line erected at $P$. It should be noted that the distance $OH = 5.7$ amp represents an effective value of $I_f$. The generated emf is found as $PB' = Q'H = 275$ volts. This is a reduction of $B'C = 26$ volts from the no-load value, due to armature reaction. The voltage drop in the windings and under the brushes is $1042\ (0.00366 + 0.00163) + 2 = 7.5$. This value as $A'B'$ is subtracted from $PB'$ to give the terminal voltage $PA'$ as $275 - 7.5 = 267.5$. The voltage regulation will be $100 \times \dfrac{300 - 267.5}{267.5} = 12.6\%$.

If the field current is adjusted to give $V = 240$ at no-load, then $I_f = OP_1 = 4.38$ amp. For rated armature current $M'_d = 1.5 = b'q'$ giving a generated emf $P_1b' = P_3q' = 178$ volts and $V = 178 - 7.5 = 170.5$. The effective $I_f = 4.38 - 1.5 = 2.88 = OP_3$. The voltage regulation will be $\dfrac{240 - 170.5}{170.5} \times 100 = 40.8\%$. The regulation is much worse than for a no-load voltage of 300, because the effect of the armature demagnetization mmf is greater: the machine operates much lower down on the saturation curve.

(d) *The Regulation Curve.* If the terminal voltage is to remain constant with increasing load current, the field current must be increased; the extent of the increase of the field current depends upon the magnitude of the armature reaction and the resistance drops. The regulation curve $I_f = f(I_a)$ shows the field current as a function of the load current for constant terminal voltage and speed (Fig. 7–6c).

The regulation curve may be determined in the following manner (see Fig. 7–6b). The terminal voltage is to remain constant at the value $OC' = PA$. At no-load the field current required is $OP$. At any assumed load current draw $AB = \Sigma I_a r + 2\Delta V$. Then $PB$ is the generated emf required and, if there were no armature reaction, the field current would need to be increased by the amount $BB' = PP'$ to the value $OP'$. However, due to armature reaction, a further increase $B'Q' = M'_d$ is required to overcome the armature reaction mmf. The total field current is now $OP''$. If the load were removed and $OP''$ maintained, the terminal voltage would rise to $P''D$. For other assumed load currents, values of $I_f$ may be obtained and plotted as shown in Fig. 7–6c.

**Example 2.** If the separately excited generator of Example 1 is to maintain $V = 240$ at no-load and at full load, the no-load field current must be $OP_1 = 4.38$. The full-load field current may be found as follows: refer to Fig. 7–6a;

$$Ab = \Sigma I_a r + 2 = 7.5 \text{ volts.}$$

The generated emf will be $P_1A + Ab = 240 + 7.5 = 247.5 = P_1b$. With no armature reaction this would require an increase in $I_f$ by the amount $bd$. Since, however, $M'_d = 1.5 = df$, the total increase in $I_f$ is $bf$, yielding a total $I_f = OK = 6.13$. If the load were entirely removed and $I_f$ kept at 6.13, the no-load voltage would be $KG = 283$ volts.

**7–4. Series Generator.** (a) *The No-load Characteristic.* For this machine the no-load characteristic can be taken only with separate excitation, because self-excitation would require the armature to carry current, and a no-load characteristic implies no armature current whatever.

(b) *The Load Characteristic.* For the series generator the load characteristic also must be taken with separate excitation, for with self-excitation the armature and field current would change at the same time. The no-load and load characteristics of the series generator are consequently identical with the no-load and load characteristics of the separately excited generator.

(c) *The External Characteristic.* The characteristic features which distinguish the series generator from other types of d-c generators are shown by its external characteristic. Fig. 7–7 shows the connections used to obtain

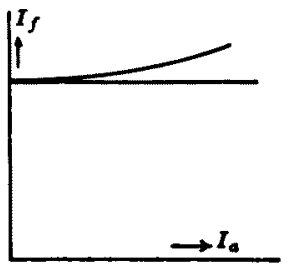


FIG. 7–6c. Regulation curve of a separately excited generator.

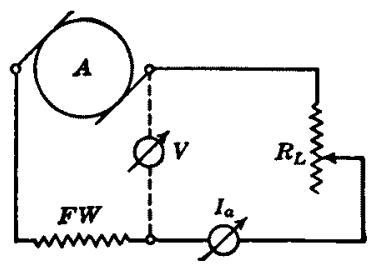


FIG. 7–7. Connection diagram for the determination of the external characteristic of a d-c series generator by test.

the external characteristic. The load current is varied by means of the load resistance $R_L$. Since the armature current is used to excite the field, the field mmf and consequently the induced emf in the armature winding and the terminal voltage $V$ increase with increasing load current. Curve III of Fig. 7–8 is the external characteristic of a series generator. Curve I is the no-load characteristic of the machine. If the voltage drop $AB = (\Sigma I_a r + 2\Delta V)$ is added to curve III, the curve II obtained is the emf induced in the armature winding by the resultant flux. The difference $BC$ between curve II and the no-load-characteristic curve $I$ is consequently the voltage drop caused by armature reaction.

**7–5. Shunt Generator.** (a) *The No-load Characteristic and Building Up of Voltage.* Fig. 7–9a shows the connections for obtaining the no-load characteristic. FW is the shunt field winding. The field current is varied by means of the shunt field rheostat $R_f$. In taking the no-load characteristic the armature supplies the field current. Since this current is only a very small percentage of the armature current under load, the voltage drop which it causes in the resistance of the armature winding and the brushes, as well as

the armature reaction produced by it, is very small. Consequently the no-load characteristic for self-excitation virtually coincides with that obtained for separate excitation. The no-load characteristic may, therefore, be obtained by separate excitation.

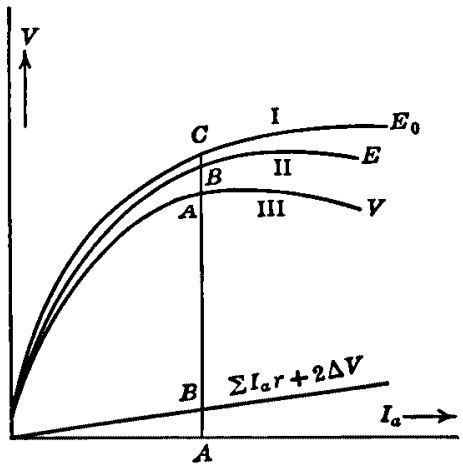


FIG. 7–8. External characteristic of a series generator.

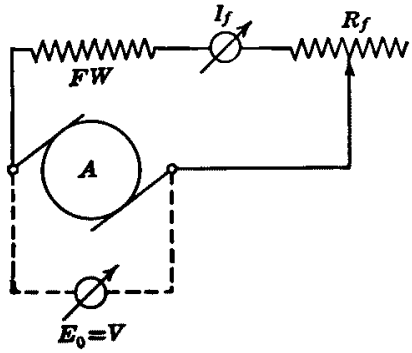


FIG. 7–9. Connection diagram for the determination of the no-load characteristic of a d-c shunt generator by test.

With respect to the build-up of the voltage in a shunt generator the following applies. In the shunt generator, Fig. 7–9a, the field circuit is connected directly across the terminals of the armature; hence the terminal voltage at the armature is the same as that applied to the shunt field circuit. The relation between $V(=E_0)$ and $I_f$ is expressed in the saturation curve $OB$ in Fig. 7–10. The relation is also expressed by the equation $V=IR_{ft}$, where $R_{ft}$ is the total resistance of the field circuit. This is shown as the straight line $OL$, Fig. 7–9b, called the *field resistance line*. For any point on this line, $R_{ft}=AP/OP$ is proportional to tan $\alpha$. The intersection at $A$ represents the graphical solution of the two functional relations $V=f(I_f)$, the saturation curve, and $V=I_fR_{ft}$, the field resistance line. *The terminal voltage must always lie on the line OL*, as will be observed in some of the discussions later on.

At no-load the voltage will always build up to the point of intersection between the field resistance line and the saturation curve—such as point $A$ in Fig. 7–10. A point $b$ will not satisfy the steady-state condition, since, with the field current $Oa$, the emf would be $ac$, whereas, with the field current $Oa$ the terminal voltage of the field circuit would only need to be $ab$, which is the voltage drop in $R_{ft}$. Hence, $bc$ may be looked upon as excess voltage, or an accelerating voltage to cause $I_f$ to increase beyond $Oa$ and $V$ beyond $ab$. The greater the intercept $cb$, the more rapid is the increase in terminal voltage, until the point $A$ is reached. If the field circuit resistance is increased as represented by $OL_1$, the voltage would only build up to $A_1$. If the field

resistance were increased to coincide with the gap line the voltage is indeterminate. This resistance is sometimes called the *critical field resistance.* If the field resistance line is $OS$, the machine will not build up at all.

(b) *Influence of Speed on the Induced Emf at No Load.* The induced emf of the shunt generator is not directly proportional to its speed when $R_{ft}$ is constant, for its field current changes with the speed. Assume in Fig. 7–11

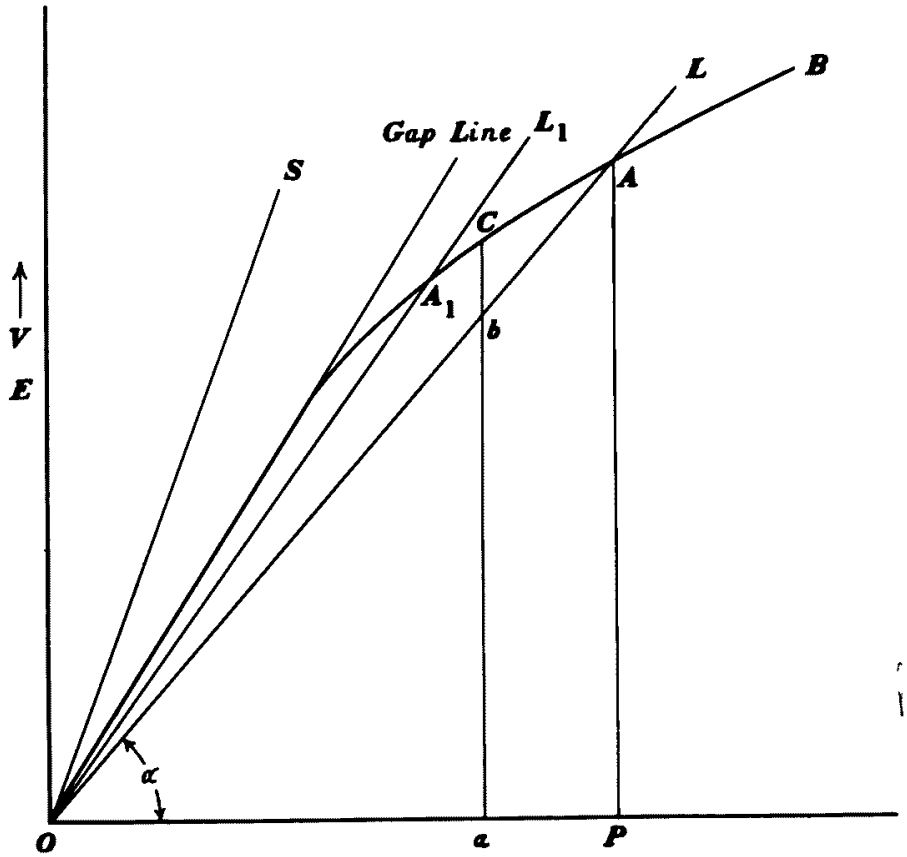


FIG. 7–10. Building up the voltage of a shunt generator.

$A\,(n_n)$ to be the no-load characteristic at rated speed $n_n$, and $OL$ to be the field-resistance line. The no-load voltage at rated speed is then $PT$ and the field current $OP$. If the speed of the machine is reduced from $n_n$ to $n'$, the no-load characteristic will be represented by the curve $A'\,(n')$ and, for the same total resistance in the field circuit, the no-load voltage will be $P_1T_1$ and the field current $OP_1$. From Fig. 7–11 the following relations are observed:

$$\frac{P_1T'_1}{P_1T_1} = \frac{n_n}{n'} = \frac{PT'}{PT}$$

or

$$PT' = PT\frac{n_n}{n'}$$

Thus, in order to determine the induced emf at the speed $n'$, compute $PT'$

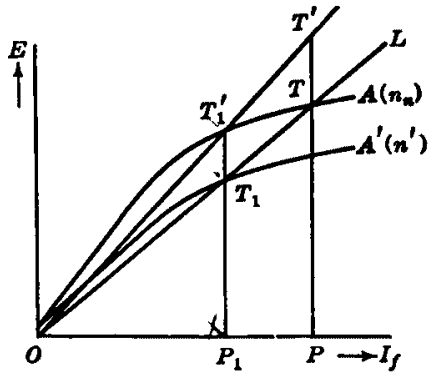


FIG. 7–11a. Influence of speed on the induced emf of a shunt generator at no-load.

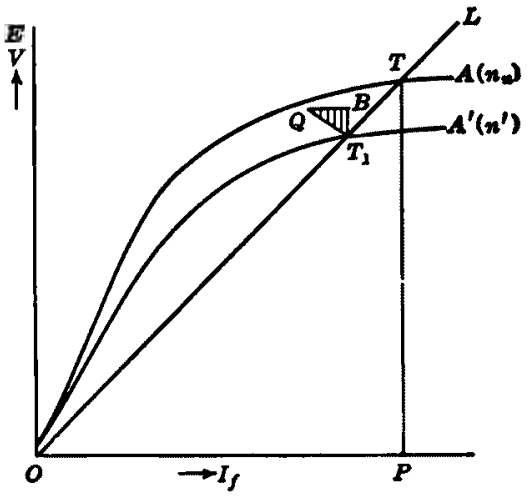


FIG. 7–11b. Influence of speed on the external characteristic of a shunt generator.

from the last equation, connect $T'$ with $O$, and draw a perpendicular through $T'_1$. The intersection point $T_1$ with the field-resistance line $OL$ will yield the desired emf $P_1T_1$, since the induced emf for all speeds must be the distance between the axis of abscissa and the field-resistance line.

(c) *The Load Characteristic.* The load characteristic of the self-excited shunt generator is almost coincident with that of the separately excited generator just as is the no-load characteristic. The trend of the load-characteristic curve, therefore, is the same as that of the separately excited generator.

(d) *The External Characteristic.* This characteristic is taken with a *constant resistance* $R_f$ in the shunt field circuit and at a constant speed, Fig. (7–12). The load current is varied by means of the rheostat $R_L$ in the external load circuit. Curve III of Fig. 7–13 shows the external characteristic of a shunt generator. The external characteristic of the same generator with separate excitation is illustrated by curve IV.

With self-excitation the external-characteristic curve is lower than that obtained with separate excitation, because in the former case the field current decreases with decreasing terminal voltage since the shunt field resistance is constant, while in the case of separate excitation the field current remains constant. At a certain value of load current, called the critical value $I_c$, the external characteristic taken with self-excitation turns back towards $D$. Up to the point $V'$ the load current increases as the external resistance $R_L$ is decreased. Below this point $V'$, the current decreases with decreasing values of the resistance $R_L$. At short circuit ($R_L = 0$) the terminal voltage is zero and the armature current is $I = OD$; this value of current is determined by the residual magnetism of the machine because when $V = 0$ the field current is also zero.

If the voltage drop $AB=(\Sigma Ir+2\Delta V)$ is added to the external characteristic, curve II is obtained. The difference $BC$ between this curve and line

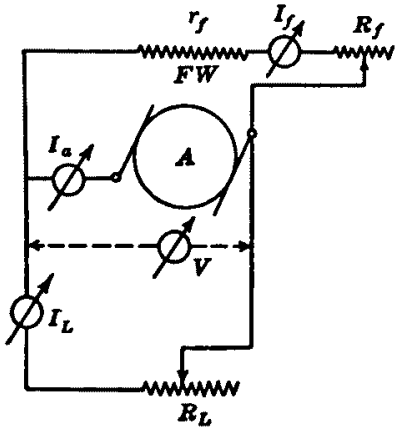


FIG. 7–12. Connection diagram for the determination of the external characteristic of a shunt generator by test.

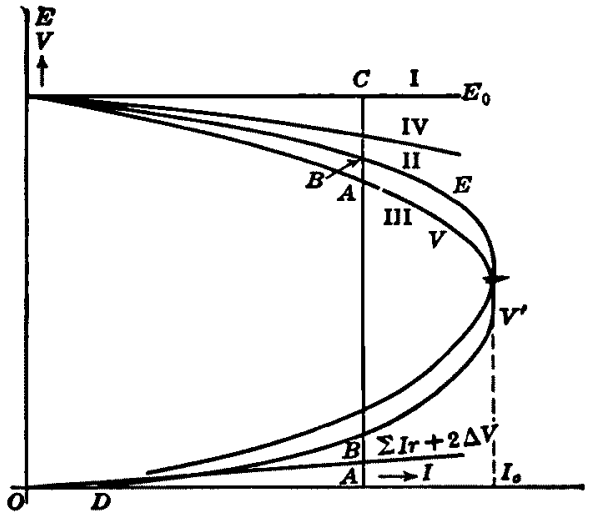


FIG. 7–13. External characteristic of a d-c shunt generator.

I which represents the no-load voltage $E_0$ of the machine is the voltage drop due to armature reaction *and* the decrease in the field current.

The voltage regulation is

$$\epsilon = 100\,\frac{E_0 - AA}{AA}\ \%$$

The external characteristic of the self-excited shunt generator is not a single-value curve: for a given value of current $I$ there are two different values of terminal voltage.

If a sudden short circuit ($R_L=0$) is applied to a shunt generator, the armature current rapidly falls to the value $OD$ which is comparatively small. On the other hand, if a short circuit is applied to a series generator, the armature current increases because the field current increases. In comparison with the series generator the shunt-connected generator has the advantage that in case of a sudden short circuit it does not feed into the short circuit but, on the contrary, the short-circuit current is decreased. However, the high instantaneous (transient) value of the short-circuit current which appears at the instant the short circuit is applied often is sufficient to damage the armature winding and commutator of the shunt generator.

With the aid of the no-load characteristic and field-resistance line, it is possible to determine the external characteristic of the shunt generator. Assume in Fig. 7–14 that the constant resistance of the field circuit is chosen

at such a value that $OL$ is the field-resistance line. $AP$ is then the no-load voltage of the generator. For the arbitrary load current $I = OS$, make

$$AB = \Sigma Ir + 2\Delta V, \quad \text{and} \quad QB = M'_d$$

The two values of the terminal voltage which correspond to the load current $OS$ will be found by first drawing a line through $Q$ parallel to the field-resistance line $OL$ and intersecting the no-load characteristic at points $Q'$

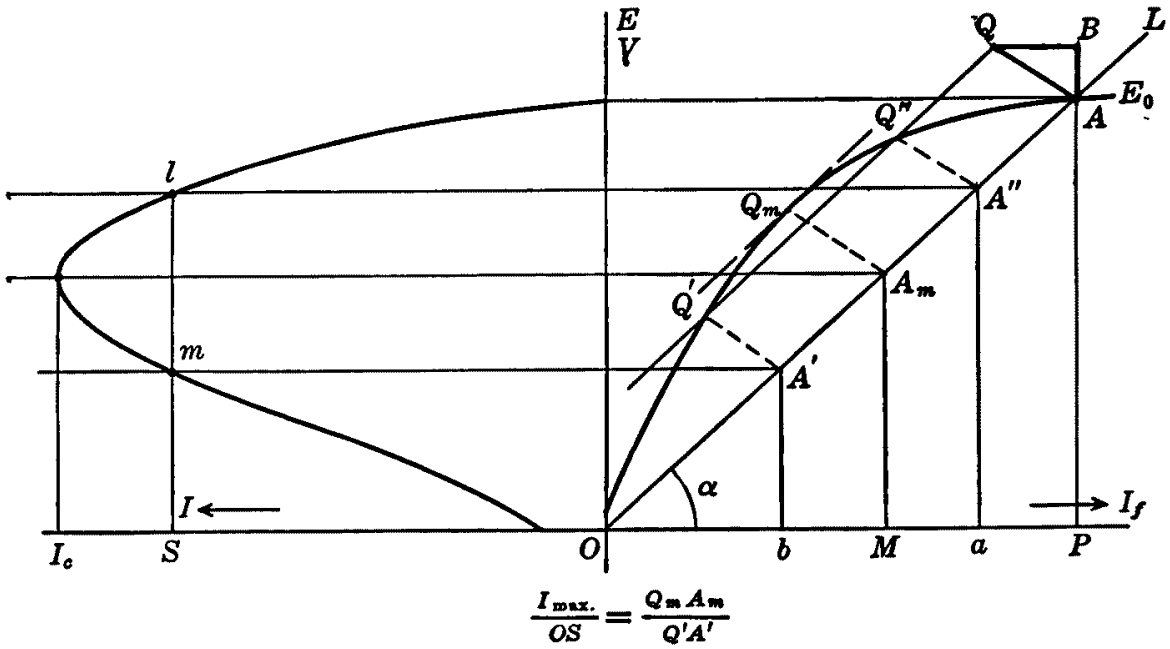


FIG. 7–14. Construction of the external characteristic of a d-c shunt generator from its no-load characteristic and field-resistance line.

and $Q''$, and then by drawing 2 lines $Q'A'$ and $Q''A''$ parallel to $AQ$. $A''a$ and $A'b$ are the two terminal voltages which correspond to the current $OS$. In the left part of Fig. 7–14 draw $Sl = A''a$ and $Sm = A'b$.

With the assumption that $M'_d = QB$ is proportional to $I$, other $ABQ$ triangles may be constructed, and corresponding values of terminal voltages determined and plotted. There will be one critical or maximum value of armature current which lies on the tangent to the no-load characteristic parallel to the field resistance line. This is shown at point $Q_m$, producing the terminal voltage $MA_m$.

The construction shown above is correct only for the upper part of the external characteristic. This is due to the fact that the armature reaction is assumed to be the same at low saturation as at high saturation. Actually, the maximum current is larger than that found in Fig. 7–14.

**Example 3.** The machine used in Examples 1 and 2 will not operate satisfactorily at 240 volts, as a shunt generator, because of the large effect of armature reaction. If we assume the armature reaction completely compensated for by a compensating winding (Art. 9–6), i.e., $M'_d = 0$, the operation as a shunt generator will be improved. Let $V = 240$ at no-load (Fig. 7–6a), $I_f = 4.38$, so that the total

field circuit resistance will be $240/4.38 = 54.8$, which requires a field rheostat of $54.8 - 47.9 = 6.9$ ohms in series with the shunt field winding. The field resistance line is $OAL$. In accordance with the method of Fig. 7–14, $P_1A = 240$ is the no-load terminal voltage and $OP_1$ the no-load field current. Since the terminal voltage $V$ must lie along $OAL$, and since $\Sigma I_a r + 2 = 7.5$, it is only necessary to find where the vertical distance between the line $OA$ and the magnetization curve is 7.5. This will occur at 2 points; one at $A_3$ giving $V = 222$ volts, and one at $A_4$ giving $V = 50$ volts. For the point $A_3$ the regulation would be $\frac{240 - 222}{222} = 8.1\%$, which is an acceptable value.

(e) *The Regulation Curve.* The regulation curve showing the field current as a function of the load current for constant terminal voltage is the same as that of the separately-excited machine, because the voltage drop produced by the field current is very small and, in comparison with the voltage drop caused by the load current, can be neglected.

(f) *Influence of Speed on the External Characteristic.* In Fig. 7–11b, curve $A(n_n)$ is the no-load characteristic at rated speed, and $OL$ is the field-resistance line. The external characteristic has been determined for rated speed, and it is to be determined at speed $n'$. Draw the no-load characteristic for speed $n'$ shown as $A'(n')$. The point $T_1$ is then the no-load voltage for the shunt generator at the speed $n'$. With the aid of the new no-load characteristic $A'(n')$ and the field resistance line $OL$ determine the external characteristic as explained in section (d). It will be observed in this case that the % regulation will be a larger value at the lower speed. If, however, the same no-load voltage were obtained at the lower speed $n'$, as at rated speed $n_n$ (by lowering the field resistance), then the regulation will be improved over its value at rated speed.

**7–6. The Cumulative Compound Generator.** (a) *The No-load Characteristic.* This characteristic of the cumulative compound generator is the same as that of the shunt generator, for at no-load the series winding is not effective.

(b) *The External Characteristic.* The characteristic features of the cumulative compound generator can be seen in its external characteristic (Fig. 7–15). The resistance drop in the armature winding and under the brushes ($\Sigma Ir + 2\Delta V$), as well as the armature reaction, act to decrease the terminal voltage with increasing load current. However, the mmf of the series winding and the flux increase with increasing load current and compensate in part or entirely for the resistance drop as well as the armature reaction. In Fig. 7–15 the mmf of the series winding predominates between $A$ and $B$ and consequently the terminal voltage is greater than the no-load voltage $OA$. For load currents greater than $OB$, the resistance drop and armature reaction predominate and the terminal voltage is less than that at no-load ($OA$). Between $A$ and $B$ the machine is overcompounded, at $B$ it is flat-compounded, and for greater currents it is undercompounded.

By a suitable adjustment of the mmf of the series winding, it is possible to obtain an external characteristic in which the terminal voltage at rated load is equal to that at no-load (regulation $\epsilon = 0$) or greater than that at no-load. If the no-load and full-load voltages are equal, the generator is said to be flat-compounded.

The series field mmf necessary to make the terminal voltage at a certain load current $I'$ equal to the no-load voltage can be determined in the following way: In Fig. 7–16a let the curve $OAQ'Q''$ be the no-load characteristic

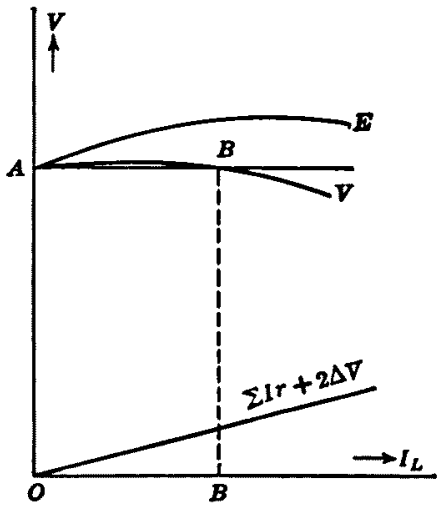


FIG. 7–15. External characteristic of a cumulative compound generator.

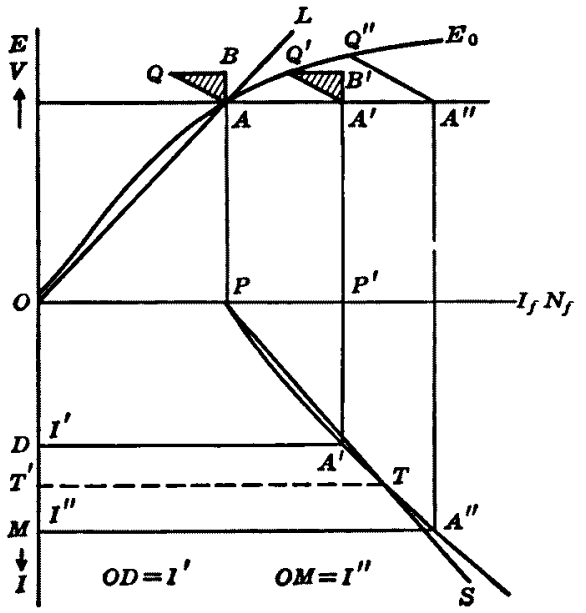


FIG. 7–16a. Determination of the series field ampere turns for a cumulative compound generator.

and $OL$ the field-resistance line. $AP$ is then the terminal voltage and $OP$ the shunt field mmf at no load. For the load current $I'$, make

$$AB = \Sigma I'r + 2\Delta V$$

and

$$BQ = M_d$$

In order that the terminal voltage shall be the same at the load current $I'$ as at no-load, the induced emf of the generator must be equal to $PB$ and the field mmf must be increased by the amount $BQ$ to compensate for the armature reaction. The series field mmf can be found by moving the triangle $ABQ$ to the right until it assumes the position $A'B'Q'$ at which $Q'$ lies on the no-load characteristic. $AA'$ is then the series field mmf necessary to obtain the voltage $PA$ at the load current $I'$. If the assumption is made that $M_d$ is proportional to the armature current, then for other values of load, other triangles, such as the one having the hypotenuse $A''Q''$, may be constructed, and corresponding values of series field mmf, such as $AA''$, be determined. In the lower part of Fig. 7–16a the series field mmf necessary for constant

terminal voltage is represented as a function of the load current. It is the curve $PA'A''$. Since the series field turns are fixed, the series field winding is only able to produce an mmf which varies linearly with the load current. If this linear mmf is chosen to be the line $PS$, then the terminal voltage $V$ will be equal to the no-load voltage only for the intersection point $T$, i.e., only for the load current $OT'$. For load currents smaller than $OT'$ the machine will be overcompounded; for load current larger than $OT'$, it will be undercompounded. The fact that the series field can produce only a linear mmf as a function of the load current, while a non-linear curve is necessary, explains why the external characteristic of the compound generator is not a straight line.

**Example 4.** The machine of Example 1 is to be flat-compounded at 240 volts. How many series turns per pole are required? Assume that the series field has a resistance of 0.0022 ohm. Then the total $\Sigma r = 0.0075$ ohm, and $\Sigma Ir + 2 = 10$ volts

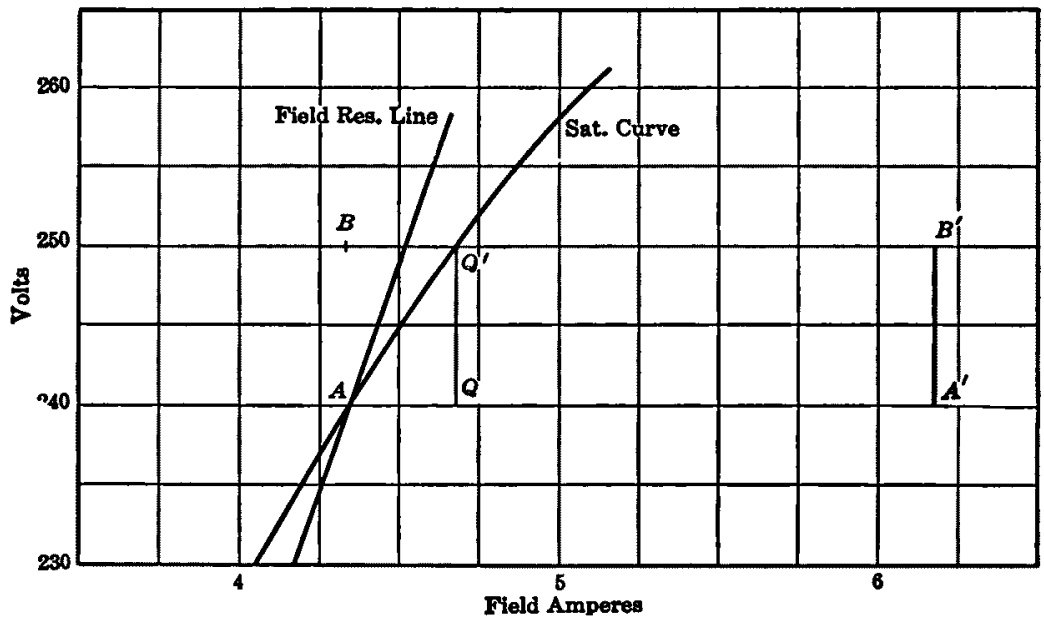


FIG. 7–16b. No-load characteristic for Example 4.

at full load. Lay off $AB = 10$ volts (Fig. 7–16b) so that the induced emf is 250 volts. With no armature reaction, the added field $AT$ would be .

$$BQ' \times 1064 = AQ \times 1064 = 0.27 \times 1064 = 277$$

However, the armature reaction $M'_d = 1.5$ still must be overcome by additional field mmf of $M'_d = QA' = 1.5$ amp, or $1.5 \times 1064 = 1600$ AT. Therefore, the total mmf to be supplied by the series field is $AA' \times 1064 = 1877$. The number of series turns required is $1877/1042 = 1.80$ turns. Therefore, 2.0 turns would be used. The machine actually was built with 2 series turns per pole.

In order to determine the external characteristic of the cumulative compound generator, consider Fig. 7–17. The parallelogram $QQ'A'A$ is the

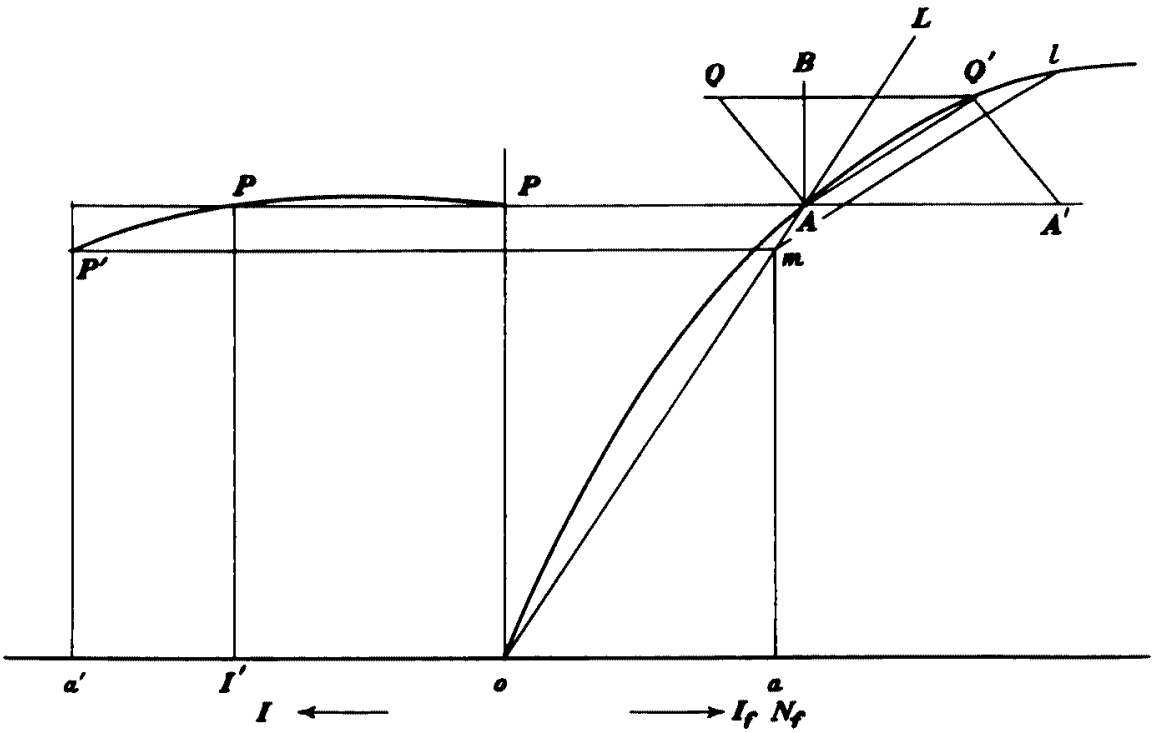


FIG. 7–17. Compound generator. External characteristic.

same as in Fig. 7–16a, i.e., for a certain current $I'$ at which the load voltage is equal to the no-load voltage,

$$AB = \Sigma I' r + 2\Delta V$$

$$BQ = M_d$$

$$AA' = QQ' = \text{mmf of the series field } (M_s)$$

and

$$BQ' = QQ' - BQ = M_s - M_d$$

With the aid of the no-load characteristic, the field-resistance line $OL$, and the triangle $ABQ'$, determine the external characteristic in the same manner as for the shunt generator. Note that the triangle $ABQ'$ in Fig. 7–17 is the same as triangle $ABQ$ of Fig. 7–14, except that it is drawn to the right of the vertical line $AB$ because $BQ'$ is a magnetizing mmf and not a demagnetizing mmf as $BQ$ is in Fig. 7–14. If the line $lm$ is drawn parallel to $AQ'$ between the no-load characteristic and the field-resistance line $OL$, then $ma = a'P'$ is the terminal voltage for the current

$$Oa' = I' \frac{ml}{AQ'}$$

**7–7. Parallel Connection and Operation of D-c Generators.** Most of the d-c generators employed are either shunt or cumulative compound machines.

If a shunt-wound or cumulative compound generator is to be connected in parallel with the other generators which are already in operation, it is first necessary to adjust the field current so that its terminal voltage is the same as that of the other generators. The armature is then connected to the bus-bars in such a manner that its positive terminal is connected to the positive bus-bar and its negative terminal to the negative bus-bar. The voltage of the incoming generator and the generators already on the bus-bars are then in opposition and equal so that no current flows in the series circuit between the machines when the switch is closed; when first connected in this manner, the incoming machine delivers no current.

If its field current is now increased so that the induced emf is greater than the terminal (line) voltage, the armature then delivers a current of such magnitude that the sum of the terminal voltage, the resistance drop in the armature and other windings, and the resistance drop under the brushes is equal to the emf induced by the resultant flux (Eq. 7–2a) and the system is then in equilibrium. As the field current of the generator is increased, the current output of its armature is also increased.

*By variation of the excitation of generators operating in parallel, it is possible to divide the load between the machines in practically any manner desired.*

It is not necessary that generators connected to operate in parallel shall have the same kw ratings. It is only essential that the total load be divided among all generators in proportion to their ratings. Fig. 7–18 shows the external characteristics $a$ and $b$ of 2 shunt generators. To the common voltage $V$ there corresponds the load current $I_a$ in generator $a$ and the load current $I_b$ in generator $b$. On the axis of abscissa is indicated the percentage of full-load current for each armature. The generators, because of the different shapes of their external characteristics, deliver different percentages of their full loads. It follows from Fig. 7–18 that, for proportional division of the load, the external characteristics must be identical if they are plotted with percentage of full-load current as abscissa.

The division of current between two generators operating in parallel can also be analyzed as follows:

Eq. 7–2b (omitting the constant voltage drop $2\Delta V$) gives $V = E - Ir$ where $Ir$ is the voltage drop in the armature winding.

For two generators in parallel, let $E_1$ and $E_2$ be the emf's of each machine, $r_1$ and $r_2$ their armature resistances, $I_1$ and $I_2$ the armature currents of each machine respectively, and $I$ the total current delivered to the common load. Neglecting the field currents of each machine, we have

$$I = I_1 + I_2; \text{ also } V = E_1 - I_1 r_1 = E_2 - I_2 r_2$$

Since $I_1 = I - I_2$, we may write

$$E_1 - r_1(I - I_2) = E_2 - I_2 r_2$$

Solving the equation for $I_2$ gives

$$I_2 = \frac{E_2 - E_1}{r_2 + r_1} + I\frac{r_1}{r_2 + r_1}$$

and

$$I_1 = \frac{E_1 - E_2}{r_2 + r_1} + I\frac{r_2}{r_2 + r_1}$$

From these equations it is seen that the current delivered by each machine may be considered to have two components. The one component (the first term on the right) is, in each case, due to a difference between the generated emf's $E_1$ and $E_2$. Therefore, this component may be adjusted by varying the relative value of $E_1$ and $E_2$. At no load ($I = 0$), there will be equal currents in

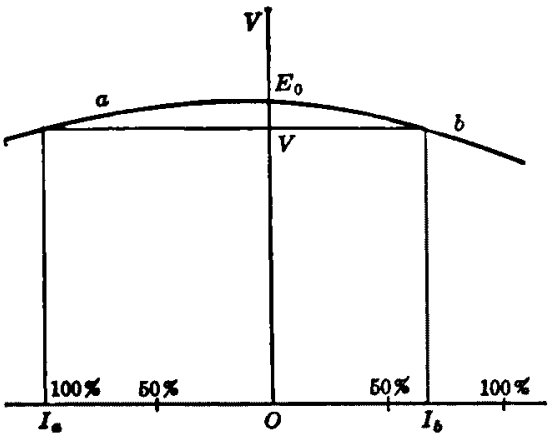


FIG. 7–18. Current distribution between 2 shunt generators operating in parallel.

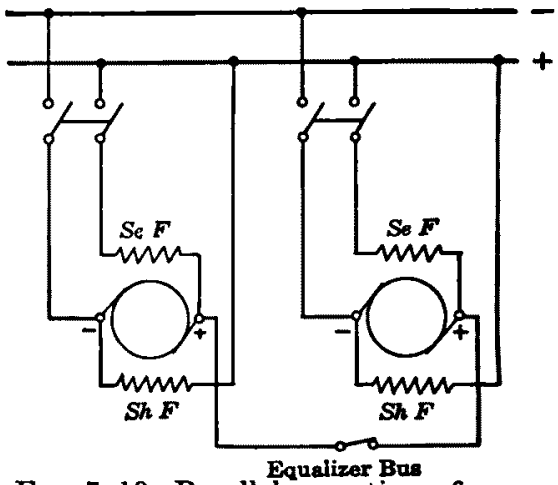


FIG. 7–19. Parallel operation of cumulative compound generators—Equalizer bus.

each machine. If each machine is to carry zero current when $I = 0$, then $E_1$ must equal $E_2$. If $E_1 \neq E_2$, a circulating current will flow between the two machines and one machine will act as a generator and the other as a motor. If $E_1 > E_2$, at $I = 0$, then machine No. 1 is the generator.

If $I \neq 0$, and $E_1 = E_2$, the currents will divide between the machines inversely proportional to the armature resistances. Thus it is seen that the division of current under load may be controlled by adjusting the emf's of the machines.

The parallel operation of cumulative compound generators is not possible without a special connection. Suppose in the case of cumulative compound generators operating in parallel that the shunt field excitation of one machine is increased somewhat. In order to restore voltage equilibrium in the armature of this machine, its armature current must be increased. However, if the armature current increases, the effect of the series field winding increases and disturbs the voltage equilibrium more and the armature current must,

in turn, increase still more. In this manner very slight variations in the shunt field circuit produce great variations in the distribution of the load current.

In order to stabilize the operation of cumulative compound generators operating in parallel, the series field windings of the machines are connected by means of an *equalizer bus* as shown in Fig. 7–19 for 2 generators. This connection places the series field windings in parallel with each other so that the voltage drop across the series fields of all generators is the same. Therefore, the line current delivered by all generators operating in parallel divides itself among the individual series field windings so that their currents are inversely proportional to their resistances; if the generators are identical, the current is divided equally among the series field windings.

If the armature current of any generator now is increased or decreased, by changing its shunt field excitation, the current in all the series field windings and the armature current of all other generators also will be increased or decreased since the voltage drop across the series field windings correspondingly increases or decreases. The equalizer bus thus enables all generators operating in parallel to take part in any change in the load on the bus-bars.

There is another reason why the equalizer bus may not be omitted: If the speed of one of the prime movers is suddenly reduced, the generator may change the direction of its emf by a reversal of current and act as a short circuit across the line. This action is prevented by the equalizer bus.

When a cumulative compound generator has to be paralleled with other cumulative compound generators, the equalizer switch (Fig. 7–19) has to be closed first or simultaneously with the armature switch.

Shunt generators in parallel are inherently stable due to the drooping form of their external characteristic. If a shunt generator drops its load, its voltage automatically rises, and vice versa. Any tendency to change the load by one machine and shift it to the other machine is neutralized by this change in the voltage. The balance of voltage (Eq. 7–2a) restores the original conditions.

If shunt generators are operating in parallel and a sudden increment of load is placed on the bus-bars, most of the added load will be taken by the generator which is operating with the lowest voltage drop: since the terminal voltage of all generators, in consequence of the added load, must decrease by the same amount, the generator with the least armature resistance produces this drop with the greatest current. In the case of cumulative compound generators operating in parallel the equalizer bus serves to divide the increment of load uniformly among the individual generators.

**7–8. Applications of the Different Types of Generators.** (a) *Separately Excited Generator and Shunt Generator.* The external characteristic of the separately excited as well as of the shunt generator (Figs. 7–4 and 7–13) shows that both machines have an inherent tendency to regulate for *nearly* constant

voltage. The regulation, i.e., the voltage drop between no-load and full load, is small in both types of generators. Since the separately excited generator needs a separate source for excitation, whereas the shunt generator is self-excited, the separately excited generator is used mainly in laboratory and commercial testing and in special regulation sets. The shunt generator is suitable for constant voltage circuits where the load is close to the generator and there is no large voltage drop in the line resistance. For example, a shunt generator may be used as an exciter for the field circuit of an alternator, for charging batteries, for supplying current to heating devices, etc.

(b) *Cumulative Compound Generator.* The cumulative compound generator is the most widely used d-c generator. Its external characteristic (Fig. 7–15) adapts it to all classes of service which require constant voltage at the point of application of the load. The shape of the external characteristic usually can be made such as to compensate for the voltage drop in the line resistance. The cumulative compound generator is used for motor drives which require d-c supply at constant voltage, for supplying current to incandescent lamps, for heavy power service such as electric railways, etc.

(c) *Differential Compound Generator.* This type of generator has an external characteristic similar to that of a shunt generator which has a large demagnetizing armature reaction. It is used in arc welding where a larger voltage drop is desirable when the current increases, in connection with electrically operated shovels where the motor may stall, etc.

(d) *Series Generator.* The external characteristic of the series generator (Fig. 7–8) shows that its voltage increases with increasing load. This makes the series generator suitable only for special purposes. For example, it is used as voltage booster in certain types of distribution systems, particularly in railway service.

## PROBLEMS

**1.** How much power is developed in the armature winding in Example 1 (p. 89)?

**2.** If the rotational loss, i.e., the sum of iron, friction and windage losses, in Example 1 is 3.5 kw, how much torque is supplied at full load for a field current of 7.2 amp?

NOTE: Before beginning the next group of problems, plot the no-load characteristic of the machine of Example 1 and Problem 3, using shunt field current as abscissa:

| | | | | | | | | | | |
|---|---|---|---|---|---|---|---|---|---|---|
| $E_0$ | 50 | 100 | 150 | 180 | 228 | 240 | 265 | 285 | 300 | 310 |
| $I_f$ | 0.8 | 1.6 | 2.38 | 2.92 | 4.0 | 4.38 | 5.28 | 6.25 | 7.2 | 7.9 |

**3.** If the armature current in Example 1 becomes 1800 amp, what will be the full-load voltage and the voltage regulation when the field current is 7.2 amp?

**4.** The machine of Example 1 operates as a shunt generator. The speed is raised to 1600 rpm. (a) What is the maximum no-load voltage obtainable? (b) What must be the resistance of the field rheostat to obtain a no-load voltage of 350 volts at 1600 rpm?

**5.** If the machine referred to in Problem 4 were to be run at 800 rpm, what would be the no-load voltage?

**6.** If the machine referred to in Problem 4 operates at 1600 rpm, and with the field rheostat set at 12 ohms, what will be the no-load terminal voltage?

**7.** The machine of Example 1 is operating (uncompensated) separately excited, at a no-load voltage of 250 and at 1200 rpm. What will be the terminal voltage for an armature current of 500 amp?

**8.** Construct the regulation curve (see Fig. 7–6b and 7–6c) for the machine of Problem 7 for: (a) constant voltage of 240; (b) constant voltage of 260. In each case get points for armature currents of 200, 400, 600, 800, 1000, and 1200 amp.

**9.** Referring to Example 3, determine the terminal voltage for armature currents of 1300 and 500 amp.

**10.** The following data apply to a d-c generator: 6 poles, 750 rpm, 600 volts, 942 amp, 565 kw, shunt field winding resistance 25.2 ohms at 75° C, commutating plus compensating field winding resistance 0.00602, armature resistance 0.01083. The armature has a simple lap winding, 1 turn per element, 87 slots, 8 conductors per slot, 2 layers (4 conductors top and bottom), 348 commutator bars, coil sides in slots 1 and 15 (chording $\frac{1}{2}$ slot). The shunt field has 924 turns per coil, commutating field $7\frac{1}{2}$ turns per coil, compensating field 5 turns per pole. The no-load characteristic data are:

| $E_0$ | 210 | 300 | 400 | 500 | 600 | 700 | 750 | 800 |
|---|---|---|---|---|---|---|---|---|
| $I_f$ | 1.6 | 2.42 | 3.55 | 4.9 | 7.2 | 11.5 | 14.5 | 18 |

Assuming that the compensation is complete, determine: (a) resistance in field rheostat for shunt excitation, at rated load, 600 volts, 942 amp, (b) the no-load voltage for this rheostat setting, (c) the % voltage regulation.

**11.** Repeat Problem 10 for speeds of 900 and 600 rpm. Compare results and explain why the results are different.

**12.** For the machine of Problem 10, the effective length of the armature $l_e$ is 10.9 in. and the equivalent pole arc $b_e$ is 9.7 in. Determine: (a) the air-gap flux per pole, (b) the air-gap density. (See Eq. 5–5).

**13.** The machine of Problem 10 has $2\frac{1}{2}$ turns per pole placed on a series coil, so that the total resistance of this series winding is 0.001 ohm. At speeds of 900, 750, and 600 rpm, the no-load voltage is adjusted to be 600 volts. What will be the full-load voltage in each case?

**14.** A compensated, interpole cumulative compound generator has 900 shunt turns and 15 series turns per pole, a full-load armature current of 72 amp, a no-load voltage of 300, and the resistance of the armature plus series field plus interpole winding plus compensating winding is 0.194 ohm. The data for the no-load characteristic are:

| $E_0$ | 192 | 256 | 298 | 338 | 365 | 383 | 398 | 410 | 421 | 430 |
|---|---|---|---|---|---|---|---|---|---|---|
| $I_f$ | 1 | 1.5 | 2 | 3 | 4 | 5 | 6 | 7 | 8 | 9 |

taken at 1150 rpm. Determine: (a) resistance of the shunt field circuit, (b) shunt ampere turns per pole at no-load, (c) series ampere turns per pole at full-load, (d) terminal voltage at full-load, (e) shunt field current at full-load, (f) total field AT per pole at full-load.

**15.** If the no-load voltage of Problem 14 is adjusted to be 360 volts, what will be the full-load voltage? For what no-load voltage will the machine be flat-compounded?

**16.** If the machine of Problem 14 operates at 920 rpm, with a no-load voltage of 300, determine: (a) total resistance of shunt field circuit, (b) full-load voltage.

**17.** Assume the machine of Problem 16 operates as a shunt generator, without the series field, at 1150 rpm, with a no-load voltage of 300, and that the series field resistance is 0.01 ohm. What will be the full-load voltage? If the speed were 920 and the no-load voltage 300, what will be the full-load voltage?

**18.** The machine of Problem 14 is to be flat-compounded at 300 volts. Determine the resistance of a diverter (shunt) for the series field. The series field resistance is 0.01 ohm.

**19.** The machine of Problem 17 now operates at 1150 rpm and a total shunt field circuit resistance of 52.8 ohms. Determine: (a) no-load terminal voltage, (b) full-load terminal voltage.

**20.** A cumulative compound generator is operated at no-load, with a shunt field current of 1.7 amp, and with 95 amp through the series winding, producing a voltage of 200 at the terminals. If the series field current is reversed, a shunt field current of 2.3 amp is required to keep the terminal voltage at 200. If the shunt field has 1400 turns per pole, how many series turns per pole are there?

**21.** The no-load voltage of a separately excited generator is 220 and the full-load voltage is 193. The armature resistance is 0.086 ohm, and the armature current is 175 amp. What is the % reduction in flux from no-load to full-load?

**22.** A 250-kw and a 750-kw, 550-volt shunt generator operate in parallel, delivering a total load of 1500 amp. The voltage regulation of the smaller machine is 0.058 in. per unit, and for the larger one 0.035. Assume the external characteristic curves are straight lines. Determine: (a) the current delivered by each machine, (b) the terminal voltage.

**23.** Two overcompounded generators operate in parallel. The external characteristic curve of machine $A$ is:

| | | | | | | | |
|---|---|---|---|---|---|---|---|
| $V$ | 220 | 225.7 | 231.2 | 235.8 | 239.7 | 243 | 245.7 |
| $I$ | 0 | 10 | 20 | 30 | 40 | 50 | 60, |

and for $B$ is

| | | | | | | | |
|---|---|---|---|---|---|---|---|
| $V$ | 220 | 227 | 233.3 | 238.7 | 243 | 246.2 | 248 |
| $I$ | 0 | 20 | 40 | 60 | 80 | 100 | 120. |

If these machines deliver a total load of 100 amp, what current will each deliver, and at what terminal voltage? When the load is such that the terminal voltage is 245, what current is each delivering?

**24.** Assume that by suitable adjustment of speed and of field current the external characteristic of $B$ of Problem 23 is moved down parallel to itself, so that at $V = 240$ volts machine $B$ takes 2 times as much load as $A$. What will be the current delivered by each machine? The adjustment of machine $A$ is unchanged.

**25.** With the adjustment of Problem 24 how much current will each machine deliver to a total load of 100 amp, and of 50 amp, and what will be the voltage at each of these loads?

**26.** Two shunt generators, $A$ and $B$, having straight-line external characteristics, are operated in parallel, and each has its no-load voltage adjusted at 240 before being paralleled. $A$ is rated 375 kw at 230 volts, $B$ rated 100 kw at 220 volts. For a total load of 400 kw, determine: (a) terminal voltage, (b) kw of each machine, (c) current of each machine.

# *Chapter 8*

## THE D-C MOTOR

**8–1. Voltage and Torque Equation of the D-c Motor.** In the generator, induced emf $E$, terminal voltage $V$, and armature current $I_a$ are all in the same direction. In a motor the terminal voltage $V$ and the armature current $I_a$ are in the same direction but opposite to the induced emf $E$. This will be explained by means of Figs. 8–1 and 8–2.

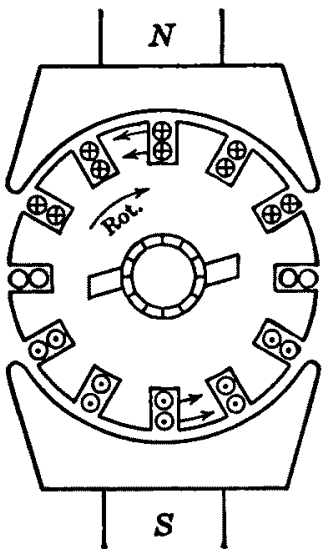


FIG. 8–1. Direction of current and induced emf in a generator.

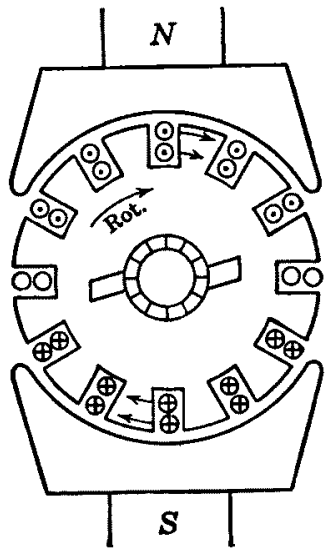


FIG. 8–2. Direction of current and induced emf in a motor.

Fig. 8–1 refers to a generator. The armature is driven in a clockwise direction. For balance of torques, the electromagnetic torque produced by the armature must have a counterclockwise direction. This can be accomplished only by currents which have the directions shown in Fig. 8–1, i.e., by currents which flow into the plane of the page under the N-pole and out of the plane under the S-pole. According to Faraday's law (see Fig. 1–2), the emf's induced in the armature conductors have the same directions as the currents shown in Fig. 8–1. Thus, in a generator, induced emf $E$ and armature current $I_a$ are in the same direction.

Fig. 8–2 refers to a motor for which it is assumed that the armature

rotates in a clockwise direction. Since the electromagnetic torque establishes the direction of rotation of the armature of a motor, this torque must also be in a clockwise direction. This can be accomplished only by currents which have the directions shown in Fig. 8–2, i.e., by currents which flow out of the plane of the page under the N-pole and flow into the plane under the S-pole. The direction of rotation of the armature is the same in Figs. 8–1 and 8–2 and, therefore, the direction of the induced emf's must be the same, namely, in the direction of the currents in Fig. 8–1 and opposite to the direction of the currents in Fig. 8–2. Thus, in a motor, induced emf $E$ and armature current $I_a$ are in opposition; the same is true of the induced emf $E$ and terminal voltage $V$. For this reason $E$ is called a *counter-emf* in the motor.

Thus applying Kirchhoff's law to the motor (see Eq. 7–1), we have

$$V - E = (\Sigma Ir + 2\Delta V) \tag{8–1a}$$

or

$$V = E + (\Sigma Ir + 2\Delta V) \tag{8–1b}$$

The difference of the signs of $V$ and $E$ in Eq. 8–1a also shows why the emf $E$ is called counter-emf in a motor.

The magnitude of the induced emf $E$ for the motor is given by the same equation as for the generator (Eq. 7–3):

$$E = Z\frac{p}{a}\frac{n}{60}\Phi 10^{-8} = C_1 n\Phi \tag{8–2}$$

where $C_1$ is a constant quantity for a given machine.

The equation for the torque is (Eq. 4–6):

$$T = 0.1174 \times 10^{-8}\frac{p}{a} Z\Phi I_a \text{ lb-ft} \tag{8–3}$$

or (Eqs. 4–7 and 4–8)

$$T = C_2\Phi I_a = 7.04C_1\Phi I_a = \frac{7.04EI_a}{n} \text{ lb-ft} \tag{8–4}$$

where $C_2 = 7.04C_1$ is a constant quantity for a given machine.

The armature current of the d-c motor, as in all other electric motors, *adjusts itself* so as to produce a balance of torques, i.e., so as to make the developed torque equal to the opposing torque. This opposing torque is equal to the sum of the load torque and the loss torque of the rotating armature. How this adjustment of $I_a$ is accomplished may be seen from Eq. 8–4 and Eq. 8–1b. From Eq. 8–4 it is noted that the product $\Phi I_a$ must adjust itself to the opposing torque $T$. If $\Phi$ is constant, as is practically the case in the shunt-motor, then $I_a$ will vary directly with the torque. If $\Phi$ varies with $I_a$, as it does in the series motor and the compound motor, then $I_a$ will not vary linearly with $T$. The factors which will cause $I_a$ to change

may be found if Eq. 8–1b is arranged as

$$I_a = \frac{V - E - 2\Delta V}{\Sigma r} = \frac{V - C_1 \Phi n - 2\Delta V}{\Sigma r}$$

If $I_a$ is to change, it can only be brought about through a variation in $\Phi$ or $n$, since the other factors are constant. In the shunt motor, since $\Phi$ is nearly constant, then $n$ must change in order for $I_a$ to change. If $I_a$ is to increase, as required for an increase in load torque then $n$ will decrease. In the series motor since $\Phi$ changes with $I_a$ the variation of speed with torque will be greater than in the shunt motor.

With a motor operating at rated power, the sum of the voltage drops $\Sigma I_a r + 2\Delta V$ is about 4 to 10% of the terminal voltage, with the larger value applicable to small motors.

Note that the torque given by Eq. 8–3 or Eq. 8–4 is the electromagnetic or *developed torque* of the machine. This torque must be distinguished from the *delivered torque*, i.e., the torque delivered to the shaft. This latter torque is smaller than the former by the loss torque.

If each term of Eq. 8–1b is multiplied by $I_a$, there results

$$VI_a = EI_a + \Sigma I_a^2 r + 2\Delta V I_a \tag{8–5}$$

In this equation, $VI_a$ is the power input to the armature, $\Sigma I_a^2 r$ is the copper loss in the armature and other series-connected windings, $2\Delta V I_a$ is the power loss in the brush contacts, and $EI_a$ is *the electromagnetic power* corresponding to the developed (electromagnetic) torque.

The electromagnetic power $E \times I_a$ and the developed (electromagnetic) torque are connected by a basic equation of mechanics (Eq. 1–26):

$$T = \frac{7.04 EI_a}{n} \text{ lb-ft} = 7.04 C_1 \Phi I_a \tag{8–6a}$$

or

$$T = \frac{5250 \text{ hp}}{n} = \frac{5250}{n} \frac{EI_a}{746} \text{ lb-ft} \tag{8–6b}$$

Eq. 8–6 can be verified readily by introducing in it the value of $E$ from Eq. 8–2: Eq. 8–3 for the torque is then obtained.

Combining Eq. 8–1 with Eq. 8–2, we obtain the speed of a motor:

$$n = \frac{V - (\Sigma I r + 2\Delta V)}{C_1 \Phi} = \frac{E}{C_1 \Phi} \tag{8–7}$$

**8–2. Characteristics of the Shunt Motor.** The flux $\Phi$ of the shunt motor is a function of the current in the shunt field winding, $I_f$:

$$\Phi = f(I_f) \tag{8–8}$$

*Starting the Shunt Motor.* When starting the motor the developed torque must be greater than the restraining torque of the load in order to provide an accelerating torque. As long as the developed torque is greater than the

load torque plus loss torque the armature will accelerate. The acceleration continues until developed torque and load torque plus loss torque are balanced;

From Eq. 8–1b, $I_a = \dfrac{V - E - 2\Delta V}{\Sigma r}$, it should be noted that $E$ is only a few % less than $V$, with the motor running under normal load. At standstill, $E = 0$, and hence

$$I_a = \frac{V - 2\Delta V}{\Sigma r} \text{ at standstill}$$

If $V$ were the rated value at standstill, a very large and damaging current would flow. To limit this current to a safe value of from 150–200% of rated current, the voltage applied to the armature must be reduced. This is accomplished by inserting a resistance in series with the armature. This resistance is gradually "cut out" as the motor comes up to speed.

**Example 1.** A 5-hp, 120-volt shunt motor has an armature resistance of 0.10 ohm, and a full-load armature current of 40 amp. Determine the value of the series resistance to add to the armature to limit the initial starting current to 150% of normal.

$I_a = 40 \times 1.5$ at starting; $V = 120$, the line voltage;

$$\Sigma r = \frac{120 - 2}{60} = 1.966 \text{ ohms.}$$

Therefore, a series resistance of $1.966 - 0.1 = 1.866$ would be required.

From Eq. 8–4, $T = 7.04 C_1 \Phi I_a$, it is observed that, in order for the starting to occur with the least value of $I_a$, it is necessary for $\Phi$ to be large; hence, in starting a shunt motor it is important to apply rated voltage to the field winding in order to produce the normal value of $\Phi$.

Eq. 8–7 shows that the speed varies inversely with the flux $\Phi$. If it should happen that *sufficient flux* $\Phi$ is not available (low field current), the motor may *accelerate to a very high speed* and the high mechanical stresses produced may cause it to fly apart. When starting a shunt motor, it therefore is not permissible to connect first the armature circuit and then the field circuit across the line. The field circuit must be excited first and then voltage impressed across the armature, or both circuits may be closed simultaneously. In order that the armature current at starting may not become too high, a starting resistance is placed in the armature circuit before the line voltage is applied. As the speed and counter-emf rise, the quantity $(\Sigma I_a r + 2\Delta V)$ decreases, the current $I_a$ decreases, and the starting resistance can be reduced. (See Chap. 13).

Fig. 8–3 shows the basic scheme for starting the shunt motor. One terminal of the field winding $a$ is connected directly to the power line, and the other terminal $b$ is connected to the line through a shunt rheostat $R_f$ and the starting resistance $R$. In this manner, both field and armature windings are

connected to the line at the same instant. The terminal *b* cannot be connected directly to the armature winding when starting, without including a part of the starting resistance. To connect the shunt field winding directly across the armature would result in a very low field flux, because the armature terminal voltage is very low at starting.

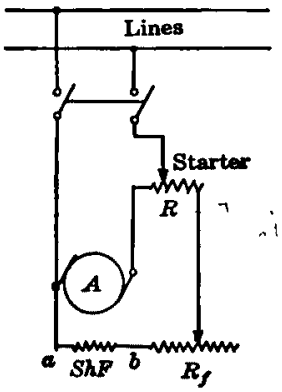


FIG. 8–3. Connections for starting a shunt motor.

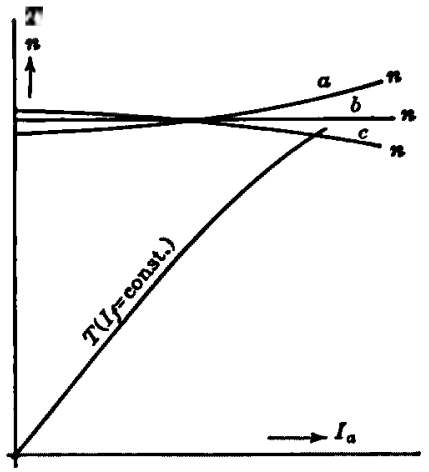


FIG. 8–4. Torque and speed of a shunt motor as a function of armature current for constant field current.

*The field winding should never be opened suddenly.* Since the field winding has a high self-inductance, a sudden breaking of this circuit may produce an emf of self-induction high enough to puncture the insulation. Therefore the connection of the field winding in parallel with the armature winding and a part of the starting resistance has another important advantage. When the connection in Fig. 8–3 is used and the motor is disconnected, the field circuit is not broken but always remains closed through the armature and a part of the starting resistance. Starting boxes are designed to accomplish this arrangement. (See Chap. 13).

Fig. 8–4 shows the speed of a shunt motor as a function of its armature current at a constant terminal voltage and for 3 different degrees of saturation (3 different field currents). Increasing the armature current increases both the armature reaction and the sum of the voltage drops. These quantities oppose each other in their effect on the speed of the motor. A larger demagnetizing armature reaction produces a smaller resultant flux, and consequently the speed must increase according to Eq. 8–7. A large voltage drop due to the resistance of armature and brushes means a lower counter-emf and therefore a lower speed. With increasing armature current, the speed of the shunt motor will vary according to curve *a* or curve *c*: If the armature reaction predominates, with increasing current, the speed follows curve *a*; if the voltage drops predominate, it follows curve *c*. For a particular excitation the above two effects may compensate each other approximately, and

the speed as a function of the armature current then becomes almost parallel to the axis of abscissae (curve *b*). The rising characteristic shown as *a* usually is not desirable, as it may lead to instability of operation.

According to Eq. 8–4 the torque of a motor is proportional to its armature current:

$$T = C_2 I_a \Phi.$$

For a constant field current the torque does not increase exactly linearly with the armature current, for as the latter increases, the armature reaction also increases and the resultant flux $\Phi$ decreases. Fig. 8–4 shows the developed torque curve for a constant field current. It deviates from a straight line because of the non-linearity of the magnetization curve.

Fig. 8–5 shows the armature current $I_a$ and efficiency $\eta$ as a function of the power output for constant field current and constant terminal voltage. Since the current and voltage drops increase with increasing power output, the counter-emf therefore decreases. It was shown above that the product $EI_a$ is a measure of the power output. Since the quantity $E$ decreases with increasing power output, the current $I_a$ must increase more than linearly with increasing power output.

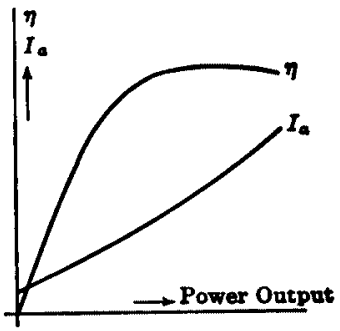


FIG. 8–5. Armature current and efficiency of a shunt motor as a function of power output for constant field current.

Fig. 8–4 shows that the shunt motor is essentially a constant-speed motor. Its developed torque as a function of the armature current is approximately linear over the normal operating range.

In determining the operating characteristics of the d-c motor, one of the important parameters is the no-load characteristic (the magnetization curve). Data for this curve may be determined either by computation (Chap. 5) or experimentally as described in Art. 7–5. In any case there will be a choice of units for the coordinates. Any of the following quantities may be used as ordinate: flux $\Phi$, or induced emf $E_0$ at some constant speed $n_0$, or $C_1\Phi = \dfrac{E_0}{n_0}$ (see Eq. 8–2); and for the abscissa: $I_f$ in the field winding (shunt or series), or the total field mmf in ampere-turns. The choice of coordinates will depend upon the particular use to be made of the curve. For most of the discussion to follow, the ordinate will be either $E_0$ at some constant speed $n_0$, or $C_1\Phi$, with $I_f$ or $N_f I_f$ as abscissae.

The torque as a function of armature current, for a constant field current, may be determined in the following manner. In Fig. 8–6, let the curve $OA'B$ be the magnetization curve, using $I_f$ as abscissa and $C_1\Phi$ as ordinate. The assumed constant field current is $OP$. The corresponding value of $C_1\Phi$ is $PB$ at no load. For the assumed value of armature current $I_a$, determine $M'_d$ and subtract this as $AP$ from $OP$. Then the effective field current for

this load is $OA = OP - AP$. The value of $C_1\Phi$ is now $AA'$. Since the developed torque is $T = 7.04 C_1 \Phi I_a$, it is now calculated as $7.04 \times (AA') \times I_a$. Assuming that $M'_d$ is directly proportional to $I_a$, then $T$ may be determined for other assumed values of $I_a$, and plotted, as in Fig. 8–4.

The speed as a function of $I_a$ for constant $I_f$ may be determined as follows: In Fig. 8–7 the curve $OFQ$ is the magnetization curve plotted with $E_0$ as

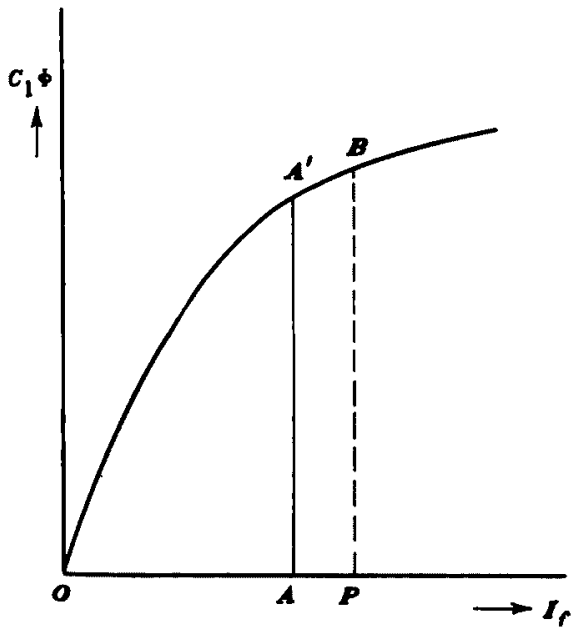


FIG. 8–6. Shunt motor. Determination of torque.

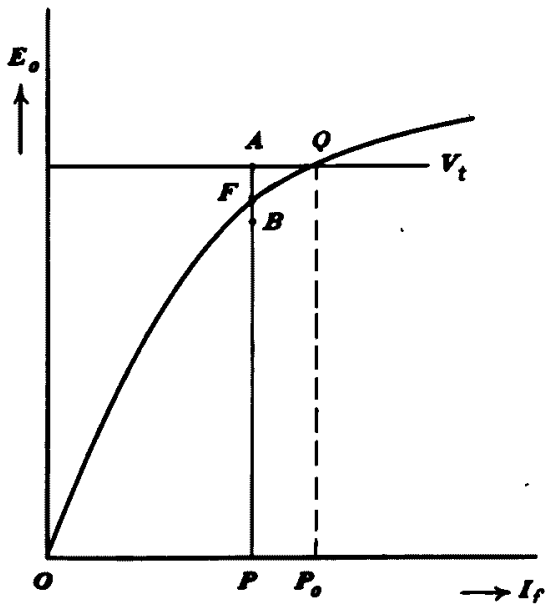


FIG. 8–7. Shunt motor. Determination of speed.

ordinate and $I_f$ as abscissa, and taken at the constant speed $n_0$ which is the no-load speed of the motor. The constant terminal voltage is $V_t = P_0Q$ and the constant field current is $I_f = \frac{V_t}{R_f} = OP_0$. At no load, the speed will be $n_0$.

For any assumed $I_a$ determine $M'_d = AQ = PP_0$. Then $OP$ is the effective field current and $PF$ would be the induced emf if the speed were constant at $n_0$. Also determine $\Sigma I_a r + 2\Delta V = AB$. Then the actual emf $E = V_t - AB = PB$. Therefore, the speed at the assumed value of $I_a$ will be

$$n_L = n_0 \times \frac{BP}{PF}$$

Assuming $M'_d$ to vary directly with $I_a$, the speed may be determined for other values of $I_a$, and the curve plotted, as in Fig. 8–4.

The speed could also have been calculated from Fig. 8–6 as follows: Having determined the value of $C_1\Phi$ as used in calculating the torque for any value of $I_a$, and also $E = V_t - (\Sigma I_a r + 2\Delta V)$, then $n_L = \frac{E}{C_1\Phi}$.

*Speed regulation* is defined as the ratio of the difference between no-load and

full-load speed to the full-load speed. Thus, the speed regulation in per cent is

$$\epsilon = 100 \frac{\text{no-load speed} - \text{full-load speed}}{\text{full-load speed}}$$

The speed regulation can be determined from the speed-armature current curve or the torque-speed curve.

**Example 2.** The data for the no-load characteristics of a 4-pole, 20-hp, 230-volt shunt motor, taken at 1800 rpm, are:

| $E_0$ | 75 | 110 | 140 | 168 | 188 | 204 | 218 | 231 | 240 | 262 | 268 |
|---|---|---|---|---|---|---|---|---|---|---|---|
| $I_f$ | 0.2 | 0.3 | 0.4 | 0.5 | 0.6 | 0.7 | 0.8 | 0.9 | 1.0 | 1.4 | 1.6 |

The combined resistance of armature and interpole winding at 75° C is 0.0814 ohm, the shunt winding has 2800 turns per pole, the total resistance of the shunt field winding circuit is 259 ohms, the full-load armature current is 76 amp, the demagnetizing effect of full-load armature current (expressed in terms of shunt field current) is $M'_d = 0.1$ amp. Determine (a) the full-load speed and (b) the full-load torque.

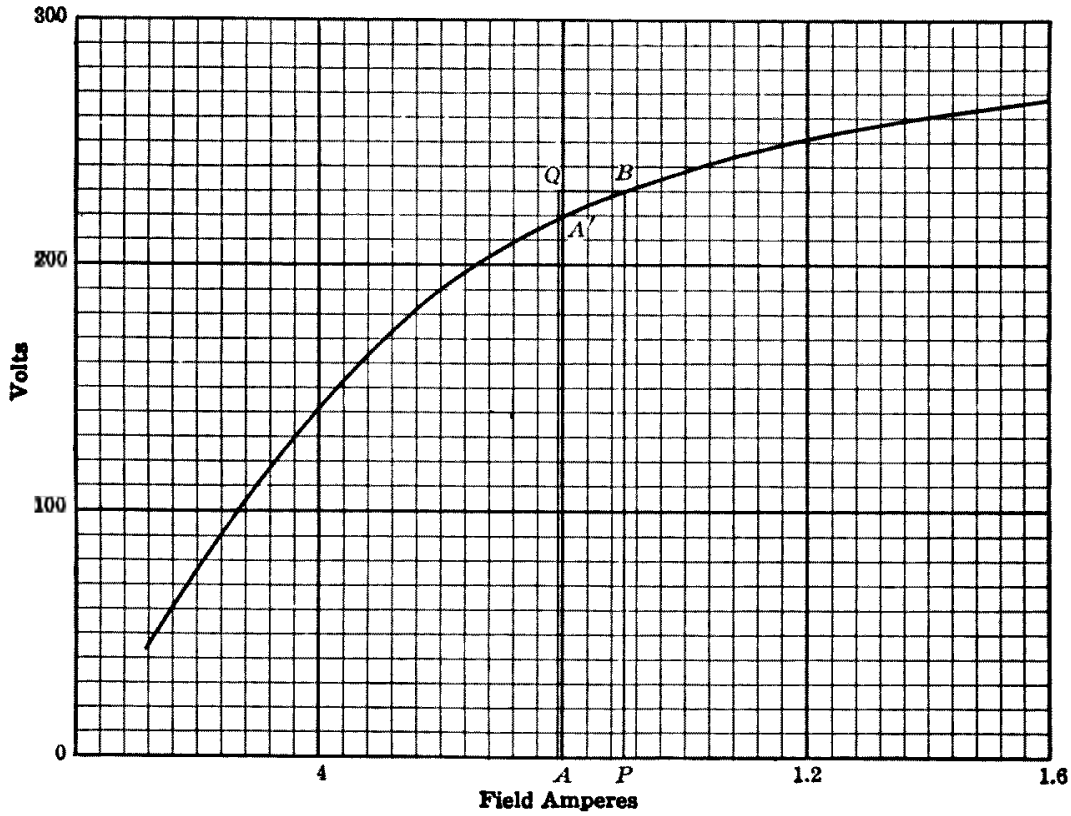


FIG. 8–7a. No-load characteristic for Example 2.

From the no-load characteristic, $I_f = 230/259 = 0.89 = OP$ (Fig. 8–7a), $E = 230$, and $C_1\Phi = 230/1800 = 0.1278$. The no-load speed, operating with $V = 230$ volts, will be 1800 rpm. At full-load current the effective field current is

$$0.89 - 0.1 = 0.79 = OA,$$

from the curve $C_1\Phi = 218 \div 1800 = 0.121$. The actual emf

$$E = 230 - (76 \times 0.0814 + 2) = 222.$$

Hence the speed at full load will be $n = E \div C_1\Phi = 222 \div 0.121 = 1834$ rpm. The torque $T = 7.04 C_1 \Phi I_a = 7.04 \times 0.121 \times 76 = 64.8$ lb-ft. It is seen that the full-load speed is higher than the no-load value. This is due to the effect of armature reaction in reducing the flux. This is equivalent, in effect, to the action of a differential compound motor. Since this is undesirable, it is usually overcome by a few series turns placed on the field poles, sometimes called the *stabilizing winding*.

**8–3. Characteristics of the Series Motor.** Eqs. (8–1) (8–2), and (8–7) also apply to the series motor. However, in place of Eq. 8–8 the equation

$$\Phi = f(I_a) \tag{8–9}$$

has to be applied, since the field and armature currents are the same in a series motor.

Fig. 8–8 shows the speed and torque of a series motor as a function of the armature current. Since the flux $\Phi$ is small for low values of armature current, the speed $n$ consequently must be high in order to satisfy Eq. 8–2. When $I_a$ is very small, the flux is also very small and the speed $n$ of the motor becomes so high that the machine may destroy itself. *A series motor should*

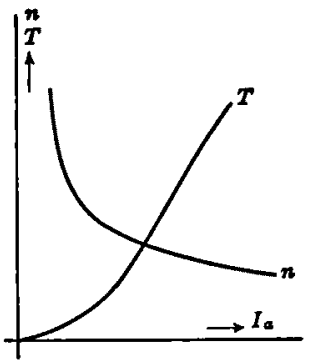


FIG. 8–8. Torque and speed curves of a series motor as a function of armature current.

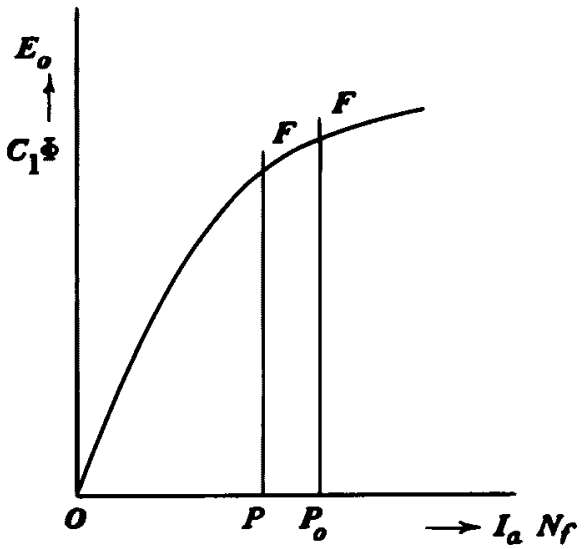


FIG. 8–9. Series motor. Determination of speed.

*never be connected to a line if there is any possibility of losing its entire load* (except in the case of fractional-horsepower motors). Even when starting the series motor, care must be taken to see that a certain opposing torque exists since at low currents the speed will assume a high value despite the starting resistance. While the speed of a shunt motor varies only a little with the armature current, the speed change of the series motor is very large.

For small values of armature current, the machine is not saturated and

the flux of the series motor is directly proportional to the armature current. Consequently, for small values of armature current, the torque increases as the square of the current (see Eq. 8–4). When the armature current is large and the machine is saturated, the flux is more nearly constant and the torque then varies nearly as the first power of the armature current. For still greater values of armature current, the flux decreases because of the armature reaction, and the torque, therefore, increases at a rate less than that of the armature current.

The developed torque of the series motor as a function of $I_a$ may be determined as follows: The curve $OFF_0$ in Fig. 8–9 is the no-load characteristic (magnetization curve) of the motor. The abscissa is the field mmf $I_aN_f$, and the ordinate is in units of $C_1\Phi$, as obtained from a no-load test. At any assumed value of $I_a$, such as full load, determine $I_aN_f = OP_0$, $M_d = P_0P$; then $OP = OP_0 - P_0P$ is the net mmf, and $PF = C_1\Phi$ at the current $I_a$. The torque is now calculated as $T = 7.04C_1\Phi I_a$. Also determine the emf as $E = V_t - (\Sigma I_a r + 2\Delta V)$. The speed may now be calculated from the relation (Eq. 8–7).

$$n = \frac{V_t - (\Sigma I_a r + 2\Delta V)}{C_1\Phi} = \frac{E}{C_1\Phi}$$

For other assumed values of $I_a$, the torque and speed may be determined in the same manner and plotted as in Fig. 8–8. In Eq. 8–7 for the speed, the flux $\Phi$ varies widely with load since $E$ is nearly equal to $V_t$. Therefore, the

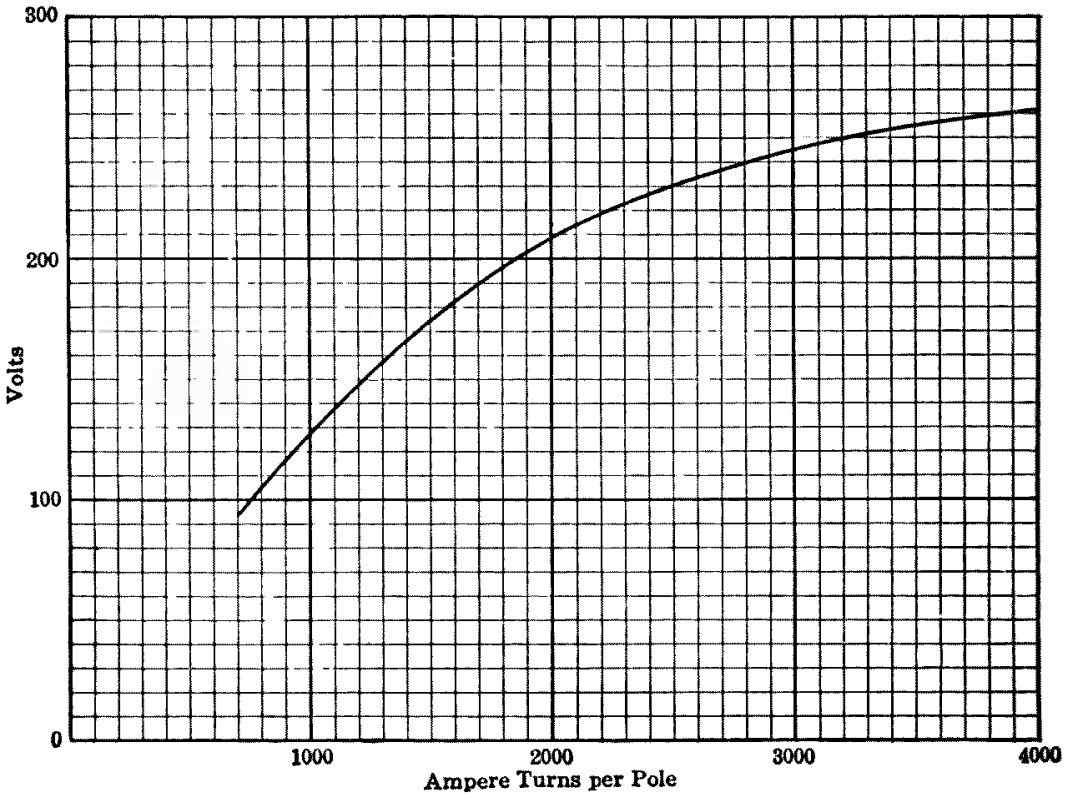


FIG. 8–9a. Ampere turns per pole.

speed of the series motor will vary widely with load due mainly to the variation in $C_1\Phi$.

**Example 3.** Assume that the motor of Example 2 had been designed as a series motor with 37.5 turns per pole, and that the resistance of the series field winding is 0.0636 ohm. Determine the speed and torque at full-load, half-load, and at 125% full-load current. Fig. 8–9a shows the no-load characteristic at 1800 rpm, using field-ampere turns as abscissa. At full-load current the armature reaction ampere-turns are $2800 \times 0.1 = 280$ (see Example 2). The effective AT per pole are

$$76 \times 37.5 - 280 = 2570.$$

From the curve (Fig. 8–9a), $E_0 = 233$. Therefore, $C_1\Phi = 233 \div 1800 = 0.1295$. Hence at full load the torque $T = 7.04 \times 0.1295 \times 76 = 69.2$ lb-ft. The emf generated at full load is $230 - 2 - 76 \times 0.155 = 217$. The speed will be $n = 217/0.1295 = 1675$ rpm. At half load the effective AT $= 38 \times 37.5 - 140 = 1285$, and from Fig. 8–9a,

$$E_0 = 148 \text{ or } C_1\Phi = 148/1800 = 0.0822.$$

The emf $E = 230 - 2 - 38 \times 0.155 = 222.5$. Therefore, $n = 222.5/0.0822 = 2710$ rpm and $T = 7.04 \times 0.0822 \times 38 = 22$ lb-ft. At 125% load the effective AT $= 3210$, $C_1\Phi = 248/1800 = 0.1377$, $E = 214.3$. Hence, $n = 214.3/0.1377 = 1555$ rpm at

$$T = 7.04 \times 0.1377 \times 95 = 92.2 \text{ lb-ft.}$$

**8–4. Characteristics of the Cumulative Compound Motor.** According to the relative strengths of the series and shunt field mmf's, the cumulative compound motor may exhibit characteristics approaching those of either the series or shunt motor. If the series motor is supplied with a shunt winding, the possibility of its running away at no load is avoided. If a shunt motor is supplied with a series winding, it is possible to obtain a speed almost independent of the load and therefore almost constant.

The variation of speed and developed torque of the cumulative compound motor as a function of armature current $I_a$ may be determined in a manner similar to that of the shunt and series motors. The curve in Fig. 8–10a is the no-load (magnetization) curve, showing the relation of the induced emf $E_0$ to the field mmf at the no-load speed of the motor $n_0$.

$V_t$ is the constant terminal voltage and $OP_0$ is the mmf of the shunt winding. For the long-shunt connection $OP_0$ is constant also. Make $P_0Q$ equal to the mmf of the series field winding for the assumed value of $I_a$; also make $PQ = M_d$; then $P_0P = P_0Q - PQ$ is the resultant mmf due to the current $I_a$ and $OP$ is the net or resultant mmf of the motor. $PF$ would then be the counter-emf if the speed were $n_0$. Now determine $AB = \Sigma I_a r_a + 2\Delta V$. Then since $E = V_t - (\Sigma I_a r + 2\Delta V)$, it will be represented on Fig. 8–10 as $PB$. Since for a given field mmf the armature emf is directly proportional to speed, the speed will be given by

$$n_L = n_0 \frac{BP}{PF}$$

For other values of $I_a$ the values of speed may be determined when $M_d = PQ$ is assumed to vary directly with $I_a$. The speed of the cumulative compound motor falls more rapidly with increasing $I_a$ than that of the shunt motor. With increasing $I_a$ the rate of decrease in speed becomes less and less as saturation of the magnetic circuit is approached. The speed-current characteristic will be greatly affected by the location of the point $F_0$ on the magnetization curve (Fig. 8–10a) as well as upon the relative number of turns on the two field windings.

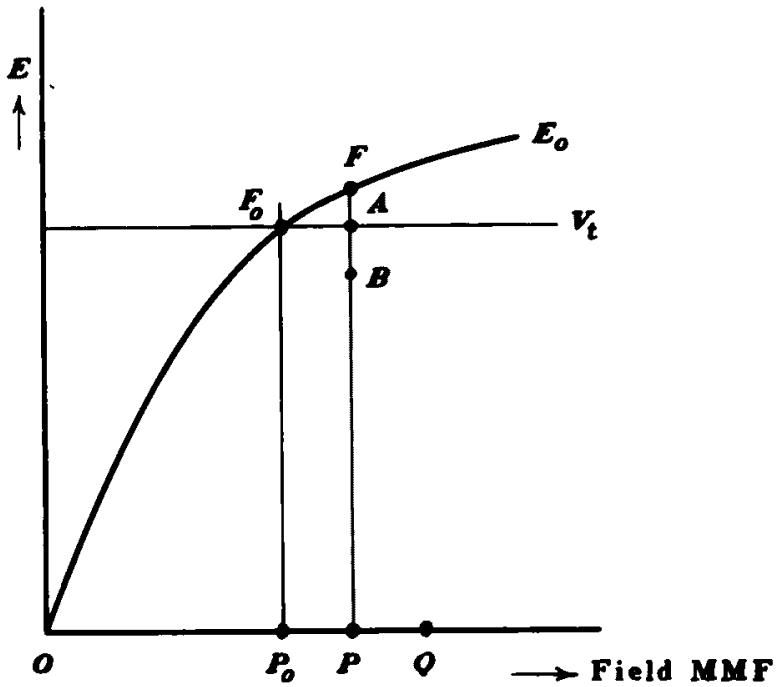


FIG. 8–10a. Determination of speed and torque for cumulative motor.

Having determined the speed $n_L$, and the counter-emf $E = PB$, the torque may be determined by Eq. 8–4 as

$$T = \frac{7.04EI_a}{n} \text{ lb-ft}$$

If the ordinates in Fig. 8–10a are plotted in terms of $C_1\Phi$, then the calculations for both speed and torque may be made as follows: $OP_0$ is the constant mmf of the shunt field; $P_0Q$ is the mmf of the series field for the assumed value of $I_a$; $M_d = QP$; then $OQ - PQ = OP$ is the net or resultant mmf of the motor. $PF$ then equals $C_1\Phi$. The torque is then $T = 7.04C_1\Phi I_a$ lb-ft. Calculate $E = V_t - (\Sigma I_a r + 2\Delta V)$, and then, from Eq. 8–7,

$$n = \frac{E}{C_1\Phi}$$

**Example 4.** Let it be assumed that a series field winding of 7.5 turns per pole be added to the motor of Example 2, and that the total resistance of the armature circuit is now 0.10 ohm (not including the brush contact). The series

$$AT = 7.5 \times 76 = 570$$

at full load. In terms of shunt field current this is equivalent to $570/2800 = 0.203$ amp. Therefore, the effective field current in terms of shunt field winding is

$$0.89 + 0.203 - 0.1 = 0.993 \text{ amp.}$$

From the curve of Fig. 8–7a, $C_1\Phi$ is determined as $238/1800 = 0.1322$. The induced emf at full load is $E = 230 - (76 \times 0.10 + 2) = 220.4$. Therefore, the speed will be $220.4/0.1322 = 1665$ rpm, and the torque (Eq. 8–4) is

$$T = 7.04 \times 0.1322 \times 76 = 70.7 \text{ lb-ft.}$$

Since the effect of the series winding is small at no-load, the speed at no-load will be practically 1800 rpm. The speed regulation as a cumulative compound motor will be

$$\frac{1800 - 1665}{1665} \times 100 = 8.1\%$$

The *differential compound* motor may be analyzed as above, if it is remembered that $P_0Q$ and $PQ$ are both to be subtracted from the shunt field mmf, $OP_0$. The construction is shown in Fig. 8–10b. The ordinates may be $E_0$ at the no-load speed $n_0$ or $C_1\Phi$. For the assumed values of $I_a$, $M_d = PQ$; the mmf of the series field is $P_0Q$; then $PP_0 = P_0Q + PQ$ is the resultant demagnetizing mmf of the load current $I_a$ and $OP = OP_0 - PP_0$ is the net or resultant mmf of the motor. $PF$ would be the emf $E_0$ if the speed were $n_0$. The actual counter emf is $V_t - (\Sigma I_a r + 2\Delta V) = V_t - AB = PB$. The speed is

$$n_L = n_0 \times \frac{PB}{\overline{PF}}$$

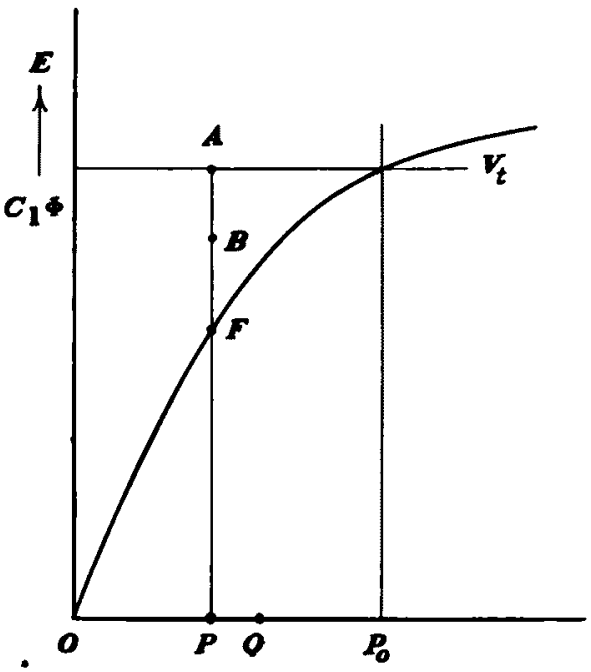


FIG. 8–10b. Determination of speed and torque of differential motor.

Observe here that the speed may be greater at load than at no-load. In fact, the speed may rise rapidly with increasing load, so that the action of the motor will be unstable and the speed will become excessive. The speed and torque may also be readily determined as for the cumulative motor, if the ordinates of the saturation curve are in units of $C_1\Phi$.

**8–5. Comparison Between the Different Types of Motors.** Figs. 8–11, 8–12, and 8–13 show the speed-current, torque-current, and speed-torque curves of shunt, cumulative compound, and series motors. These curves permit a comparison between the various types of motors. They show that the differences between the torque-current curves are not so marked as the differences between the speed-current and speed-torque curves. Fig. 8–13 can be helpful in deciding the type of motor suitable for a given application.

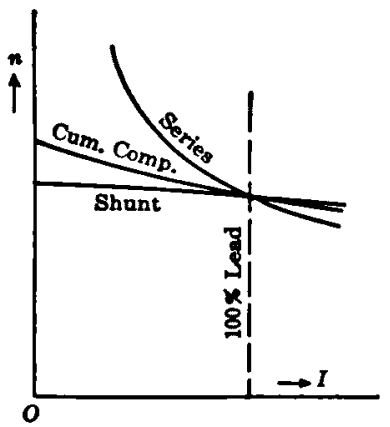


FIG. 8–11. Speed as a function of load current for the different kinds of d-c motors.

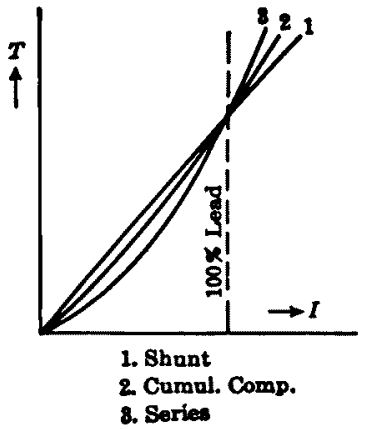


FIG. 8–12. Torque as a function of load current for the different kinds of d-c motors.

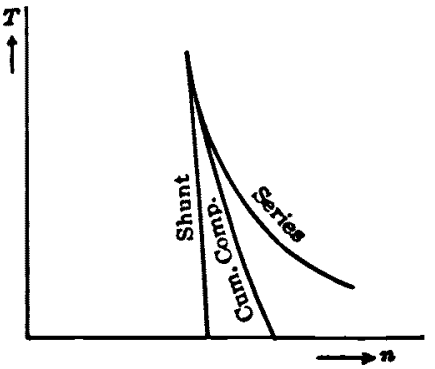


FIG. 8–13. Torque as a function of speed for the different kinds of d-c motors.

The characteristic features of the shunt motor are: approximately a constant speed between no-load and full load, a torque nearly proportional to the armature current (since the flux is almost constant), and the ability to operate as a generator in the same direction of rotation without any change of polarity or connections. The last property mentioned makes dynamic braking possible with the shunt motor: if the opposing torque of the load is lost and the armature is *driven in the same direction* as before, the machine acts as a generator, delivers power to the line, produces a torque opposite to the previous motor torque, and therefore acts as a brake.

The outstanding properties of the series motor are: decreasing speed with increasing torque, a high starting torque varying nearly as the square of the current at low saturation, and a power output *comparatively* unaffected by voltage drops in the line conductors.

The characteristics of the cumulative compound motor lie between those of the shunt and series motors. It has a definite no-load speed as does the shunt motor, but on the other hand its speed decreases more with increasing torque than that of the shunt motor.

The reaction of shunt and cumulative compound motors to the variation of the terminal voltage is shown in the accompanying table.

## GENERAL EFFECT OF VOLTAGE VARIATION ON D-C MOTOR CHARACTERISTICS

+ = Increase  – = Decrease

| Voltage Variation % | Starting and Max. Run Torque % | Full-load Speed % | EFFICIENCY | | | Full-load Current % | Temperature Rise, Full load | Maximum Overload Capacity % | Magnetic Noise |
|---|---|---|---|---|---|---|---|---|---|
| | | | Full Load | ¾ Load | ½ Load | | | | |
| **SHUNT-WOUND** | | | | | | | | | |
| 120 | +30 | 110 | Slight + | No change | Slight – | –17 | Main field +. Commutator, c. field and armature – | +30 | Slight + |
| 110 | +15 | 105 | Slight + | No change | Slight – | –8.5 | Main field +. Commutator, c. field and armature – | +15 | Slight + |
| 90 | –16 | 95 | Slight – | No change | Slight + | +11.5 | Main field –. Commutator, c. field and armature + | –16 | Slight – |
| **COMPOUND-WOUND** | | | | | | | | | |
| 120 | +30 | 112 | Slight + | No change | Slight – | –17 | Main field +. Commutator, c. field and armature – | +30 | Slight + |
| 110 | +15 | 106 | Slight + | No change | Slight – | –8.5 | Main field +. Commutator, c. field and armature – | +15 | Slight + |
| 90 | –16 | 94 | Slight – | No change | Slight + | +11.5 | Main field –. Commutator, c. field and armature + | –16 | Slight – |

NOTES: Starting current is controlled by starting resistor.

This table shows general effects, which will vary somewhat for specific ratings.

In comparison to the a-c motors, the d-c motors, especially the shunt and compound motor, have the advantage that their speed can be varied over wide limits by simple and economic means. The speed control of d-c motors is discussed in Art. 8–7. The applications of the different types of d-c motors is discussed in Art. 8–8.

**8–6. Stability of a Motor.** Consider a motor operating at a speed $n_1$ and developing the torque $T_1$ at this speed. Whether the motor is stable or not at this condition of operation depends upon the shape of the speed-torque curves of the motor and load. The motor will be stable, if both curves intersect each other in such a manner that with increasing speed the load torque is larger than the motor torque (Fig. 8–14a) (i.e., the motor is retarded),

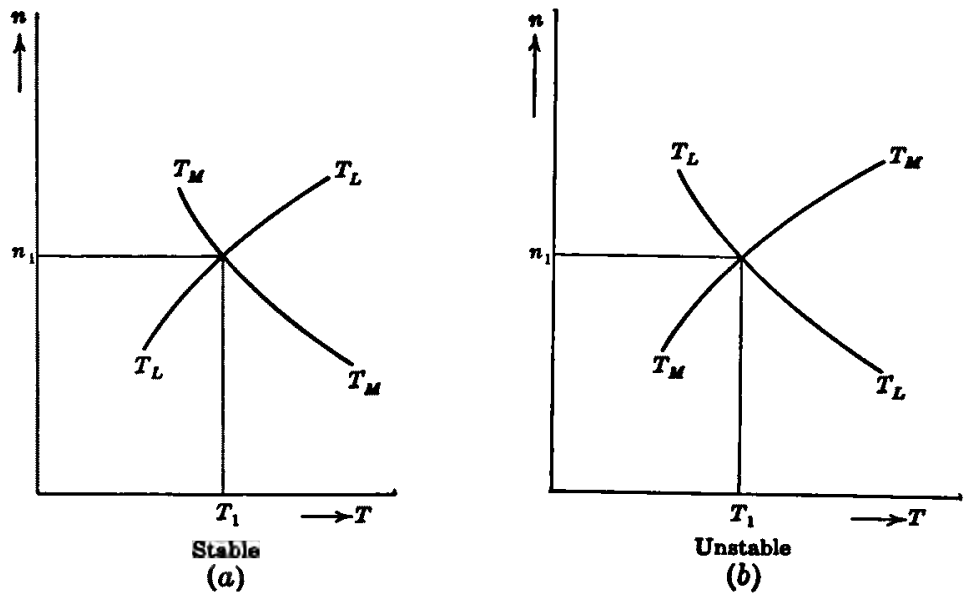


FIG. 8–14. Determination of the stability of a motor.
Stable (a) Unstable (b)

and with decreasing speed the motor torque is larger than the load torque (i.e., the motor is accelerated). Otherwise (Fig. 8–14b), with increasing speed, the motor will be accelerated more and more and may reach a dangerous speed; with decreasing speed, the motor will be retarded more and more and may come to standstill unless the speed-torque curves intersect at another point where the condition for stability (Fig. 8–14a) is satisfied.

**8–7. Speed Control of the D-c Motors.** It follows from the speed equation of the motor (Eq. 8–7)

$$n = \frac{V - (\Sigma I_a r + 2\Delta V)}{C_1 \Phi}$$

that there are 3 methods for regulating its speed, namely, by varying the

voltage $V$ (*voltage control*), by varying the resistance of the armature circuit (*rheostatic control*), and by varying the flux $\Phi$ (*flux* or *field control*).

(a) *Separately Excited, Shunt and Cumulative Compound Motor.* Rheostatic control necessitates an external resistor in the armature circuit. This resistor produces a drop in the speed characteristic. Fig. 8–15 shows speed-torque characteristics for 2 different values of external resistance. At very small loads the resistance is not very effective. Therefore this method makes the regulation, i.e., the change of speed between no-load and full-load, large. Furthermore, the efficiency is reduced by this method of speed control, since the copper losses of the armature circuit are increased. For this reason the *rheostatic-control method seldom is used* in industrial installations.

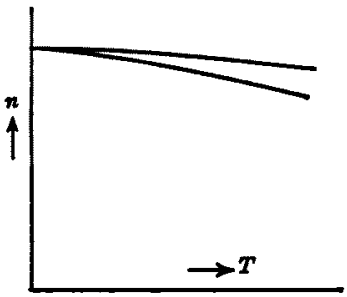


FIG. 8–15. Speed-torque characteristics obtained by rheostatic speed control. (Separately excited, shunt, and cumulative compound motor.)

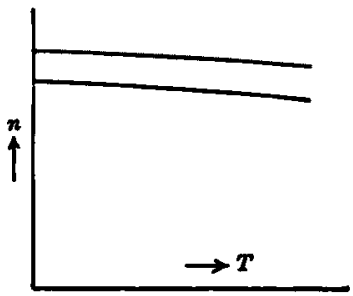


FIG. 8–16. Speed-torque characteristics obtained by flux control. (Separately excited, shunt, and cumulative compound motor.)

The simplest and cheapest method of speed control is the flux control by means of a rheostat in the shunt field circuit. Since the energy required by this circuit is only a small percentage of the machine output, the rheostat is small in size. This method is therefore an efficient one. In machines without interpoles, where the main flux is used to improve the commutation, the speed may be increased approximately in the ratio 2 : 1. A further weakening of the main flux may interfere with the commutation, since the armature reaction may reduce the field density at the pole tips beyond the value necessary for good commutation. In machines with interpoles a ratio of maximum to minimum speed of 5 : 1 or 6 : 1 is fairly common. To a given change in flux (shunt field current) there is a definite shift of the speed characteristic as shown in Fig. 8–16. The speed regulation is affected only slightly by this method of speed control. These considerations apply to the cumulative compound motor only when the series field is small in comparison to the shunt field. In general a shunt motor is used with this type of speed control.

Voltage control is used under certain conditions, in connection with separate excitation, in the arrangement known as the *Ward-Leonard system.*

In Fig. 8–17, $M$ is the main motor the speed of which is to be regulated. It is supplied with power from the generator $G$ which is driven by another motor $M'$. The field of the generator $G$ is excited from a constant voltage source and may be adjusted from zero to a maximum, in both directions,

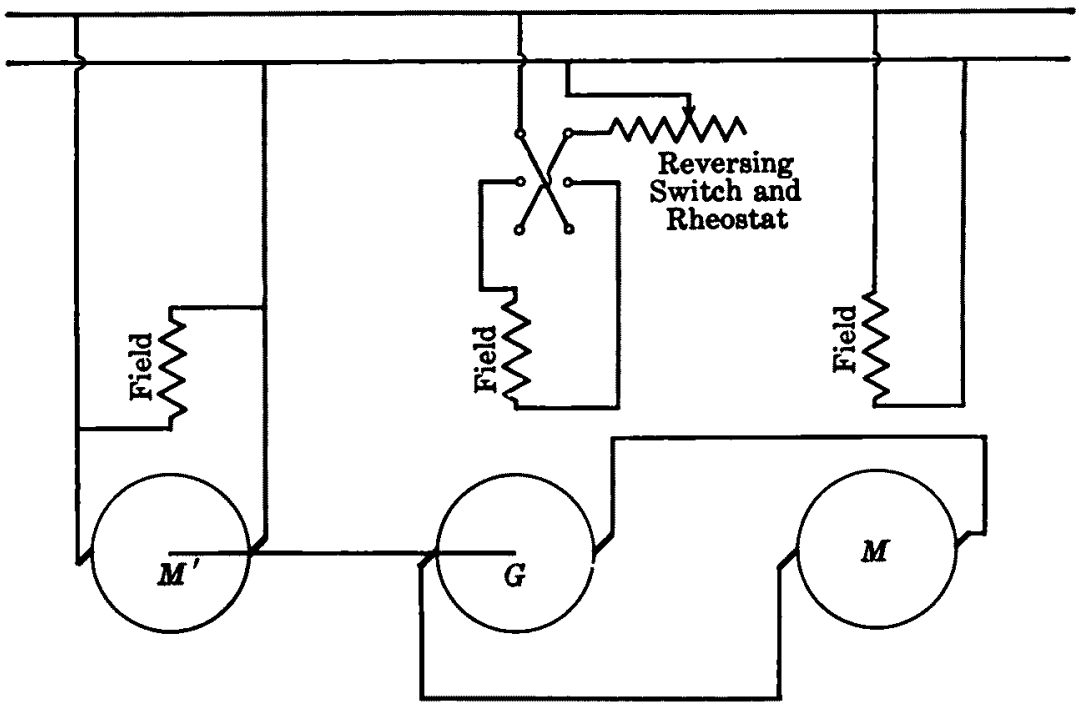


FIG. 8–17. Ward-Leonard system for speed control.

by means of a rheostat and reversing field switch. In this way a smooth variation of the voltage impressed on the main motor is obtained. The motor $M'$ is very often an a-c motor, though it may be any suitable prime motor.

(b) *Series Motor.* Rheostatic control is used for speed variation of the railway series motor. The resistor produces a drop in the speed curve similar to that in the shunt motor. Fig. 8–18 shows speed characteristics for 2 different values of resistance in the armature circuit. When a car is equipped with 2 or more motors, as is usually the case, series-parallel control (Fig. 8–19) is applied. This is a combined rheostatic and voltage control. For full speed the resistor is cut out entirely and both motors run in parallel at the line voltage. In S1 the motors are in series with each other and with all of the starting rheostat. In S2 some of the starting rheostat has been cut out; and in S3 the rheostat has been cut out entirely and each motor operates at one-half line voltage. In T1 one motor is short-circuited, and all of the starting rheostat is in series with the other. The control continues until at P3 both motors receive full

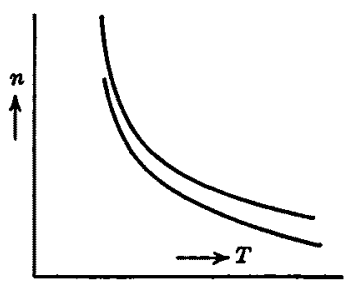


FIG. 8–18. Rheostatic speed control of a series motor.

line voltage. Positions S3 and P3 are known as *running positions*, because all the rheostat is cut out.

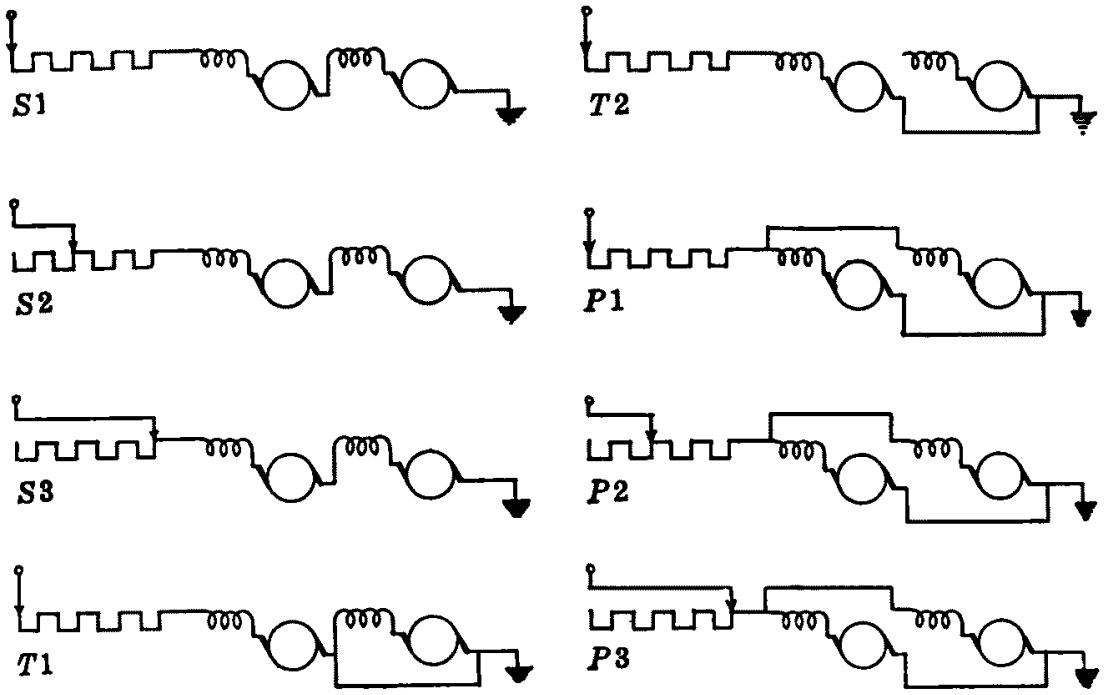


FIG. 8–19. Series-parallel speed control of series motors.

**8–8. Motor Application.** The problem of motor application consists essentially in finding first the requirements of the load, such as horsepower, variation of speed, torque, starting torque, acceleration characteristics, the duty cycle, and the surrounding or operating conditions. In order to specify the motor to fit these requirements, the character of the power supply must be known, as well as the operating characteristics of the various motors which are available. If the motor and its control have been properly chosen and applied, it will be possible to start the load from rest and accelerate to full speed without injury to the motor or the load and without putting an undue strain on the power lines. The load will be carried satisfactorily through whatever duty cycle is required, and the capacity of the motor will be adequate for such momentary overloads as may be required by the load without shutting down the motor or overheating it. Many installations are served satisfactorily by general-purpose motors, which are readily available and standardized according to generally accepted standards set up by N.E.M.A. (National Electrical Manufacturers Association). The discussion to follow considers only the general fundamentals of motor application.

**8–9. Characteristics of Load.** An important characteristic of motor loads is the relation of torque to speed. Many industrial loads are essentially constant speed, that is, a variation in speed of 5 to 15 % is of no particular importance. Such loads are constant-speed conveyors, pumps, fans, blowers,

woodworking machines, metal-working machines, motor generator sets, line shafting, compressors, power-plant auxiliaries, grinders, concrete mixers, laundry machinery, looms in textile mills. Since these loads are essentially constant-speed loads, the increase in load is brought about by increased torque requirements, such as are produced by adding load to a motor-generator set, adding material to a conveyor, etc. In this type of load, the output, therefore, is proportional to the load torque. The d-c shunt motor is adapted to this type of load.

On the other hand, many loads require that the speed be adjustable over a wide range for various conditions of operation, but that the speed regulation still be within 10 to 15%. Such loads are fans, blowers, machine tools, some types of printing presses, some textile machinery, and paper machines. Adjustable speed loads are of three general types: (1) in which the torque is essentially constant at all speeds; (2) in which the output requirements are practically constant at all speeds; and (3) in which the torque is inherently variable. Typical of (1) are conveyors (when variable speed is needed) and automatic machine tools; in this type of load the output varies directly with the speed and the motor is called a constant-torque adjustable-speed motor. The best type of control for these devices, i.e., the one requiring the smallest motor, is the d-c shunt motor with an adjustable armature voltage supply. This is not always practical, so that a d-c shunt motor designed for adjustable speed by field control may be used for such loads. Type (2) loads include most machine tools, where the speed is reduced as the size of cut is increased. A d-c shunt motor designed for adjustable speed by field control is well suited for this type of load. Type (3) loads include fans, blowers, and centrifugal pumps. In these loads the torque increases with about the square of the speed, so that the power output required varies as the cube of the speed. Loads of this type usually require low starting torque. A d-c shunt motor with field control is best suited for wide speed ranges.

The starting torque required by the load is an important factor in determining the type of motor. Loads such as fans, blowers, centrifugal pumps, unloaded compressors, machine tools, etc., usually require a low starting torque, i.e., one considerably less than full-load torque, perhaps 30 to 50%. Other loads, such as loaded compressors, pumps, ball mills used for grinding ore, and conveyors, start under load. In addition to the load there may be considerable standing friction to be overcome, where the machinery has been standing idle for some time. This type of load requires high starting torque to break away from standstill, and the starting torque required may be as high as 300% for some loads. Certain loads, such as band saws, centrifugal compressors, wood chippers, and others, have high inertia. While these machines may be started unloaded, the high inertia may require long starting periods and consequent heating of the motor, unless adequate torque is provided for quick acceleration. If high inertia as well as high load torque is encountered, the starting requirement is especially difficult. High starting

torques are required in railway application, and the series motor is best adapted to this service.

Another important factor in motor application is the surrounding conditions under which the motor must operate. If the ambient temperature is high, special motor insulation may be required or in any case a larger-sized motor than for normal ambient temperature (40° C); or perhaps special ventilating methods may be required. The new type of plastic insulation (silicon) evidently will make possible operating under higher temperatures. If the surrounding air contains dust, corrosive or explosive gases, salt air, or excessive moisture, the motor will require special enclosures to protect the windings and any sliding contacts such as a commutator or slip rings. Motor enclosures are available that are splash-proof, drip-proof, dust-proof, explosion-proof, etc. (see Definitions, p. 188), to take care of these conditions.

The manner of connecting the load to the motor also must be considered. A belt or chain connection requires that the bearings of the motor be adequate to stand the strain caused by the belt or chain. Direct connection through couplings or by gear does not put as much strain on motor bearings as the belt or chain connection, and the former methods are used when possible. The V-belt drive usually is preferred over the flat belt for short shaft centers.

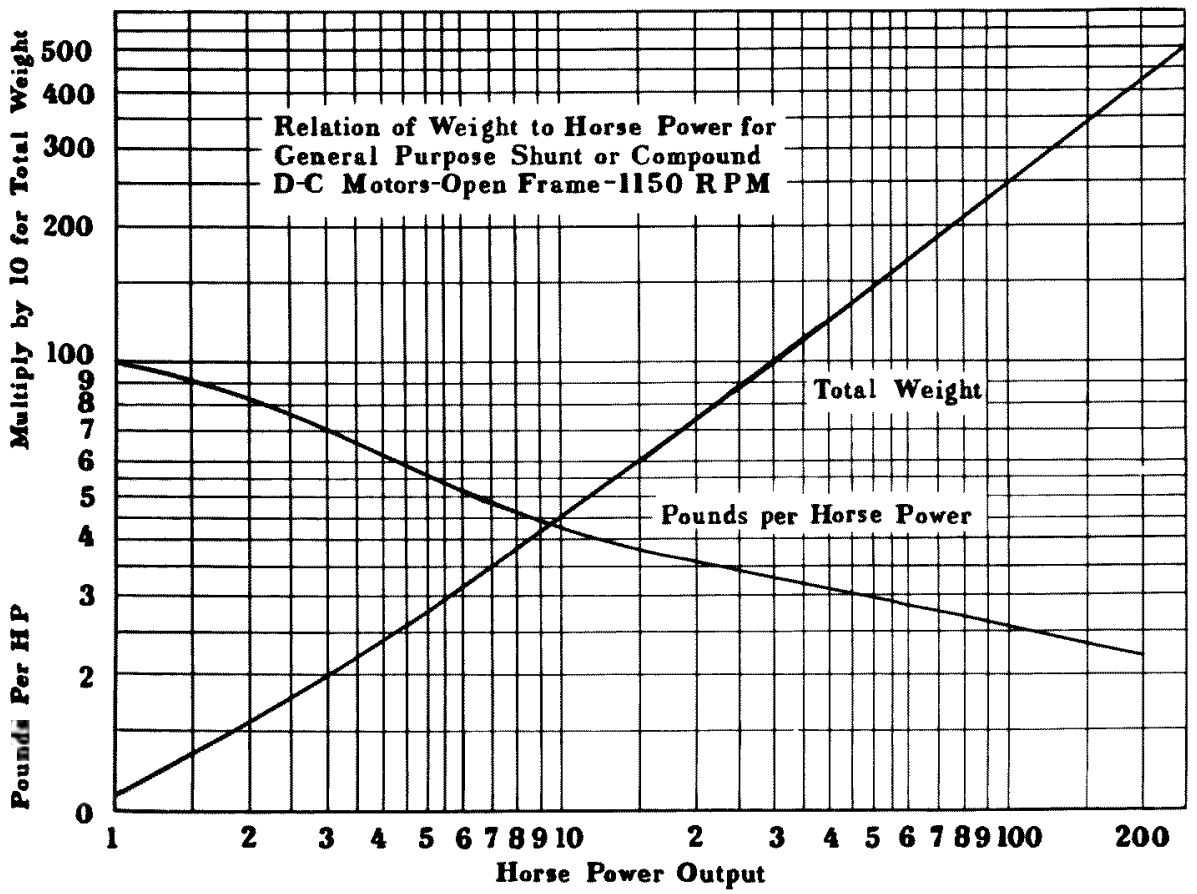


FIG. 8–20. Relation of weight to horsepower for general purpose motors, shunt or compound, open frame, 1150 rpm.

**8–10. Motor Types, Sizes, and Costs.** The frame size of a motor depends basically upon such factors as horsepower, speed, temperature (both ambient and the allowable rise), the duty cycle of operation, and type of motor enclosure. The horsepower rating required for a driven machine usually can be obtained from the manufacturer. In some cases, such as hoists, pumps, fans, etc., the horsepower can be calculated with considerable accuracy, while in other cases an actual load test may be required. The cost of a motor depends basically upon the horsepower, speed, type of enclosure, and type of bearings. Generally speaking, higher-speed motors are lighter in weight

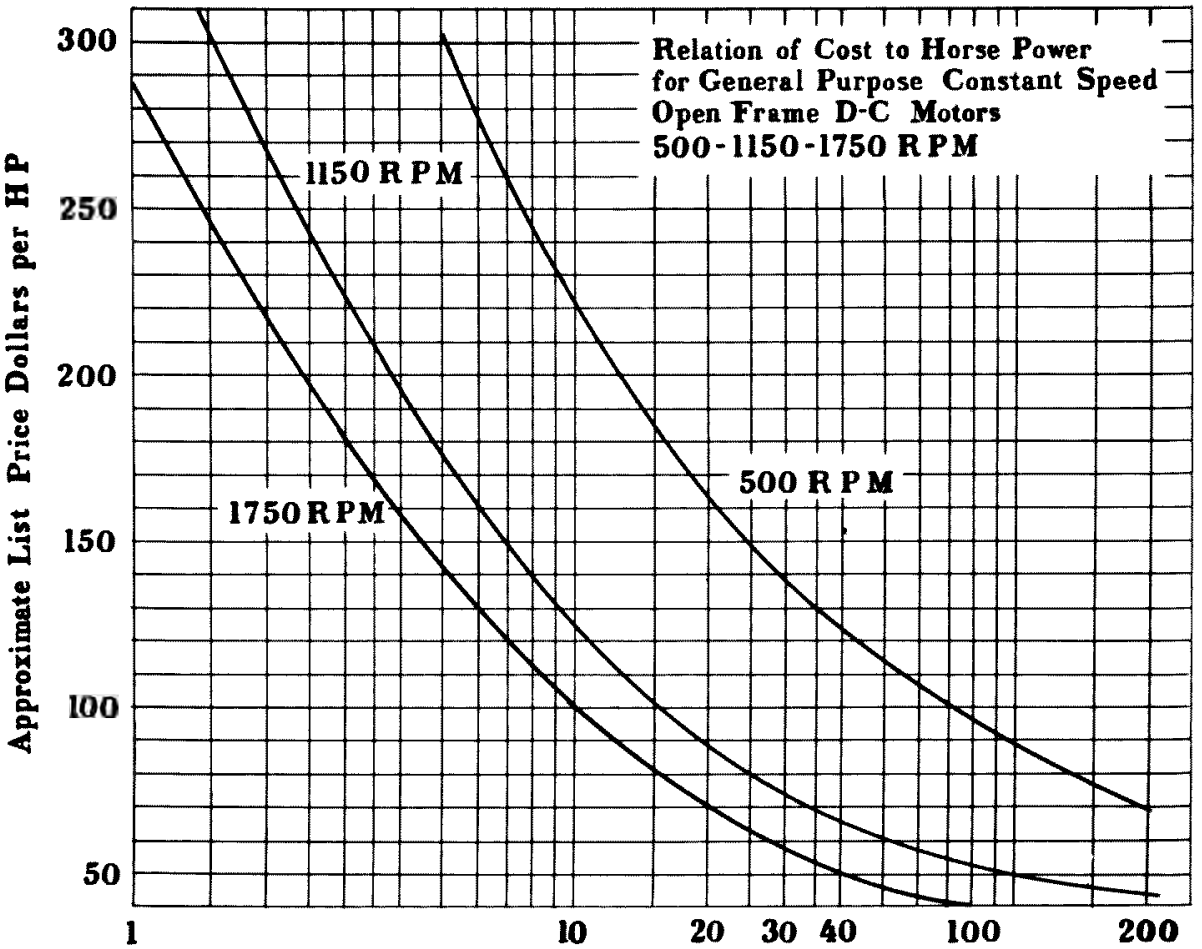


FIG. 8–21. Relation of cost to horsepower for general purpose, 500–1150–1750 rpm, constant speed, open frame motors.

and less expensive than lower-speed motors. Very-high-speed motors have high costs due to the special mechanical features necessary at the high speeds. Fig. 8–20 shows the relation of horsepower and weight for d-c shunt or compound motors, constant speed. It will be seen that the weight in pounds per horsepower decreases with increase in horsepower. This is a general characteristic for practically all electric machines.

Fig. 8–21 shows the relation of cost to horsepower for constant-speed motors of 500, 1150, and 1750 rpm. Fig. 8–22 shows the relation of weight and cost to speed for a 25-hp, open-frame, d-c motor. The list prices are

representative of a competitive line of N.E.M.A. standardized motors. The increase in weight and cost with reduction in speed is clearly shown. The implication of these curves is that, other things being equal, the higher-

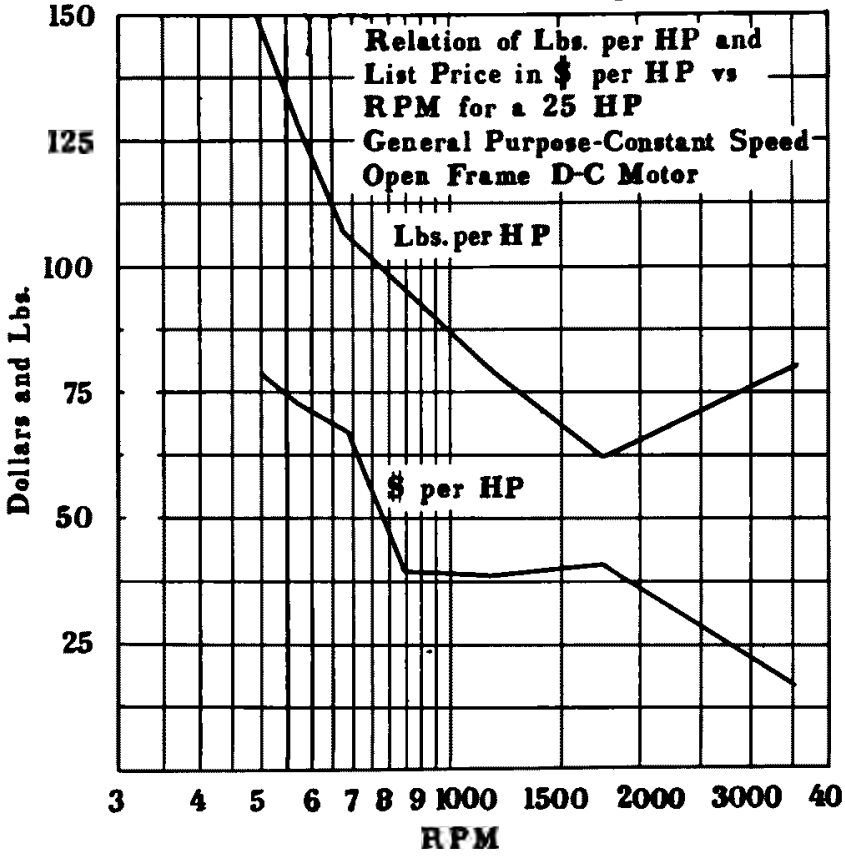


FIG. 8–22. Relation of lbs/hp and list price in $ per hp vs rpm for a 25-hp general purpose, constant speed, open frame motor.

speed motor should be chosen. In many cases it is possible and desirable to get lower speeds, when required, by gears or pulleys. With speeds below 700 rpm at low output, a gear motor usually will be lighter in weight and less expensive than a regular low-speed motor.

Table 8–1 shows the general characteristics and application of d-c motors.

## PROBLEMS

1. Determine the value of the starting resistance to limit the starting current in the motor of Example 2, to 150% of rated value. Determine the value to limit the current to 200%.

2. Assume the shunt motor of Example 2 operates at a terminal voltage of 250. Determine the torque and speed at full-load current, and the speed at no-load.

3. Assume the motor of Problem 2 now operates at a terminal voltage of 210. What will be the speed at no-load and at full-load current, and the full-load torque?

4. Assume the motor of Example 4 to operate at a terminal voltage of 250. Determine the no-load speed, the speed and torque at full-load current.

## TABLE 8–1

CHARACTERISTICS AND APPLICATIONS OF D–C MOTORS

| Type | Starting Torque % | Max. Running Torque, Momentary % | Speed Regulation or Characteristic % | Speed Control % | Typical Application and General Remarks |
|---|---|---|---|---|---|
| Shunt, constant speed | Medium — usually limited to less than 250 by a starting resistor but may be increased | Usually limited to about 200 by commutation | 5–10 | Increase up to 200 by field control; decrease by armature voltage control | Essentially for constant-speed applications requiring medium starting torque. May be used for adjustable speed not greater than 2 to 1 range. For centrifugal pumps, fans, blowers, conveyors, woodworking machines, machine tools, printing presses. |
| Shunt adjustable speed | Same as above | Same as above | 10–15 | 6 to 1 range by field control, lowered below base speed by armature voltage control | Same as above, for applications requiring adjustable speed control, either constant torque or constant output. |
| Compound | High — up to 450, depending upon degree of compounding | Higher than shunt — up to 350 | Varying, depending upon degree of compounding — up to 25–30 | Not usually used but may be up to 125 by field control | For drives requiring high starting torque and only fairly constant speed ; pulsating loads with flywheel action. For plunger pumps, shears, conveyors, crushers, bending rolls, punch presses, hoists. |
| Series | Very high — up to 500 | Up to 400 | Widely variable, high at no-load | By series rheostat | For drives requiring very high starting torque and where adjustable—varying speed is satisfactory. This motor is sometimes called the *traction motor*. Loads must be positively connected, not belted. For hoists, cranes, bridges, car dumpers. To prevent over-speed, lightest load should not be much less than 15 to 20% of full-load torque. |

**5.** Assume the motor of Problem 4 to operate at a terminal voltage of 210. Repeat the calculations of Problem 4.

**6.** How much resistance would have to be inserted in series with the shunt field winding of the motor of Problem 5 in order to produce a full-load speed of 1800 rpm?

**7.** Assume a resistance of 0.3 ohm inserted in series with the armature of the motor of Example 4. What will be the speed and torque at full-load current?

**8.** For armature currents of 20, 40, 60, 80, and 100 amp, determine the torque and speed for the machine of Example 4.

**9.** A resistor of 0.240 ohm is shunted across the series field of the motor in Example 3. Determine the speed and torque at rated armature current.

**10.** The full-load speed of the series motor of Example 3 is to be raised to 2000 rpm. What value of resistance must be placed in parallel with the series field?

**11.** A 230-volt series motor has a combined armature plus interpole plus series field winding resistance of 0.4 ohm. What current will be required to develop 60-ft-lb torque at 1200 rpm?

**12.** If the motor of Example 2 is to run at 1850 rpm and develop 70-ft-lb torque, what armature current must it carry? What shunt field current will be required and what will be the resistance of the field rheostat?

**13.** The motor of Example 2 is to develop 70-ft-lb torque at 1600 rpm. How much armature current must flow? How many series turns must be added per pole?

**14.** A 7.5-hp 115-volt shunt motor has a full-load speed of 1750 rpm, and takes a line current of 57.6 amperes. The shunt field resistance is 144 ohms and that of the armature 0.15 ohm. It is desired that this motor run at 900 rpm, when developing 20-ft-lb torque. How much resistance should be inserted in series with the armature?

**15.** The 7.5-hp motor of Problem 14 is operating under normal load conditions. If a resistance of 0.5 ohm is *suddenly* inserted in series with the armature, determine for the *instant* at which this resistance is inserted: (a) the induced emf, (b) the armature current, (c) the developed torque. Explain what happens to the operation of the motor, and determine the final steady value of speed.

**16.** The shunt motor of Problem 14 is operating at normal rated load conditions, and the field flux is *suddenly reduced* 15%. For the *first instant after* the reduction in flux, determine: (a) the induced emf, (b) the armature current, (c) the developed torque. Explain what happens to the operation of the motor and determine the final speed. Compare the action with that of Problem 15.

**17.** The motor of Example 2 is operating at rated load and voltage. If the terminal voltage is raised to 250, and the torque demands remain constant, determine for the final constant conditions: (a) the field current, (b) armature current, (c) speed. Compare results with Example 2, and explain differences. Why is the speed not directly proportional to the terminal voltage?

**18.** Repeat Problem 17 for a terminal voltage of 210.

**19.** A 10-hp 230-volt shunt motor takes a line current of 38 amp, and runs at 1750 rpm at full load. The armature resistance is 0.2 ohm, and the field resistance 383 ohms. Determine: (a) counter-emf, (b) developed torque, (c) efficiency of the motor. If the required torque is reduced 60% and the motor is to run at 900 rpm, with a 20% increase in flux, determine: (d) armature current, (e) resistance to be inserted in series with the armature.

**20.** A 25-hp 120-volt shunt motor has at rated speed of 900 rpm an armature current of 175 amp. The armature resistance is $r_a = 0.026$ ohm. What is the developed torque of the motor? What resistance must be inserted in the armature circuit in order that the motor will develop half of the rated torque at 700 rpm? The flux can be assumed constant.

**21.** A 120-volt shunt motor has at rated speed of 900 rpm an armature current of 150 amperes. The armature resistance is 0.025 ohm. What will be the speed of the motor if, at constant developed torque and constant flux, the armature voltage is: (a) increased by 15%, (b) decreased by 15%?

**22.** Solve Problem 21 with the assumption that the flux is changed proportionally to the armature voltage by changing the field resistance.

**23.** A 220-volt shunt motor at 1200 rpm has an armature current of 25 amp. The armature resistance is $r_a = 0.2$ ohm. What will be the speed of the motor if, at constant developed torque, a resistance of 0.8 ohm is inserted in the armature circuit?

**24.** A 220-volt shunt motor operating at 1000 rpm has an armature current of 25 amp. The armature resistance is $r_a = 0.5$ ohm. How much (in percent) has the flux been changed if, at 200 volts and 5 amp of armature current, the speed is 900 rpm? Also determine the ratio between the developed torques.

**25.** A series motor runs at 200 rpm and takes a current of 75 amp at 500 volts. Resistance of armature and series field equals 0.22 ohm. What will be the speed of the motor if, at constant torque, the voltage is: (a) increased by 20%, (b) decreased by 20%? Assume no saturation.

**26.** A series motor draws a current of 40 amp at 500 volts and runs at 1000 rpm. How much has the flux been reduced (in percent) if, at reduced load, the motor takes 19 amp at 1600 rpm? The series resistance of armature and field is 0.4 ohm.

**27.** A motor is operating as a cumulative compound motor. How must the connections be changed in order to change the direction of rotation, if the motor is to emain cumulatively compounded? Assume that the series field winding is cut out and the motor runs as a shunt motor. How must the connections be changed in this case, in order to change the direction of rotation?

**28.** A cumulative compound motor draws $I_a = 10$ amp at 220 volts and runs at 1000 rpm. Resistance of armature and series field equals 0.4 ohm. Determine the developed torque. How much (in percent) must the flux be changed, in order that the speed be 750 rpm when the armature current is 30 amp and the voltage 200 volts?

**29.** A cumulative compound motor draws $I_a = 50$ amp at 230 volts and runs at 1000 rpm. Resistance of armature and series field equals 0.12 ohm. What is the speed of the motor, if the armature current is 22 amp and the developed torque 32 lb-ft?

**30.** A 25-hp 120-volt shunt motor has at rated speed of 900 rpm an armature current of 175 amp. The armature resistance is $r_a = 0.026$ ohm. A braking resistance of 1.5 ohms is inserted in series with the armature circuit, in order to stop the motor. Determine the armature current and retarding torque immediately after the braking begins.

**31.** A cumulative compound motor has an armature resistance of 0.2 ohm, series field plus commutating field resistance of 0.05 ohm, shunt field 55 ohms. The shunt winding has 1200 turns per pole, the series 10.5 turns per pole. At a line

voltage of 110. the line current is 50.0 amp, and the speed 800 rpm. Assuming a linear saturation curve, what will be the torque and speed for a line current of 30 amp? Compare with conditions at 50 amp.

**32.** The data for the no-load characteristic of a shunt dynamo, taken at 450 rpm, are:

| | | | | | | | | |
|---|---|---|---|---|---|---|---|---|
| $E_0$ | 20 | 40 | 60 | 70 | 80 | 90 | 100 | 110 |
| $I_f$ | 1.8 | 3.6 | 5.7 | 7 | 8.8 | 11.3 | 15.7 | 22 |

This machine operates as a shunt motor from 240-volt lines, the field resistance is 15 ohms, the armature plus commutating field resistance is 0.04 ohm, the full-load armature current is 500 amp, the demagnetizing effect of armature reaction is equivalent to 1 amp of shunt field current. There are 400 shunt field turns per pole. Determine for full-load current: (a) field current, (b) speed, (c) developed torque.

**33.** The motor of Problem 32 now has 6.5 series turns per pole added to give cumulative action. Assume long-shunt connection, and that the series field has a resistance of 0.01 ohm. Determine the speed and torque for full-load armature current.

**34.** A 5-hp 230-volt adjustable-speed motor has 2500 shunt turns per pole, and 9 series or stabilizing turns per pole. The armature reaction $M'_d = 0.05$ in terms of shunt field current, the armature resistance is 0.298 ohm, and the shunt field equals 240 ohms. The full-load armature current is 20 amp. The data for the no-load saturation curve taken at 525 rpm are:

| | | | | | | | | | |
|---|---|---|---|---|---|---|---|---|---|
| $E_0$ | 40 | 60 | 80 | 100 | 120 | 140 | 160 | 180 | 200 |
| $I_f$ | 0.075 | 0.12 | 0.165 | 0.21 | 0.27 | 0.35 | 0.49 | 0.75 | 1.23 |

When operating at full-load current, the following speeds are desired: 615, 800, 1000, 1200, 1400, 1600, and 1800 rpm. Determine the values of the resistance for the shunt field rheostat to accomplish this result.

**35.** The armature of the motor of Example 2 is built as follows: 35 slots, 10 conductors per slot, 1 turn per coil, simple progressive wave winding, area of each conductor is 0.0158 square inch. The mean length of each turn is 29 inches. The coil width is 9 slots. Determine: (a) the number of commutator bars, (b) the winding pitch, the back and front pitch, in terms of slots and also in terms of commutator bars; (c) is the winding symmetrical? (d) What is the flux in the air-gap per pole at no load?

**36.** The armature winding of Problem 35 is reconnected as a lap winding, and the same field coils are used. The flux per pole is unchanged, and the terminal voltage reduced to 115. Determine: (a) how to connect the shunt field coils, (b) the no-load speed, (c) the rated armature current.

**37.** Determine the full-load developed torque of Problem 36 and compare it with Example 2.

**38.** The motor of Example 2 is to have a new wave-wound armature designed for operation at the same speed, but with a line voltage of 440 volts. Give the specifications for the new winding, assuming the same commutator to be used.

**39.** The sum of the core loss and the friction and windage losses for the motor of Example 4 is 1203 watts, and the stray load losses are 150 watts. What will be the efficiency for rated armature current, with full field current, and 230-volt line?

**40.** A shunt motor is tested with a Prony brake and the following data are obtained: terminal voltage is 120, line current is 90 amperes, rpm is 1250, length of brake arm is 25 inches, scale reading is 23 pounds. The resistance of the shunt field winding is 27.3 ohms, and the armature plus interpole resistance is 0.07 ohm. Assuming the stray load loss is 150 watts, and that the core loss and the friction and windage losses are constant, determine: (a) the efficiency of the motor, (b) the sum of the friction and windage losses, (c) the armature current at no load, (d) the power (hp) developed by the electromagnetic action of the armature.

**41.** From the data given in Problem 35, calculate the armature resistance at 75° C using specific resistance of 0.678 microhm per inch$^3$ at 20° C.

# *Chapter 9*

## COMMUTATION

**9–1. The Short-circuited Winding Elements.** It has been pointed out previously (see Fig. 5–8) that the position of the brushes on the commutator determines the direction of current in the individual winding elements. The conductors lying in any one path between two brushes all have the same direction of current and this direction is different under consecutive poles. Since the brushes are at standstill and the conductors move, the latter change their current direction, i.e., *commutate*, when they pass the brushes.

If $I_a$ is the total armature current and the winding has $a$ parallel paths, the current per path is

$$i_a = \frac{I_a}{a} \tag{9–1}$$

and the current of each individual winding element as a function of time has the wave shape of Fig. 9–1.

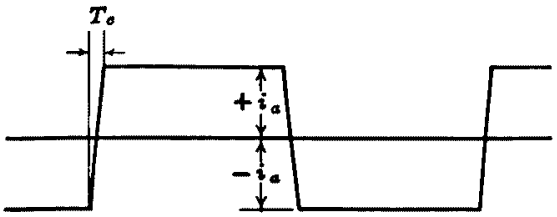


FIG. 9–1. Current in a single winding element.

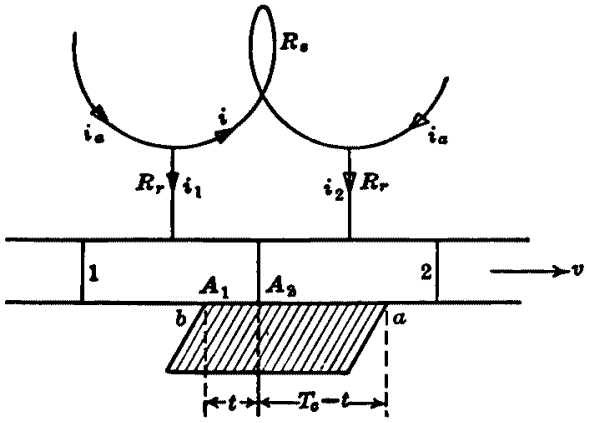


FIG. 9–2. Short-circuited winding element.

The connection between the individual elements of a d-c armature winding is such that, *when they commutate, they are short-circuited* by one or two brushes. As is evident from Figs. 3–13 and 3–14 a winding element of a lap winding is short-circuited by one brush. In the wave winding with only two brush studs, $p/2$ winding elements are simultaneously short-circuited by one brush. If the wave winding has $p$ brush studs, as is usually the case,

then each brush short-circuits $p/2$ winding elements and in addition each winding element is short-circuited by two brushes of the same polarity (see Figs. 3–17 and 3–18) which are connected externally.

The fact that the winding elements are short-circuited for a certain time may lead to sparking under the brushes. This must be avoided. Since the sparking period of a winding element coincides with the commutation period, the word "commutation" has become the meaning of sparking itself and a machine with "good commutation" is to be understood as one which has no sparking at the brushes.

The brush width is usually equal to from 2 to 3.5 commutator bars. The short-circuit period is proportional to the width of the brush. In Fig. 9–1 the short-circuit time is denoted by $T_c$ (commutation time).

Fig. 9–2 shows a coil (winding element) of a lap winding with its connections to the commutator bars. It is assumed that the width of the brush is equal to the width of a commutator pitch. In this case the brush can short-circuit only one winding element. In Fig. 9–2 the short circuit of the coil begins when brush edge $b$ touches bar 1, and ends when the brush edge $a$ leaves bar 2; $b$ is the *leading brush edge* and $a$ the *trailing brush edge*.

Before the beginning of the short-circuit period $T_c$, the current in the coil is $i_a$; the brush is then on bar 2 only and carries a current $2i_a$; the current density is uniform over the entire cross section of the brush. At the end of the time $T_c$, the current in the coil is $-i_a$; the brush now contacts only commutator bar 1 and again carries a current $2i_a$; the current density is again uniform over the entire cross section of the brush just as at the beginning of commutation.

During the short-circuit time $T_c$, the coil carries a current the magnitude of which depends upon the position of the brush and upon conditions to be given in the discussion that follows. Only a part of this current reaches the external circuit; the other part is an internal current which circulates in the short-circuit path made up of the coil, both commutator risers, both commutator bars, and the brush. The current density over the brush cross section is no longer uniform, for the brush now carries not only the current $2i_a$ but in addition carries the circulating current $i$. *If the current density in the trailing brush edge a at the instant when the short circuit is removed* (end of short-circuit period $T_c$) *becomes too large, then sparking appears under the brush.* As a result of this, the commutator is pitted and the sparking becomes progressively worse because of the poor surface contact between the brush and the commutator.

Besides being dependent upon the efficiency and the heating of the windings, *the usefulness of the commutator machine is, above all, dependent upon its commutation.* It therefore is necessary to have the current density under the trailing brush edge as low as possible. Although the current density should not be too high in any part of the brush, owing to the danger of melting the carbon or the copper, a high current density in the

trailing brush edge is most dangerous because of the sparking which it produces.

**9–2. The Commutation Curve.** In order to determine the current density in the trailing brush edge *a* knowledge of the current $i$ in the short-circuited winding element as a function of time, i.e., a knowledge of the commutation curve $i=f(t)$, is necessary. The factors upon which $i$ depends first will be made clear.

During the time of short circuit, $T_c$, the short-circuited winding element moves a fixed distance. It moves in the armature *cross flux* (Fig. 5–10) and, if the brushes are displaced from the neutral axis, it also moves in the *pole flux* (Fig. 5–9). The armature flux is determined by *all* of the armature conductors; it has a fixed axis determined by the position of the brushes and is fixed in space just as the pole flux is. *The armature flux as well as the pole flux induces an emf in the short-circuited winding element.*

However, another emf appears in the short-circuited winding element, namely, one which is due to the change in current from $+i_a$ to $-i_a$; this is an *emf of self-induction.*

It has been explained previously that the field winding of the d-c machine produces a leakage flux, Fig. 5–1, i.e., a flux which does not go through the main magnetic path of the machine (gap, teeth, and core). The same is true of the armature winding embedded in the armature slots. This winding produces several fluxes which do not go through the main path. One of these leakage fluxes is that which crosses the slots without crossing the gap. Another leakage flux is that between the tooth tops in the gap without going through the pole iron. These two leakage fluxes are shown in Fig. 9–3.

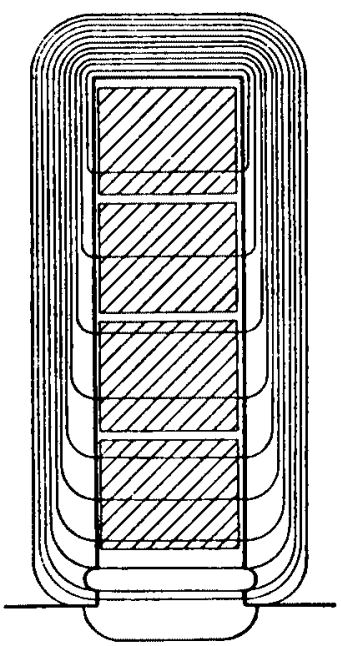

FIG. 9–3. Slot and tooth top leakage fluxes.

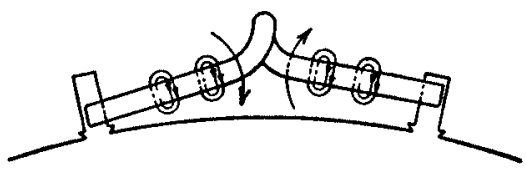

FIG. 9–4. End winding leakage flux.

A third leakage flux is that around the end-windings, i.e., around the external connections between the conductors, Fig. 9–4.

These three leakage fluxes have no influence on the winding elements as long as their current remains constant (equal to $+i_a$ or $-i_a$). However, when a winding element goes through the commutation period, i.e., when its current changes from $+i_a$ to $-i_a$, or vice versa, these leakage fluxes, which are proportional to the armature current, undergo changes and induce an emf of self-induction in the short-circuited winding element.

As has been mentioned, the brush width is usually greater than one commutator bar. In this case several winding elements are short-circuited by the brush at the same time and there is *mutual induction* between the simultaneously short-circuited winding elements. It will be seen later that the self-induction of the short-circuited winding element and the mutual induction are the most important with respect to good commutation.

The magnitude of the emf of self- and of mutual-induction is larger the shorter the time $T_c$ (Fig. 9–1) during which the current changes from $+i_a$ to $-i_a$. If $b_b$ is the brush width and $v_c$ is the surface velocity of the commutator, then the duration of the short-circuit of the winding element is given by

$$T_c = \frac{b_b}{v_c} \tag{9–2}$$

The emf's of self- and mutual-induction in high-speed machines are greater than those in low-speed machines because of the shorter time $T_c$.

In the case where an interpole field is not used (see Art. 9–5), the variation of the current $i$ in the short-circuited winding element depends upon the following emf's and resistances:

(1) Emf's of self- and mutual-induction.
(2) Emf due the armature cross flux.
(3) Emf due the pole flux.
(4) Resistance of the brush contact.
(5) Resistance of the commutator risers (connections from coils to commutator).
(6) Resistance of the short-circuited winding element.

**9–3. Resistance Commutation.** The conditions necessary for good commutation, i.e., low current density in the trailing brush edge, will now be investigated.

First, the ideal case will be considered in which the emf's of self- and mutual-induction and the emf's produced in the short-circuited winding element by the armature cross flux and pole flux are equal to zero. This would be the case only if the velocity of the armature were zero. Let

$R_s$ = resistance of short-circuited winding element,
$R_r$ = resistance of a commutator riser,
$R_b$ = contact resistance between the brush and commutator,

$i$ = current in short-circuited winding element,
$i_1, i_2$ = currents in the commutator risers,
$A_b$ = contact surface area of brush,
$A_1$ = contact surface area of brush with commutator bar 1,
$A_2$ = contact surface area of brush with commutator bar 2.

From Fig. 9–2 which represents the position of brush and commutator bars at a time $t$ seconds after the short circuit begins, the following relations may be obtained:

$$i_1 = i_a - i, \quad i_2 = i_a + i, \tag{9–3}$$

$$A_1 = A_b \frac{t}{T_c}, \quad A_2 = A_b \frac{T_c - t}{T_c} \tag{9–4a}$$

and for the contact resistances between brush and bar 1 ($R_1$) and brush and bar 2 ($R_2$)

$$R_1 = R_b \frac{A_b}{A_1} = R_b \frac{T_c}{t} \tag{9–4b}$$

$$R_2 = R_b \frac{A_b}{A_2} = R_b \frac{T_c}{T_c - t} \tag{9–4c}$$

From these it is seen that, when $t = 0$, $R_1 = \infty$ and $R_2 = R_b$, and when $t = T_c$, then $R_1 = R_b$ and $R_2 = \infty$.

With the assumption that no emf's are present in the short-circuited path, the sum of all voltage drops, according to Kirchhoff's law, must be equal to zero. Therefore,

$$iR_s + i_2 R_r + i_2 R_b \frac{T_c}{T_c - t} - i_1 R_b \frac{T_c}{t} - i_1 R_r = 0 \tag{9–5}$$

If the values of $i_1$, $i_2$, as given in Eq. 9–3, are substituted in Eq. 9–5 and we let

$$k_1 = \frac{R_s + 2R_r}{R_b} \tag{9–6}$$

the short-circuit current $i$ as a function of time $t$ is given by the equation:

$$i = i_a \frac{T_c(T_c - 2t)}{T_c^2 + k_1 t(T_c - t)} \tag{9–7a}$$

Curve II of Fig. 9–5 is the curve of the short-circuit current $i$ drawn for a value of $k_1 = \frac{1}{5}$. If $k_1$ is assumed zero, i.e., if the resistance of the coil and commutator risers is assumed negligible in comparison to the brush contact resistance (and this is usually permissible), Eq. 9–7a becomes

$$i = i_a - \frac{2i_a t}{T_c} \tag{9–7b}$$

and the curve of the short-circuit current $i$ is the straight line I (Fig. 9–5). For $t = 0$ and $t = T_c$, i.e., for the beginning and end of the commutation period, Eq. 9–7a yields $i = i_a$ and $i = -i_a$, respectively, as it should.

Therefore, if the resistance of the brush contact is the exclusive factor influencing the commutation (*resistance commutation*), the commutation curve $i=f(t)$ is approximately a straight line.

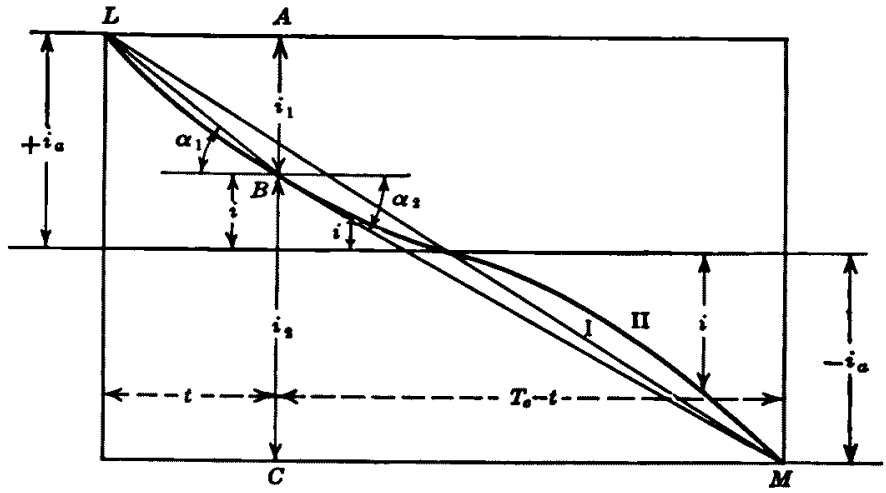


FIG. 9–5. Resistance commutation and linear commutation.

However, the current density at the leading and trailing brush edges is of more concern than the shape of the current curve during the entire commutation period.

At time $t$ the current density at the contact area of the brush with bar 1 is

$$s_1=\frac{i_1}{A_1}=\frac{T_c}{A_b}\frac{i_1}{t} \tag{9–8}$$

and at the contact area of the brush with bar 2

$$s_2=\frac{i_2}{A_2}=\frac{T_c}{A_b}\frac{i_2}{T_c-t} \tag{9–9}$$

The currents $i_1$ and $i_2$ are (Eq. 9–3)

$$i_1=i_a-i \quad \text{and} \quad i_2=i_a+i$$

In Fig. 9–5 the value of $i_1$ is represented by the distance from a point on the commutation curve $i=f(t)$ to the top of the rectangle which is located at a distance $+i_a$ from the axis of abscissa. In the same manner $i_2=i_a+i$ is the distance from the point on the commutation curve to the bottom of the rectangle which is located at a distance $-i_a$ from the axis of abscissa. Thus, in Fig. 9–5, at time $t$, $i_1=AB$ and $i_2=BC$. Since $s_1=\text{const}\times i_1/t$ (Eq. 9–8) and $s_2=\text{const}\times i_2/(T_c-t)$, (Eq. 9–9),

$$s_1=\text{const}\times\frac{i_1}{t}=\text{const}\times\tan\alpha_1 \tag{9–10}$$

and

$$s_2=\text{const}\times\frac{i_2}{T_c-t}=\text{const}\times\tan\alpha_2 \tag{9–11}$$

(Fig. 9–5). Therefore, the current densities $s_1$ and $s_2$ at the contact areas of the brush with bars 1 and 2 at the time $t$ are found by drawing a horizontal line through the point in consideration (point $B$, Fig. 9–5) on the commutation curve and connecting this point with the corners $L$ and $M$ of the rectangle. The tangents of the angles $\alpha_1$ and $\alpha_2$ formed by this construction are then a direct measure of the current densities $s_1$ and $s_2$. Fig. 9–5, curve I, shows that a value of $k_1=(R_s+2R_r)/R_b=0$ (*linear commutation*) gives a current density that remains constant during the entire commutating period. The resistances of the short-circuited winding element $R_s$ and the commutator risers $2R_r$ cause the current density in the leading part of the brush (bar 1) as well as in the trailing part of the brush (bar 2) to be greater than the constant value which corresponds to linear commutation (curve I). Thus, neither the resistance—nor the linear commutation satisfies the condition for zero current density at the trailing edge of the brush at the end of the short-circuit period $T_c$.

It has been assumed, in the consideration just made, that the brush width is equal to a commutator pitch. If the brush covers several commutator bars and $k_1=0$, the commutation curve is also a straight line, provided no emf's act on the short-circuited winding element.

**9–4. Conditions Necessary for Zero Current Density at the Trailing Brush Edge.** In order to find the conditions for zero current density at the trailing brush edge, it is apparently necessary to set up Kirchhoff's mesh equation for the short-circuit path, taking into account the three emf's enumerated in Art. 9–2. In order to express these emf's as a function of the time $t$, some rough approximations have to be made. Furthermore, the solution of the mesh equation becomes involved. For this reason another approach to the solution of the problem will be used: namely, the *magnitude of the resultant emf* which is necessary to produce zero current density at the trailing edge of the brush at $t=T_c$ will be determined.

Designating this resultant emf by $e_r$ and disregarding the resistances of the short-circuited winding element and commutator risers, Eq. 9–5 may be written:

$$i_2R_b\frac{T_c}{T_c-t}-i_1R_b\frac{T_c}{t}+e_r=0 \tag{9–12}$$

By substituting the values of $i_1$, $i_2$ (Eq. 9–3) and letting

$$-\frac{e_r}{2i_aR_b}=k_2 \tag{9–13}$$

the equation for the short-circuit current $i$ becomes

$$i=i_a\frac{2k_2(T_c-t)t-T_c(2t-T_c)}{T_c^2} \tag{9–14}$$

At times $t=0$ and $t=T_c$, this equation yields values of $i$ equal to $+i_a$ and $-i_a$, respectively, as expected.

The current at the *trailing part* of the brush (bar 2) is at time $t$

$$i_2 = i + i_a = 2i_a \frac{k_2(T_c - t)t + T_c(T_c - t)}{T_c^2} \tag{9–15}$$

and the current *density* at the trailing part of the brush at time $t$ is

$$\frac{i_2}{A_2} = s_2 = \frac{T_c}{A_b} \frac{i_2}{T_c - t} = 2i_a \frac{k_2 t + T_c}{T_c A_b} \tag{9–16}$$

In order to determine the current density in the trailing brush edge, the time $T_c$ is substituted for $t$ in this last equation. This gives

$$s_{2(t=T_c)} = \frac{2i_a}{A_b}(k_2 + 1) \tag{9–17}$$

It is seen from this equation that the current density under the trailing brush edge ($t=T_c$) is zero, when $k_2 = -1$. *This is the most favorable condition for good commutation.* It occurs when the resultant of all emf's ($e_r$) acting on the short-circuited winding element is equal to the voltage drop produced by the contact resistance between brush and commutator ($2i_a R_b$).

This analysis, derived under the assumption that the width of the brush is equal to the width of 1 commutator pitch, also holds approximately when the width of the brush is greater than 1 commutator pitch.

Fig. 9–6 shows the commutation curve $i=f(t)$ for $k_2 = -1$. Near the end

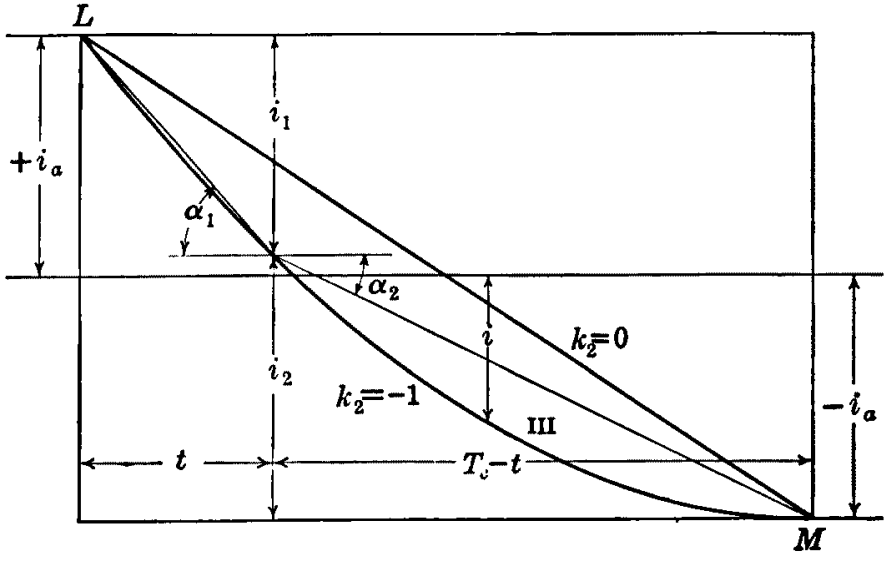


FIG. 9–6. Accelerated commutation corresponding to current density zero at the trailing edge of the brush.

of the short-circuit period the current curve is almost tangent to the line $i=-i_a$; consequently $i_2$ and also $s_2 = \text{const} \times \tan \alpha_2$ are almost zero at the end of the short-circuit period. At $t=T_c$, $s_2$ becomes zero.

Comparing the commutation curve for $k_2 = -1$ (curve III, Fig. 9–6) with the straight line representing the linear commutation, we see that for $k_2 = -1$ the positive values of $i$ are smaller and the negative values of $i$ are larger than in the case of linear commutation, i.e., $k_2 = -1$ means *accelerated commutation.*

**9–5. Effects of the Various Emf's on the Commutation.** The effects of the individual emf's acting on the short-circuited winding element will now be considered.

(a) *Influence of the Emf of Self-induction on the Commutation.* During the short-circuit period $T_c$ the current in the short-circuited winding element changes from $+i_a$ to $-i_a$. This causes a corresponding *variation* in the leakage fluxes of the coil and consequently an emf of self-induction. This emf opposes any change of the current and therefore *delays* the change of the current from $+i_a$ to $-i_a$. Fig. 9–7 again shows the straight line curve I for linear commutation and also a delayed commutation curve IV due to the emf of self-induction. For each value of time $t$ the short-circuit current $i$ shown in curve IV is greater than the corresponding current of curve I. Near the end of the short-circuit period $T_c$ the absolute value of current in the short-circuited winding element is considerably less than $i_a$; and thus the current density under the trailing brush edge, $s_2 = \text{const} \times (\tan \alpha_2)$, is quite large. *The chief cause of sparking in the d-c machine lies in the detrimental effect of the emf's of self- and mutual-induction on the short-circuited winding element during commutation.*

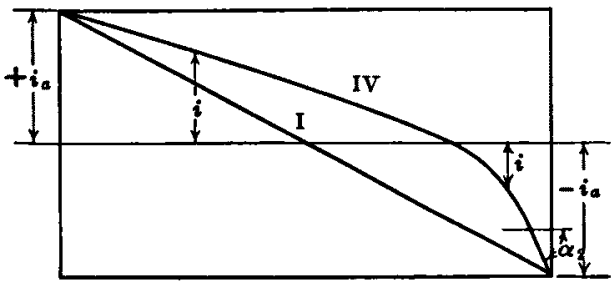


FIG. 9–7. Delayed commutation due to the emf of self-induction in the short-circuited winding element.

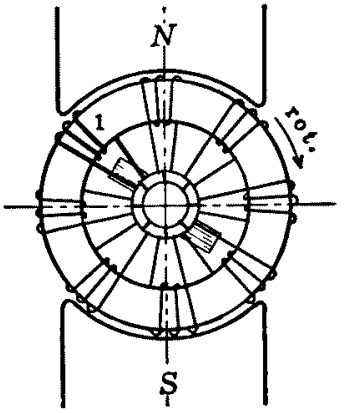


FIG. 9–8. Influence of main pole flux on commutation. (Winding elements shown schematically)

(b) *Influence of the Main Flux on Commutation.* The emf induced in the short-circuited element by the main flux either delays or accelerates commutation, according to the position of the coil in the main flux during the commutation period, i.e., according to the position of the brushes on the commutator. This can be understood easily by reference to Fig. 9–8 which

shows a 2-pole generator. The brushes are displaced far enough in the direction of rotation so that commutation in a coil such as coil 1 takes place in the strong field of the north pole. Consider coil 1. It moves from the lower to the upper armature path, and its direction of current, which corresponds to the south pole, will be changed to that of the north pole. However, since the coil lies under a north pole *during the commutation period*, an emf already is induced in it in the direction which it should have *after* the commutation period is completed. This accelerates the commutation. If the brushes in Fig. 9–8 were shifted opposite to the rotation, the direction of the emf induced in the coil during the period of commutation by the south pole would be opposite to that which it should have at the end of commutation; i.e., for this position of the brushes the commutation is delayed.

*In general, commutation is accelerated by shifting the brushes of a generator in the direction of rotation and shifting the brushes of a motor opposite to the rotation*; commutation is delayed by shifting the brushes of a generator opposite to the direction of rotation and the brushes of a motor in the direction of rotation.

Thus the delaying effect of the emf of self-induction may be compensated for by a suitable shift of the brushes in the direction of rotation for a generator or opposite to rotation for a motor; this shift may change the delayed commutation (*undercommutation*) of curve IV (Fig. 9–7) to the accelerated commutation (*overcommutation*) of curve III (Fig. 9–6).

(c) *Influence of the Armature Flux on Commutation.* In order to determine the effect of the third emf on the short-circuited winding element, i.e., of the emf induced by the armature flux, reference will be made to Fig. 5–10. It already has been mentioned that the armature flux is stationary in space and its position independent of the rotation of the armature. The velocity of the armature conductors relative to the armature flux and to the main pole flux is the same. The emf's induced in the individual armature coils by the armature flux *oppose each other in each path* as can be seen if Faraday's law is applied to the flux distribution of Fig. 5–10. (Notice that the current distribution shown in this figure is due to the main flux.) Therefore, these armature emf's cannot produce a current between + and − brushes. On the other hand, the emf induced by the armature flux in the short-circuited winding element can produce a current in the short-circuit path made up of winding element, commutator risers, commutator bars, and the brush.

Considering the left side of the armature in Fig. 5–10, the lines of force produced by the armature leave the armature just as do those produced by the poles at the south pole of the machine; thus the emf induced by the armature flux in the armature conductors lying in the neutral zone to the left is the same as that of the armature path which the conductors leave behind them. The same is true of the conductors lying in the neutral zone to the right. *The armature flux*, therefore, *delays commutation* exactly as does the emf of self-induction.

Summarizing, it can be said that the emf of self-induction as well as the emf produced by the armature flux delays the commutation and consequently gives rise to high current densities at the trailing brush edge. In order to prevent sparking at the brushes and improve the commutation, either the main flux (by moving the brushes) or a special commutating flux (interpoles) has to be employed. This then compensates not only for the effect of the emf of self-induction and the emf produced by the armature flux, but in addition compensates for the voltage drop in the contact resistance of the brushes. If the main flux is used to improve commutation, the brushes are shifted in the direction of rotation in generators and opposite to rotation in motors.

In the foregoing discussion, the effects of the armature flux and of the main flux on the short-circuited winding element have been considered separately. Since the effect of these fluxes in the commutating zone, i.e., in the *air*, has to be investigated, separate consideration of both fluxes is permissible. Actually only one flux, which is the resultant of both of these fluxes, is present (Fig. 5–11).

As previously explained (see Art. 5–4), the effect of the armature flux manifests itself in a displacement of the neutral zone—ahead (in the direction of rotation) in the case of the generator and behind in the case of the motor. Considering the left half of Fig. 5–11 which represents a generator, it is seen that commutation takes place in the flux of a south pole which the coil left behind it. Commutation, therefore, is taking place in an improper flux and, as a result, is delayed. Thus, with respect to the influence of the armature flux, the same result will be obtained regardless of whether this flux is considered independently or whether the total flux which includes it is considered.

Too strong an armature flux is to be avoided, not only because of its effect on commutation and distortion of the flux, but also because of the associated danger of ring fire (flash-over). By a suitable selection of the ratio of pole arc to pole pitch and the ratio of armature mmf to field mmf, the effect of the armature flux can be limited. The greater the ratio of field mmf to armature mmf the less noticeable is the effect of the armature flux. The desired ratio of field mmf to armature mmf can be obtained by a satisfactory selection of the air-gap and saturation of the iron. A relatively large air-gap is especially necessary in small machines without interpoles.

**9–6. Production of a Commutating Flux by Means of Interpoles. Compensating Winding.** In order to obtain good commutation, interpoles, rather than the main flux and a shift of the brush axis, are used to produce the necessary commutating flux. Reasons for this use will be discussed later. Since the *purpose of the interpoles is acceleration of commutation*, each generator interpole must have the same polarity as the main pole ahead of it in the direction of rotation. For motors the interpole polarity is opposite to that of the main pole ahead in the direction of rotation. Fig. 9–9 shows the

arrangement of the interpoles for a 2-pole generator, Fig. 9–10 for a 2-pole motor. The interpole axis coincides with the perpendicular to the pole axis. As Figs. 9–9 and 9–10 show, the interpole flux opposes the armature flux; in

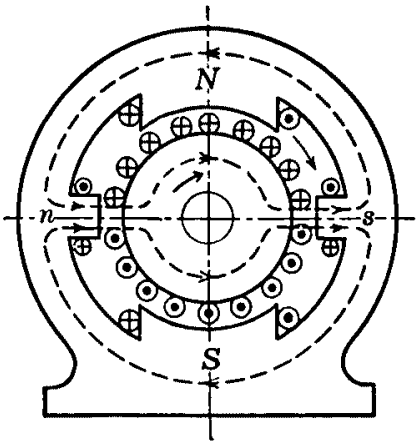


FIG. 9–9. Interpole arrangement for a 2-pole generator.

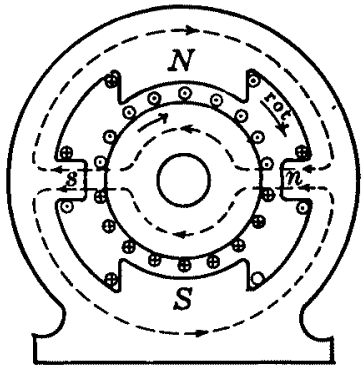


FIG. 9–10. Interpole arrangement for a 2-pole motor.

the neutral zone it completely cancels the armature flux. The interpole flux must be stronger than the armature flux in the neutral zone, for in addition to canceling this flux it must induce an emf in the short-circuited winding element which opposes the emf of self- and mutual-induction and the voltage drop $2i_aR_b$ under the brushes.

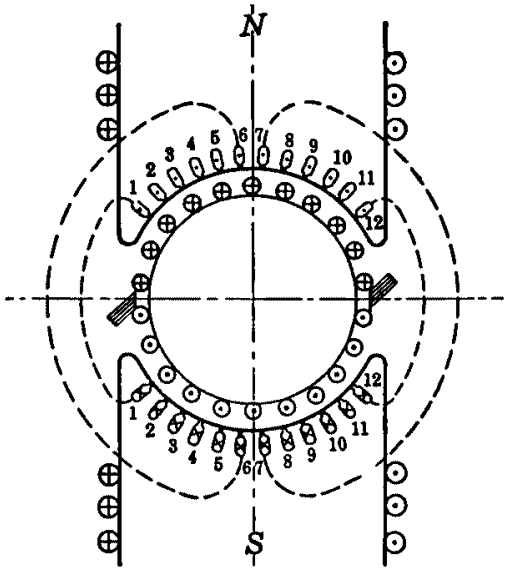


FIG. 9–11. Schematic diagram of a compensating winding in a 2-pole d-c machine.

The interpoles cancel the armature cross flux *only in the commutation zone*. The non-uniform distribution of the flux in the pole and the concentration of flux in the air-gap under 1 pole half is not affected by the interpoles; therefore the danger of ring fire still exists. In the case of large machines and heavy-duty machines, as for example steel-mill rolling motors which are subject to sudden heavy loads and require rapid reversal of rotation, a special winding called a *compensating winding* is used to suppress the armature flux. The complete suppression of the armature flux would be possible only by the use of a winding distributed over the whole surface just as the armature winding is. For this reason the compensating winding is *placed in the pole shoes* near to the surface. Fig. 9–11 shows the schematic diagram of the compensating winding for a 2-pole machine. Back connections are made as follows: top conductor 1 with bottom

conductor 1, top conductor 2 with bottom conductor 2, etc. The front connections are: bottom conductor 1 with top conductor 2, bottom conductor 2 with top conductor 3, etc. This results in a solenoid having an axis coincident with the neutral axis and the axis of the armature flux. Figs. 9–12a and 9–12b show the position of the compensating winding relative to the

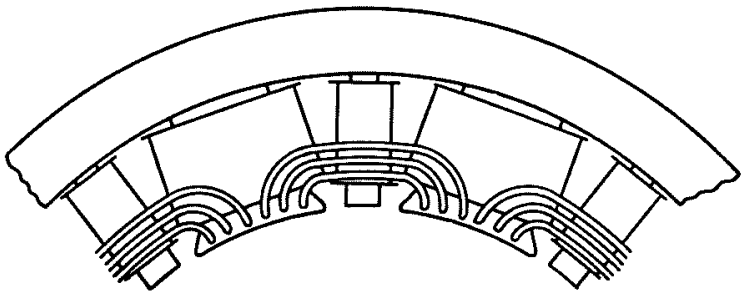

FIG. 9–12a. End connections of a compensating winding.

main poles and interpoles. Since the armature mmf is proportional to the armature current, the mmf of the compensating winding also must be proportional to the armature current. Consequently the armature and com-

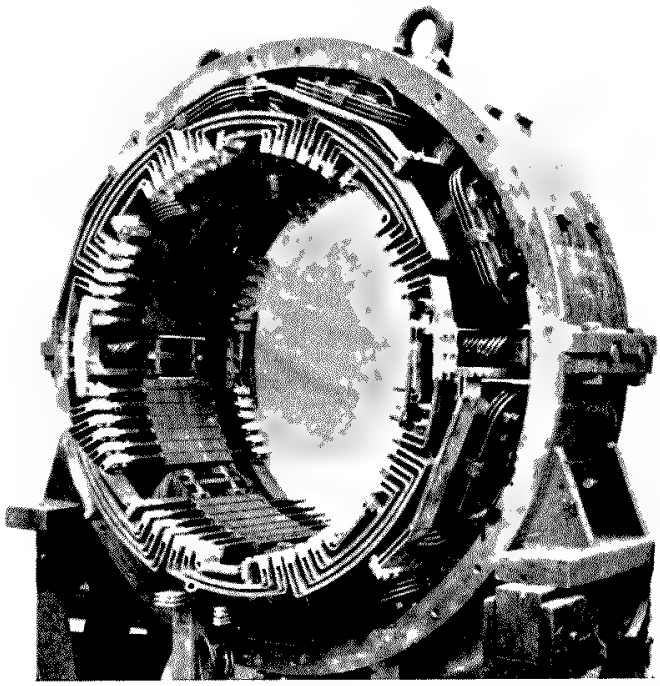

FIG. 9–12b. Larger d-c machine with interpoles and compensating winding.

pensating windings must be connected in series in such a manner that the armature and compensating winding conductors lying within the same pole pitch carry the armature current in different directions.

If a compensating winding is used, it will suppress the mmf of those armature conductors which lie under the pole shoes. The remaining armature

mmf (about 30%) as well as the emf of self- and mutual-induction and the voltage drop under the brushes must be suppressed by the interpoles. Machines having a compensating winding can be built with a smaller air-gap than those without compensating windings. It will be shown that the interpole also must carry the armature current if it is to improve the commutation at all loads.

**9–7. The Magnitude of the Emf of Self- and Mutual-Induction in the Short-Circuited Winding Element. The Magnitude of Interpole Flux —Density.** In the previous considerations (Art. 9–5a) the emf of self-induction in the short-circuited winding element due to the change in the current from $+i_a$ to $-i_a$ has been discussed. Usually several winding elements commutate at the same time and, therefore, the mutual inductance between the short-circuited winding elements also has to be taken into account. Fig. 9–13 shows a 4-pole lap winding with 1 conductor per layer

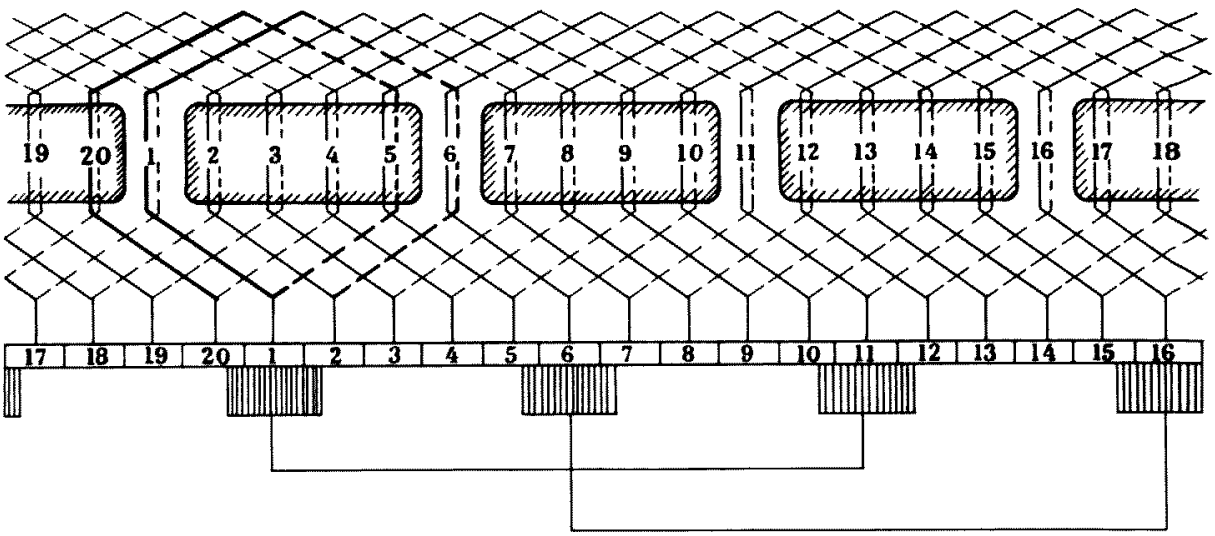


FIG. 9–13. Commutation when brush width is larger than one commutator pitch.

and a brush width greater than 1 commutator pitch. The sides of the winding elements which are short-circuited by the positive and negative brushes (indicated by heavier lines) lie near to each other and consequently induce mutual emf's in each other. The total emf induced in the short-circuited winding element is thus:

$$e = -\left(L\frac{di}{dt} + \Sigma M_x \frac{di_x}{dt}\right) \tag{9–18}$$

It was mentioned that the magnitude of $L$ is determined by the leakage fluxes of the armature, i.e., by the slot leakage, tooth-top leakage, and end winding leakage. The same leakage fluxes also determine the magnitude of $M$.

The currents $i$ and $i_x$ as functions of $t$ (Eq. 9–18), i.e., the commutation

curves, are not known. The *average* change of current during the period $T_c$ *is known*. It is $2i_a/T_c$, for the current in the winding element must change during the time $T_c$ from $+i_a$ to $-i_a$. This average current-change in connection with the simple expression $e = -L\frac{di}{dt}$ is used in order to determine the emf of self- and mutual-induction in the short-circuited winding element. This $L$ includes then the coefficients of self- *and* mutual-induction. Thus

$$e_s = L\frac{2i_a}{T_c} \text{ volts} \tag{9–19}$$

In this formula $L$, $T_c$, and $i_a$ will be expressed by other quantities in order to demonstrate clearer the factors which most influence the commutation.

From Eq. 1–13

$$L = \frac{N\phi}{i} \tag{9–20a}$$

and from Eq. 1–21

$$\phi = \frac{0.4\pi Ni}{R_m} = 0.4\pi Ni \times \Lambda_m$$

Thus

$$L = 0.4\pi N^2 \times \Lambda_m \tag{9–20b}$$

With the number of turns per winding element $N_e$ and the armature length $l$, the equation for $L$ of the short-circuited winding element can be written as

$$L = N_e{}^2 2l\xi \times 10^{-8} \text{ henry} \tag{9–21}$$

where $\xi$ is the magnetic permeance of the leakage fluxes per unit length of armature. $\xi$ takes into account the self- and mutual-inductance.

If $b'_b$ is the brush width referred to the circumference of the armature and $v_a$ is the surface velocity of the armature, the short-circuit period $T_c$ is (see Eq. 9–2)

$$T_c = \frac{b'_b}{v_a} \tag{9–22}$$

To the brush width $b'_b$ there correspond $Ab'_b$ ampere-conductors on the armature surface (for the definition of $A$, see Art. 5–4c). Assuming that the brush width is equal to 1 commutator bar, then, since $2N_e i_a$ ampere-conductors are associated with 1 commutator bar,

$$Ab'_b = 2N_e i_a \tag{9–23}$$

Inserting Eqs. 9–21, 9–22, and 9–23 into Eq. 9–19, there results

$$e_s = N_e A v_a l\xi \times 10^{-8} \text{ volts} \tag{9–24}$$

where $A$ is measured in ampere-conductors per inch circumference, $v_a$ in ft/min, and $l$ in inches.

Eq. 9–24 has been derived under the assumption that the brush width is equal to 1 commutator bar. It also holds with good approximation when the brush covers several commutator bars. In this case the short-circuit period $T_c = \frac{b'_b}{v_a}$ in Eq. 9–22 becomes larger, but $L$, which comprises the mutual inductance, also becomes larger since the number of simultaneously short-circuited winding elements increases with increasing $b'_b$.

It follows from Eq. 9–24 that, in order to reduce the magnitude of $e_s$, the quantities $N_s$, $A$, $v_a$, and $\xi$ must be small. For this reason, medium-sized and larger d-c machines have only one turn per winding element ($N_s = 1$) and are designed with a relatively shorter core and a relatively shallower slot than the a-c machines. The shallow slot reduces the permeance of the slot leakage flux and, therefore, $\xi$ the value of which normally lies between 4 and 7. The speed of even medium-sized d-c machines does not exceed 2400 rpm, whereas a-c machines of all sizes can be built for 3600 rpm. In general, d-c machines cannot be built for the large output which a-c machines are built for.

While the effect of the armature flux on the short-circuited winding element can be nullified by the use of interpoles or interpoles and a compensating winding which suppress the armature flux itself, the effect of the emf of self- and mutual-induction can be opposed only by employing an external flux and inducing an emf in the winding element which is equal to, but opposite in direction to, the emf of self- and mutual-induction. The cause of the emf of self- and mutual-induction, namely, the variation of the leakage fluxes during commutation, cannot be removed.

If the flux density under the interpole is $B_i$, then, according to Eq. 1–2b, the emf induced in the short-circuited winding element by the interpole flux is

$$e_i = \tfrac{1}{5} \times 2B_i l v_a N_s 10^{-8} \text{ volts} \qquad (9\text{–}25)$$

If the only purpose of the interpole is to compensate for the emf of self- and mutual-induction, the interpole flux density would be adjusted so that $e_i = e_s$. By equating Eqs. 9–24 and 9–25 there results:

$$B_i = \xi A \times 2.54 \text{ lines per in.}^2 \qquad (9\text{–}26)$$

As a matter of fact, $B_i$ *must be somewhat larger* in order to compensate for the voltage drop $2i_a R_b$ due to the brush contact resistance.

Since the emf's of self- and mutual-induction are proportional to $A$, i.e., to the armature current, the interpole flux, according to Eq. 9–26, also must increase with increasing armature current. This is possible only if the interpole winding carries the armature current and the saturation of the interpoles is low enough so that a direct proportionality exists between interpole flux and armature current. Therefore, the interpole winding, just as the compensating winding, must be connected in series with the armature.

Eq. 9–26 also shows why improvement of commutation by shifting the brushes and making use of the main flux is not as good as the improvement that can be obtained by using interpoles. This is due to the fact that no direct proportionality exists between the main flux and the armature current. If the brushes are set in a position to give good commutation for a certain load, then a lighter load will produce overcommutation and a heavier load will produce undercommutation. Each load, therefore, requires a different brush position. In general, for a machine which operates at various loads, good commutation cannot be obtained by shifting the brushes. For this reason, only small machines are constructed today without interpoles.

From the foregoing, the conclusion could be drawn that an emf of self- and mutual-induction of any magnitude in the short-circuited winding element is permissible, provided an interpole flux as given by Eq. 9–26 exists. It should not be forgotten, however, that the calculations have been based on an *average* value of the emf of self- and mutual-induction. Actually the difference between the *instantaneous* value of $e_s$ and $e_i$ is of great importance for the commutation. With respect to this matter, the average value of the emf of self- and mutual-induction, according to Eq. 9–26, is not permitted in practice to exceed 8 to 12 volts.

As has been explained in Art. 3–9, circulating currents may arise in the armature winding under certain conditions which load the brushes and produce high current densities. For this reason, only symmetrical windings are employed in order to obtain good commutation and, by means of equalizer connections provided for the purpose, the circulating currents due to mechanical unsymmetries are prevented from following a path through the brushes.

Bouncing of the brushes or a loose commutator likewise can lead to high local current densities under the brushes. Therefore, a rigid construction of the brush studs and commutator is also one of the necessary conditions for good commutation. Brushes having a high contact resistance are more desirable for good commutation than those having a low contact resistance since the high resistance diminishes the short-circuit current; however, they give rise to greater losses and a greater heating effect of the commutator.

**9–8. The Brush Curve.** The brush curve represents the voltage drop between brush and commutator for different points on the commutator under the brush. The voltage drop is measured usually on four points, as shown in Fig. 9–14a. The brush curve gives an indication of the shape of the commutating curve, for the voltage drop between brush and commutator is greater where the current density is greater. Fig. 9–14b shows three different shapes of brush curves. Curve A indicates nearly uniform current density all along the brush and, therefore, corresponds to nearly linear commutation. Curve *B* shows a large decrease of current density from the leading edge to the trailing edge of the brush, indicating overcommutation (curve IV, Fig.

9–16). Curve $C$ shows a large increase of current density from the leading to the trailing edge of the brush, indicating undercommutation (curve III, Fig. 9–16) and too weak a commutating flux.

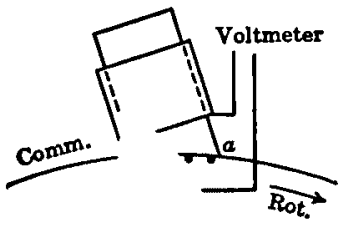


FIG. 9–14a. Determining the brush curve by test.

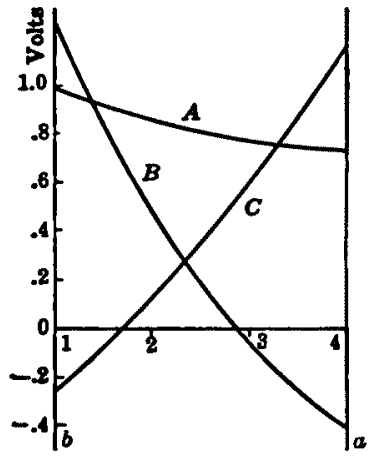


FIG. 9–14b. Brush curve.

**9–9. Reaction of Current in the Short-Circuited Winding Elements upon Main Flux.** Fig. 9–15 shows the initial and final positions of a winding element undergoing commutation in a generator. In the initial position $ab$

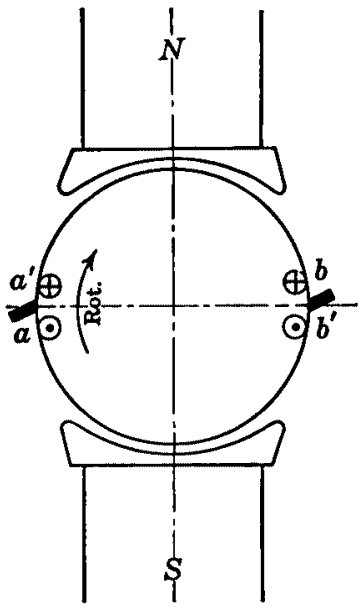


FIG. 9–15. Influence of short-circuited winding elements on the main flux.

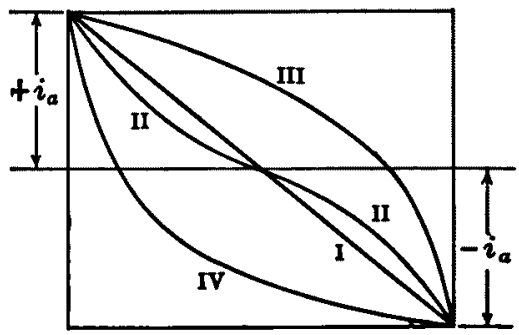


FIG. 9–16. Linear commutation (I), undercommutation (III), and overcommutation (IV).

it exerts a demagnetizing mmf on the main flux; in the final position $a'b'$ it is magnetizing. If the commutation is linear (line I, Fig. 9–16) or if the commutation curve $i=f(t)$ is symmetrical with respect to the straight line I

(curve II, Fig. 9–16), the *average effect* of the short-circuited winding element on the main flux during the commutation is zero. If the commutation is delayed (undercommutation, curve III, Fig. 9–16), the effect on the main flux is the same as if the coil were in the position *ab*. On the other hand, if the commutation is accelerated (overcommutation, curve IV, Fig. 9–16), the effect of the short-circuited winding element on the main flux is the same as if the coil were in the position *a'b'*. Thus steady undercommutation (curve III) produces a demagnetizing effect on the main flux; steady overcommutation (curve IV, Fig. 9–16) produces a magnetizing effect. Steady *delayed* commutation has the same effect on the main flux of a generator as a brush shift in the direction of rotation; steady *accelerated* commutation has the same effect as a brush shift opposite to the direction of rotation. Steady delayed commutation weakens the main flux in a generator and increases it in a motor; steady accelerated commutation produces the opposite effect. The magnitude of the magnetizing or demagnetizing effect depends upon the difference between the commutation curve (curve III or IV, Fig. 9–16) and the straight line I, i.e., upon the average value of the additional short-circuit current in the winding element.

In small machines, the influence of the short-circuit currents on the main flux may be noticeable. In the previous discussions it has been disregarded.

# *Chapter 10*

# SPECIAL D-C MACHINES AND ROTATING AMPLIFIERS

## A. Special D-C Machines

**10–1. Three-Wire Generator.** A great economy in the use of copper can be realized when power transmission is accomplished at a high voltage and a low current rather than at low voltage and high current. Assume $V$ to be the voltage at the generator end, $I$ the current transmitted, and $R$ the total resistance of the line wires. The power loss in the line is then $I^2R$. If the same power is transmitted at the voltage $2V$, the current is $I/2$, and, for the same power loss, the resistance of the lines is 4 times larger and therefore the weight of the copper in the line wires is only one-fourth of its value at the voltage $V$.

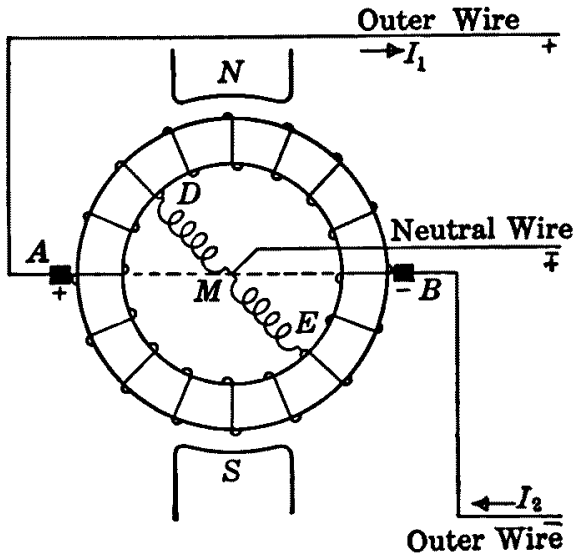


Fig. 10–1. Three-wire generator.

However, in incandescent lighting, lamps designed for 115 and 120 volts are more efficient than those designed for higher voltage. The *3-wire system* makes it possible to connect lamps and small loads (small motors) to a low voltage, while larger loads (larger motors) can be connected to a voltage 2 times that of the lamps.

Fig. 10–1 shows the scheme of a 3-wire generator devised by *Dolivo-Dobrowolsky* (see Ref. D1). A coil of wire $DE$ wound on an iron core and thus

having a high reactance is connected into the armature winding between points $D$ and $E$ which lie 180 electrical degrees apart. The voltage between points $D$ and $E$ is alternating (Art. 3–8). The current in the coil $DE$ has the frequency $pn/120$, and it is very small due to the high reactance of the coil. The mid-point $M$ of the coil is connected through a slip ring to a third wire or *neutral* wire. Lamps and small motors are connected between the outer wires and the neutral wire, while larger motors are connected between the outer wires.

When both halves of the system are loaded equally, $I_2 = I_1$, and no current flows through the middle wire. Thus, at no-load and at symmetrical load,

$$V_{AD} = V_{EB} \quad \text{and} \quad V_{MD} = V_{EM} \tag{10–1}$$

$$V_{AD} + V_{DM} = V_{ME} + V_{EB} \tag{10–1a}$$

for any position of the coil (of the taps $D$ and $E$). Since the voltage $V_{AB}$ is the terminal voltage of the generator $V$,

$$V_{AM} = V_{MB} = \frac{V}{2} \tag{10–1b}$$

The power output at any symmetrical load is

$$P = VI_1 = VI_2 = V\frac{I_1 + I_2}{2} \tag{10–2}$$

When both halves of the system are loaded unsymmetrically, a direct current will flow through the coil superimposed on the small alternating current and the voltages of both circuits will not be equal. The voltage difference between both circuits must not exceed a certain magnitude. This difference will be determined in the following analysis.

The total power output is

$$P = V_1 I_1 + V_2 I_2 \tag{10–3}$$

where

$$V_1 + V_2 = V = V_{AB} \tag{10–4}$$

Introducing the total voltage $V$ in the output equation, there results:

$$P = (V_1 + V_2)\left(\frac{I_1 + I_2}{2}\right) + (V_1 - V_2)\left(\frac{I_1 - I_2}{2}\right) \tag{10–5}$$

For $I_1 = I_2$, this equation yields Eq. 10–2.

Eq. 10–5 can be rewritten as

$$P = V\frac{I_1 + I_2}{2} + V_1\frac{I_1 - I_2}{2} - V_2\frac{I_1 - I_2}{2} \tag{10–6}$$

The current distribution in the different parts of the system, corresponding

to Eq. 10–6, is shown in Fig. 10–2. Both circuits have the common current $(I_1+I_2)/2$, which determines the total voltage $V$:

$$V=E-\frac{I_1+I_2}{2}r_a \tag{10–7}$$

The current in the neutral wire is

$$I_n=2\frac{I_1-I_2}{2}=I_1-I_2 \tag{10–8}$$

This current divides into two equal parts in the coil $DE$ and goes through

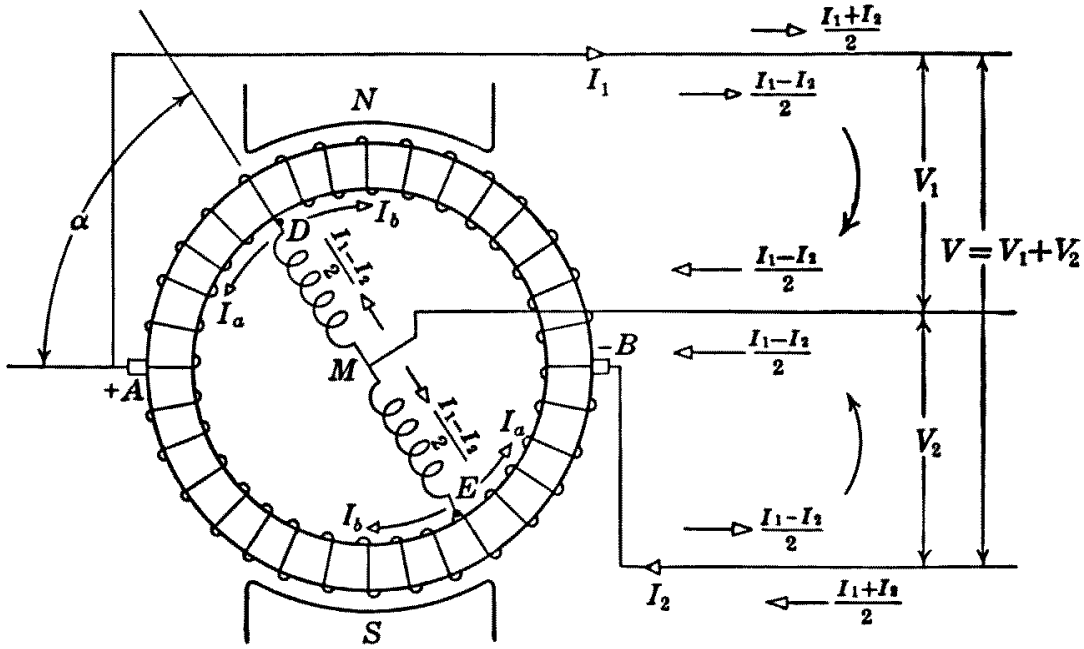


FIG. 10–2. Determination of the voltage drop between the outer wires of a three-wire generator.

the armature to the positive as well as to the negative brush; it produces the difference between the voltages $V_1$ and $V_2$.

The voltage drop in the coil is

$$\epsilon_c=\frac{I_1-I_2}{2}\frac{R_c}{2} \tag{10–9}$$

where $R_c$ is the resistance of the entire coil $DE$.

The voltage drop in the part of the armature winding $AD$, due to the neutral-wire current, varies during rotation of the armature. If $r_a$ is the armature resistance, the resistance of the part $AD$ (Fig. 10–2) is

$$x=\frac{\alpha}{\pi}2r_a \tag{10–10}$$

and the resistance of the part $DB$ is $2r_a-x$.

Assume that the current $(I_1-I_2)/2$ divides into the components $I_a$ and $I_b$

at the point $D$ (Fig. 10–2). Then the current at the point $E$ also divides into $I_a$ and $I_b$ in such a manner that the current between $E$ and $B$ is equal to $I_a$ and the current between $E$ and $A$ is equal to $I_b$.

Kirchhoff's laws, when applied to the complete closed armature circuit, yield:

$$I_a x - I_b(2r_a - x) + I_a x - I_b(2r_a - x) = 0 \tag{10–11}$$

and

$$I_a + I_b = \frac{I_1 - I_2}{2} \tag{10–11a}$$

Thus

$$I_a x = \frac{I_1 - I_2}{2}\left(\frac{2r_a x - x^2}{2r_a}\right) \tag{10–11b}$$

This is the voltage drop in the part $DA$ of the armature due to the current in the neutral wire. The average voltage drop is

$$\epsilon_a = \frac{1}{\pi}\int_0^{\pi} V_{AD}\,d\alpha = \frac{1}{\pi}\int_0^{\pi} I_a x\,d\alpha = \frac{1}{\pi}\int_0^{\pi} \frac{I_1 - I_2}{2}\left(\frac{2r_a x - x^2}{2r_a}\right)\,d\alpha \tag{10–12}$$

Inserting $\alpha = x\pi/2r_a$ from Eq. 10–10, the average voltage drop is

$$\epsilon_a = \frac{I_1 - I_2}{2}\frac{1}{2r_a}\int_0^{2r_a} \frac{2r_a x - x^2}{2r_a}\,dx$$

$$\epsilon_a = \frac{1}{3}\frac{I_1 - I_2}{2} r_a \tag{10–13}$$

The total voltage drop between $M$ and $A$ is equal to $\epsilon_c + \epsilon_a$. Thus,

$$\epsilon = \frac{I_1 - I_2}{2}\left(\frac{R_c}{2} + \frac{1}{3} r_a\right) \tag{10–14}$$

The total voltage drop between $M$ and $B$ has the same magnitude as the total voltage drop between $M$ and $A$ but is opposite in direction since it adds to $V/2$ when the other subtracts from it. Therefore, the total voltage difference between both circuits is equal to 2 times $\epsilon$, i.e.,

$$\Delta V = (I_1 - I_2)(\tfrac{1}{3} r_a + \tfrac{1}{2} R_c) \tag{10–15}$$

**10–2. Train-Lighting Generators.** A train-lighting generator must satisfy the condition that the lamp voltage shall be constant, independent of the number of lamps in use, and also of the speed and direction of motion of the train, since the generator is driven from the axle. The same condition applies to generators for automobile lighting except that there is no need to provide for a reversal of direction of rotation, since in automobiles the generator is driven from the engine which always runs in the same direction.

The normal d-c generator has as many brush studs as poles. However, it is possible to arrange more brush studs than poles in the d-c machine and

to use a part of the brush studs for the production of another flux in addition to the main flux (*4-brush generator by Rosenberg*) or for the excitation of the main poles (*3rd-brush generator by Sayers*). In the following, a 4-brush generator suitable for train-lighting storage-battery systems and a 3-brush generator suitable for automobile-lighting storage-battery systems will be described.

Fig. 10–3 shows the Rosenberg generator (see Ref. D3). The battery serves two purposes: it excites the shunt field winding *ShF*, i.e, the main poles *N* and *S*, and supplies current to the lamps which are connected through suitably controlled contractors or relays to $T_1T_2$, when the train is at rest. Besides the normal brushes $B_1B_1$ perpendicular to the pole axis, there are 2 brushes $B_2B_2$ in the pole axis. The brushes $B_1B_1$ are short-circuited. When the

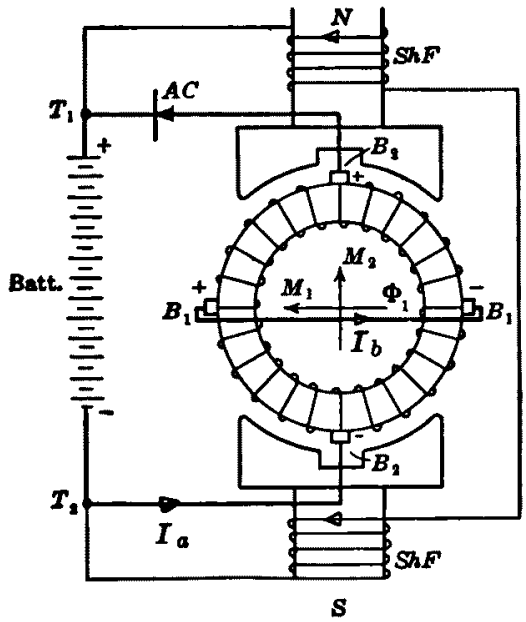


FIG. 10–3. Rosenberg generator for constant current.

machine rotates, the pole flux induces an emf and a current ($I_b$) between these brushes. The armature mmf $M_1$ due to this short-circuit produces a flux $\Phi_1$ the axis of which is perpendicular to the pole axis. The path for this flux $\Phi_1$ is through the interpolar space and the pole shoes. The flux $\Phi_1$ induces an emf between the brushes $B_2B_2$ which are connected to the load circuit. A contact rectifier *AC* which has the property of permitting current to flow in only one direction is placed between one of the brushes $B_2B_2$ and the battery, and is connected so that current can flow only from the armature to the battery and load, thus preventing the discharge of the battery through the armature when the train is at rest or running at low speed.

The current $I_a$ which flows through the armature between the brushes $B_2B_2$ produces an mmf $M_2$ which opposes the mmf of the field winding. The flux in the pole axis therefore becomes weak. This fact in connection

with a notching of the poles in the pole axis facilitates the commutation of load brushes $B_2B_2$ which short-circuit winding elements directly under the poles.

It can be seen from Fig. 10–3 that when the direction of rotation is reversed, the cross flux $\Phi_1$ also reverses its direction and, as result of the double reversal, the polarity of the load brushes $B_2B_2$ remains unchanged.

There is a limit beyond which the current $I_a$ delivered by the load brushes $B_2B_2$ cannot increase. This limit is reached when the armature mmf $M_2$ neutralizes the mmf of the shunt field winding. Therefore, beyond a certain speed the machine will deliver a practically constant current (Fig. 10–4).

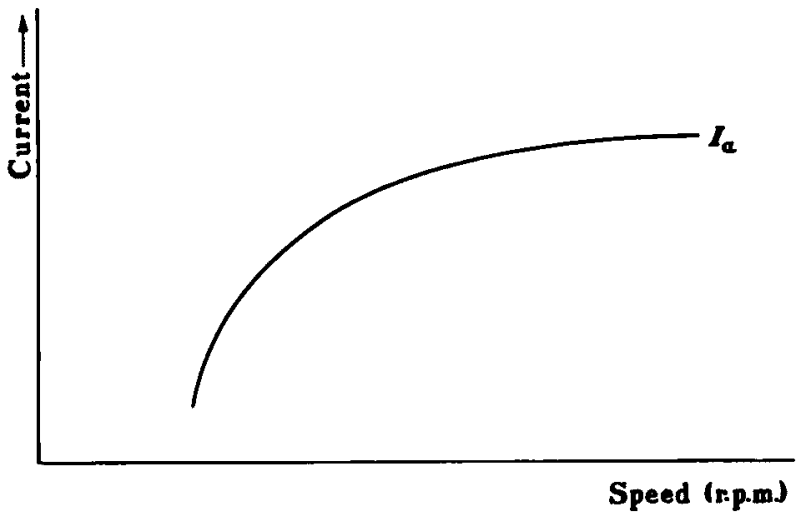


FIG. 10–4. Current-speed curve of the Rosenberg generator.

The magnitude of this current can be regulated by a rheostat in the shunt field circuit. Independence of the polarity of the load brushes on the direction of rotation, and practically a constant current beyond a certain speed are the distinctive properties of the Rosenberg generator.

Provided with a series field winding and with a special control device, the Rosenberg generator can be converted into a constant-voltage instead of a constant-current generator. Fig. 10–5 shows this arrangement. The series field winding $SF$ is in series with the load brushes $B_2B_2$. The shunt field winding is not connected directly to the storage battery as in Fig. 10–3 but through a Wheatstone bridge. The resistances $RR$ of the bridge are constant while the resistances $R'R'$ have negative temperature coefficients. The design of the bridge is such that at a fixed voltage the bridge is balanced and therefore no current flows through the shunt field winding $ShF$. When the voltage is smaller or larger than the fixed value, current flows through the shunt field winding in one direction or the other, adding to or subtracting from the mmf of the series field winding. Here also a cutout or automatic switch is necessary, in order to prevent the battery from discharging through the generator at standstill or under low-speed conditions.

Fig. 10–6 shows the diagram of connections of the Sayers generator (3rd-brush generator), designed to produce automatic compounding action in a constant-speed machine. The shunt winding is not connected between the main brushes $B_1B_2$ as usual, but between an auxiliary brush $B_3$, which is placed about halfway between the main brushes, and the main brush which lies nearer to the trailing pole shoe tip ($B_2$, Fig. 10–6). Under load conditions

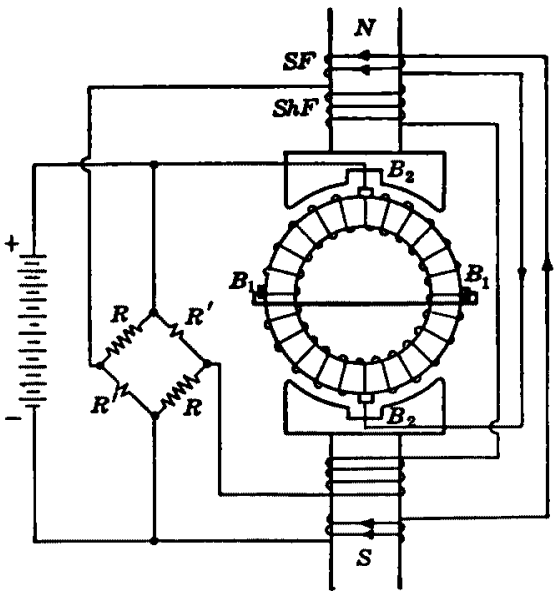


FIG. 10–5. Rosenberg generator for constant voltage.

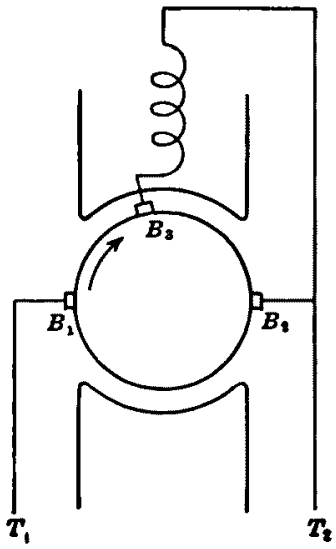


FIG. 10–6. Third-brush generator (Sayers generator).

the cross flux produced by the current flowing between the main brushes $B_1B_2$ will increase the flux in the trailing half of the pole, thus increasing the emf in the part of the armature winding included between the brushes $B_3B_2$, and increasing the field current.

The principles of the Sayers generator are embodied in the *3-brush generator* used in automobiles with the difference that the field winding in the latter machine is connected between the auxiliary brush and the main brush which lies nearer to the leading pole shoe tip ($B_1$, Fig. 10–6). The load current between $B_1B_2$ now will decrease the field current with increasing load. This sets a limit to the current which the machine is able to deliver although its speed may be very high. With increasing speed the emf between the main brushes $B_1B_2$ and the load current would increase if the field remained constant; however, the increased load current reduces the field. The current-speed curve of the 3-brush generator has the form shown in Fig. 10–7. The speed at which the maximum current occurs as well as the magnitude of the maximum current can be changed by shifting the auxiliary brush $B_3$.

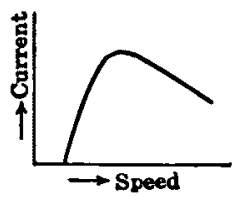


FIG. 10–7. Current-speed—curve of the third-brush generator.

As for the Rosenberg generator, an automatic switch or cutout is necessary, in order to prevent the battery from discharging through the generator at standstill or under low-speed conditions.

**10–3. Arc-Welding Generators.** The volt-ampere characteristic of a d-c welding generator should have the drooping form shown in Fig. 10–8. It is

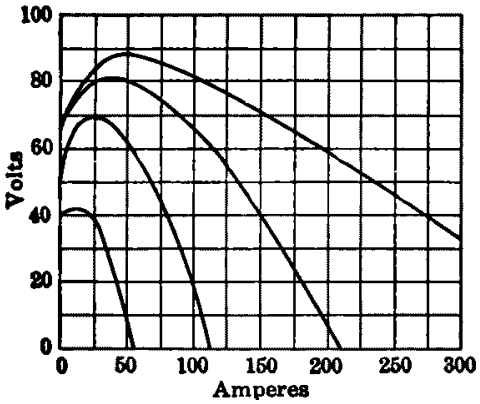


FIG. 10–8. Volt-ampere characteristics of a d-c 200-ampere welding generator.

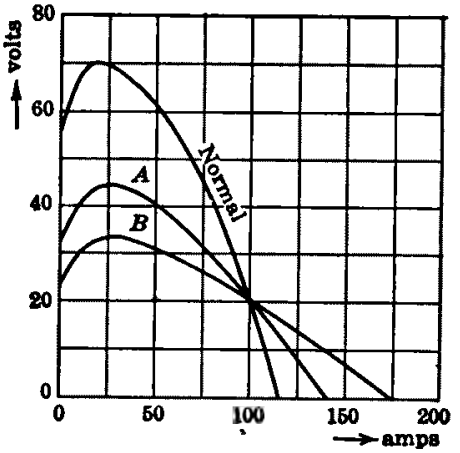


FIG. 10–9. Change of the slope of the volt-ampere characteristic of a d-c welding generator corresponding to the kind of welding: Normal (downhand, large electrodes), A (overhead and vertical, short arc), B (overhead and vertical, very short arc).

further necessary to change the slope of the volt-ampere curves as shown in Fig. 10–9, in order to control the arc according to the kind of welding. The higher initial value of voltage is necessary to ignite the arc.

Of the different types of arc-welding generators, two will be described, namely a 4-brush generator of the Rosenberg type and a 3-brush generator.

Fig. 10–10 shows the schematic diagram of the 4-brush welding generator (see Ref. D4). *SF* is a series field winding, *CF* is a commutating field winding. The commutating poles for the brushes $B_2B_2$ are parts of the main poles as shown in Fig. 10–11. The brushes $B_1B_1$ are connected together through a variable resistance. The principle of operation is the same as that of the Rosenberg generator (see Art. 10–2). A small battery takes care that the polarity is maintained and delivers the initial flux in the pole axis. This flux produces a current between the brushes $B_1B_1$. The cross flux due to this current in-

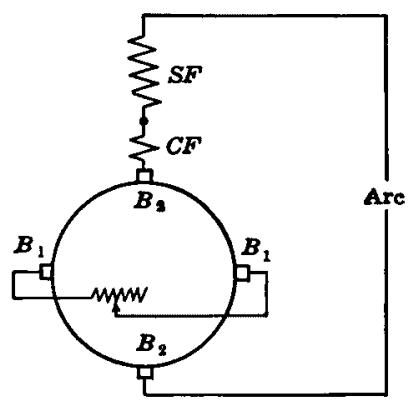


FIG. 10–10. Connection diagram of the 4-brush welding generator.

duces an emf in the armature winding between the load brushes $B_2B_2$. A flux leakage block (Fig. 10–11) is arranged so that the air-gap between it and the main poles can be changed over a wide range. This makes it possible to produce the volt-ampere characteristics shown in Fig. 10–8. The change in the slope of the volt-ampere curves is achieved through variation of the resistance between the brushes $B_1B_1$.

Fig. 10–12 shows the 3-brush welding generator (see Ref. D5, 6). It is a 2-pole

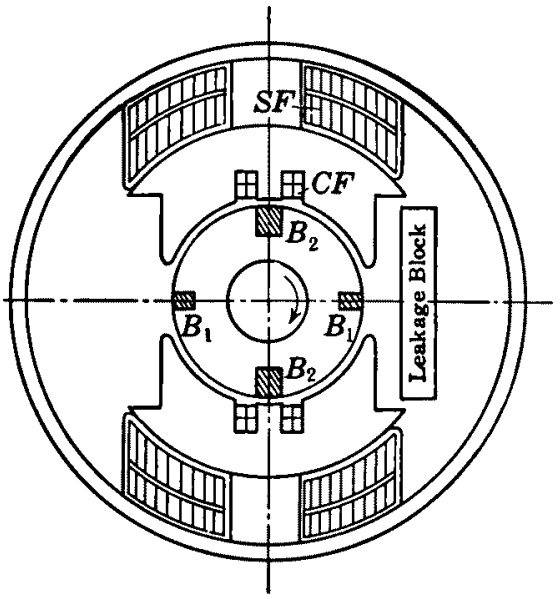


FIG. 10–11. Coil arrangement of the 4-brush welding generator.

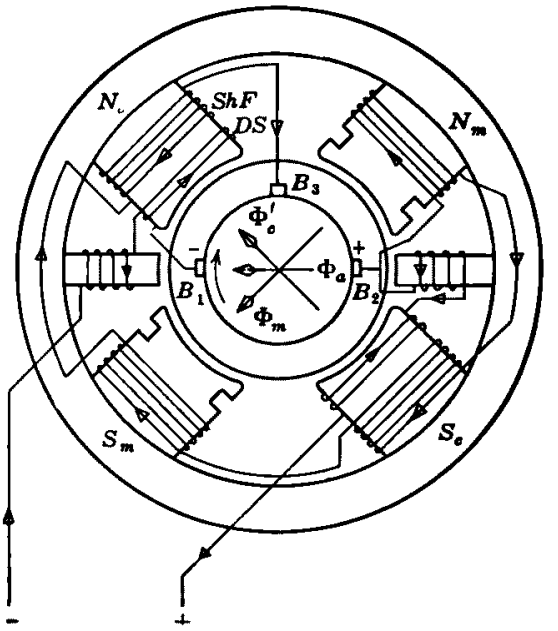


FIG. 10–12. Three-brush welding generator.

machine with 2 commutating poles and a 2-pole armature winding, but the main poles are split into 2 parts. The third brush $B_3$ is located in the middle between the main brushes $B_1B_2$. The shunt field winding *ShF* is connected between the auxiliary brush $B_3$ and the positive main brush $B_2$. A differential compound winding *DS* is placed on only half of each main pole.

For the direction of rotation assumed in Fig. 10–12 the armature flux $\Phi_a$ due to the current between the main brushes $B_1B_2$ has the direction from $B_2$ to $B_1$. This flux can be resolved in two components $\Phi_{am}$ and $\Phi_{ac}$, $\Phi_{am}$ coinciding with the axis of the pole halves $N_m$ and $S_m$ (*main* poles) and $\Phi_{ac}$ coinciding with the axis of the pole halves $N_c$ and $S_c$ (*cross* poles). The main poles $N_m$ and $S_m$ are constricted so that they are saturated at all loads. Therefore, the component of the armature mmf which produces the flux $\Phi_{am}$ will have little influence on the main flux $\Phi_m$ produced in the axis $N_mS_m$ by the shunt field winding, and $\Phi_m$ remains substantially constant and independent of the load.

The magnetic path of the cross poles $N_c$ and $S_c$ is not saturated so that the component of the armature flux $\Phi_{ac}$ reduces the flux $\Phi_c$ produced in this

axis by the shunt field winding. Thus the armature reaction flux $\Phi_{ac}$ supports the differential compound winding on the pole halves $N_c$ and $S_c$; and if the latter winding is sufficiently strong, the cross flux $\Phi_c$ produced by the shunt field may reverse its direction at a large load.

The armature voltage between the load brushes $B_1B_2$ consists of two parts, one induced in the part of the armature winding between the brushes $B_2B_3$ and the other induced in the part of the armature winding between the brushes $B_3B_1$. It can be seen from Fig. 10–12 that the first part of the armature is interlinked with the flux $\Phi_m$, while the other part is interlinked with the resultant cross flux $\Phi'_c$. Since $\Phi_m$ is practically constant, the emf induced between $B_2$ and $B_3$ remains constant and with it also the shunt field current (the shunt field winding is connected between $B_2$ and $B_3$). The emf induced between the brushes $B_3B_1$ varies with the resultant flux $\Phi'_c$; it reverses in direction at large loads. In the actual machine, the no-load emf's between $B_2B_3$ and $B_3B_1$ are each equal to 30 volts, giving a no-load terminal voltage of 60 volts. At a load of 200 amperes the emf between $B_3$ and $B_1$ reverses and becomes $-10$ volts, resulting in a terminal voltage of 20 volts needed to maintain the arc.

The differential compound winding has several taps in order to adjust the volt-ampere curve of the generator (see Figs. 10–8 and 10–9).

**10–4. Diverter-Pole Generator.** The construction of the diverter-pole generator is shown in Fig. 10–13 for a 2-pole machine (see Ref. D7). The main

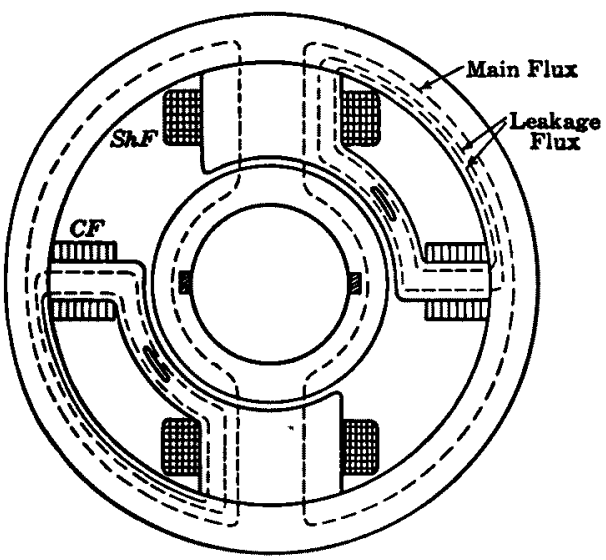


FIG. 10–13. Diverter pole generator. Flux distribution at no-load.

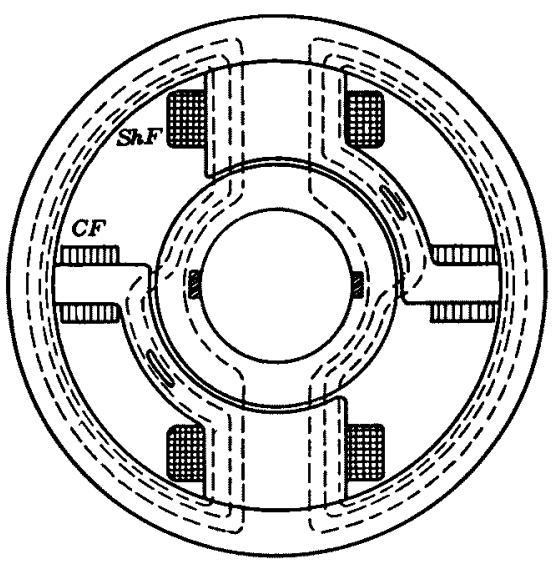


FIG. 10–14. Diverter pole generator. Flux distribution at load.

poles which are excited by a shunt field winding are connected by magnetic bridges to the commutating poles. The flux distribution at no-load is indicated in Fig. 10–13. At no-load the commutating winding is not excited and a larger part of the pole flux is diverted away from the armature and

goes through the bridge and the diverter (commutating) pole. With increasing load, the mmf of the diverter pole presses more and more flux back into the armature (Fig. 10–14), thus increasing the emf induced in the generator.

The bridges between the main poles and diverter poles have constricted sections. This, in connection with a proper mmf on the diverter poles and a proper area of the bridge, produces constant voltage for a certain range of the load current, making the diverter-pole generator useful for battery charging in telephone exchanges and in power stations where batteries are used to operate circuit breakers and relays.

**10–5. Dynamotor.** A generator is often called a *dynamo*. The *dynamotor* is a combination of a d-c generator and d-c motor in a single unit. The pole structure and armature core are common for both machines but there are two separate armature windings and two separate commutators with brushes. If voltage is impressed on one of the two armature windings, this machine runs as a motor. The common flux induces emf's in both windings. Therefore, the second armature winding can be loaded as a generator. The speed of the motor is determined by its counter-emf which is approximately equal to the impressed voltage (see Eq. 8–7). Since speed and flux are the same for both windings, the emf induced in the generator winding is nearly equal to the voltage impressed on the motor times the ratio of number of conductors ($Z_g/Z_m$), i.e., the generator voltage cannot be regulated independently.

The dynamotor has a higher efficiency than a 2-unit motor generator. It has practically no armature reaction, since the currents in the windings are opposite in direction and the mmfs of the 2 windings are nearly equal.

Dynamotors are used mostly for radio and other communication services in ratings of a few hundred watts. The motor power is taken from a battery at low voltage. The generator voltage may be as high as 1500 volts.

**10–6. Tuned Generators (Rototrol** = Rotating Control, **Regulex).** It has been explained in Art. 7–5 that a shunt generator is able to build up to a fixed voltage only when its resistance line intersects the no-load characteristic, Fig. 10–15. If the resistance line lies to the left of the no-load characteristic (straight line II) the generator will not build up. If it coincides with the gap characteristic, i.e., with the lower straight part of the no-load characteristic, its voltage will be undetermined; it may be any value between $O$ and $A$. The slope of the resistance line is determined by the resistance of the field circuit.

The same applies to the series generator. Since in this generator the field current and load current are the same, the slope of its resistance-line is determined by the total resistance of the armature circuit. In order that the generator may operate on the straight part of its characteristic, the total resistance of its armature circuit must be adjusted so that the $\Sigma Ir$ is equal to the voltage induced by the current $I$ as a field current.

A generator which is adjusted so that it operates on its gap characteristic is called a *tuned generator*. A tuned generator is not able to determine its voltage by itself, but it is able to assume any voltage on its gap characteristic if this voltage is dictated by some outside means. It is, therefore, adapted to control purposes where a certain quantity, such as voltage, current, speed, etc., has to be kept on a predetermined standard, either constant or variable. If a mechanical quantity has to be controlled, it must be converted into voltage or current; for example, speed has to be converted into voltage by a pilot generator.

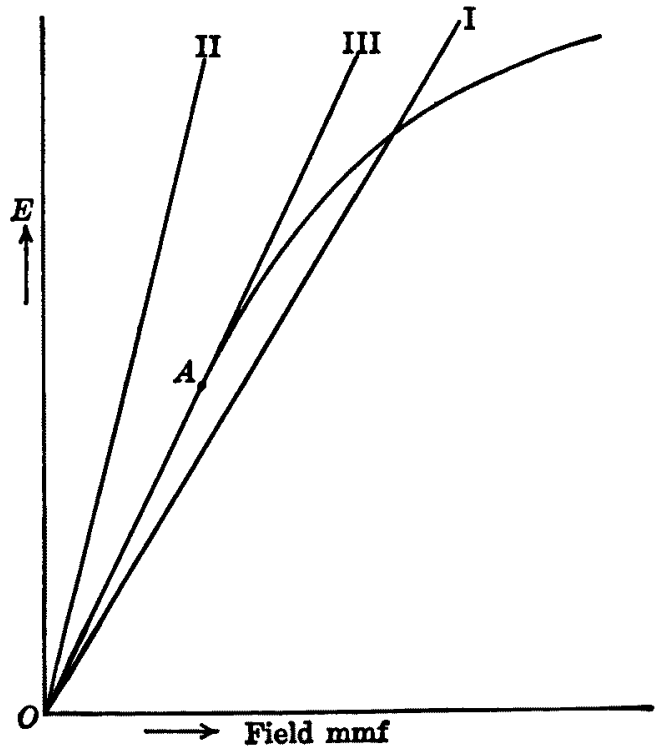


FIG. 10–15. Tuning of a generator.

In the successful operation of any regulating device it is necessary that the apparatus be capable of comparing the actual value of the quantity being controlled with the standard value desired. If there be any difference between the actual and desired quantities, the regulating device must supply power of the correct magnitude and direction to eliminate the difference, i.e., the regulating means must measure a certain quantity, compare this quantity with the standard, and if the two are not equal, initiate some means for equalizing them. The regulating means which take care of this in a regulating system with a tuned generator are *special field windings* on its poles. The general appearance and construction of a tuned generator is that of a normal d-c generator, except that the field windings are different.

The simplest form of a regulating system with tuned generator, of the Rototrol type, has three fields: a self-exciting field, generally series wound, and two separately excited control fields. One of these control fields is the

*pattern field* which is excited from a *standard source*. The other field measures the quantity to be regulated, and is referred to as the *pilot field*. The pilot field is usually connected in opposition to the pattern field, and is called in this case the differential field. To explain how a generator with these three fields operates, a simple arrangement for speed regulation will be considered.

Fig. 10–16 shows such an arrangement for speed control of a d-c motor (see Ref. D9). It is desired to maintain the speed constant irrespective of load variations, temperature changes, etc. The motor is excited from a constant

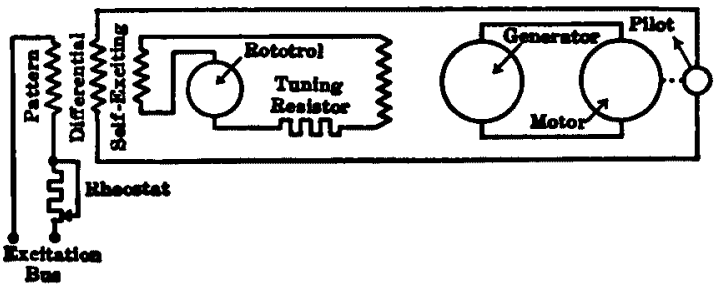


FIG. 10–16. Speed-control circuit using the Rototrol.

source of power, its armature voltage is regulated by a generator which is excited by the Rototrol. A *pilot generator* coupled with the motor produces a voltage proportional to the motor speed. This voltage is impressed on the differential field. A standard voltage is impressed on the pattern field, and these two fields are connected in opposition. The armature circuit of the Rototrol contains the self-excited series coils, the field winding of the generator (the load) and in addition a tuning resistor. The Rototrol is driven by a separate motor.

It will be assumed at first that the self-exciting series field is taken out from the armature circuit and that the main motor is at standstill. If now the pattern field is excited, the voltage of the generator builds up and the main motor accelerates. The pilot generator being in rotation energizes the differential field of the Rototrol, and thus influences the field of the generator. A balance is reached when the difference between the ampere turns of the two fields on the Rototrol is just enough to supply the necessary excitation to the generator field to maintain the generator voltage.

Now if the load on the motor increases, the speed tends to decrease just as in any separately excited motor. This decrease in motor speed, however, causes a decrease in the pilot-generator voltage and, therefore, a decrease in strength of the differential field of the Rototrol. This results in an increase in net field strength in the Rototrol, since the pattern field is constant. This, in turn, increases the Rototrol voltage, generator field strength, generator voltage, and motor speed until a balance is again reached. However, the speed under the changed load conditions can never be precisely the same as it was originally. This is due to the fact that the pattern and differential

fields must be different in order to supply the Rototrol with excitation since there is no other field winding.

For complete accuracy of regulation it is necessary that the pattern and differential fields control the Rototrol output without having to supply any of the power required to effect the regulation. *To supply this power is the function of the self-exciting field.* This field has to deliver the total exciting power necessary under steady state conditions and the aim of the two control fields (pattern and differential) becomes that of *locating the proper operating point on the gap characteristic* of a series generator consisting of a self-exciting field and an armature, and keeping this operating point constant.

Assume that the motor is at standstill. With the rheostat in the pattern field set at some position and its circuit closed, the voltage in the Rototrol armature rises rapidly because the excitation of the pattern field is added to that of the self-exciting field. This voltage excites the generator field, causing the main motor and pilot generator to rotate and thus producing a voltage across the differential field of the Rototrol, which neutralizes the effect of the pattern field. When the differential field completely neutralizes the pattern field, the Rototrol reaches a steady point of operation because there is no more forcing of the field and the self-exciting field can just maintain this steady-state condition.

Consider an increase of load on the motor that causes its speed to drop. This decreases the differential field strength and because the pattern field is constant, the Rototrol voltage and thus the generator-field current and voltage increase. This increase in voltage continues until the differential field again neutralizes the pattern field and the self-exciting field again maintains this new condition. At this time the speed is exactly the same as before the load changed, because the Rototrol can be at balance only if the pattern and the differential fields are equal. The differential field, which is the same as before, measures the speed of the motor and the speed, therefore, must be exactly the same in the two cases.

On the other hand, if the speed of the motor rises for any reason, the differential field becomes stronger than the pattern field and the excess ampere turns cause the Rototrol to seek a lower operating point until balance is restored between the pattern and differential fields, i.e., until the speed is lowered to the former value.

It follows from the foregoing that the setting of the pattern field determines the point on the gap characteristic on which the generator operates, and also the speed of the main motor. The pattern field determines the magnitude which the differential field must have and, therefore, the speed of the pilot generator and main motor. On the other hand, the speed of the main motor is determined by the generator voltage which in turn is fixed by its field, i.e., the magnitude of the voltage of the Rototrol.

The arrangement shown in Fig. 10–16 with certain modifications permits

a speed variation as high as 120 : 1, while the ordinary d-c motor with field control has a speed range control of about 6 : 1.

Similar arrangements to that shown in Fig. 10–16 can be used to maintain constant torque of a d-c motor or constant horsepower of a d-c motor, or constant voltage of a generator, etc.

It will be explained in the next section where the rotating amplifiers are treated that each d-c generator can be considered as an amplifier of power since the power of its armature which is much larger than that of its field can be controlled by the small field power. If the gap is small and the machine unsaturated the field power may be as low as only 1% of the armature power. This corresponds to an amplification of 1 : 100. In certain applications this amplification is not sufficient. In these cases the rotating amplifiers described in the following articles are used for control purposes.

## B. Rotating Amplifiers

### (amplidyne, 2-stage and multi-stage rototrol)

An amplifier is a device which, operated by very little power, is able to control the flow of a much larger quantity of power. With this definition a d-c generator may be considered as a power amplifier. Consider Fig. 10–17. A prime mover $M$ drives a d-c generator $G$ which delivers the power $P_2$ to the load. This power is delivered by the prime mover but the generator field can be used to control the power flow to the load, since the voltage and current of the generator depend upon the power of the field.

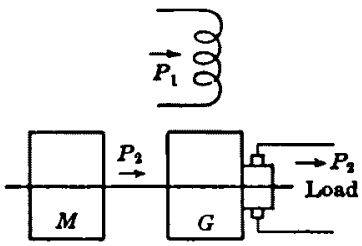


Fig. 10–17. D-c generator as a power amplifier.

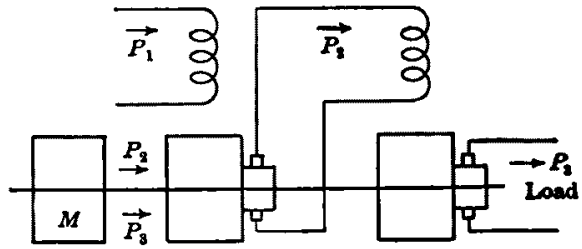


Fig. 10–18. Increase of amplification by using 2 d-c machines.

The field power of a d-c generator with low saturation and a relatively small air-gap is about 1% of the power transmitted to the load. Such a d-c generator thus has an amplification of 100 : 1 = 100, i.e., 1 watt in the field circuit is able to increase the output by 100 watts. This amplification is too small for many industrial applications. The amplification can be increased by using two d-c machines in series as shown in Fig. 10–18. Here an amplification of $100 \times 100 = 10{,}000$ can be achieved. However, an amplifier must have not only a certain amplification but also a certain rapidity of response; and a system as shown in Fig. 10–18 is sluggish in this respect due to the fact

that it has two separate magnetic circuits. The rotating amplifier should have only one magnetic circuit and at least two electric circuits on the armature in order to be useful in industrial applications.

There are different solutions to this problem. One of them is provided by the Rosenberg machine (Fig. 10–3) and this will be described first.

**10–7. Two-Stage Amplifier with the Pole-Ratio 1 : 1 Based on the Rosenberg Machine (Amplidyne).** Consider Fig. 10–19 in which the Rosenberg machine is separately excited by coils $C$, called *control coils*. Further, a compensating winding (*Comp. W.*) is arranged in order to nullify

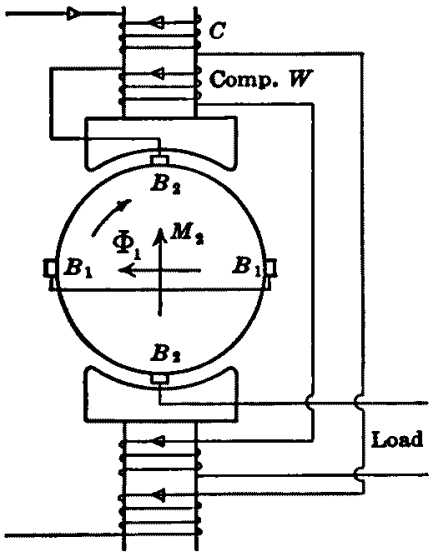


FIG. 10–19. Rotating amplifier of the amplidyne type (Rosenberg generator with compensating winding).

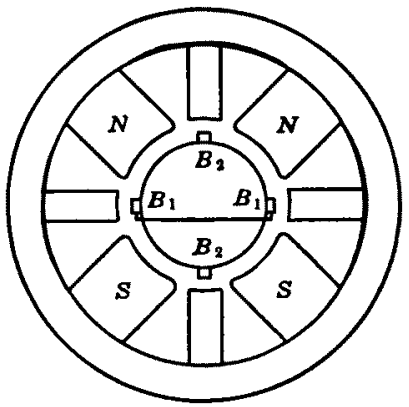


FIG. 10–20. Rotating amplifier of the amplidyne type with split poles.

the armature mmf $M_2$ in the pole axis. Then the field produced by the control coils will induce an emf between the brushes $B_1B_1$, as in the normal d-c machine. Since these brushes are connected together, a current will flow between them. This is the first stage of amplification. The current flowing between the brushes $B_1B_1$ produces an armature flux $\Phi_1$ which induces an emf between the brushes $B_2B_2$ which are connected to the load. This is the second stage of amplification. For a power of 1 watt in the control coil there will be a corresponding power of about $100 \times 100 = 10{,}000$ watts at the load brushes $B_2B_2$.

The main difference between this amplifier and the Rosenberg machine, as used for train lighting, is that in the Rosenberg machine the armature mmf in the pole axis $M_2$ is an essential part necessary for the functioning of the machine, while here this mmf must be compensated very completely (see Ref. D11). Since the volt-amperes which correspond to $M_2$ are 10,000

times as great as the volt-amperes in the control circuit, then if the compensation is not complete, a part of the control field will be nullified and the amplification will be reduced.

In the Rosenberg generator (Fig. 10–3) the field under the poles is weak. Therefore, satisfactory commutation could be obtained with the aid of notches in the poles. Here the field under the poles (Fig. 10–19) is much stronger due to the fact that $M_2$ is compensated. The practical amplifier therefore has split poles, as shown in Fig. 10–20, and 4 interpoles, 2 for each brush axis. The coils which compensate $M_2$ are wound around the poles $NN$ and $SS$ so that their axis coincides with the axis of the brushes $B_2B_2$.

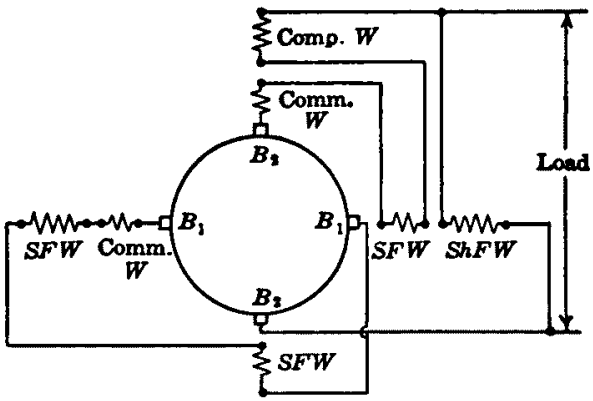


FIG. 10–21. Field coil arrangement of the rotating amplifier of the amplidyne type.

Besides the control coils and compensating winding, the amplifier may have a shunt winding for the axis $B_1B_1$ connected to the load terminals, and also series windings in both axes as shown in Fig. 10–21. The flux produced by the control coils and by all windings having the same axis as the control coils goes (Fig. 10–20) from $N$ to $S$ and from $N$ to $S$. The flux produced by the current flowing through the brushes $B_1B_1$ and by all windings having the same axis as the brushes $B_1B_1$ goes from $N$ to $N$ and from $S$ to $S$.

**10–8. Two-Stage Amplifier with the Pole-Ratio 1 : 2 (Two-Stage Rototrol) and Three-Stage Amplifier with the Pole-Ratios 1 : 1 : 2 (Three-Stage Rototrol).** While the two-stage amplifier described in the foregoing has the same number of poles in both stages, i.e., a pole-ratio 1 : 1, the two-stage amplifier described below has a different number of poles in the two stages, with a pole-ratio 1 : 2. The first stage has the smaller number of poles, the second stage the larger number. The smallest numbers of poles of this amplifier are, therefore, 2 for the first stage and 4 for the second stage. With these numbers of poles the machine has a 4-pole field structure, 4 interpoles, a 4-pole armature, and 4 brush studs. The appearance is that of a normal 4-pole generator, except that the field windings are different.

Fig. 10–22 shows schematically the armature, the main poles, and brushes. The interpoles are omitted for the sake of simplicity. The 4 main poles are designated by 1, 2, 3, and 4, and the 4 brushes by $B_1$, $B_2$, $B_3$ and $B_4$. The first stage is made by field coils on the poles 1 and 3, i.e., by control coils, and the armature between the brushes $B_1B_3$. The second stage is made by field coils on all four poles, 1, 2, 3, and 4, excited from the brushes $B_1B_3$, and by the armature between the brushes $B_1B_3$ and $B_2B_4$. Fig. 10–23 shows this

arrangement schematically. The operation of this amplifier is similar to that of the amplidyne. (See Ref. D16, 17.)

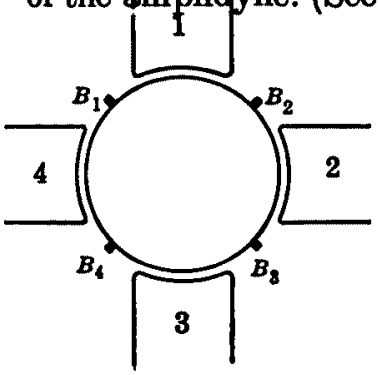


FIG. 10–22. Main poles and brushes of the 2-stage amplifier with the pole ratio 1:2 (interpoles not shown).

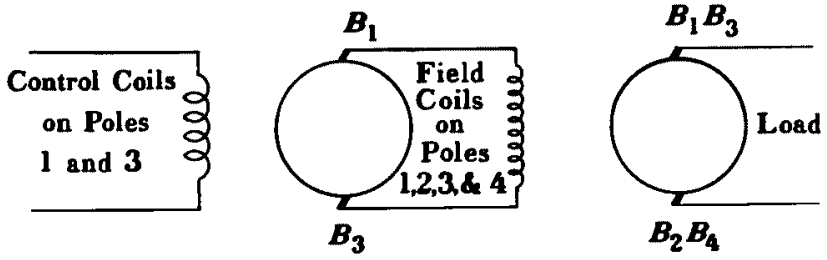


FIG. 10–23. Two-stage amplifier with the pole-ratio 1:2 (schematic arrangement).

The same machine (Fig. 10–22) can be arranged to operate as a three-stage amplifier. Fig. 10–24 shows schematically the three stages. The first stage is made by control coils on poles 1 and 3 and the armature between the brushes $B_1B_3$. The second stage is made by field coils on poles 2 and 4, excited from the brushes $B_1B_3$, and the armature between the brushes $B_2B_4$. The third stage is made by field coils on all four poles, excited from the brushes $B_2B_4$, and the armature between the brushes $B_1B_3$ and $B_2B_4$.

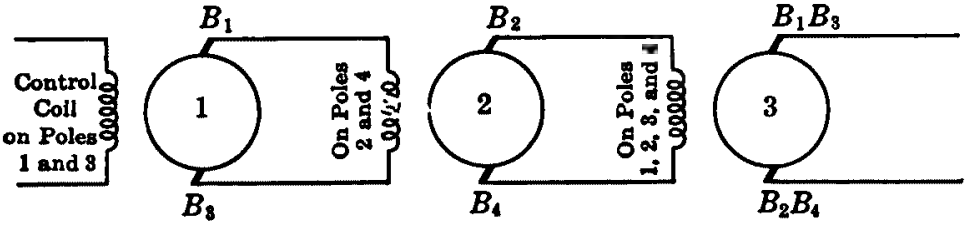


FIG. 10–24. Arrangement of the field coils of second and third stage of the 3-stage amplifier with the pole ratios 1:1:2.

Additional information about the fluxes, voltages and operation of the two-stage and three-stage Rototrols is given in Chap. 21.

# *Chapter 11*

# LOSSES

Both main elements of the electric machine, the magnetic flux and the current in the armature conductors, produce a certain amount of heat in the machine.

Each electric machine is a *converter of power*: the generator converts mechanical power into electrical, the motor converts electrical power into mechanical, the motor generator and rotary converter convert electrical power into electrical power. The heat produced in the machine by the flux and currents is a loss of power which reduces the efficiency of the machine. Due to this heat the input of the machine must be larger than its output. The *efficiency* of a machine is defined as:

$$\eta = \frac{\text{output}}{\text{input}} = \frac{\text{input} - \text{losses}}{\text{input}} = \frac{\text{output}}{\text{output} + \text{losses}} = 1 - \frac{\text{losses}}{\text{input}}$$

The different kinds of losses which appear in the electric machine are considered in the following articles.

## 11–1. Losses Due to the Main Flux

(a) *Iron Losses in the Armature.* Since the armature must rotate relative to the magnetic field, in order that the emf be induced in the conductors, the particles of the armature iron are magnetized alternately, first in one direction and then in the other. This leads to hysteresis losses. The magnitude of the hysteresis loss depends upon the area of the hysteresis loop, the number of magnetic cycles per second, and the volume of iron.

As has been explained in Chap. 2, the armature iron is laminated perpendicular to the direction of the current in the armature conductors, in order to avoid parasitic or eddy currents in the iron running parallel to the conductors and causing losses. However, eddy currents do appear in the single laminations and produce heat. The eddy-current losses depend upon the field density, number of magnetic cycles per second, thickness of the laminations, the quality of the iron, and the volume of iron.

According to Steinmetz, the hysteresis losses per unit weight can be represented by the following equation:

$$p_h = \sigma_h f B^{1.6} \tag{11–1}$$

where $B$ is the maximum value of flux density and $f=pn/120$ is the number of magnetic cycles per second. $\sigma_h$ which Steinmetz called the hysteretic coefficient is a constant depending upon the quality of the iron. Steinmetz's equation yields low values for the losses when $B>65{,}000$ lines/in.$^2$. A more accurate equation proposed by R. Richter is:

$$p_h = afB + bfB^2 \tag{11-2}$$

$a$ and $b$ are constants similar to $\sigma_h$. In practice $B>65{,}000$ lines/in.$^2$. In this case the first term of Eq. 11–2 can be disregarded and the following equation used:

$$p_h = \sigma_h \frac{f}{60}\left(\frac{B}{64{,}500}\right)^2 \text{ watts/lb} \tag{11-3}$$

The eddy-current losses are

$$p_e = \sigma_e \left(\Delta \frac{f}{60}\frac{B}{64{,}500}\right)^2 \text{ watts/lb} \tag{11-4}$$

The constant $\sigma_e$ depends upon the electric resistivity of the iron. $\Delta$ is the thickness of the laminations in inches. The total iron losses per pound are

$$p_{h+e} = \sigma_h \frac{f}{60}\left(\frac{B}{64{,}500}\right)^2 + \sigma_e \left(\Delta \frac{f}{60}\frac{B}{64{,}500}\right)^2 \text{ watts/lb} \tag{11-5}$$

The constants $\sigma_h$ and $\sigma_e$ for different kinds of iron are given in the following tabulation.

| $\Delta$ inch | Si % approx. | Loss per pound at 60 cycles and $B=64{,}500$ | $\sigma_h$ | $\sigma_e$ |
|---|---|---|---|---|
| 0.0185 | 1 | 1.29 | 0.79 | 1,470 |
| 0.025 | 2½ | 1.07 | 0.77 | 800 |
| 0.0185 | 3½ | 0.89 | 0.62 | 800 |
| 0.014 | 4½ | 0.49 | 0.33 | 800 |

In practice iron-loss curves are used which represent the total iron loss in watts per pound as a function of the flux density $B$. Fig. 11–1 represents such curves for the same kinds of iron which are tabulated above. It follows from Eq. 11–5 that the iron loss is proportional to the square of the induction $B$.

However, the specific loss taken from Fig. 11–1 or determined from Eq. 11–5 and multiplied by the weight of the teeth and core, respectively, will yield only a part of the iron losses produced by the main flux. This is due to many additional factors which increase the hysteresis as well as the eddy-current losses but mainly the latter losses.

Eq. 11–5, as well as Fig. 11–1, assumes that the flux density is sinusoidally distributed in the gap. This is not the case in the d-c machine (see Fig. 1–4).

If the flux distribution curve of the d-c machine is resolved into a Fourier series it will show a fundamental with harmonics of considerable amplitude. These harmonics produce additional losses so that the eddy-current losses in the teeth are about twice as large as those determined by Fig. 11–1.

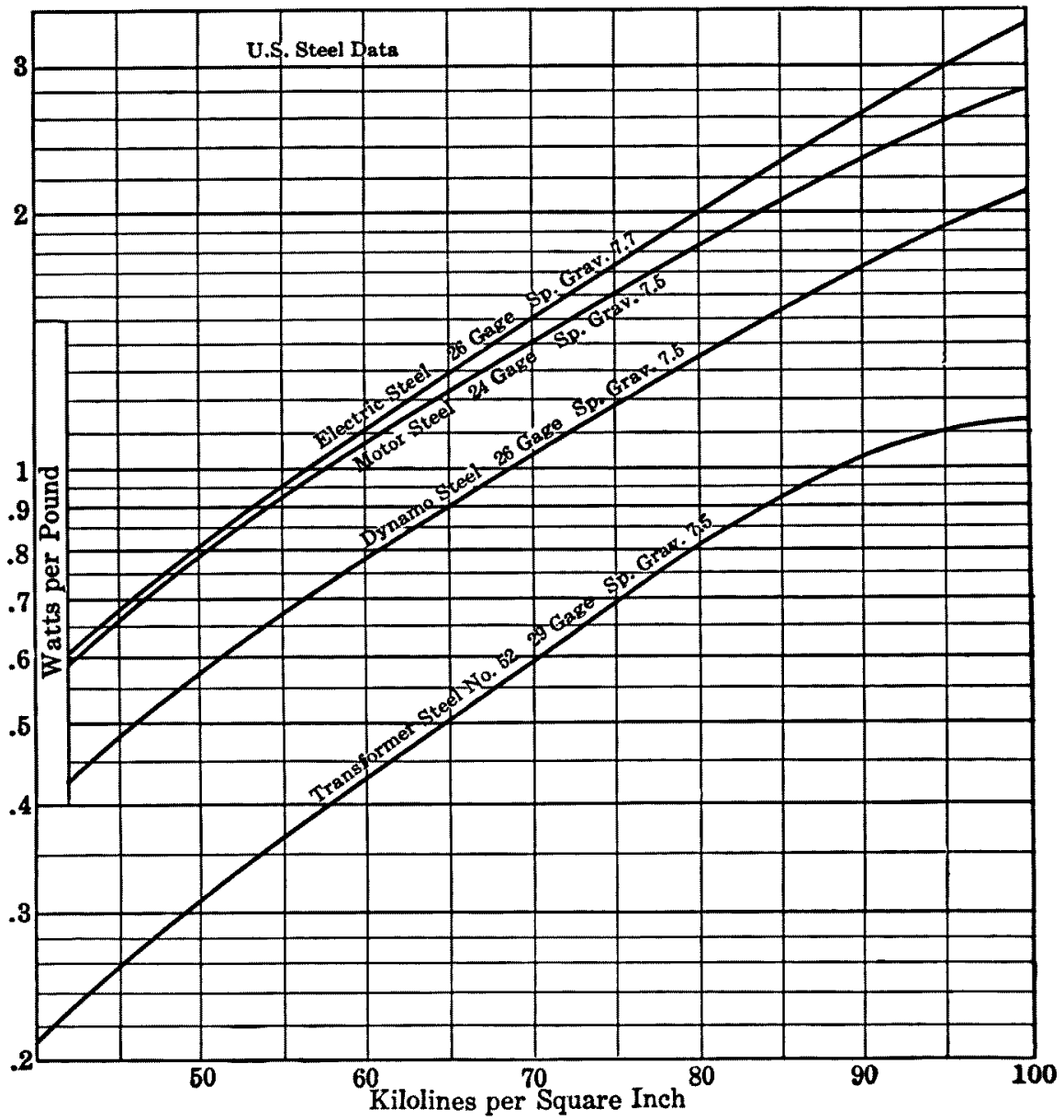


FIG. 11–1. Loss curves at 60 cycles for transformer steel and dynamo steel.

The non-uniform distribution of the flux over the cross section of the armature core is a further factor which increases the iron losses. While this factor may increase the hysteresis losses of the core by 5% to 30%, the eddy-current losses in the core may increase by 20% to 80%. The rate of increase depends upon the ratio between the inside diameter of the core and the outside diameter.

The process of punching the laminations increases the iron losses by 7% to 15%; filing, in order to remove the burrs, increases the losses by 5% to 8%. Re-annealing after punching decreases the losses by 10% to 15%, but this entails additional manufacturing costs. It can be assumed that all these factors increase the iron losses due to the main flux by 40% to 60%.

(b) *Pole-Face Losses.* Iron losses appear not only in the armature iron but also in the pole iron. Because of the slot openings the flux distribution curve becomes distorted (Fig. 11–2). The flux density is larger at points opposite the teeth than at points opposite the slots, owing to the difference of magnetic reluctance. On the average flux density, there is superimposed a ripple, the wave length of which is equal to a slot pitch. This ripple moves with respect to the poles and induces eddy currents in the pole surface. Since a full cycle corresponds to a slot pitch, the frequency of this pulsation is

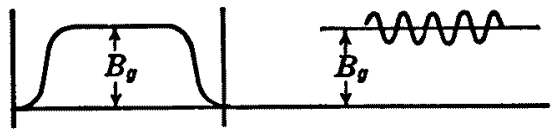


FIG. 11–2. Ripple in the field curve due to slot openings.

$$f_t = \frac{Qn}{60} \tag{11–6}$$

where $Q$ is the number of slots on the armature. The amplitude of the flux pulsations, i.e., the difference between maximum and average flux density, depends upon the slot opening. It is much larger in machines with open slots than in machines with semi-closed slots; for a given slot opening it decreases with increasing air-gap. The pole-surface losses thus depend upon slot opening, air-gap, and frequency $f_t$, i.e., number of slots and speed $n$. Whether the pole is laminated or solid is also of importance. The poles of d-c machines are usually laminated. The pole-face losses are 15% to 40% of the losses due to the main flux (Eq. 11–5).

(c) *Copper Losses.* The main flux is associated with copper losses in the field winding and also in the armature winding. In order to produce the pole flux a certain current in the field winding is necessary. The losses due to the field current are

$$P_{Cuf} = I_f^2 R_f$$

where

$$R_f = \rho \frac{N_f l_t}{cA} \tag{11–7}$$

$N_f$ is the total number of field turns, $l_t$ the mean length of a turn, $A$ the area of the conductor, $c$ the number of parallel circuits, and $\rho$ the resistivity of the material. $\rho$ depends upon the temperature. It is:

$$\rho_t = \rho_{20}[1 + \alpha(t - 20)] \tag{11–8}$$

$\rho_{20}$ is the resistivity at 20° C and $\alpha$ the temperature coefficient of resistance.

| | | |
|---|---|---|
| Copper: | $\rho_{20} = 0.68 \times 10^{-6}$ ohm/in.$^3$; | $\alpha = 0.00393$ |
| Aluminium: | $\rho_{20} = 1.114 \times 10^{-6}$ ohm/in.$^3$; | $\alpha = 0.0039$ |
| Brass: | $\rho_{20} = 2.76 \times 10^{-6}$ ohm/in.$^3$; | $\alpha = 0.002$ |

In d-c machines which usually are more highly saturated than the other electric machines, a small part of the main flux goes through the slots and conductors as shown in Fig. 11–3. Since the flux interlinkage with the armature copper changes with the position of the poles with respect to the conductors, eddy currents are induced in the conductors and mainly in those which lie in the top of the slot near the air gap. These additional copper losses are 10% to 30% of the copper losses due to the armature current.

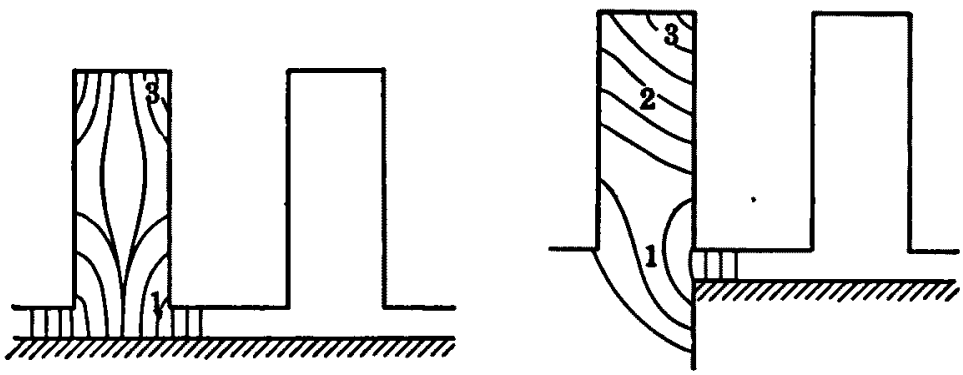


FIG. 11–3. Main flux in the slots of a highly saturated d-c machine.

(d) *Eddy-Current Losses in Structural Parts.* In d-c machines the armature winding is often held in place by bands which are placed in grooves made in the armature core. The main flux induces eddy currents in these steel-wire bands.

## 11–2. Losses Due to the Armature Current (Load)

(a) *$I^2R$-losses in the Armature, Interpole, Series Field, and Compensating Windings.* The resistance of the armature winding is

$$r_a = \rho \frac{Zl_t}{2a^2A} \tag{11–9}$$

where $l_t$ is the mean length of a turn and $A$ is the area of cross section of the conductor.

All d-c machines except the smallest have an interpole winding. This winding is excited by the armature current. Its losses have to be added to those of the armature winding. If there is a series field and a compensating winding, the losses of these windings also have to be added to those of the armature winding.

(b) *Skin-Effect Losses.* It should be remembered that the current flowing in the *armature conductors* of a d-c machine is not a d-c but an *a-c current* of the shape shown in Fig. 9–1. This current goes through a full cycle during the

time the conductor passes a pole pair. If $n$ is the rpm of the armature, the frequency of the conductor current, in cycles per second, is

$$f=\frac{p}{2}\frac{n}{60}=\frac{pn}{120} \tag{11-10}$$

Consider now Fig. 11–4a which shows a single bar in a slot. The line of force at the distance $x_1$ from the bottom of the conductor is interlinked with the current which flows in the lower part of the conductor determined by the

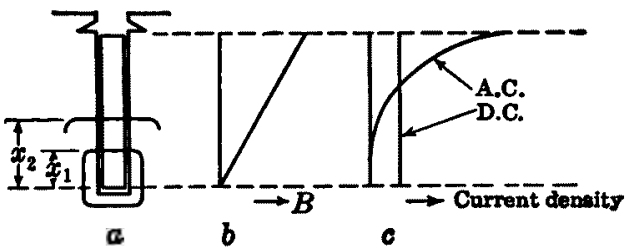


FIG. 11–4. Explanation of the skin effect in conductors due to the cross flux in the slot.

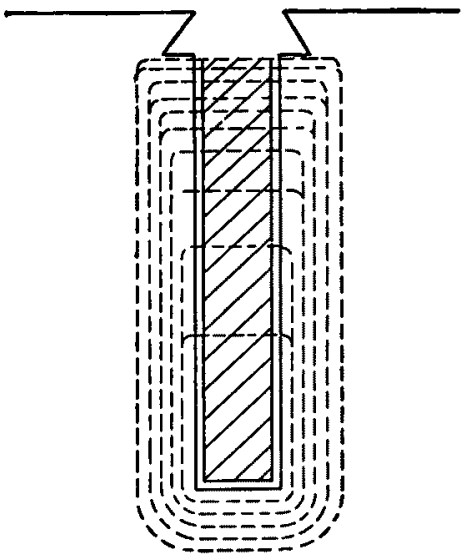

FIG. 11–5. Explanation of the skin effect in conductors due to the cross flux in the slot.

height $x_1$. The line of force at the distance $x_2$ from the bottom is interlinked with a larger current than the line of force at $x_1$. Therefore, the flux density at $x_2$ is larger than that at $x_1$. If the magnetic reluctance of the iron is neglected, the magnetic reluctance for all lines of force is determined solely by the width of the slot, and the flux density for low frequency current increases linearly from the bottom to the top of the conductor as shown in Figs. 11–4b and 11–5.

Assume that the conductor is stranded perpendicular to the slot depth, in an infinite number of strands. The strand at the bottom of the conductor is interlinked with the total flux produced by the entire conductor (Fig. 11–4a). Each strand which lies above the bottom strand is interlinked with only a part of the total flux, and the strand at the top of the conductor is linked with relatively little flux. It should be noted that the flux considered here is *the slot leakage flux* produced by the currents in the conductor (Fig. 9–3). The main flux, the path of which is through the core, is interlinked equally with all strands and induces the same emf in all strands. But due to the fact that the leakage flux interlinkage ($L$) is not the same for the different strands,

the leakage reactance ($2\pi fL$) produced by an a-c current in the conductor is different for each separate strand, and, while the emf induced by the main flux is the same for all strands, the current in each is different. The current is very small in the bottom strand and is a maximum in the upper strand (Fig. 11–4c). The current appears to be moved from the bottom to the top of the slot. This is the skin effect phenomenon. Due to this effect the current flowing through the conductor is not distributed uniformly over the cross section of the conductor. The skin effect increases with the height of the conductor and the frequency. There is no skin effect when low frequency or direct ($f=0$) current flows through a conductor. In this case the current is distributed uniformly over the cross section of the conductor. Fig. 11–4c applies to a single conductor in a slot. The current distribution for 2 conductors in the slot is shown in Fig. 11–6. Thus the conductor current is concen-

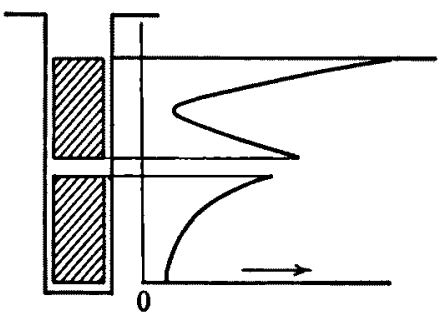


FIG. 11–6. Current distribution in a slot with 2 conductors (due to skin effect).

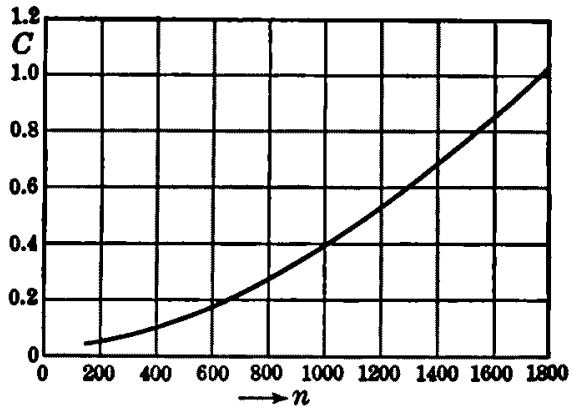


FIG. 11–7. Friction plus windage losses in d-c machines up to 100 hp.

trated more or less in the top part of the conductor, depending upon the height of the conductor and frequency. The effect is the same as though only a part of the conductor cross section were effective or as though the resistance of the conductor were increased. For this reason it is customary to distinguish between the d-c ($f=0$) resistance and *a-c resistance* of a conductor (winding). The latter takes into account the skin effect and is larger than the d-c ($f=0$) resistance. Thus the skin effect increases the $I^2R$ losses of the armature winding.

Since the skin effect increases with the height of the conductor, it is possible to reduce it by dividing the conductor, perpendicular to its height, into strands. This stranding however, is effective only when the strands are insulated from each other.

The skin-effect loss in the armature winding is 5% to 25% of its d-c copper loss. The resistance for the latter loss is given by Eq. 11–9.

(c) *Copper Losses in the Armature Winding Due to Flux Distortion.* It has been shown in Art. 5–4 that the armature mmf distorts the pole flux, making the flux density higher under one half of the pole and lower under the other

half of the pole. This causes eddy-current losses in the armature conductors of the same kind as those produced by the main flux at no load (see Fig. 11–3). These losses are negligible in d-c machines with compensating winding because there is no flux distortion. The amount of these losses in non-compensated machines is about 0.5 to 0.6% of the machine output.

**11–3. Friction and Windage Losses.** Owing to rotation, bearing friction losses occur in all machines. The amount of the bearing friction losses depends upon the pressure on the bearing, the peripheral speed of the shaft at the bearing, and the coefficient of friction between bearing and shaft.

In commutator machines, brush friction losses must be considered in addition to the bearing friction losses. These brush friction losses are quite large. Like the bearing friction losses they depend upon the brush pressure, the peripheral speed of the commutator, and the coefficient of friction between commutator and brush.

The A.I.E.E. standards recommend as average values for brush friction losses: 8 watts per sq. in. of brush contact per 1000 ft/min peripheral speed for carbon and graphite brushes, and 5 watts per sq. in. of brush contact per 1000 ft/min peripheral speed for metal graphite brushes.

The windage losses produced by rotation depend upon the peripheral speed of the rotor, the rotor diameter, the core length, and largely upon the construction of the machine. While the friction losses can be calculated more or less accurately, the windage losses have to be estimated on the basis of tests on similar machines or determined by actual test. Figs. 11–7 and 11–8 give the windage and bearing friction losses for smaller and larger d-c machines. The values given in these figures are average values found by tests on a large number of machines.

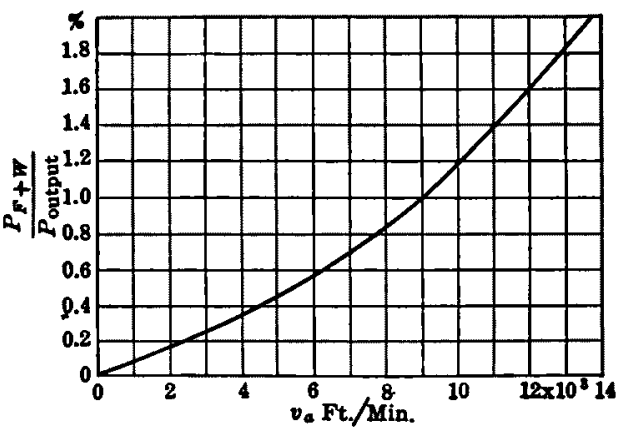


FIG. 11–8. Friction and windage losses in larger d-c machines.

**11–4. No-Load and Load Losses; Stray Load Losses.** A part of the losses considered above occur when the machine operates at no-load, and the remainder appears when the machine is loaded. The first part is called *no-load losses*; the latter part, *load losses*. Table 11–1 gives the losses which appear at no load and the losses which are due to the load.

TABLE 11–1

*No-Load Losses*

1. Iron losses in the armature due to the main flux
2. Pole-surface losses due to slot-openings
3. Losses in conductors due to the main flux
4. Windage and bearing friction losses
5. Brush friction losses at the commutator
6. Losses in banding wires due to the main flux
7. $I^2R$ loss in shunt field windings

*Load Losses*

1. $I^2R$ losses in all windings
2. Skin-effect losses in the armature conductors
3. Losses in armature conductors due to flux distortion
4. Electric loss in the contact resistance under the brushes
5. Losses in short-circuited coils during commutation

The *additional* losses due to the load, namely, the skin-effect losses in the armature conductors, the losses in the armature conductors due to flux distortion, and the losses in the short-circuited winding elements, are called *stray load losses.*

The standards of the A.I.E.E. recommend that the stray load losses of d-c generators and motors be taken as equal to 1% of the output, except for motors 200 hp, 575 rpm, and smaller, in which case they shall be omitted.

In accordance with the standards of the A.I.E.E., the copper losses in all windings are to be calculated for a temperature of 75° C for all loads.

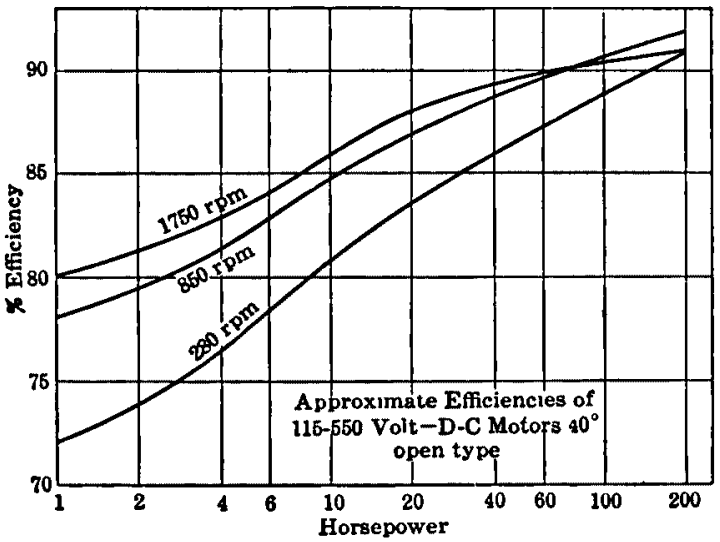


FIG. 11–9. Approximate efficiencies of 115–550-volt 40°C open type d-c motors.

**11–5. Examples of Loss Distribution and Efficiencies.** The following tabulation shows the loss distribution for four d-c machines. Approximate efficiencies of motors of various speed and output are given in Fig. 11–9.

*Compound Motor*

3 hp, 115 volts, 1150 rpm
4 poles, open type
Armature current = 24 amp
Shunt field current = 0.7 amp

| | |
|---|---|
| Armature $I^2R$ | 210 watts |
| Interpole field $I^2R$ (2 interpoles) | 35 |
| Series field $I^2R$ | 25 |
| Brush contact loss | 48 |
| Stray load loss | 0 |
| Shunt field loss | 80 |
| Iron loss | 100 |
| Brush friction loss | 20 |
| Bearing friction and windage loss | 80 |
| | 598 watts |

Input = (24 + 0.7)115 = 2840 watts
Output = 2840 − 598 = 2242 = 3.0 hp

$$\eta = 100\,\frac{2242}{2840} = 78.9\,\%$$

*Compound Generator*

250 kw, 240 volts, 1200 rpm
6 poles, open type
Armature current = 1040 amp
Shunt field current = 4.25 amp

| | |
|---|---|
| | 3,800 watts |
| (6 interpoles) | 1,600 |
| | 400 |
| | 2,100 |
| | 2,500 |
| | 1,000 |
| | 4,400 |
| | 2,000 |
| | 2,500 |
| | 20,300 watts |

Output = 240 × 1040 = 250 kw

$$\eta = 100\,\frac{250}{250 + 20.3} = 92.5\,\%$$

*Shunt Motor with Compensating Winding*

800 hp, 250 volt, 500/800 rpm, 8 poles, 500 rpm

| | |
|---|---|
| Armature $I^2R$ | 10.7 kw |
| Interpole and $I^2R$ comp. wind. | 7.03 |
| Brush contact loss | 5.2 |
| Stray load loss | 6.0 |
| Shunt field loss | 2.9 |
| Iron loss | 9.7 |
| Brush friction loss | 2.2 |
| Bearing friction and windage loss | 3.0 |
| | 47.0 kw |

$$\eta = 100\,\frac{597}{597 + 47} = 92.7\,\%$$

*Compound Generator with Compensating Winding*

3000kw, 720 volt, 360 rpm, 12 poles

| | |
|---|---|
| Armature $I^2R$ | 40.6 kw |
| Interpole and $I^2R$ comp. wind. | 30.3 |
| Series field | 19.5 |
| Brush contact loss | 8.3 |
| Stray load loss | 30.0 |
| Shunt field loss | 4.7 |
| Iron loss | 23.0 |
| Brush friction loss | 6.9 |
| Bearing friction and windage loss | 14.5 |
| | 177.8 kw |

$$\eta = 100\,\frac{3000}{3000 + 177.8} = 94.4\,\%$$

# *Chapter 12*

# HEATING AND COOLING OF THE D-C MACHINE

**12–1. Influence of the Heat Conductivity of the Materials and of the Heat Transfer to the Air.** It has been shown in the previous chapter that, in the conversion of energy from mechanical into electrical or vice versa, certain losses are produced in the machine. These losses are of different kinds, but all of them appear in the electric machine in the form of heat. Since the losses are produced mainly in the active parts of the machine, i.e., in the iron which carries the flux and in the conductors which carry the currents, the heat appears mainly in these machine parts. The result is an increase in the temperature of the iron and copper above that of the surroundings.

Tests on various kinds of insulating materials have shown that for each material there is a safe continuous-operating temperature which cannot be exceeded without impairing the life of the material. The following Table 12–1 shows the limiting temperatures for the different kinds of insulation as specified by the A.I.E.E.

The table distinguishes four classes of insulation. Class O insulation consists of cotton, silk, paper, and similar organic materials when neither impregnated nor immersed in oil. Class A insulation consists of cotton, silk, paper, and similar organic materials when impregnated or immersed in oil; also enamel, as applied to conductors. Class B insulation consists of inorganic materials, such as glass, or mica and asbestos in built-up form, combined with binding substances.

A relatively new development in the field of insulating materials is represented by the *silicon* binders and varnishes. These binders and varnishes when used together with the inorganic materials of Class B insulation yield an insulation which is able to withstand much higher temperatures than the standard Class B insulation for the *same life* of the winding. The use of the silicon resins permits a reduction in the size of the machine at a given output. Since the copper resistance increases with the temperature (see Eq. 11–8), the copper losses of the silicon-insulated machines are higher than those insulated according to Class A or B, i.e., the use of silicon insulation results in a reduction of the efficiency of the machine; this reduction decreases with the size of the machine.

TABLE 12–1

| | | Limiting Temperatures, ° C for Industrial Apparatus | | |
|---|---|---|---|---|
| | | Thermometer | Embedded Detector | Hot-Spot |
| 0 Untreated organics | Untreated fabrics of cotton, silk, linen. Untreated paper, fiber, wood, etc. | 75 | 85 | 90 |
| A Treated or impregnated organics | Oil, varnish, wax, or compound impregnated fabrics or sheets of cotton, silk, linen, paper, wood, fiber; oil, varnish, bakelite, organic filler compounds. | 90 | 100 | 105 |
| B Treated or impregnated inorganics | Asbestos, Fiberglas, mica tape, oxide films, inorganic fillers, asbestos boards. (A limited amount of organic materials may be used for binding purposes.) | 110 | 120 | 130 |
| H Treated or impregnated inorganics | Mica, asbestos, Fiberglas and similar inorganic materials in built-up form with binding substances composed of silicone compounds, or materials with equivalent properties; silicone compounds in rubbery and resinous forms, or materials with equivalent properties in minute proportions. Class A material may be used only where essential for structural purposes during manufacture. | — | — | 180 |

The temperature rise of any part of the machine increases as the heat conductivity to the surface of the machine part and the heat transfer of the surface of the machine part to the cooling medium (air) is decreased. High heat conductivity of all materials used, i.e., of the laminations, conductor material, and insulating materials, and high heat transfer from the surfaces of windings and iron to the cooling medium are the necessary conditions for low temperature rises.

The heat conductivity of some materials is given in Chap. 19. The heat

conductivity of copper is higher than that of the other metals. The heat conductivity of the insulating materials is low.

There are two ways for the heat transfer to occur from the surface to the cooling medium: (1) through radiation and (2) through convection, i.e., heat transportation by the moving air. The radiation is effected by the frame. In totally enclosed machines without an air supply from the outside, convection also is effected only by the frame. In open-type machines and in totally enclosed machines with an air supply from the outside, the winding and the laminations, as well as the frame, are included in the heat transfer by convection.

Consider, for example, the end winding on the armature of a d-c machine. Let $\vartheta$ be the temperature of the copper in the end winding, where the losses originate; $\vartheta_s$ the temperature at the surface of the end winding; and $\vartheta_{air}$ the temperature of the cooling air. Then

$$\vartheta - \vartheta_{air} = (\vartheta - \vartheta_s) + (\vartheta_s - \vartheta_{air})$$

$(\vartheta - \vartheta_{air})$ is the temperature rise of the winding the magnitude of which is limited by the properties of the insulating materials, as has been explained above. The temperature rise consists of two terms. The magnitude of the first term $(\vartheta - \vartheta_s)$ depends upon the heat conductivity of the copper and the insulating materials used for the insulation of the single conductors and the total coil. The magnitude of the second term $\vartheta_s - \vartheta_{air}$ depends upon the heat-transfer coefficient from the coil surface to the air.

The insulation of the end winding consists of three different parts: the conductor insulation, the coil (ground) insulation, and the varnish. Therefore, $(\vartheta - \vartheta_s)$ consists of several terms, i.e., $(\vartheta - \vartheta_s) = \Sigma \Delta\vartheta$. If $I_h$ is the heat flow from the copper to the surface of the end winding per unit surface, then

$$\vartheta - \vartheta_s = \Sigma \Delta\vartheta = I_h \Sigma \frac{d}{\lambda_h}$$

where $d$ is the thickness of the insulation material and $\lambda_h$ its heat conductivity. Thus, in order to obtain a small temperature rise $(\vartheta - \vartheta_s)$, the ratio $d/\lambda_h$ must be as small as possible for all insulating materials, i.e., the thickness of the insulation must not be larger than is necessary with respect to the dielectric strength of the insulation, and the heat conductivities of all insulating materials must be as large as possible.

The temperature rise $(\vartheta_s - \vartheta_{air})$ is determined by the heat-transfer coefficient from the surface of the end winding to the air, which depends upon the velocity of the air between the end windings. Approximate values for the heat-transfer coefficient are given in Chap. 19.

**12–2. Heating and Cooling of a Homogeneous Body.** In the preceding article, the temperature rise of the end winding has been considered as an example. It should be noted that the temperature rise of each part of the

machine depends not only upon the heat produced in it but also upon the heat produced *in other parts* of the machine, since a heat flow from one part to another takes place within the machine. For example, the heat produced in the embedded part of the winding, i.e., in the part which lies in the slots, flows partially through the insulation to the laminations and partially to the end windings. Thus the end windings must transfer to the air not only the heat produced in them but also a part of the heat produced in the slot portion of the winding.

The electric machine *is not a homogeneous body.* Its parts are made of different materials, iron, copper, and insulating materials, with different heat conductivities and different heat-transfer coefficients. Because of the heat flow between the machine parts, the temperature rise of one part depends upon the heat produced in the other parts. However, it is useful to consider the heating and cooling of a homogeneous body since the results obtained from such considerations are, to a certain degree, applicable to the different parts of the machine as well as to the machine as a whole.

For the homogeneous body let:

$Q$ = heat produced in the body per second in kg-cal,
$W$ = weight of the body in kg,
$S$ = cooling surface of the body in cm$^2$,
$c$ = specific heat of the substance, i.e., the amount of heat required to raise 1 kg 1° C,
$h$ = heat-transfer coefficient, i.e., the amount of heat in kg-cal, dissipated per cm$^2$ surface per 1° C difference of temperature between the body and the surrounding medium,
$\vartheta$ = temperature rise of the body, i.e., the temperature of the body above that of the surrounding medium.

Then

$$Q\,dt = Wc\,d\vartheta + Sh\vartheta\,dt \tag{12–1}$$

i.e., the heat produced in the body during the time $dt$ is equal to the heat $Wc\,d\vartheta$ which, during this time, increases its temperature by $d\vartheta$ plus the heat $Sh\vartheta\,dt$ transferred to the cooling medium during this same period.

Under steady-state conditions, i.e., when the temperature of the body becomes stationary, $d\vartheta = 0$ and $\vartheta = \vartheta_{max}$. This happens when the rate of heat production is equal to the rate of heat dissipation. Thus, according to Eq. 12–1,

$$\vartheta_{max} = \frac{Q}{Sh} \tag{12–2}$$

Introducing this relation in Eq. 12–1,

$$dt = \frac{\frac{Wc}{Sh}}{\vartheta_{max} - \vartheta}\,d\vartheta = \frac{I}{\vartheta_{max} - \vartheta}\,d\vartheta \tag{12–3}$$

The quantity

$$T = \frac{Wc}{Sh} \tag{12–4}$$

is a constant having the dimension of time and is called the *thermal time constant.*

The solution of the differential Eq. 12–3 is

$$t = -T \ln (\vartheta_{max} - \vartheta) + C \tag{12–5}$$

At $t = 0$, let the temperature rise $\vartheta$ be equal to $\vartheta_0$. Then

$$C = T \ln (\vartheta_{max} - \vartheta_0)$$

and

$$t = T \ln \frac{\vartheta_{max} - \vartheta_0}{\vartheta_{max} - \vartheta} \tag{12–6}$$

or

$$\vartheta = \vartheta_{max} (1 - \epsilon^{-t/T}) + \vartheta_0 \epsilon^{-t/T} \tag{12–7}$$

If $\vartheta_0$ starts with the value zero, i.e., if the heat production in the body starts at $t = 0$, then

$$\vartheta = \vartheta_{max} (1 - \epsilon^{-t/T}) \tag{12–8}$$

The heating curve which corresponds to this equation is shown in Fig. 12–1. $t/T$ is plotted along the axis of abscissae, $\vartheta/\vartheta_{max}$ along the axis of ordinates.

At the time $t = T$, the temperature rise is equal to

$$\vartheta_{t=T} = \vartheta_{max} \frac{\epsilon - 1}{\epsilon} = 0.633 \vartheta_{max} \tag{12–9}$$

The thermal time constant is thus the time required for $\vartheta$ to reach 63% of its final value.

At the time $t = 3T$, the temperature rise $\vartheta = 0.95 \vartheta_{max}$. Theoretically, $\vartheta$ becomes equal to $\vartheta_{max}$ at the time $t = \infty$.

The rate of change of $\vartheta$ is (see Eq. 12–3)

$$\frac{d\vartheta}{dt} = \frac{\vartheta_{max} - \vartheta}{T} \tag{12–10}$$

At any point of the heating curve it is proportional to the difference $(\vartheta_{max} - \vartheta)$. In Fig. 12–2 the heating curve is plotted again, using $t$ as the abscissa and $\vartheta$ as the ordinate. It follows from Eq. 12–10 that the subtangent of this curve with respect to the line $\vartheta = \vartheta_{max}$ is constant and equal to the thermal time constant $T$. This makes it possible to determine easily the thermal time constant when a heating curve taken from test is available and $\vartheta_{max}$ is given.

$\vartheta_{max}$ can be determined from the heating curve in the following way. It follows from Eq. 12–10 that $\vartheta$, as a function of $d\vartheta/dt$, is a straight line which intersects the axis of abscissae at the point $\vartheta_{max}/T$, and the axis of ordinates at the point $\vartheta_{max}$ (Fig. 12–2). Therefore, if $d\vartheta/dt$ is determined for 2 points of

the heating curve, the straight line $\vartheta = f(d\vartheta/dt)$ can be drawn and $\vartheta_{max}$ determined.

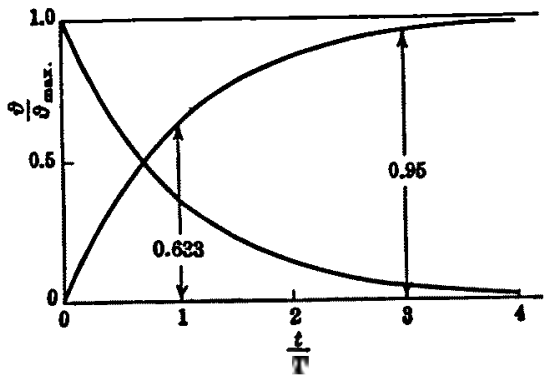


FIG. 12–1. Heating curve and cooling curve of a homogeneous body.

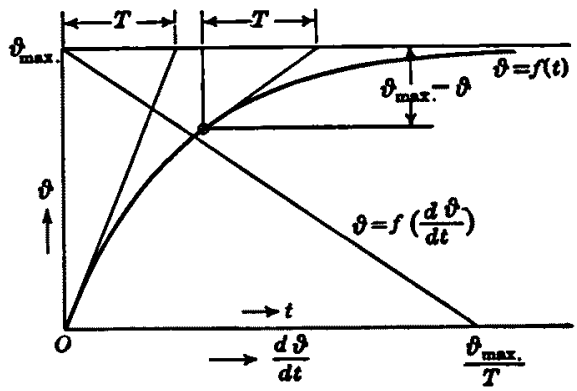


FIG. 12–2. Determination of the thermal time constant.

It follows further from Fig. 12–2 that the thermal time constant is the time during which the body would reach $\vartheta_{max}$ if there were no heat dissipation, i.e., if there were no heat transfer to the surrounding medium.

If in Eq. 12–1 $Q\,dt$ is assumed to be zero, the *cooling* curve of the homogeneous body is obtained:

$$t = T \ln \frac{\vartheta_0}{\vartheta}$$

or

$$\frac{\vartheta}{\vartheta_0} = \epsilon^{-t/T} \tag{12–11}$$

where $\vartheta_0$ is the temperature at $t = 0$. The cooling curve for $\vartheta_0 = \vartheta_{max}$ is shown in Fig. 12–1. It is the mirror image of the heating curve with respect to the line of symmetry

$$\frac{\vartheta}{\vartheta_{max}} = \frac{1}{2}$$

The numerator of Eq. 12–4, $Wc$, is the amount of heat required to raise the temperature of the body by 1° C, i.e., the thermal capacity of the body. The denominator $Sh$ of this equation is the heat transferred by the body to the cooling medium per second per 1° C temperature difference. The thermal time constant $T$ which is a measure of the rate of heating or cooling of the homogeneous body is thus the ratio between the thermal capacity of the body and its heat transfer. The larger the heat-transfer coefficient $h$, the smaller will be the thermal time constant $T$. The more intensive the cooling of the machine, the smaller is its thermal time constant, and the sooner the stationary condition is achieved. Large electric machines have a time constant of several hours.

**12–3. Temperature Rise of the Windings.** The calculation of the temperature rises of the copper and iron in the electric machine is not simple, due to the fact that several heat conductivities, several heat-transfer coefficients, and the heat flow from one part of the machine to other parts are involved. For this reason, in practical design, the designer uses specific heat constants based on experience, in order to determine whether or not the machine will meet the A.I.E.E. standards. A method for calculating the temperature rises of the windings and iron, and the heat flow in electrical machines, based on Fourier's heat flow equation, is given in Chap. 19.

**12–4. Cooling (Ventilation) of D-c Machines. Different Types of Enclosures.** Sufficient cooling is achieved when care is taken that good heat transfer exists from the active iron and copper, where the losses originate, to the cooling medium (*air*). For this purpose either the armature (except the short ones) is divided into stacks of laminations about 2 inches wide, separated by $\frac{3}{8}$-inch ducts or the armature is provided with axial ducts, or both kinds of ducts are used. Forcing air through the ducts facilitates the transfer, to the air, of the heat due to the losses in the iron and in the embedded parts of the windings. Sufficient air circulation must be present also around the end windings and field coils, in order to transfer the heat developed there to the air.

Among all kinds of machines the one used most widely is the *open machine*, i.e., one in which there is no restriction to ventilation other than that necessitated by good mechanical construction. However, on account of the environment, more or less complete enclosure may be necessary.

The different types of enclosures as defined by N.E.M.A. (National Electrical Manufacturers Association) are listed in the following (number in parenthesis is N.E.M.A. number):

1. *Tight.* Water-tight, dust-tight, etc., when so constructed that the enclosing case will exclude the specified material (IC50–18).
2. *Proof.* Splash-proof, dust-proof, etc., when so constructed, protected, or treated that its successful operation is not interfered with when subjected to the specified material or condition (IC50–20).
3. *Resistant.* Moisture-resistant, fume-resistant, etc., when so constructed, protected or treated that it will not be readily injured when subjected to the specified material (IC50–23).
4. *Self-Ventilated Machine.* A machine which has its ventilating air circulated by means integral with the machine (MG50–41).
5. *Separately Ventilated Machine.* A machine which has its ventilating air supplied by an independent fan or blower external to the machine (MG50–45).
6. *Open Machine.* A self-ventilated machine having no restriction to ventilation other than that necessitated by mechanical construction (MG50–40).

NOTE: In the sense of this definition, an open machine, when the term is used without qualification, is understood not to be splash-proof or drip-proof.

**7.** *Drip-Proof Machine.* A machine in which the ventilating openings are so constructed that drops of liquid or solid particles falling on the machine at any angle not greater than 15° from the vertical cannot enter the machine either directly or by striking and running along a horizontal or inwardly inclined surface (MG50–14).

**8.** *Splash-Proof Machine.* A machine in which the ventilating openings are so constructed that drops of liquid or solid particles falling on the machine or coming towards it in a straight line at any angle not greater than 100° from the vertical cannot enter the machine either directly or by striking and running along a surface (MG50–16).

**9.** *Totally Enclosed Machine.* A machine so enclosed as to prevent exchange of air between the inside and the outside of the case but not sufficiently enclosed to be termed air-tight (MG50–43).

**10.** *Totally Enclosed Fan-Cooled Machine.* A totally enclosed machine equipped for exterior cooling by means of a fan or fans, integral with the machine, but external to the enclosing parts (MG50–44).

**11.** *Explosion-Proof Machine.* A machine in an enclosing case which is designed and constructed to withstand an explosion of a specified gas or dust which may occur within it, and to prevent the ignition of the specified gas or dust surrounding the motor by sparks, flashes, or explosions of the specified gas or dust, which may occur within the machine casing (MG50–18).

**12.** *Water-Proof Machine.* (1) A totally enclosed machine so constructed that it will exclude water applied in the form of a stream from a hose.

(2) A totally enclosed machine so constructed that a stream of water from a hose (not less than 1 inch in diameter) under a head of 35 feet and from a distance of about 10 feet can be played on the machine without leakage, except that leakage which may occur around the shaft may be considered permissible, provided it is prevented from entering the oil reservoir and provision is made for automatically draining the machine (MG50–20).

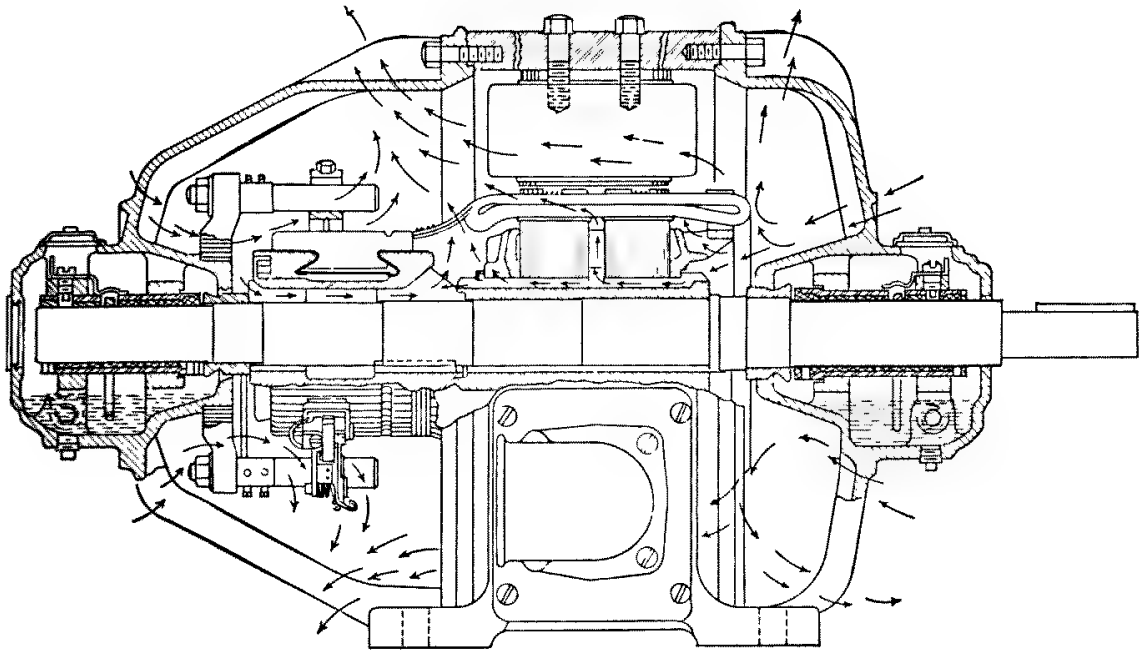

FIG. 12–3. Air-flow in an open-type d-c machine.

**13.** ***Dust-Tight Machine.*** A machine so constructed that the enclosing case will exclude dust (MG50–22).

The air flow in an open-type d-c machine provided with radial and axial ducts is shown by Fig. 12–3.

Fig. 12–4 shows an open-type, d-c motor. Note that either end may be covered with plates, screens, or louvres.

Fig. 12–5 shows a splash-proof d-c motor. Note that air flows in through the bottom opening at the left-hand end, and out at the louvre-protected opening at the right-hand end. This construction protects the motor from splashing or dripping liquid, but not from contaminated air or dust.

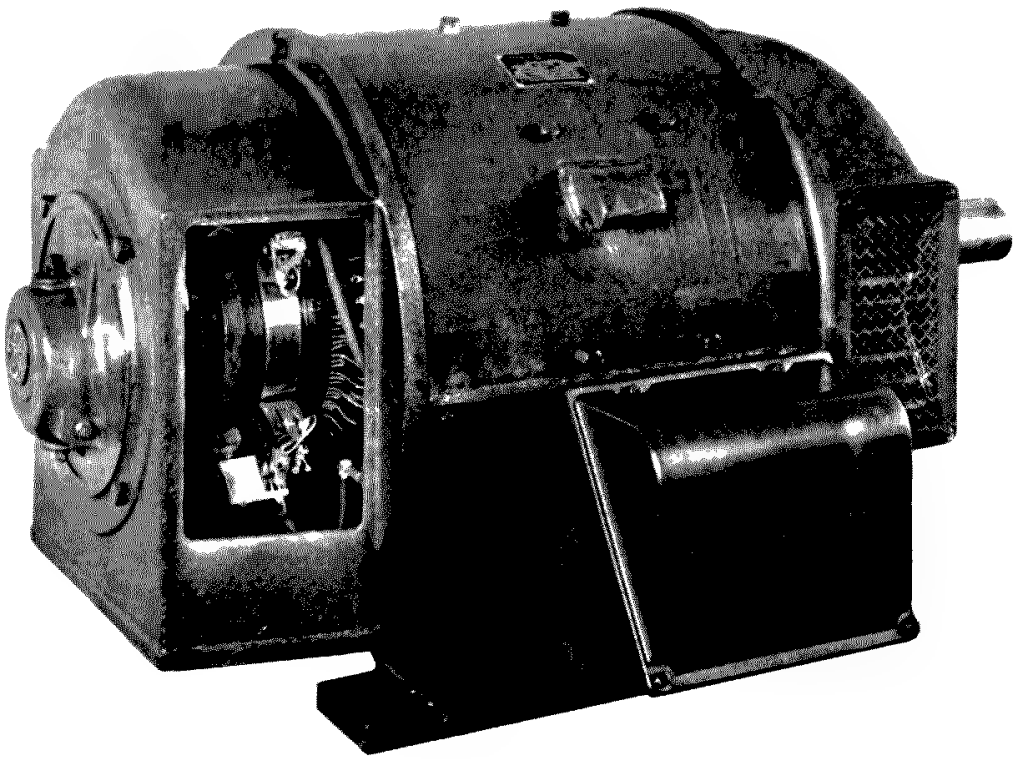

FIG. 12–4. Open frame motor.

Fig. 12–6 shows a typical totally enclosed, non-ventilated d-c motor. In this motor none of the internal moving parts or windings are in contact with air from the surroundings. All heat is conveyed away only from the outside of the frame directly to the surrounding air. For a given horsepower rating this type of motor requires a larger machine than an open type.

Fig. 12–7 shows a totally enclosed, fan-cooled d-c motor, and Fig. 12–8 shows the internal construction of the motor. The motor is essentially the same as shown in Fig. 12–6 except that a fan and an enclosure have been added at the commutator end. Air is forced over the end enclosure and over the outside of the frame without coming in contact with the commutator

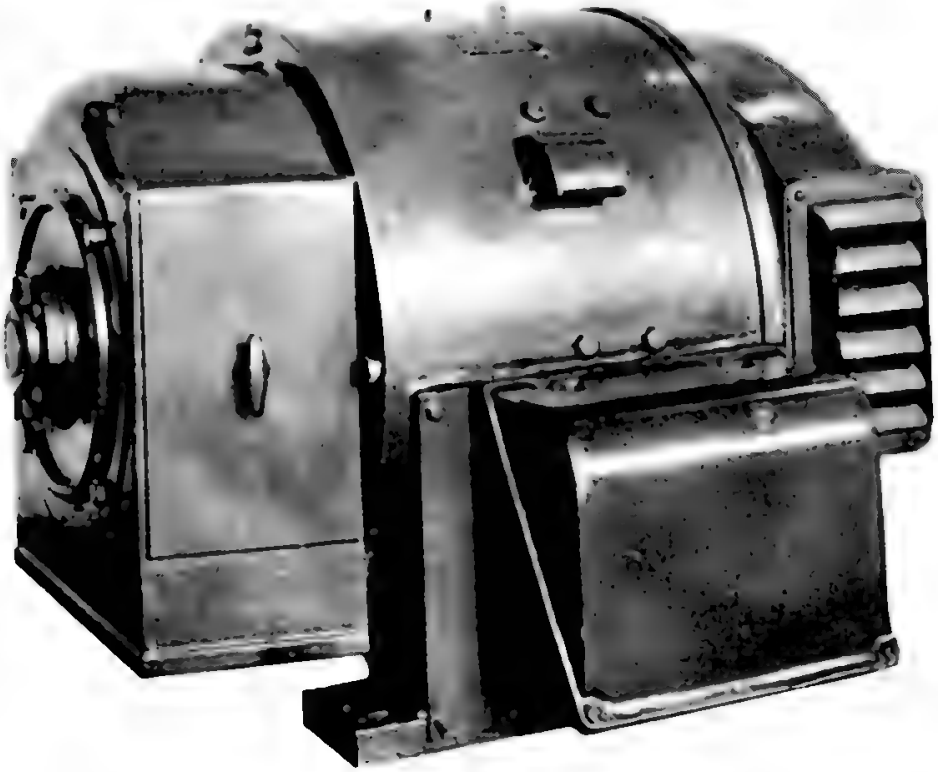

FIG. 12–5. Splash-proof motor

FIG. 12–6. Totally enclosed, non-ventilated motor.

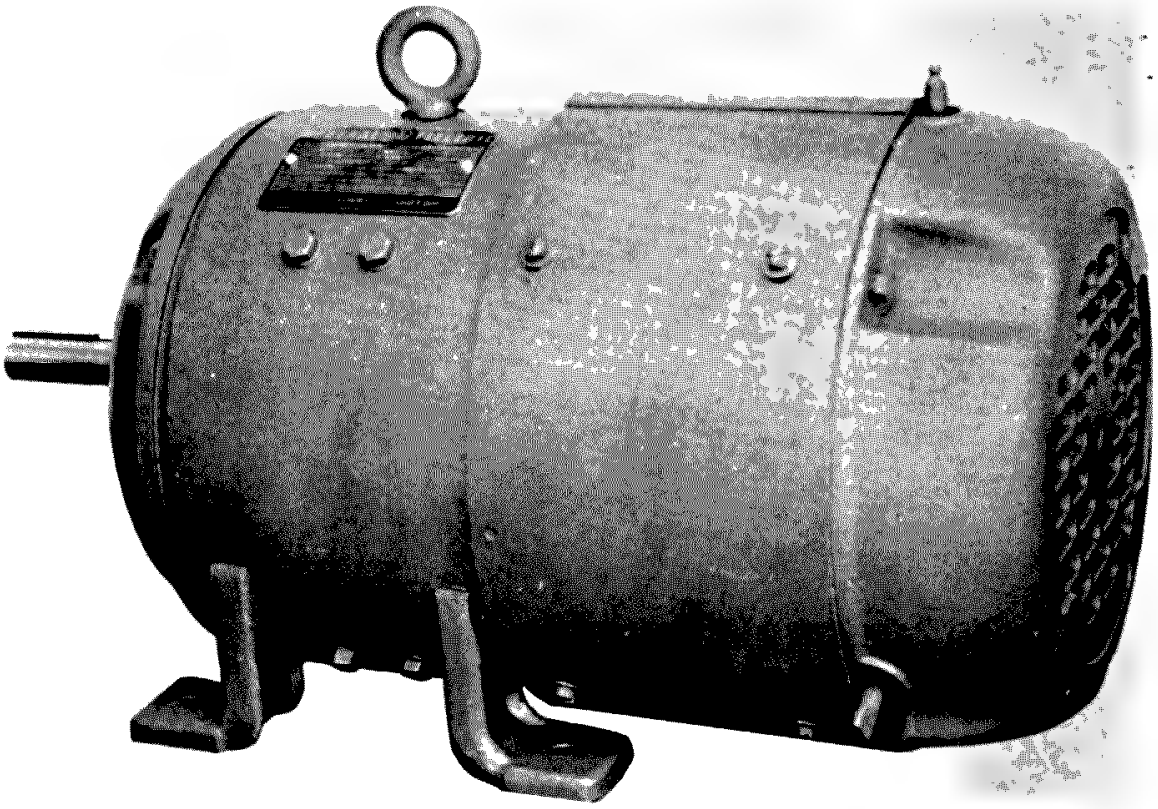

FIG. 12–7. Totally enclosed, fan-cooled motor.

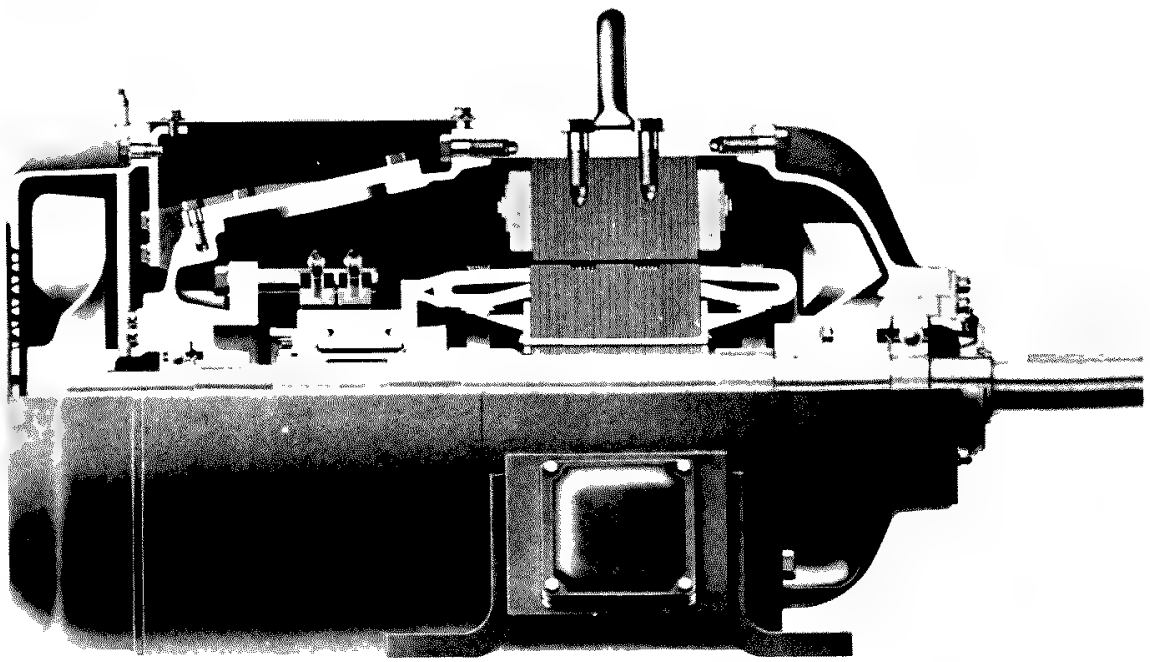

FIG. 12–8. Internal section of fan-cooled, totally enclosed motor.

This enables the machines to operate in a contaminated atmosphere, without damage, as well as to provide good cooling.

Fig. 12–9 shows a motor arranged for forced ventilation. This type is used when the ambient temperature is high. Note that the general construction is the same as for the splash type, except for the addition of the fan at the top of end housing. Many other special types of enclosures are available to take care of special surrounding or operating conditions.

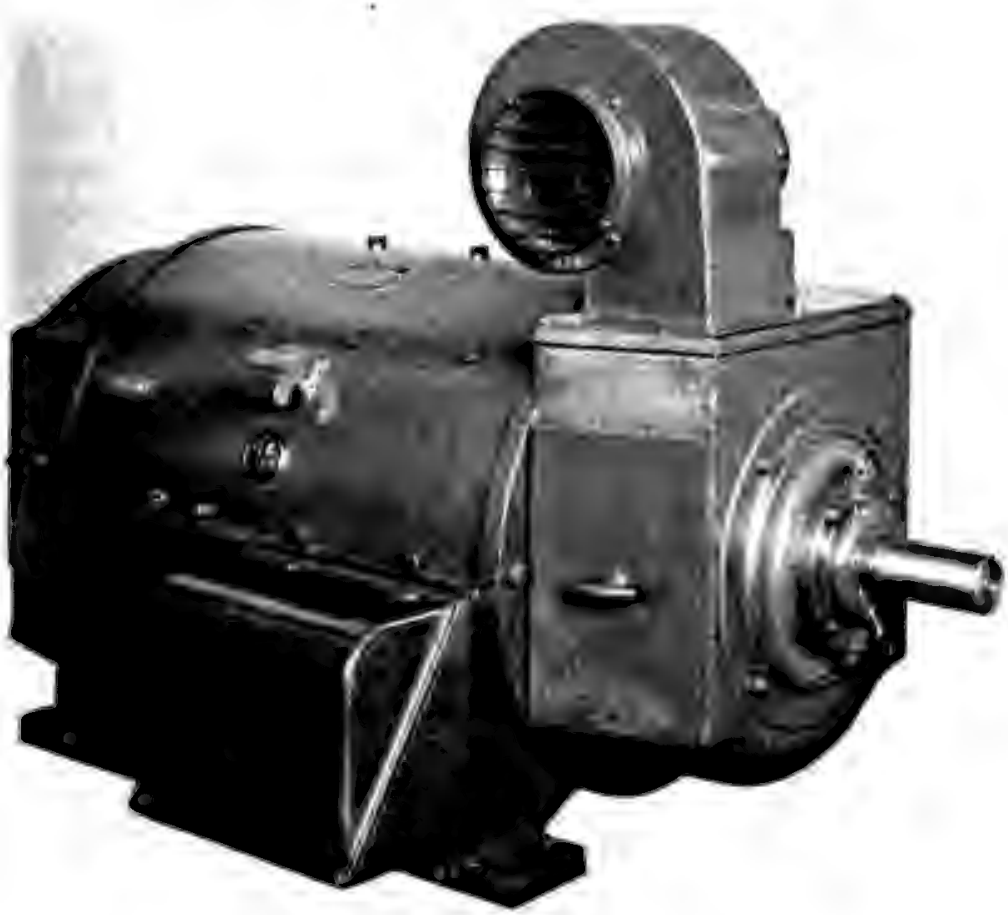

FIG. 12–9. Separately ventilated motor.

# *Chapter 13*

## STARTING OF D-C MOTORS

All electric motors, when running, develop an emf of rotation. This emf together with the impedance drop due to the current balances the applied voltage at all times. Since this *emf is absent at standstill,* the applied voltage is balanced by the impedance drop only. If rated voltage is applied at standstill, excessive currents may flow and cause damage to the motor. Also this excessive current may cause a large voltage fluctuation in the power lines. Excessive torque or too-rapid acceleration also may damage the load. In order to limit the amount, and often the duration of the starting current, many motor installations require a starting device. This device usually reduces the voltage applied at the motor terminals during the starting period, and controls the time used for acceleration, either manually or automatically. N.E.M.A. defines a starter as a controller designed for accelerating a motor to normal speed in one direction of rotation; and an electric controller as a device or group of devices, which serves to govern, in some predetermined manner, the electric power delivered to the apparatus to which it is connected. All d-c motors above 2 hp require a starter to reduce the armature voltage. Fractional-horsepower motors generally do not require a starter to reduce the voltage.

**13–1. Starting a D-c Motor.** (a) *Shunt Motor.* The armature current of a shunt motor is $I_a=(V-C_1\Phi n)/R_a$ where $R_a$ includes the total resistance of the armature circuit. At standstill $n$ is zero, and in order to limit the starting current to safe values, resistance must be added in series with the

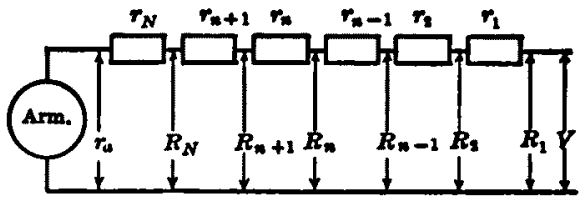


FIG. 13–1. Armature with starting rheostat for a d-c motor.

armature. The maximum current at start is usually limited to between 150% and 200% of full-load current, although under certain conditions it may be greater or less. As the motor accelerates, the current decreases, until

the speed is constant. The resistance is then reduced in order to increase the current and produce further acceleration. This reduction of resistance is made in steps, to fit the required conditions. The accleration of a shunt motor may be studied by the use of the diagrams of Figs. 13–1 and 13–2. Fig. 13–1 shows the schematic diagram of the armature circuit, and Fig. 13–2 the speed-current curves, or counter-emf-current curves, for different values of total armature circuit resistance. The following nomenclature applies to this discussion:

$I_r$ = armature current at rated load.

$V$ = line voltage; $R_a$ = armature resistance including leads, brushes, and commutating field. This may be conveniently expressed as $R_a = Z(V/I_r)$, where it may be assumed that $Z \approx 0.1$ for a wide range of motor sizes. It will be less than 0.1 for very large motors and greater for fractional-horsepower motors.

$I_p$ = maximum or peak starting current.

$I_v$ = minimum starting current, i.e., when switching takes place.

$I_p/I_r = Y$, where $Y$ is usually 1.5 to 2.0, but may be as high as 4.0.

$I_p/I_v = X$, where $X$ is commonly equal to $Y$ for a loaded motor, but may be greater for a lightly loaded motor during starting.

$E_c$ = counter-emf; $E_{cn}$ = counter-emf at end of an accelerating period just prior to cutting out resistor $r_n$.

$R_1$ = total resistance of starting circuit. $R_1 = V/I_p$.

$R$ = total resistance of starting rheostat. $R = R_1 - R_a$.

$R_n$ = total resistance of circuit with resistor $r_n$ still in the circuit.

$r_n$ = resistance of one of the steps in the starting resistor.

$N$ = number of steps in the starting resistor.

$n$ = speed in rpm.

It is assumed for this discussion that the total load torque is constant.

For the shunt motor, $V = I_a R_a + K_1 n$, where $K_1$ may be found from normal full-load conditions, by test or from the design.

$$K_1 = \frac{V - I_a R_a}{n} \tag{13–1}$$

For $I_a$ = zero, the speed is $n_0 = V/K_1$. This may be called the *limiting no-load speed*, and is shown in Fig. 13–2 as *Om*. In Fig. 13–2 the scales for the ordinates are speed and voltage, and the abscissa is armature current. Assume that the curve *klm* is the normal speed-current curve of the motor, *Oa* is the initial starting current $I_p = YI_r$, *Os* is the minimum value of starting current $I_v$, *Om* is the speed or counter-emf (= terminal voltage) at no load. With the total resistance $R_1$, the initial current at standstill will be *Oa*. The motor will accelerate along the line *abm* as long as the delivered torque is greater than the load torque. If at point *b* the delivered torque is just equal to the load torque, the current will remain equal to $I_v$, and the speed and counter-emf

equal to $Sb$. The total resistance drop in the circuit is then $wb$. This resistance drop is divided as $wl$ within the armature and $lb$ in the resistance $R$. Hence $R = lb/I_v$. If the first step of resistance $r_1$ is now cut out by switching, the current will rise again to $I_p$, provided the resistance $r_1$ had been properly chosen, as will be shown later. The motor then accelerates along $cdm$ to

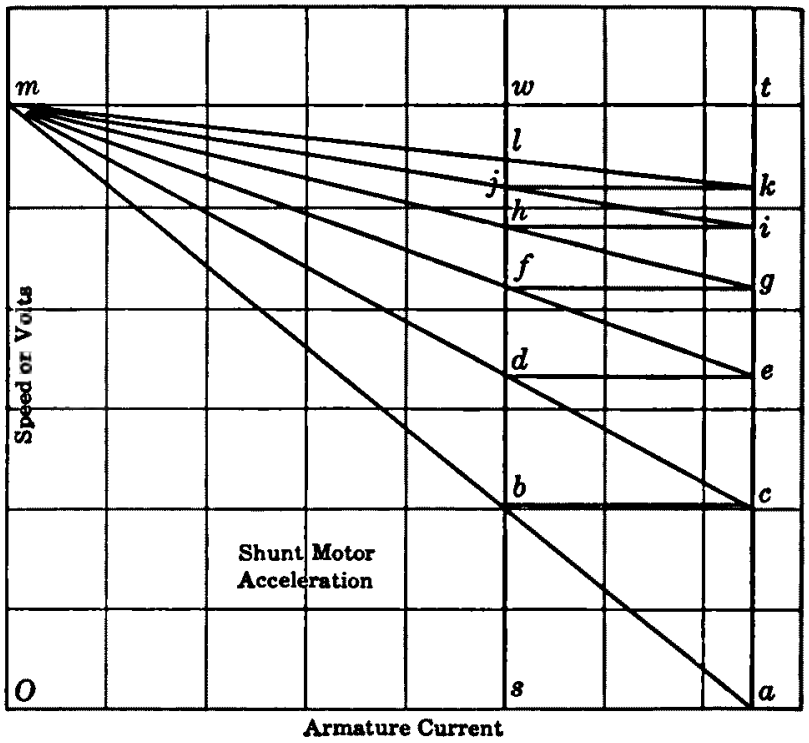


FIG. 13–2. Speed-current curves for shunt motor acceleration.

point $d$. Cutting out $r_2$ raises the current to $I_p = Oa$ again. This process continues until full line voltage is impressed across the armature terminals and the motor is operating on its normal speed-current curve $klm$. If $I_v$ is full-load current, the speed will be $sl$ at full-load.

From Figs. 13–1 and 13–2 it is seen that

$$R_1 = \frac{V}{I_p} = \frac{V}{Oa} = \frac{ws}{I_p} = \frac{wb}{I_v} \quad \text{and} \quad R_2 = \frac{tc}{I_p} = \frac{wd}{I_v} \tag{13–2}$$

and

$$r_1 = \frac{ws}{I_p} - \frac{wb}{I_p} = \frac{bs}{I_p}, \quad \text{or} \quad r_1 = \frac{wb}{I_v} - \frac{wd}{I_v} = \frac{bd}{I_v}, \quad \text{and} \quad r_2 = \frac{bd}{I_p} = \frac{fd}{I_v} \tag{13–3}$$

If the curves of Fig. 13–2 are plotted accurately to scale, the resistance and number of steps of the starting rheostat may be determined graphically as suggested in the foregoing, or analytically as shown in the following paragraphs.

With the line voltage $V$ applied to $R_1$ at start, the current will be

$$I_p = \frac{V}{R_1} \quad \text{or} \quad R_1 = \frac{V}{I_p}, \quad \text{and} \quad I_p = YI_r \tag{13–4}$$

The motor will accelerate with this resistance $R_1$ as has been shown. When the acceleration has ended with $R_1$, the counter-emf will be $E_{c1}$ and the current $I_v$:

$$E_{c1} = V - I_v R_1 \quad \text{or} \quad V - E_{c1} = I_v R_1 \tag{13–5}$$

In order that the current may rise to $I_p$ after cutting out the first resistor $r_1$, the following equation must be satisfied:

$$I_p = \frac{V - E_{c1}}{R_2} = \frac{I_v R_1}{R_2} \quad \text{or} \quad R_2 = \frac{R_1}{X} \quad \text{or} \quad R_1 = R_2 X \tag{13–6}$$

Acceleration again takes place, until the current again is reduced to $I_v$; then

$$E_{c2} = V - I_v R_2 \quad \text{or} \quad V - E_{c2} = I_v R_2 \tag{13–7}$$

and upon cutting out $r_2$,

$$I_p = \frac{V - E_{c2}}{R_3} = \frac{I_v R_2}{R_3} \quad \text{or} \quad R_3 = \frac{R_2}{X} \quad \text{or} \quad R_3 = \frac{R_1}{X^2} \tag{13–8}$$

This process is continued until all of the starting resistance has been cut out and full line voltage applied to the armature.

From these relations it follows that the total resistance for any accelerating point is

$$R_n = \frac{R_{n-1}}{X} = X R_{n+1} = \frac{R_1}{X^{n-1}} \tag{13–9}$$

and

$$R_a = \frac{R_1}{X^N} \quad \text{or} \quad X^N = \frac{R_1}{R_a} = \frac{V}{Y I_r} \times \frac{I_r}{Z V} = \frac{1}{YZ} \tag{13–10}$$

so that

$$\log X = \frac{\log \frac{1}{YZ}}{N} \quad \text{or} \quad N = \frac{\log \frac{R_1}{R_a}}{\log X} = \frac{\log \frac{1}{YZ}}{\log X} \tag{13–11}$$

Hence, if $Z = 0.1$ then,

$$N = \frac{1 - \log Y}{\log X} \tag{13–12}$$

or if $Y = X$ as is usually the case, then

$$N = \frac{1}{\log Y} - 1 \quad \text{or} \quad \log Y = \frac{1}{N+1} \tag{13–12a}$$

For a starter with only 1 step, $N = 1$, and $Y = 3.17$. This means that if $I_p = 3.17$ and $I_v = 1.0$, then only 1 step is required. On the other hand, if $N = 2$, $Y = 2.15$; or if $N = 3$, $Y = 1.75$; or if $N = 4$, $Y = 1.6$.

From these equations the number of steps in the starting resistor is determined for given values of $X$, $Y$, and $Z$. It will be unlikely that the solution for $N$ will yield a whole number, but since $N$ must be a whole number, the values of $X$ and of $Y$ may be readjusted.

From Fig. 13–1 and Eqs. 13–9 and 13–10 it follows that

$$r_n = R_n - R_{n+1} = R_n - \frac{R_n}{X} = \frac{R_n}{X}(X-1) = \frac{R_1}{X^n}(X-1) \tag{13–13}$$

From Eq. 13–13 it may be determined also that

$$r_n = \frac{r_{n-1}}{X} \tag{13–13a}$$

Hence,

$$r_1 = \frac{R_1}{X}(X-1) \tag{13–14}$$

The total resistance in the starting resistor is

$$R = R_1 - R_a = R_1 - \frac{R_1}{X^N} = \frac{R_1}{X^N}(X^N - 1) = \frac{V}{YI_r} - \frac{ZV}{I_r} = \frac{V}{I_r}\left(\frac{1}{Y} - Z\right) \tag{13–15}$$

The units of the starting rheostat must be chosen to withstand the heating conditions imposed by the particular starting-duty cycle required of the motor, and in this connection reference should be made to N.E.M.A. Industrial Control Standards. Some of the methods and apparatus used to start the motor will be discussed in a later part of the chapter.

**Example:** Determine the number of steps and resistance of each step, in a manual-type starting rheostat to accelerate a 5-hp 230-volt shunt motor under full load. Assuming

$$Z = 0.1, \quad Y = 1.5, \quad X = 1.5$$

solving Eq. 13–12

$$N = \frac{1 - \log 1.5}{\log 1.5} = 4.68$$

This will require 5 steps, and an adjustment of $X$ so that $\log X = \frac{1 - \log 1.5}{5}$, $X = 1.46$ instead of 1.5 as assumed, and $I_v = 20.5$ which is but slightly greater than 20, the full-load current.

$$R_1 = \frac{230}{30} = 7.67, \qquad R = 7.67 - 1.15 = 6.52,$$

$$R_a = \frac{0.1 \times 230}{20} = 1.15, \quad r_1 = \frac{7.67}{1.46} \times 0.46 = 2.42,$$

$$r_2 = \frac{r_1}{X} = 1.66, \quad r_3 = \frac{r_2}{X} = 1.14, \quad r_4 = 0.78, \quad r_5 = 0.53$$

If $Y = X = 3.5$, then $N = 0.85$, so only 1 step is required, and $R_1 = \frac{230}{70} = 4.72$ and $R = 4.72 - 1.15 = 3.57$ ohms.

(b) *Series Motor.* The process of accelerating a series motor is essentially the same as for a shunt motor. The details of choosing the steps of the starting rheostat are a little different, due to the dependence of the field flux on the

armature current. Using the same nomenclature as for the shunt motor and assuming a linear magnetization curve, the following analysis yields the necessary information. At the end of the first accelerating step, the counter-emf will be

$$E_1 = V - I_v R_1 = K_1 n I_v \quad \text{or} \quad n = \frac{V - I_v R_1}{K_1 I_v} \tag{13–16}$$

Just after switching out the first step, and before the speed has changed,

$$V = I_p R_2 + K_1 n I_p = I_p R_2 + \frac{K_1 I_p (V - I_v R_1)}{K_1 I_v} \tag{13–17}$$

Solving Eq. 13–17 gives:

$$R_2 = \frac{V}{I_p} + R_1 - \frac{V}{I_v} = R_1 + R_1 - \frac{VX}{I_p} = 2R_1 - XR_1 = R_1(2 - X) \tag{13–18}$$

and since $r_1 = R_1 - R_2$,

$$r_1 = R_1(X - 1) \tag{13–19}$$

In a similar manner it will be found that all steps are alike so that

$$r_n = R_1(X - 1) = V\left(\frac{1}{I_v} - \frac{1}{I_p}\right) \tag{13–20}$$

and

$$R = NR_1(X - 1) = R_1 - R_a \tag{13–21}$$

and

$$N = \frac{R_1 - R_a}{R_1(X - 1)} = \frac{1}{X - 1} - \frac{R_a}{R_1(X - 1)}$$

$$= \frac{1}{X - 1} - \frac{VZI_p}{I_r V(X - 1)} = \frac{1 - ZY}{X - 1} \tag{13–22}$$

In the case of the series motor, the value of $Z$ is greater than for a shunt motor, about 0.15. If the magnetization curve is not assumed linear, then a graphical analysis similar to Fig. 13–2, using speed-current curves for different values of armature circuit resistance, may be used.

**13–2. Manual-Type Starters for D-c Motors.** Cutting out steps of the starting rheostat may be done *manually* or *automatically*. When done manually, the most common type of starting device for motors of not greater than 75 hp at 115 volts, or 150 hp at 230 volts, is the *face-plate starting box*. For larger motors the manual *drum-type* or an *automatic starter* is used. The face-plate type (Fig. 13–3) consists of stationary contacts or buttons, mounted on an insulated panel, and arranged on the arc of a circle. A series of resistors are connected between the buttons, and a sliding arm moves over these buttons. The number of steps in the manual starter is greater than in the automatic type. This is considered necessary in order to take into account the possibility of abuse by the operator. The number of steps in the manual type

depends upon the horsepower, and is about as follows: Up to 1 hp, 5 to 7 steps; 1 hp through 5 hp, 7 or 8 steps; 5 through 20 hp, about 10 steps; and above 20 hp, 10 to 13 steps. Two types of these boxes are available: a 3-terminal or no-field release, and a 4-terminal or no-voltage release. The operation of these boxes is described in the following paragraphs.

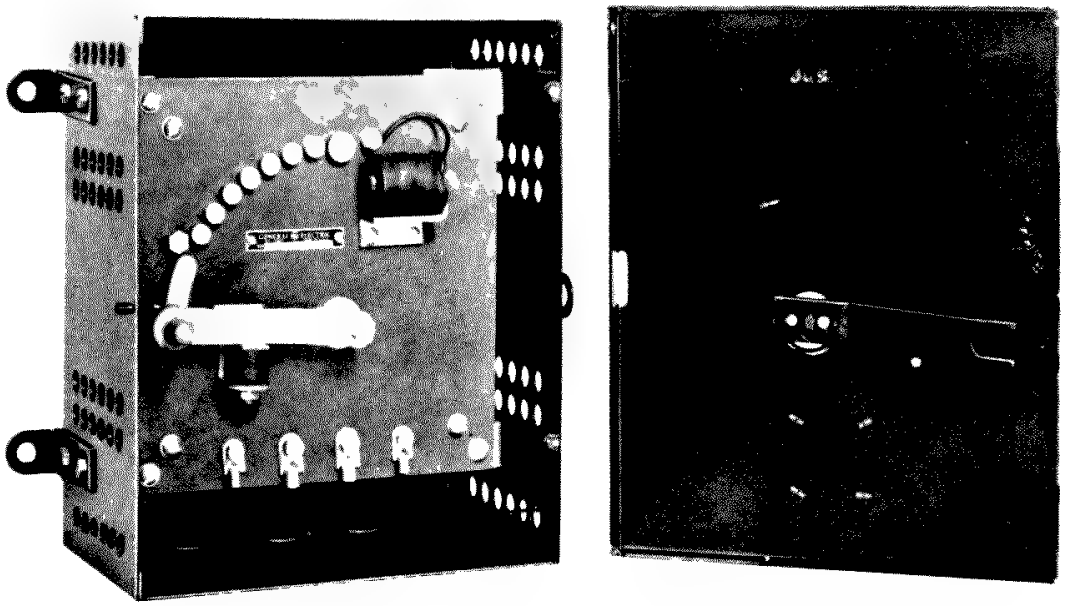

FIG. 13–3. Manual-type 4-terminal starting rheostat for a 5-hp d-c motor.

(a) *Three-Terminal Starter.* Fig. 13–4 shows a *3-terminal starter* connected to a shunt motor, although it is equally suitable for compound motors. The movable arm swings about the post $P$, and makes contacts with the taps on the resistor. This arm is held in the *off* or starting position by a coil spring around the post $P$. It is held in the running position on the last button $N$ by the holding coil $C$, this coil being in series with the shunt-field coil of the motor. When the arm is on button 1, all of the starting resistor is in series with the armature, and this is gradually cut out as the arm moves towards the last button $N$ where the armature is connected directly to the line. One end of the holding coil $C$ is connected to the frame of the holding magnet, so that the field current of the motor does not pass through the starting resistor when the arm is in the running position. If the field current should fail, due to an open circuit, the arm will be returned to the *off* position by the spring very quickly, and the motor disconnected from the line. Should the line voltage fail, the motor will slow down gradually; and when the counter-emf is not large enough to provide sufficient holding coil current, the arm will release and return to the *off* button $S$. This type of box is not well suited for use with adjustable-speed motors, in which shunt field control requiring a wide range of field current is used. It is also evident that the design of the holding magnet coil must be co-ordinated with the field current of the motor.

This type of box also is not suitable for series motors, and is not as universal in its application as the 4-terminal box.

(b) *Four-Terminal Starter.* Fig. 13–5 shows a *4-terminal face-plate starter* connected to a shunt motor, although it may be used with compound or series motors. In the latter case, no use is made of the terminal *F*. The

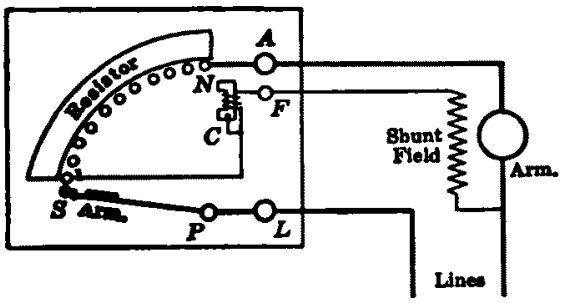


FIG. 13–4. Schematic diagram of a 3-terminal manual-type face plate starter for shunt or compound d-c motors.

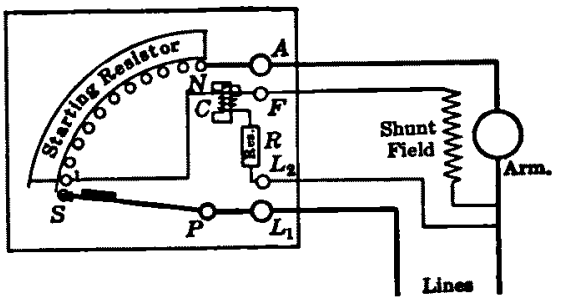


FIG. 13–5. Schematic diagram for a 4-terminal manual-type face plate starter for shunt or compound d-c motors.

essential difference between the 3-terminal and 4-terminal starters is in the connections to the holding magnet coil *C*. In the 4-terminal starter, the holding coil is not in series with the shunt field coil of the motor, but is connected to the supply lines through a resistance *R*. As in the 3-terminal starter, one end of the holding coil is connected to the frame of the holding magnet, so that the field current of the motor and the holding coil current do not pass through the starting resistor when the arm is in the running position. The holding coil is not designed for full line voltage, because, being rather small, it would require a large number of turns of very small wire—an expensive and fragile construction. Moreover, different coils would be required for different line voltages. In order to minimize these difficulties, the coil is designed for a low voltage and wound with heavier wire. A resistor *R* is connected in series with it. This type of starter does not provide the *no-field* (field failure) protection available in the 3-terminal starter. When needed, this protection may be provided by other means, such as a field relay. This starter does provide *low-voltage protection*, as the arm will be returned to the *off* position upon failure of line voltage.

It should be noted that the terminal marked $L_1$ is connected internally to the arm of the starter and externally to only 1 of the lines. The terminal $L_2$ is connected internally through the resistor *R* to 1 end of the holding magnet coil, and externally to the other line, to which is connected also 1 side of the armature and the field coils of the motor. Since the terminal $L_1$ carries a large current, and $L_2$ only a small current, the former usually will be larger in size than the latter. These designations $L_1$ and $L_2$, in the order suggested, are the accepted designations. This type of starter is more universal in application, where manual starters are suitable, than the 3-terminal

starter, as it may be used on any type of d-c motor; whereas the 3-terminal starter is not adapted for series motors, or for variable-speed shunt motors. Fig. 13–3 shows the appearance of a 4-terminal starter for a 5-hp motor. It is common practice to enclose the front of the panel, in order to protect it and the operator. Both types of starters just described have *low-voltage* protection, provided by the holding magnet. Overload protection may be provided by line fuses or a series relay, the coil of which carries the motor line current, and the contacts of which are in series with the holding coil and normally are closed. Currents greater than the setting of the relay open these contacts, releasing the arm which returns to the *off* position. This relay action may be provided by a *thermal-type* relay. The contacts of this overload relay may be connected directly across the terminals of the holding coil and normally are open, but closed when sufficient overload current flows, thus short-circuiting the holding coil. In fact, any protective feature may be incorporated to cut out the holding coil when some undesirable operating condition of the motor occurs.

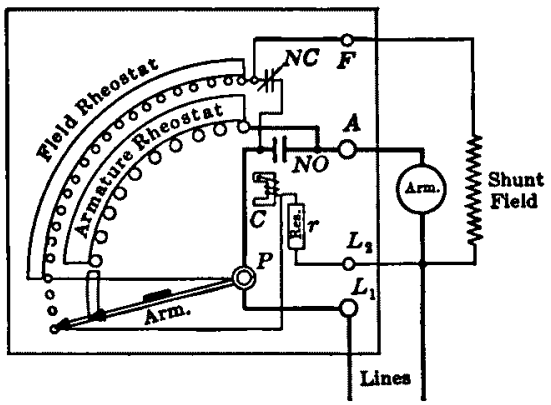


FIG. 13–5a. Schematic diagram for manual-type face plate starter and speed regulator for shunt or compound d-c motors.

*Adjustable speed features*, by means of shunt field control, may be incorporated in the 4-terminal starter, as shown in Fig. 13–5a. The arm rotating about $P$ is made to move over 2 sets of contact buttons: the outer one provides field current control and the inner one is for starting. The contacts $NC$ normally are closed (with the starting arm in *off* position), and are opened by the starting arm as it reaches the full *on* position. Contacts $NC$ being closed except when the lever is in running position provide *full field* for starting. The contacts $NO$ are open until closed by the arm reaching the full *on* position. This is accomplished, as shown in Fig. 13–5b, by the arm engaging the lever shown at the right. This lever then is held in the *running* position by the holding coil $C$. The arm now may be moved back over the outer row of contacts, thus inserting resistance in the shunt field circuit, and increasing the speed. The resistor $r$ (Fig. 13–5a) is connected across the shunt field terminals when the arm is at *off*, thus acting as a field discharge resistor. With the arm in running position, this resistor $r$ is in series with the holding coil $C$. During the starting operation no current flows in coil $C$ until the arm reaches the final or operating position *on*. This type of controller provides only for an increase of speed above the base speed. If desired, provision may be made for the starting resistor to be used to reduce the speed, by inserting it in series with the armature. In this case the resistor units are designed for continuous operation.

The design of the starting rheostat must fit the starting-duty cycle required by the motor, and normally starters of the face-plate type are designed to start the motor when the starting torque is not greater than 150% of full-load torque and the time required to attain full speed not greater than 30 seconds. If more severe starting-duty cycles are necessary, the manufacturer of the starter should be consulted. For further information on the question of ratings refer to N.E.M.A. Industrial Control Standards.

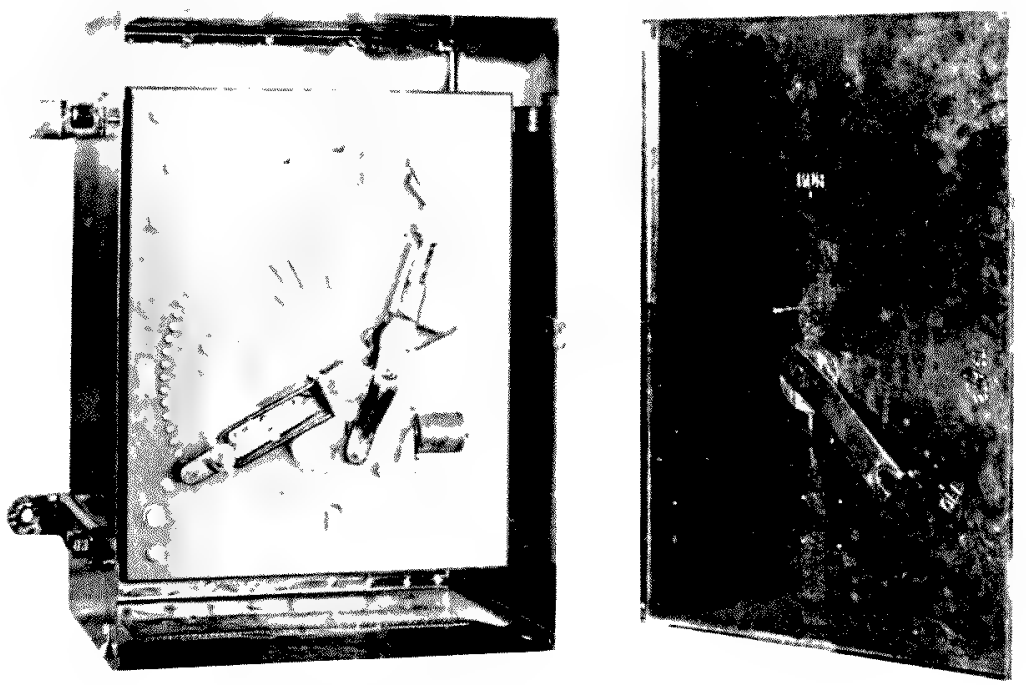

FIG. 13–5b. Starting and field-regulating rheostat for d-c shunt and compound motors.

(c) *Drum-Type Starter.* For certain types of starting and control duty, where speed control is required, where starting and operating cycles are repeated at short intervals, where large currents are commutated, and where reversing and breaking service is required, *the drum type of manual control* is more suitable than the face-plate type just described. The essential features of the simple drum-type switch or controller are shown in Fig. 13–6. The moving contacts consist of copper segments or discs of various arc lengths assembled on a central vertical steel shaft, but insulated from it and from each other. One of these is shown in Fig. 13–6a. At the top of the shaft is keyed an operating handle, and just beneath this handle usually is placed a notched or star wheel. A stationary roller is forced into these notches by a suitable spring to insure that the handle will be stopped in the proper position to make the internal contacts. Suitable bearings are provided at the top and bottom ends of the shaft, to maintain alignment and provide proper operation. Stationary contact fingers (Fig. 13–6a) are arranged to contact

with the rotating segments for whatever position is required. These fingers are insulated from each other, and are connected to the motor, lines, or starting resistors in order to complete the proper sequence of electrical connection as the shaft is rotated. The stationary fingers are assembled over a supporting shaft, insulated from it and from each other, and are

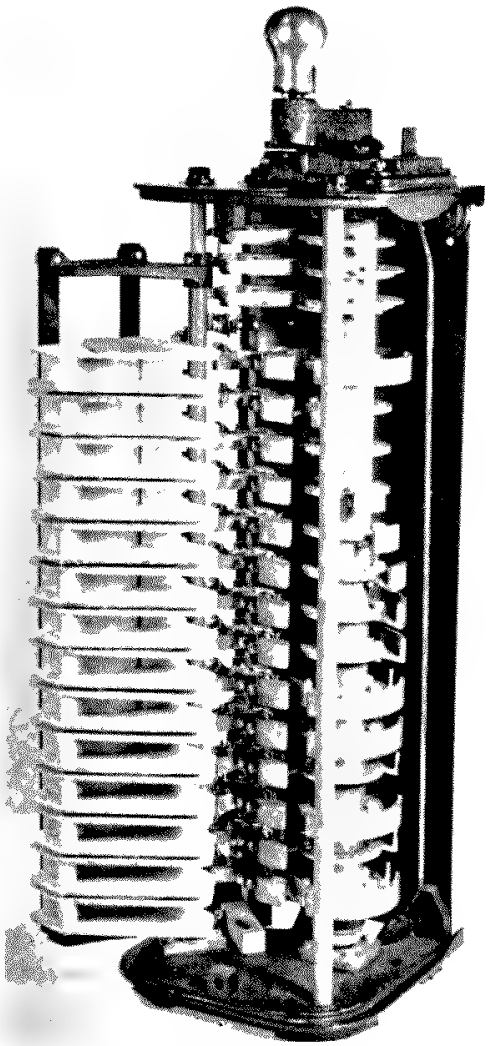

FIG. 13–6. Drum-type switch for a d-c motor starter.

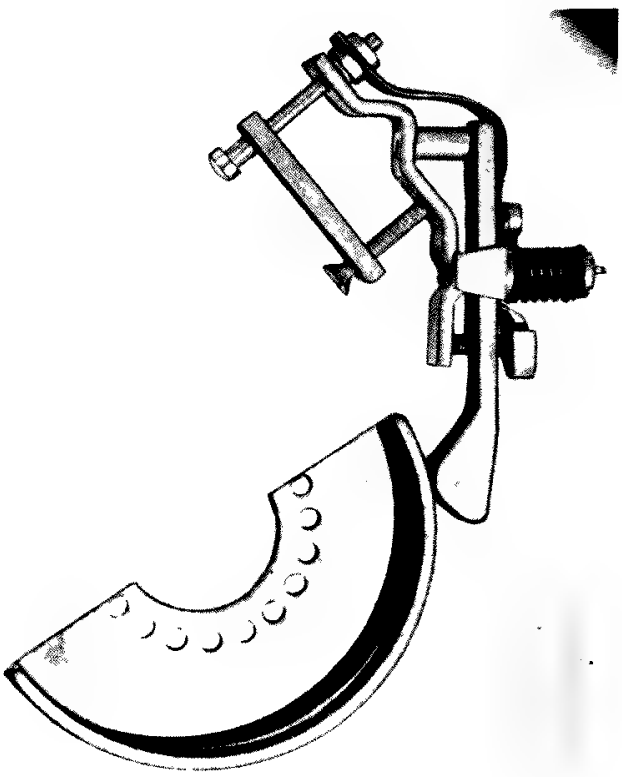

FIG. 13–6a. Contact finger and rotating segment of a drum-type switch.

pressed into contact with the moving segments by adjustable springs. All wiring is done to these fingers, and no wires connect to the rotating drum. Thus, upon the rotation of the vertical shaft, one or more of the stationary fingers are connected electrically together, in this way closing circuits to the motor and control resistors. The *off* position of the operating handle usually is in the center of the arc of rotation, and forward control is on one side of *off* and reverse on the other side. In addition to starting duty, this type of controller may be used for speed control through armature resistance, provided

the starting resistors are designed properly for continuous operation. Speed control through field resistance also may be provided for shunt or compound motors.

To prevent arc-over between adjacent segments or fingers, insulating barriers usually are provided as shown in Fig. 13–6. Also, to reduce arcing when the contacts separate, magnetic blow-out coils are provided as shown in Fig. 13–7.

Instead of using contacts between stationary fingers and rotating segments, a cam-type drum controller may be used for more severe operation. In this type (Fig. 13–8) cams are mounted on the rotating shaft, insulated from the

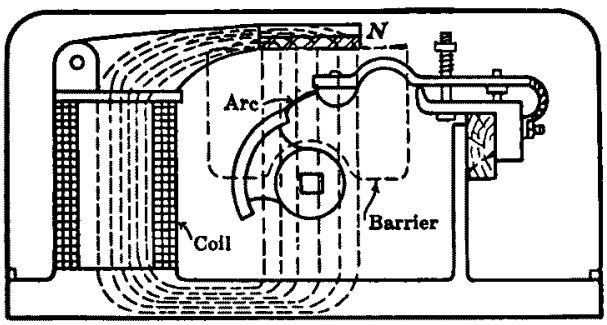


FIG. 13–7. Magnetic blow-out coil for drum-type switch.

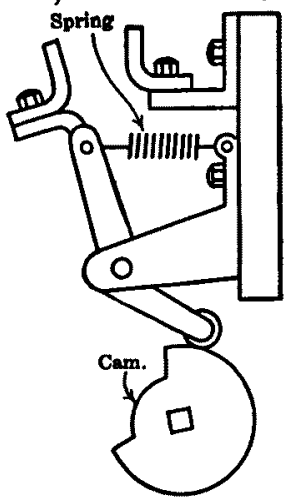


FIG. 13–8. Cam-type drum switch for d-c drum-type controller.

shaft and from each other. When the high portion of the cam engages the rollers of the movable contact assembly, the contacts are forced open. When the depressed section is beneath the roller, the spring closes the contacts. In some designs the operation takes place in reverse fashion, the spring opening the contacts. The cam type is much quicker and more positive in closing and opening the contacts and therefore is preferred for large currents or where operation is continuous. Also the blow-out feature is applied here more readily.

Fig. 13–9 is a schematic connection diagram of a reversing, cam-type drum controller applied to a cumulative compound motor. A main line contactor *M* with its operating coil *Mc* controlled through a push-button station is provided. Overload protection is provided by the thermal element *OL* which, when overloaded, opens the normally closed contact *q*; this in turn opens the circuit of the operating coil *Mc* and shuts down the motor. The auxiliary contacts *k* at the top of the drum switch are closed when the handle is in the *off* position, but open in all other positions. Thus the contacts *M* cannot close unless the starting handle is placed in the *off* position. This prevents the closing of *M* when the motor is not running, with the handle

in any operating position except *off*. The contacts *a* to *h* are operated by moving the handle of the controller. These contacts are open when the handle is in the *off* position, and closed for the positions marked *X*. At the right are shown the magnetic blow-out coils *B*.

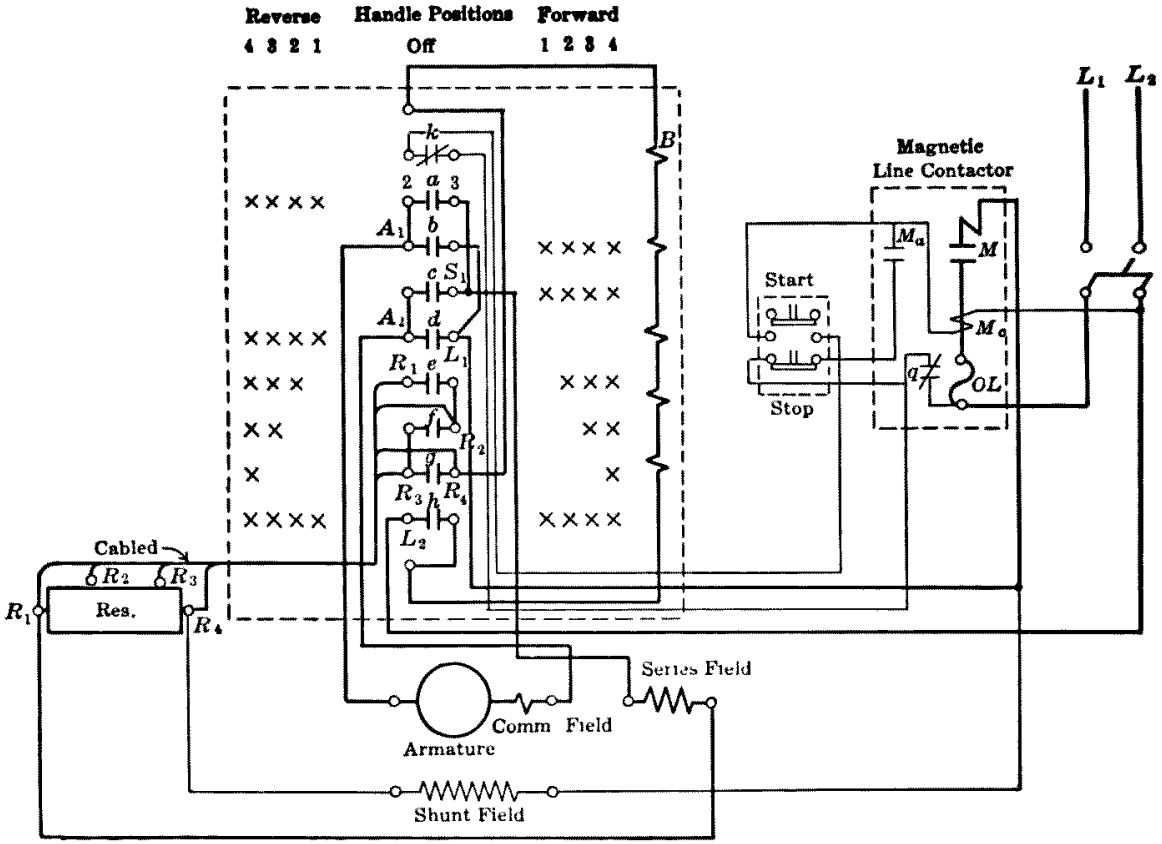


FIG. 13–9. Schematic diagram for drum-type starter and reversing controller for d-c motors.

To close the contactor *M*, the starting handle must be placed in *off* position. When the *start* button is pressed, the line voltage is applied to operating coil *Mc*, closing main contacts *M* and also the normally open auxiliary contacts *Ma*. These contacts *Ma* are in parallel with the starting-button contacts and thus maintain the current in coil *Mc* when the start button is released, and also when contacts *k* open, due to the operation of the controller. Full shunt field current is provided as soon as the contacts *M* close, but no armature current flows until the operating handle is moved to position 1 in either forward or reverse. Moving the operating handle first to forward position, armature current flows through all of the starting resistor points $R_1$ to $R_4$. Moving the operating handle to position 2 closes contacts *e*, shorting out section $R_1R_2$ of the starting resistor. On the last position, 4, the entire starting resistor is shorted out and the motor operates at full line voltage.

When the starting handle is turned to the first position in reverse, the same condition prevails as before, except that armature current flows in a

reverse direction and the motor rotates in reverse direction. To stop the motor either the controller handle may be returned to *off* or the *stop* button pushed. In any case the handle must be returned to *off* before the motor can be started again.

The advantages of the drum-type controller over the face-plate type are:

(1) Better mechanical construction, and easier maintenance under severe service conditions.

(2) Good contact pressure easily provided by spring action.

(3) Entire structure easy to enclose.

(4) Blow-out magnets and arc barriers easily applied.

(5) Lends itself to more complicated control operation. The drum type is used almost exclusively for crane and hoist control, and for machine-tool control, when manual operation is applied.

**13–3. Automatic Starters for D-c Motors.** The operation of the starters described in the foregoing is manual, except for the line contactor described in connection with the drum controller. Cutting out the starting resistor in steps may be done *automatically instead of manually*. In this connection the word *automatic* means *self-acting*, operating by its own mechanism when actuated or "signalled" to by some impersonal influence, as for example, by a change in current strength, variation in voltage, passage of time. In this case the operator merely presses a start, stop, reverse, or other push button, and the functions of starting and control are taken over entirely by automatic means. The actuating mechanism of an automatic controller is usually the electromagnetic contactor. Before reading further, it is advisable to study the list of symbols, Fig. 13–16, and the definitions in Art. 13–4.

The important parts of any automatic starter are: The magnetic contactors used to make connections to the line and to cut out starting resistors; the various auxiliary electrical and mechanical interlocks and relays associated with the contactor; the control switches or push buttons; and the units of starting resistors. If control features other than starting are provided, there will be the necessary rheostats and switches to operate these features. Various relays, such as overload relays, are usually integral parts of automatic starters.

A most important part of any automatic starter or controller is the *magnetic contactor*. A contactor, as defined by N.E.M.A. is a device for repeatedly establishing and interrupting an electric power circuit; and a magnetic contactor is one actuated by electromagnetic means. Fig. 13–10 shows a 300-ampere d-c contactor with arcing terminals, main contacts, blow-out coil, operating coil, and with half of the arc chute removed.

In the automatic starter the starting resistors are cut out by contactors called *accelerating contactors*, the operating coils of which are controlled according to the accelerating method chosen. The three common methods are: (1) *definite-time limit*, (2) *counter-emf acceleration*, and (3) *current-limit*

*acceleration*. As suggested by their names, in the definite-time-acceleration method, the resistors are cut out in sequence, at the end of definite time intervals, regardless of the motor speed, current, or load; in the counter-emf method, the operating coils of each accelerating contactor are connected across the armature terminals, and adjusted to close in succession as the counter-emf rises; in the current-limit method the accelerating contactors operate in sequence, in direct response to the variation in armature current. Each method has certain advantages as well as limitations. The most common industrial method now in use is time limit, although in some small d-c motors counter-emf is used. Sometimes a combination of time and current limit is applied. The time limit method is equally suitable for both a-c and d-c motors of all types. In order to understand the operation of the automatic acceleration methods and the diagrams which have been developed to illustrate them, the operation of a simple counter-emf type and a time-limit type will be described in detail.

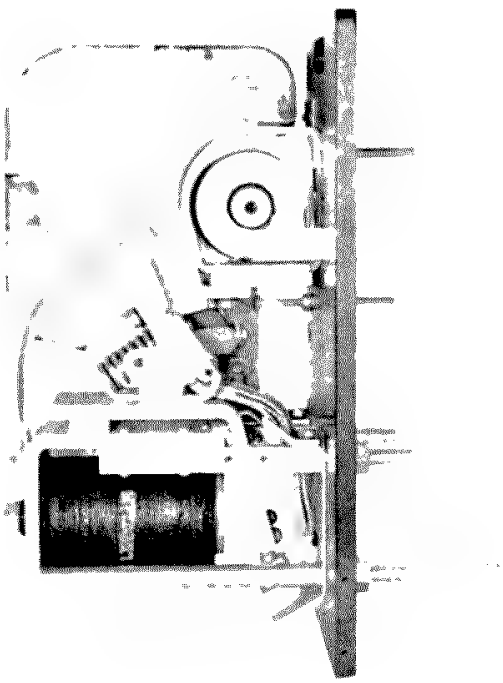

FIG. 13–10. Magnetic d-c contactor.

(a) *Counter-Emf Type*. The diagram and description of this automatic starter is quite standardized, and is in accordance with N.E.M.A. and A.S.A. Referring to Fig. 13–11, the line terminals are 17 and 18. $M_1$ is the normally open line contactor, its operating coil being marked (M) shown at 13. Mechanically associated with the operating mechanism of *M* are the auxiliary or normally open control contacts *Ma*, marked 11 and 16. The accelerating contactors are 1*A* and 2*A*, marked 4 and 5, they are operated by coils (1A) and (2A) , marked 9 and 10.

To start the motor, the *start* button 15 is pressed momentarily. Current then flows in coil (M) and this closes the main line contactor *M* and connects the shunt field directly across the line. At the same time the armature is connected to the line, through the starting resistor. When *M* closes, the 2 associated control contacts *Ma* close. Control contact 16 shunts the *start* button contacts 15, and the *start* button may be released. Closing of control contacts *Ma* (11), connects the coils of the accelerating contactors 1*A* and 2*A* across the armature. Coil (1A) usually is set to close at about 50% line voltage, and coil (2A) at about 80%. As the motor accelerates, the voltage across coil (1A) soon rises to the value required

to operate it, and as contacts 1*A* close, part of the starting resistor is shorted out, and the armature current rises. Further acceleration eventually raises the voltage across coil (2A) to its closing value. Contactor 2*A* then closes, cutting out the remaining part of the starting resistor. The motor now operates at full line voltage. In case of overload, the thermal element *OL* opens control contacts *OL* (12), which in turn open main contactor coil (M) (13), and shut down the motor.

To stop the motor, the *stop* button 14 is pressed momentarily. This opens the line contactor *M* and with it the control contacts *Ma*, marked 16 and 11, also open, before the motor has stopped, thus preventing the application of full voltage across the armature, except by going through the normal starting cycle. Also with control contact *Ma* (16) open, the circuit through operating coil (M) (13) is open, when the *stop* button is released.

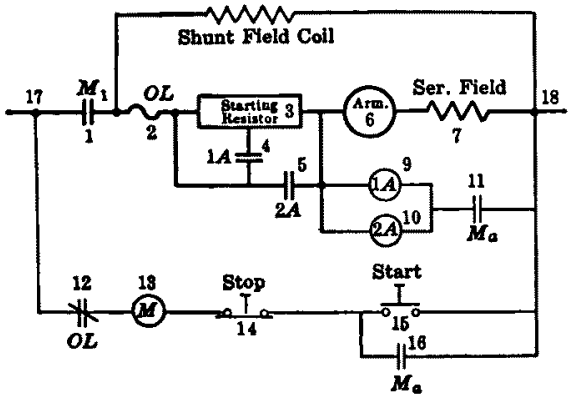


FIG. 13–11. Schematic diagram of a counter-emf starter for a d-c motor.

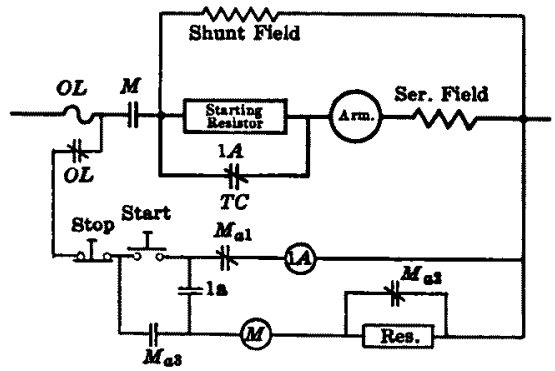


FIG. 13–12. Schematic diagram of a definite-time starter for a d-c motor.

The counter-emf starter is quite simple in construction, but is not very adaptable to more than 2 or 3 starting steps or for large motors. It is limited usually to motors of less than 10 hp. Also it is not very reliable when the line voltage fluctuates widely. Furthermore, large contactors are too sluggish on a rising applied voltage, and the contacts may close so slowly and with such light pressure that they will weld together. The method is well adapted to small motors starting under light load. If the load is too heavy, the motor may never accelerate high enough to produce enough voltage to operate the first accelerating contactor. In this case the starting resistor may burn out.

(b) *Definite-Time Starter.* Fig. 13–12 shows the schematic connections for a definite-time starter, with 1 step of starting resistance. Fig. 13–13 shows the appearance of one type of such a starter. The accelerating contactor 1*A* is spring-closed, and magnetically opened by the coil (1A). After being opened, by closing of the circuit through coil (1A), the subsequent closing by spring action is time-controlled, through control of the decay of flux in the magnetic circuit of the contactor 1*A*. In Fig. 13–13 the contactor

at the left is the accelerating contactor, and the main contactor *M* is shown in the center.

It is to be noted that the accelerating contactor 1*A* is normally closed, except when coil (1A) is energized; the line contactor *M* is operated by coil (M) and it has the two normally closed control contacts *Ma*1 and *Ma*2, together with the normally open contact *Ma*3 mechanically associated with it; the accelerating contactor 1*A* has the normally open control contact 1*Aa* mechanically associated with it; the thermal overload device *OL* has normally closed contacts in series with the control circuits.

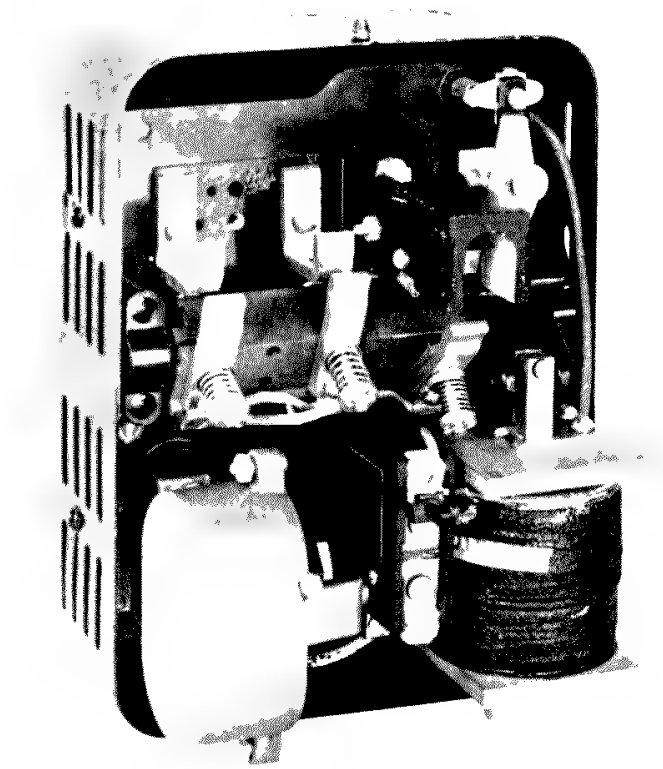

FIG. 13–13. Magnetic definite-time starter of mechanical escapement type with 3 accelerating points.

To start, press the *start* button momentarily. This first energizes the accelerating contactor coil (1A) and opens contacts 1*A*, removing the short around the starting resistor. This action also closes control contact 1*Aa*, which in turn completes the circuit for main contactor coil (M) and closes contacts *M*. This in turn closes contact *Ma*3 maintaining circuit through (M) when *start* button is released; it also opens contact *Ma*2, inserting holding resistance in series with (M), thus cutting down its current (this feature is often omitted, then the coil (M) operates at full line voltage); it also opens contact *Ma*1 by removing current from coil (1A) and allowing the time closing contacts 1*A* to close at the end of the time intervals for which the action is adjusted. This puts the motor directly across the line. An over-

load causes the contacts *OL* to open and shut down the motor. To stop the motor, the *stop* button is pressed momentarily, opening line contactor *M* and shutting down the motor. As many steps of starting resistor may be provided as conditions require. These are cut out in sequence by time-controlled contactors, as discussed in the foregoing.

This method of starting is generally adaptable for use with all types and sizes of both d-c and a-c motors. The number of interlocked control contacts increases materially with the number of starting steps, but their adjustment is not critical or difficult. This starter will always cut out starting steps, whether or not the acceleration of the motor responds. In this way it makes the motor do its utmost to start the load. The current peaks may be large if the motor starts under an excessive load, but a correspondingly large torque is produced. The motor protective device must take care of overload conditions. If the rotor becomes locked, the overload device must protect the motor, since the starter offers no protection. Since the accelerating time is fixed, several operations requiring sequence of operation may be accomplished by an operator. This type of starter does not require readjustment of timing because of change in motor loading, in order for the starter to function satisfactorily. It is generally the most economical in the use of power, during acceleration, and at present is the most widely used of all accelerating means. Several devices have been developed to produce the time element in the closing of the accelerating contactors. They are: (1) mechanical escapement similar to a clock escapement mechanism, in which the time is adjustable by adjusting the length of a pendulum; (2) dashpot time delay; (3) motor-driven mechanism on large starters; (4) magnetic delay. In the smaller and medium-size starters the most common methods are (1) and (4) with some use of (2).

Fig. 13–13 shows a time starter, with 3 accelerating points, operated by solenoid-type multifinger contactor, controlled by a mechanical escapement. The line contacts at the right of the center have a magnetic blow-out coil, and an arc chute to interrupt the arc quickly. Energizing the solenoid coil causes the plunger to rise, setting in rotary motion the shaft on which the fingers are mounted and instantly closing the main line contact at the right, thus inserting all the starting resistance and providing full field. The further motion of the shaft is restrained or *timed* by the escapement device. The other contacts then close in timed sequence, until the starting resistor is completely cut out. The time required for starting is adjustable, up to 10 seconds, by changing the length of pendulum on the escapement mechanism enclosed in the case at the lower left. The thermal-overload device is shown in the lower center.

Fig. 13–14 shows a definite-time starter of the *magnetic flux-delay type.* The accelerating contactor shown at the lower left has its action controlled by the delayed decay of flux. The operation of the starter is explained in connection with Fig. 13–12. Definite-time starters are in some cases controlled

or timed by a small motor, which governs the sequence of closing of the contactors. These are used usually in the larger size motors, when very accurate timing is required.

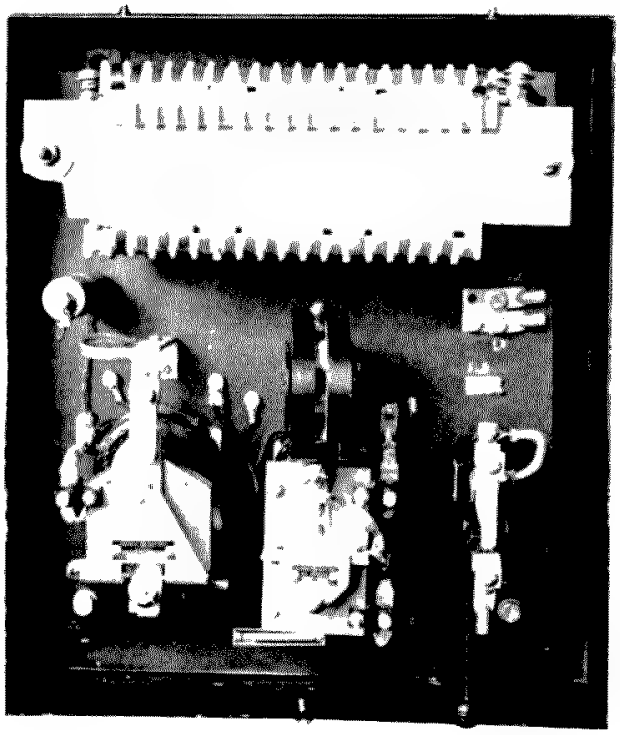

FIG. 13–14. Magnetic definite-time starter of the flux-delay type.

(c) *Dynamic Braking Controller.* Many motor applications require control of stopping time as well as of starting time. In this case *dynamic braking*, *regenerative braking*, or *mechanical braking may be used.* In hoisting applications a mechanical holding brake is always required, and in addition dynamic or regenerative braking may be used. In dynamic braking the energy stored in the inertia of the rotating parts of motor and load is dissipated by allowing the motor to operate as a generator, and absorbing the energy in a resistor load. If the energy if fed back into the supply line, it is called *regenerative braking.* Fig. 13–15 shows the schematic connections for a time starter, equipped for dynamic braking. The following points are to be noted: The spring-closed accelerating contactor *A* has normally open control contacts

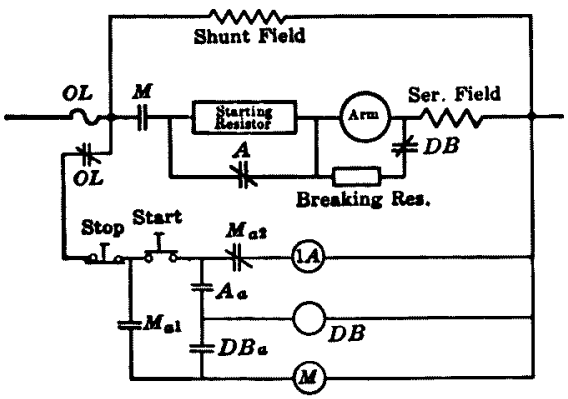


FIG. 13–15. Schematic diagram of a definite-time starter with dynamic braking.

*Aa* associated with it; dynamic-braking contactor *DB* has normally open control contacts *DBa*; the main line contactor *M* has normally open control contacts *Ma*1 and normally closed contacts *Ma*2; the operating coils are shown as (1A), (DB), and (M). Dynamic-braking contactor *DB* is spring-closed and is opened by the magnetic action of coil (DB).

To start the motor the *start* button is pressed momentarily. This first energizes coil (1A), then opens contacts *A* and removes the short from starting resistor. Control contacts *Aa* close. This energizes coil (DB) and opens contacts *DB* to disconnect the braking resistor. Control contacts *DBa* on the contactor *DB* now close. This energizes coil (M) and closes line contactor *M* and along with it the control contacts *Ma*1, and opens contacts *Ma*2. Current now flows to the motor through the starting resistor. Coil (1A) being now open, the contacts *A* are closed by a spring at the end of the time limit. This shorts out the starting resistor and opens control contacts *Aa*. Since control contacts *Ma*1 and *DBa* are closed, current is maintained in coils (DB) and (M), keeping contacts *DB* open and *M* closed, while the *start* button contacts and contacts *Aa* are open.

To stop, the *stop* button is pressed momentarily. This de-energizes coils (M) and (DB), opening contacts *M* while contacts *DB* are spring closed. This action disconnects the motor from the line and connects the braking resistor across the armature, and the motor decelerates due to the loading action of the braking resistor.

There are many electronic controls now available for use with d-c motors. For further detailed information on starters and controls, references E will be helpful.

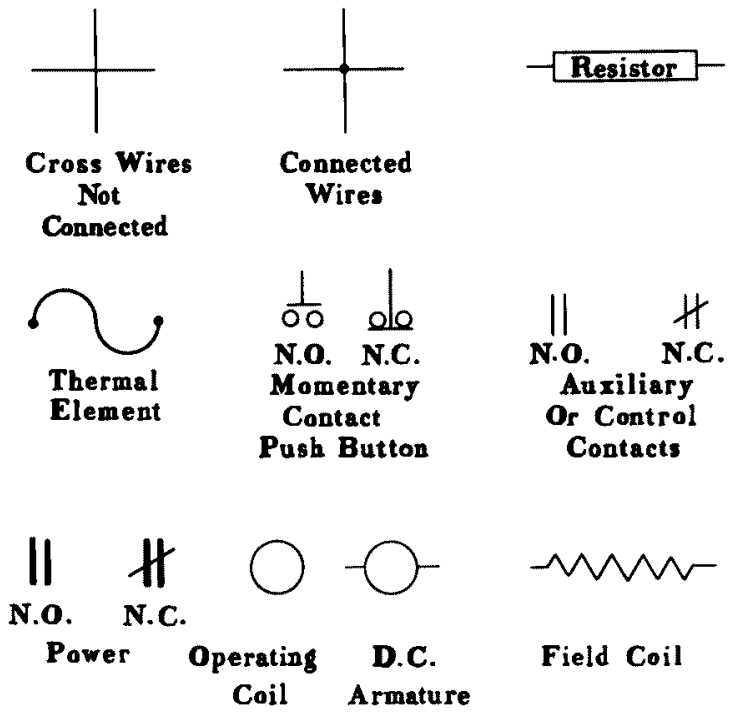


FIG. 13–16. Symbols and designations.

## 13–4. Definitions.

1. *Undervoltage Protection.* The effect of a device operative on the reduction or failure of voltage to cause and maintain the interruption of power to the main circuit. (N.E.M.A. IC50–230.)

2. *Undervoltage Release.* The effect of a device operative on the reduction or failure of voltage to cause the interruption of power to the main circuit but not to prevent the re-establishment of the main circuit on return of voltage. (IC50–232).

3. *Phase-Failure Protection.* The effect of a device operative upon the failure of power in one wire of a polyphase circuit, to cause and maintain the interruption of power in all the wires of the circuit. (IC50–234.)

4. *Phase-Reversal Protection.* The effect of a device operative on the reversal of the phase-rotation in a polyphase circuit, to cause and maintain the interruption of power in all the wires of the circuit. (IC50–236.)

5. *Overload Protection.* The effect of a device operative on excessive current, but not necessarily on short-circuit, to cause and maintain the interruption of current flow to the device governed.

NOTE: By operating overload is meant a current not in excess of 4 times the rated current for a-c motors, nor in excess of 4 times the rated current for d-c motors. (IC50–238.)

6. *Resistor.* A device used primarily because it possesses the property of electrical resistance. A resistor as used in electric circuits for purposes of operation, protection or control, commonly consists of an aggregation of units. (IC50–248.)

7. *Constant Torque Resistor.* A resistor for use in the armature or rotor circuit of a motor in which the current remains practically constant throughout the entire speed range. (IC50–254.)

8. *Fan Duty Resistor.* A resistor for use in the armature or rotor circuit of a motor in which the current is approximately proportional to the speed of the motor. (IC50–256.)

9. *Relay.* A device that is operative by a variation in the conditions of one electric circuit to effect the operation of other devices in the same or another electric circuit.

NOTE: Where relays operate in response to changes in more than one condition, all functions should be mentioned. (IC50–275.)

10. *Notching.* A qualifying term indicating that a predetermined number of separate impulses are required to complete operation. (IC50–300.)

11. *Inverse Time.* A qualifying term indicating that there is purposely introduced a delayed action, which delay decreases as the operating force increases. (IC50–302.)

12. *Definite Time.* A qualifying term indicating that there is purposely introduced a delay in action, which delay remains substantially constant regardless of the magnitude of the quantity that causes the action. (IC50–304.)

13. *Instantaneous.* A qualifying term indicating that no delay is purposely introduced in the action of the device. (IC50–306.)

14. *Magnetic Contactor.* A contactor actuated by electromagnetic means. (IC50–322.)

15. *Electric Controller.* A device, or group of devices, which serves to govern,

in some predetermined manner, the electric power delivered to the apparatus to which it is connected. (IC50–324.)

**16.** *Manual Controller.* A controller operated by hand. (IC50–332.)

**17.** *Drum Controller.* A controller which utilizes a drum switch as the main switching element.

NOTE: A drum controller usually consists of a drum switch and a resistor. (IC50–334.)

**18.** *Starter.* A controller designed for accelerating a motor to normal speed in one direction of rotation.

NOTE: A device designed for starting a motor in either direction of rotation includes the additional function of reversing and should be designated a controller.

NOTE: By basic functions is usually meant acceleration, retardation, line closing, reversing, etc. (IC50–336.)

**19.** *Automatic.* Automatic means self-acting, operating by its own mechanism when actuated by some impersonal influence, as, for example, a change in current strength; not manual, without personal intervention. Remote control that requires personal intervention in not automatic, but manual. (IC50–338.)

**20.** *Automatic Starter.* A starter designed to control automatically the acceleration of a motor during the acceleration period. (IC50–340.)

**21.** *Autotransformer Starter.* A starter having an autotransformer to furnish a reduced voltage for starting. The device includes the necessary switching mechanism and frequently is called a compensator or autostarter. (IC50–342.)

**22.** *Control Cutout Switch.* A switch that isolates the control circuit of a motor controller. (IC50–344.)

**23.** *Magnet Brake.* A friction brake controlled by electromagnetic means. (IC50–350.)

**24.** *Sealing Gap.* The distance between the armature and center of the core of a magnetic contactor when the contacts first touch each other. (IC50–352.)

**25.** *Sealing Voltage (or Current).* The voltage (or current) necessary to seat the armature of a magnetic contactor from the position at which the contacts first touch each other. (IC50–354.)

**26.** *Pick-Up Voltage (or Current).* The voltage (or current) at which a magnetic contactor starts to close. (IC50–356.)

**27.** *Drop-Out Voltage (or Current).* The voltage (or current) at which a magnetic contactor will release to its de-energized position. (IC50–358.)

**28.** *Normally Open and Normally Closed.* The terms *normally open* and *normally closed* when applied to a magnet-operated switching device, such as a contactor or relay, or to the contacts thereof, signify the position taken when the operating magnet is de-energized. These terms apply only to non-latching types of devices. (IC50–360.)

**29.** *Jogging. Jogging* or *inching* is the quickly repeated closure of the circuit to start a motor from rest for the purpose of accomplishing small movements of the driven machine. (IC50–374.)

# SOME ADVANCED TOPICS ON D-C MACHINES

# *Chapter 14*

# TANGENTIAL FORCES IN THE ELECTRICAL MACHINES

**14–1. Biot-Savart's Law.** In Chap. 4 the tangential force on the armature and the torque was derived on the basis of Biot-Savart's law (Art. 1–4)

$$F = \text{const} \times BlI$$

where $I$ is the current of a conductor lying *within* the $B$-flux. Accordingly, it was assumed for the derivations of Chap. 4 that the armature conductors lie *directly within the gap flux.* In reality this is not the case. The armature conductors are placed in slots, i.e., they are moved away from the gap and, therefore, lie in a flux the density of which is much smaller than that in the gap. If the tangential force of the machine were calculated with the *actual* value of $B$ in which the conductors lie, a much smaller force would be obtained than that measured by tests.

In Art. 1–5 the electromagnetic power of a machine was derived from Biot-Savart's law. Vice versa, Biot-Savart's law can be derived from the electromagnetic field energy. This law and the derivations made in Chap. 4 are correct and are in agreement with tests. Thus, Biot-Savart's law, applied under the assumption that the conductors lie within the gap flux and that the forces are exerted on the conductors themselves, yields accurate results, but in reality the forces are exerted not upon the conductors. It follows from this, that there must be *another kind of mutual influence* between the $B$-flux in the gap and the conductors carrying the current $I$, i.e., the two elements of Biot-Savart's law, which accounts for the tangential force of the electrical machine. This other combination effect of $B$ and $I$ can be found by applying Faraday-Maxwell's conception of the stresses in the magnetic field. This yields the result that the tangential forces are exerted upon the teeth.

**14–2. Stresses in the Magnetic Field.** Faraday-Maxwell's conception of the forces in the electromagnetic field is based upon the idea that a stress exists along the lines of force which tends to make them shorter and that this shortening produces a lateral force across the lines of force which makes them wider. On the basis of the fundamental laws, Maxwell determined the magnitudes of the stress and the lateral force. Both forces have the same

magnitude and this is equal to the field energy per unit volume, i.e., in the magnetic field, the forces are

$$f = \tfrac{1}{2}BH = \tfrac{1}{2}\mu_0\mu H^2 \tag{14–1}$$

This value of $f$ is the stress per unit surface (*perpendicular* to the lines of force) and also the lateral force per unit surface (*parallel* to the lines of force).

The validity of Eq. 14–1 with respect to the stress will be proved by an example of a toroidal iron core with a small cross section $c$ and with the length of the lines of force $l$. The ampere turns around the core are $NI$, the current $I$ being constant. Applying Ampère's law

$$\int_0 H_l \, dl = NI,$$

which can be written

$$Hl = NI \quad \text{or} \quad H = \frac{NI}{l} \tag{14–2}$$

the flux density becomes

$$B = \frac{\mu_0\mu}{l} NI \tag{14–3}$$

The flux in the core is

$$\Phi = Bc$$

and the flux interlinkages per unit current, i.e., the coefficient of self-inductance,

$$L = \frac{N\Phi}{I} = N^2 \frac{\mu_0\mu}{l} c \tag{14–4}$$

Kirchhoff's mesh equation of the electric circuit is here

$$v - L\frac{di}{dt} = ir$$

Multiplying by $idt$ and rearranging, we have

$$vidt - ri^2dt = Lidi = d(\tfrac{1}{2}Li)$$

The right term of this equation is the excess of energy supplied by the source over the heat loss in the resistance $r$, i.e., the right term is the change of the magnetic energy of the core during the time $dt$. Since constant d-c current $I$ is assumed, magnetic energy is supplied to the core only during the period in which the current rises from the value 0 to the value $I$. At the end of this period the magnetic energy is $\frac{1}{2}LI^2$. Thus the magnetic energy of the core is

$$E_m = \tfrac{1}{2}LI^2$$

The energy per element $dl$ of the core is

$$dE_m = \tfrac{1}{2}I^2 \frac{\partial L}{\partial l} dl$$

If $f$ is the stress along the lines of force, then the work corresponding to this stress along the distance $dl$ in the direction of the lines of force is $fdl$ and this work must be equal to $dE_m$ (Compare this with a stretched spring: the work put in to stretch the spring appears as potential energy of the spring.) Thus

$$fdl = dE_m = \tfrac{1}{2} I^2 \frac{\partial L}{\partial l} dl$$

or, with Eq. 14–4,

$$f = -\tfrac{1}{2} N^2 \frac{\mu_0 \mu}{l^2} c \tag{14–5}$$

The minus sign indicates that the force is opposite to the direction of the lines of force, i.e., that the force tends to shorten the lines of force.

Inserting into Eq. 14–5, Eqs. 14–2, and 14–3, the force becomes

$$f = -\tfrac{1}{2} BHc$$

or per unit cross-sectional area

$$f = -\tfrac{1}{2} BH \tag{14–6}$$

This is the same as Eq. 14–1.

**14–3. Forces at the Boundary Surface Between Air and Iron.** Consider Fig. 14–1. $dS$ is an element of the boundary surface. The angle between the

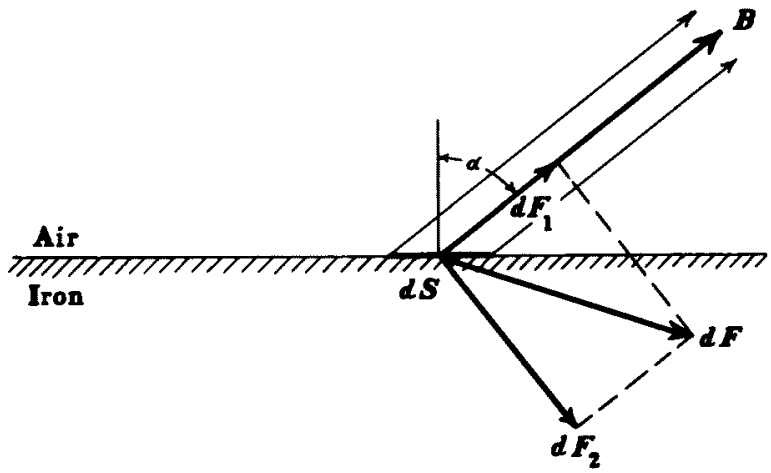


FIG. 14–1. Forces at the boundary surface between air and iron.

lines of force $B$ in the air and the normal to the boundary surface is $\alpha$. Two forces affect the surface element $dS$. One, $dF_1$, is due to the stress along the lines of force; its magnitude is

$$dF_1 = (fds) \times \cos \alpha \tag{14–7}$$

since the perpendicular to the lines of force and the plane of $dS$ are displaced

by the angle $\alpha$. The other force on $dS$, $dF_2$, is due to the lateral force across the lines of force; its magnitude is

$$dF_2 = (fds) \times \sin \alpha \tag{14–8}$$

The resultant of these two forces is $dF$. The tangential (to $dS$) component of $dF$, in the direction from the left to the right, is

$$dF_t = dF_1 \cos (90 - \alpha) + dF_2 \cos \alpha = 2fds \cos \alpha \sin \alpha = fdS \sin 2\alpha \tag{14–9}$$

The normal (to $dS$) component of $dF$, in upward direction, is

$$dF_n = dF_1 \cos \alpha - dF_2 \cos (90 - \alpha) = fdS \cos^2 \alpha - fdS \sin^2 \alpha = fdS \cos 2\alpha \tag{14–10}$$

Introducing Eq. 14–1 for $f$ and for $B$ and $H$ their normal and tangential components *in the air*,

$$dF_t = 2 \times \tfrac{1}{2} B \cos \alpha \, H \sin \alpha \, dS = B_n H_t \, dS = \frac{1}{\mu_0} B_n B_t \, dS \tag{14–11}$$

$$dF_n = \tfrac{1}{2} B \cos \alpha \, H \cos \alpha \, dS - \tfrac{1}{2} B \sin \alpha \, H \sin \alpha \, dS = \frac{1}{2\mu_0} (B_n^2 - B_t^2) \, dS \tag{14–12}$$

$dF_t$ and $dF_n$ are the forces in the air. Corresponding forces appear in the iron.

First the normal and tangential components of $B$ in the iron ($B'_n$ and $B'_t$) will be determined. Consider Fig. 14–2. In the medium with the permeability

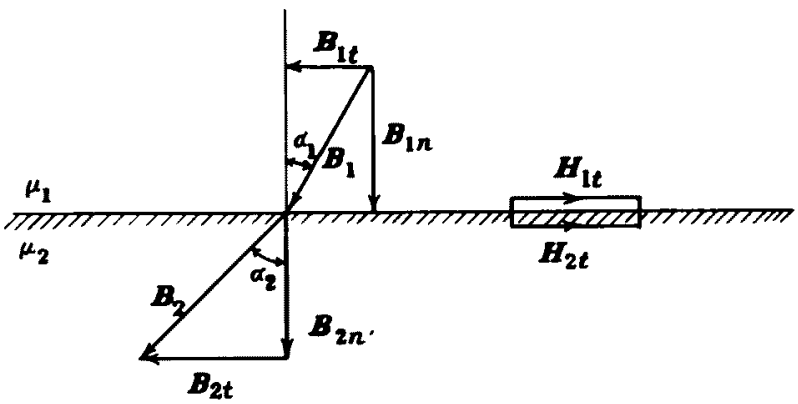


FIG. 14–2. Normal and tangential components of $B$ at a boundary surface between 2 media with different permeabilities.

$\mu_1$, the lines of force make an angle $\alpha_1$ with the vertical to the boundary surface. They enter the medium with the permeability $\mu_2$ under an angle $\alpha_2$ with the vertical to the boundary surface. If $B_1$ is resolved into its normal and tangential components $B_{1n}$ and $B_{1t}$, the normal component $B_{1n}$ represents the flux per unit surface which passes the boundary surface. The same applies to $B_2$. Only its normal component $B_{n2}$ is the flux (per unit surface) which enters the medium with the permeability $\mu_2$. Since there are no magnetic

charges or electric currents present, the ingoing flux must be equal to the outgoing flux, i.e.,

$$B_{1n} = B_{2n} \tag{14–13}$$

Consider again Fig. 14–2 and apply Ampère's law to a closed loop two sides of which lie so close to the boundary surface that the two components $H_t\,dl$ perpendicular to the boundary surface can be neglected. Since no mmf $(NI)$ is present, $\int_0 H_t\,dl = 0$ and the tangential components $H_{1t}$ and $H_{2t}$ must be equal and have the same direction, i.e., at the boundary surface

$$H_{1t} = H_{2t} \tag{14–14}$$

It follows from this equation, with $B_{1t} = \mu_0\mu_1 H_{1t}$ and $B_{2t} = \mu_0\mu_2 H_{2t}$

$$\frac{B_{1t}}{B_{2t}} = \frac{\mu_1}{\mu_2} \tag{14–15}$$

and

$$\frac{\tan\alpha_1}{\tan\alpha_2} = \frac{B_{1t}}{B_{2t}} = \frac{\mu_1}{\mu_2} \tag{14–16}$$

If $\mu_1 = \mu_0$ (air) and $\mu_2 = \mu_0\mu$ large (iron), then $\tan\alpha_1$ becomes small, i.e., the lines of force enter the boundary surface between air and iron almost perpendicular to the surface.

It follows from the Eqs. 14–13 and 14–15 that, for the example considered in Fig. 14–1, the normal and tangential components of $B$ in iron are

$$B'_n = B_n \qquad B'_t = \mu B_t \tag{14–17}$$

Inserting these relations in Eq. 14–11, and introducing in the denominator the permeability of iron $\mu_0\mu$ instead of that of air $\mu_0$, the tangential force on the surface element $dS$ in the iron, from the right to the left, is

$$dF'_t = \frac{1}{\mu_0\mu} B_n \mu B_t\,dS = \frac{1}{\mu_0} B_n B_t\,dS \tag{14–18}$$

This is the same value as that of Eq. 14–11, i.e., the tangential forces on both sides of the boundary surface cancel each other and the force on the surface is always perpendicular to the boundary surface.

Inserting Eq. 14–17 into Eq. 14–12 and introducing in the denominator $\mu_0\mu$ instead of $\mu_0$, the normal component of the force on the iron, in downward direction, is

$$dF'_n = \frac{1}{2\mu_0\mu}(B_n^2 - \mu^2 B_t^2)\,dS \tag{14–19}$$

The total pull on the surface of the iron, in *upward* direction, per unit surface, is

$$f = \frac{dF_n}{dS} - \frac{dF'_n}{dS} = \frac{\mu - 1}{2\mu_0\mu}(B_n^2 + \mu B_t^2) \tag{14–20}$$

where $B_n$ and $B_t$ are the normal and tangential components of $B$ *in the air*. Since the lines of force enter the boundary surface between air and iron almost perpendicular to the surface, $B_t$ is very small and approximately

$$f \approx \frac{\mu - 1}{2\mu_0 \mu} B_n^2 \tag{14–21}$$

**14–4. Forces on the Teeth.** Eq. 14–21 will be used in order to demonstrate the source of the tangential (driving) force in the electric machine. Consider Fig. 14–3. It shows the boundary surface of a north pole and below an open slot with conductors. Fig. 14–3a refers to no-load. The flux in the slot is produced by the field current alone. The flux density at the teeth decreases rapidly from the top to the bottom of the slot. For this flux density the symbol $B_{n0}$ will be used, the subscript 0 indicating no-load. The curve to the left of Fig. 14–3a gives an idea about the magnitude of $B_{n0}$ along the teeth.

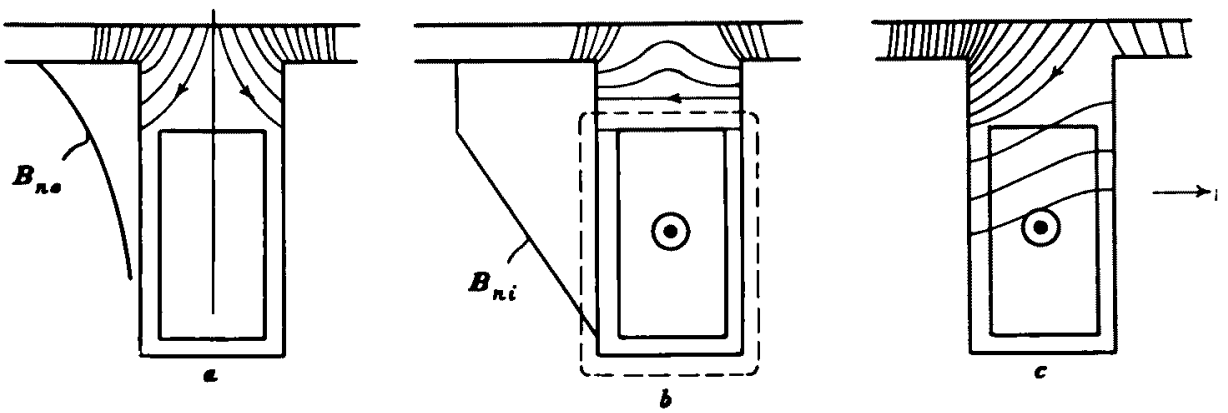


FIG. 14–3. Flux in the slot :
(a) At no-load.
(b) Armature carries current. Field not excited.
(c) At load.

Fig. 14–3b shows the flux produced by the conductors in the slot, when the field is not excited. It is assumed that the current in the conductors is directed towards the observer. The lines of force shown in the slot close themselves through the teeth and core (indicated by a dashed line). Applying Ampère's law to these closed circuits and assuming that the field intensity in the iron is small ($\mu$ high), the flux density in the slot produced by the armature current ($B_{ni}$) increases linearly from the bottom of the conductors to their top and then remains constant up to the armature surface. This is shown to the left of Fig. 14–3b. The flux distribution in the slot at load can be obtained through superposition of the fluxes of Figs. 14–3a and 14–3b. The superposition is permissible because the reluctance of these two fluxes lies mainly in the air. The result obtained is shown in Fig. 14–3c.

Examining the three flux distributions, Figs. 14–3a, 3b, and 3c, with respect to the forces on the teeth, it is seen that at no-load (Fig. 14–3a) or

with the poles not excited (Fig. 14–3b) the pull on the two teeth flanks making the slot cancels out. Contrary to this the pull on the two teeth flanks and the teeth edges is entirely different when the excited machine is loaded (Fig. 14–3c). The pull on the left tooth flank is much larger than on the right tooth flank, i.e., for the assumed polarity of the pole and direction of the armature current, a force, perpendicular to the teeth, drives the armature in clockwise direction. The same direction of the force is obtained by applying Biot-Savart's law (see Art. 1–4).

If $B_{n0}$ is the flux density at the tooth flank at no-load, and $B_{ni}$ the flux density at no excitation, then the flux density at load is $B_{n1}=B_{n0}+B_{ni}$ at the left tooth flank (Fig. 14–3c) and $B_{n2}=B_{n0}-B_{ni}$ at the right tooth flank. Eq. 14–21 yields for the resultant pull, per unit surface,

$$f_{res}=\frac{\mu-1}{2\mu_0\mu}(B_{n1}^2-B_{n2}^2) \tag{14–22}$$

Inserting for $B_{n1}$ and $B_{n2}$ their values, we have

$$f_{res}=\frac{\mu-1}{2\mu_0\mu}(B_{n1}+B_{n2})(B_{n1}-B_{n2})=\frac{\mu-1}{2\mu_0\mu}\times 2B_{n0}\times 2B_{ni} \tag{14–22}$$

In order to find the total pull on the teeth, the latter equation has to be integrated over the tooth height and the result multiplied by the number of teeth. This yields the same force as Biot-Savart's law does. It is evident that the computation of the forces is much simpler on the basis of Biot-Savart's law than on the basis of the magnetic pull on the teeth. The latter method requires exact flux mapping which is a tedious procedure yielding not entirely accurate results.

A flux distribution picture as that of Fig. 14–3c, made for a semi-closed slot, shows large forces on the tooth edges. The flux distribution under load

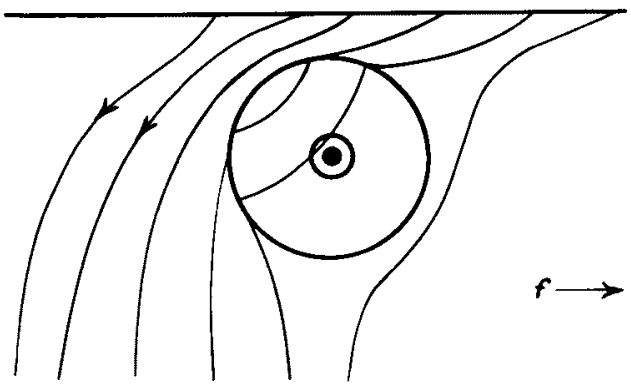


FIG. 14–4. Flux in a closed slot at load.

for a closed slot is shown in Fig. 14–4. Here lines of force penetrate the slot with a slope thus producing the pull on the teeth.

Corresponding to the law "action = reaction", the force which drives the

armature must appear also at the poles but with negative sign. Fig. 14–5 shows the flux distribution at the edges of the pole-shoes of a north pole with the same direction of the armature current as in Fig. 14–3. This flux distribution is due to armature reaction (see Art. 5–4). It is seen from Fig. 14–5 that a pull is produced on the pole shoes in counter-clockwise direction, i.e., in opposite direction to the pull on the armature.

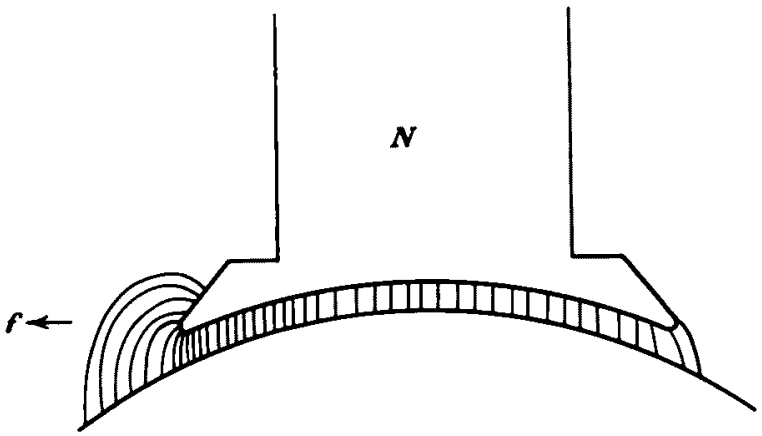


FIG. 14–5. Flux at the pole at load.

If a d-c machine has a compensating winding, the flux distribution is the same at both pole-shoes and the pole pull is exerted on the teeth of the poles. For the same pole polarity, the pull on the pole teeth is opposite to the pull on the armature teeth, because the compensating winding and armature winding carry currents of opposite direction. (See Ref. A6, 7.)

# *Chapter 15*

## LIMITATIONS OF THE WAVE WINDING WITH RESPECT TO THE NUMBER OF WINDING ELEMENTS PER LAYER PER SLOT

If $u$ is the number of winding elements lying side by side in a layer of a slot (in Fig. 3–7, $u=3$; in Fig. 3–8, $u=2$), then

$$K=uQ$$

On the other hand, for the wave winding (Eq. 3–7)

$$K=y\frac{p}{2}\pm\frac{a}{2}$$

Therefore,

$$\frac{Q}{a/2}=\frac{y\frac{p}{a}\pm 1}{u}$$

Since $\frac{Q}{a/2}$ must be an integer (see Eq. 3–9), the value of $u$ cannot be chosen arbitrarily, when $u>1$. The following table gives values of $u$ for different values of $p$ and $a$.

| $p=$ | 4 | 6 | 8 | 10 | 12 | 14 | 16 | 18 | 20 | 24 |
|---|---|---|---|---|---|---|---|---|---|---|
| $a=2$ | 3;5 | 2;4;5 | 3;5 | 2;3;4 | 5 | 2;3;4;5 | 3;5 | 2;4;5 | 3 | 5 |
| $a=4$ | L | (5) | 3;5 | (3) | 2;4;5 | (3;5) | 3;4 | (5) | 3;4 | 5 |
| $a=6$ | — | L | — | — | 3;5 | — | — | 4;5 | — | 3;5 |
| $a=8$ | — | — | L | — | — | — | 3;5 | — | — | 2;4;5 |

A dash — indicates that the winding is not symmetrical; parentheses () indicate that the winding is not entirely symmetrical but can be used. The letter L indicates the cases in which the lap winding should be used.

# *Chapter 16*

## DETERMINATION OF THE NO-LOAD FIELD MMF

It has been explained in Chap. 5 how to determine the ampere-turns on the poles necessary to force a given flux through a given machine structure (given magnetic circuit). Simplifying assumptions were made there for which more accurate methods will be given in this chapter.

It follows from Eq. 5–2 that the cross-sectional areas of the 5 components of the magnetic circuit must be known.

**16–1. Cross-sectional Area of the Gap. Gap Mmf.** This area is determined by a certain arc, $b_e$ (Fig. 16–1), called *effective pole* arc and a certain

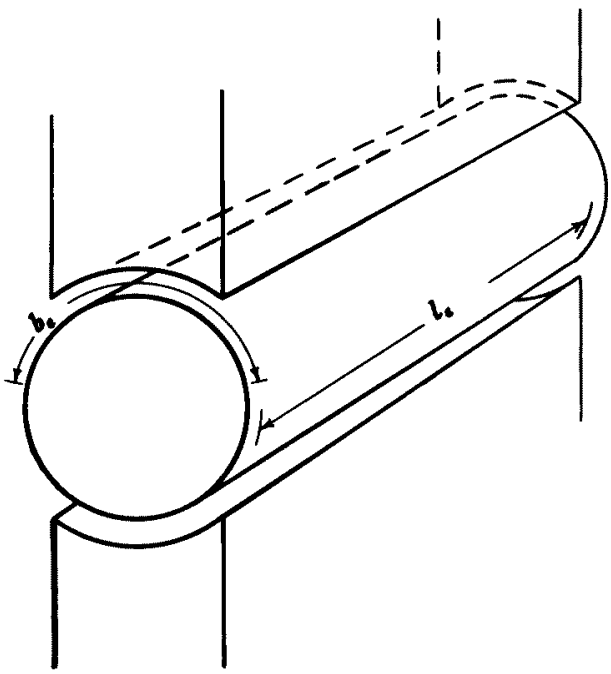


FIG. 16–1. Explanation of effective pole arc and effective armature length.

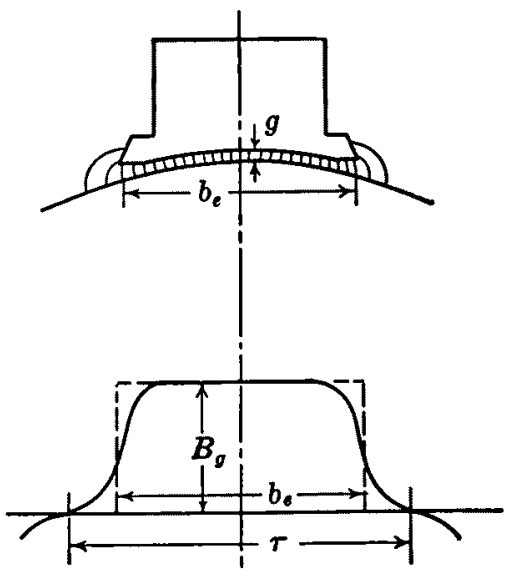


FIG. 16–2. Flux-distribution curve of a d-c machine.

length, $l_e$, called *effective armature length*. The effective pole arc is determined from the flux distribution curve (Fig. 16–2) by defining a width $b_e$ in such a manner that this width times the height of the curve, $B_g$, is equal to the area

of the flux distribution curve. As has been pointed out, the latter area is the armature flux per unit armature length. The evaluation of a large number of flux distribution curves shows that, with satisfactory accuracy,

$$b_e = b_p + 2g \tag{16-1}$$

where $b_p$ is the actual pole arc and $g$ the length of the gap under the center of the pole. The flux distribution curve is determined either from a flux map or experimentally by means of a full-pitch search coil placed on the armature. The emf of such a coil has exactly the same shape as the $B$-curve.

The effective core length $l_e$ is smaller than the gross core length $L$ (Fig. 16–3) and larger than the net core length $l = L - n_v b_v$. The fringing at the ends

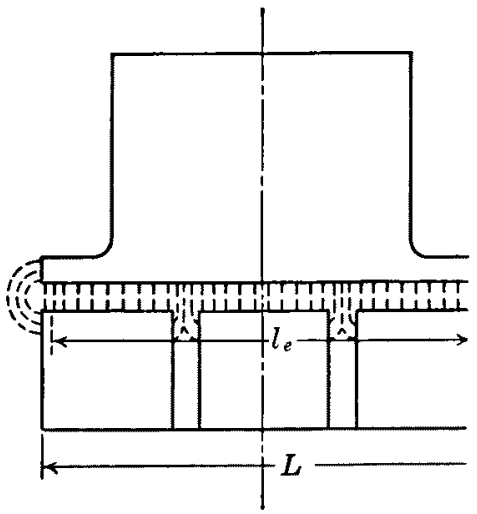


FIG. 16–3. Determination of the equivalent armature length.

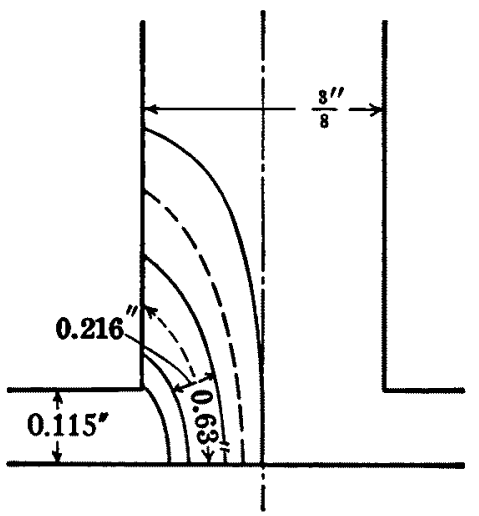


FIG. 16–4. Determination of the equivalent width of an air duct.

of the pole is small. The width of the vents ($n_v \times b_v$) can be up to 15% of the gross core length $L$ and the flux within the vents must be taken into account. The magnitude of this flux will be determined by an example, using a flux map.

Fig. 16–4 shows the case of a machine with an air-gap $g$ equal to 0.115 inch and a duct width $b_v$ equal to $\frac{3}{8}$ inch. The flux going through the duct can be divided into two equal parts, one for each side of the duct. The flux of one of these two parts is represented in Fig. 16–4 by three tubes of force, the widths of which are 0.137, 0.216, and 0.233 inch, and the lengths 0.315, 0.63, and 0.985 inch.

The permeance (reciprocal to reluctance) for the flux going through the gap into a stack of laminations, per unit of the armature circumference, is

$$\frac{(\tau_v - b_v) \times 1}{g} = \frac{(\tau_v - b_v) \times 1}{0.115}$$

where $\tau_v$ is the vent pitch; $\mu$ here is 1. The permeance for the flux going

through a duct into the armature, also per unit circumference of the armature, is

$$\Sigma\left(\frac{b_x}{g_x}\right)=2\left(\frac{0.137}{0.315}+\frac{0.216}{0.63}+\frac{0.233}{0.985}\right)=2.03$$

Assuming as an example $\tau_v=2$ inches, the permeances are 14.13 and 2.03

It is expedient to replace all tubes of force in a duct by a *single* tube of the length $g$, i.e., of the same length which the tubes have between pole and the stack of laminations. The width of this single tube then will be determined by the relation

$$\frac{b'}{g}=\Sigma\left(\frac{b_x}{g_x}\right) \quad \text{or} \quad b'=g\Sigma\left(\frac{b_x}{g_x}\right)$$

$b'$, defined in this manner, is a width of iron equivalent to the air duct, with respect to the flux entering the armature.

In the example considered $b'=0.115\times 2.03=0.234$ inch and the radial duct of the width $b_v=0.375$ inch is equivalent to a length of iron equal to 0.234 inch, with respect to the flux entering the armature. The loss in the length $L$ per duct is then

$$b_v-b'=0.375-0.234=0.141 \text{ inch}$$

and the effective core length, $l_e$,

$$l_e=L-n_v(b_v-b') \tag{16–2}$$

If, with the aid of flux plots, $b'$ is determined for different values of $g$, it is observed to depend upon the ratio $b_v/g$ and becomes smaller as this ratio increases. For *a constant value of* $b_v$, if the loss of iron per duct $(b_v-b')$ is drawn as a function of $g$, a curve is obtained for which the following relation holds

$$b_v-b'=\frac{b_v/g}{5+b_v/g}\,b_v \tag{16–3}$$

The ratio of the permeance of a stack without duct $(b_v=0)$ to that with a duct of the width $b_v$ is

$$k_v=\frac{\tau_v\times 1}{g}\Big/\frac{[\tau_v-(b_v-b')]\times 1}{g}=\frac{\tau_v}{\tau_v-(b_v-b')}$$

Introducing Eq. 16–3, we have

$$k_v=\frac{\tau_v(5g+b_v)}{\tau_v(5g+b_v)-b_v^2} \tag{16–4}$$

There is one more stack than ducts. With

$$\tau_v=\frac{L+b_v}{n_v+1} \tag{16–5}$$

approximately,

$$l_e=L\frac{n_v+1}{1+n_vk_v} \tag{16–6}$$

The effective core length $l_e$ can be calculated either from Eqs. 16–2 and 16–3 or from Eq. 16–6. The factor $k_v$ as a function of $b_v/g$ and $b_v/\tau_v$ is given in Fig. 16–5.

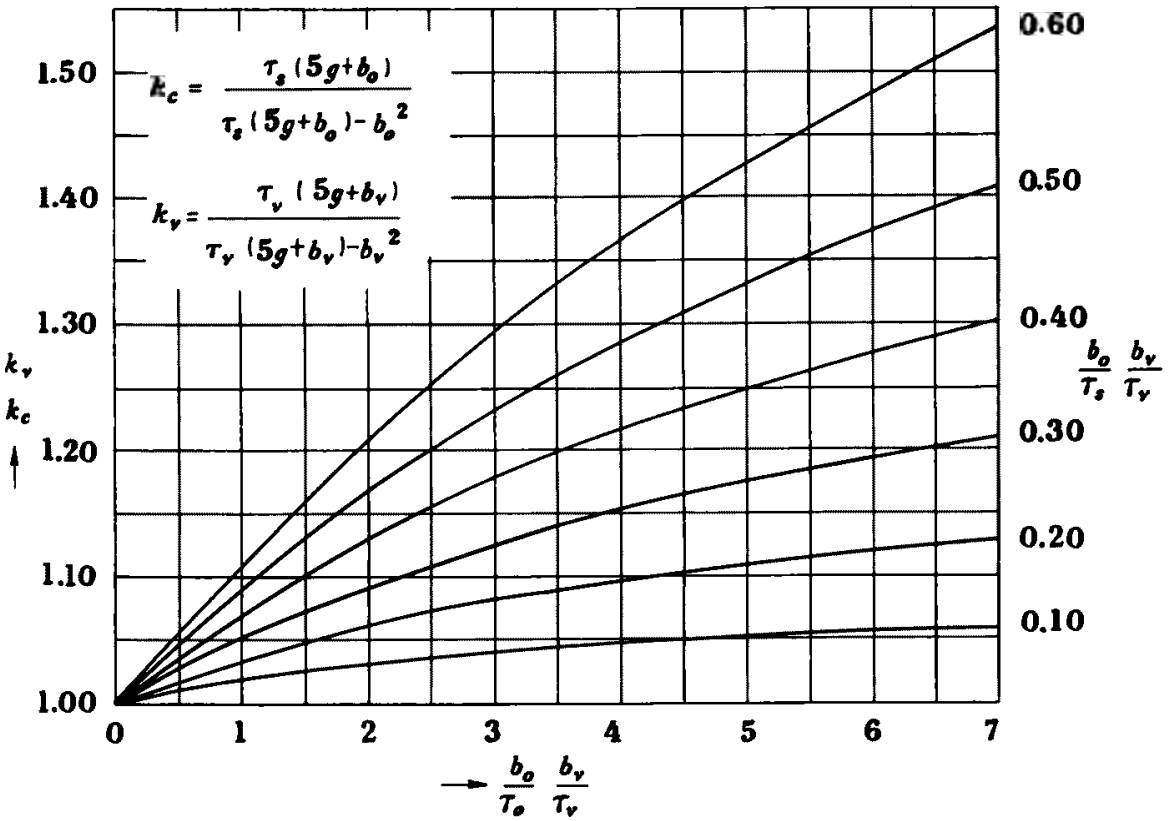


FIG. 16–5. Vent factor $k_v$ and Carter factor $k_c$.

For the example considered in Art. 5–1

$$L=7.0, \quad n_v=2, \quad b_v=\tfrac{3}{8}, \quad g=0.218$$

From Eqs. 16–3 and 16–2

$$b_v - b' = \frac{0.375/0.218}{5+0.375/0.218} \times 0.375 = 0.0961$$

$$l_e = 7.0 - 2 \times 0.0961 = 6.81 \text{ inches}$$

From Eq. 16–5, $\tau_v = \frac{7.375}{3} = 2.46$. From Fig. 16–5, $k_v = 1.04$. From Eq. 16–6

$$l_e = 7.0 \, \frac{2+1}{1+2 \times 1.04} = 6.81 \text{ inches}$$

The fringing at the end of the pole can be taken into account by adding 0.1 inch to $l_e$.

One more important factor has to be taken into account. This is the influence of the slot openings of the armature upon $b_e$. Apparently the slot-openings decrease $b_e$ in the same manner as the ducts decrease the core length

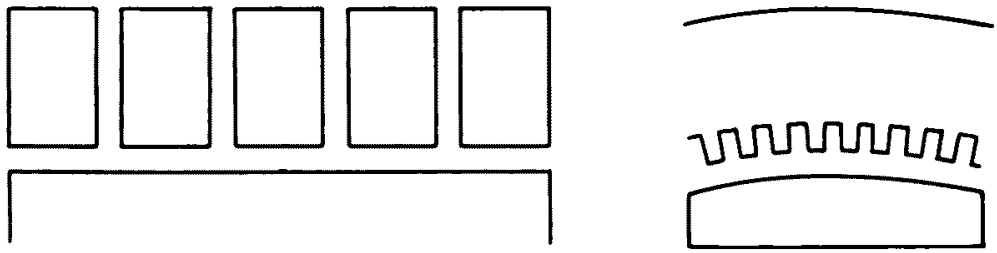

FIG. 16–6. Explanation of Carter Factor $k_c$.

$L$. An observer placed on a pole (Fig. 16–6), and looking circumferentially around the armature sees the same picture as looking axially along the armature, namely, iron alternating with air. Therefore, Eq. 16–4 for the vent (duct) factor $k_v$ applies also to the slot openings, if the slot-pitch $\tau_s$ is introduced for $\tau_v$ and the slot opening $b_0$ is introduced for $b_v$. This yields the slot-openings factor

$$k_c = \frac{\tau_s(5g + b_0)}{\tau_s(5g + b_0) - b_0^2} \tag{16–7}$$

This factor is called *Carter factor* because it was derived first (analytically) by F. W. Carter. $k_c$ as a function of $b_0/g$ and $b_0/\tau_s$ is given in Fig. 16–5.

Summarizing, the cross-sectional area of the gap is

$$A_g = \frac{b_e}{k_c} l_e \tag{16–8}$$

where $b_e$ is given by Eq. 16–1.

The flux density in the gap is

$$B_g = \frac{\Phi}{A_g} = \frac{\Phi}{b_e l_e} \times k_c$$

The field intensity in the gap is

$$H_g = \frac{B_g}{0.4\pi} = \frac{\Phi}{b_e l_e} \times \frac{k_c}{0.4\pi}$$

and the gap mmf necessary to produce this field intensity is (for both gaps)

$$M_g = H_g \times 2g = 2g \times \frac{B_g}{0.4\pi}$$

In this equation $B_g$ is expressed in Gausses (lines per square centimeter) and $g$ in centimeters. If $B$ is expressed in lines per square inch and $g$ in inches, then

$$M_g = 2g \frac{B_g}{0.4\pi} \frac{2.54}{2.54^2} = 2g \left(\frac{\Phi}{b_e l_e}\right) \times \frac{k_c}{0.4\pi} \times \frac{1}{2.54} = \frac{1}{1.595} \left(\frac{\Phi}{b_e l_e}\right) (g k_c) \tag{16–9}$$

Though the Carter factor $k_c$ has been derived in connection with the pole arc

$b_e$, it is customary to associate it with the gap and to call the quantity $gk_c$ the *effective gap*. Correspondingly the flux density in the gap is defined as

$$B_g = \frac{\Phi}{b_e l_e} \tag{16–10}$$

where $b_e$ is given by Eq. (16–1). The introduction of an effective gap $gk_c$ is justified by the fact that, at the slot openings, the gap between pole and armature is larger than between pole and teeth, resulting in a gap larger than that between pole and teeth.

**16–2. Teeth Mmf.** With the value of $B_g$ from Eq. 16–10 the tooth density can be determined as

$$B_t = \frac{\tau_{sg} l_e B_g}{b_t k_i l} \tag{16–11}$$

where $\tau_{sg}$ is the slot pitch at the air gap, $b_t$ the tooth width, $l = L - n_v b_v$ the axial length of the armature iron, including the insulation between the laminations, and $k_i$ the stacking factor which takes into account the insulation between laminations. $k_i = 0.92$ for waterglass or lacquer insulation; $k_i = 0.96$ for oxide-film insulation. The numerator of Eq. 16–11, $\tau_{sg} l_e B_g$, is the flux which enters the armature through a slot pitch.

The length of the magnetic path in the two teeth is $2h_t$, where $h_t$ is the height of the tooth.

Eq. 16–11 assumes that the flux entering the armature through a slot pitch passes only through the iron (through the tooth). This is the case when $B_t$ is equal to or smaller than about 118,000 lines/in$^2$. When $B_t$ is larger than this value, a part of the flux $\tau_{sg} l_e B_g$ takes a path also through slot, i.e., parallel to the tooth iron. With respect to the flux $\tau_{sg} l_e B_g$, tooth and slot are magnetically in parallel. In the case of low saturation, the reluctance of the tooth is small in comparison to that of the slot so that practically no lines of force go through the slot. On the other hand, if the tooth is saturated, its permeability will be low, the reluctance will be comparatively large, and a part of the lines of force will go through the slot. In this latter case, Eq. 16–11 would yield too high a value for the tooth density.

For high tooth saturation, the value of $B_t$ yielded by Eq. 16–11 will be called the fictitious tooth density $B'_t$. The *actual tooth density* $B_t$ is determined as follows:

The flux through a slot pitch is

$$\tau_{sg} l_e B_g = \Phi' \tag{16–12}$$

For high tooth saturation, it divides into two parts:

$$\Phi' = \Phi_t + \Phi_s \tag{16–13}$$

The flux $\Phi_t$ goes through the tooth and the flux $\Phi_s$ through the slot.

The ratio of the cross section of the slot, $A_s$, to the cross section of the tooth, $A_t$, is

$$k_t = \frac{A_s}{A_t} = \frac{\tau_s l_e - b_t k_i l}{b_t k_i l} \tag{16–14}$$

Dividing Eq. 16–13 by $A_t$, we obtain

$$\frac{\Phi'}{A_t} = \frac{\Phi_t}{A_t} + \frac{\Phi_s}{A_s} k_t$$

or

$$B'_t = B_t + B_s k_t$$

Thus the actual tooth density is

$$B_t = B'_t - B_s k_t \tag{16–15}$$

$B'_t$, the fictitious tooth density is given by Eq. 16–11. Introducing $B_s = 0.4\pi H$, we have

$$B_t = B'_t - 0.4\pi k_t H \tag{16–16}$$

Since $H$ is the same along the slot as along the tooth, $H$ and $B_t$ in Eq. 16–16 are *coordinated* to each other by the magnetization curve of the tooth iron.

The axis of abscissa of the magnetization curve is usually given in ampere turns per unit length (AT $= H$). Furthermore, $B$ and AT are drawn to different scales. If $S_{at}$ is the number of ampere turns per cm per unit length in the axis of at and $S_B$ the number of lines per cm$^2$ per unit length in the axis of $B$, then

$$B_t = B'_t - 0.4\pi k_t \frac{S_{at}}{S_B} \times \text{AT} \tag{16–17}$$

If, further, the magnetization curve is given in the units

$$B/\text{in.}^2 = f(\text{AT} = \text{AT/in.})$$

and $S'_{at}$ is the number of ampere turns per inch per unit length in the axis of at and $S'_B$ the number of lines per in.$^2$ per unit length in the axis of $B$, then

$$B_t = B'_t - 0.4\pi k_t \frac{S'_{at}}{S'_B} \times 2.54 \times \text{AT} = B'_t - 3.19 k_t \frac{S'_{at}}{S'_B} \times \text{AT} \tag{16–18}$$

In order to determine the actual tooth density $B_t$, draw the quantity

$$3.19 k_t (S'_{at}/S'_B) \times \text{AT}$$

as a function of at below the magnetization curve $B = f(\text{at})$, AT shown in Fig. 16–7. This is a straight line. If the fictitious tooth density $B'_t$ (Eq. 16–11) is equal to $DA$ and from $A$ a line is drawn parallel to the line

$$3.19 k_t (S'_{at}/S'_B) \times \text{AT},$$

the distance $BC$ is equal to the actual tooth density $B_t$ and the distance $OC$ is the corresponding value of $H_t = \text{AT}$.

The tooth mmf is then

$$M_t = 2h_t H_t \tag{16–19}$$

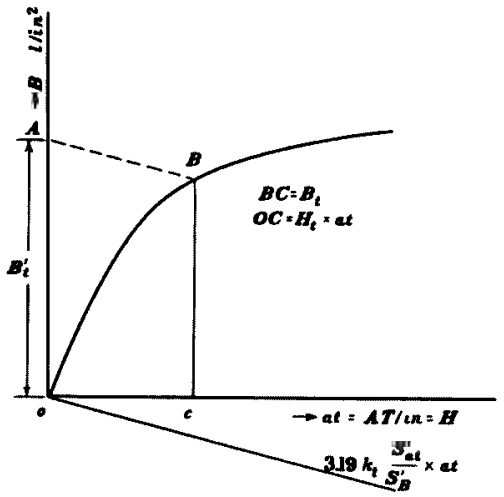


FIG. 16–7. Determination of the actual tooth density from the fictitious tooth density.

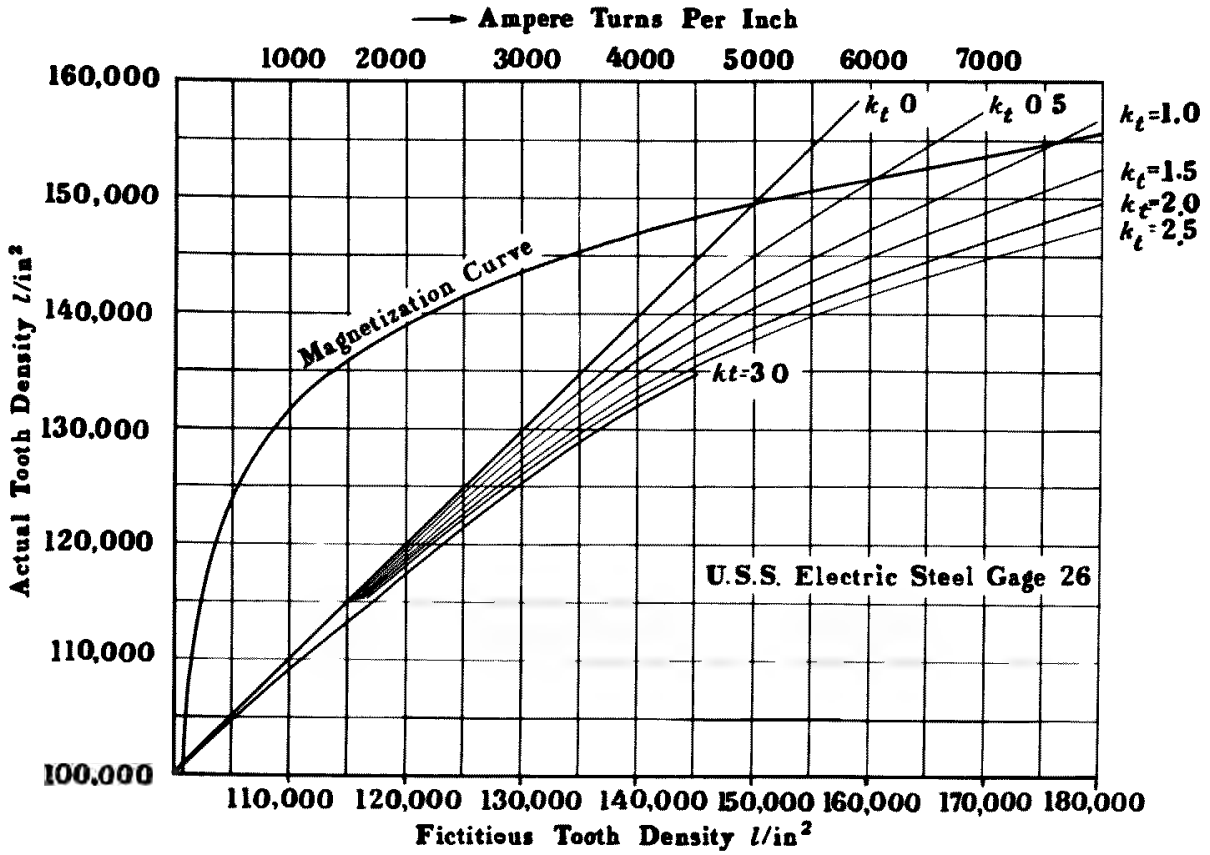


FIG. 16–8. Actual tooth density as a function of the fictitious tooth density for different values of $k_t$.

Fig. 16–8 shows the corresponding values of the fictitious tooth density, the actual tooth density, and the field intensity $H = at$ for USS Electrical Steel, Grade 26.

When the width of the tooth at its top is different from that at its base, the

tooth density varies along the tooth. In this case, it is often satisfactory to compute with the tooth density at $\frac{1}{3}h_t$ measured from base of the tooth; i.e., for $b_t$ in Eq. 16–11 and for $\tau_s$ and $b_t$ in Eq. 16–14 the values at this place are to be used. A more accurate value for $M_t$ than the $\frac{1}{3}h_t$-computation yields is obtained by applying *Simpson's* rule. Here the values of tooth density and corresponding $H_t$ are calculated for top, middle, and base of the tooth by substituting the value of $b_t$ in Eq. 16–11 and the values $\tau_s$ and $b_t$ in Eq. 16–14 for each of these places. The tooth mmf is then

$$M_t = 2h_t \frac{(H_{t,\text{top}} + 4H_{t,\text{mi.}} + H_{t,\text{base}})}{6} \tag{16–20}$$

**16–3. Armature Core Mmf.** The flux density in the armature core is

$$B_c = \frac{\Phi}{2h_c k_i l} \tag{16–21}$$

where $h_c$ is the height of the core behind the teeth. The length of the magnetic path is

$$l_c = \frac{\pi D'}{p} \tag{16–22}$$

where $D'$ is the diameter in the middle of the core. The core mmf is

$$M_c = H_c l_c \tag{16–23}$$

**16–4. Pole Leakage. Pole and Yoke Mmf's.** Just as the slot offers a path for the lines of force parallel to the tooth, the interpolar space offers a parallel path for the lines of force which enter the armature through the pole; Fig. 16–9 shows the course of the lines of force for half of a pole. The continuation of the lines of force into the armature is not drawn. A part of the lines of force do not enter the armature, but take a path from pole shoe to pole shoe, pole body to pole body, and a small part also from pole body to yoke. Although the reluctance of the interpolar space is large, the flux which takes a path through this region cannot be disregarded: it is about $\frac{1}{10}$ to $\frac{1}{5}$ of the armature flux. Since only the flux $\Phi$ which enters the armature induces an emf in the armature winding, the flux which passes through the space between the poles is not a useful flux and is called the *pole leakage flux*; it is a disadvantage in that it requires the flux in the pole and yoke to be greater than that in the arma-

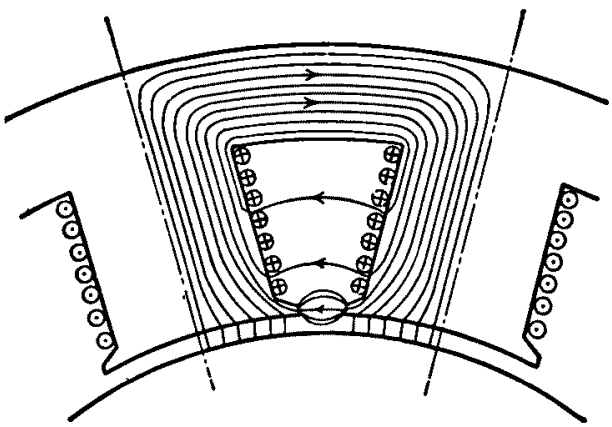

FIG. 16–9. Main flux and leakage flux of salient poles.

ture. This requires a greater mmf to magnetize the yoke and poles than if no leakage whatever were present.

The leakage flux can be calculated with the aid of Ampère's law, Eq. 1–18. The same mmf which acts upon 2 air-gaps, 2 armature teeth, and armature core, i.e., $(M_g + M_t + M_c)$, is influential in determining the magnitude of the leakage flux between the pole shoes. This fact follows without further discussion from Eq. 5–4. If the line integral $\oint H_l \, dl$ is set up, beginning at a pole surface adjacent to the air-gap and going through the pole, the pole yoke, a second pole, air-gap, armature teeth, armature core, armature teeth, and air-gap (see Fig. 2–2), the result will be exactly the same as for a path following through the first pole, pole yoke, second pole, and the distance in the air between the pole shoes; the contribution to this integral furnished by the air-gap and the armature must be the same as that furnished by the dis-

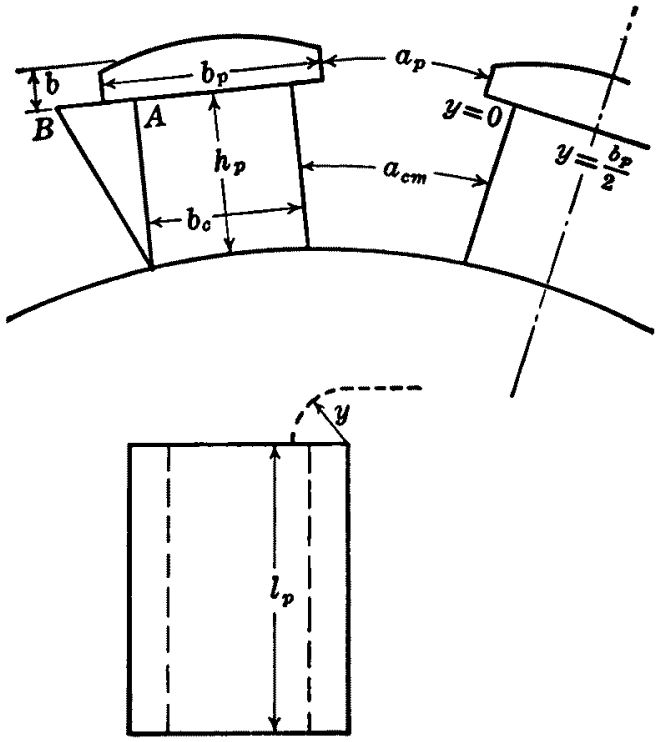


FIG. 16–10. Determination of the leakage flux of salient poles.

tance in the air between the pole shoes, for other terms in the summation are equal in both cases. By similar considerations, the mmf acting between the pole cores decreases linearly from the pole shoe to the yoke and is equal to $(M_g + M_t + M_c) = AB$ (Fig. 16–10) at the pole shoe and nearly zero at the yoke.

The leakage flux consists of the following four parts:

(a) Leakage flux between the inside surfaces of the pole shoes.
(b) Leakage flux between the end surfaces of the pole shoes.
(c) Leakage flux between the inside surfaces of the pole cores.
(d) Leakage flux between the end surfaces of the pole cores.

If

$$M_l = M_g + M_t + M_c \tag{16–24}$$

the flux between the internal surfaces of the pole shoes is (Fig. 16–10)

$$\Phi_a = \frac{0.4\pi M_l}{\mathscr{R}_a} = \frac{0.4\pi M_l l_p b}{a_p} \times 2.54 \tag{16–25}$$

The significance of the individual quantities follows from Fig. 16–10. If it is assumed that the lines of force between the external surfaces of the pole shoes go part of the way in the arc of a circle of radius $y$ (Fig. 16–10), and part of the way in a straight line (along the line $a_p$), then

$$\begin{aligned}\Phi_b &= 2M_l \int_{y=0}^{y=b_p/2} \frac{0.4\pi\, b dy}{(a_p + \pi y)} \\ &= 2 \times 0.4\pi M_l b \times \frac{2.3}{\pi} \log\left(1 + \frac{\pi}{2}\frac{b_p}{a_p}\right) \times 2.54 \\ &= 1.84 M_l b \log\left(1 + \frac{\pi}{2}\frac{b_p}{a_p}\right) \times 2.54 \end{aligned} \tag{16–26}$$

The factor 2 takes into account both ends of the machine.

If the leakage flux between the pole cores is calculated using the average value of the mmf which prevails between the cores, that is, with

$$(M_l + 0)/2 = M_l/2,$$

then

$$\Phi_c = 0.4\pi \frac{M_l}{2} \frac{l_p h_p}{a_{\text{cm}}} \times 2.54 \tag{16–27}$$

With the same considerations as for $\Phi_b$

$$\begin{aligned}\Phi_d &= \frac{2 \times 0.4\pi M_l}{2} h_p \times \frac{2.3}{\pi} \log\left(1 + \frac{\pi}{2}\frac{b_c}{a_{\text{cm}}}\right) \times 2.54 \\ &= 0.92 M_l h_p \log\left(1 + \frac{\pi}{2}\frac{b_c}{a_{\text{cm}}}\right) \times 2.54 \end{aligned} \tag{16–28}$$

The entire leakage flux $\Phi_l$ for both pole sides is

$$\Phi_l = 2(\Phi_a + \Phi_b + \Phi_c + \Phi_d) \tag{16–29}$$

The flux in the pole core and yoke is

$$\Phi_p = \Phi + \Phi_l \tag{16–30}$$

The flux density in the pole core is

$$B_p = \frac{\Phi_p}{A_c} \tag{16–31}$$

and the pole mmf is

$$M_p = 2h_p H_p \tag{16–32}$$

The flux density in the yoke is

$$B_y = \frac{\Phi_p}{2A_y} \tag{16–33}$$

The length of the magnetic path in the yoke is

$$l_y = \frac{\pi D''}{p} \tag{16–34}$$

where $D''$ is the diameter in the middle of the yoke. The yoke mmf is

$$M_y = l_y H_y \tag{16–35}$$

Thus, the calculation of the mmf necessary to produce the armature flux $\Phi$ in the d-c machine is as follows: First, the air-gap flux density $B_g$, the tooth flux density $B_t$, and armature-core flux density $B_c$ are calculated, and from these values $(M_g + M_t + M_c)$ is obtained. With this, the mmf $M_l$ which produces the leakage flux is known, and the leakage flux $\Phi_l$ and pole flux $\Phi_p = \Phi_l + \Phi$ can be calculated. From this, $B_p$ and $B_y$ and the mmf necessary to magnetize the pole and yoke can be determined.

# *Chapter 17*

# COMMUTATION

## A. Self- and Mutual Inductance of the Leakage Fluxes

**17–1. General Formulae for $L$ and $M$.** It has been mentioned in Art. 9–1 that the armature conductors produce three kinds of leakage fluxes (Figs. 9–3 and 9–4), namely,

slot leakage flux,
tooth-top leakage flux,
end-winding leakage flux.

The magnetic paths of these fluxes are different and, therefore, their reluctances are different. Each of the three kinds of leakage flux will be considered in turn.

It should be mentioned that *each of the leakage fluxes is directly proportional to the current* which produces it, since its reluctance is principally in air, for which $\mu = 1$. It is only in the case of the main flux, where the path is through iron, that the relationship between flux and current is determined by the magnetization curve of the particular iron used; this is not the case, however, for the leakage fluxes.

As has been explained in Art. 9–1, the leakage fluxes induce, during the time of commutation, emf's of self- and mutual induction in the short-circuited winding elements. The coefficients of self- and mutual induction will be determined in the following:

According to Eq. 9–20a, in general,

$$L = \frac{\Sigma(N_x \Phi_x)}{i} \tag{17–1}$$

This equation assumes that not all turns are interlinked with the same flux and, therefore, the total flux interlinkage has to be determined as the sum of the partial flux interlinkages.

Since $\Phi_x$ is produced by the mmf $iN_x$, it follows from Eq. 1–21 that

$$\Phi_x = \frac{0.4\pi i N_x}{\mathscr{R}_x} \quad \text{and} \quad \mathscr{R}_x = \frac{l_x}{\mu_x \mathscr{A}_x} \tag{17–2}$$

where $\mathscr{R}_x$ is the reluctance applying to the path of the flux $\Phi_x$. Thus,

$$L = 0.4\pi \Sigma \frac{N_x^2}{\mathscr{R}_x} = 0.4\pi \Sigma N_x^2 \Lambda_x \tag{17-3}$$

$\Lambda_x$ is the permeance of the flux $\Phi_x$.

Corresponding to Eq. 17–1, in general,

$$M_{12} = M_{21} = \frac{\Sigma(n_{x1}\Phi_{x2})}{i_2} = \frac{\Sigma(n_{x2}\Phi_{x1})}{i_1} \tag{17-4}$$

$\Sigma(n_{x1}\Phi_{x2})$ is the sum of all flux interlinkages with the circuit 1 due to a current $i_2$ in circuit 2; vice versa, $\Sigma(n_{x2}\Phi_{x1})$ is the sum of all flux interlinkages with the circuit 2 due to a current $i_1$ in circuit 1. In order to determine $M_{12} = M_{21}$, *either* a current of one ampere is assumed to flow in circuit 1 and the sum of flux interlinkages with circuit 2 is computed *or* a current of one ampere is assumed to flow in circuit 2 and the sum of flux interlinkages with circuit 1 is computed.

**17–2. The Slot Leakage Flux.** (a) *Single-layer Winding.* First a semi-closed slot (Fig. 17–1) with a single coil of $n_c$ turns will be treated. The slot is divided

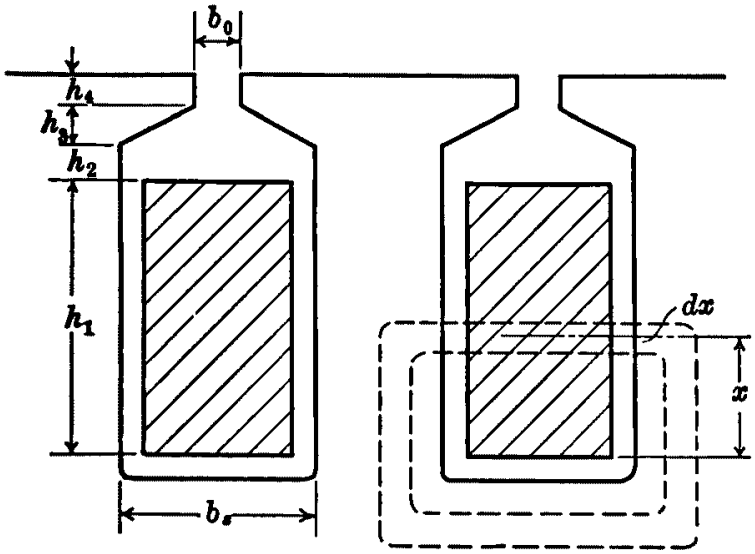


FIG. 17–1. Determination of the slot leakage permeance.

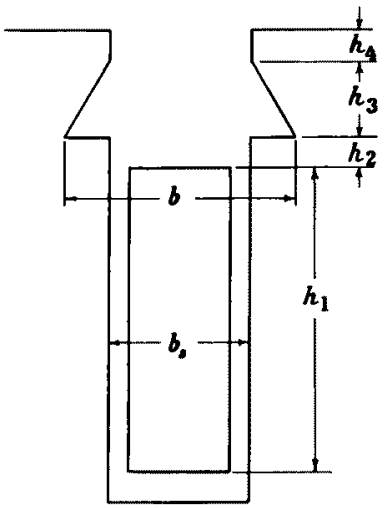


FIG. 17–2. Determination of the slot leakage permeance.

into four parts with the heights $h_1$, $h_2$, $h_3$, and $h_4$. Consider a tube of force crossing part 1 at the distance $x$ from the bottom of the coil; the height of the tube of force is $dx$. Then for this tube of force (Eq. 17–3)

$$N_x = \frac{x}{h_1} n_c \quad \text{and} \quad \Lambda_x = \frac{dx l_s}{b_s} \tag{17-5}$$

$l_s$ is the length of the iron effective for the slot leakage flux; its value will be determined in the following.

The sum $\Sigma N_x^2 \Lambda_x$ for part 1 is found by integrating $N_x^2 \Lambda_x$ in Eq. 17–5 from $x=0$ to $x=h_1$. Thus, for part 1,

$$L_1 = 0.4\pi n_c^2 l_s \frac{1}{b_s h_1^2} \int_{x=0}^{x=h_1} x^2\, dx = 0.4\pi n_c^2 l_s \frac{h_1}{3b_s} \tag{17–6}$$

For part 2

$$N_x = n_c, \quad \Lambda_x = dx \frac{l_s}{b_s}$$

For part 3

$$N_x = n_c, \quad \Lambda_x = \frac{dx l_s}{(b_s + b_0)/2}$$

For part 4

$$N_x = n_c, \quad \Lambda_x = \frac{dx l_s}{b_0}$$

thus

$$L_2 = 0.4\pi n_c^2 l_s \frac{h_2}{b_2} \tag{17–7}$$

$$L_3 = 0.4\pi n_c^2 l_s \frac{2h_3}{b_s + b_0} \tag{17–8}$$

$$L_4 = 0.4\pi n_c^2 l_s \frac{h_4}{b_0} \tag{17–9}$$

and the total slot-leakage inductance for *one coil side* is

$$L_s = L_1 + L_2 + L_3 + L_4 = 0.4\pi n_c^2 l_s \left[\frac{h_1}{3b_3} + \frac{h_2}{b_s} + \frac{2h_3}{b_s + b_0} + \frac{h_4}{b_0}\right] \times 2.54 \times 10^{-8} \text{ henry} \tag{17–10}$$

$l_s$ is measured in inches. The quantity in brackets is called the *permeance per unit length* of the slot leakage flux and is denoted by $\lambda_s$. Eq. 17–10 is usually written in the form

$$L_s = 0.4\pi n_s^2 l_s \lambda_s \times 2.54 \times 10^{-8} \text{ henry} \tag{17–10a}$$

Hence for a semi-open slot

$$\lambda_s = \frac{h_1}{3b_s} + \frac{h_2}{b_s} + \frac{2h_3}{b_s + b_0} + \frac{h_4}{b_0} \tag{17–11}$$

For an open slot (Fig. 17–2) the part 2 and 4 can be combined, so that, for this slot

$$\lambda_s = \frac{h_1}{3b_s} + \frac{h_2 + h_4}{b_s} + \frac{2h_3}{b + b_s} \tag{17–12}$$

The quantity $l_s \lambda_s = \Lambda_s$ is the *total permeance* of the slot leakage flux.

Consider Fig. 17–3 which shows a coil in a slot. The core consists of three stacks separated by two radial ducts of the width $b_v$. It is seen that, due to

the ducts, the effective length for the slot leakage flux is smaller than the gross length of the armature $L$, but it is larger than the iron length $L - n_v b_v$ ($n_v$ = number of ducts) due to the fringing within the ducts.

In Art. 16–1 equations were derived for the loss of iron per radial vent (Eq. 16–3) and for a vent factor $k_v$ (Eq. 16–4). These equations apply to the case when radial vents are arranged in one machine part only (Fig. 16–3).

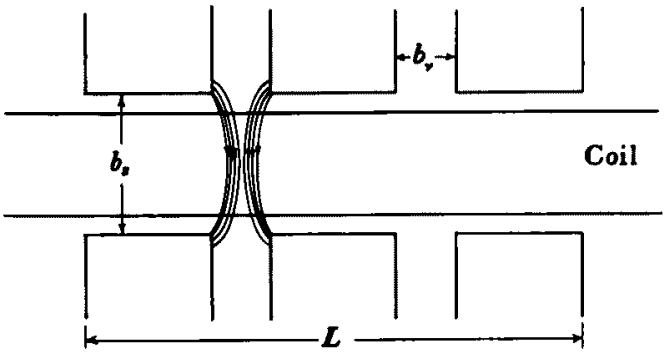


FIG. 17–3. Explanation of the slot-leakage factor $k_s$.

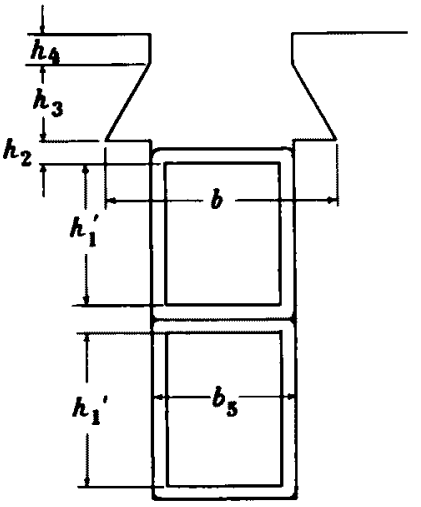


FIG. 17–4. Determination of the slot leakage permeance for a 2-layer winding.

If both machine parts have radial vents and these vents are opposite one another, then, in the same manner as in Art. 16–1, it is found that the vent factor is

$$k_v = \frac{\tau_v(5g + 2b_v)}{\tau_v(5g + 2b_v) - 2b_v^2}$$

As can be seen from Fig. 17–3, this equation can be used for the determination of a slot-leakage factor $k_s$, if $b_s$ is substituted for $g$, i.e.,

$$k_s = \frac{\tau_v(5b_s + 2b_v)}{\tau_v(5b_s + 2b_v) - 2b_v^2} \tag{17–13}$$

and

$$l_s = \frac{L}{k_s} \tag{17–14}$$

(b) *Two-layer Winding with One Winding Element per Layer.* A two-layer winding in an open slot with one winding element per layer (Fig. 17–4) will be considered. There is in the slot a bottom and a top coil side belonging to different winding elements. The coefficients of self-inductance are different for both coil sides, and mutual inductance exists between them.

The permeance per unit-length for the *top* coil side is (Eq. 17–12)

$$\lambda_{st}=\frac{h'_1}{3b_s}+\frac{h_2+h_4}{b_s}+\frac{2h_3}{b+b_s} \tag{17–15}$$

Therefore, the slot-leakage inductance of the *top coil side* is

$$L_{st}=0.4\pi N_e^2 l_s\lambda_{st}\times 2.54\times 10^{-8}\text{ henry} \tag{17–16}$$

$N_e$ is the number of turns per winding element. For the permeance of the *bottom coil side* the space taken by the upper coil side has to be considered as air space. Thus

$$\lambda_{sb}=\frac{h'_1}{3b_s}+\frac{h'_1+h_2+h_4}{b_s}+\frac{2h_3}{b+b_s}=\frac{4h'_1}{3b_s}+\frac{h_2+h_4}{b_s}+\frac{2h_3}{b+b_s} \tag{17–17}$$

and

$$L_{sb}=0.4\pi N_e^2 l_s\lambda_{sb}\times 2.54\times 10^{-8}\text{ henry} \tag{17–18}$$

It is seen that $L_{sb}$ is much larger than $L_{st}$.

The coefficient of mutual inductance between both coil sides is, according to Eq. 17–4,

$$M_{tb}=M_{bt}=\frac{\Sigma(n_{xt}\Phi_{xb})}{i_b}=\frac{\Sigma(n_{xb}\Phi_{xt})}{i_t} \tag{17–19}$$

It will be assumed that one ampere flows in the top coil side and the sum of all flux interlinkages $\Sigma(n_{xb}\Phi_{xt})$ with the bottom coil side will be determined. Since current flows only in the top coil side, there are no tubes of force below this coil side and, therefore, for all tubes of force interlinked with the bottom coil side, $n_{xb}=N_e$. Further, for a tube of force crossing the top coil side at the distance $x$ from the bottom of this coil side

$$\Phi_{xt}=\frac{0.4\pi n_{xt}\times 1}{b_s/l_s\,dx}, \quad n_{xt}=\frac{x}{h'_1}N_e \tag{17–20}$$

Inserting into Eq. 17–19, $n_{xb}=N_e$, $\Phi_{xt}$ from Eq. 17–20 and integrating from $x=0$ to $x=h'_1$, there results, for all tubes of force crossing the top coil side,

$$0.4\pi N_e^2 l_s\frac{h'_1}{2b_s}$$

The tubes of force which are produced by the current of one ampere in the top coil side and which lie above this coil side yield the flux interlinkage with the bottom *coil side*

$$0.4\pi N_e^2 l_s\left[\frac{h_2+h_4}{b_s}+\frac{2h_3}{b+b_s}\right]$$

so that

$$M_{tb}=M_{bt}=0.4\pi N_e^2 l_s\lambda_{bt}\times 2.54\times 10^{-8}\text{ henry} \tag{17–21}$$

where

$$\lambda_{bt}=\lambda_{tb}=\frac{h'_1}{2b_s}+\frac{h_2+h_4}{b_s}+\frac{2h_3}{b+b_s} \tag{17–22}$$

$\lambda_{bt}=\lambda_{tb}$ is the permeance per unit length for mutual induction.

(c) *Two-layer Winding with Several Winding Elements per Layer.* Fig. 17–5 shows a 2-layer winding with three winding elements per layer. Considering conductor* 1, its slot-leakage inductance is given by Eq. 17–10a. There is mutual inductance between conductor 1 and conductors 2, 3, 1′, 2′, and 3′. It is seen from Fig. 17–5 that the coefficient of mutual inductance between 1 and 2 and 1 and 3 is the same as the coefficient of self-inductance of conduc-

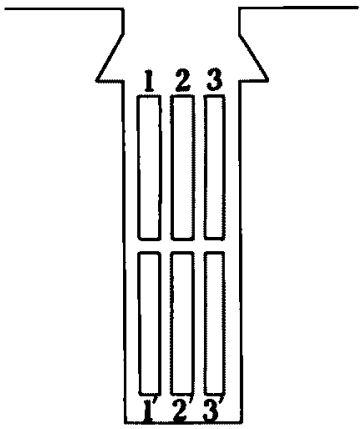


FIG. 17–5. Two-layer winding with three conductors per layer.

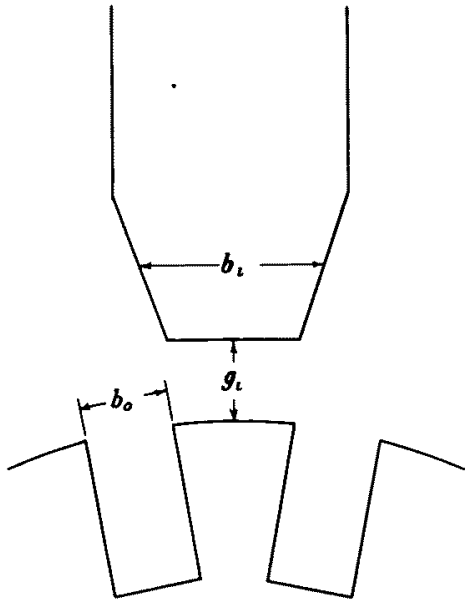


FIG. 17–6. Explanation of the interpole-shoe arc.

tor 1, because one ampere flowing in conductor 2 or 3 will produce the same flux interlinkage with 1 as a current of one ampere flowing in 1. Therefore

$$M_{1\text{-}2} = M_{1\text{-}3} = L_{s1} \tag{17–23}$$

It is also seen from Fig. 17–5 that the mutual inductance between conductor 1 and conductors 2′ and 3′ is the same as between conductor 1 and conductor 1′. Thus

$$M_{1\text{-}1}' = M_{1\text{-}2}' = M_{1\text{-}3}' = M_{tb} \tag{17–24}$$

where $M_{tb}$ is given by Eq. 17–21.

**17–3. The Tooth-top Leakage Fluxes.** With the symbols

$\tau$ = pole pitch
$b_p$ = main pole-shoe arc
$b_i$ = interpole-shoe arc or average width of the interpole bevel (Fig. 17–6)
$k_{ci}$ = Carter factor for the interpole air-gap

* The word "conductor" is used here for "winding-element side," although the latter may contain several conductors.

and Fig. 17–6, the permeance for the tooth-top leakage per unit length is with sufficient approximation (Ref. C4).

$$\lambda_{tt} = \frac{2.3}{\pi} \log \left[ 1 + \frac{\pi(\tau - b_p)}{2b_0} \right] \quad \text{for machines without interpoles} \tag{17–25}$$

$$\lambda_{tt} = 0.5 \left[ \frac{b_i + 2g_i - b_0}{3k_{ci}g_i} \right] \quad \text{for machines with interpoles} \tag{17–26}$$

The first of the two equations (Eq. 17–25) is obtained by assuming that the

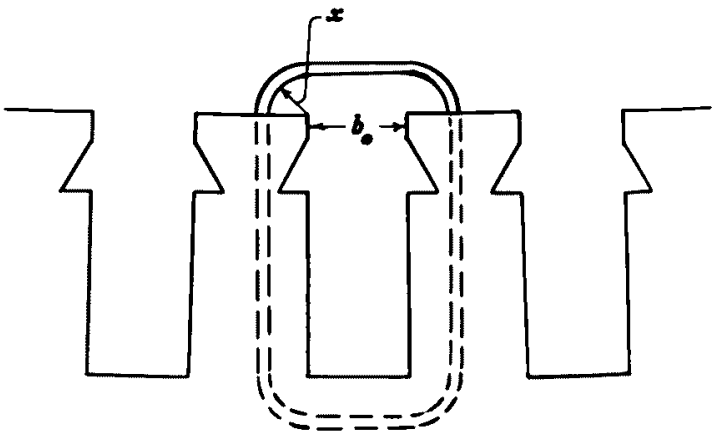


FIG. 17–7. Determination of the tooth-top leakage permeance.

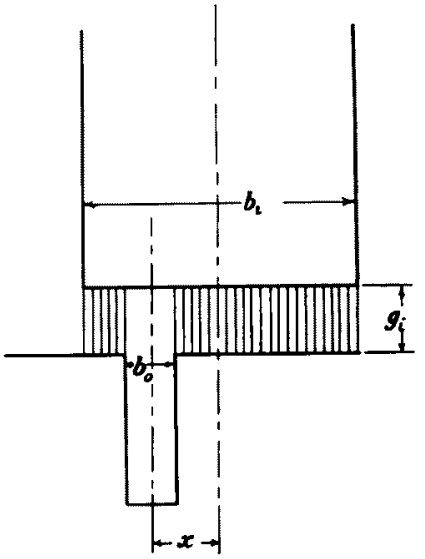


FIG. 17–8. Determination of the tooth-top leakage permeance for a machine with interpoles.

tubes of force consist of a straight portion $b_0$ and two quadrants of a circle, as shown in Fig. 17–7. The permeance of such a tube per unit length is $dx/(b_0 + \pi x)$. Since the winding element lies close to the middle of the interpolar space during commutation, the integration has to be extended from $x = 0$ to $x = (\tau - b_p)/2$. This yields Eq. 17–25.

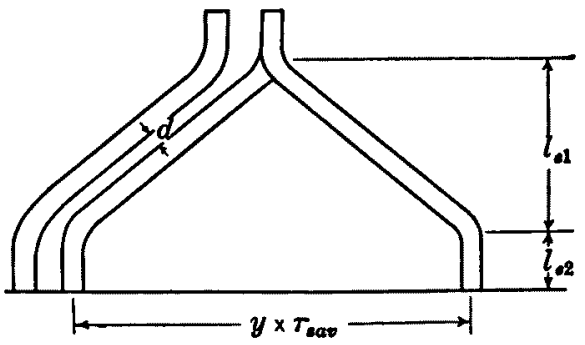


FIG. 17–9. Determination of the end-winding leakage.

In machines with interpoles, the tooth-top leakage flux depends upon the position of the slot with respect to the interpole. For the position shown in Fig. 17–9, the reluctance for the tooth-top leakage flux, per unit length of armature, is

$$\frac{g_i k_{ci}}{b_i/2 - (x + b_0/2)} + \frac{g_i k_{ci}}{b_i/2 + (x - b_0/2)} = 4g_i k_{ci} \frac{b_i - b_0}{(b_i - b_0)^2 - 4x^2}$$

and the permeance, per unit length,

$$\lambda_{tt,x}=\frac{1}{4g_ik_{ci}}\left[(b_i-b_0)-\frac{4x^2}{b_i-b_0}\right]$$

The average value is determined by integrating from $x=0$ to $x=(b_i-b_0)/2$ and dividing by $(b_i-b_0)/2$. This yields Eq. 17–26.

With Eqs. 17–25 and 17–26, the tooth-top leakage inductance *per coil side* becomes

$L_{tt}=0.4\pi N_c^2 l_s\lambda_{tt}\times 2.54\times 10^{-8}$ henry for machines without interpoles, and (17–27)

$L_{tt}=0.4\pi N_c^2 l_{si}\lambda_{tt}\times 2.54\times 10^{-8}$ henry for machines with interpoles (17–28)

where

$$l_{si}=\frac{l_i}{k_s} \tag{17–29}$$

$l_i$ is the length of the interpole and $k_s$ is given by Eq. 17–13.

Consider, as an example, conductor 1 in Fig. 17–5. Its tooth-top leakage inductance is given by Eq. 17–27 or Eq. 17–28. However, it is seen that there exists mutual induction from the other conductors 2, 3, 1′, 2′, and 3′ due to their tooth-top leakage fluxes. A current of one ampere in each of these five latter conductors produces the same tooth-top leakage flux as one ampere in conductor 1 produces. Hence, the coefficient of mutual inductance for the tooth-top leakage flux is equal to $L_{tt}$ as given by Eqs. 17–25 and 17–26.

While the mutual inductance due to the *slot* leakage flux is different for conductors lying in the same layer (Eq. 17–23) and conductors lying in the other layer (Eq. 17–24), the mutual inductance due to the tooth-top leakage flux is the same for conductors of both layers.

It should be noted that a winding element, for example element 1 in Fig. 17–5, is influenced also by the tooth-top leakage fluxes of the conductors lying in adjacent slots. The mutual inductance due to tooth-top leakage fluxes of adjacent slots will be taken into account by a 20% increase of the values obtained for self-inductance from the Eqs. 17–27 or 17–28.

**17–4. The End-Winding Leakage Fluxes.** With the symbols

$l_e$ = length of a coil end, i.e., average length of a half-turn minus gross core length
$\tau_c$ = commutator pitch
$b_b$ = brush width
$i$ = thickness of insulation between two commutator bars
$u$ = number of winding elements side by side in the slot
$\delta'$ = distance between two conductors in the same slot (Fig. 17–9)
$\delta''$ = distance between two conductors of two adjacent slots (Fig. 17–9)
$h_c$ = height of the conductor
$d_c$ = width of the conductor

$$b' = b_b - i + \left(1 - \frac{a}{p}\right)\tau_c \tag{17–30}$$

$$\delta_{av} = \frac{(u-1)\delta' + \delta''}{u} \tag{17–31}$$

The end-winding leakage self- *and* mutual inductance *per coil side* is given by the empirical formula

$$L_e = 0.4\pi N_c^2 \times 0.1 l_e \frac{b'}{\tau_c} \sqrt{\frac{l_e + \tau}{h_c + \frac{b'}{\tau_c}(d_c + \delta_{av}) - \delta_{av}}} \times 2.54 \times 10^{-8} \text{ henry} \tag{17–32}$$

Notice that this equation takes into account the mutual inductance from the end-windings of the conductors lying in the same slot as well as of those lying in adjacent slots.

## B. Time of Mutual Induction; Average Value of $(L + \Sigma M)$

**17–5. Standard (Non-split) Coil.** Consider again, as example, conducter 1 of Fig. 17–5. This conductor is influenced by mutual induction from the conductors 2, 3, 1′, 2′, and 3′. The time of mutual induction is not the same for these five conductors. In order to determine the average value of $(L + \Sigma M)$ for a winding element, the time of mutual induction by the other conductors must be known.

The *short-circuit time* is

$$T_c = \frac{b'}{v_c} \tag{17–33}$$

where $b'$ is given by Eq. 17–30. In Chap. 9, Eq. 9–2, the short-circuit time was defined as $T_c = \frac{b_b}{v_c}$ with $b_b$ being the brush width. This is corrent only for the lap winding $(a = p)$ and the simple wave winding $(a = 2)$ with only two brush studs. In both cases the short-circuit time is determined by a *single* brush and it is equal to the brush width $b_b$ divided by $v_c$ or, more accurate, if the insulation between the commutator bars (i) is taken into account, to $(b_b - i)/v_c$.

It has been mentioned in Art. 9–1 that, when the wave winding is provided with $p$ brush studs, as is usually the case, a winding element is short-circuited not only by a single brush but also by two consecutive brushes of same polarity. This adds, to the short-circuit time corresponding to one brush width $(b_b - i)$, the additional time $\left(1 - \frac{a}{p}\right)\tau_c$, as can be seen from Fig. 17–10 which is derived from Figs. 3–21 and 3–22. Fig. 17–10 refers to a simple wave winding with $a = 2$. The winding element $D$, in series with $\left(\frac{p}{2} - 1\right)$ winding

elements following it to the right, starts its short-circuit period produced by brush $A$. This brush will short-circuit the winding element $D$ until the edge $d$ of the commutator bar $b$ will reach the edge $d'$ of brush $A$. This time is given by the brush width $b_b - i$. After the short-circuit period by brush $A$ is finished, the commutator bar $a$ still lies under the brush $A$. At the same time the commutator bar $c$, to which the end of the winding element $D$ is connected,

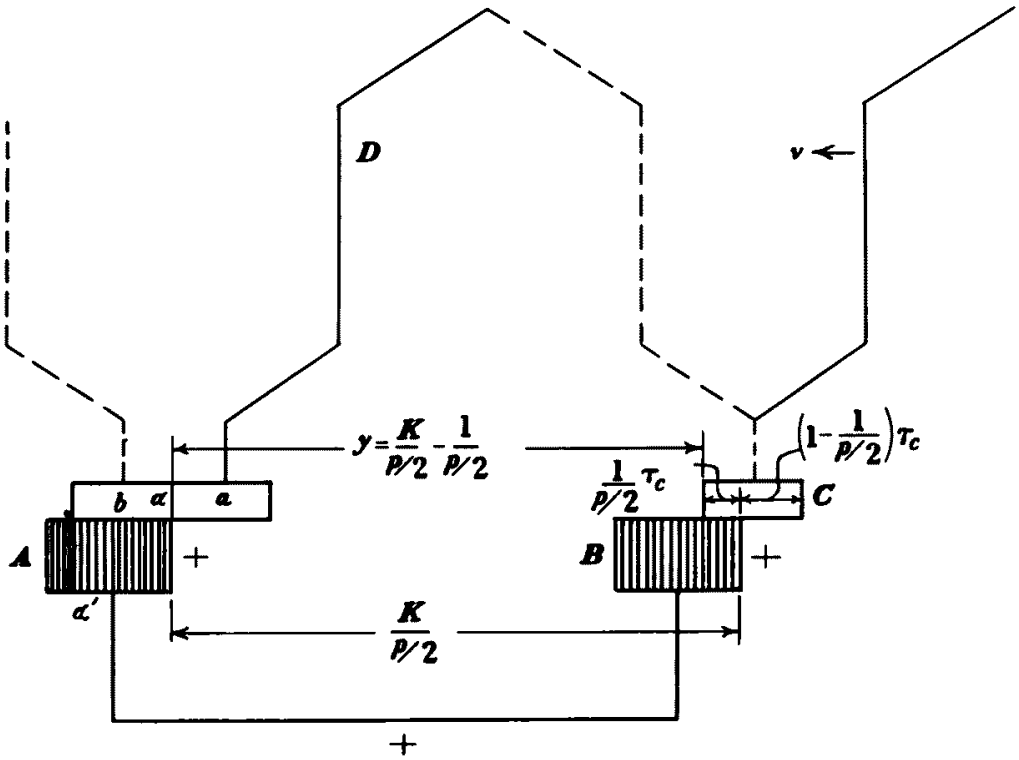


FIG. 17–10. Determination of the short-circuit time.

lies under the brush $B$. Since brush studs $A$ and $B$ are solidly connected, the winding element $D$, after having finished the short-circuit period by brush $A$, continues to be short-circuited by brushes $A$ and $B$ and normally during the time corresponding to

$$\tau_c\left(1-\frac{1}{p/2}\right)=\tau_c\left(1-\frac{2}{p}\right)$$

For the simple wave winding $a=2$, so that the additional short-circuit time can be written as $\tau_c\left(1-\frac{a}{p}\right)$. In this form the additional time applies also to the wave winding with $a$ larger than two (duplex and triplex wave winding), as can be seen from Figs. 3–22 and 3–26. Thus for the wave windings with $a$ parallel paths

$$T_c=\frac{b_b-i+\left(1-\frac{a}{p}\right)\tau_c}{v_c} \qquad (17\text{–}34)$$

Since for the lap winding $a = p$, Eq. 17–34 applies also to the lap winding and is general.

Since $v_c$ in Eq. 17–34 is a constant, the short-circuit time $T_c$ can be represented by the brush width $b'$. Then the times of mutual induction can be expressed as fractions of $b'$.

This can be best explained by an example. Consider a 4-pole lap winding in $Q = 18$ slots. The number of conductors per slot is 6, 3 in each layer ($u = 3$).

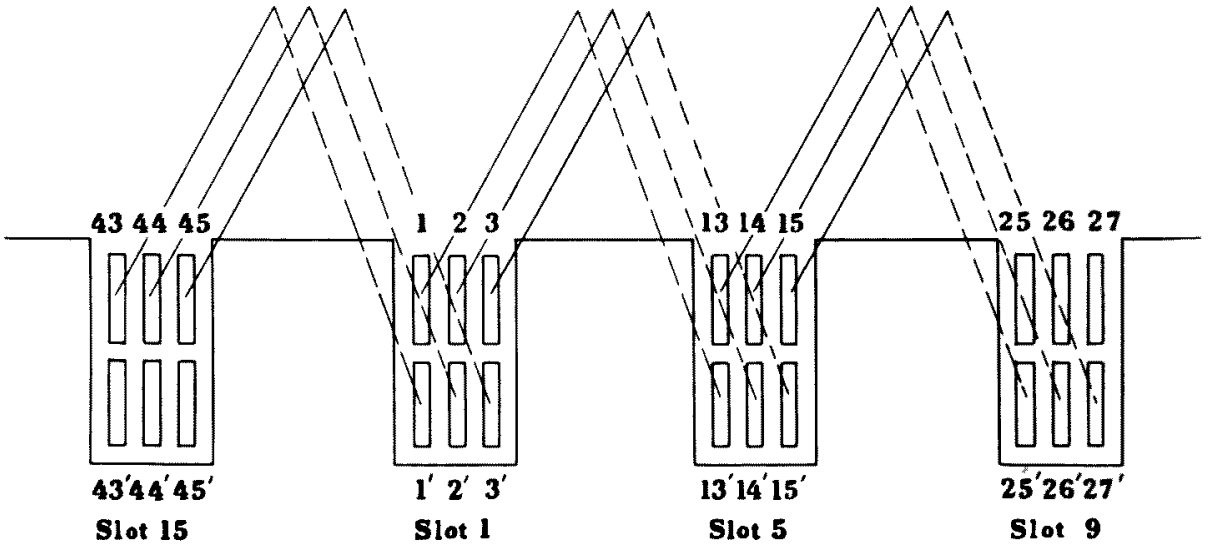


FIG. 17–11. Part of a 4-pole lap winding in 18 slots. $u = 3$, $y_b = 4$ slot pitches, $c = 1\frac{1}{2}$

The coil pitch ($y_b$) is chosen to be four slot pitches (from slot 1 to slot 5, Fig. 17–11). Therefore, the chording in slot pitches is

$$c = \frac{18}{4} - 4 = \frac{1}{2} \text{ slot pitch}$$

Since $u = 3$, the number of commutator bars is $Q \times u = 18 \times 3 = 54$. The coil width, $y_b$, which is equal to four slot pitches, can be measured also in *upper conductors* or *commutator bars*, since the sequence of the commutator bars is the same as that of the upper conductors. It is seen from Fig. 17–11 that $y_b$ is equal to 12 conductors, i.e., to 12 commutator pitches. Thus the chording expressed in commutator bars is

$$c = \frac{54}{4} - 12 = 1\frac{1}{2}$$

In general,

$$c = \frac{K}{p} - y_b \qquad (17\text{–}35)$$

Fig. 17–12 shows the connection to the commutator of some winding elements of the winding considered. The *numbering* of the conductors in Figs. 17–11 and 17–12 is chosen to go *clockwise* and the direction of *rotation* of the armature is chosen to be *counterclockwise*.

The times of mutual induction will be determined for one of the winding elements and, as such, the winding element 1-13′ will be chosen. The result obtained applies to all other winding elements.

Upper conductor 1 of the winding element in consideration is influenced by conductor 2, 3, 1′, 2′, and 3′. Its lower conductor 13′ is influenced by the conductors 14′, 15′, 13, 14, and 15.

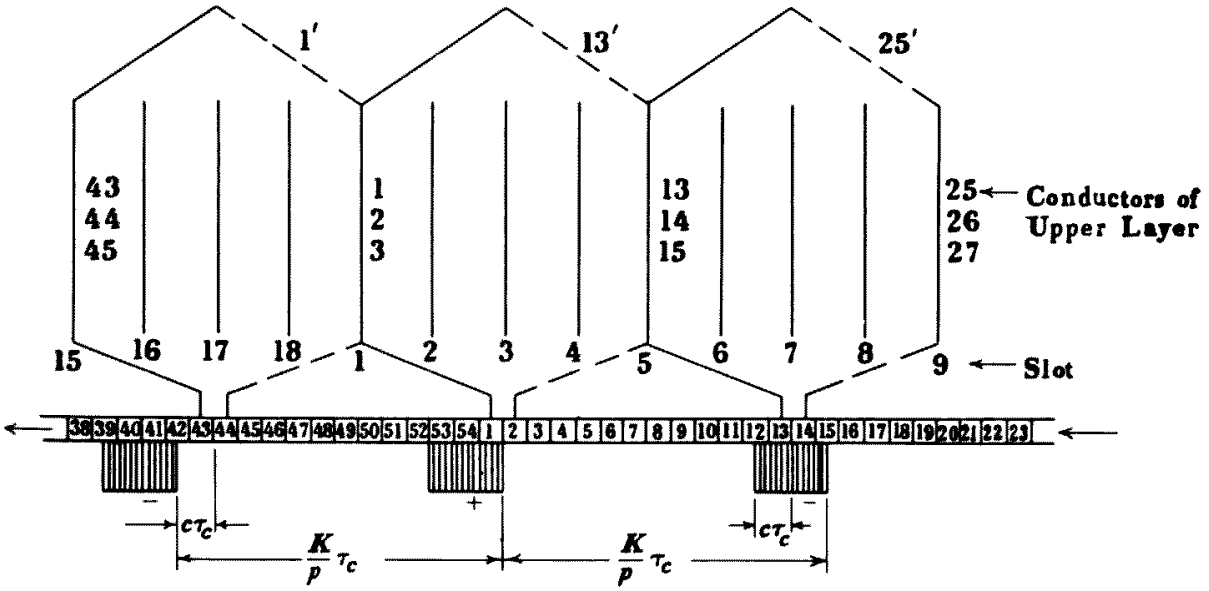


FIG. 17–12. Winding of Figure 17–11 with connections to commutator and bushes.

Since the armature moves to the left, the winding element 2-14′ will start its commutation period one commutator pitch (bar) later than winding element 1-13′ and winding element 3-15′ will start its commutation period two commutator pitches later than winding element 1-13′. If now in Fig. 17–13 the width of the rectangle 1-13′ is chosen equal to $b'$, then the rectangle for the winding element 2-14′ has to be placed the distance $\tau_c$ behind the rectangle 1-13′ and the rectangle for the winding element 3-15′ has to be placed $2\tau_c$ behind the rectangle 1-13′. All rectangles have the same length, since the short-circuit time is the same for all winding elements.

It can be seen from Fig. 17–11 that conductor 14 will start its commutation one commutator pitch later than conductor 13 and that conductor 15 will start its commutation two commutator pitches later than conductor 13. The same applies to conductor 2′ and 3′ with respect to conductor 1′. Thus it remains to determine in Fig. 17–13 the time position of conductors 1′ and 13, in order to complete it.

If the winding was not chorded, then the coil span ($y_b$) 1′-43 would be equal to $\tau$. Since the distance between consecutive brushes also is equal to $\tau$, conductor 1 and conductor 43 would start their commutation at the same instant. Since the winding is chorded by the amount $c\tau_c$, conductor 43 is moved clockwise towards conductor 1 by this distance and, for the assumed

counterclockwise rotation of the armature, will start its commutation $c\tau_c$ later than conductor 1. Accordingly, conductor 1′ appears in Fig. 17–13 $c\tau_c$ behind conductor 1.

If the winding was not chorded, then the distance 13′-1 would be equal to $\tau$ and conductor 13 would start its commutation simultaneously with conductor 1. Since the winding is chorded 13′ and 13 are moved counterclockwise towards conductor 1. Since the armature also moves counterclockwise, conductor 13′ will start its commutation $c\tau_c$ earlier than conductor 1. This is shown in Fig. 17–13.

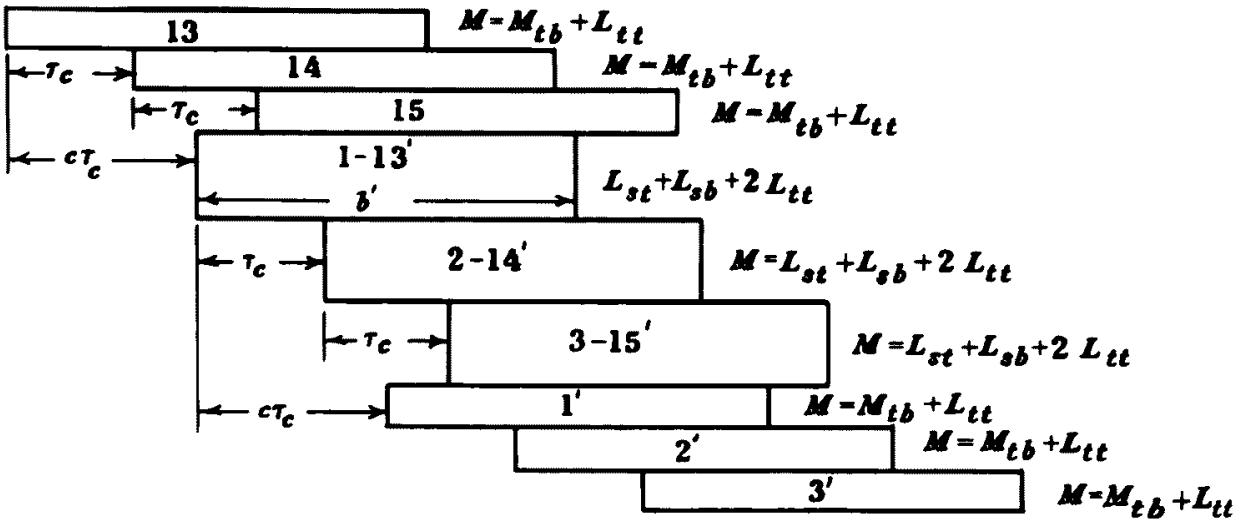


FIG. 17–13. Times of self- and mutual-induction of the winding of Fig. 17–11.

To the right of winding element 1-13′ is given its self-inductance due to the slot-leakage flux, $L_{st}+L_{sb}$, according to Eqs. 17–16 and 17–18, and its self-inductance due to the tooth-top leakage flux, $2L_{tt}$, according to Eq. 17–27 or 17–28.

It has been explained previously that the mutual-inductance between a conductor which lies in the same layer as the conductor in consideration and this latter conductor is equal to the self-inductance of this conductor considered; i.e., the mutual inductance between the winding elements 2-14′ and 1-13′ and also between the winding elements 3-15′ and 1-13′ is equal to the self-inductance of winding element 1-13′. For this reason, to the right of winding elements 2-14′ and 3-15′ the quantities are given as for winding element 1-13′.

The mutual inductance between conductor 1′ and conductor 1 is given by the sum $M_{tb}+L_{tt}$ (Eqs. 17–21 and 17–27 or 17–28). The same is true of the mutual inductance between conductors 2′ and 3′ and conductor 1 and also between conductors 13, 14, and 15 and conductor 13′, i.e., the six conductors 1′, 2′, 3′, 13, 14, and 15 have the same value of $M$. This is shown in Fig. 17–13.

Fig. 17–13 shows the time relations between the winding elements undergoing commutation and the coefficients of self- and mutual inductance due

to slot leakage fluxes and tooth-top leakage fluxes. The considerations which led to this figure are summarized in Table 17–1. Comparing this Table with Fig. 17–13, it is seen that, for practical calculations, it is necessary to fill in only columns *a*, *d*, *e*, and *f*. The average value of $(L+\Sigma M)$ of the winding element considered for the commutation period $b'$ is then obtained from the following equation:

$$(L+\Sigma M)_{av}=\left[1+(u-1)-\frac{(u-1)u}{2}\times\frac{\tau_c}{b'}\right](L_{st}+L_{sb}+2L_{tt})+\left[2u-\Sigma\mid d\mid\frac{\tau_c}{b'}\right](M_{tb}+L_{tt}) \qquad (17\text{–}36)$$

$\Sigma\mid d\mid$ means the sum of the *absolute* values of all quantities contained in column *d* for parts *B* and *C*, except those terms for which $\mid d\mid\tau_c>b'$. This will be explained later in an example.

Table 17–1 and Eq. (17–36) derived from it apply to lap as well as to wave windings with standard non-split coils. Notice that Table 17–1 is based on clockwise numbering of the slots and commutator segments and on counter-clockwise rotation of the armature.

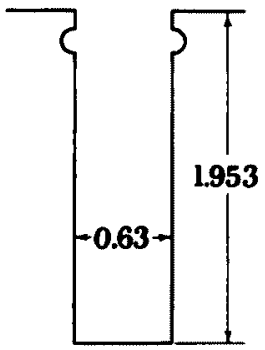


FIG. 17–14. 10-pole lap winding in 155 slots. Slot dimensions.

**17–6. Example of Calculation of $(L+\Sigma M)_{av}$.** The method of calculation described above will be illustrated by an example of a 10-pole lap winding in $Q=155$ slots. There are two conductors per layer, i.e., $u=2$, $K=310$, $N_e=1$. The coil pitch $y_b$ is equal to 15 slot pitches $=30$ commutator pitches. The chording is (Eq. 17–35)

$$c=\frac{310}{10}-30=1 \text{ commutator pitch}$$

The brush covers 3.25 commutator pitches ($b_b=3.25\tau_c$). Since $a=p$, from Eqs. 17–33 and 17–34 with i neglected,

$$b'\approx b_b=3.25\tau_c$$

Armature diameter = 66 in. Number of air vents = 5
Core length = 16 in. Width of an air vent = $\frac{3}{8}$ in.

Length of the interpole = $15\frac{1}{2}$ in.
Average width of interpole = 1.75 in.
Interpole-gap = 0.5 in.
The slot dimensions are given in Fig. 17–14.
Conductor dimensions: $h_c=0.75$ in., $d_c=0.25$ in.

Vent pitch $\tau_v=\dfrac{L+b_v}{n_v}=\dfrac{16+0.375}{6}=2.73$ in.

TABLE 17–1

| *a* Mutual induction by winding element or conductor | | *b* To consider upper conductor | *c* Distance of *b* from conductor 1 | *d* Distance *c* minus 0 for *A* and minus $K/p$ for *B* and *C* | *e* Commutation Starts | *f* Value of *M* | *g* Equations for *M* |
|---|---|---|---|---|---|---|---|
| *A* | | | | | | | |
| Winding elements lying in both layers side by side with the winding element considered | $2 \rightarrow (2+y_b)'$ | 2 | $1r$ | $+1r$ | $\tau_c$ later | $L_{st}+L_{sb}+2L_{tt}$ | (17–16) |
| | $3 \rightarrow (3+y_b)'$ | 3 | $2r$ | $+2r$ | $2\tau_c$ later | | (17–18) (17–27) |
| | $u \rightarrow (u+y_b)'$ | $u$ | $(u-1)r$ | $+(u-1)r$ | $(u-1)\tau_c$ later | | (17–28) |
| *B* | | | | | | | |
| Upper conductors lying to the right of conductor 1 in slot $1+y_{bs}$* | $1+y_b$ | $1+y_b$ | $y_b \quad r$ | $-c \quad r$ | $-c\tau_c \quad r$† | $M_{tb}+L_{tt}$ | (17–21) |
| | $2+y_b$ | $2+y_b$ | $(1+y_b)r$ | $(-c+1)r$ | $(-c+1)\tau_c \quad r$† | | (17–27) |
| | $u+y_b$ | $u+y_b$ | $[(u-1)+y_b]r$ | $[-c+(u-1)]r$ | $(-c+u-1)\tau_c \quad r$† | | (17–28) |
| *C* | | | | | | | |
| Lower conductors lying in same slot as conductor 1 | $1'$ | $1+K-y_b$ | $y_b \quad l$ | $-c \quad l$ | $-c\tau_c \quad l$† | $M_{tb}+L_{tt}$ | (17–21) |
| | $2'$ | $2+K-y_b$ | $(y_b-1)l$ | $(-c-1)l$ | $(-c-1)\tau_c \quad l$† | | (17–27) |
| | $u'$ | $u+K-y_b$ | $[y_b-(u-1)]l$ | $[-c-(u-1)]l$ | $(-c-u+1)\tau_c l$† | | (17–28) |

* $y_{bs}$=back pitch in slot pitches; $y_b$=back pitch in commutator pitches

† A positive quantity means later for $r$, earlier for $l$;
a negative quantity means earlier for $r$ later for $l$.

From Eq. 17–13

$$k_s=\frac{2.73(5\times 0.63+2\times 0.375)}{2.73(5\times 0.63+2\times 0.375)-2\times 0.375^2}=1.03$$

From Eq. (17–14)

$$l_s=\frac{16}{1.03}=15.55 \quad l_{si}=\frac{15.5}{10.3}=15.05$$

From Eqs. 17–15, 17–17, and 17–22, with $b=b_s$,

$$\lambda_{st}=\frac{0.796}{3\times 0.63}+\frac{0.211}{0.63}=0.756$$

$$\lambda_{sb}=\frac{0.796}{3\times 0.63}+\frac{0.055+0.819+0.211}{0.63}=2.14$$

$$\lambda_{tb}=\frac{0.796}{2\times 0.63}+\frac{0.211}{0.63}=0.968$$

From Eq. 16–7, the Carter factor for the interpole,

$$\tau_s=\frac{\pi\times 66}{155}=1.335, \quad k_{ci}=\frac{1.335(5\times 0.5+0.63)}{1.335(5\times 0.5+0.63)-0.63^2}=1.105$$

and from Eq. 17–26

$$\lambda_{tt}=0.5\,\frac{1.75+2\times 0.5-0.63}{3\times 1.105\times 0.5}=0.64$$

Adding 20% to the tooth-top leakage, in order to take into account the influence of adjacent slots (see Art. 17–2), the total permeance for the self-inductance is (see Eq. 17–28)

$$\Lambda_{st}+\Lambda_{sb}+2\Lambda_{tt}=15.55\left(0.756+2.14+2\times 1.2\times\frac{15.05}{15.55}\times 0.64\right)=68.2$$

The total permeance for the mutual inductance between conductors of different layers is

$$\Lambda_{bt}+\Lambda_{tt}=15.55\left(0.968+\frac{15.05}{15.55}\times 0.64\right)=24.8$$

From Eqs. 17–16, 17–18, and 17–28, with $N_e=1$,

$$L_{st}+L_{sb}+2L_{tt}=0.4\pi\times 68.2\times 2.54\times 10^{-8}=217.5\times 10^{-8}\text{ henry}$$

and from Eqs. 17–21 and 17–28,

$$M_{bt}+L_{tt}=0.4\pi\times 24.8\times 2.54\times 10^{-8}=79.1\times 10^{-8}\text{ henry}$$

Table 17–1 becomes for the winding in consideration as shown in Table 17–2. The reference winding element is 1→31′.

TABLE 17–2

| *a* | *d* | *e* | Value of $M \times 10^8$ |
|---|---|---|---|
| *A* | | | |
| 2→32′ | $+1r$ | $\tau_c$ later | 217.5 |
| *B* | | | |
| 31 | $-1r$ | $\tau_c$ earlier | 79.1 |
| 32 | $0r$ | simultaneous | 79.1 |
| *C* | | | |
| 1′ | $-1l$ | $\tau_c$ later | 79.1 |
| 2′ | $-2l$ | $2\tau_c$ later | 79.1 |

The time relations and values of $M$ of Table 17–2 are represented in Fig. 17–15. Adding up $L$ and the $M$'s for winding element 1-31′, 4 regions are

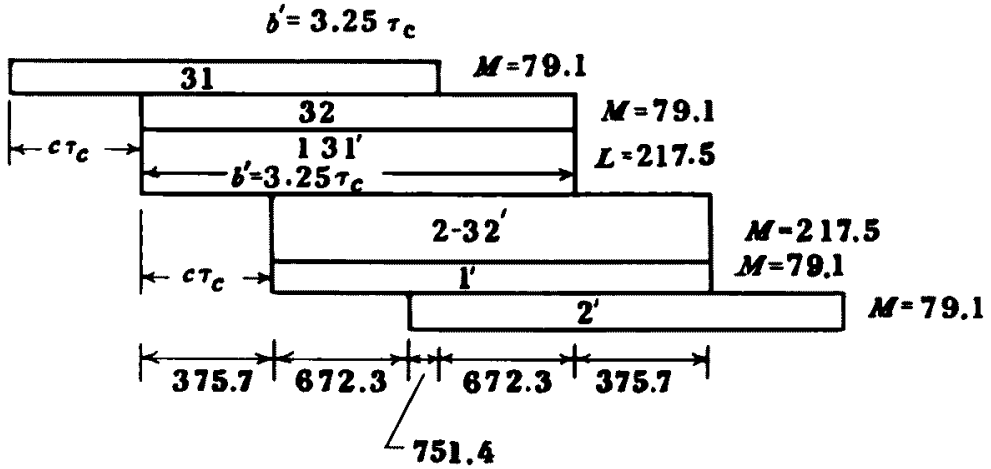


FIG. 17–15. Time relations and values of $L$ and $M$ for the 10-pole lap winding.

obtained the values of which are given at the bottom of Fig. 17–15. The average value for $(L + \Sigma M)$ is

$$\frac{(375.7 + 672.3 + 0.25 \times 751.4 + 672.3)\tau_c}{3.25\tau_c} = 587$$

This figure refers to the slot and tooth top leakage fluxes only. The total average permeance is obtained by adding to this figure $2L_e$, i.e., the self-

and mutual inductance of the end-winding leakage (Eq. 17–32). There is

$$\tau_c = 0.41'' \quad b' = 1.33 - 0.04 = 1.29 \quad l_e = 28.5 \quad \tau = 20.7$$

$$\delta' = \frac{0.63}{2} - 0.25 = 0.065 \quad \delta'' = 0.065 + 0.125 = 0.19$$

$$\delta_{av} = \frac{(2-1)(0.065+0.19)}{2} = 0.127$$

$$2L_e = 2 \times 0.4\pi \times 0.1 \times 28.5 \frac{1.29}{0.41} \times \sqrt{\frac{28.5+20.7}{0.75+\frac{1.29}{0.41}(0.25+0.127)-0.127}} \times 2.54 \times 10^{-8}$$

$$= 298 \times 10^{-8} \text{ henry}$$

and, therefore,

$$(L + \Sigma M)_{tot,av} = (587 + 298)10^{-8} = 885 \times 10^{-8} \text{ henry}$$

It can be seen, from Fig. 17–15, that the same result is obtained for the winding element 2-32′. If $u > 2$, then $(L + \Sigma M)$ is not necessarily the same for all winding elements lying side by side in both layers. For the example of Art. 17–5 with $u = 3$, the same value of $(L + \Sigma M)$ is obtained for the winding elements 1-13′ and 3-15′, but a different value is obtained for the winding element 2-14′. In this case $(L + \Sigma M)$ is to be calculated for each of the $u$ winding elements separately and the average value determined. To this latter average value, $2L_e$ is then to be added.

Checking the value obtained for winding element 1-31′ from Fig. 17–15 with Eq. 17–36, we have

$$(L + \Sigma M)_{av} = \left(1 + 1 - \frac{1}{3.25}\right) 217.5 \times 10^{-8} + \left(4 - 4 \times \frac{1}{3.25}\right) 79.1 \times 10^{-8}$$

$$= 587 \times 10^{-8} \text{ henry}$$

**17–7. Split Coils.** Fig. 17–16 refers to a split-coil, 4-pole, lap winding in $Q = 14$ slots. $u = 3$, $K = 42$. The back pitch is equal to 3 and 4 slot pitches but equal to 10 upper conductors, i.e., to 10 commutation bars.

Winding elements 1-11′ and 2-12′ lie all along together. Winding element 3-13′ lies only in slot 1 together with winding elements 1-11′ and 2-12′. Its lower conductor, 13′, does not lie in the slot in which conductors 11′ and 12′ lie, because of splitting of the coils. The mutual inductance between winding elements 1-11 and 3-13′ is, therefore, different from that between winding elements 1-11′ and 2-12′.

The value of $(L + \Sigma M)$ will be different for the short winding elements

1-11′, 2-12′ than for the long winding element 3-13′. The short winding elements will be considered first.

(a) *Short Winding Elements.* The $(L+\Sigma M)_{av}$ of the winding element 1-11′ will be determined. The value of $L$ for this winding element is determined

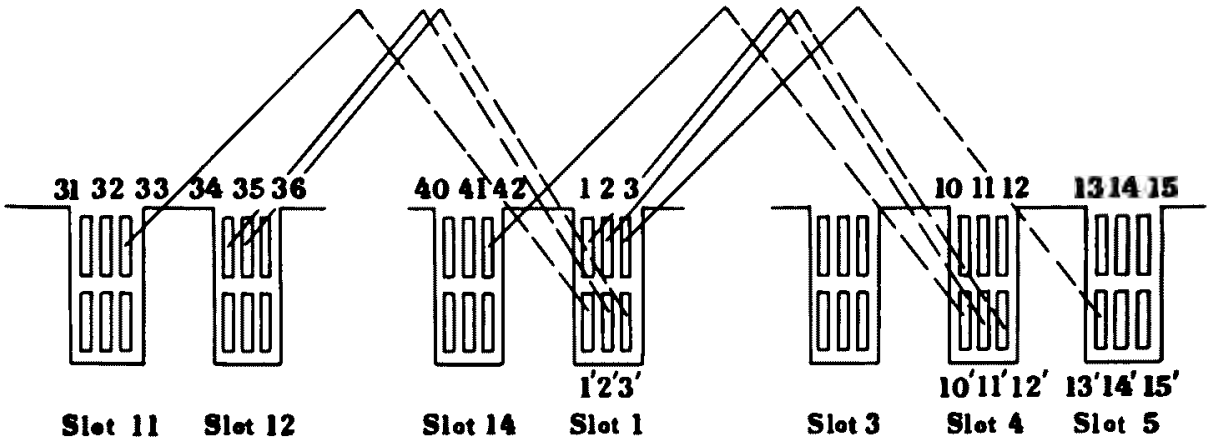


Fig. 17–16. Part of a 4-pole lap winding with split coils. $Q=14$, $u=3$, $K=42$.

by Eqs. 17–16, 17–18, and 17–27 or 17–28 ($L=L_{st}+L_{sb}+2L_{tt}$). It is influenced by mutual induction from the

| | |
|---|---|
| winding element . . . 2-12′ | upper conductor . . . . . 3 |
| lower conductors . . 1′, 2′, 3′ | lower conductor . . . . . 10′ |
| upper conductors . . 10, 11, 12 | |

The mutual inductance due to winding element 2-12′ is equal to $L$ of the winding element considered. The mutual inductance due to conductors 1′, 2′, 3′, 10, 11, and 12 is, as before, equal to

$$M_{tb}+L_{tt}$$

where $M_{tb}$ is given by Eq. 17–21 and $L_{tt}$ by Eq. 17–27 or 17–28. The mutual inductance due to upper conductor 3 is

$$L_{st}+L_{tt}$$

where $L_{st}$ is given by Eq. 17–16, and the mutual inductance by the lower conductor 10′ is

$$L_{sb}+L_{tt}$$

where $L_{st}$ is given by Eq. 17–18.

It is now necessary to determine the times of mutual induction. This can be done by a table similar to Table 17–1, as shown below in Table 17–3. The graphical representation of the time relations of this Table is given in Fig. 17–17.

(b) *Long Winding Element.* This winding element is influenced by mutual induction from the

| | |
|---|---|
| upper conductors . . 1 and 2 | lower conductors . . . 1′, 2′, 3′ |
| upper conductors . . 13, 14, 15 | lower conductors . . . 14′, 15′ |

TABLE 17–3. SHORT WINDING ELEMENTS (1–11 and 2–12)

| *a* Mutual induction by winding element or conductor | | *b* To consider upper conductor | *c* Distance of *b* from conductor 1 | *d* Distance *c* minus 0 for *A*, *D*, and *E* and minus $K/p$ for *B* and *C* | *e* Commutation starts | *f* Value of *M* | *g* Equations for *M* |
|---|---|---|---|---|---|---|---|
| *A* Winding elements lying in both layers side by side with winding elem. 1–11′ | 2–12′ | 2 | $1r$ | $+1r$ | $\tau_c$ later | $L_{st}+L_{sb}+2L_{tt}$ | (17–16) (17–18) (17–27) (17–28) |
| *B* Upper conductors lying to the right of winding elem. 1–11′ but not in the same slot | 10<br>11<br>12 | 10<br>11<br>12 | $9r$<br>$10r$<br>$11r$ | $9-\frac{42}{4}=-1.5r$<br>$-0.5r$<br>$+0.5r$ | $1.5\,\tau_c$ earlier<br>$0.5\,\tau_c$ earlier<br>$10.5\,\tau_c$ later | $M_{tb}+L_{tt}$ | (17–21) (17–27) (17–28) |
| *C* Lower conductors lying in the same slot as conductor 1 | 1′<br>2′<br>3′ | 33<br>34<br>35 | $1+42-33=10l$<br>$9l$<br>$8l$ | $10-\frac{42}{4}=-0.5l$<br>$-1.5l$<br>$-2.5l$ | $0.5\,\tau_c$ later<br>$1.5\,\tau_c$ later<br>$2.5\,\tau_c$ later | $M_{tb}+L_{tt}$ | (17–21) (17–27) (17–28) |
| *D* Upper conductors lying side by side with conductor 1, in the same slot | 3 | 3 | $2r$ | $+2r$ | $2\,\tau_c$ later | $L_{st}+L_{tt}$ | (17–16) (17–27) (17–28) |
| *E* Lower conductors lying side by side with conductor 11′, in the same slot | 10′ | 42 | $1+42-42=1l$ | $+1l$ | $\tau_c$ earlier | $L_{sb}+L_{tt}$ | (17–18) (17–27) (17–28) |

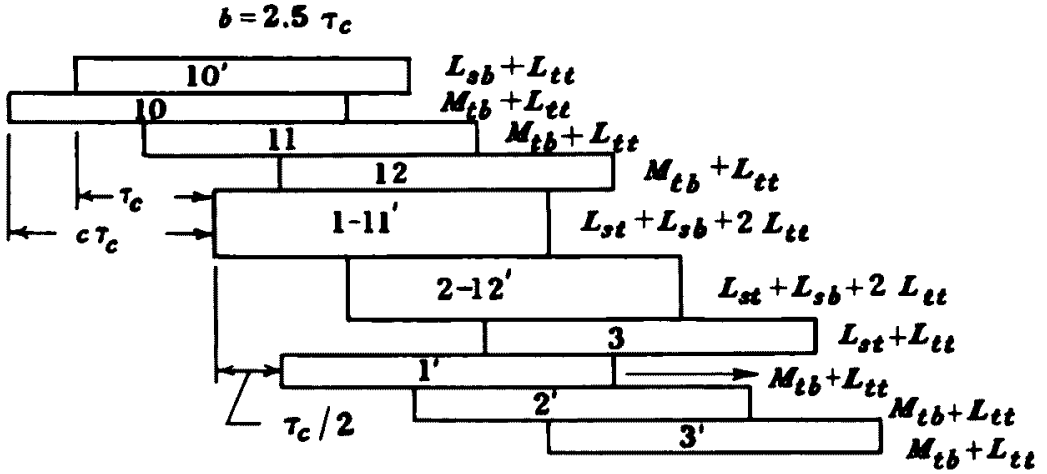


FIG. 17–17. Time relations for the short winding elements of the winding Fig. 17–16.

The mutual inductance between the long winding element 3-13′ and upper conductors 1 and 2 is equal to $L_{st}+L_{tt}$ and is determined by Eqs. 17–16 and 17–27 or 17–28. The mutual inductance due to conductors 13, 14, 15, 1′, 2′, and 3′ is equal to $(M_{tb}+L_{tt})$ and is determined by Eqs. 17–21 and 17–27 or

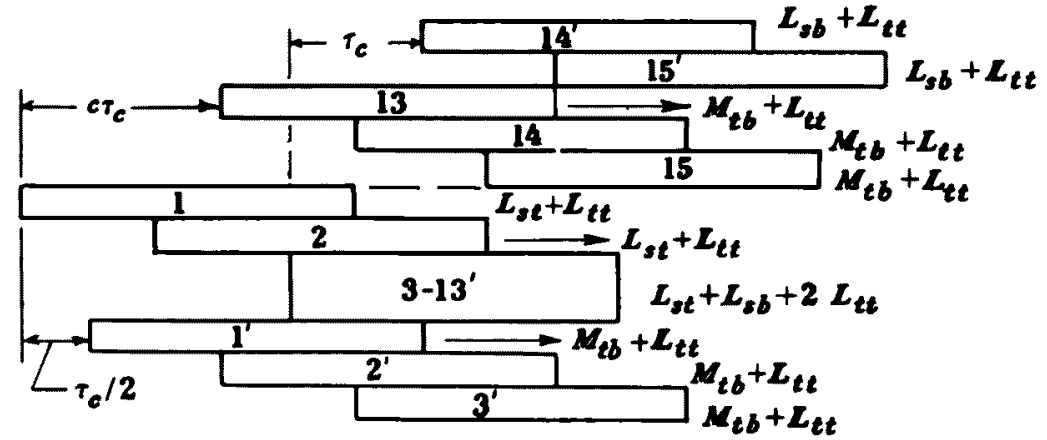


FIG. 17–18. Time relations for the long winding elements of the winding Fig. 17–16.

17–28. The mutual inductance due to the lower conductors 14′ and 15′ is equal to $L_{sb}+L_{tt}$, where $L_{sb}$ is given by Eq. 17–18.

The time relations are shown in Table 17–4 and Fig. 17–18.

**17–8. Comparison Between Not-chorded Standard Coil, Chorded Standard Coil, and Split Coil.** For comparison, the time relations and the change of $(L+\Sigma M)$ as a function of time have been calculated for a low-speed machine with the following data:

20 poles, $a=p=20$, $b'=4.5\tau_c$,

$Q=330$, $u=3$, $K=990$ for the chorded standard winding and split-coil winding; $Q=320$, $u=3$, $K=960$ for the standard not-chorded winding.

| *a* Mutual induction by winding element or conductor | | *b* To consider upper conductor | *c* Distance of *b* from conductor 1 | *d* Distance *c* minus 0 for *A*, *D*, and *E* and minus $K/p$ for *B* and *C* | *e* Commutation starts | *f* Value of $M$ | *g* Equations for $M$ |
|---|---|---|---|---|---|---|---|
| *A*<br>Winding elements lying in both layers side by side with winding element 3–13′ | — | — | — | — | — | — | — |
| *B*<br>Upper conductors lying to the right of winding element 3–13′ but not in the same slot | 13<br>14<br>15 | 13<br>14<br>15 | $12r$<br>$13r$<br>$14r$ | $12-\frac{42}{4}=+1.5r$<br>$+2.5r$<br>$-3.5r$ | $1.5\,\tau_c$ later<br>$2.5\,\tau_c$ later<br>$3.5\,\tau_c$ later | $M_{tb}+L_{tt}$ | (17–21)<br>(17–27)<br>(17–28) |
| *C*<br>Lower conductors lying in the same slot as conductor 3 | 1′<br>2′<br>3′ | 33<br>34<br>35 | $1+42-33=10l$<br>$9l$<br>$8l$ | $10-\frac{42}{4}=-0.5l$<br>$-1.5l$<br>$-2.5l$ | $0.5\,\tau_c$ later<br>$1.5\,\tau_c$ later<br>$2.5\,\tau_c$ later | $M_{tb}+L_{tt}$ | (17–21)<br>(17–27)<br>(17–28) |
| *D*<br>Upper conductors lying side by side with conductor 3, in the same slot | 1<br>2 | 1<br>2 | 0<br>$1r$ | 0<br>$+1r$ | $\tau_c$ later | $L_{st}+L_{tt}$ | (17–16)<br>(17–27)<br>(17–28) |
| *E*<br>Lower conductors lying side by side with conductor 13′, in the same slot | 14′<br>15′ | 4<br>5 | $3r$<br>$4r$ | $+3r$<br>$+4r$ | $3\,\tau_c$ later<br>$4\,\tau_c$ later | $L_{sb}+L_{tt}$ | (17–18)<br>(17–27)<br>(17–28) |

For the standard winding, back pitch = 16 slot pitches = 48 commutator pitches. Chording $c$, therefore,

$$c = \frac{960}{20} - 48 = 0, \quad \text{standard not chorded winding}$$

$$c = \frac{990}{20} - 48 = 1.5\tau_c, \quad \text{standard chorded winding}$$

The arrangement of the split-coil winding is shown in Fig. 17–19.

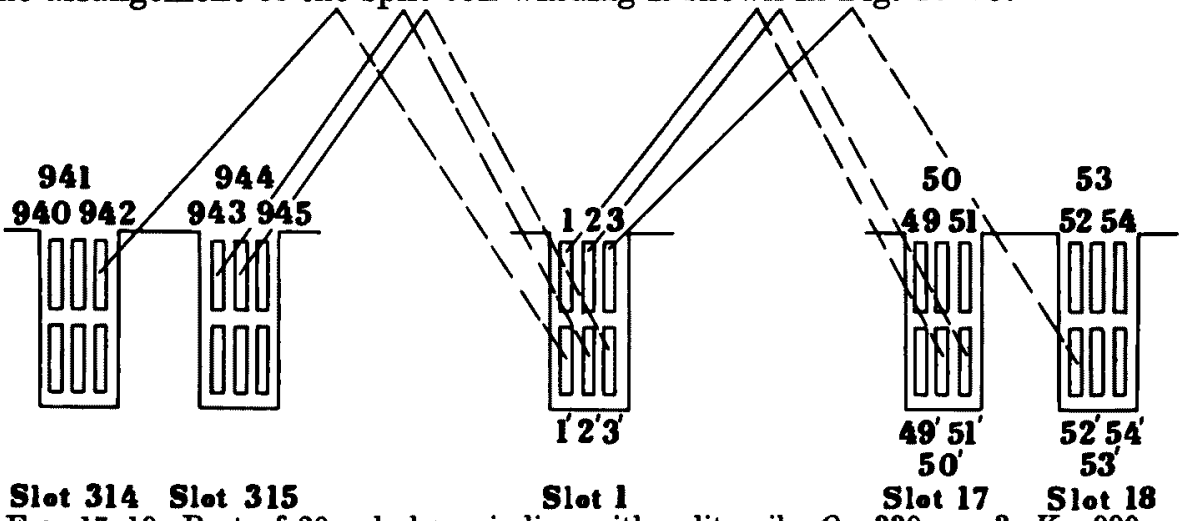


FIG. 17–19. Part of 20-pole lap winding with split coils. $Q = 330$, $u = 3$, $K = 990$.

It is assumed that the coefficient of self-inductance of a winding element $(L_{st} + L_{sb} + 2L_{tt})$ is equal to 100. Then for the machine considered

$$M_{bt} + L_{tt} = 35, \quad L_{st} + L_{tt} = 30 \quad \text{and} \quad L_{sb} + L_{tt} = 70$$

The time relations for the three types of windings and the variation of

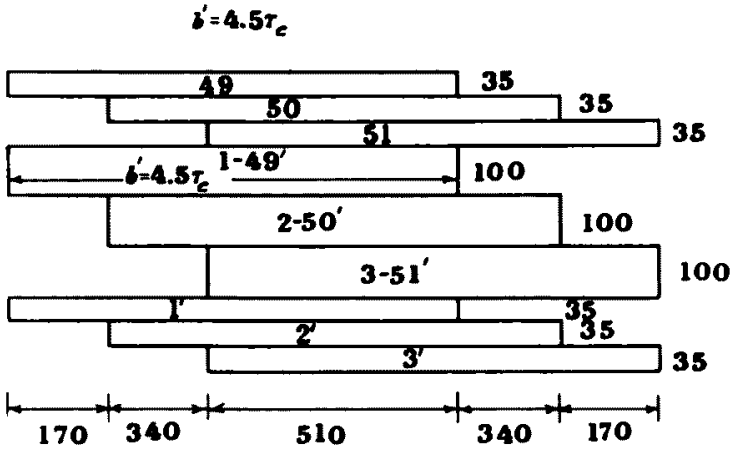


FIG. 17–20. Time relations and values of $L$ and $M$ for a 20-pole not chorded lap winding in 320 slots. $u = 3$, $K = 960$.

$(L + \Sigma M)$ as a function of time for the three winding elements is shown in Figs. 17–20 to 17–25. It is seen that the peak value of $(L + \Sigma M)$ is larger for

the standard not-chorded winding than for the standard chorded winding. Also the average value of $(L + \Sigma M)$ for the three coils is smaller for chorded winding.

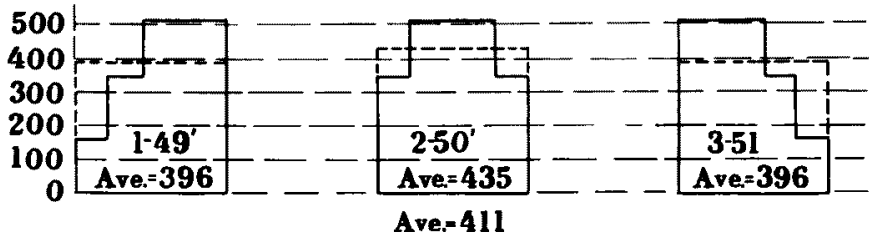


FIG. 17–21. $(L + \Sigma M)$ for the 3 winding elements of Fig. 17–20.

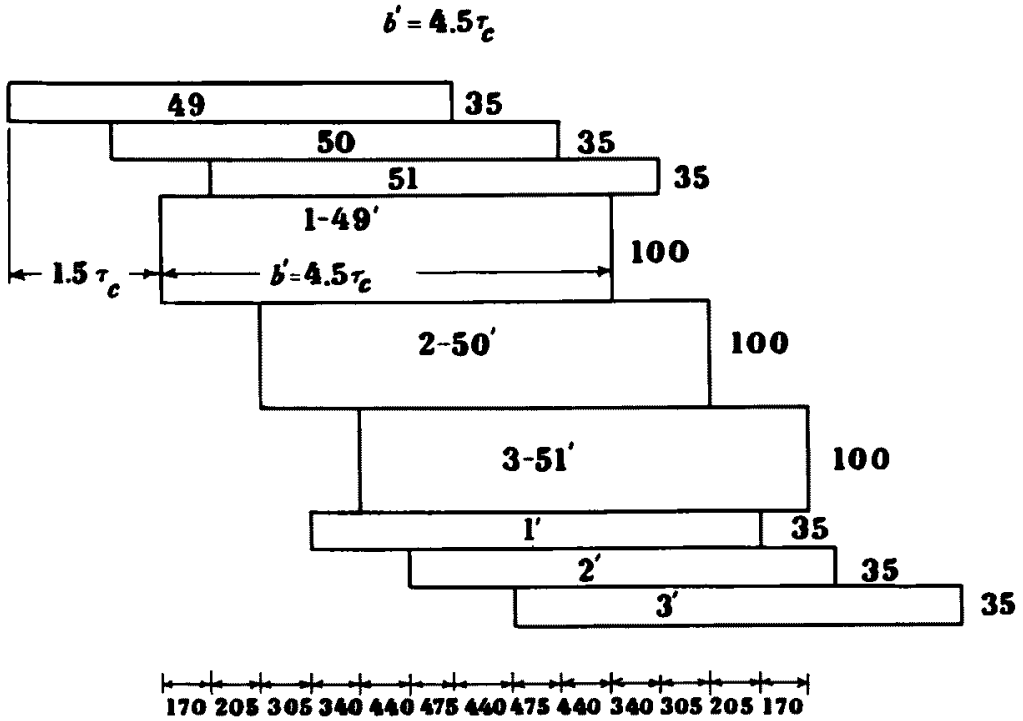


FIG. 17–22. Time relations and values of $L$ and $M$ for a 20-pole chorded lap winding in 330 slots. $u = 3$, $K = 990$.

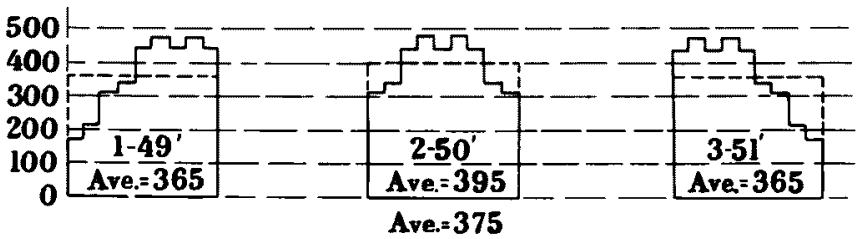


FIG. 17–23. $(L + \Sigma M)$ for the 3 winding elements of Fig. 17–22.

It is further seen from Figs. 17–20 to 17–25 that the variation of $(L + \Sigma M)$ during the commutation period is smaller for the split-coil winding than for the standard winding. A further advantage of the split-coil winding is that it often has a shorter commutation time for *all conductors of a slot*, i.e., a smaller

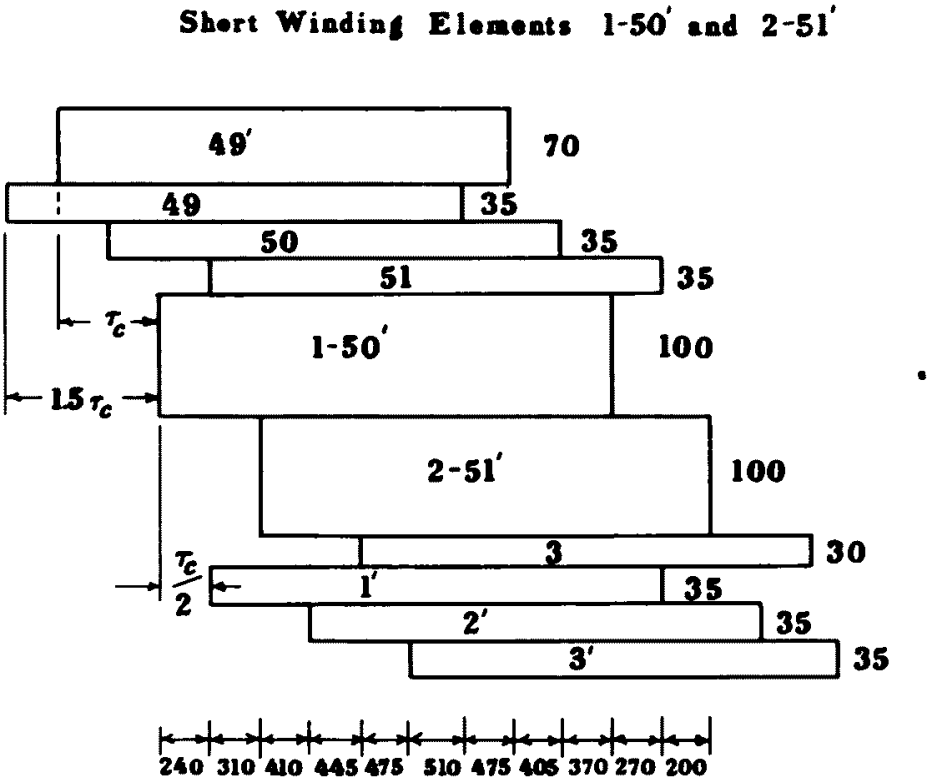


FIG. 17–24. Time relations and values of $L$ and $M$ for the long winding elements of the winding Fig. 17–19.

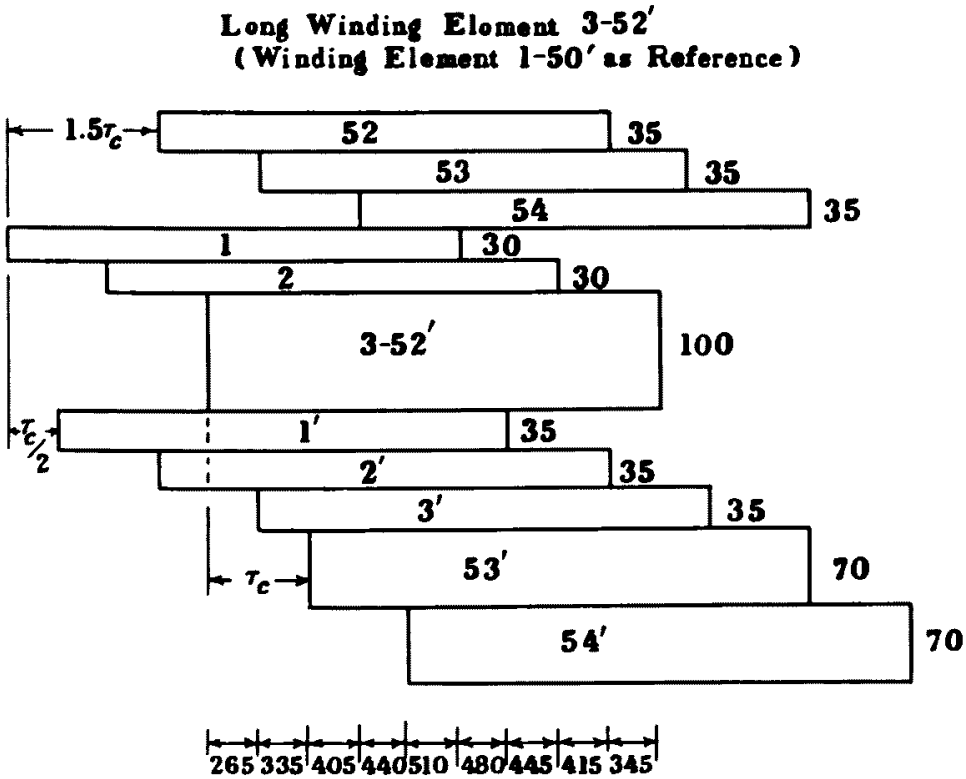


FIG. 17–24a. Time relations and values of $L$ and $M$ for the short winding elements of the winding Fig. 17–19.

width of the interpole zone (see Art. 17–10) than the standard winding. For the machine under consideration this total time is $b' + 2\tau_c + 1.5\tau_c$ for the standard chorded winding (Fig. 17–22) and $b' + 2\tau_c + 0.5\tau_c$ for the split-coil winding (Fig. 17–24a).

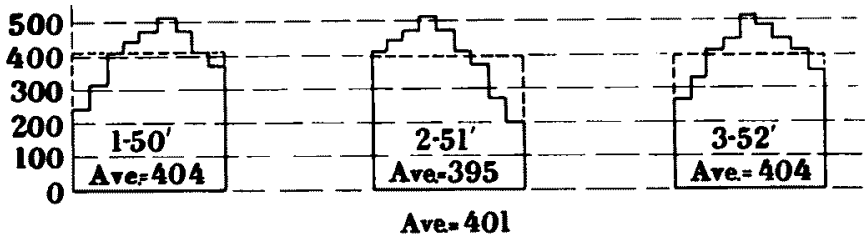


FIG. 17–25. $(L + \Sigma M)$ for the 3 winding elements of Fig. 17–19.

## C. AVERAGE EMF OF THE SHORT-CIRCUITED WINDING ELEMENT DUE TO LEAKAGE FLUXES. INTERPOLE AT.

**17–9. Reactance Voltage.** With $(L + \Sigma M)$ determined in the manner explained in Arts. 17–6 and 17–7, the emf induced in the short-circuited winding element by the leakage fluxes (often called *reactance* voltage) is (see Eq. 9–19)

$$e_r = \frac{2i_a}{T_c}(L + \Sigma M)_{\text{tot. av}} \tag{17–37}$$

where $i_a = \dfrac{I_a}{a}$ and $T_c = \dfrac{b'}{v_c}$ (Eq. 17–34).

If in the latter equation $b'$ is measured in inches, $v_c$ must be expressed in in./sec. Introducing the peripheral velocity of the armature $v_a$ in ft/min, we have

$$T_c = \frac{b'}{v_a \dfrac{D_c}{D}\dfrac{12}{60}} = \frac{5b'}{v_a}\frac{D}{D_c}$$

and

$$e_r = 0.4\frac{I_a}{a}\frac{v_a}{b'}\frac{D_c}{D}(L + \Sigma M)_{\text{tot. av}} \text{ volts} \tag{17–38}$$

The motor treated in Art. 17–6 has the following data: 2500 hp,

$$(L + \Sigma M)_{\text{tot. av}} = 885 \times 10^{-8} \text{ henry},$$

$$v_a = \frac{\pi \times 66 \times 514}{12} = 8870 \text{ ft/min}$$

Thus

$$e_r = 0.4 \times \frac{3290}{10}\frac{8870}{1.29}\frac{40.5}{66} \times 885 \times 10^{-8} = 4.91 \text{ volts}$$

The motor operates with heavy overloads; for this reason $e_r$ is relatively low at rated load.

**17–10. Interpole AT.** Eq .17–38 for $e_r$ yields the average value for the interpole flux density, as explained in Art. 9–7. The emf induced through rotation under the interpole is

$$e_i = 2B_{i\,av}N_e l_{ie} v_a 10^{-8} \text{ volt}$$

where $B$ is in gausses, $l_{ie}$ in cm and $v_a$ in cm/sec. If $B$ is expressed in lines/in.$^2$, $l_{ie}$ in in. and $v_a$ in ft/min,

$$e_i = \tfrac{2}{5}B_{i\,av}N_e l_{ie} v_a 10^{-8} \text{ volt} \tag{17–39}$$

Setting $e_r$ equal to $e_i$ yields

$$B_{i\,av} = 2.5\,\frac{e_r \times 10^{-8}}{N_e l_{ie} v_a} \text{ lines/in.}^2 \tag{17–40}$$

The effective length of the interpole is

$$l_{ie} = \frac{l_i}{k_v} + \frac{L - l_i}{2} \tag{17–41}$$

$k_v$ is given by Eq. 16–4.

Eq. 17–40 represents the *average* value of the flux density under the interpole. Experience shows that, if the interpole flux density is kept constant according to Eq. 17–40 over the whole effective width of the interpole, satisfactory commutation is achieved. The effective width of the interpole is made equal to the commutating zone, i.e., to the distance on the armature which corresponds to the short-circuit time of the conductors of a slot. It can be seen from Fig. 17–13 that this distance for the standard winding is

$$b_{cz} = [b' + (u-1)\tau_c + c\tau_c]\frac{D}{D_c}$$

or inserting for $b'$ the value of Eq. 17–30

$$b_{cz} = \frac{D}{D_c}\left[b_b - i + \left(u + c - \frac{a}{p}\right)\tau_c\right] \tag{17–42}$$

In this equation the *absolute* value of $c$ from Eq. 17–35 is to be introduced. Eq. 17–42 applies also to the split-coil winding.

If the shape of the interpole is such that $B_i$ is not constant, along the commutating zone, as is the case, for example, with a bevel-shaped interpole, then the interpole AT must correspond to the maximum value of the interpole flux density. The ratio of maximum to average value can be found approximately from a time-relation sketch, as that shown in Fig. 17–15. As a maximum take the average value for the middle of the sketch; as an

average, take the average value for the top conductors of the slot in consideration.

This will be explained again on the motor treated in Art. 17–6. For this motor, with $l_{ie}=15$ in.,

$$B_{i\,\mathrm{av}}=2.5\,\frac{4.91\times10^{8}}{1\times15\times8870}=9200\ \text{lines/in.}^2$$

From Fig. 17–15, the maximum value (neglecting the peak) is 672.3 and the average value

$$\frac{(375.7+672.3+0.25\times751.4+672.3+375.7)}{4.25\tau_c}\tau_c=537$$

Thus the approximate ratio $B_{i\,\mathrm{max}}/B_{i\,\mathrm{av}}=672.3/537=1.25$ and $B_{i\,\mathrm{max}}=1.25\times9200=11{,}500$ lines/in.$^2$ The AT per interpole, necessary to produce $B_i$($B_{i\,\mathrm{av}}$ or $B_{i\,\mathrm{max}}$), are

$$N_iI_a=\frac{B_ig_ik_{ci}}{3.19} \tag{17–43}$$

where $N_i$ are the turns per interpole and $k_{ci}$ the Carter factor for the interpole gap. This assumes that the saturation of the iron for the path of the interpole flux is small, *as it should be.*

If $A$ denotes the ampere-conductors per inch armature circumference, then the total AT per interpole are

$$\mathrm{AT}_{i\,\mathrm{tot.}}=N_iI_a+\frac{\mathrm{A}\tau}{2} \tag{17–44}$$

for machines without compensating winding and

$$\mathrm{AT}_{i\,\mathrm{tot.}}=N_iI_a+\left(\frac{\mathrm{A}\tau}{2}-N_cI_a\right) \tag{17–45}$$

for machine with compensating winding. $N_c$ is the number of turns of the compensating winding per pole.

# *Chapter 18*

## LOSSES DUE TO SLOT-OPENINGS AND SKIN-EFFECT

**18–1. Pole-face Losses.** It has been pointed out in Art. 11–1a that the iron losses in the teeth and core, due to the main flux, must be multiplied by a factor 1.4 to 1.6, if they are determined from loss-curves (Fig. 11–1). This factor takes into account the non-sinusoidal flux distribution in the gap, the non-uniform flux distribution over the cross section of the armature core, and the influence of punching and removing the burrs.

In Art. 11–1b the influence of the slot-openings was discussed. Due to the latter, the flux density under the pole is not uniform and additional high frequency eddy-current losses are caused in the pole-face by a flux ripple (Fig. 11–2). The frequency of the eddy currents is determined by the number of armature slots and by the rpm of the armature.

$$f_e = \frac{Qn}{60} \tag{18–1}$$

At high frequencies the flux ripple does not penetrate the iron of the pole face to the same degree as at low frequencies. This is due to the *reaction* of the eddy currents which makes the flux density in the laminations non-uniform: it is larger at the side surfaces than in the middle of the lamination. This results in a reduction of the eddy-current loss.

If $\rho$ is the resistivity of the iron (in micro ohms/in.$^3$) and $\mu$ its average permeability, then

$$\xi = 0.316 \Delta \sqrt{\frac{\mu f}{\rho}} \tag{18–2}$$

and the reduction factor for the eddy-current loss (Eq. 11–4)

$$r_e = \frac{3}{\xi} \frac{\sinh \xi - \sin \xi}{\cosh \xi - \cos \xi} \tag{18–3}$$

For $\xi < 2$, $r_e \approx 1$; for $\xi > 4$, $r_e \approx \frac{3}{\xi}$.

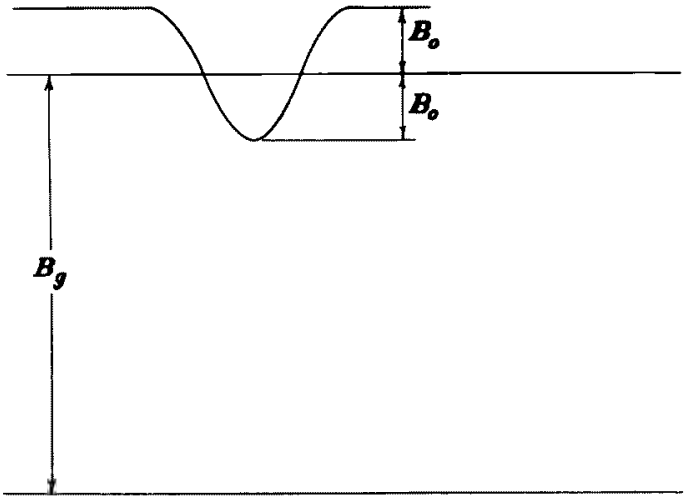


FIG. 18–1. Variation of flux density due to slot-openings.

The slot opening produces a dip in the flux distribution curve. The method of conformal mapping yields for the *variation* of the flux density $B_0$ (Fig. 18–1)

$$B_0 = \beta k_c B_g \tag{18–4}$$

where $\beta$ is a function of the ratio of the slot opening at the gap ($b_{sg}$) and length of the gap ($g$). $B_g$ is the average flux density (Fig. 11–2). The quantity $\beta$ as a function of $b_{sg}/g$ is given in Fig. 18–2.

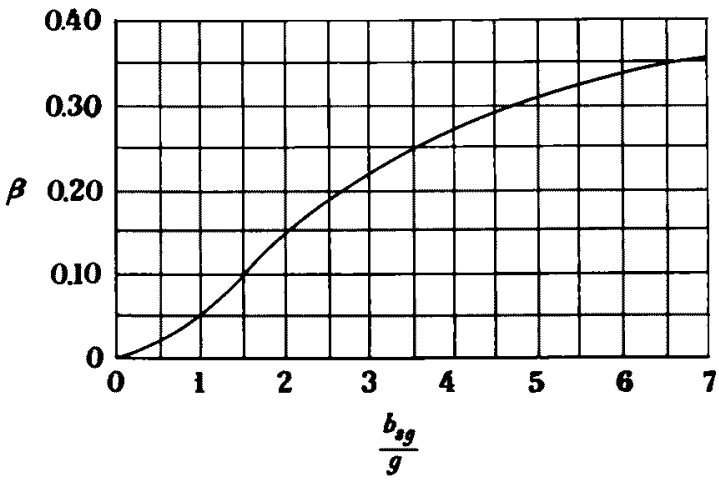


FIG. 18–2. The quantity $\beta$ as a function of $b_{sg}/g$

Since the distance between the positive and negative amplitudes of $B_0$ is equal to half of the slot pitch $\tau_s/2$, the width of the eddy-current path in a solid pole-shoe is also equal to $\tau_s/2$. Introducing into Eq. 11–4 $\tau_s/2$ for $\Delta$ and

multiplying this equation by $r_e = 3/\xi$, because the frequency is high, the pole-face loss, in watts per square inch, becomes

$$l_s = k_s \left(\frac{Qn}{1000}\right)^{1.5} \left(\frac{B_0 \tau_s}{1000}\right)^2 \text{ watts/in.}^2 \tag{18–5}$$

For solid steel, $k_s = 24 \times 10^{-4}$. This factor is much smaller for laminated pole-shoes:

$k_s = 6 \times 10^{-4}$ for steel sheet, 1/16 in. thick

$k_s = 5 \times 10^{-4}$ for dynamo steel, 0.04 in. thick

The total pole-face loss is

$$L_s = p l_s b_p l_p \text{ watts} \tag{18–6}$$

**18–2. Copper Losses Due to the Main Flux.** It has been explained in Art. 11–1c that a part of the main flux goes through the slots (Fig. 11–3) and causes eddy-current losses in the top conductors. These losses can be expressed by equivalent losses produced by a current flowing in the *embedded part* of the total winding. The current density corresponding to this latter current is, for larger d-c machines,

$$d_M = 16 \frac{hf}{\rho} \left(\frac{B'_t}{6450} - 16\right) \text{ amp/in.}^2 \tag{18–7}$$

where $h$ = height of the conductor, in in.

$\rho$ = resistivity of the conductor material, in micro ohms/in.$^3$

$f = \dfrac{pn}{120}$

$B'_t$ = fictitious flux density at the root of the tooth, in lines/in.$^2$

The additional loss in the conductors due to the main flux, as a *fraction of the* $I^2R$*-loss* of the armature, is thus

$$_M = \left(\frac{d_M}{d_r}\right)^2 \lambda \tag{18–8}$$

and in watts

$$\epsilon_M = \epsilon_M \times I^2R \tag{18–9}$$

where $d_r$ = current density corresponding to rated load

$$\lambda = \frac{l(=\text{net core length})}{1/2 \text{ mean length turn}} \tag{18–10}$$

$I^2R$ = copper loss at rated current.

**18–3. Skin-effect Losses.** In Art. 11–26 the skin-effect losses in the conductors due to the slot flux were discussed. In order to compute these losses, determine first (Ref. C3)

$$\xi = 0.316h\sqrt{\frac{b_{cu}}{b_s}\frac{f}{\rho}} \tag{18–11}$$

where $h$ = height of the conductor

$b_{cu}$ = width of all conductors in the slot width

$b_s$ = width of the slot

$f = \frac{pn}{120}$

$\rho$ = resistivity of the conductor material, in micro ohms/in.[3]

Further

$$\sigma = \frac{b_b + (u-1)\tau_c}{\tau(D_c/D)}\frac{1}{\xi^2} \tag{18–12}$$

where $b_b$ = brush width

$u$ = number of conductors lying side by side in the slot

$\tau_c$ = commutator pitch

$\tau$ = pole pitch

$D_c$ = diameter of commutator

$D$ = diameter of armature

With the value of $\sigma$ compute

$$F = \frac{0.116}{0.13 + \sigma} \tag{18–13}$$

and finally the skin-effect loss as a fraction of the $I^2R$-*loss* of the armature

$$\epsilon_{sk} = \frac{4}{3\pi} m^2\xi^2\lambda F \tag{18–14}$$

where $m$ = number of conductors in the depth of the slot

$\lambda$ = (see Eq. 18–9)

This loss in watts is

$$L_{sk} = \epsilon_{sk} \times I^2R \tag{18–15}$$

The quantity $F$ takes into account the short-circuit time of the winding element. Linear commutation has been assumed for the derivation of the skin-effect loss.

**18–4. Example of calculation.** A 560-kw, $n=375$ rpm, 8-pole generator has the following dimensions:

Armature dia.: 39.5 in.
Gross core length: 14.5 in.
Radial vents: 4
Width of a vent: $\frac{3}{8}$ in.
Number of slots: 82
Slot pitch: 1.513 in.
Length of the gap: 0.315 in.
Carter factor: 1.14
Flux density in the gap $B_g$: 62,500 lines/in.$^2$
Slot width: 0.605 in.
Pole pitch: 15.5 in.
$I^2R$-loss in the armature: 11,500 watts
Fictitious tooth density at root of the tooth: 141,400 lines/in.$^2$

Pole arc $b_p$: 9.5 in.
Length of pole: 14.5 in.
Conductors per slot: 6
3 conductors per layer: $(u=3)$
Upper conductor: $0.157\times0.51$ in.
Lower conductor: $0.157\times0.67$ in.
Av. height of cond.: 0.59 in.
Av. current density: 2975 amp/in.$^2$
Commutator dia.: 33.5 in.
Commutator pitch: 0.427 in.
Brush width: 1.0 in.
Half mean length turn: 34.4 in.
Net core length: 13 in.

(a) *Pole-face Loss.* $\beta=0.14$ corresponds to $\frac{b_s}{g}=\frac{0.605}{0.315}=1.92$ (Fig. 18–2). From Eq. 18–4

$$B_0=0.14\times1.14\times62{,}500=10{,}000 \text{ lines/in.}^2$$

Eq. 18–5 yields for 1/16 in. thick steel sheet

$$l_s=6\times10^{-4}\left(\frac{82\times375}{10{,}000}\right)^{1.5}\left(\frac{10{,}000\times1.513}{1000}\right)^2=0.745 \text{ watts/in.}^2$$

The total pole-face loss is (Eq. 18–6)

$$L_s=8\times14.5\times9.5\times0.745=820 \text{ watts}$$

(b) *Copper Loss Due to the Main Flux.* The frequency is

$$f=\frac{8\times375}{120}=25$$

Eq. 18–7 yields for $\rho=0.825$ (at 75° C)

$$d_M=16\,\frac{0.59\times25}{0.825}\left(\frac{141{,}400}{6450}-16\right)=1690 \text{ amp/in.}^2$$

$\lambda$ is equal to $13/34.4=0.378$. Eqs. 18–8 and 18–9 yield for this loss

$$\epsilon_M=\left(\frac{1690}{2975}\right)^2\times0.378=0.122$$

$$L_M=0.122\times11{,}500=1400 \text{ watts}$$

(c) *Skin-effect Loss.* From Eq. 18–11

$$\xi = 0.316 \times 0.59 \sqrt{\frac{3 \times 0.157}{0.605}} \times \frac{25}{0.825} = 0.906$$

From Eqs. 18–12 and 18–13

$$\sigma = \frac{1 + (3 - 1) \times 0.427}{15.5 \times 33.5/39.5} = 0.172$$

$$F = \frac{0.116}{0.13 + 0.172} = 0.384$$

Eqs. 18–14 and 18–15 yield for this loss ($m = 2$)

$$\epsilon_{sk} = \frac{4}{3\pi} 4 \times 0.906^2 \times 0.378 \times 0.384 = 0.202$$

and

$$L_{sk} = 0.202 \times 11{,}500 = 2220 \text{ watts}$$

# *Chapter 19*

# HEAT FLOW AND TEMPERATURE RISES OF THE WINDINGS AND IRON

**19–1. Data on Heat Conductivities and Heat Transfer Coefficients.** The importance of high heat conductivity of all materials used and of high heat transfer constants from the surfaces to the cooling medium has been pointed out in Chap. 12.

The heat conductivities of some metals and insulating materials are given in Table 19–1. The heat conductivity of the iron in the axial direction is much less than that in the radial direction due to the insulation and voids between the laminations. The heat conductivity of the insulating materials is low.

Approximate values of the heat transfer coefficients for air as a cooling medium (in watts/in.$^2$/° C) are given in Table 19–2. The air velocities which correspond to the two extreme values of the heat-transfer coefficient also are given in the table.

TABLE 19–1

HEAT CONDUCTIVITIES OF SOME METALS AND INSULATING MATERIALS

(in Watts/in.$^2$/in./°C)

| | |
|---|---|
| Laminations in radial direction | 0.80 to 1.2 |
| Laminations in axial direction | 0.013 to 0.014 |
| Copper | 9.75 |
| Brass (70 Cu:30 Zn) | 2.80 |
| Aluminium | 5.35 |
| Organic varnishes | 0.0035 to 0.0045 |
| Shellac | 0.0063 |
| Air | 0.0006 |
| Cotton tape, untreated | 0.0019 |
| Cambric, varnished | 0.004 |
| Mica, sheet | 0.014 |
| Micafolium | 0.0044 |

TABLE 19–1—*continued*

| | |
|---|---|
| Micanite (for commutator) | 0.0104 |
| Paper, board, varnished | 0.0073 |
| Paper, Kraft tissue | 0.001 |
| Pressboard | 0.0046 |
| Silk, untreated | 0.0012 |
| Silk, varnished | 0.0042 |
| Micarta with paper and cotton fillers | 0.0046 to 0.008 |
| Micarta with fiberglas and asbestos filler | 0.006 to 0.010 |
| Micarta (0.125 in.) | 0.0066 |
| Asbestos, paper (0.025 in.) | 0.0040 |
| Quartz | 0.0380 |
| Asphalt | 0.00175 |
| Powdered graphite (through 20- to 40-mesh sieve) | 0.034 |
| Powdered graphite (through 40-mesh sieve) | 0.011 |
| Rope paper | 0.0029 |
| Rope paper, impregnated in oil | 0.0037 |
| Rope paper, impregnated in varnish | 0.0043 |
| Cement paper | 0.0034 |
| Fish paper | 0.0046 |
| Cotton, untreated | 0.0012 to 0.00175 |
| Cotton, impregnated in varnish | 0.0061 to 0.0068 |

TABLE 19–2

HEAT-TRANSFER COEFFICIENTS FOR AIR AS COOLING MEDIUM

| End Winding and Parts of the Winding in the Radial Vents | Laminations in Radial Vents | Laminations in Axial Channels | Field Winding |
|---|---|---|---|
| 0.025 to 0.10 watts/in.$^2$/°C<br>600 to 6000 ft/min | 0.025 to 0.07 watts/in.$^2$/°C<br>800 to 4000 ft/min | Length of channel = 2 in.<br>0.03 to 0.11 watts/in.$^2$/°C<br>1200 to 5000 ft/min<br><br>Length of channel = 20 in.<br>0.02 to 0.08 watts/in.$^2$/°C<br>1200 to 5000 ft/min | 0.008 to 0.025 watts/in.$^2$/°C<br>800 to 8000 ft/min |

**19–2. Assumptions for the Investigation.** The method of calculating the heat flow and temperature rises of copper and iron described below is applicable to stators and rotors of machines with radial as well as with axial

cooling; it is applicable to distributed as well as to concentrated windings.

The assumptions on which the theoretical derivations are based are:

1. The height and width of the coil are small in comparison to its length so that there is no heat flow within the cross section of the coil. A temperature gradient then exists only along the centerline of the coil.
2. The radial heat conductivity of the iron is large so that there is no temperature gradient within a single lamination.

With these two assumptions, the heat flow problem becomes a linear one.

**19–3. The Equation of Heat Flow.** For the unidimensional heat flow, the heat balance, under steady-state conditions, is given by the equation

$$v_0(1+\alpha\vartheta)-\frac{uw}{f}+k\frac{\partial^2\vartheta}{\partial x^2}=0 \qquad (19\text{–}1)$$

where $v_0$ = heat (in watts) developed in a cubic inch of the substance at ambient temperature

$\alpha$ = temperature coefficient of the heat conductor ($\alpha = 0.004$ for copper, $\alpha$ is assumed equal to 0 for iron)

$\vartheta$ = temperature rise above ambient temperature in °C

$u$ = circumference of the heat conductor in inches (of both coil sides in 2-layer windings, measured in the middle of the ground insulation)

$f$ = cross section of the heat conductor in in.$^2$ (without ground insulation)

$w$ = heat (in watts) transferred per unit surface of the heat conductor

$k$ = heat conductivity of the heat conductor in watts/in./°C

Eq. 19–1 means that the heat developed in the unit volume of the heat conductor is equal to the sum of the heat conducted to the neighboring space elements and the heat transferred through its surface.

**19–4. Temperature Rises of Stator Copper and Iron.** Applying the equation of heat flow (Eq. 19–1) to the stator of the electrical machine, the end-winding and the part of the coil embedded in iron are to be considered separately. Subscript 1 will be used for the end-winding and the origin of the coordinates will be placed in its middle. The length of the end-winding is assumed to be $L_1$ (Fig. 19–1). Subscript 2 will be used for the part of the coil embedded in iron and subscript Fe will be used for the iron. The origin of the coordinates for the embedded part of the coil will be placed in the middle of

the machine. The length of the iron (including vents, in the case of radial ventilation) is assumed to be $L$ (Fig. 19–1).

(a) *End-winding.* The heat transferred per unit surface of the end-winding is proportional to the difference between the temperature rise of the con-

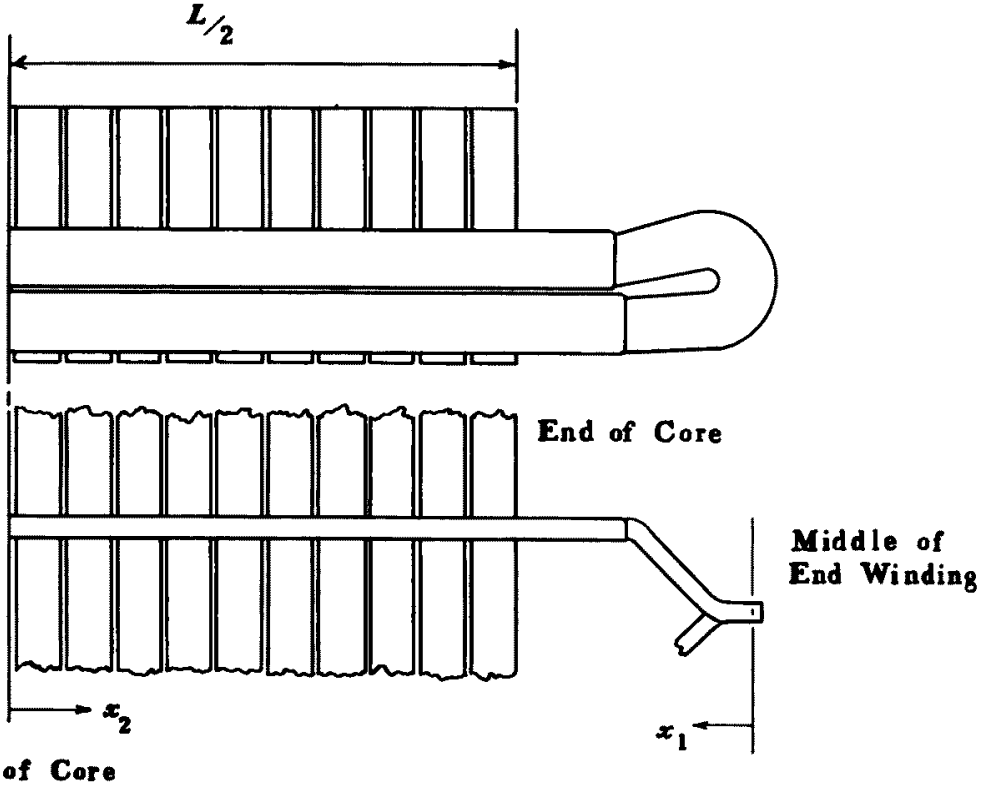


FIG. 19–1. Explanation of $L_1$ and $L$. Locating origins of coordinates for the end-winding and embedded part of the coil.

ductor material, $\vartheta$, and the temperature rise of the outer surface of the insulation of the end-winding, $\vartheta_1$, i.e.,

$$w_1 = \frac{k_1}{\delta_1}(\vartheta - \vartheta_1) \tag{19–2}$$

where $k_1$ is the heat conductivity of the insulation (including air layers) and $\delta_1$ is the thickness of the insulation.

The heat $w_1$ is transferred to the air (in general, to cooling medium). It is true that

$$w_1 = h_1(\vartheta_1 - \vartheta_{A1}) \tag{19–3}$$

where $h_1$ is the heat transfer constant of the end-winding and $\vartheta_{A1}$ the temperature rise of the air at the end-windings. It follows from Eqs. 19–2 and 19–3 that, with

$$\lambda_1 = \frac{k_1 h_1}{k_1 + h_1 \delta_1} \tag{19–4}$$

$w_1$ becomes

$$w_1 = \lambda_1(\vartheta - \vartheta_{A1}) \tag{19–5}$$

$\lambda_1$ is the thermal conductivity of the end-winding. Combining Eq. 19–5 with Eq. 19–1, we have

$$\frac{\partial^2 \vartheta}{\partial x^2} - a_1^2 \vartheta + b_1 = 0 \tag{19–6}$$

where

$$a_1^2 = \frac{1}{k_{co}} \left( \lambda_1 \frac{u_1}{f} - \alpha v_{10} \right) \tag{19–7}$$

$$b_1 = \frac{1}{k_{co}} \left( v_{10} + \lambda_1 \frac{u_1}{f} \vartheta_{A1} \right) \tag{19–8}$$

The solution of the differential Eq. 19–6 is

$$\vartheta = A_1 e^{a_1 x} + B_1 e^{-a_1 x} + \frac{b_1}{a_1^2} \tag{19–9}$$

The temperature rise of the conductor, $\vartheta$, as a function of $x$, is symmetrical with respect to the middle of the end-winding, i.e., with respect to $x_1 = 0$. This yields $A_1 = B_1$, and the differential Eq. 19–9 becomes

$$\vartheta = 2A_1 \cosh a_1 x_1 + \frac{b_1}{a_1^2} \tag{19–9a}$$

(b) *Embedded Part of the Winding and the Stator Iron.* The heat transferred from the surface of the winding material to the iron within a stack of laminations of the length $l'$ (for axial ventilation $l' = L$) is

$$W_{Fe} = \Lambda_{Fe}(\vartheta - \vartheta_{Fe}) \tag{19–10}$$

where

$$\Lambda_{Fe} = \lambda_{Fe} u_2 l' N, \quad \lambda_{Fe} = \frac{k_2}{\delta_2} \tag{19–11}$$

and $k_2$ = heat conductivity of the insulation in the slot (including air layers)

$\delta_2$ = thickness of the insulation in the slot

$u_2$ = average circumference of the insulation in the slot

$N$ = number of slots

$\vartheta - \vartheta_{Fe}$ = average temperature gradient in the slot insulation within a stack of laminations

The iron losses in a stack of laminations will be denoted by $L'_{Fe}$. Then the total heat in the stack is $W_s = W_{Fe} + L'_{Fe}$. This heat is to be carried away by the cooling medium.

Due to the fact that the axial heat conductivity of the laminations is small, the temperature rise of the side surfaces of the stack of laminations is smaller than that in the middle of the stack. In accordance with the assumption that the radial heat conductivity of the iron is infinite, the temperature rise $\vartheta_{Fe}$ is the same for the inner and outer cylinder surfaces of the stack.

Let $\vartheta_{A2}$ = temperature rise of the air in the radial vents (at the root of the tooth)

$\vartheta_s$ = temperature rise of the side surfaces of the stack of laminations

$h_s$ = heat transfer constant of the side surfaces of the stack of laminations

$A_s$ = area of both side surfaces of the stack

The heat transferred to the air by the side-surfaces is then

$$W_s = h_s(\vartheta_s - \vartheta_{A2})A_s \tag{19–12}$$

If $\vartheta_{Fe}$ = *average* temperature rise of the iron of the stack of laminations

$h_c$ = heat transfer constant of the inner cylinder surface of the stack

$A_c$ = area of the inner cylinder surface of the stack,

$h'_c$ = heat transfer constant of the outer surface of the stack

$A'_c$ = area of the outer cooling surface of the stack

$h_{ax}$ = heat transfer constant of the axial vents

$A_{ax}$ = area of the axial cooling vents of a stack

$\vartheta_{A3}$ = temperature rise of the air at the inner cylinder surface

$\vartheta_{A4}$ = temperature rise of the air at the outer surface of the core

$\vartheta_{A5}$ = temperature rise of the air in the axial vents

then the heat transferred to the air by the *inner cylinder-surface* of the stack is

$$W_c = h_c(\vartheta_{Fe} - \vartheta_{A3})A_c \tag{19–13}$$

the heat transferred to the air by the *outer* cooling surface of the stack is

$$W'_c = h'_c(\vartheta_{Fe} - \vartheta_{A4})A'_c \tag{19–13a}$$

and the heat transferred to the air by the *axial vents* of the stack is

$$W_{ax} = h_{ax}(\vartheta_{Fe} - \vartheta_{A5})A_{ax} \tag{19–13b}$$

Under steady-state conditions, the heat produced must be equal to the heat transferred to the cooling medium, i.e.,

$$\begin{aligned} W_{Fe} + L'_{Fe} &= W_s + W_c + W'_c + W_{ax} \\ &= h_s(\vartheta_s - \vartheta_{A2})A_s + h_c(\vartheta_{Fe} - \vartheta_{A3})A_c + h'_c(\vartheta_{Fe} - \vartheta_{A4})A'_c \\ &\quad + h_{ax}(\vartheta_{Fe} - \vartheta_{A5})A_{ax} \end{aligned} \tag{19–14}$$

With the aid of this equation, it is possible to set up the equation of heat flow in the stack of laminations and to determine the temperature rise across the stack as a function of the coordinate $x$, the origin of which is placed in the centerline of the stack. Then $\vartheta_{Fe}$ can be eliminated from Eq. 19–14 and the equation for the heat flow in the embedded part of the winding can be set up.

The *total heat transferred through the side-surfaces of the stack* is

$$W_s = W_{Fe} + L'_{Fe} - h_c(\vartheta_{Fe} - \vartheta_{A3})A_c - h'_c(\vartheta_{Fe} - \vartheta_{A4})A'_c - h_{ax}(\vartheta_{Fe} - \vartheta_{A5})A_{ax} \tag{19–15}$$

and the heat transferred *per unit volume* is

$$w_s = \frac{W_s}{\left(\frac{A_s}{2}\right)l'} \tag{19–16}$$

Therefore, the equation of heat flow for the stator iron is

$$w_s + k_q \frac{\partial^2 \vartheta}{\partial x^2} = 0 \tag{19–17}$$

The solution of this equation is

$$\vartheta = -\frac{w_s}{2k_q}x^2 + Ax + B \tag{19–18}$$

The constants $A$ and $B$ can be determined from the boundary conditions:

$$x = -\frac{l'}{2} \quad \vartheta = \vartheta_s$$

$$x = +\frac{l'}{2} \quad \vartheta = \vartheta_s \tag{19–19}$$

Thus

$$A = 0 \quad B = \vartheta_s + \frac{w_s l'^2}{8k_q} \tag{19–20}$$

and

$$\vartheta = \vartheta_s + \frac{w_s l'^2}{8k_q}\left[1 - \left(\frac{2x}{l'}\right)^2\right] \tag{19–21}$$

$\vartheta_s$ is different for the different stacks of laminations.
Setting $d\vartheta/dx = 0$, the maximum temperature rise of the stack is obtained

$$\vartheta_{Fe,m} = \vartheta_s + \frac{w_s l'^2}{8k_q} \tag{19–22}$$

The average temperature rise of the iron of the stack is

$$\vartheta_{Fe} = \vartheta_s + \frac{w_s l'^2}{12k_q} \tag{19–23}$$

Thus, independent of the magnitude of the quantity $\frac{w_s l'^2}{8k_q}$

$$\vartheta_{Fe,m} = 1.5\vartheta_{Fe} - 0.5\vartheta_s \tag{19–24}$$

The average temperature rise $\vartheta_{Fe}$ as well as the maximum temperature rise $\vartheta_{Fe,m}$ is different for the different stacks of laminations.

From Eqs. 19–23, 19–16, and 19–15

$$\vartheta_{Fe} = \vartheta_s + \frac{1}{\Lambda_s}[W_{Fe} + L'_{Fe} - h_c(\vartheta_{Fe} - \vartheta_{A3})A_c - h'_c(\vartheta_{Fe} - \vartheta_{A4})A'_c - h_{ax}(\vartheta_{Fe} - \vartheta_{A5})A_{ax}] \tag{19–25}$$

where

$$\frac{1}{\Lambda_s} = \frac{l'^2}{12k_q\frac{A_s}{2}l'} = \frac{l'}{6A_sk_q} \tag{19–26}$$

Substituting Eqs. 19–10, 19–25, and 19–26 into Eq. 19–14,

$$W_{Fe} = \Lambda_{Fe}\left[c\vartheta - \frac{1}{\Lambda}L'_{Fe} - \frac{1}{d\Lambda}h_sA_s\vartheta_{A2} - \frac{1}{\Lambda}(h_cA_c\vartheta_{A3} + h'_cA'_c\vartheta_{A4} + h_{ax}A_{ax}\vartheta_{A5})\right] \tag{19–27}$$

where

$$c = \frac{\Lambda_p}{\Lambda_p + d\Lambda_{Fe}}$$

$$d = 1 + \frac{h_sA_s}{\Lambda_s}$$

$$\Lambda_p = h_sA_s + d(h_cA_c + h'_cA'_c + h_{ax}A_{ax}) \tag{19–28}$$

$$\frac{1}{\Lambda} = \frac{d}{\Lambda_p + d\Lambda_{Fe}}$$

If $b_v$ = width of a radial vent

$\vartheta - \vartheta_2$ = temperature gradient between the inner and outer surfaces of the insulation in the vent

then the heat which flows through the insulation into a radial vent is

$$W_A = \frac{k_2}{\delta_2}(\vartheta - \vartheta_2)\,u_2Nb_v \tag{19–29}$$

This heat is carried away by the air. Therefore,

$$W_A = h_2(\vartheta_2 - \vartheta_{A6})u_2Nb_v \tag{19–30}$$

where $h_2$ is the heat-transfer constant of the slot insulation and $\vartheta_{A6}$ the temperature rise of the air in the radial vent at the middle of the tooth. It follows from Eqs. 19–29 and 19–30 for $W_A$

$$W_A = \lambda_A(\vartheta - \vartheta_{A6})u_2Nb_v \tag{19–31}$$

where

$$\lambda_A = \frac{k_2h_2}{k_2 + h_2\delta_2} \tag{19–32}$$

$\lambda_A$ is the thermal conductivity of the winding in the vent.

The heat conduction from the coil to the air in the vent is different from that from the coil to the iron in the slot. An exact mathematical treatment would make it necessary to consider both coil parts separately and to set up two different differential equations for the heat flow. However, for the sake of simplicity, an average value for the heat transferred over the length $l' + b_v$ (stack + vent) will be introduced:

$$w = \frac{W_A + W_{Fe}}{u_2(l' + b_v)N} \tag{19–33}$$

With this value of the transferred heat, the differential equation of the heat flow in the coil part embedded in iron becomes the same as for the end-winding (Eq. 19–6), and its solution is

$$\vartheta = 2A_2 \cosh a_2 x_2 + \frac{b_2}{{a_2}^2} \tag{19–34}$$

where

$${a_2}^2 = \frac{1}{k_{co}} \left( \lambda_2 \frac{u_2}{f} - \alpha v_{20} \right) \tag{19–35}$$

$$b_2 = \frac{1}{k_{co}} \frac{u_2}{f} \left[ \frac{\lambda_{Fe} L'_{Fe}}{\Lambda} \frac{l'}{l' + b_v} + \lambda_2 \frac{b_v}{l' + b_v} \vartheta_{A6} + \lambda_{Fe} \frac{l'}{l' + b_v} \frac{c}{\Lambda_p} \right.$$
$$\left. \times (h_s A_s \vartheta_{A2} + dh_c A_c \vartheta_{A3} + dh'_c A'_c \vartheta_{A4} + dh_{ax} A_{ax} \vartheta_{A5}) + \frac{f}{u_2} v_{20} \right] \tag{19–36}$$

$$\lambda_2 = \frac{b_v \lambda_A + c l' \lambda_{Fe}}{l' + b_v} \tag{19–37}$$

Differential Eq. 19–9 for the end-winding must yield at $x_1 = L_1/2$ the same temperature rise and the same temperature gradient $d\vartheta/dx$, with opposite sign, as differential Eq. 19–34 yields at $x_2 = L/2$. It follows from this for the integration constants $A_1$ and $A_2$

$$2A_1 = \left( \frac{b_2}{{a_2}^2} - \frac{b_1}{{a_1}^2} \right) \frac{a_2}{e} \sinh \frac{a_2 L}{2} \tag{19–38}$$

$$2A_2 = \left( \frac{b_1}{{a_1}^2} - \frac{b_2}{{a_2}^2} \right) \frac{a_1}{e} \sinh \frac{a_1 L_1}{2} \tag{19–39}$$

where

$$e = a_1 \sinh \frac{a_1 L_1}{2} \times \cosh \frac{a_2 L}{2} + a_2 \sinh \frac{a_2 L}{2} \times \cosh \frac{a_1 L_1}{2} \tag{19–40}$$

With these values of the integration constants, the temperature rises of the copper in the middle of the machine and in the middle of the end-windings become

$$\vartheta_{max} = \frac{b_2}{{a_2}^2} + 2A_2 \tag{19–41}$$

$$\vartheta_{min} = \frac{b_1}{{a_1}^2} + 2A_1 \tag{19–42}$$

The average temperature rise of the winding, as determined by the resistance test, is

$$\vartheta_{av} = \frac{2}{L+L_1}\left[\int_0^{L_1/2} \vartheta\, dx_1 + \int_0^{L/2} \vartheta\, dx_2\right]$$

$$= \frac{2}{L+L_1}\left[\frac{2A_1}{a_1}\sinh\frac{a_1 L_1}{2} + \frac{b_1 L_1}{2a_1^2} + \frac{2A_2}{a_2}\sinh\frac{a_2 L}{2} + \frac{b_2 L}{2a_2^2}\right] \qquad (19\text{–}43)$$

In order to determine the *average* temperature rise of the stack of laminations $\vartheta_{Fe}$ the assumption is made that the temperature rise of the winding within the stack is constant and equal to the temperature rise in the middle of the stack $\vartheta_m$. Eqs. 19–10 and 19–27 then yield

$$\vartheta_{Fe} = (1-c)\vartheta_m + \frac{c}{\Lambda_p}[h_s A_s \vartheta_{A2} + d(h_c A_c \vartheta_{A3} + h'_c A'_c \vartheta_{A4} + h_{ax} A_{ax} \vartheta_{A5}] + \frac{L'_{Fe}}{\Lambda} \qquad (19\text{–}44)$$

The average temperature rise of the side surfaces of the stack of laminations is then, according to Eqs. 19–25 and 19–27,

$$\vartheta_s = \vartheta_{Fe} + \frac{1}{\Lambda_s}[h_c A_c(\vartheta_{Fe} - \vartheta_{A3}) + h'_c A'_c(\vartheta_{Fe} - \vartheta_{A4}) + h_{ax} A_x(\vartheta_{Fe} - \vartheta_{A5})$$

$$- \frac{\Lambda_{Fe}}{\Lambda_s} c\left[\vartheta_m - \frac{h_s A_s}{\Lambda_p}\vartheta_{A2} - \frac{d}{\Lambda_p}(h_c A_c \vartheta_{A3} + h'_c A'_c \vartheta_{A4} + h_{ax} A_{ax} \vartheta_{A5}\right]$$

$$+ \frac{L'_{Fe}}{\Lambda_s}\left(\frac{\Lambda_{Fe}}{\Lambda} - 1\right) \qquad (19\text{–}45)$$

The maximum temperature rise of the stack of laminations is, according to Eq. 19–24,

$$\vartheta_{Fe\,m} = 1.5\vartheta_{Fe} - 0.5\vartheta_s \qquad (19\text{–}46)$$

**19–5. Temperature Rise of Rotor Copper and Iron.** In order to determine the equation of heat flow and the temperature rises of copper and iron of the rotor, the same considerations can be applied as above to the stator. It must be taken into account that the parts of the end-windings which lie under the bands or retaining rings of induction motors, d-c machines, and turbogenerators do not contribute to the cooling surface and heat transfer. However, in d-c machines, the *commutator risers* contribute to the heat transfer. Experience shows that the risers have a *temperature rise of 25 to 30°C*. Therefore, the integration constants $2A_1$ and $2A_2$, (Eqs. 19–38 and 19–39) become for the rotor of the d-c machine

$$2A_1 = \vartheta_R - \frac{b_1}{a_1^2} \qquad (19\text{–}47)$$

$$2A_2 = \left[\left(\vartheta_R - \frac{b_1}{a_1^2}\right)\cosh\frac{a_1 L_1}{2} + \left(\frac{b_1}{a_1^2} - \frac{b_2}{a_2^2}\right)\right]\frac{1}{\cosh\frac{a_2 L}{2}} \qquad (19\text{–}48)$$

where $\vartheta_R$ is the temperature rise of the commutator risers, and $L_1$ *is the free length of the end-winding*, i.e., the part of the end-winding not covered by the band or retaining ring.

**19–6. Temperature Rise of Concentric Field Windings.** The concentric field windings of d-c machines and salient pole synchronous machines can be treated as coils placed in slots and the *same method* of calculation can be applied *as to a winding embedded in slots.*

The method of calculation of the temperature rises of copper and iron developed above will be demonstrated by examples.

**19–7. Example of Calculation.** In the following, the temperature rise of the armature winding of the machine treated in Art. 18–4 will be computed. Some necessary additional data are:

| | |
|---|---|
| Depth of the slot: 1.656 in. | Length of core: 14.5 in. |
| Height of core: 4.45 in. | Length of end-winding: 19.9 in. |
| Inside diameter: 27.3 in. | Length of a stack of laminations: 2.6 in. |

The heat conductivities, in watts/in.$^2$/in./°C, are

$$k_1 = 0.0043 \qquad k_{co} = 9.1$$

$$k_2 = 0.0038 \qquad k_q = 0.025$$

The thickness of the insulation is

$$\delta_1 = 0.048 \text{ in.} \qquad \delta_2 = 0.055 \text{ in.}$$

The cross section of the copper in a slot is

$$f = 0.555 \text{ in.}^2$$

The total $I^2R$-losses are 11,500 watts. The embedded part of these losses is $11{,}500 \times (14.5/34.4) = 4850$ watts. To these losses must be added the copper losses which are due to the skin effect and to the main flux (Art. 18–4), so that the total embedded copper losses are

$$L_{co,\,emb} = 4850 + 2200 + 1400 = 8450 \text{ watts}$$

The iron losses in core and teeth are

$$L_{Fe} = 2850 + 1620 = 4470 \text{ watts}$$

The air through the radial vents must carry away $L_{co,\,emb} + L_{Fe}$ + a part of the end-winding losses. This necessitates about 1900 ft$^3$/min air through the vents. This air volume and the available area for the air flow yield the following heat-transfer constants

$$h_c = 0.038 \qquad h'_c = 0.034$$

$$h_{s,\,av} = 0.036 = h_2$$

Furthermore,

$$h_1 = 0.03 \qquad \vartheta_{A1} = 0$$

$$\vartheta_{A3} = 0 \quad \vartheta_{A2} = 4°\text{C} \qquad \vartheta_{A4} = 12°\text{C}, \qquad \vartheta_{A6} = 8°\text{C}$$

The iron loss in a stack of laminations is

$$L_{\text{Fe}} = \frac{4470}{5} = 894 \text{ watts}$$

The copper losses per in.$^3$ of copper are

$$v_{10} = \frac{6650}{82 \times 0.555 \times 19.9} = 7.33 \text{ watts/in.}^3$$

$$v_{20} = \frac{8450}{82 \times 0.555 \times 14.5} = 12.8 \text{ watts/in.}^3$$

Further

$$A_s = 2\left[\frac{\pi}{4}(39.5^2 - 27.3^2) - 82 \times 0.605 \times 1.656\right] = 1156 \text{ in.}^2$$

$$A'_c = (\pi \times 39.5 - 82 \times 0.605)2.6 = 194.5 \text{ in.}^2; \quad A_c = 180 \text{ in.}^2$$

$$u_1 = 2(0.605 - 0.048) + 2(1.42 - 0.048) = 3.85 \text{ in.}^2$$

$$u_2 = (0.605 - 0.055) + 2(1.42 - 0.055) = 3.3 \text{ in.}^2$$

$$\lambda_1 = \frac{0.0043 \times 0.03}{0.0043 + 0.03 \times .048} = 0.0224$$

$$a_1^2 = \frac{1}{9.1}\left(0.0224 \times \frac{3.85}{0.555} - 0.004 \times 7.33\right) = 0.01385$$

$$a_1 = 0.118; \quad b_1 = 0.805$$

$$\lambda_{\text{Fe}} = \frac{0.0038}{0.055} = 0.0692$$

$$\Lambda_{\text{Fe}} = 0.0692 \times 3.3 \times 2.6 \times 82 = 48.7$$

$$\frac{1}{\Lambda_s} = \frac{2.6}{6 \times 1156 \times 0.025} = 0.015$$

$$d = 1 + 0.036 \times 1156 \times 0.015 = 1.625$$

$$\Lambda_p = 0.036 \times 1156 + 1.625(0.038 \times 180 + 0.034 \times 194.5) = 63.5$$

$$c = \frac{63.5}{63.5 + 1.625 \times 48.7} = 0.445$$

$$\frac{1}{\Lambda} = \frac{1.625}{63.5 + 1.625 \times 48.7} = 0.0114$$

$$\lambda_A = \frac{0.0038 \times 0.036}{0.0038 + 0.036 \times 0.055} = 0.0236$$

$$\lambda_2 = \frac{0.375 \times 0.0236 + 0.445 \times 2.6 \times 0.0692}{2.6 + 0.375} = 0.0298$$

$$a_2^2 = \frac{1}{9.1}\left(0.0298 \times \frac{3.3}{0.555} - 0.004 \times 12.8\right) = 0.01385$$

$$a_2 = 0.118$$

$$b_2 = \frac{1}{9.1} \times \frac{3.3}{0.555}\left[0.0692 \times 894 \times 0.0114 \frac{2.6}{2.975}\right.$$

$$+ 0.0298 \frac{2.6}{2.975} \times 8 + 0.0692 \frac{2.6}{2.975} \frac{0.445}{63.5}$$

$$\times (0.036 \times 1156 \times 4 + 1.625 \times 0.038 \times 180 \times 0 + 1.625$$

$$\left. \times 0.034 \times 194.5 \times 12) + \frac{0.555}{3.3} \times 12.8\right] = 1.976$$

$$2A_1 = 30 - \frac{0.805}{0.01385} = -28.1$$

$$2A_2 = \left[-28.1 \cosh \frac{0.118 \times 7}{2} + \left(\frac{0.805}{0.01385} - \frac{1.976}{0.01385}\right)\right]$$

$$\times \frac{1}{\cosh \dfrac{0.118 \times 14.5}{2}} = -83.$$

$$\vartheta_{max} = \frac{1.976}{0.01385} - 83 = 59.8°C$$

The average temperature rise of the winding and the temperature rise of the iron is obtained from Eqs. 19–43 to 19–46.

## List of Symbols for Chapter 19

$A_s$ = area of both sides of a stack of laminations, in in.$^2$
$A_c$ = area of the inner cylinder of a stack of laminations, in in.$^2$
$A'_c$ = area of the outer cooling surface of a stack of laminations, in in.$^2$
$A_{ax}$ = area of axial cooling vents of a stack $j$ in in.$^2$
$A_1$ = integration constant
$A_2$ = integration constant
$b_v$ = width of a radial vent, in in.
$f$ = cross section of the copper (of both coil sides, without ground insulation), in in.$^2$
$h$ = heat-transfer constant, in watts/in.$^2$/°C

$h_1$ = heat-transfer constant from the end-windings to the air at the end-windings

$h_2$ = heat-transfer constant from the coil to the air in the radial vent

$h_s$ = heat-transfer constant from the side surfaces of the stack of laminations to the air in the vent

$h_c$ = heat-transfer constant from the inner cylinder surface of the stack to the air

$h'_c$ = heat-transfer constant from the outer surface of the stack to the air

$h_{ax}$ = heat-transfer constant from the surface of the axial vents to the air

$k$ = heat conductivity, in watts/in./°C

$k_1$ = heat conductivity of the insulation of the end-windings

$k_2$ = heat conductivity of the insulation in the slot

$k_{cu}$ = heat conductivity of the conductor copper

$k_q$ = heat conductivity of the laminations in axial direction

$l'$ = length of a stack of laminations, in in.

$L$ = length of the core (including radial vents), in in.

$L_1$ = length of the end-winding, in in. ($L_1 = 1/2$ MLT − L)

$L'_{Fe}$ = iron loss in a stack of laminations (in watts)

$N$ = number of slots

$u_1$ = circumference of both coil sides, measured in the middle of the end-winding insulation, in in.

$u_2$ = circumference of both coil sides, measured in the middle of the ground insulation, in in.

$v_{10}$ = heat developed in a cubic inch of the copper of the end-windings, in watts

$v_{20}$ = heat developed in a cubic inch of the copper embedded in the slots, in watts

$w_1$ = heat transferred to the air by the end-windings, in watts/in.$^2$

$w$ = heat transferred by the embedded part of the winding (average value for a stack of laminations and a vent), in watts/in.$^2$

$W_{Fe}$ = heat transferred by the embedded part of the winding to a stack of laminations, in watts

$W_s$ = heat transferred to the air by the side-surfaces of a stack of laminations, in watts

$W_c$ = heat transferred to the air by the inner cylinder surface of a stack of laminations

$W'_c$ = heat transferred to the air by the outer surface of a stack of laminations

$W_{ax}$ = heat transferred to the air by the axial vents in a stack of laminations

$W_A$ = heat transferred to the air in a radial vent by the winding

$\delta_1$ = thickness of the end-winding insulation, in in.

$\delta_2$ = thickness of the slot-insulation, in in.

$\lambda_A$ = thermal conductivity of the winding in the radial vents (Eq. 19–32), in watts/in.$^2$/°C

$\lambda_1$ = thermal conductivity of the end-winding, in watts/in.$^2$/°C
$\vartheta$ = temperature rise, in °C
$\vartheta$ = temperature rise of winding or iron as a function of $x$
$\vartheta_{A1}$ = temperature rise of the air at the end-windings
$\vartheta_{A2}$ = temperature rise of the air in the radial vent at the root of the tooth
$\vartheta_{A3}$ = temperature rise of the air at the inner cylinder surface
$\vartheta_{A4}$ = temperature rise of the air at the outer surface of the core
$\vartheta_{A5}$ = temperature rise of the air in the axial vents
$\vartheta_{A6}$ = temperature rise of the air in the radial vent (at the middle of the tooth)
$\vartheta_1$ = temperature rise of the outer surface of the insulation of the end-windings
$\vartheta_2$ = temperature rise of the outer surface of the slot-insulation in the vent
$\vartheta_{Fe}$ = temperature rise of a stack of laminations (average value)
$\vartheta_s$ = temperature rise of the side-surfaces of a stack of laminations
$\vartheta_{Fe,m}$ = temperature rise of the iron in the middle of the stack
$\vartheta_{max}$ = temperature rise of the copper in the middle of the core
$\vartheta_{min}$ = temperature rise of the copper in the middle of the end-winding
$\vartheta_{av}$ = temperature rise of the copper, average value as found by resistance test
$\vartheta_R$ = temperature rise of the commutator risers

# *Chapter 20*

## APPROXIMATE DETERMINATION OF THE FIELD-DISTRIBUTION CURVE

In order to determine the flux distribution curve, i.e., $B=f(x)$, in the air-gap, the following approximate method can be applied. Draw several equipotential lines (1, 2, and 3) (Fig. 20–1), i.e., lines between which the magnetic potential (mmf) is constant, in such a manner that the total mmf between pole and armature is divided into *equal* parts. Since the equipotential lines are perpendicular to the lines of force ($B$ lines), the pole-face surface, and the armature surface in Fig. 20–1 are also equipotential lines. Thus in Fig. 20–1 the space between the pole-shoe tip and the armature is divided into 4 parts by 5 equipotential lines. The distances between the end-points of the equipotential lines 1, 2, and 3 are equal since the mmf increases linearly from the bottom to the top of the pole (see Fig. 16–10).

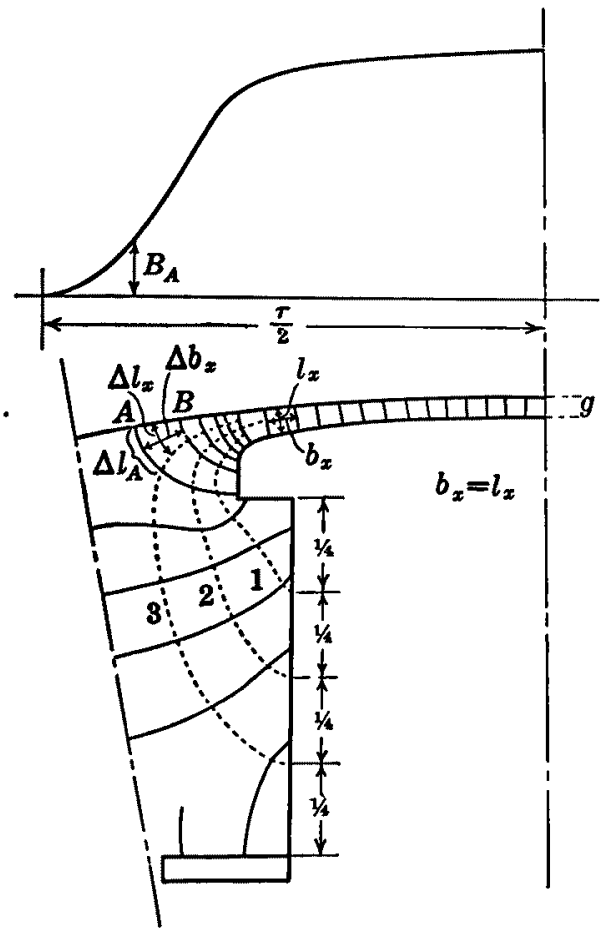


FIG. 20–1. Determination of the field distribution curve.

Draw the lines of force perpendicular to the equipotential lines in such a manner that the quadrangles obtained show the same distances between the mid-points of the lines of force as between the mid-points of the equipotential lines, i.e., make $b_x=l_x$. With this kind of division, the flux between each two adjacent lines of force is *constant*.

For the part of the pole-face where the air-gap is constant, the quadrangles are squares and the equipotential lines given by the pole-face line and armature surface line suffice to draw the lines of force. At the pole-tips the

additional equipotential lines (1, 2, and 3 in Fig. 20–1) are necessary, and a finer subdivision along the equipotential lines increases the accuracy of the method. For this part of the pole the equipotential lines and the lines of force have to be drawn several times until the width and height of each quadrangle are equal, and at the same time the lines of force are perpendicular to the equipotential lines.

In this way the real value of $B$ between the pole-shoe and the armature is obtained. In order to determine the flux-distribution curve, i.e., $B=f(x)$ in the air-gap, consider Ohm's law of the magnetic circuit (Eq. 1–21). For any point at distance $x$ from the centerline of the pole,

$$B_x=\frac{\phi_x}{a_x}=0.4\pi NI\,\frac{1}{l_x\times 1} \tag{20–1}$$

i.e., the induction $B$ as function of $x$ is inversely proportional to the length of the tube of force, since the mmf $NI$ is the same for all tubes of force. Consider, for example, the tube of force between the points $A$ and $B$. This tube consists of 4 quadrangles on each of which the same mmf ($\frac{1}{4}$ of the total mmf) acts. Since $b_x=l_x$ for each quadrangle, the same flux goes through all parts of the tube. This also follows from Ohm's law of the magnetic circuit: for a unit length of the armature,

$$\phi_x=\frac{1}{4}\times 0.4\pi NI\,\frac{b_x\times 1}{l_x}$$

and $b_x=l_x$ makes $\phi_x$ a constant.

The tube of force considered between $A$ and $B$ is wider at the armature surface than at the pole-shoe, and the flux density is, therefore, smaller at the armature than at the pole. With respect to the induction at the armature surface, the tube can be replaced by one which consists of four parts equal to that adjacent to the armature. Thus the flux density $B_A$ at the point $A$, with the notations of Fig. 20–1, is

$$B_A=B_g\,\frac{g}{4\Delta l_x}$$

or, in general,

$$B_x=B_g\,\frac{g}{n\Delta l_x} \tag{20–2}$$

where $n$ is the number of quadrangles into which the tube of force is divided. (For bibliography on flux mapping.)

# *Chapter 21*

# THE TWO-STAGE AND THREE-STAGE ROTOTROLS

**21–1. The Two-Stage Rototrol.** It has been mentioned in Art. 10–8 that the two-stage Rototrol is an amplifier with a pole ratio 1:2. The smallest numbers of poles of this amplifier are, therefore, 2 and 4; 2 for the first stage, 4 for the second stage. A Rototrol with these numbers of poles has the appearance of a normal 4-pole generator, except that the field windings are different and that the armature winding has no equalizers, though it is of lap type.

Referring to Fig. 10–22, which shows schematically the main poles, the armature, and the brushes, and also to Fig. 21–1, the first stage is made by field coils on the poles 1 and 3, i.e., by control coils, and by the armature between the brushes $B_1B_3$. (Fig. 21–1.) The second stage is made by field coils on all 4 poles 1, 2, 3, and 4, and by the 4 brushes $B_1B_3$ and $B_2B_4$. This becomes clear from the following consideration.

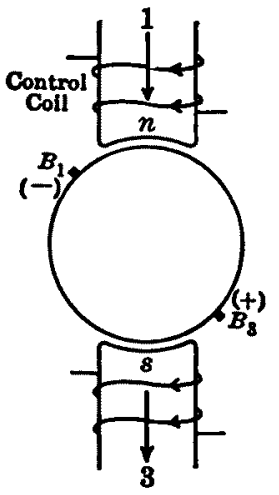


FIG. 21–1. First stage of the 2-stage amplifier with the pole ratio 1:2.

It must be noted first that the control coils on poles 1 and 3 will not produce a flux in the poles 2 and 4. In order that the control coils shall be effective, rotating amplifiers must operate at very low magnetic densities, i.e., on their gap characteristic. Since in this case the superposition of fluxes is admissible, the fluxes produced by the control coils and the 4-pole excitation coils are as shown in Fig. 21–2. In this figure it is assumed that the 4-pole excitation makes poles 1 and 3 north poles ($N$) and poles 2 and 4 south poles ($S$), while the control coils make pole 1 a north pole ($n$) and pole 3 a south pole ($s$). For the 4-pole excitation, the polarity of the brushes $B_1$ and $B_3$ will be assumed minus, and that of the brushes $B_2$ and $B_4$ plus. For the 4-pole machine, brush $B_1$ can be directly connected to brush $B_3$ and brush $B_2$ to brush $B_4$. Since there is but one armature winding rotating in the two fields, the 2-pole excitation, i.e., the control coils, will make brush $B_1$ minus ( − ) and brush $B_3$ plus ( + ). It will be shown presently that the control field does not induce an emf between brushes $B_2$ and $B_4$.

While the armature winding which is wound 4-pole is normal with respect

to the 4-pole field, it is abnormal with respect to the 2-pole control field: with respect to this field it is chorded 50%, i.e., with respect to this field, the upper and lower conductors which together make up a winding element are only nearly 90 electrical degrees apart instead of nearly 180°. In a normal 2-pole machine the brush position for maximum voltage is perpendicular to the pole axis. This is not the case here due to the fact that the winding is 50% chorded.

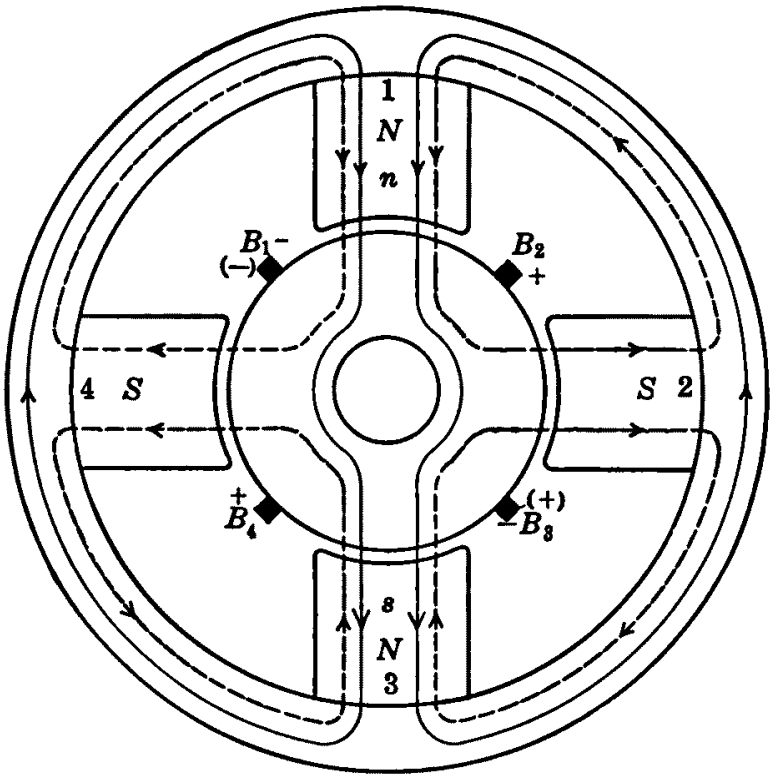


FIG. 21–2. Pole fluxes of the 2-stage amplifier with the pole ratio 1:2.

Fig. 21–3 shows the emf's induced by the 2-pole control flux between the brushes $B_1$ and $B_3$. The upper and lower layer of only one of the 2 parallel circuits are shown. The conductors which lie in the interpolar space of the 2-pole field, between $a$ and $B_3$, have practically no emf induced in them. The emf between the brushes $B_1$ and $B_3$ is made up of the emf's induced in the upper conductors which lie between $B_1$ and $a$ and the lower conductors which lie between $B_3$ and $b$. The position of the brushes $B_1$ and $B_3$ shown in Fig. 21–3 is the normal position of these brushes with respect to the 4-pole field, i.e., these brushes are each shifted 90 electrical degrees with respect to the axes of the poles $N$ and $S$ (Fig. 21–2). With respect to the pole axis $ns$, however, they are shifted only 45 electrical degrees. If any other position for the brushes $B_1$ and $B_3$ is assumed than that shown in Fig. 21–3, it will be found that the emf between them is smaller than that obtained in Fig. 21–3,

i.e., the brush position shown in Fig. 21–3 is the brush position for maximum voltage with respect to the 2-pole control flux and, thus, the brush position for maximum voltage is the *same* for the 2-pole control flux and the 4-pole flux. It is normal (shifted 90°) with respect to the axis of the 4-pole field and abnormal (shifted 45°) with respect to the axis of the 2-pole control field.

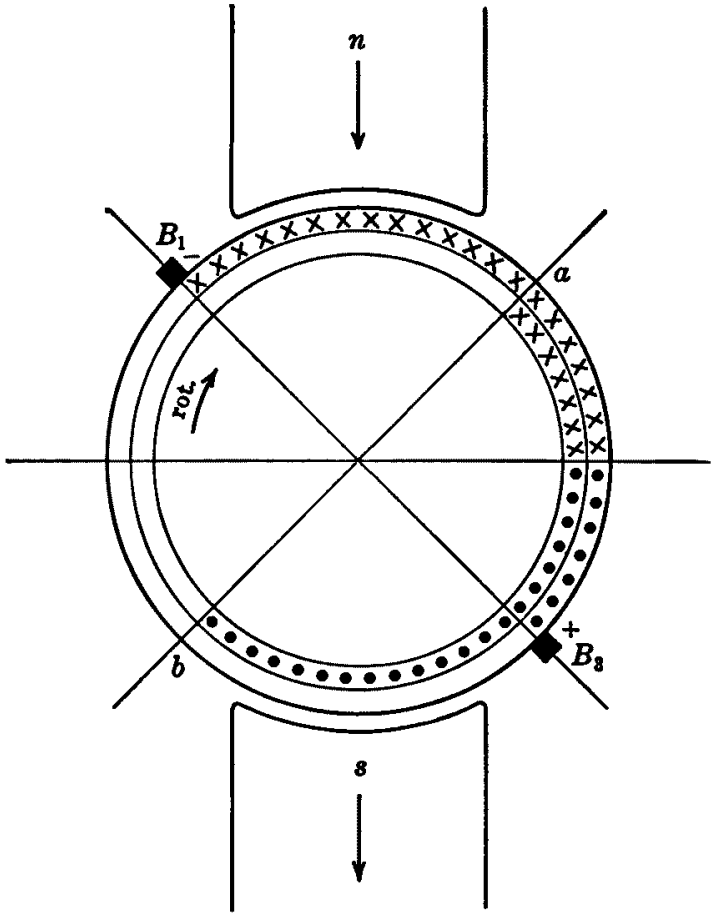


FIG. 21–3. Emfs induced between the brushes $B_1B_3$ by the control flux.

In a normal 2-pole machine the brush position for zero voltage is shifted 90 electrical degrees with respect to the brush position for maximum voltage. The same applies here. Fig. 21–4 shows the emf's induced by the 2-pole control flux between the brushes $B_2B_4$ which are shifted 90° with respect to the brushes $B_1B_3$. Disregarding the conductors which lie in the interpolar spaces of the 2-pole field (between $B_2a'$ and $a''B_4$), in the remaining conductors, between $a''B_2$, the emf's of the conductors of the lower layer have the same direction as the emf's of the conductors of the upper layer and since they all lie in the same path there is no emf between the brushes $B_2B_4$.

Summarizing, the 2-pole control field induces an emf only between the brushes $B_1B_3$ while the 4-pole flux induces emf's between each 2 neighboring brushes. The brushes $B_1B_3$ have opposite polarity with respect to the 2-pole

control field while they have the same polarity with respect to the 4-pole field (Fig. 21–2). The *voltage between* $B_1B_3$ due to the 2-pole control field *is now used to excite the field coils of the* 4*-pole field*, on the poles 1, 2, 3, and 4. Thus, the first stage of amplification is made by the control coils on poles 1 and 3 and the armature between the brushes $B_1B_3$, and the second stage is made by the field coils on poles 1, 2, 3, and 4 and the armature between the brushes $B_1B_2B_3B_4$.

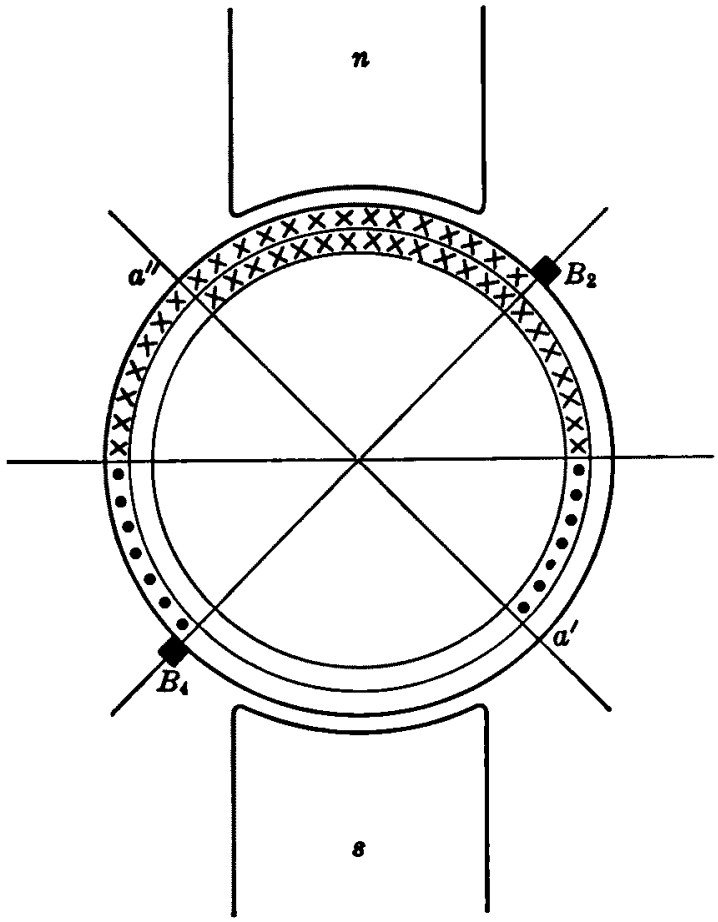


FIG. 21–4. Emfs induced between the brushes $B_2B_4$ by the control flux.

Since the 4-pole excitation of the second stage must follow only the control flux and not be influenced by the load, the 4-pole field coils must be arranged accordingly. Fig. 21–5 shows a series 4-pole excitation which is independent of the load. The coils 1 to 8 are field coils placed on the 4 poles (1, 2, 3, and 4) of the 4-pole machine, 2 on each pole. All 8 coils have the same number of turns. 4 of the 8 coils are marked by $C$, 4 by $D$. On each pole is placed one $C$- and one $D$-coil. The 4 $C$-coils as well as the 4 $D$-coils are connected in series. The 8 coils are connected to the brushes $B_1B_3$ which are the negative terminal of the 4-pole machine. The negative load terminal of this machine is connected to a tap between the coils $C$ and coils $D$. The current

of the 2-pole machine is denoted by $I_{2B_1B_3}$, that of the 4-pole machine is denoted by $2I_4$. It can be seen from Fig. 21–5 that the load current ($I_4$) flows through the $C$-coils in opposite direction to that through the $D$-coils. If the $C$- and $D$-coils are wound in the same direction, the resultant mmf on each pole, due to the current $I_4$, will be zero, i.e., if this current makes the 4 $C$-coils cumulative compound, the 4 $D$-coils will be differential compound, and the load current $I_4$ will have no effect on the excitation of the 4-pole machine.

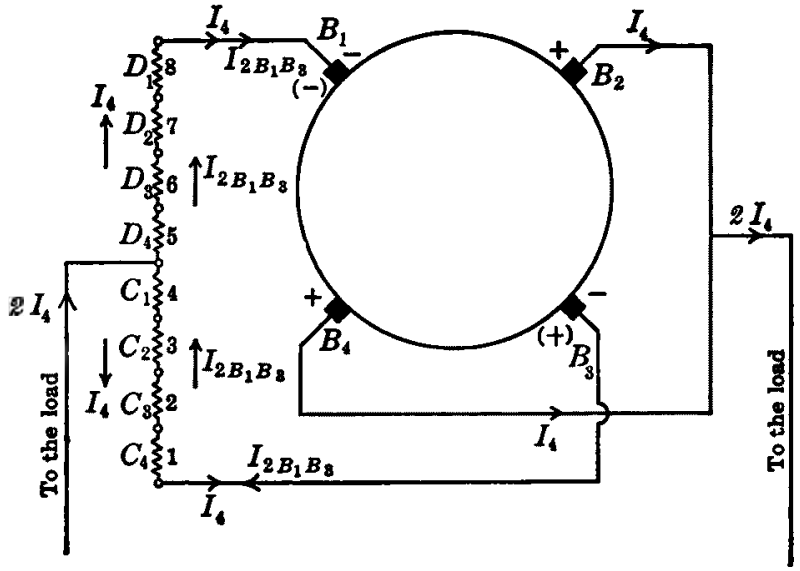


FIG. 21–5. Arrangement of the field coils of the second stage.

Consider now the current $I_{2B_1B_3}$ produced by the control field in the 2-pole machine between the brushes $B_1B_3$ (Fig. 21–5). This current flows through the $C$-coils and $D$-coils in the same direction. Since all coils are wound in the same direction, their mmf's *add up* on each pole producing a strong field for the 4-pole machine, i.e., for the second stage of amplification.

The arrangement described in the foregoing represents a pure amplifier, i.e., the load of the second stage is controlled exclusively by the excitation of the first stage (by the control coils). When the current in the control coils is zero, the output current ($2I_4$) of the machine is zero, i.e., under steady state conditions the amplifier delivers no power. It is usually desirable to use the machine as an amplifier for control purposes under transient conditions and as a normal generator under steady-state conditions. Consider the case where a pure amplifier is used to control the voltage of an a-c generator. When a change of the a-c load and, therefore, of the a-c voltage occurs, a *reference* or *pattern* circuit connected with the a-c generator transmits power to the control coils which, by means of the amplifier armature and of special field coils on the poles of the exciter of the generator, takes care of the voltage adjustment. Under steady-state conditions neither the control coils nor the armature of the amplifier, nor the special field coils of the exciter carry current. If, however, the coils $C$ and $D$ in Fig. 21–5 are given different

numbers of turns, the 4-pole machine is able to operate as a series generator under steady state conditions and can then replace the exciter. Instead of making the coils $C$ and $D$ different, additional special series coils can be arranged on the 4 poles 1, 2, 3, and 4, and placed in the load circuit (for example, in the negative load lead connected between coils 4 and 5, Fig. 21–5). Instead of series coils also shunt coils on the poles 1, 2, 3, and 4 can be used, in order to make the 4-pole machine self-excited. In either case the machine must be tuned (see Art. 10–6), i.e., be able to operate on its gap characteristic.

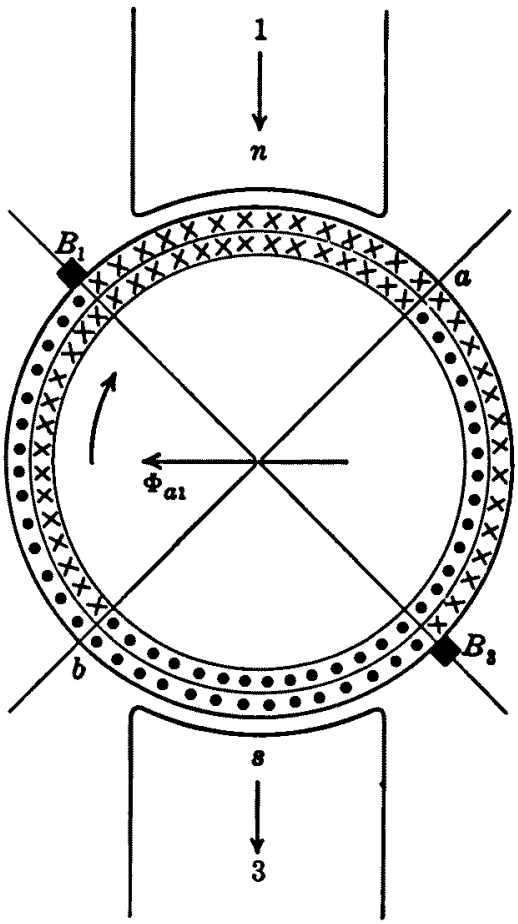


FIG. 21–6. Current distribution due to the circulating current $I_{2B_1B_3}$ between the brushes $B_1B_3$.

It has been pointed out that the neutralization of armature reaction is of primary importance in the 2-stage amplifier with the pole-ratio 1 : 1. The armature reaction must also be given special consideration here. Consider Fig. 21–6 which shows the distribution of the circulating current $I_{2B_1B_3}$ between the brushes $B_1B_3$. This figure corresponds to the emf distribution of Fig. 21–3. It can be seen that this current distribution produces a flux $\Phi_{a1}$ perpendicular to the pole axis $ns$, i.e., to the axis of poles 1 and 3. It is directed from the right to the left and takes its magnetic path through the poles 2 and 4, as shown in Fig. 21–7. This is a 2-pole flux superimposed on poles 2 and 4 which produces a north pole ($n'$) in pole 2 and a south pole ($s'$) in pole 4. The brushes $B_2B_4$ have, with respect to the poles $n's'$, exactly the same position as the brushes $B_1B_3$ have with respect to the poles $ns$ of the control flux. Therefore, the flux $\Phi_{a1}$ will induce maximum emf between the brushes $B_2B_4$ and zero emf between the brushes $B_1B_3$. Since the brushes $B_2B_4$ are connected together (see Fig. 21–5) a circulating current $I_{2B_2B_4}$ will flow between the brushes $B_2B_4$. The polarities of the brushes $B_2$ and $B_4$ due to the flux $n's'$ are respectively the same as the polarities of the brushes $B_1$ and $B_3$ due to the control flux ($ns$). The distribution of the current $I_{2B_2B_4}$ in the armature is shown in Fig. 21–8. It has the same distribution as in Fig. 21–6, except that it is shifted 90° to the right. It can be seen that the flux $\Phi_{a2}$ due to this current distribution is directed upwards, opposite to the control coil flux. Thus the circulating current $I_{2B_1B_3}$ causes a flux $\Phi_{a2}$ which would practically destroy the control flux if no means were taken to prevent this.

To counteract the armature reaction, either the flux $\Phi_{a1}$ can be eliminated and then no opposing flux $\Phi_{a2}$ will exist, or the opposing flux $\Phi_{a2}$ can be destroyed, or a part of the flux $\Phi_{a1}$ and the flux $\Phi_{a2}$ produced by the remainder of flux $\Phi_{a1}$ can then be eliminated. In order to eliminate the flux $\Phi_{a1}$ either a distributed compensated winding (see Art. 9–6) in the pole shoes of the poles 1 and 3 or simpler concentrated coils on the poles 2 and 4 can be used. In either case the coils must be fed by the current $I_{2B_1B_3}$. In order to eliminate

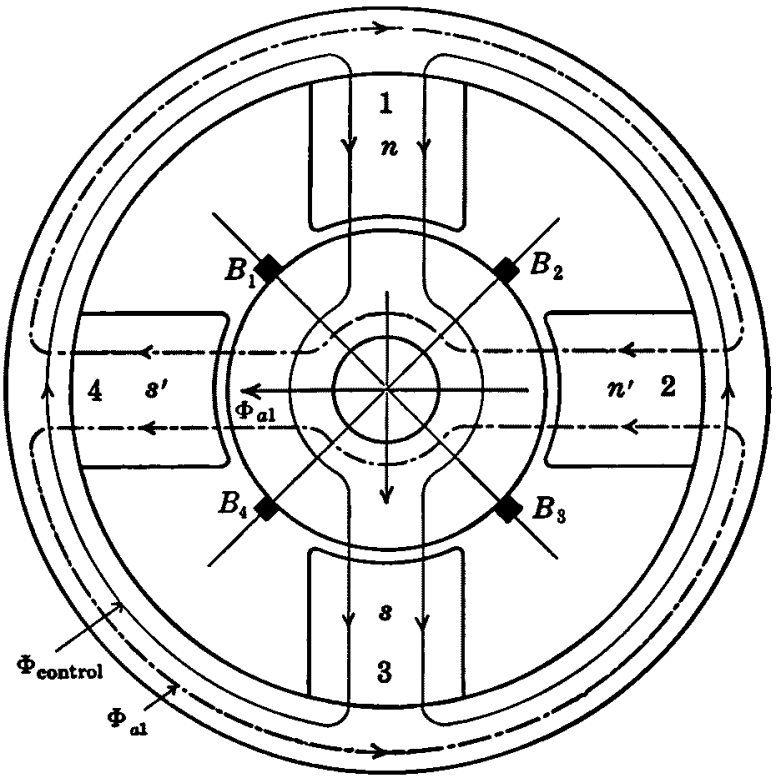


FIG. 21–7. Armature flux $\Phi_{a1}$ produced by the circulating current between the brushes $B_1B_3$.

the flux $\Phi_{a2}$ either a distributed compensating winding in the pole shoes of the poles 2 and 4 or simpler concentrated coils on the poles 1 and 3 can be used. In either case the coils must be fed by the current $I_{2B_2B_4}$. A combination of concentrated coils on poles 2 and 4 fed by the current $I_{2B_1B_3}$, concentrated coils on poles 1 and 3 fed by the current $I_{2B_2B_4}$, and concentrated coils on poles 2 and 4 fed by the current $I_{2B_2B_4}$ may be used to provide satisfactory reduction of armature reaction. The latter coils are less effective than the first ones but they also contribute to the reduction of the flux $\Phi_{a1}$.

During transients the current distribution (Fig. 21–6) due to the circulating current $I_{2B_1B_3}$ is superimposed on the current distribution of the 4-pole machine. The resultant current distribution is not symmetrical. In order to achieve satisfactory commutation, 4 different coils are necessary on each interpole.

**21–2. Multi-Stage Amplifier (Multi-Stage Rototrol).** Consider Figs 21–1 and 21–5. In the 2-stage amplifier with the pole ratio 1 : 2 the voltage

induced between the brushes $B_1B_3$ by the control flux is used to excite the 4 poles 1, 2, 3, and 4 of the second stage. The armature current $I_{2B_1B_3}$ due to this voltage produces an armature flux $\Phi_{a1}$ in the axis of the poles 2 and 4 (Fig. 21–7). As has been explained in the foregoing, such a flux induces an emf between the brushes $B_2B_4$. Therefore, if the voltage induced by the control flux between the brushes $B_1B_3$ is used in order to excite field coils on the

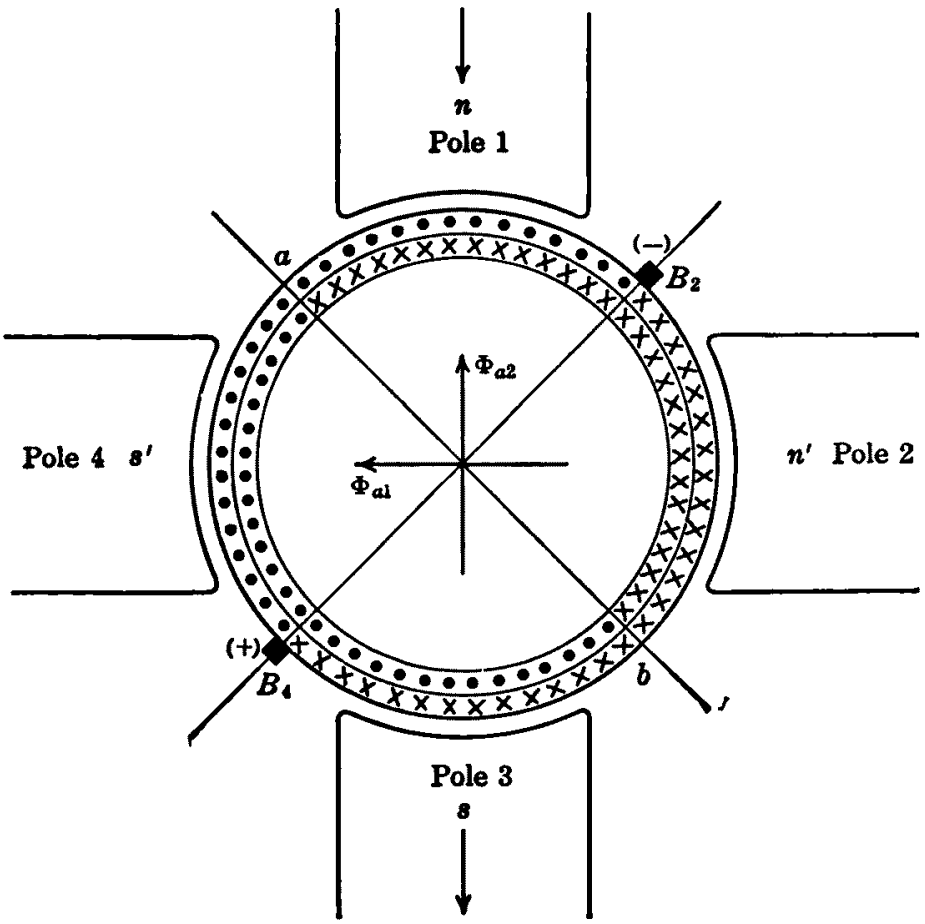


FIG. 21–8. Current distribution and armature flux ($\Phi_{a2}$) produced by a circulating current between the brushes $B_2B_4$.

poles 2 and 4, an emf will be induced between the brushes $B_2B_4$ which in turn can be used in order to excite the 4 poles 1, 2, 3, and 4 of the 4-pole machine (see Ref. D17).

In this way 3 stages of amplification (Fig. 10–24) will be obtained, namely

first stage: 2-pole control flux in the poles 1 and 3—armature between the brushes $B_1B_3$.

second stage: 2-pole flux produced by the circulating current between brushes $B_1B_3$ in the poles 2 and 4—armature between the brushes $B_2B_4$.

third stage: 4-pole flux produced by the circulating current between the brushes $B_2B_4$ in the poles 1, 2, 3, and 4—armature between the brushes $B_1B_2B_3B_4$.

The pole-ratios of this 3-stage amplifier are 1 : 1 : 2. The coil arrangement for this amplifier is shown in Fig. 21–9. Care must be taken that the load current does not influence the excitation of the second stage, i.e., the field coils on the poles 2 and 4 fed by the current $I_{2B_1B_3}$. This can be achieved in the same manner as for the second stage of the 2-stage amplifier (see Fig. 21–5). On each of the poles 2 and 4, 2 coils are placed, $D_2$ and $C_2$ and $D_4$ and $C_4$, respectively, which have the same number of turns. The 2 $D$-coils as well as

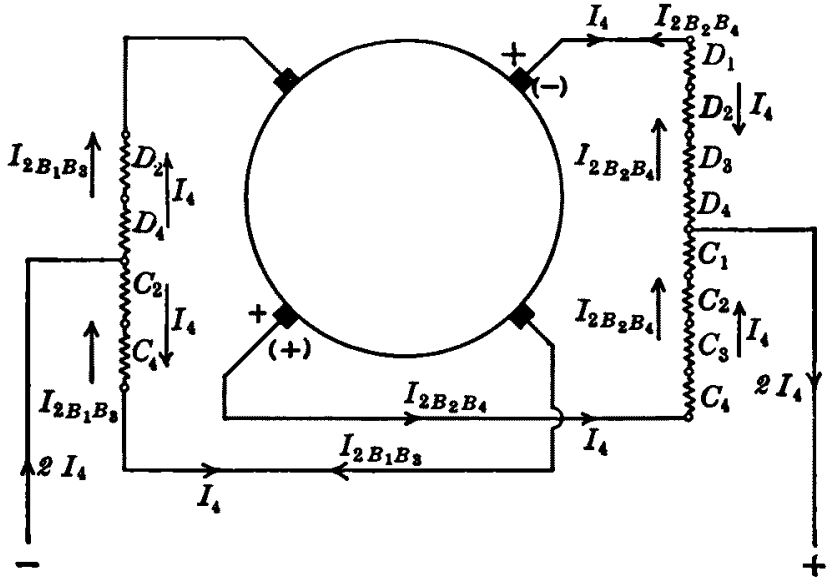


FIG. 21–9. Schematic representation of the 3 stages of the amplifier with the pole ratios 1:1:2.

the 2 $C$-coils are connected in series and the lead to the load is connected to a tap between the $D$-coils and $C$-coils. The 4 coils are wound in the same direction so that they cancel out on each pole with respect to the load current $I_4$, while all 4 coils add up with respect to the exciting current $I_{2B_1B_3}$.

The armature flux $\Phi_{a1}$ produced by the circulating current $I_{2B_1B_3}$ lies in the axis of the poles 2 and 4. Therefore, the field coils of the second stage on the poles 2 and 4 fed by the circulating current $I_{2B_1B_3}$ should be excited in such a manner as to produce a flux in the direction of the flux $\Phi_{a1}$, i.e., increasing this flux. This will increase the voltage between the brushes $B_2B_4$ and, therefore, the amplification.

It has been mentioned in the foregoing that the 2-stage amplifier with the pole ratio 1 : 1 has an amplification $100^2$ under certain conditions. The same applies to the 2-stage amplifier with the pole ratio 1 : 2. The 3-stage amplifier will have under the same conditions an amplification $100^3$. Since such an amplification is usually unnecessary, the field coils of the second stage on the poles 2 and 4 can be omitted, i.e., the brushes $B_1$ and $B_3$ can be short-circuited and the armature flux $\Phi_{a1}$ produced by the circulating current $I_{2B_1B_3}$ in the

poles 2 and 4 used as excitation for the second stage. The coil arrangement for this case is shown in Fig. 21–10.

If operation as a generator under steady-state conditions is desired, then either the coils $C_1$ to $C_4$ and the coils $D_1$ to $D_4$ have to be given different numbers of turns or otherwise 4 special coils have to be placed on the 4 poles 1, 2, 3, and 4. If these coils are fed by the current $2I_4$, i.e., placed in the load circuit, the 3rd stage will behave as a series generator under steady state conditions. Also shunt coils or both shunt and series coils can be used for self-excitation. The machine must be tuned.

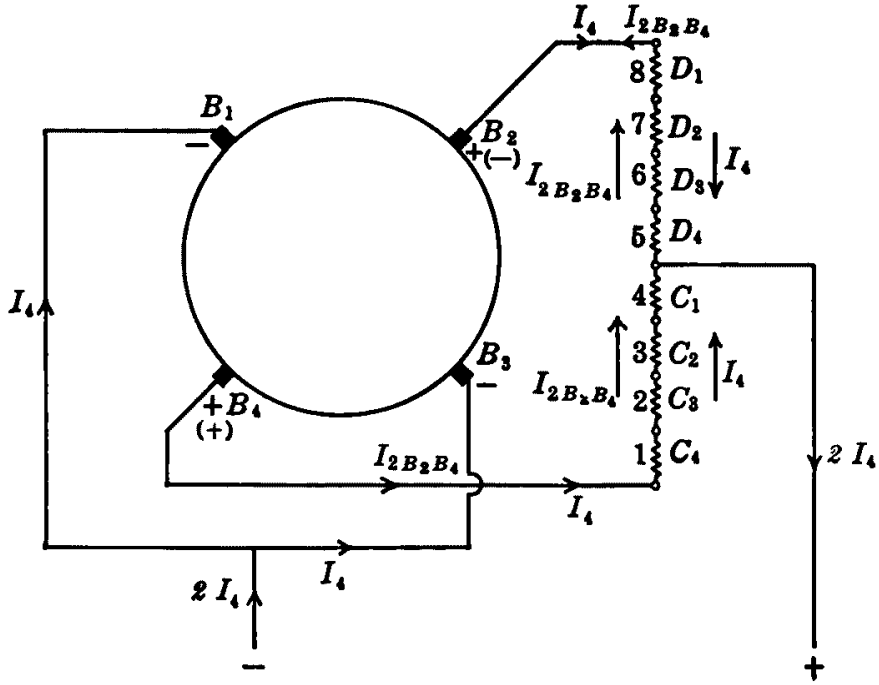


FIG. 21–10. Connections of the 3-stage amplifier with the pole ratios 1:1:2 when the armature reaction of the first stage is used to excite the second stage.

Contrary to the 2-stage amplifier, the armature flux $\Phi_{a1}$ due to the circulating current $I_{2B_1B_3}$ between the brushes $B_1$ and $B_3$ is a necessary flux in the 3-stage amplifier but not the flux $\Phi_{a2}$ produced in the axis of the poles 1 and 3 by the circulating current $I_{2B_2B_4}$ between the brushes $B_2$ and $B_4$. This flux opposes the control flux and must be eliminated. This can be done by arranging a distributed compensating winding in the pole-shoes of poles 2 and 4 or simpler by placing concentrated coils on the poles 1 and 3. In both cases the coils must be fed by the current $I_{2B_2B_4}$ which produces the flux $\Phi_{a2}$. Since the amplification of the 3-stage amplifier is very high, the compensation of the armature reaction is not so critical as in the 2-stage amplifier.

The machine considered in the foregoing is a 4-pole machine. As has been shown, 3 stages of amplification can be achieved. More stages of amplification can be obtained if a machine with a higher number of poles than 4 is used.

# REFERENCES

## A. Electromagnetic Field Theory


1. *The Electromagnetic Field.* M. Mason and W. Weaver. University of Chicago Press, 1929.
2. *Classic Theory of Electricity and Magnetism.* M. Abraham and R. Becker. Blackie and Sons, 1932.
3. *Electromagnetic Theory.* J. A. Stratton. McGraw-Hill, 1941.
4. *Electric and Magnetic Fields.* S. S. Atwood. Wiley, 1941.
5. *Two Dimensional Fields in Electrical Engineering.* L. Bewley. Macmillan, 1948.
6. *Electromagnetic Fields.* E. Weber. Vol. I and Vol. II. Wiley, 1951.
7. *The Origin of the Torque in Electric Machines.* K. Humburg. Elektrotechnische Zeitschrift, 1950, p. 311.
8. Arrangement for Testing the Location of the Electromagnetic Forces in Slotted Armatures. L. Fleischmann. *ETZ,* Vol. 42, 1921, p. 287.
9. Power Flow in Electrical Machines. J. Slepian. *El. J.,* Vol. 31, 1926, p. 61.
10. Notes on Air-Gap and Interpolar Induction. F. W. Carter. *IEE Proc.* (British), Vol. 29, 1900, p. 925.
11. Air Gap Induction. F. W. Carter. *El. Works,* Vol. 38, 1901, p. 884.
12. The Reluctance of Some Irregular Magnetic Fields. J. F. H. Douglas. *AIEE Proc.,* Vol. 34, 1915, p. 1067.
13. The Graphical Determination of Two-Dimensional Magnetic Fields in Regions Where Laplace's Equation Is Satisfied and Also in Regions Where the Curl of the Field Is Not Zero. Th. Lehmann. *Rev. Gen. El.,* Vol. 14, 1923.
14. Sketches of Magnetic Fields in Iron. Th. Lehmann. *Rev. Gen. El.,* Vol. 17, 1926.


## B. Flux Mapping


1. Mapping Magnetic and Electrostatic Fields. A. D. Moore, *El. J.,* Vol. 23, 1926, p. 355.
2. Fundamental Theory of Flux Plotting. A. R. Stevenson. *G.E. Rev.,* Vol. 29, 1926, p. 797.
3. Graphical Determination of Magnetic Fields. R. W. Wieseman. *AIEE Trans.,* Vol. 46, 1927, p. 430.
4. Graphical Determination of Magnetic Fields. E. E. Johnson and C. H. Green. *AIEE Trans.,* Vol. 46, 1927, p. 136.
5. Graphical Determination of Magnetic Fields. A. R. Stevenson and R. H. Park. *AIEE Trans.,* Vol. 46, 1927, p. 112.
6. The Interpolar Fields of Saturated Magnetic Circuits. Th. Lehmann. *AIEE Trans.,* Vol. 46, 1927, p. 1411.
7. A Practical Application of Graphical Flux Mapping. J. F. Calvert. *El. J.,* Vol. 24, 1927, p. 543.
8. Graphical Flux Mapping. J. F. Calvert and A. M. Harrison. *El. J.,* Vol. 25, 1928. Theory and General Discussion, p. 147; Fields of Non-Salient Pole Synchronous Machines, p. 179; D-C Motors and Generators, p. 399; D-C Motor, Salient Pole Synchronous Machine, Universal Motor, etc., p. 510.

9. Analytical Determination of Magnetic Fields. B. L. Robertson and I. A. Terry. *AIEE Trans.*, Vol. 48, 1929, p. 1242.
10. Magnetic Fields in Machinery Windings. J. F. H. Douglas. *AIEE Trans.*, Vol. 54, 1935, p. 959.

### C. Textbooks on D-C Machines

1. *D-C Machines.* E. Arnold and J. L. La Cour. Vol. I and II. Springer, Germany, 1927.
2. *Electric Machinery.* R. Richter. Vol. I. Springer, Germany, 1924.
3. *Electric Machinery.* Vol. I, II, III. M. Liwschitz-Garik, Teubner, Germany, 1926/1931/1934.
4. *Principles of D-C Machines.* A. S. Langsdorf. McGraw-Hill, 1940.
5. *Direct-Current Machinery.* R. G. Kloeffler, R. M. Brenneman and J. L. Kerchner. Macmillan, 1948.

### D. Special D-C Machines

1. D-C Machine for Three-Wire System. M. Dolivo-Dobrowolsky. *ETZ*, Vol. 15, 1894, p. 323.
2. *D-C Machines.* E. Arnold and J. L. La Cour. Vol. 2. Springer, Germany, 1927.
3. A New D-C Machine and Its Application to Train-Lighting. E. Rosenberg. *ETZ*, Vol. 26, 1905, p. 393.
4. New Welding Generator of Cross-Field Design. J. H. Blankenbuhler. *The Welding Engineer*, 1935.
5. A New Type of Arc-Welding Generator. S. R. Bergman. *G.E. Rev.*, Vol. 23, 1920, p. 442.
6. New System for D-C Arc-Welding. S. R. Bergman. *AIEE Trans.*, Vol. 50, 1931, p. 678.
7. The Diverter-Pole Generator. E. D. Smith. *J. AIEE*, Vol. 48, 1929, p. 11.
8. Electrical Drives for Wide Speed Ranges. G. A. Caldwell and W. H. Formhals. *AIEE Trans.*, Vol. 61, 1942.
9. Wide Speed Control with the Rototrol. W. H. Formhals. *Westinghouse Engineer*, Vol. 2, 1942.
10. Industrial Application of Rototrol Regulators. W. R. Harris. *AIEE Trans.*, Vol. 65, 1946, p. 118.
11. The Amplidyne Generator—A Dynamoelectric Amplifier for Power Control. E. F. Alexanderson, M. A. Edwards, and K. K. Bowman. *AIEE Trans.*, Vol. 59, 1940.
12. Design Characteristics of Amplidyne Generators. A. Fisher. *AIEE Trans.*, Vol. 59, 1940.
13. Industrial Applications of Amplidyne Generators. D. R. Shoults, M. A. Edwards, and F. E. Clever. *AIEE Trans.*, Vol. 59, 1940.
14. Steady State Theory of the Amplidyne Generator. T. D. Graybeal. *AIEE Trans.*, Vol. 61, 1942.
15. Fundamentals of the Amplidyne Generator. J. L. Bower. *AIEE Trans.*, Vol. 64, 1945.
16. The Two-Stage Rototrol. A. W. Kimball. *AIEE Trans.*, Vol. 66, 1947.
17. The Multi-Stage Rototrol. M. Liwschitz. *AIEE Trans.*, Vol. 66, 1947.

### E. Control and Starters

1. *Control of Electric Motors.* P. B. Harwood. Wiley, 1944.
2. *Electric Motors in Industry.* D. R. Shoults and C. J. Rife. Wiley, 1942.

3. Theory and Design of NEMA Resistors for Motor Starting and Speed Control. G. C. Armstrong. *AIEE Trans.*, Vol. 59, 1940, p. 277.
4. Variable Voltage or Field Control of Speed for D-C Drives. T. B. Montgomery and J. F. Sellers. *Allis Chalmers El. Rev.*, 1937, p. 17.
5. NEMA Industrial Control Standards.

## CONVERSION TABLE

| *Multiply* | *by* | *to obtain* |
|---|---|---|
| Centimeters | 0.3937 | Inches |
| Centimeters | 0.01 | Meters |
| Circular mils | $0.7854 \times 10^{-6}$ | Square inches |
| Square centimeters | 0.1550 | Square inches |
| Square centimeters | $10^{-4}$ | Square meters |
| Square inches | 6.45 | Square centimeters |
| Dynes | $10^{-5}$ | Newtons |
| Dynes | $2.25 \times 10^{-6}$ | Pounds |
| Dyne-centimeters | $10^{-7}$ | Newton-meters |
| Dyne-centimeters | $7.38 \times 10^{-8}$ | Pound-feet |
| Ergs | $10^{-7}$ | Joules or watt-seconds |
| Joules | 0.738 | Foot-pounds |
| Foot-pounds | $3.77 \times 10^{-7}$ | Kilowatt hours |
| Kilowatt-hours | 3413 | B.T.U. |
| Kilowatt-hours | 1.34 | Horsepower-hours |
| Kilowatt-hours | $3.6 \times 10^{6}$ | Joules |
| Kilowatt-hours | 860 | Kilogram-calories |
| Foot-pounds per second | $1.356 \times 10^{-3}$ | Kilowatts |
| Horsepower | 746 | Watts |
| Abamperes | 10 | Amperes |
| Abvolts | $10^{-8}$ | Volts |
| Abohms | $10^{-9}$ | Ohms |
| Ohm-centimeters | 0.01 | Ohm-meters |
| Ohm-centimeters | $6.02 \times 10^{6}$ | Ohms "per mil foot" |
| Kilolines | 1000 | Maxwells (lines) |
| Maxwells (lines) | $10^{-8}$ | Webers |
| Gausses | 6.45 | Lines per square-inch |
| Gausses | $10^{-4}$ | Webers per square-centimeter |
| Ampere-turns | 1.257 | Gilberts |
| Ampere-turns per inch | 39.37 | Ampere-turns per meter |
| Ampere-turns per inch | 0.495 | Oersteds |
| Abhenries | $10^{-9}$ | Henries |
| Abfarads | $10^{9}$ | Farads |

# INDEX


Air gap, area, 228
  mmf for, 228
Air gap line, 67
Ampére's Law, 1, 8, 61
Application of generators, 103-104
Amplidyne, 168
Amplifiers, rotating, 164, 168, 170, 291-300
Armature core, 19
Armature paths, number of, 31, 38
Armature reaction, 67, 70-75
Armature windings, 26-53
  emf in, 55-57
Application of motors, 120-129
Arc-welding generators, 161-163
Automatic starters for motors, 207-213

Back pitch, 29
Biot-Savart Law, 10, 57, 219
Brushes, current density in, 84, 141
Brush curve, 151
Brush resistance, 84, 138
Brush rigging, 22

Carter factor, 232
Characteristic curves of generators, 83-100
Circuital law of magnetic field, 8, 61, chap. 16
Compound generators, 97-100
Cumulative compound motor, 117
Coefficient of self-inductance, 6, 143
Coefficient of mutual-inductance, 7, 148
Cooling and ventilation of machines, 186
Commutation, 135-153, 240-267
  accelerated, 142-143
  curve of, 137
  delayed, 143
  effect of brush position on, 144
  effect of emf's on, 143, 149
  linear, 140
  resistance, 140
  resistance commutation, 138
  short-circuited winding element, 135
  time of commutation, 136
Compensating windings, 146
Compound winding, 78
Cross-magnetizing, armature reaction, 67

Differential compound motor, 119
Demagnetizing effect of arm, 74
Direction of rotation, 2, 80
Diverter pole generator, 163
Drum controller, 203
Duplex windings, 42
Dynamic braking, 212
Dynamotor, 164

Eddy current losses, 173
Electromagnetic power, 12
Electromagnetic torque, 57
Emf induced in armature, 55
Emf of self-inductance, 149
Emf of short-circuited element, 265
Enclosed motor, 24
Enclosures, types of, 188
Equalizer connections, 49
External characteristics of generators, 83, 86, 91, 94, 97
Excitation, methods of, 77-80

Faraday's Law, 1, 55
Field coils, 21
Field displacement, 38, 43
Field distribution curve, determination of, 289
Field mmf, load, 73
  no-load, 61
Forces on conductors, 10, 219-226
Forces on the iron, 221, 224
Fundamental laws, 1

Generator
  application of, 103
  characteristic curves, 83-100
  compound, 67
  diverter pole, 163
  homopolar, 26

parallel operation, 100
Rosenberg generator, 158
separately excited, 84
series, 91
shunt, 91
third-brush, 160
tuned, 164
welding, 161

Heat conductivity, 182, 274
Heating and cooling of d-c machines, 182-193
Heating and cooling of a homogenous body, 184
Heat flow equations, 276
Heat transfer coefficients, 274
Homopolar generator, 26

Insulation of windings, 51
Interpoles, 145
Interpole ampere-turns, 266
Interpole flux density, 148
Iron losses, 173

Kirchhoff's Mesh Law, 8

Laminations, 18
Lap winding, 26-50
Leakage flux
of end winding, 247
of slots, 241
of tooth top, 245
Linear commutation, 140
Load characteristics, 85, 91, 94
Losses due to slot openings, skin effect, 268
Losses in d-c machines, 172-181
copper, 175
distribution of, 180
due to main flux, 172
examples, 181
friction and windage, 179
no-load, 179
pole face, 175
stray load, 179

Magnetic circuit of d-c machines, 61
Manual starters, 199
Mechanical elements, 17-25
Mill motor, 24
Mmf of armature, 67
of field, 61
Motor application, 123-129
Motor control, definitions used in, 214
Motor starters, 199
Motor types of frames, definitions used in, 188
Motors, comparison of types, 120
sizes and costs, 128, 130
Mutual inductance, 240
time of in commutation, 248

Neutral axis, 48, 71
No-load characteristics, 67, 83, 84
accurate determination of, 228-239

Parallel operation of generators, 100-103
Parallel paths in armature, 31, 38
Phasor diagrams of emf's, 41, 45
Polar diagrams of armature windings, 35, 37
Pole face losses, 268
Pole leakage, 230
Pole mmf, 236

Regulation curve of generators, 87, 90
Regulex, 164-168
Resistance of brushes and contact, 84, 138-139
Resistance commutation, 138
Rosenberg generator, 158-160
Rotating amplifiers, 168-171
Rototrol, 164-168
Rototrol, 2-stage and 3-stage, 291-300

Saturation curve, 9, 67
Separately excited generators, 84-90
Series generator, 91
Series motor, 115-117
Short-circuited winding elements, 152
Shunt generator, 91-97
Shunt motor, 109-114
Skin-effect losses, 271
Special d-c machines, 154-171
Speed-current of shunt motors, 112
Speed control of motors, 122-125
Speed equation of motor, 109
Split coil winding, 46
Stability of motors, 122
Starting a motor, 109
Starting of motors, 194-215
automatic, 207

dynamic braking and starter, 212
manual starter, 199
series motor, 198
shunt motor, 194
Stresses in the magnetic field, 219
Symmetry of armature windings, 49

Tangental forces in machines, 219-226
Teeth, forces on, 224
mmf for, 233
Temperature rise in copper and iron, 186, 188, 276, 283
Third brush generator, 160
Three-wire generator, 154
Torque-current of shunt motor, 113
Torque in d-c machines, 57
Torque in motors, 108
Train lighting generators, 157
Tuned generators, 164-168

Ventilation of machines, 188
Voltage, equation, 82
equation for motors, 107
Voltage polygon, 47

Wave winding, 26-50, 227
Welding generators, 161
Winding element, 27, 29
Winding pitch, 29
Windings, armature, 26-51